frontiers | Research Topics

Plant growth-promoting bacteria as key tool for future agriculture: Agronomic, molecular and omics approaches

Edited by
José David Flores Félix, Reiner Rincón Rosales,
Víctor Manuel Ruíz-Valdiviezo and Clara Ivette Rincón Molina

Published in
Frontiers in Microbiology

FRONTIERS EBOOK COPYRIGHT STATEMENT

The copyright in the text of individual articles in this ebook is the property of their respective authors or their respective institutions or funders. The copyright in graphics and images within each article may be subject to copyright of other parties. In both cases this is subject to a license granted to Frontiers.

The compilation of articles constituting this ebook is the property of Frontiers.

Each article within this ebook, and the ebook itself, are published under the most recent version of the Creative Commons CC-BY licence. The version current at the date of publication of this ebook is CC-BY 4.0. If the CC-BY licence is updated, the licence granted by Frontiers is automatically updated to the new version.

When exercising any right under the CC-BY licence, Frontiers must be attributed as the original publisher of the article or ebook, as applicable.

Authors have the responsibility of ensuring that any graphics or other materials which are the property of others may be included in the CC-BY licence, but this should be checked before relying on the CC-BY licence to reproduce those materials. Any copyright notices relating to those materials must be complied with.

Copyright and source acknowledgement notices may not be removed and must be displayed in any copy, derivative work or partial copy which includes the elements in question.

All copyright, and all rights therein, are protected by national and international copyright laws. The above represents a summary only. For further information please read Frontiers' Conditions for Website Use and Copyright Statement, and the applicable CC-BY licence.

ISSN 1664-8714
ISBN 978-2-8325-3895-1
DOI 10.3389/978-2-8325-3895-1

About Frontiers

Frontiers is more than just an open access publisher of scholarly articles: it is a pioneering approach to the world of academia, radically improving the way scholarly research is managed. The grand vision of Frontiers is a world where all people have an equal opportunity to seek, share and generate knowledge. Frontiers provides immediate and permanent online open access to all its publications, but this alone is not enough to realize our grand goals.

Frontiers journal series

The Frontiers journal series is a multi-tier and interdisciplinary set of open-access, online journals, promising a paradigm shift from the current review, selection and dissemination processes in academic publishing. All Frontiers journals are driven by researchers for researchers; therefore, they constitute a service to the scholarly community. At the same time, the *Frontiers journal series* operates on a revolutionary invention, the tiered publishing system, initially addressing specific communities of scholars, and gradually climbing up to broader public understanding, thus serving the interests of the lay society, too.

Dedication to quality

Each Frontiers article is a landmark of the highest quality, thanks to genuinely collaborative interactions between authors and review editors, who include some of the world's best academicians. Research must be certified by peers before entering a stream of knowledge that may eventually reach the public - and shape society; therefore, Frontiers only applies the most rigorous and unbiased reviews. Frontiers revolutionizes research publishing by freely delivering the most outstanding research, evaluated with no bias from both the academic and social point of view. By applying the most advanced information technologies, Frontiers is catapulting scholarly publishing into a new generation.

What are Frontiers Research Topics?

Frontiers Research Topics are very popular trademarks of the *Frontiers journals series*: they are collections of at least ten articles, all centered on a particular subject. With their unique mix of varied contributions from Original Research to Review Articles, Frontiers Research Topics unify the most influential researchers, the latest key findings and historical advances in a hot research area.

Find out more on how to host your own Frontiers Research Topic or contribute to one as an author by contacting the Frontiers editorial office: frontiersin.org/about/contact

Plant growth-promoting bacteria as key tool for future agriculture: Agronomic, molecular and omics approaches

Topic editors

José David Flores Félix — University of Salamanca, Spain
Reiner Rincón Rosales — Tuxtla Gutierrez Institute of Technology, Mexico
Víctor Manuel Ruíz-Valdiviezo — Tecnológico Nacional de México/Instituto Tecnológico de Tuxtla Gutiérrez, Mexico
Clara Ivette Rincón Molina — Instituto Tecnológico de Tuxtla Gutiérrez/TecNM, Chiapas, Mexico

Citation

Félix, J. D. F., Rosales, R. R., Ruíz-Valdiviezo, V. M., Molina, C. I. R., eds. (2023). *Plant growth-promoting bacteria as key tool for future agriculture: Agronomic, molecular and omics approaches*. Lausanne: Frontiers Media SA.
doi: 10.3389/978-2-8325-3895-1

Table of contents

05 Editorial: Plant growth-promoting bacteria as a key tool for future agriculture: Agronomic, molecular and omics approaches
Clara Ivette Rincón-Molina, Víctor Manuel Ruíz-Valdiviezo, Reiner Rincón-Rosales and José David Flores Félix

08 *Serratia plymuthica* MBSA-MJ1 Increases Shoot Growth and Tissue Nutrient Concentration in Containerized Ornamentals Grown Under Low-Nutrient Conditions
Nathan P. Nordstedt and Michelle L. Jones

22 Assessment of Bacterial Inoculant Delivery Methods for Cereal Crops
Yen Ning Chai, Stephanie Futrell and Daniel P. Schachtman

36 Newly Isolated *Paenibacillus monticola* sp. nov., a Novel Plant Growth-Promoting Rhizobacteria Strain From High-Altitude Spruce Forests in the Qilian Mountains, China
Hui-Ping Li, Ya-Nan Gan, Li-Jun Yue, Qing-Qing Han, Jia Chen, Qiong-Mei Liu, Qi Zhao and Jin-Lin Zhang

51 Identification of the Phosphorus-Solubilizing Bacteria Strain JP233 and Its Effects on Soil Phosphorus Leaching Loss and Crop Growth
Haiyang Yu, Xiaoqing Wu, Guangzhi Zhang, Fangyuan Zhou, Paul R. Harvey, Leilei Wang, Susu Fan, Xueying Xie, Feng Li, Hongzi Zhou, Xiaoyan Zhao and Xinjian Zhang

63 Volatile Organic Compounds of *Streptomyces* sp. TOR3209 Stimulated Tobacco Growth by Up-Regulating the Expression of Genes Related to Plant Growth and Development
Yuxi He, Wenyu Guo, Jieli Peng, Jinying Guo, Jia Ma, Xu Wang, Cuimian Zhang, Nan Jia, Entao Wang, Dong Hu and Zhanwu Wang

76 Melatonin Attenuates the Urea-Induced Yields Improvement Through Remodeling Transcriptome and Rhizosphere Microbial Community Structure in Soybean
Renhao Xiao, Qin Han, Yu Liu, Xuehai Zhang, Qingnan Hao, Qingqing Chai, Yongfang Hao, Junbo Deng, Xia Li and Hongtao Ji

92 Broad-spectrum resistance mechanism of serine protease Sp1 in *Bacillus licheniformis* W10 *via* dual comparative transcriptome analysis
Lina Yang, Chun Yan, Shuai Peng, Lili Chen, Junjie Guo, Yihe Lu, Lianwei Li and Zhaolin Ji

111 *Rhizobium etli* CFN42 proteomes showed isoenzymes in free-living and symbiosis with a different transcriptional regulation inferred from a transcriptional regulatory network
Hermenegildo Taboada-Castro, Jeovanis Gil, Leopoldo Gómez-Caudillo, Juan Miguel Escorcia-Rodríguez, Julio Augusto Freyre-González and Sergio Encarnación-Guevara

134 Molecular mechanisms of plant growth promotion for methylotrophic *Bacillus aryabhattai* LAD
Chao Deng, Xiaolong Liang, Ning Zhang, Bingxue Li, Xiaoyu Wang and Nan Zeng

148 Study of the effect of bacterial-mediated legume plant growth using bacterial strain *Serratia marcescens* N1.14 X-45
Jiaxin Zheng, Chao Liu, Jiayi Liu and Jia Yao Zhuang

161 Effect of the application of vermicompost and millicompost humic acids about the soybean microbiome under water restriction conditions
Maura Santos Reis de Andrade da Silva, Lucas Amoroso Lopes de Carvalho, Lucas Boscov Braos, Luiz Fernando de Sousa Antunes, Camilla Santos Reis de Andrade da Silva, Cleudison Gabriel Nascimento da Silva, Daniel Guariz Pinheiro, Maria Elizabeth Fernandes Correia, Ednaldo da Silva Araújo, Luiz Alberto Colnago, Nicolas Desoignies, Everaldo Zonta and Everlon Cid Rigobelo

176 Application of data integration for rice bacterial strain selection by combining their osmotic stress response and plant growth-promoting traits
Arun Kumar Devarajan, Marika Truu, Sabarinathan Kuttalingam Gopalasubramaniam, Gomathy Muthukrishanan and Jaak Truu

194 Potential of *Bacillus pumilus* to directly promote plant growth
Jakub Dobrzyński, Zuzanna Jakubowska and Barbara Dybek

200 Combination of *Aspergillus niger* MJ1 with *Pseudomonas stutzeri* DSM4166 or mutant *Pseudomonas fluorescens* CHA0-*nif* improved crop quality, soil properties, and microbial communities in barrier soil
Haiping Ni, Yuxia Wu, Rui Zong, Shiai Ren, Deng Pan, Lei Yu, Jianwei Li, Zhuling Qu, Qiyao Wang, Gengxing Zhao, Jianzhong Zhao, Lumin Liu, Tao Li, Youming Zhang and Qiang Tu

frontiers | Frontiers in Microbiology

TYPE Editorial
PUBLISHED 17 March 2023
DOI 10.3389/fmicb.2023.1168891

Check for updates

OPEN ACCESS

EDITED AND REVIEWED BY
Trevor Carlos Charles,
University of Waterloo, Canada

*CORRESPONDENCE
José David Flores Félix
✉ jdflores@usal.es

SPECIALTY SECTION
This article was submitted to Microbe and Virus Interactions with Plants, a section of the journal Frontiers in Microbiology

RECEIVED 18 February 2023
ACCEPTED 07 March 2023
PUBLISHED 17 March 2023

CITATION
Rincón-Molina CI, Ruíz-Valdiviezo VM, Rincón-Rosales R and Flores Félix JD (2023) Editorial: Plant growth-promoting bacteria as a key tool for future agriculture: Agronomic, molecular and omics approaches. *Front. Microbiol.* 14:1168891. doi: 10.3389/fmicb.2023.1168891

COPYRIGHT
© 2023 Rincón-Molina, Ruíz-Valdiviezo, Rincón-Rosales and Flores Félix. This is an open-access article distributed under the terms of the Creative Commons Attribution License (CC BY). The use, distribution or reproduction in other forums is permitted, provided the original author(s) and the copyright owner(s) are credited and that the original publication in this journal is cited, in accordance with accepted academic practice. No use, distribution or reproduction is permitted which does not comply with these terms.

Editorial: Plant growth-promoting bacteria as a key tool for future agriculture: Agronomic, molecular and omics approaches

Clara Ivette Rincón-Molina[1], Víctor Manuel Ruíz-Valdiviezo[1], Reiner Rincón-Rosales[1] and José David Flores Félix[2]*

[1]Instituto Tecnológico de Tuxtla Gutiérrez/Tecnológico Nacional de Mexico, Tuxtla Gutiérrez, Mexico, [2]CICS-UBI - Health Sciences Research Centre, University of Beira Interior, Covilhã, Portugal

KEYWORDS

plant growth-promoting bacteria, rhizosphere, biostimulant, omics, biofertilizer

Editorial on the Research Topic
Plant growth-promoting bacteria as a key tool for future agriculture: Agronomic, molecular and omics approaches

Plant growth-promoting bacteria (PGPB) are a fundamental tool in the agriculture of the future because the mechanisms they exhibit are key in improving agricultural efficiency, increasing the integration of agriculture into the environment, and reducing the ecological footprint of agriculture (Bizos et al., 2020). These bacteria have shown to be capable of interacting at different levels with crops, both through direct mechanisms, such as nitrogen fixation or phosphate solubilization, and indirect mechanisms, such as induction of systemic resistance (ISR) or competition for space through the formation of biofilms (Haskett et al., 2020). In recent years, and through the incorporation of omics techniques (genomics, transcriptomics, proteomics, ionomics, and metabolomics), we are starting to understand the depth of plant-microorganism interactions and define a holobiont with the implications that this has for design strategies in agriculture (Riva et al., 2022). These new approaches have shown that an in-depth study of the interactions between PGPB and crops is necessary to understand how to modulate and direct nutrient acquisition and plant improvement to biotic and abiotic stresses through the application of PGPB. The main objective of this Research Topic is to elucidate plant-microorganism interactions through the application of omic techniques and the use of multidisciplinary approaches. Within this topic, 14 articles have been published, providing a deeper understanding of plant-microorganism interactions in agricultural systems and the implications for improving crop productivity.

Nordstedt and Jones studied the potential of *Serratia plymuthica* MBSA-MJ1 as a PGPB, showing the usefulness of genomic analysis and the ability of this strain to improve the development and vigor of flower crops of *Petunia* × *hybrida* (petunia), *Impatiens walleriana* (impatiens), and *Viola* × *wittrockiana* (pansy), as well as increased root, shoot, and leaf development, and nutrient absorption. Dobrzyński et al. also evaluated the capacity of the *Bacillus pumilus* species through the study of the strains *B. pumilus* W8, *B. pumilus* LZP02, *B. pumilus* JPVS11, *B. pumilus* TUAT-1, *B. pumilus* TRS-3, and *B. pumilus* EU927414 for better plant production. The authors observed improvements in vegetative parameters, substance content (amino acids, proteins, and fatty acids), and oxidative enzymes. Some strains also showed an important capacity to modulate the rhizosphere of the hosts. On the other hand,

the study of the rhizosphere, whose diversity is not yet known, is essential in the search for new inoculants. Li et al. described *Paenibacillus monticola*, a novel bacteria that presented important capacities to promote development in *Arabidopsis* and *Trifolium repens*.

Ni et al. evaluated the capacity of the consortium of *Aspergillus niger* MJ1, *Pseudomonas stutzeri* DSM4166, and *P. fluorescens* CHA0-nif mutant strain on the quality of lettuce and cucumber. The authors discovered a positive effect on the production of these vegetables and modulation of the associated microbial populations to these crops, with enrichment in *Pyrinomonadaceae* and *Blastocatellia*. The application of PGPB in agriculture is a tool to improve crop efficiency, as shown by Yu et al. through the application of *Pseudomonas* sp. JP233, a phosphate solubilizing bacterium, which improved the absorption of this nutrient in corn without increasing P leaching.

The inoculation of certain PGPB strains can have a decisive effect on the rhizosphere, such as *Serratia marcenscens* X-45, whose inoculation not only improves vegetative and productive parameters in *Indigofera pseudotinctoria*, but also increases the abundance of *Bradyrhizobium*, an endosymbiont of this legume, from 1 to 42% in its rhizosphere, as demonstrated by Zheng et al.. This work strategy was also used by Deng et al. to study *in silico* the potential of *B. aryabhattai* LAD as a PGPB, identifying the main genes involved in growth promotion mechanisms and correlating with improvements in maize development.

Chai et al. studied the assessment method of PGPB, determining that due to the production of lipopeptidoglycans, as well as the need to adapt the inoculation method to the culture, Gram-positive bacteria are less sensitive to the adhesion method used than Gram-negative bacteria. The use of vermicompost and millicompost in conjunction with *Bradyrhizobium* sp. was studied by da Silva et al.. The authors showed an increase in taxa belonging to *Sphingobacteriaceae*, *Chitinophaga,* and *Actinobacteria*, thus enrichment in *Erysiphe diffusa* and *Thanatephorus cucumeris* related to phytopathogens. However, no disease was observed in soybean plants.

Devarajan et al. evaluated the use of statistical data integration methods, namely, principal component analysis (PCA) of concatenated data, multiple co-inertia analysis (MCIA), and multiple kernel learning (MKL), to improve PGPB selection. They demonstrated that data integration methods could complement the single-table data analysis approach and provide better insight into the microbial strain selection process.

The complexity of plant-microorganism interactions is proving to be significant, with elements such as enzymes (i.e., serine protease Sp1 from *B. licheniformis)* involved in biocontrol processes being capable of inducing upregulation of 150 differentially expressed genes (DEGs) and downregulation of 209 DEGs by RNA-seq technology. Yang et al. demonstrated that new application strategies for bacterial biofertilizers or their derivatives are possible. Another aspect studied in recent years is the role of volatile organic compounds (VOCs) in promoting plant growth and plant health. He et al. showed that the production of VOCs by *Streptomyces* sp. TOR3209 increases the expression of genes related to the improvement of plant development, such as UDP-glycosyltransferase or glutamate receptors.

In addition, not only are applied assays precise but the use of metatranscriptomic techniques allowed for the proteomic study of symbiosomes in *Phaseolus vulgaris* inoculated with *Rhizobium etli* CFN42. Taboada-Castro et al. showed differences in the production of isoenzymes associated with the development conditions of the endosymbiont, allowing us to understand the transcriptional regulations and the design of inoculation strategies.

Regarding the application of treatments to improve crop adaptation, Xiao et al. demonstrated that foliar application of melatonin induced transcriptomic modification on soybean leaves and changed rhizosphere microbial community species but not in alpha diversity, which is different from urea treatment. Their research indicates how foliar application of melatonin might influence soybean yields.

In conclusion, the study of the potential of new biofertilizers is essential for the development of biofertilizers that improve the efficiency of agriculture through *in silico* and in planta studies. This aspect should be complemented by a transcriptional study to understand and clarify the plant promotion mechanisms used by these bacteria and whose knowledge will allow the establishment of new bacterial biostimulation strategies.

Author contributions

CR-M and VR-V wrote the first draft of the manuscript. RR-R and JF revised the manuscript and wrote the final version of the manuscript. All authors contributed to the article and approved the submitted version.

Funding

This research was funded by the European Union's Horizon 2020 research and innovation program under the Marie Skłodowska-Curie grant agreement No. 101003373.

Conflict of interest

The authors declare that the research was conducted in the absence of any commercial or financial relationships that could be construed as a potential conflict of interest.

Publisher's note

All claims expressed in this article are solely those of the authors and do not necessarily represent those of their affiliated organizations, or those of the publisher, the editors and the reviewers. Any product that may be evaluated in this article, or claim that may be made by its manufacturer, is not guaranteed or endorsed by the publisher.

References

Bizos, G., Papatheodorou, E. M., Chatzistathis, T., Ntalli, N., Aschonitis, V. G., and Monokrousos, N. (2020). The role of microbial inoculants on plant protection, growth stimulation, and crop productivity of the olive tree (*Olea europea* L.). *Plants* 9, 743. doi: 10.3390/plants9060743

Haskett, T. L., Tkacz, A., and Poole, P. S. (2020). Engineering rhizobacteria for sustainable agriculture. *ISME J.* 15, 949–964. doi: 10.1038/s41396-020-00835-4

Riva, V., Mapelli, F., Bagnasco, A., Mengoni, A., and Borin, S. (2022). A meta-analysis approach to defining the culturable core of plant endophytic bacterial communities. *Appl. Environ. Microbiol.* 88, e0253721. doi: 10.1128/aem.02537-21

frontiers in Microbiology

ORIGINAL RESEARCH
published: 02 December 2021
doi: 10.3389/fmicb.2021.788198

Serratia plymuthica MBSA-MJ1 Increases Shoot Growth and Tissue Nutrient Concentration in Containerized Ornamentals Grown Under Low-Nutrient Conditions

*Nathan P. Nordstedt and Michelle L. Jones**

Department of Horticulture and Crop Science, Ohio Agricultural Research and Development Center, The Ohio State University, Wooster, OH, United States

OPEN ACCESS

Edited by:
José David Flores Félix, Universidade da Beira Interior, Portugal

Reviewed by:
Gayathri Ilangumaran, McGill University, Canada
Sowmyalakshmi Subramanian, McGill University, Canada
Naeem Khan, University of Florida, United States

***Correspondence:**
Michelle L. Jones
jones.1968@osu.edu

Specialty section:
This article was submitted to Microbe and Virus Interactions With Plants, a section of the journal Frontiers in Microbiology

Received: *01 October 2021*
Accepted: *10 November 2021*
Published: *02 December 2021*

Citation:
Nordstedt NP and Jones ML (2021) Serratia plymuthica MBSA-MJ1 Increases Shoot Growth and Tissue Nutrient Concentration in Containerized Ornamentals Grown Under Low-Nutrient Conditions. Front. Microbiol. 12:788198. doi: 10.3389/fmicb.2021.788198

High fertilizer rates are often applied to horticulture crop production systems to produce high quality crops with minimal time in production. Much of the nutrients applied in fertilizers are not taken up by the plant and are leached out of the containers during regular irrigation. The application of plant growth promoting rhizobacteria (PGPR) can increase the availability and uptake of essential nutrients by plants, thereby reducing nutrient leaching and environmental contamination. Identification of PGPR can contribute to the formulation of biostimulant products for use in commercial greenhouse production. Here, we have identified *Serratia plymuthica* MBSA-MJ1 as a PGPR that can promote the growth of containerized horticulture crops grown with low fertilizer inputs. MBSA-MJ1 was applied weekly as a media drench to *Petunia* × *hybrida* (petunia), *Impatiens walleriana* (impatiens), and *Viola* × *wittrockiana* (pansy). Plant growth, quality, and tissue nutrient concentration were evaluated 8 weeks after transplant. Application of MBSA-MJ1 increased the shoot biomass of all three species and increased the flower number of impatiens. Bacteria application also increased the concentration of certain essential nutrients in the shoots of different plant species. *In vitro* and genomic characterization identified multiple putative mechanisms that are likely contributing to the strain's ability to increase the availability and uptake of these nutrients by plants. This work provides insight into the interconnectedness of beneficial PGPR mechanisms and how these bacteria can be utilized as potential biostimulants for sustainable crop production with reduced chemical fertilizer inputs.

Keywords: biofertilizer, biostimulant, floriculture, genome analysis, horticulture, nutrient stress, nutrient solubilization, PGPR

INTRODUCTION

The plant rhizosphere, the microscopic environment surrounding plant roots, hosts a diversity of microorganisms. Plants secrete a variety of root exudates into the rhizosphere including sugars, vitamins, and amino acids, which assist in recruiting specific microbial populations (Lugtenberg and Kamilova, 2009; Martín-Sánchez et al., 2020). In return, many of these microbes

play essential roles in the rhizosphere ecosystem by influencing both plant and soil health (Vessey, 2003). The study of these beneficial plant growth promoting rhizobacteria (PGPR) and their contribution to agriculture has gained significant interest in recent years (Bhardwaj et al., 2014). PGPR can stimulate plant growth through a variety of mechanisms including modulating phytohormone levels, inhibiting growth of plant pathogens, producing secondary metabolites, and increasing the availability and uptake of nutrients for their plant host (Raklami et al., 2019; Martín-Sánchez et al., 2020).

Plants require 14 essential mineral nutrients to support proper growth and development, and agricultural systems often rely on the addition of chemical fertilizers to provide adequate nutrients to support crop production (Marschner, 2011). However, high rates of fertilizer are frequently attributed to surface and groundwater pollution due to nutrient leaching and runoff (Adesemoye and Kloepper, 2009). The bioavailability of nutrients for plant uptake plays a significant role in plant nutrient use efficiency (NUE), and therefore, the lack of bioavailability increases the susceptibility of nutrients to leaching and runoff (Adesemoye and Kloepper, 2009; Bindraban et al., 2015). This is of particular concern for horticulture crops grown in peat-based soilless substrates, which have lower ion exchange capacities than field soil, increasing the possibility that nutrients will be removed from the substrate *via* leaching (Bachman and Metzger, 2008). Therefore, it is important that crop producers find sustainable ways to produce crops with high yield and quality while minimizing chemical fertilizer inputs.

Studies have shown that the application of PGPR can increase the NUE of plants, thereby reducing the amount of nutrients that are leached into the environment (Khan, 2005; Adesemoye et al., 2008, 2010; Shaharoona et al., 2008; Arif et al., 2017; Pereira et al., 2020). A meta-analysis of studies evaluating PGPR application on plant NUE showed an average increase in NUE of 5.8 kg yield per kg nitrogen fertilizer applied (Schütz et al., 2018). Direct mechanisms that PGPR can utilize to facilitate increased nutrient bioavailability and uptake by plants include nitrogen fixation, nutrient solubilization, sulfur oxidation, and chelation of metals (Lugtenberg and Kamilova, 2009).

The availability of essential plant nutrients including phosphorus, potassium, and zinc is dependent on their solubility in the rhizosphere (Ruzzi and Aroca, 2015). When these nutrients are bound by other salts and metals, plants are unable to access them for growth and development. However, bacterial solubilization can make them readily accessible for plant utilization and less likely to be removed from the growing substrate *via* leaching (Adesemoye and Kloepper, 2009). Many bacterial species that are plant growth promoters have been identified as efficient solubilizers of phosphorus, potassium, and zinc (Sharma et al., 2013, 2016; Kamran et al., 2017; Borgi et al., 2020). The application of phosphorus-solubilizing *Bacillus* and *Aspergillus* strains reduces the level of fertilizer required for optimal yield and tissue nutrient content in strawberry (Güneş et al., 2014). Although many different bacterial enzymes can solubilize these nutrients, bacterial-produced organic acids are thought to be the primary mechanism involved in increasing the availability of insoluble phosphorus, potassium, and zinc (Rodríguez et al., 2006; Hussain et al., 2015; Parmar and Sindhu, 2019).

Iron is an essential nutrient for both plants and bacteria; however, it is not readily available in the required concentrations in its predominant form as a ferric ion (Gupta et al., 2015). Bacteria can produce siderophores that act as chelating agents to make the element available for uptake by plants (Crowley et al., 1988; Sharma et al., 2003; Lurthy et al., 2020). Additionally, siderophores can act similarly to chelate other essential metals, such as copper (Yoon et al., 2010). Application of the siderophore-producing PGPR *Chryseobacterium* C138 increased the iron content of tomato plants supplied solely with ferric iron (Radzki et al., 2013). Siderophore production by PGPR allows for reduced chemical inputs to meet the demand of available iron to plants (Gupta et al., 2015).

It is advantageous to crop producers and the environment that PGPR increase the availability or uptake of multiple essential plant nutrients, allowing for a reduction in total fertilizer inputs. Formulation of these PGPR into biostimulant products would then make them widely available for commercial greenhouse operations. Therefore, in this work, we have evaluated the model PGPR strain *Serratia plymuthica* MBSA-MJ1 for its ability to increase plant growth and tissue nutrient concentration of three economically important horticulture crop species produced with low fertilizer inputs. MBSA-MJ1 was previously evaluated for its ability to increase plant growth during recovery from severe water stress (Nordstedt and Jones, 2021). In addition, we have characterized the *in vitro* and genomic characteristics of this PGPR to begin elucidating different putative mechanisms used to promote plant growth with an emphasis on nutrient availability. This work demonstrates the potential of this PGPR as a commercial biostimulant, allowing growers to reduce chemical fertilizer inputs without sacrificing crop health or quality.

MATERIALS AND METHODS

Bacterial Strain

Serratia plymuthica MBSA-MJ1 originated from a bacteria collection in the laboratory of Dr. Christopher Taylor (Aly et al., 2007), although the environmental source of this strain is unknown. MBSA-MJ1 was recently evaluated for its ability to reduce *Botrytis cinerea* infection in *Petunia* × *hybrida* (South et al., 2020) and to stimulate the growth of plants recovering from severe water stress (Nordstedt and Jones, 2021).

Low-Nutrient Greenhouse Trial

A previously established greenhouse trialing protocol was utilized to evaluate the ability of *S. plymuthica* MBSA-MJ1 to increase the growth of three economically important ornamental plant species produced with low fertilizer inputs (Nordstedt et al., 2020). *Petunia* × *hybrida* 'Picobella Blue' (petunia; Syngenta Flowers Gilroy, CA), *Impatiens walleriana* 'Super Elfin Ruby' (impatiens; PanAmerican Seed, West Chicago, IL), and *Viola* × *wittrockiana* 'Delta Pure Red' (pansy; Syngenta Flowers) seeds were sown in Pro-Mix PGX soilless media (Premier Tech Horticulture, Quakertown, PA) and grown for 3 weeks.

Seedlings were then transplanted to 11.4 cm diameter pots containing Pro-Mix PGX. All plants were fertilized with 25 mg L^{-1} N from 15N–2.2P–12.5K–2.9Ca–1.2Mg water soluble fertilizer (JR Peters Inc., Allentown, PA) at each irrigation to provide low-nutrient conditions. Plants were arranged in a Randomized Complete Block Design by species. Each block contained one bacterial-treated and one untreated control plant with $n = 13$ for petunia, $n = 14$ for pansy, and $n = 18$ for impatiens. Greenhouse temperatures were set at 24/18°C (day/night) and supplemental lighting was provided by high-pressure sodium and metal halide lights (GLX/GLS e-systems GROW lights, PARSource, Petaluma, CA, United States) to maintain light levels above 250 mmol m^{-2} s^{-1} and provide a 16 h photoperiod.

Each plant was treated weekly with 120 ml working inoculum of *S. plymuthica* MBSA-MJ1. Working inoculum was prepared by diluting an overnight culture grown in LB media ($OD_{595} = 0.8$) 1:100 in reverse osmosis (RO) water as described previously (Nordstedt et al., 2020). Diluted uninoculated LB media was used as the control. Plants were grown under low-nutrient conditions with weekly bacterial treatments for 8 weeks, at which point all plants had open flowers. Plant performance was then evaluated by counting flower number (open flowers and flower buds showing color) and collecting shoots (including stems and leaves) and flowers for biomass measurements. Shoot and flower biomass was combined to get the total shoot biomass. Potting media was removed from the roots by rinsing in water, and root tissue was collected separately from shoot tissue. Roots, shoots, and flowers were dried at 49°C for at least 96 h and then weighed to determine dry weights. Root dry weights and shoot dry weights were used to calculate the root:shoot ratio.

Tissue Nutrient Concentration

Dried leaf and stem tissue (shoots minus the flowers) collected from the low-nutrient greenhouse trial were pooled for tissue nutrient analysis. Each sample consisted of tissue pooled separately for each plant species and treatment (MBSA-MJ1 and control) and contained tissue from three blocks located spatially together in the greenhouse ($n = 3$). Tissue nutrient analyses were conducted at the Service Testing and Research Laboratory (The Ohio State University/OARDC, Wooster, OH). Total tissue nitrogen (N) concentration was determined from a 100 mg sample using the Dumas combustion method (Vario Max combustion analyzer, Elementar America, Inc., Germany; Sweeney, 1989). The phosphorus (P), potassium (K), magnesium (Mg), calcium (Ca), sulfur (S), boron (B), copper (Cu), iron (Fe), sodium (Na), molybdenum (Mo), manganese (Mn), and zinc (Zn) concentration of the tissue was then determined by inductively coupled plasma spectrometry (model PS3000, Leeman Labs Inc., Hudson, NH) of a 250 mg tissue sample following nitric acid microwave digestion (Discover SP-D, CEM Corporation; Isaac and Johnson, 1985).

In vitro Characterization

Sole Carbon Source Utilization

Growth of *S. plymuthica* MBSA-MJ1was evaluated on media containing different sole sources of carbon, including cellobiose, fructose, galactose, glucose, glycerol, mannitol, sucrose, and ribose. Basal media was prepared according to Pridham and Gottlieb (1948) supplemented with 1% w/v (1% w/w for glycerol) of each carbon source. Cells from an overnight culture of MBSA-MJ1 were resuspended in PBS buffer, and 5 µl of inoculum was struck out into each carbon source plate in triplicate ($n = 3$). Plates were incubated at 28°C for 96 h and growth on each carbon source was recorded as yes/no.

Phosphate Solubilization

Phosphate solubilization capabilities of *S. plymuthica* MBSA-MJ1 were evaluated according to Mehta and Nautiyal (2001). An overnight culture grown in LB media was diluted to $OD_{595} = 0.2$ and 80 µl was used to inoculate 8 ml NBRIP media in triplicate ($n = 3$). Uninoculated LB in NBRIP media was used for the negative control. NBRIP media consisted of (per liter): 10.0 g glucose, 5.0 g $Ca_3(PO_4)_2$, 5.0 g $MgCl_2 \cdot 6H_2O$, 0.25 g $MgSO_4 \cdot 7H_2O$, 0.2 g KCl, and 0.1 g $(NH_4)_2SO_4$. The pH of the media was adjusted to 7.0 before autoclaving. Following inoculation, samples were incubated at 30°C for 72 h with 200 rpm shaking. After incubation, samples were centrifuged at 4°C and 5,000 rpm for 10 min to collect bacterial cells and remaining insoluble phosphate. The supernatant was collected, and the pH was measured as an indicator of solubilized phosphate.

Potassium Solubilization

The potassium solubilization ability of *S. plymuthica* MBSA-MJ1 was evaluated according to a modified protocol adapted from Rajawat et al. (2016). Cultures were prepared similar to those described above for the phosphate solubilization assay, and 80 µl was used to inoculate 8 ml Aleksandrov (AKV) liquid media. Uninoculated LB in AKV media served as the negative control. AKV media consisted of (per liter): 5.0 g glucose, 2.0 g $Ca_3(PO_4)_2$, 0.5 g $MgSO_4 \cdot 7H_2O$, 0.1 g $CaCO_3$, 0.005 g $FeCl_3$, and 2.0 g montmorillonite as the insoluble form of potassium. The pH of the media was adjusted to 7.2 before autoclaving. After inoculation, samples were incubated at 30°C for 72 h with 200 rpm shaking. Following incubation, bacterial cells and insoluble montmorillonite were collected by centrifugation at 4°C and 5,000 rpm for 10 min, and the supernatant was collected. The pH of the supernatant was measured as an indicator of solubilized potassium.

Quantification of Solubilized Phosphate and Potassium

Total solubilized orthophosphate and potassium in defined media were measured as validation of the nutrient solubilization capabilities of *S. plymuthica* MBSA-MJ1. Cultures were grown and inoculated in NBRIP and AKV media to evaluate phosphate and potassium solubilization, respectively. Samples were prepared similar to the solubilization assays, and after incubation and centrifugation, the supernatant was filtered through a 0.45 µm nylon filter and total orthophosphate (PO_4) or potassium in the filtrate was determined using Dionex ICS-6000 Ion Chromatograph (Thermo Fisher Scientific Inc., Waltham, MA).

Iron and Copper Chelation

The iron and copper chelation capabilities of *S. plymuthica* MBSA-MJ1 were evaluated according to Schwyn and Neilands (1987). All labware for media preparation and culturing the samples was washed in a 6 M HCl acid bath for at least 24 h prior to use. Succinic acid (SA) media consisted of (per liter): 6.0 g K_2HPO_4, 3.0 g KH_2PO_4, 1.0 g $(NH_4)_2SO_4$, 0.2 g $MgSO_4 \cdot 7H_2O$, and 4.0 g succinic acid disodium salt, and the pH of the media was adjusted to 7.0 before autoclaving. The chrome azurol S (CAS) assay solution was prepared in two solutions. Solution one contained 20 ml H_2O, 6.0 ml 10 mm hexadecyltrimethylammonium bromide, 7.5 ml 2 mm CAS, and 1.5 ml 1 mm $FeCl_3$ or $CuCl_2$ to test for iron and copper chelation, respectively. Solution two contained 4.307 g anhydrous piperazine in 30 ml H_2O, pH adjusted to 5.6 with 12 M HCl. Once prepared, solution one was added to solution two and the final volume was brought to 100 ml with H_2O to make up the working CAS assay solution. The CAS assay solution was stored in a dark polyethylene bottle.

For the assay, 5 ml SA media was inoculated with a single colony of MBSA-MJ1 and incubated for 24 h. After incubation, cultures were diluted to $OD_{595} = 0.5$, and 80 µl diluted culture was inoculated in 8 ml SA media in triplicate ($n = 3$). Uninoculated SA media was used as the negative control. Samples were incubated at 28°C for 24 h with 200 rpm shaking. After incubation, bacterial cells were collected by centrifugation at 4°C and 5,000 rpm for 10 min. After centrifugation, 750 µl supernatant was mixed with 750 µl CAS assay solution and incubated in the dark for 15 min with 100 rpm shaking to allow for color development. Absorbance of each sample was then measured at 630 nm, with a decrease in absorbance corresponding to chelation of the respective metal and a color change from blue to orange. The chelation percentage of the MBSA-MJ1 sample was calculated using $[(Ac\text{-}Ab)/Ac] \times 100\%$, where *Ac* is the absorbance at 630 nm of the control sample, and *Ab* the absorbance at 630 nm of the MBSA-MJ1 sample (Dimkpa, 2016).

Statistical Analysis

Statistical analyses for the greenhouse trial and *in vitro* characterization experiments were conducted in R Studio version 3.5.2 using an ANOVA with the model: $Y = \mu + \text{treatment} + \text{block}$. The Tukey's HSD test was used to determine statistical significance between MBSA-MJ1 treatment and the negative control. For the greenhouse trial, each plant species was analyzed independently of each other.

Genome Analyses

Genome sequence data for *S. plymuthica* MBSA-MJ1 (Nordstedt and Jones, 2021) were used to search for genes putatively involved in increasing nutrient availability, carbon and amino acid metabolism, and heavy metal resistance. Genome sequence data can be found in the National Center for Biotechnology Information data base accession # PRJNA669647. AntiSMASH (v 5.0) was used to identify secondary metabolite biosynthetic gene clusters within the genome of MBSA-MJ1 (Blin et al., 2019). BlastKOALA was used for annotation of KEGG pathways involved in nutrient transport, amino acid synthesis, and carbon metabolism and transport (Kanehisa et al., 2016).

RESULTS

Low-Nutrient Greenhouse Trial

Application of *S. plymuthica* MBSA-MJ1 increased the visual quality of all three plant species. Overall, plants treated with MBSA-MJ1 were larger and had greener leaves than the control plants that were not treated with bacteria (**Figure 1**). In addition to increasing the visual quality of plants, impatiens treated with MBSA-MJ1 had significantly more flowers than the uninoculated control, an average increase of six flowers per plant (**Figure 2A**). Application of MBSA-MJ1 significantly increased the total shoot biomass of all three plant species. Petunia, impatiens, and pansy grown under low-nutrient conditions and treated with MBSA-MJ1 had 24, 41, and 51% greater biomass, respectively (**Figure 2B**). Petunia and pansy plants treated with MBSA-MJ1 also had significantly lower root:shoot biomass ratio, whereas there was no statistically significant difference in impatiens (**Figure 2C**).

Tissue Nutrient Concentration

Plants grown under low-nutrient conditions and treated with *S. plymuthica* MBSA-MJ1 had significantly higher concentrations of certain nutrients in the shoot tissue; however, differences varied depending on plant species (**Figures 3, 4**). Petunia, impatiens, and pansy plants had an increase of 32, 74, and 82% in tissue nitrogen concentration when treated with MBSA-MJ1, respectively. No other nutrients were significantly greater in petunia plants treated with MBSA-MJ1 when compared to the control. The concentrations of potassium, calcium, and sulfur were significantly greater in bacteria-treated impatiens and pansy plants. Only impatiens showed a significant increase in magnesium, boron, copper, molybdenum, and zinc when treated with MBSA-MJ1. Phosphorus was the only element where an increase was only observed in pansy. No significant differences in iron concentration were observed in any of the three plant species, and manganese concentration was found to be significantly greater in the control plants of petunia and pansy compared to those treated with MBSA-MJ1.

In vitro Characterization

S. plymuthica MBSA-MJ1 was able to grow on basal media containing either cellobiose, fructose, galactose, glucose, glycerol, mannitol, sucrose, or ribose as the sole carbon source, indicating its ability to utilize each as an energy source.

In vitro characterization of MBSA-MJ1's ability to increase the availability of nutrients showed that the strain was able to solubilize phosphate and potassium. Media containing insoluble forms of phosphorus and potassium had a significant decrease in pH when inoculated with MBSA-MJ1 compared to the uninoculated control (**Table 1**). The pH of the media decreased by 29 and 32% for the phosphate and potassium solubilization assays when inoculated with MBSA-MJ1,

FIGURE 1 | *Petunia* × *hybrida* (petunia), *Impatiens walleriana* (impatiens), and *Viola* × *wittrockiana* (pansy) plants grown under low-nutrient conditions had increased visual quality when treated with *Serratia plymuthica* MBSA-MJ1. Plants were treated weekly for 8 weeks with *S. plymuthica* MBSA-MJ1 or uninoculated LB (control) as a media drench and fertilized at each irrigation with 25 mg L^{-1} N from 15N–2.2P–12.5K–2.9Ca–1.2Mg water soluble fertilizer to induce low-nutrient conditions.

respectively. In addition, defined media with insoluble forms of phosphorus or potassium had a significant increase in available orthophosphate and potassium after inoculation with MBSA-MJ1 (**Table 1**). MBSA-MJ1 was also able to chelate copper and iron *in vitro* as indicated by sample color change when evaluated with the CAS assay. Absorbance values of the bacteria and control samples converted to chelation percentages show that MBSA-MJ1 was able to chelate over 62 and 63% of the iron and copper in the media, respectively (**Table 1**).

Genomic Analyses to Identify Genes Putatively Involved in Growth Promotion

Nitrogen Availability and Transport

Annotation files for *S. plymuthica* MBSA-MJ1 were used to identify genes within the genome that are putatively involved in nutrient metabolism and increasing availability to plants (**Supplementary Table S1**). Genes encoding for the nitrogen starvation transcription regulation system that are also involved in ammonium transport (*glnD*, *glnK*, and *amtB*) were identified in the genome of MBSA-MJ1(**Supplementary Table S1**). The genome of MBSA-MJ1 encodes for genes involved in nitrate transport (*nrtA*), nitrite uptake and reduction to ammonium (*nirC*), nitrate reduction (*nasA*), nitrite reduction (*nirD*) and its cofactor (*cysG*), and the operons responsible for nitrate and nitrite reductase (*narLXKGHJI*) and fumarate reductase (*frdABCD*; **Supplementary Table S1**). Genes involved in nitrogen assimilation (*gdhA*, *glnA*, *glnB*, *glnD*, *glnL*, *gltB*, and *gltD*) and periplasmic nitrate reductase (*napA*) were also identified (**Supplementary Table S1**).

Phosphate Availability and Transport

Bacteria can convert phosphorus to inorganic bioavailable forms *via* nonspecific phosphatases, phytases, and phosphonatases (Liu et al., 2018). The genome of MBSA-MJ1 encodes for the *appA* enzyme, which has both acid phosphatase and phytase activity, a polyphosphate kinase (*ppk*), exopolyphosphatases (*ppx* and *gppA*), a pyrophosphatase (*ppa*), alkaline phosphatase (*phoA*), and a nonspecific acid phosphatase (*phoC*; **Supplementary Table S1**). Genes encoding for both low-affinity (*pitA*) and high-affinity phosphate transporters (*phnCDE*$_1$*E*$_2$ and *pstSCAB*) were identified within the genome (**Supplementary Tables S1** and **S3**). We identified components of the bacterial P signaling pathway including the phosphate starvation two-component system (*phoBR*) and the negative regulator of phosphate transport (*phoU*; **Supplementary Table S1**). Genes involved in the catabolism of phosphonates and phosphites (*phnGHIJKLMOP*) and the negative regulator of PhnCDE (*phnF*) were also identified (**Supplementary Table S1**).

Zinc Availability and Transport

The MBSA-MJ1 genome encodes for the high-affinity ABC zinc transporter (*znuABC*) and its regulator (*zur*), which are responsible for zinc transport under low-zinc conditions (**Supplementary Table S1**). Genes encoding for both constitutive (*zitB*) and regulated (*zntABR*) zinc export were also identified (**Supplementary Tables S1** and **S3**).

Organic Acid Synthesis

Mineral nutrient solubilization is most often attributed to the production of organic acids (Rodríguez and Fraga, 1999;

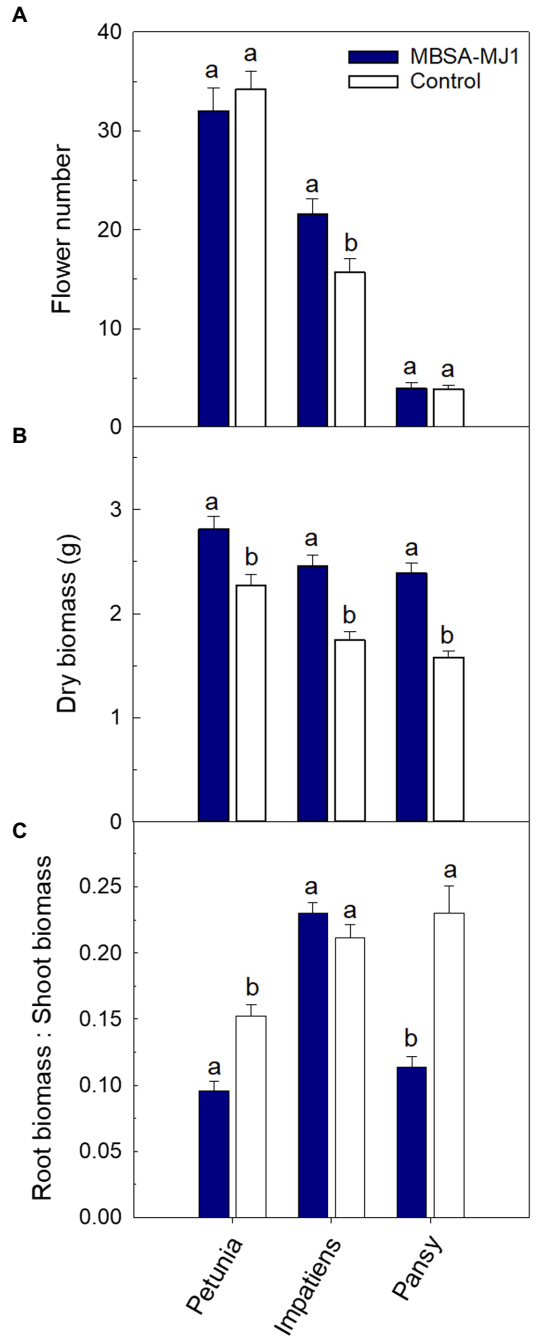

FIGURE 2 | Treatment with *S. plymuthica* MBSA-MJ1 influenced plant growth parameters for *Petunia* × *hybrida* (petunia), *Impatiens walleriana* (impatiens), and *Viola* × *wittrockiana* (pansy) plants grown under low-nutrient conditions. Plants were treated weekly with a media drench of *S. plymuthica* MBSA-MJ1 (blue bars) or uninoculated LB (control; white bars). Total number of flowers **(A)** and total shoot biomass (dry weight) **(B)** was measured 8 weeks post-transplant. The root:shoot ratio **(C)** was calculated with root and total shoot dry weights. Bars represent mean (±SE) with different letters representing significant differences ($p < 0.05$), and $n = 13$ for petunia, $n = 14$ for pansy, and $n = 18$ for impatiens.

Rodríguez et al., 2006). Genes involved in the metabolism of gluconic, ketogluconic, acetic, glyoxylic, lactic, and glycolic acid were identified (**Supplementary Table S1**). In particular, the genome included multiple genes putatively involved in the synthesis of gluconic acid (*pqqB*, *pqqC*, *pqqD*, *gcd*, *gdh*, *gnl*, *kdgK*, *gnd*, *gntR*, and *ylil*; **Supplementary Table S1**).

Sulfur Availability and Transport

The genome of MBSA-MJ1 encodes for the master regulator and transcriptional activator under sulfur starvation (*cysB*) and the sulfate ABC-type transporter complex (*sbp* and *cysPWAT*; **Supplementary Table S1**). The operon responsible for alkanesulfonate transport under sulfur limiting conditions (*ssuACBDE*), which includes an ABC-like transport system, was also identified (**Supplementary Table S1**). Additionally, the genome encodes for multiple genes involved in sulfur metabolism (*cysND*, *cysC*, and *cysHIJ*; **Supplementary Tables S1** and **S3**).

Iron Chelation and Transport

The antiSMASH analysis predicted two biosynthetic gene clusters that encode for the siderophores malleobactin and amonabactin (**Supplementary Table S2**). The genome of MBSA-MJ1 also encodes for other genes involved in iron transport, such as the two-component system to transport ferric iron (*basSR*), the operon responsible for ferric hydroxamate uptake (*fhuADCB*), the ferrous iron transporters (*feoABC* and *efeUOB*), and two copies of the ferrous ion efflux pump (*fieF*; **Supplementary Table S1**). Additionally, the KEGG pathway analysis identified ABC transporters for iron (II; *sitACDB*), iron (III; *afuABC*), iron-enterobactin complex (*fepBDGC*), and the iron (III) hydroxamate complex (*fhuDBC*; **Supplementary Table S3**).

Amino Acid and Carbon Metabolism

KEGG pathway analysis identified genes responsible for the synthesis of several amino acids within the genome of MBSA-MJ1, including isoleucine, valine, leucine, lysine, arginine, proline, phenylalanine, tryptophan, and tyrosine. Further, amino acid uptake systems were identified for tryptophan, tyrosine, phenylalanine (*aroP*), isoleucine (*brnQ*), asparagine (*gltP*), glutamate (*gltP* and *gltS*), and serine and threonine (*sstT*; **Supplementary Table S1**). ABC transporters were also identified for lysine/arginine/ornithine (*argT* and *hisMQP*), histidine (*hisJMQP*), glutamine (*glnHPQ*), arginine (*artJMIQP*), glutamate/aspartate (*gltIKJL*), cystine (*tcyABC*), methionine (*metQIN*), proline (*proVWX*), and branched-chain amino acids (*livKHMGF*; **Supplementary Table S3**). In addition to amino acids, genes were identified for both the transport and metabolism of a variety of sugars (**Table 2**).

Heavy Metal Resistance

Multiple copper resistance proteins were identified (*copA*, *cueO*, *cueR*, and *pcoC*; **Supplementary Table S1**). Additionally, the genome of MBSA-MJ1 encodes for two lead/cadmium/zinc/mercury resistance proteins (*zntA* and *zntR*), two copies of the chromate resistance protein (*chrR*), two nickel transporters (*hypA* and *hypB*), and the two-component system involved in response to heavy metals (*basRS*; **Supplementary Table S1**).

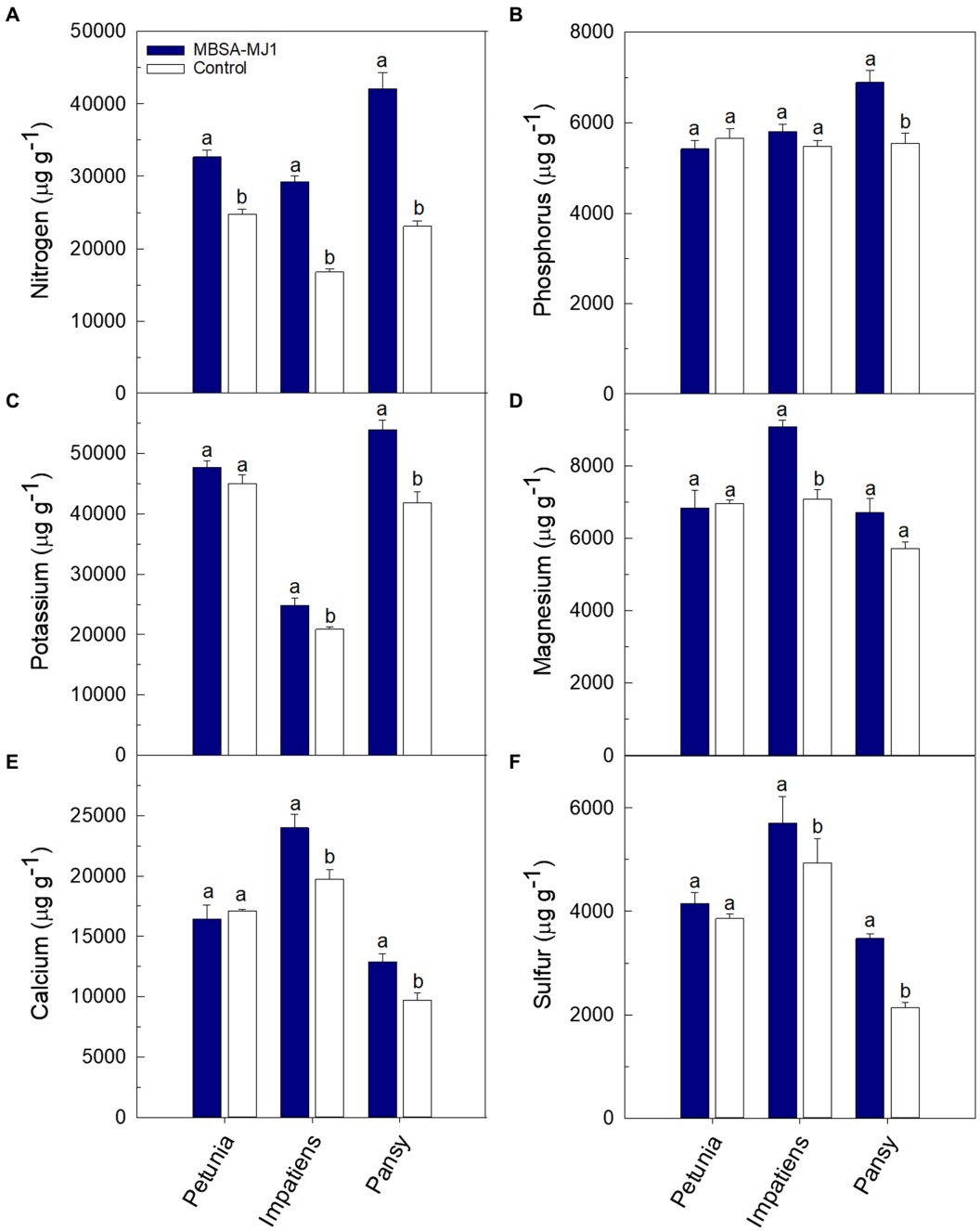

FIGURE 3 | Tissue macronutrient concentration of *Petunia* × *hybrida* (petunia), *Impatiens walleriana* (impatiens), and *Viola* × *wittrockiana* (pansy) plants grown under low-nutrient conditions: nitrogen **(A)**, phosphorus **(B)**, potassium **(C)**, magnesium **(D)**, calcium **(E)**, and sulfur **(F)**. Plants were treated weekly with a media drench of *S. plymuthica* MBSA-MJ1 (blue bars) or uninoculated LB (control; white bars). Tissue nutrient concentration was evaluated 8 weeks post-transplant. Bars represent the mean (±SE) with different letters representing significant differences ($p < 0.05$) and $n = 3$.

DISCUSSION

Although the benefits of fertilizer application are easily recognizable in agricultural production systems, excessive application of these chemicals has negative effects on the environment. Negative environmental impacts of fertilization can often be attributed to low bioavailability and uptake by plants, leaving excess nutrients more prone to leaching (Yang et al., 2009). Therefore, it is important for crop producers to have sustainable options to ensure plants have an adequate supply of nutrients for proper growth and development, without relying on increasing applications of chemical fertilizers. We used

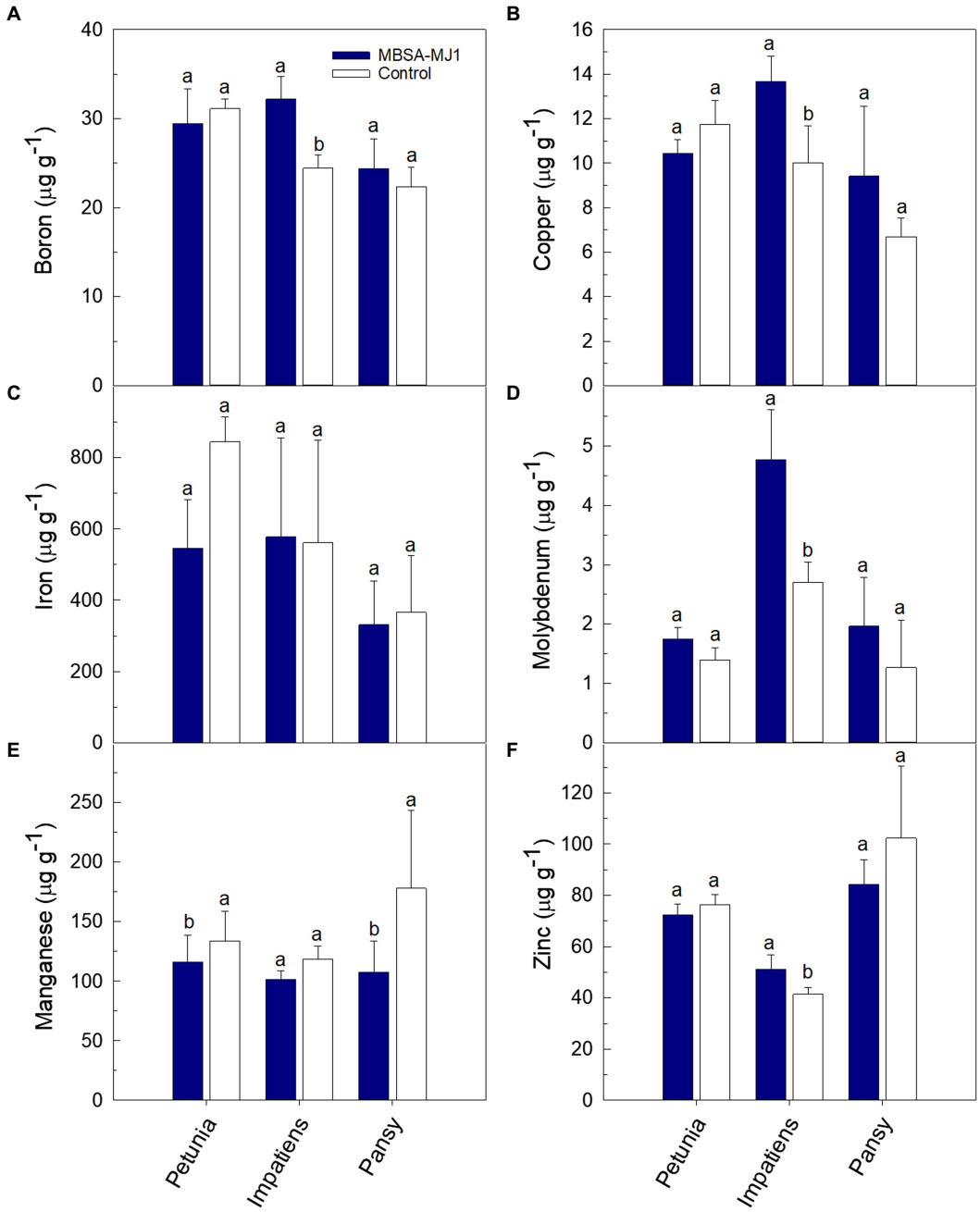

FIGURE 4 | Tissue micronutrient concentration of *Petunia* × *hybrida* (petunia), *Impatiens walleriana* (impatiens), and *Viola* × *wittrockiana* (pansy) plants grown under low-nutrient conditions: boron **(A)**, copper **(B)**, iron **(C)**, molybdenum **(D)**, manganese **(E)**, and zinc **(F)**. Plants were treated weekly with a media drench of *S. plymuthica* MBSA-MJ1 (blue bars) or uninoculated LB (control; white bars). Tissue nutrient concentration was evaluated 8 weeks post-transplant. Bars represent the mean (±SE) with different letters representing significant differences ($p < 0.05$) and $n = 3$.

a rate of 25 mg L^{-1} N from 15 N–2.2P–12.5 K–2.9Ca–1.2 Mg fertilizer in our greenhouse experiments because it is less than 20% of the average recommended fertilizer rate for ornamental crop species (150–200 mg L^{-1} N; Beytes and Hamrick, 2003). The application of biostimulant products containing plant growth promoting bacteria (PGPR) with the ability to increase the bioavailability of nutrients provides a sustainable approach for growers to ensure proper nutrient supply while reducing chemical inputs (Saravanan et al., 2007; Park et al., 2009; Kraiser et al., 2011; Gupta et al., 2015; Ruzzi and Aroca, 2015; Drobek et al., 2019; Kramer et al., 2020). In this work, we determined that *S. plymuthica* MBSA-MJ1 can increase the growth and quality of containerized horticulture crops produced with low fertilizer inputs. Our work has utilized the biological and genomic

TABLE 1 | *In vitro* characterization of nutrient solubilization and chelation abilities of *S. plymuthica* MBSA-MJ1.

	Phosphate solubilization[z]		Potassium solubilization[z]		Iron chelation[y]	Copper chelation[y]
	pH	Solubilized PO_4 (mg/L)	pH	Solubilized K (mg/L)	Chelation (%)	Chelation (%)
MBSA-MJ1	4.32 b	150.40 a	4.66 b	4.07 a	62.17	63.36
Control	6.08 a	11.33 b	6.89 a	1.74 b	–	–

[z]*The pH and concentration (mg/L) of solubilized PO_4 and K were measured in defined media containing insoluble forms of phosphorus and potassium, respectively, and inoculated with MBSA-MJ1 or the uninoculated control.*

[y]*Iron and copper chelation percentages were calculated from the CAS assay using absorbance values of samples inoculated with MBSA-MJ1 and the negative control. Values in each column with different letters indicate statistically significant differences.*

TABLE 2 | Genes identified in the genome of *S. plymuthica* MBSA-MJ1 involved in sugar transport and metabolism.

Sugar	Transport	Metabolism
Arabinose	*araE*	*araBAD*
Arabinogalactan	*cycB*	*ganB*
Galactose	*galP*	*galK, galT*
Glycerol	*glpF*	*glpK, glpD*
Lactose	*lacY*	*lacZ*
Maltose/Maltodextrin	*malGFEK*	*malP, malQ, malS, malZ*
Melibiose, raffinose, and sucrose	*scrY*	*rafA, rafR, scrB, scrK*
Ribose	*rbsACB, rbsD*	*rbsK, rbsD, rbsR*
Xylose	*xylFGH*	*xylAB*
Cellulose and cellobiose	–	*bcsZ, bglB, ylil*
Citric acid	*citT*	*citABCDEFXG*
Glucose	*galP, glk*	*pgm, yihX, glk, pgi*
Glycosides	–	*bglB, bglA, ascG*

characteristics of this beneficial bacteria to identify different putative mechanisms that MBSA-MJ1 may utilize to increase the availability of nutrients to plants and promote growth under otherwise limiting conditions.

The results obtained from the low-nutrient greenhouse trial provide evidence that MBSA-MJ1 can significantly improve the growth and quality of different plant species grown under low-nutrient conditions (**Figures 1, 2**). Multiple factors influence host specificity of both endophytic and rhizospheric bacteria, including attraction to plant root exudates, root colonization, and functioning of plant growth promoting mechanisms, contributing to varied host specificity between strains (Drogue et al., 2012; Tabassum et al., 2017; Afzal et al., 2019). Broad host specificity is particularly important for application in greenhouse production, which is characterized by the production of many different plant species. Although the application of MBSA-MJ1 only increased the flower number of impatiens compared to the uninoculated control, application did significantly increase the shoot biomass of all three plant species. Similarly, previous work with the same plant species showed application of *Pseudomonas poae* 29G9 or *Pseudomonas fluorescens* 90F12-2 increased the flower number of impatiens, while also increasing the total biomass of petunia, impatiens, and pansy plants grown under similar low-nutrient conditions (Nordstedt et al., 2020).

The growth differences observed between plants treated with MBSA-MJ1 and the uninoculated control are likely a result of MBSA-MJ1's ability to increase plant nutrient levels. This is particularly apparent with the difference in the tissue nitrogen concentration, where all three plant species had a very large increase in foliar nitrogen when treated with MBSA-MJ1 (**Figure 3A**), with up to 82% more nitrogen in pansy. This is similar to other reports that show *Serratia* spp. increase tissue nitrogen and leaf chlorophyll content compared to uninoculated control plants (Martínez et al., 2018). Due to high concentrations of carbon but low concentrations of other nutrients in soilless media, microorganisms have the potential to deplete available nitrogen sources leading to plant nutrient deficiency (Jackson et al., 2009). Nitrogen deficiency in plants often leads to a decrease in leaf chlorophyll content, and therefore a yellowing of the leaves (Boussadia et al., 2010). In our study, leaf yellowing was observed in the uninoculated control plants, but not in the three plant species treated with MBSA-MJ1, even though all plants were grown under similar low-nutrient conditions (**Figure 1**). Although bacterial nitrogen fixation can be very complex, our genomic analyses identified a variety of genes involved in ammonium, nitrate, and nitrite transport and reduction that likely play a role in MBSA-MJ1's ability to increase bioavailable nitrogen to the plant when grown under low-nutrient conditions, contributing to the growth promotion observed in the greenhouse trial.

Following nitrogen, phosphorus is the second most important element in plant nutrition. Although phosphorus is often present in abundant amounts, the total phosphorus that is available to plants is typically at very low concentrations due to its poor solubility (Gupta et al., 2015; Wang et al., 2018; Borgi et al., 2020). Phosphorus is usually applied in excess in greenhouse production and is more easily leached from the soilless substrates, leading to increasing environmental pollution (Kim and Li, 2016). Bacterial phosphate solubilization has been widely accepted as a mechanism for PGPR to increase phosphorus bioavailability to plants (Rodríguez et al., 2006; Park et al., 2009; Chen et al., 2014; Goswami et al., 2016), and *Serratia* spp. have been reported to be phosphate solubilizers (Ben Farhat et al., 2009). Our *in vitro* characterization of MBSA-MJ1 showed that the strain is an efficient phosphate solubilizer, as indicated by its ability to convert insoluble phosphorus to bioavailable orthophosphate in defined media (**Table 1**). The tissue nutrient analyses confirmed

that this increased availability resulted in increased total phosphorus in the shoots of pansy plants (**Figure 3B**). Similarly, *S. plymuthica* BMA1 is an efficient phosphate solubilizer that increased plant growth of *Vicia faba* (Borgi et al., 2020). The pH reduction observed in the *in vitro* phosphate solubilization assay (**Table 1**), coupled with the identification of multiple genes involved in gluconic acid synthesis (Silva et al., 2021), indicates that MBSA-MJ1 could be producing organic acids as a mechanism to solubilize phosphate (Rodríguez et al., 2006). This mechanism for phosphate solubilization has been previously reported in *Serratia marcescens* strains (Chen et al., 2006; Selvakumar et al., 2008; Ben Farhat et al., 2009). Impatiens and pansy plants treated with MBSA-MJ1 also had significantly greater tissue potassium concentration than the uninoculated control (**Figure 3C**). Application of *Serratia marcescens* strains NBRI1213 and MTCC 8708 similarly show increases of phosphorus and potassium tissue nutrient content in maize and wheat plants (Selvakumar et al., 2008; Lavania and Nautiyal, 2013). Our *in vitro* characterization showed a similar decrease in media pH and increase in soluble potassium in defined media when inoculated with MBSA-MJ1 (**Table 1**); therefore, it is probable that MBSA-MJ1 is able to utilize organic acid production as a mechanism to solubilize and increase the bioavailability of potassium similar to phosphate (Sharma et al., 2016).

Zinc is essential to many plant physiological processes including chlorophyll synthesis, and zinc deficiency can negatively impact plant growth and development (Hussain et al., 2015). In our work, we showed that impatiens grown under low-nutrient conditions had significantly higher levels of zinc in shoot tissues when treated with MBSA-MJ1 as compared to the uninoculated control (**Figure 4F**). Bacterial zinc solubilization is one mechanism that can increase the bioavailability of this valuable nutrient to plants, and research has shown that zinc solubilizing bacteria can increase plant growth (Ramesh et al., 2014; Kamran et al., 2017). Similar to phosphate and potassium, zinc becomes more soluble and available to plants at a lower pH (Hussain et al., 2015). Research has shown that phosphate solubilizing bacteria can also increase plant zinc uptake (Salimpour et al., 2012). Considering MBSA-MJ1's ability to solubilize phosphate and potassium through a reduction in pH, the production of organic acids by MBSA-MJ1 is a potential mechanism allowing this strain to solubilize phosphorus, potassium, and zinc, making them more bioavailable and increasing tissue nutrient levels.

Iron is usually present in abundant amounts in soil, but its availability to plants is often dependent on the production of iron chelators, such as bacterial-produced siderophores (Powell et al., 1980). Microbial-produced siderophores have been shown to increase iron acquisition and reduce iron deficiency symptoms in multiple crops grown under iron-deficient conditions (Sharma et al., 2003; Jin et al., 2006; Zhou et al., 2018; Lurthy et al., 2020). Our *in vitro* characterization showed that MBSA-MJ1 acts as an efficient iron chelator (**Table 1**). Additionally, genomic analyses identified biosynthetic gene clusters for two siderophores and multiple genes involved in bacterial iron transport and metabolism. However, our tissue nutrient analysis did not show any significant differences between bacterial-treated plants and the control (**Figure 4C**). Lurthy et al. (2020) suggests that the impact of siderophores on plant iron acquisition is highly dependent on the type of siderophore and the plant host. Therefore, it is probable that MBSA-MJ1 could assist in iron acquisition when colonizing plant hosts not evaluated in this study.

Copper is another essential metal element; however, it can be toxic to cells above certain levels (Vita et al., 2016). Our tissue nutrient analysis showed that impatiens plants treated with MBSA-MJ1 had significantly higher copper levels than the untreated control. However, the plants did not exhibit any signs of copper toxicity, such as stunted growth or the inhibition of photosynthesis, as these plants were larger and greener than untreated plants (**Figures 1, 2**). The optimal tissue copper concentration in impatiens is 10–15 $\mu g g^{-1}$ (Dole and Wilkins, 1999). The control plants had only 10 $\mu g g^{-1}$, whereas plants treated with MBSA-MJ1 had 13.7 $\mu g g^{-1}$ (**Figure 4B**). This indicates that MBSA-MJ1 can increase levels of this essential plant nutrient without reaching toxic levels. Our *in vitro* characterization of MBSA-MJ1 showed that like iron, the strain could efficiently chelate copper (**Table 1**). This likely provides a mechanism for MBSA-MJ1 to provide safe levels of copper to its plant host and augment growth under low-nutrient conditions. Notably, our genome analyses also identified four copper resistance proteins that may be involved in protecting the bacteria from potentially toxic exposure to copper (**Supplementary Table S1**; Lee et al., 2002).

Recent work has shown that application of sulfur oxidizing bacteria increases soil sulfate concentration and increases plant growth and sulfur uptake in maize and garlic (Youssif et al., 2015; Pourbabaee et al., 2020). In our study, we observed that impatiens and pansy plants grown under low-nutrient conditions and treated with MBSA-MJ1 had significantly greater levels of sulfur when compared to the uninoculated control (**Figure 3F**). Additionally, our genomic analyses identified both the master transcriptional regulator under sulfur starvation (*cysB*) and the sulfate transporter complex (*sbp-cysPWAT*) encoded in the genome of MBSA-MJ1 (**Supplementary Table S1**). These genes could potentially play a role in MBSA-MJ1's ability to sense limited sulfur in the rhizosphere and supply bioavailable sulfur to the plant host, corroborating the increase in plant tissue concentration that was observed.

In addition to the nutrients already discussed in detail, it should be noted that treatment with MBSA-MJ1 significantly increased the tissue concentration of other essential nutrients, such as boron, calcium, magnesium, and molybdenum (**Figures 3, 4**). Impatiens and pansy treated with MBSA-MJ1 also had significantly greater tissue sodium concentration (data not shown). Interestingly, the untreated plants had higher manganese content than bacterial-treated plants (**Figure 4E**). When plants are grown under phosphorus-deficient conditions, as were induced by our low fertilizer treatment, many plant species increase root exudation of carboxylates, which increase the availability and uptake of manganese (Lambers et al., 2014). Bacteria that increase the availability of phosphorus in the rhizosphere may prevent the release of carboxylates from the roots and subsequently these plants will have reduced Mn uptake and Mn tissue concentration. Although the emphasis on understanding bacterial nutrition-related plant growth promoting mechanisms have focused on nutrients, such as

nitrogen and phosphorus, our work has shown the bacterial application can increase the tissue levels of these other important macro and micronutrients. Therefore, these results provide justification for future work to begin understanding bacterial mechanisms involved in increasing the availability or uptake of nutrients to plants grown under low-nutrient conditions.

Amino acids and carbon secreted by plant roots serve as an important method to recruit and sustain beneficial rhizospheric bacteria. Therefore, bacteria with robust amino acid and carbon source metabolism are more likely to persist in the rhizosphere and be able to positively influence the growth of their host (Lugtenberg and Kamilova, 2009). Genomic analyses conducted in this work identified a series of genes related to amino acid and carbon metabolism and transport. In addition to the genomic analyses, our *in vitro* characterization assays provided evidence that MBSA-MJ1 could utilize a variety of carbon sources for growth. Not only is this robust carbon metabolism useful for persistence in the rhizosphere, but it also has the potential to increase MBSA-MJ1's host range, a valuable trait for potential commercial biostimulant products.

CONCLUSION

Serratia plymuthica MBSA-MJ1 significantly increased the shoot biomass of all three plant species, the flower number of impatiens plants, and the tissue concentrations of certain nutrients in different plant species grown under low-nutrient conditions. In addition, the comprehensive genomic analyses shed light on different genes encoded within MBSA-MJ1's genome that are putatively involved in mechanisms conferring plant growth promotion under low-nutrient conditions. Plant growth promotion by rhizospheric bacteria is likely the result of multiple coordinated mechanisms, and this work begins to highlight how interconnected mechanisms can increase overall plant health and quality. Increasing plant health under low-nutrient conditions without increasing chemical inputs provides an exciting option for crop producers to improve environmental sustainability. Formulation of biostimulant products containing well-characterized PGPR is a viable solution to accomplish this goal. Using MBSA-MJ1 as a model strain, future work should be invested in characterizing how PGPR increase the bioavailability or uptake of different essential nutrients by plants. Our work has defined the biology and genomic characteristics of this agriculturally important PGPR, contributing to a comprehensive understanding of this strain's ability to increase plant growth under low-nutrient stress and the mechanisms that might be allowing this interaction to take place.

DATA AVAILABILITY STATEMENT

The datasets presented in this study can be found in online repositories. The names of the repository/repositories and accession number(s) can be found at: https://www.ncbi.nlm.nih.gov/genbank/, PRJNA669647.

AUTHOR CONTRIBUTIONS

NN and MJ conceived the project and experimental design. NN performed the greenhouse production trial, *in vitro* assays, genomic analyses, and led the writing of the manuscript. MJ acquired funding and resources, served as project administrator, and edited the manuscript. All authors contributed to the article and approved the submitted version.

FUNDING

Salaries and research support were provided in part by the State and Federal funds appropriated to the OARDC, the Ohio State University. Journal Article Number HCS 21–01. This work was financially supported, in part, by the American Floral Endowment, the Floriculture and Nursery Research Initiative, USDA-ARS cooperative agreement #58–5082–0-006 as part of the Application Technology Research Unit project #5082–21000-001-00D, and the OSU D.C. Kiplinger Floriculture Endowment. Support was also provided to NN by the Ohio State University Distinguished Fellowship, the OARDC Director's Graduate Associateship, and the Altman Family Scholarship.

ACKNOWLEDGMENTS

We thank Laura Chapin for assistance with the greenhouse experiments, Dr. Chris Taylor for his advice and for sharing his bacteria collections, and Dr. James Altland and Leslie Morris from the USDA-ARS Application Technology Research Unit (Wooster, OH) and Juan Quijia Pillajo for assistance with the *in vitro* nutrient measurements. We also thank Ball Horticultural Company and Syngenta Flowers for providing seeds for the greenhouse experiment.

SUPPLEMENTARY MATERIAL

The Supplementary Material for this article can be found online at https://www.frontiersin.org/articles/10.3389/fmicb.2021.788198/full#supplementary-material

REFERENCES

Adesemoye, A. O., and Kloepper, J. W. (2009). Plant-microbes interactions in enhanced fertilizer-use efficiency. *Appl. Microbiol. Biotechnol.* 85, 1–12. doi: 10.1007/s00253-009-2196-0

Adesemoye, A. O., Torbert, H. A., and Kloepper, J. W. (2008). Enhanced plant nutrient use efficiency with PGPR and AMF in an integrated nutrient management system. *Can. J. Microbiol.* 54, 876–886. doi: 10.1139/W08-081

Adesemoye, A. O., Torbert, H. A., and Kloepper, J. W. (2010). Increased plant uptake of nitrogen from 15N-depleted fertilizer using plant growth-promoting rhizobacteria. *Appl. Soil Ecol.* 46, 54–58. doi: 10.1016/j.apsoil.2010.06.010

Afzal, I., Shinwari, Z. K., Sikandar, S., and Shahzad, S. (2019). Plant beneficial endophytic bacteria: mechanisms, diversity, host range and genetic determinants. *Microbiol. Res.* 221, 36–49. doi: 10.1016/j.micres.2019.02.001

Aly, H., Kamalay, J., Walter, N., Okubara, P., and Taylor, C. (2007). "Characterization of the pseudomonas genus of bacteria for plant-parasitic nematode control." in *ASM Conferences "Pseudomonas 2007"*; August 26, 2007 (Seattle, WA, USA).

Arif, M. S., Shahzad, S. M., Riaz, M., Yasmeen, T., Shahzad, T., Akhtar, M. J., et al. (2017). Nitrogen-enriched compost application combined with plant growth-promoting rhizobacteria (PGPR) improves seed quality and nutrient use efficiency of sunflower. *J. Plant Nutr. Soil Sci.* 180, 464–473. doi: 10.1002/jpln.201600615

Bachman, G. R., and Metzger, J. D. (2008). Growth of bedding plants in commercial potting substrate amended with vermicompost. *Bioresour. Technol.* 99, 3155–3161. doi: 10.1016/j.biortech.2007.05.069

Ben Farhat, M., Farhat, A., Bejar, W., Kammoun, R., Bouchaala, K., Fourati, A., et al. (2009). Characterization of the mineral phosphate solubilizing activity of *Serratia marcescens* CTM 50650 isolated from the phosphate mine of Gafsa. *Arch. Microbiol.* 191, 815–824. doi: 10.1007/s00203-009-0513-8

Beytes, C., and Hamrick, D. (2003) in *Ball Redbook. 17th Edn*. eds. C. Beytes and D. Hamrick Batavia (IL: Ball Publishing).

Bhardwaj, D., Ansari, M. W., Sahoo, R. K., and Tuteja, N. (2014). Biofertilizers function as key player in sustainable agriculture by improving soil fertility, plant tolerance and crop productivity. *Microb. Cell Factories* 13, 1–10. doi: 10.1186/1475-2859-13-66

Bindraban, P. S., Dimkpa, C., Nagarajan, L., Roy, A., and Rabbinge, R. (2015). Revisiting fertilisers and fertilisation strategies for improved nutrient uptake by plants. *Biol. Fertil. Soils* 51, 897–911. doi: 10.1007/s00374-015-1039-7

Blin, K., Shaw, S., Steinke, K., Villebro, R., Ziemert, N., Lee, S. Y., et al. (2019). antiSMASH 5.0: updates to the secondary metabolite genome mining pipeline. *Nucleic Acids Res.* 47, W81–W87. doi: 10.1093/nar/gkz310

Borgi, M. A., Saidi, I., Moula, A., Rhimi, S., and Rhimi, M. (2020). The attractive *Serratia plymuthica* BMA1 strain with high rock phosphate-solubilizing activity and its effect on the growth and phosphorus uptake by *Vicia faba* L. plants. *Geomicrobiol J.* 37, 437–445. doi: 10.1080/01490451.2020.1716892

Boussadia, O., Steppe, K., Zgallai, H., Ben El Hadj, S., Braham, M., Lemeur, R., et al. (2010). Effects of nitrogen deficiency on leaf photosynthesis, carbohydrate status and biomass production in two olive cultivars "Meski" and "Koroneiki". *Sci. Hortic.* 123, 336–342. doi: 10.1016/j.scienta.2009.09.023

Chen, Y., Fan, J. B., Du, L., Xu, H., Zhang, Q. H., and He, Y. Q. (2014). The application of phosphate solubilizing endophyte *Pantoea dispersa* triggers the microbial community in red acidic soil. *Appl. Soil Ecol.* 84, 235–244. doi: 10.1016/j.apsoil.2014.05.014

Chen, Y. P., Rekha, P. D., Arun, A. B., Shen, F. T., Lai, W. A., and Young, C. C. (2006). Phosphate solubilizing bacteria from subtropical soil and their tricalcium phosphate solubilizing abilities. *Appl. Soil Ecol.* 34, 33–41. doi: 10.1016/j.apsoil.2005.12.002

Crowley, D. E., Reid, C. P. P., and Szaniszlo, P. J. (1988). Utilization of microbial siderophores in iron acquisition by oat. *Plant Physiol.* 87, 680–685. doi: 10.1104/pp.87.3.680

Dimkpa, C. (2016). Microbial siderophores: production, detection and application in agriculture and environment. *Endocytobiosis Cell Res.* 27, 7–16.

Dole, J. M., and Wilkins, H. F. (1999). *Floriculture Priciples and Species*. New Jersey: Prentice-Hall, Inc..

Drobek, M., Frąc, M., and Cybulska, J. (2019). Plant biostimulants: importance of the quality and yield of horticultural crops and the improvement of plant tolerance to abiotic stress-A review. *Agronomy* 9:9060335. doi: 10.3390/agronomy9060335

Drogue, B., Doré, H., Borland, S., Wisniewski-Dyé, F., and Prigent-Combaret, C. (2012). Which specificity in cooperation between phytostimulating rhizobacteria and plants? *Res. Microbiol.* 163, 500–510. doi: 10.1016/j.resmic.2012.08.006

Goswami, D., Thakker, J. N., and Dhandhukia, P. C. (2016). Portraying mechanics of plant growth promoting rhizobacteria (PGPR): A review. *Cogent Food Agric.* 2, 1–19. doi: 10.1080/23311932.2015.1127500

Güneş, A., Turan, M., Güllüce, M., and Şahin, F. (2014). Nutritional content analysis of plant growth-promoting rhizobacteria species. *Eur. J. Soil Biol.* 60, 88–97. doi: 10.1016/j.ejsobi.2013.10.010

Gupta, G., Parihar, S. S., Ahirwar, N. K., Snehi, S. K., and Singh, V. (2015). Plant growth promoting rhizobacteria (PGPR): current and future prospects for development of sustainable agriculture. *J. Microb. Biochem. Technol.* 07, 96–102. doi: 10.4172/1948-5948.1000188

Hussain, A., Arshad, M., Zahir, Z. A., and Asghar, M. (2015). Prospects of zinc solubilizing bacteria for enhancing growth of maize. *Pakistan J. Agric. Sci.* 52, 915–922.

Isaac, R. A., and Johnson, W. C. (1985). Elemental analysis of plant tissue by plasma emission spectroscopy: collaborative study. *J. Assoc. Off. Anal. Chem.* 68, 499–505. doi: 10.1093/jaoac/68.3.499

Jackson, B. E., Wright, R. D., and Alley, M. M. (2009). Comparison of fertilizer nitrogen availability, nitrogen immobilization, substrate carbon dioxide efflux, and leaching in peat-lite, pine bark, and pine tree substrates. *HortScience* 44, 781–790. doi: 10.21273/hortsci.44.3.781

Jin, C. W., He, Y. F., Tang, C. X., Wu, P., and Zheng, S. J. (2006). Mechanisms of microbially enhanced Fe acquisition in red clover (*Trifolium pratense* L.). *Plant Cell Environ.* 29, 888–897. doi: 10.1111/j.1365-3040.2005.01468.x

Kamran, S., Shahid, I., Baig, D. N., Rizwan, M., Malik, K. A., and Mehnaz, S. (2017). Contribution of zinc solubilizing bacteria in growth promotion and zinc content of wheat. *Front. Microbiol.* 8:2593. doi: 10.3389/fmicb.2017.02593

Kanehisa, M., Sato, Y., and Morishima, K. (2016). BlastKOALA and GhostKOALA: KEGG tools for functional characterization of genome and metagenome sequences. *J. Mol. Biol.* 428, 726–731. doi: 10.1016/j.jmb.2015.11.006

Khan, A. G. (2005). Role of soil microbes in the rhizospheres of plants growing on trace metal contaminated soils in phytoremediation. *J. Trace Elem. Med. Biol.* 18, 355–364. doi: 10.1016/j.jtemb.2005.02.006

Kim, H. J., and Li, X. (2016). Effects of phosphorus on shoot and root growth, partitioning, and phosphorus utilization efficiency in *lantana*. *HortScience* 51, 1001–1009. doi: 10.21273/hortsci.51.8.1001

Kraiser, T., Gras, D. E., Gutiérrez, A. G., González, B., and Gutiérrez, R. A. (2011). A holistic view of nitrogen acquisition in plants. *J. Exp. Bot.* 62, 1455–1466. doi: 10.1093/jxb/erq425

Kramer, J., Özkaya, Ö., and Kümmerli, R. (2020). Bacterial siderophores in community and host interactions. *Nat. Rev. Microbiol.* 18, 152–163. doi: 10.1038/s41579-019-0284-4

Lambers, H., Hayes, P. E., Laliberte, E., Oliveira, R. S., and Turner, B. L. (2014). Leaf manganese accumulation and phosphorus-acquisition efficiency. *Trends Plant Sci.* 20, 83–90. doi: 10.1016/j.tplants.2014.10.007

Lavania, M., and Nautiyal, C. S. (2013). Solubilization of tricalcium phosphate by temperature and salt tolerant *Serratia marcescens* NBRI1213 isolated from alkaline soils. *African J. Microbiol. Res.* 7, 4403–4413. doi: 10.5897/AJMR2013.5773

Lee, S. M., Grass, G., Rensing, C., Barrett, S. R., Yates, C. J. D., Stoyanov, J. V., et al. (2002). The *Pco* proteins are involved in periplasmic copper handling in *Escherichia coli*. *Biochem. Biophys. Res. Commun.* 295, 616–620. doi: 10.1016/S0006-291X(02)00726-X

Liu, J., Cade-Menun, B. J., Yang, J., Hu, Y., Liu, C. W., Tremblay, J., et al. (2018). Long-term land use affects phosphorus speciation and the composition of phosphorus cycling genes in agricultural soils. *Front. Microbiol.* 9, 1–14. doi: 10.3389/fmicb.2018.01643

Lugtenberg, B., and Kamilova, F. (2009). Plant-growth-promoting rhizobacteria. *Annu. Rev. Microbiol.* 63, 541–556. doi: 10.1146/annurev.micro.62.081307.162918

Lurthy, T., Cantat, C., Jeudy, C., Declerck, P., Gallardo, K., Barraud, C., et al. (2020). Impact of bacterial siderophores on iron status and ionome in pea. *Front. Plant Sci.* 11, 1–12. doi: 10.3389/fpls.2020.00730

Marschner, P. (2011). *Mineral Nutrition of Higher Plants*. *3rd Edn*. London: Academic press.

Martínez, O. A., Encina, C., Tomckowiack, C., Droppelmann, F., Jara, R., Maldonado, C., et al. (2018). *Serratia* strains isolated from the rhizosphere of raulí (*Nothofagus alpina*) in volcanic soils harbour PGPR mechanisms and promote raulí plantlet growth. *J. Soil Sci. Plant Nutr.* 18, 804–819. doi: 10.4067/S0718-95162018005002302

Martín-Sánchez, L., Ariotti, C., Garbeva, P., and Vigani, G. (2020). Investigating the effect of belowground microbial volatiles on plant nutrient status:

perspective and limitations. *J. Plant Interact.* 15, 188–195. doi: 10.1080/17429145.2020.1776408

Mehta, S., and Nautiyal, C. S. (2001). An efficient method for qualitative screening of phosphate-solubilizing bacteria. *Curr. Microbiol.* 43, 51–56. doi: 10.1007/s002840010259

Nordstedt, N. P., Chapin, L. J., Taylor, C. G., and Jones, M. L. (2020). Identification of *pseudomonas spp.* that increase ornamental crop quality during abiotic stress. *Front. Plant Sci.* 10, 1–12. doi: 10.3389/fpls.2019.01754

Nordstedt, N. P., and Jones, M. L. (2021). Genomic analysis of *Serratia plymuthica* MBSA-MJ1, a plant growth promoting rhizobacteria that improves water-stress tolerance in greenhouse ornamentals. *Front. Microbiol.* 12:653556. doi: 10.3389/fmicb.2021.653556

Park, K. H., Lee, C. Y., and Son, H. J. (2009). Mechanism of insoluble phosphate solubilization by *Pseudomonas fluorescens* RAF15 isolated from ginseng rhizosphere and its plant growth-promoting activities. *Lett. Appl. Microbiol.* 49, 222–228. doi: 10.1111/j.1472-765X.2009.02642.x

Parmar, P., and Sindhu, S. S. (2019). The novel and efficient method for isolating potassium solubilizing bacteria from rhizosphere soil. *Geomicrobiol J.* 36, 130–136. doi: 10.1080/01490451.2018.1514442

Pereira, S. I. A., Abreu, D., Moreira, H., Vega, A., and Castro, P. M. L. (2020). Plant growth-promoting rhizobacteria (PGPR) improve the growth and nutrient use efficiency in maize (*Zea mays* L.) under water deficit conditions. *Heliyon* 6:e05106. doi: 10.1016/j.heliyon.2020.e05106

Pourbabaee, A. A., Koohbori Dinekaboodi, S., Seyed Hosseini, H. M., Alikhani, H. A., and Emami, S. (2020). Potential application of selected sulfur-oxidizing bacteria and different sources of sulfur in plant growth promotion under different moisture conditions. *Commun. Soil Sci. Plant Anal.* 51, 735–745. doi: 10.1080/00103624.2020.1729377

Powell, P. E., Cline, G. R., Reid, C. P. P., and Szaniszlo, P. J. (1980). Occurrence of hydroxamate siderophore iron chelators in soils. *Nature* 287, 833–834. doi: 10.1038/287833a0

Pridham, T. G., and Gottlieb, D. (1948). The utilization of carbon compounds by some *Actinomycetales* as an aid for species determination. *J. Bacteriol.* 56, 107–114. doi: 10.1128/jb.56.1.107-114.1948

Radzki, W., Gutierrez Mañero, F. J., Algar, E., Lucas García, J. A., García-Villaraco, A., and Ramos Solano, B. (2013). Bacterial siderophores efficiently provide iron to iron-starved tomato plants in hydroponics culture. *Antonie Van Leeuwenhoek* 104, 321–330. doi: 10.1007/s10482-013-9954-9

Rajawat, M. V. S., Singh, S., Tyagi, S. P., and Saxena, A. K. (2016). A modified plate assay for rapid screening of potassium-solubilizing bacteria. *Pedosphere* 26, 768–773. doi: 10.1016/S1002-0160(15)60080-7

Raklami, A., Bechtaoui, N., Tahiri, A. I., Anli, M., Meddich, A., and Oufdou, K. (2019). Use of rhizobacteria and mycorrhizae consortium in the open field as a strategy for improving crop nutrition, productivity and soil fertility. *Front. Microbiol.* 10, 1–11. doi: 10.3389/fmicb.2019.01106

Ramesh, A., Sharma, S. K., Sharma, M. P., Yadav, N., and Joshi, O. P. (2014). Inoculation of zinc solubilizing *bacillus aryabhattai* strains for improved growth, mobilization and biofortification of zinc in soybean and wheat cultivated in Vertisols of Central India. *Appl. Soil Ecol.* 73, 87–96. doi: 10.1016/j.apsoil.2013.08.009

Rodríguez, H., and Fraga, R. (1999). Phosphate solubilizing bacteria and their role in plant growth promotion. *Biotechnol. Adv.* 17, 319–339. doi: 10.1016/S0734-9750(99)00014-2

Rodríguez, H., Fraga, R., Gonzalez, T., and Bashan, Y. (2006). Genetics of phosphate solubilization and its potential applications for improving plant growth-promoting bacteria. *Plant Soil* 287, 15–21. doi: 10.1007/s11104-006-9056-9

Ruzzi, M., and Aroca, R. (2015). Plant growth-promoting rhizobacteria act as biostimulants in horticulture. *Sci. Hortic.* 196, 124–134. doi: 10.1016/j.scienta.2015.08.042

Salimpour, S., Khavazi, K., Nadian, H., Besharati, H., and Miransari, M. (2012). Canola oil production and nutrient uptake as affected by phosphate solubilizing and sulfur oxidizing bacteria. *J. Plant Nutr.* 35, 1997–2008. doi: 10.1080/01904167.2012.716892

Saravanan, V. S., Kalaiarasan, P., Madhaiyan, M., and Thangaraju, M. (2007). Solubilization of insoluble zinc compounds by *Gluconacetobacter diazotrophicus* and the detrimental action of zinc ion (Zn^{2+}) and zinc chelates on root knot nematode *Meloidogyne incognita*. *Lett. Appl. Microbiol.* 44, 235–241. doi: 10.1111/j.1472-765X.2006.02079.x

Schütz, L., Gattinger, A., Meier, M., Müller, A., Boller, T., Mäder, P., et al. (2018). Improving crop yield and nutrient use efficiency *via* biofertilization—A global meta-analysis. *Front. Plant Sci.* 8, 1–13. doi: 10.3389/fpls.2017.02204

Schwyn, B., and Neilands, J. B. (1987). Universal chemical assay for the detection and determination of siderophore. *Anal. Biochem.* 160, 47–56. doi: 10.1016/0003-2697(87)90612-9

Selvakumar, G., Mohan, M., Kundu, S., Gupta, A. D., Joshi, P., Nazim, S., et al. (2008). Cold tolerance and plant growth promotion potential of *Serratia marcescens* strain SRM (MTCC 8708) isolated from flowers of summer squash (*Cucurbita pepo*). *Lett. Appl. Microbiol.* 46, 171–175. doi: 10.1111/j.1472-765X.2007.02282.x

Shaharoona, B., Naveed, M., Arshad, M., and Zahir, Z. A. (2008). Fertilizer-dependent efficiency of *pseudomonads* for improving growth, yield, and nutrient use efficiency of wheat (*Triticum aestivum* L.). *Appl. Microbiol. Biotechnol.* 79, 147–155. doi: 10.1007/s00253-008-1419-0

Sharma, A., Johri, B. N., Sharma, A. K., and Glick, B. R. (2003). Plant growth-promoting bacterium *pseudomonas sp.* strain GRP3 influences iron acquisition in mung bean (*Vigna radiata* L. Wilzeck). *Soil Biol. Biochem.* 35, 887–894. doi: 10.1016/S0038-0717(03)00119-6

Sharma, S. B., Sayyed, R. Z., Trivedi, M. H., and Gobi, T. A. (2013). Phosphate solubilizing microbes: sustainable approach for managing phosphorus deficiency in agricultural soils. *Springerplus* 2, 1–14. doi: 10.1186/2193-1801-2-587

Sharma, A., Shankdhar, D., and Shankhdhar, S. C. (2016). "Potassium-solubilizing microorganisms: Mechanism and their role in potassium solubilization and uptake," in *Potassium Solubilizing Microorganisms for Sustainable Agriculture*. eds. V. Meena, B. Maurya and J. Verma (New Delhi: Springer), 1–17.

Silva, U. C., Cuadros-Orellana, S., Silva, D. R. C., Freitas-Junior, L. F., Fernandes, A. C., Leite, L. R., et al. (2021). Genomic and phenotypic insights into the potential of rock phosphate solubilizing bacteria to promote millet growht *in vivo*. *Front. Microbiol.* 11:574550. doi: 10.3389/fmicb.2020.574550

South, K. A., Hand, F. P., and Jones, M. L. (2020). Beneficial bacteria identified for the control of *Botrytis cinerea* in petunia greenhouse production. *Plant Dis.* 104, 1801–1810. doi: 10.1094/PDIS-10-19-2276-RE

Sweeney, R. A. (1989). Generic combustion method for determination of crude protein in feeds: collaborative study. *J. Assoc. Off. Anal. Chem.* 72, 770–774. doi: 10.1093/jaoac/72.5.770

Tabassum, B., Khan, A., Tariq, M., Ramzan, M., Iqbal Khan, M. S., Shahid, N., et al. (2017). Bottlenecks in commercialisation and future prospects of PGPR. *Appl. Soil Ecol.* 121, 102–117. doi: 10.1016/j.apsoil.2017.09.030

Vessey, J. K. (2003). Plant growth promoting rhizobacteria as biofertilizers. *Plant Soil* 255, 571–586. doi: 10.1023/A:1026037216893

Vita, N., Landolfi, G., Baslé, A., Platsaki, S., Lee, J., Waldron, K. J., et al. (2016). Bacterial cytosolic proteins with a high capacity for cu(I) that protect against copper toxicity. *Sci. Rep.* 6, 1–11. doi: 10.1038/srep39065

Wang, F., Deng, M., Xu, J., Zhu, X., and Mao, C. (2018). Molecular mechanisms of phosphate transport and signaling in higher plants. *Semin. Cell Dev. Biol.* 74, 114–122. doi: 10.1016/j.semcdb.2017.06.013

Yang, J., Kloepper, J. W., and Ryu, C. M. (2009). Rhizosphere bacteria help plants tolerate abiotic stress. *Trends Plant Sci.* 14, 1–4. doi: 10.1016/j.tplants.2008.10.004

Yoon, S., Kraemer, S. M., DiSpirito, A. A., and Semrau, J. D. (2010). An assay for screening microbial cultures for chalkophore production. *Environ. Microbiol. Rep.* 2, 295–303. doi: 10.1111/j.1758-2229.2009.00125.x

Youssif, B. D., Hosna, M. A. F., and Mervat, A. A. T. (2015). Effect of Sulphur and Sulphur oxidizing bacteria on growth and production of garlic (*Allium sativum*, L.) under saline conditions. *Middle East J. Agric. Res.* 4, 446–459.

Zhou, C., Zhu, L., Ma, Z., and Wang, J. (2018). Improved iron acquisition of *Astragalus sinicus* under low iron-availability conditions by soil-borne bacteria *Burkholderia cepacia*. *J. Plant Interact.* 13, 9–20. doi: 10.1080/17429145.2017.1407000

Conflict of Interest: The authors declare that the research was conducted in the absence of any commercial or financial relationships that could be construed as a potential conflict of interest.

Publisher's Note: All claims expressed in this article are solely those of the authors and do not necessarily represent those of their affiliated organizations, or those of the publisher, the editors and the reviewers. Any product that may

be evaluated in this article, or claim that may be made by its manufacturer, is not guaranteed or endorsed by the publisher.

Copyright © 2021 Nordstedt and Jones. This is an open-access article distributed under the terms of the Creative Commons Attribution License (CC BY). The use, distribution or reproduction in other forums is permitted, provided the original author(s) and the copyright owner(s) are credited and that the original publication in this journal is cited, in accordance with accepted academic practice. No use, distribution or reproduction is permitted which does not comply with these terms.

frontiers in Microbiology

ORIGINAL RESEARCH
published: 26 January 2022
doi: 10.3389/fmicb.2022.791110

Assessment of Bacterial Inoculant Delivery Methods for Cereal Crops

*Yen Ning Chai, Stephanie Futrell and Daniel P. Schachtman**

Department of Agronomy and Horticulture and Center for Plant Science Innovation, University of Nebraska – Lincoln, Lincoln, NE, United States

Despite growing evidence that plant growth-promoting bacteria can be used to improve crop vigor, a comparison of the different methods of delivery to determine which is optimal has not been published. An optimal inoculation method ensures that the inoculant colonizes the host plant so that its potential for plant growth-promotion is fully evaluated. The objective of this study was to compare the efficacy of three seed coating methods, seedling priming, and soil drench for delivering three bacterial inoculants to the sorghum rhizosphere and root endosphere. The methods were compared across multiple time points under axenic conditions and colonization efficiency was determined by quantitative polymerase chain reaction (qPCR). Two seed coating methods were also assessed in the field to test the reproducibility of the greenhouse results under non-sterile conditions. In the greenhouse seed coating methods were more successful in delivering the Gram-positive inoculant (*Terrabacter* sp.) while better colonization from the Gram-negative bacteria (*Chitinophaga pinensis* and *Caulobacter rhizosphaerae*) was observed with seedling priming and soil drench. This suggested that Gram-positive bacteria may be more suitable for the seed coating methods possibly because of their thick peptidoglycan cell wall. We also demonstrated that prolonged seed coating for 12 h could effectively enhance the colonization of *C. pinensis*, an endophytic bacterium, but not the rhizosphere colonizing *C. rhizosphaerae*. In the field only a small amount of inoculant was detected in the rhizosphere. This comparison demonstrates the importance of using the appropriate inoculation method for testing different types of bacteria for their plant growth-promotion potential.

Keywords: inoculation, plant growth promoting bacteria, rhizosphere, endosphere, *Chitinophaga*, *Caulobacter*, *Terrabacter*, sorghum

OPEN ACCESS

Edited by:
Reiner Rincón Rosales, Tuxtla Gutierrez Institute of Technology, Mexico

Reviewed by:
Alice Checcucci, University of Bologna, Italy
Bert Ely, University of South Carolina, United States
Monyck Jeane dos Santos Lopes, Museu Paraense Emílio Goeldi, Brazil

****Correspondence:***
Daniel P. Schachtman
daniel.schachtman@unl.edu

Specialty section:
This article was submitted to Microbe and Virus Interactions With Plants, a section of the journal Frontiers in Microbiology

Received: *07 October 2021*
Accepted: *04 January 2022*
Published: *26 January 2022*

Citation:
Chai YN, Futrell S and Schachtman DP (2022) Assessment of Bacterial Inoculant Delivery Methods for Cereal Crops. Front. Microbiol. 13:791110. doi: 10.3389/fmicb.2022.791110

INTRODUCTION

Plants and soil microbiomes have interacted and co-evolved for over a million years. Many soil-inhabiting microbes are capable of improving plant growth (Delaux and Schornack, 2021). For example, arbuscular mycorrhizal fungi and certain bacteria improve plant nutrient uptake (Parniske, 2008; Zaidi et al., 2009; Santi et al., 2013; Lopes et al., 2021b), biocontrol microbes suppress plant pathogens (Weller, 2007), while certain bacteria produce phytohormones to improve plant growth (Egamberdieva et al., 2017). To facilitate close interactions with these microbes, plants release rhizodeposits from plant roots into the rhizosphere, a soil layer adhering to the root, to serve as carbon sources and also as signaling cues to these microbes

(Mendes et al., 2013). Apart from interacting with plants, some microbes can further colonize the inner root zone termed endosphere and those microbes are known as root endophytes. The intimate association between root endophytes and root tissues may enhance the exchange of nutrients between plants and microbes (Harman and Uphoff, 2019). For instance, the colonization of rhizobia inside root nodules allows these bacteria to fix N more efficiently due to the hypoxic conditions in the nodules, the fixed N is then supplied to the host plant in exchange for carbon (Ledermann et al., 2021).

Due to the advantages conferred by plant growth-promoting bacteria on plant vigor, using these bacteria as bioinoculants can potentially substitute or supplement chemical fertilizers that bring many adverse effects on the environment (Santos et al., 2019). The method of inoculation is an important factor that can affect the colonization of the inoculant in the host plant and impact its downstream effect on plant growth (Ciccillo et al., 2002; Müller and Berg, 2007; Fukami et al., 2016; O'Callaghan, 2016; Vassilev et al., 2020; Lopes et al., 2021b). Numerous methods have been used to deliver microbes to host plants, including soil drench, seed inoculation, and plant inoculation (Rocha et al., 2019). Seed inoculation is the most widely used on a commercial scale since it is suited to agricultural production and requires less inoculant than the other two under field conditions. To enhance the survival of the bacteria coated on the seeds, a carrier such as peat slurry or a film coat consisting of alginate polymers are often mixed with bacteria during the coating process as a layer protecting inoculants from environmental stresses such as desiccation and temperature perturbations (O'Callaghan, 2016; Lobo et al., 2019; Santos et al., 2019). Soil drench or in-furrow inoculation, on the other hand, is performed by applying the inoculants in soil before or after planting (Campo et al., 2010; Hungria et al., 2013). It has several advantages over seed inoculation as it prevents the inoculants from being inhibited by the chemicals coated on seeds (e.g., fungicides and pesticides) and can be used to deliver inoculants at higher density without being constrained by seed size (Rocha et al., 2019). However, this method is relatively impractical for field-scale compared to seed coating because higher inoculant concentration is usually required for soil inoculation to obtain desirable outcomes for plant growth (Rocha et al., 2019). Foliar spray and root dipping are two of the most commonly used methods for plant inoculation (Rocha et al., 2019). Plant inoculation is usually performed at the seedling stage because the earlier the inoculant colonizes the plant, the more likely it can persist in the plant tissues even if the plant is later colonized by other microbes (Carlstrom et al., 2019; Wippel et al., 2021). One of the greatest advantages of seedling inoculation is that it greatly enhances the plant colonization of the inoculant, but it also has the drawback of being highly impractical for use under field conditions.

Commercialization of bioinoculants began in the late 1980s and microbial inoculants have been widely applied in India and South America, especially Brazil where approximately 78% of crops planted are inoculated annually (Santos et al., 2019). Among these commercial bioinoculants, *Pseudomonas* and *Bacillus* are the most commonly used while rhizobia are the most studied bacterial inoculants (Rocha et al., 2019). Rhizobia are not only commonly used to improve the productivity of leguminous plants as they can establish endosymbiotic relationships with legumes to fix nitrogen (Andrews and Andrews, 2017), but also have the potential to enhance non-legume growth since many of them possess other plant growth-promoting abilities such as phosphorus solubilization and phytohormone production (García-Fraile et al., 2012). Despite being widely studied, rhizobial inoculants suffer from the drawback of having a short shelf life especially when coated on seeds (O'Callaghan, 2016). Endospore-forming bacteria like *Bacillus* are often preferred as seed inoculants as they can better withstand unfavorable conditions (Price et al., 2010). Gram-positive bacteria which have thicker peptidoglycan layer on their cell wall are also good for bioinoculants because the cell wall renders them less susceptible to desiccation in the seed coating process compared to the Gram-negative bacteria (Viaene et al., 2016; Xu et al., 2018). *Pseudomonas* strains, despite being non-spore-forming and Gram-negative, are often used against phytopathogens such as *Pythium* and *Fusarium* due to their biocontrol properties (O'Callaghan, 2016). Although there are many bioinoculants with different plant growth-promoting potentials, the methods for delivering these bacteria under greenhouse conditions for basic research have not been compared or published.

Three bacteria isolated from field-grown sorghum were used in this study (Chai et al., 2021), with *Chitinophaga pinensis* (Gram-negative) originating from the root endosphere while *Caulobacter rhizosphaerae* (Gram-negative) and *Terrabacter* sp. (Gram-positive) were from the soil. Despite being widely distributed and abundant in the soil and/or rhizosphere of various crops, the genera *Chitinophaga* (Chung et al., 2012; Li et al., 2014; Chiniquy et al., 2021) and *Caulobacter* (Gao et al., 2018; Lopes et al., 2021a) are rarely tested for their plant growth-promoting abilities. Compared to these two genera, the genus *Terrabacter* has also been detected in many plant species, including maize (Dohrmann et al., 2013), sorghum (Lopes et al., 2021a), and napa cabbage (Bhattacharyya et al., 2018), but in very low abundance and is understudied. Therefore, we sought to determine whether these bacteria could promote plant growth and their host colonization efficiency with different inoculation methods since they are phylogenetically distinct and exhibit different cell wall structure.

In this study, we used *Sorghum bicolor* which is the fifth most widely grown cereal crop in the world to compare five bacterial inoculation methods. Sorghum is widely grown in marginal environments where microbial inoculation may provide strong benefits, particularly on parts of the African continent where inputs such as fertilizer are scarce (Tonitto and Ricker-Gilbert, 2016). Our aim was to compare seedling priming, soil drench, and three seed coating methods (direct seed coating, alginate seed coating, and 12-h coating) for their efficacy of delivering three different bacterial strains to sorghum under sterile and field conditions. While it is possible to find these methods in the literature (Lopes et al., 2021b), a direct comparison under the same conditions along with a molecular analysis is not available. Our findings highlight the importance of tailoring

the inoculation method to the specific type of bacteria being studied to get optimal plant growth-promoting results.

MATERIALS AND METHODS

Bacteria Strains

Chitinophaga pinensis isolated from sorghum root endosphere, as well as *Terrabacter* sp. and *C. rhizosphaerae* isolated from soil where sorghum was growing, were used for inoculation in this study. These bacteria have been used in a previous study (Chai et al., 2021). The draft genome sequences and gene annotations of these bacteria are available through the IMG portal at the Joint Genome Institute under the taxon ID 2818991442, 2818991454, and 2818991462, for *C. pinensis*, *C. rhizosphaerae*, and *Terrabacter* sp., respectively.

Sorghum Seed and Potting Mix Sterilization

A sweet sorghum variety, Grassl, was used throughout this experiment (Boyles et al., 2019). Grassl seeds were surface-sterilized for 6 h with chlorine gas generated by adding 3.3 ml of hydrochloric acid to 100 ml of sodium hypochlorite in a desiccator. Surface-sterilized seeds were then washed with sterile water and plated on YPD medium (Costanzo et al., 2001) to verify that there were no bacteria on the seed surface. The potting mix used in the greenhouse experiment consisted of two parts of peat and one part of vermiculite. To sterilize the pot and potting mix, 325 g of the potting mix were added to a pot with a diameter of 12.7 cm and autoclaved three times. After autoclaving, the potting mix was plated on YPD to ensure there were no viable microbes.

Bacteria Inoculation

All bacteria were grown in R2A broth (Reasoner and Geldreich, 1985) except for *C. rhizosphaerae*, which was grown in peptone-yeast extract broth (Hottes et al., 2004) because it did not grow well in R2A. Two days before planting, each bacterial strain was grown on a rotary shaker at 180 rpm at room temperature (24°C). After a day of growth, a portion of each liquid culture was transferred to a fresh medium to allow for continued growth. On the day of the experiment, each bacterial culture was pelleted at 4,000 rpm for 10 min and resuspended in phosphate-buffered saline (PBS, 8 g/L NaCl, 0.2 g/L KCl, 1.44 g/L Na_2HPO_4, and 0.24 g/L KH_2PO_4). The optical density (OD) of each of the bacterial/PBS suspensions was measured at 600 nm with a spectrophotometer and adjusted to an OD_{600} of 1 that corresponded to 10^9 colony forming units (CFUs) for each of these bacteria before inoculation. The CFU number was derived by plating 200 µl of diluted bacterial cultures with an OD_{600} of 1 on R2A medium.

Soil Drench

Soil drench was performed with the bacterial suspension 1 day after the plant shoot emerged from the soil. One part of each bacterial solution was added to 69 parts of 1× plant nutrient solution (Hoagland and Arnon, 1950) to achieve a final OD_{600} of 0.002. Bacteria/nutrient mix equivalent to 30% of the soil volume was then added to each pot in a laminar flow hood.

Direct Seed Coating

Surfaced-sterilized seeds were dipped into the bacteria suspension in PBS and air-dried for 20 min in the laminar flow hood before planting.

Twelve Hours Seed Coating

Surface-sterilized seeds were immersed in bacteria suspension in PBS and put on a rotary shaker shaking at 180 rpm for 12 h at room temperature and air-dried for 20 min in the laminar flow hood before planting.

Alginate Seed Coating

Surface-sterilized seeds were dipped into bacteria suspension in 2% (wt/vol) alginate followed by transferring the seeds into 0.1 M $CaCl_2$ to solidify. The alginate-coated seeds were then air-dried in the laminar flow hood for 20 min before planting.

Seedling Priming

Surface-sterilized seeds were germinated at 30°C in a sterilized petri dish with wet filter paper for 24 hours. When seeds germinated they were carefully transferred to a new petri dish filled with bacteria suspension in PBS and placed on a rotary shaker at 20 rpm for 12 h. The inoculated seedlings were then sowed carefully in soil in a laminar flow hood.

No Microbe Control

In a laminar flow hood, 1:69 of PBS in 1X Hoagland solution was added to each pot right after germination.

To measure the concentration of viable bacteria on inoculated sorghum seeds, 10 inoculated seeds were placed in 10 ml of PBS and vortex vigorously for 10 min followed by a 4-fold serial dilution in PBS. About 200 µl of each dilution was then plated on R2A medium and allowed to grow at room temperature. Approximately 10^3–10^4 CFU per seed were detected for the three bacteria with seed inoculation.

Experimental Design

Greenhouse Experiment

This experiment was comprised of a total of 240 pots (three bacterial strains × five inoculation methods × five replicate pots × three sampling time points + five uninoculated control × three sampling time points). Pots were planted on March 1, 2019. In a sterile laminar flow hood, three seeds were planted into the sterile soil in each pot and the pots were covered with saucers before transferring to the greenhouse to minimize airborne contamination. Pots were arranged in the greenhouse in a completely randomized design. Seedlings were thinned to one plant per pot and a small hole was made on each saucer covering the pot to allow for shoot growth. The greenhouse was 27°C during the day and 21°C at night, with a photoperiod of 16 h. Sterilized water and 1X Hoagland nutrient solution were applied

to each pot to keep the soil evenly wet through a sterile plastic tube into the hole on the saucers covering the pot. Three samplings were conducted at 4-, 6-, and 8-week after planting. For each harvest, fresh and dry weights of both shoot and root were measured. Roots were washed to remove the soil prior to weighing. To obtain the dry weight, fresh plant material was dried in an oven at 60°C for 3 days. Rhizosphere and root tissues were collected for qPCR analysis to quantify the colonization of inoculated microbes.

Field

Grassl seeds were inoculated with each of the three bacteria using alginate and 12 h coating and were planted in a field (40.85475, −96.61) on June 1, 2019. The field soil was a silty loam with 3.9% organic matter, and the concentrations of some major chemical components of the soil were: pH: 5.55; 28 ppm nitrate-N; 446 ppm potassium; 10.7 ppm sulfate; 1,657 ppm calcium; and 253 ppm magnesium. Seed inoculation was carried out on the day before planting and planted immediately the next morning. A total of 64 plots (3.7 m × 1.5 m) were included in this experiment (three bacteria and no-microbe control × two inoculation methods × eight replicates) and arranged in complete randomized design. Early in the field study, 78.5 kg/ha of nitrogen fertilizer was applied in the form of urea. Weeding was carried out frequently and a weed score was assigned for each plot early on during the experiment with a range from 0 to 3, with the score of zero indicating no weeds and three designating severe weed infestation. The rhizosphere and root samples were collected twice, once at the vegetative (July 10, 2019) stage and a second time at flowering (August 23, 2019) for qPCR analysis to quantify the number of bacteria colonizing the rhizosphere and root. Shoot fresh weight and dry weight were measured twice during the course of the experiment. Biomass was measured on July 10 (30 days after germination) and October 8, 2019 (120 days after germination). Additionally, grain yield was also measured in October.

Sampling and Processing of Rhizosphere and Root Tissue for qPCR

Sampling

To collect root and rhizosphere, we removed the bulk soil from the root system, chose a range of root types, and put them in a 50 ml tube filled with 35 ml of phosphate buffer (6.33 g/L NaH_2PO_4 and 8.5 g/L Na_2HPO_4 anhydrous) supplemented with 0.01% of Silwet and shook them vigorously for 3 min on a vortexer. The roots were then transferred to a clean 50 ml tube, the remaining phosphate buffer with rhizosphere soil was collected (McPherson et al., 2017).

Rhizosphere Processing

The rhizosphere soil samples were filtered through a sterile 100 µm mesh filter unit (Fisher Scientific, United States) into a clean 50 ml tube and pelleted at 6,000 × *g* for 5 min at room temperature using a centrifuge. The pellet was resuspended in 1.5 ml phosphate buffer and transferred to a sterile 2 ml tube. The rhizosphere was re-pelleted by spinning tubes for 2 min at full speed. The supernatant was drained from the tube and stored at −20°C until DNA extraction.

Root Processing

Roots were surface sterilized by rinsing for 1 min in 50% sodium hypochlorite + 0.005% Tween 20, followed by a 1 min rinse in 70% ethanol, and three rinses in sterile ultrapure water for 1 min each. Roots were blotted dry, placed in a 2 ml microfuge tube, and frozen at −80°C prior to being ground in liquid N for DNA extraction.

DNA Extraction of the Rhizosphere, and Root Samples

Rhizosphere DNA was extracted using MagAttract® PowerSoil®DNA KF Kit (Qiagen) and root DNA using MagMAX™ Plant DNA Kit (ThermoFisher Scientific), with a KingFisher Flex Robot (ThermoFisher Scientific) following the manufacturer's protocol. DNA concentration was quantified using QuantiFluor® dsDNA System (Promega) with CLARIOstar® Plus microplate reader (BMG LABTECH) following the manufacturer's protocol.

qPCR

Different primer pairs were used for each bacterium to provide adequate specificity for each of the three bacteria used in this study. These primer pairs were constructed from the corresponding genome sequence of each isolate (**Table 1**). Standard curves were constructed by serial dilutions of the genomic DNA of each bacterium from 10^6 to 10^1 pg DNA μl^{-1} using molecular grade water. The genome copy number of each bacteria was computed using their genome sizes, (*C. rhizosphaerae*: 5563326 bp, *Terrabactor* sp.: 4320267 bp, and *C. pinensis*: 8318214 bp), DNA molecular weight of 650 Da bp^{-1}, and Avogadro's constant of 6.022×10^{23}. The detection limit of *C. rhizosphaerae*, *C. pinensis*, and *Terrabacter* sp. were 13, 7, and 7 genome copies, respectively. All qPCR was carried out using CFX Connect (Bio-Rad Laboratories Inc., Hercules, CA, United States) in a final volume of 10 ml, which contained 5 ml of Power Sybr Green PCR Master Mix (Applied Biosystems, Foster City, CA, United States), 0.5 ml of each of the forward and reverse primers (10 pM each), 1 ng of template DNA, and water. The same amplification

TABLE 1 | Primer pairs used to amplify the three bacterial isolates.

	Primer sequence (5'–3')	Amplicon size (bp)
Chitinophaga pinensis		
1204_1F	TTCCGTGCCTCATACTCAGA	
1204_1R	CCTCAGGAGCAAGTCCATTC	157
Caulobacter rhizosphaerae		
3260_2F	GCTTCAACTTAGGCCTGTCG	
3260_2R	GGGCGGTCTACTAAACATCG	150
***Terrabacter* sp.**		
3264_2F	ATTCAAGTGCATGGTGAACG	
3260_2R	GTCAAAGCCACAGTCGATGA	165

conditions were used for all three bacteria with an initial incubation at 95°C for 10 min, followed by 40 cycles of denaturation at 95°C for 15 s, annealing at 60°C for 30 s, and extension at 72°C for 15 s. The specificity of amplification was determined using a melting curve analysis at the end of the amplification by ramping the temperature up to 95°C for 1 min followed by a 0.5°C s^{-1} increment from 60 to 95°C. Three technical replicates were performed for each sample in the qPCR. The average of the three Ct values from the technical replicates was calculated and reported.

Statistical Analysis

All the statistical analyses in this study were performed using R v3.6.0 (R Developmental Core Team, 2018). A one-way ANOVA was performed to determine whether the colonization of the inoculated bacteria (logarithm of bacterial copy number) in the rhizosphere and root endosphere was influenced by inoculation method. Tukey's HSD *post hoc* pairwise comparison was then conducted to compare the mean difference between inoculation methods. These analyses were performed on both the greenhouse and field datasets.

Linear models were constructed using *lm* function to determine the changes in sorghum shoot and root dry biomass for each combination of inoculation method, bacterial strain, sampling time point, and degree of colonization (log copy number). Prior to model construction, root and shoot dry weight were power-transformed by 0.222 and 0.303, respectively, which were determined using *boxcox* function in "MASS" package (Venables and Ripley, 2002) to homogenize the residual variances. Backward selection was performed to eliminate the interactions that were not significant in affecting sorghum biomass from the global models. The marginal means for each treatment and strain combination were computed and subjected to Tukey's HSD pairwise comparisons using the *emmeans* function in "emmeans" package (Lenth, 2021). Plots were generated using *ggboxplot* and *ggplot* function in "ggpubr" (Kassambara, 2020) and "ggplot2" package (Wickham, 2016), respectively.

RESULTS

Primer Specificity

To construct primer pairs specific for each bacterial isolate, we first mapped each genome sequence to the NCBI database to identify the genomic regions that were unique to each of the three bacterial isolates and not found in their close relatives. As a result, we identified the genomic regions that exhibited zero matches when searched using the BLAST alignment tool. Using these unique genomic regions, we constructed three primer pairs for these isolates (**Table 1**). We further confirmed the specificity of these primers on the targeted strains by performing specificity tests on their closely related isolates in our culture collection from sorghum in the same field, some of which have a perfect match (100% similarity) with our targeted bacteria in their full-length 16S rRNA regions (**Table 2; Supplementary Table 1**).

Quantification of Bacterial Colonization in Rhizosphere and Root Endosphere Under Sterile Greenhouse Conditions

All three bacteria were detectable in the rhizosphere of the inoculated plants up to 8 weeks after planting (**Figure 1**). The colonization of *C. rhizosphaerae* in the rhizosphere was greater (10^4–10^5 copies per ng of rhizosphere DNA) when the seedling priming and soil drench method were used as compared to the seed coating approaches (10^2–10^3 copies per ng of rhizosphere DNA; **Figure 1A**). Similar trend was also found for *C. pinensis* where seedling priming and soil drench method promoted its colonization in the rhizosphere (**Figure 1B**). Prolonged seed coating for 12 h enhanced the colonization of *C. pinensis* (**Figure 1B**) but did not improve the colonization of *C. rhizosphaerae* in the rhizosphere (**Figure 1A**). The colonization of *Terrabacter* sp. in sorghum rhizosphere was consistent in all five inoculation methods; although its abundance was lower (10^2 copies per ng of rhizosphere DNA) as compared to the other two strains which reached as high as 10^5 copies per ng of rhizosphere DNA (**Figure 1C**). *C. pinensis* and *C. rhizosphaerae* but not *Terrabacter* sp. were detected in the rhizosphere of the uninoculated control at week 8 after planting (**Figures 1A,B**).

C. pinensis was the only strain that could robustly colonize the root endosphere starting from week 6 after planting (**Figures 2A–C**). The colonization of *C. pinensis* in the root endosphere was greater when inoculated with seedling priming

TABLE 2 | Bacterial strains used to test the specificity of each primer pair.

Bacteria strain	Similarity of 16S rRNA to the targeted strain	Primer tested	Amplification	Origin
Caulobacter segnis 1776	97%	3260_2F, 2R	Not detected	Isolated from sorghum rhizosphere
Caulobacter rhizosphaerae 2154	100%		Not detected	Isolated from sorghum soil
Chitinophaga pinensis 1232	100%	1204_1F, 1R	Not detected	Isolated from sorghum root from low-nitrogen field
Chitinophaga sancti 3198	97%		Not detected	Isolated from sorghum root from low-nitrogen field
Chitinophaga pinensis 1209	100%		Not detected	Isolated from sorghum root from low-nitrogen field
Terrabacter sp. 3211	99%	3264_2F, 2R	Not detected	Isolated from sorghum root from full-nitrogen field
Terrabacter lapilli 3265	98%		Not detected	Isolated from sorghum root from full-nitrogen field

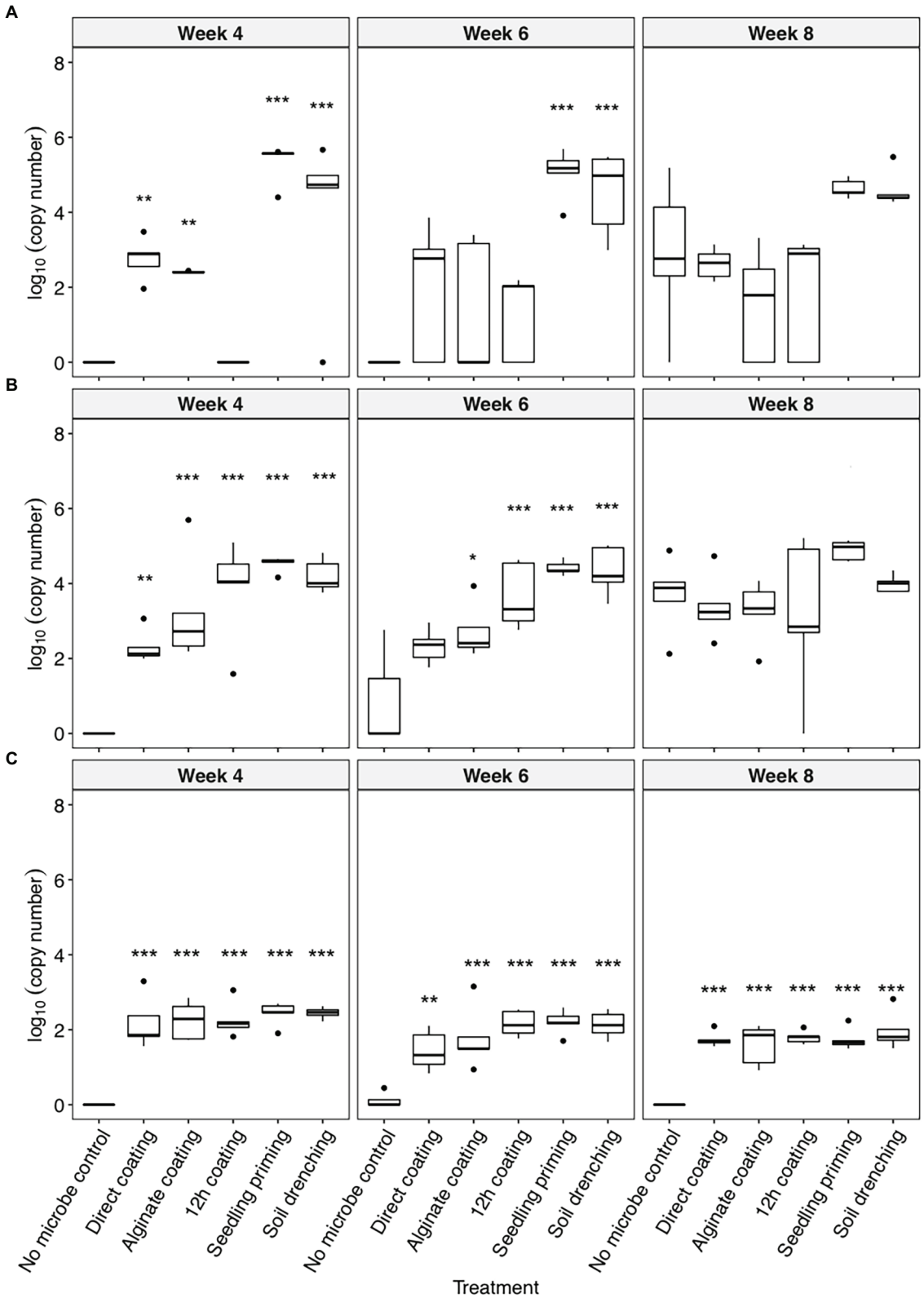

FIGURE 1 | The colonization [$\log_{10}$(bacterial DNA copy number)/ng of rhizosphere DNA] of **(A)** *Caulobacter rhizosphaerae*, **(B)** *Chitinophaga pinensis*, and **(C)** *Terrabacter* sp. in the rhizosphere of *Sorghum bicolor* inoculated using different methods at week 4, 6, and 8 after planting. ANOVA was performed with Tukey's HSD correction for multiple comparisons. Asterisks denote significant difference in the bacteria DNA copy number between inoculated samples and uninoculated controls. $^{*}p \leq 0.05$, $^{**}p \leq 0.01$, $^{***}p \leq 0.001$.

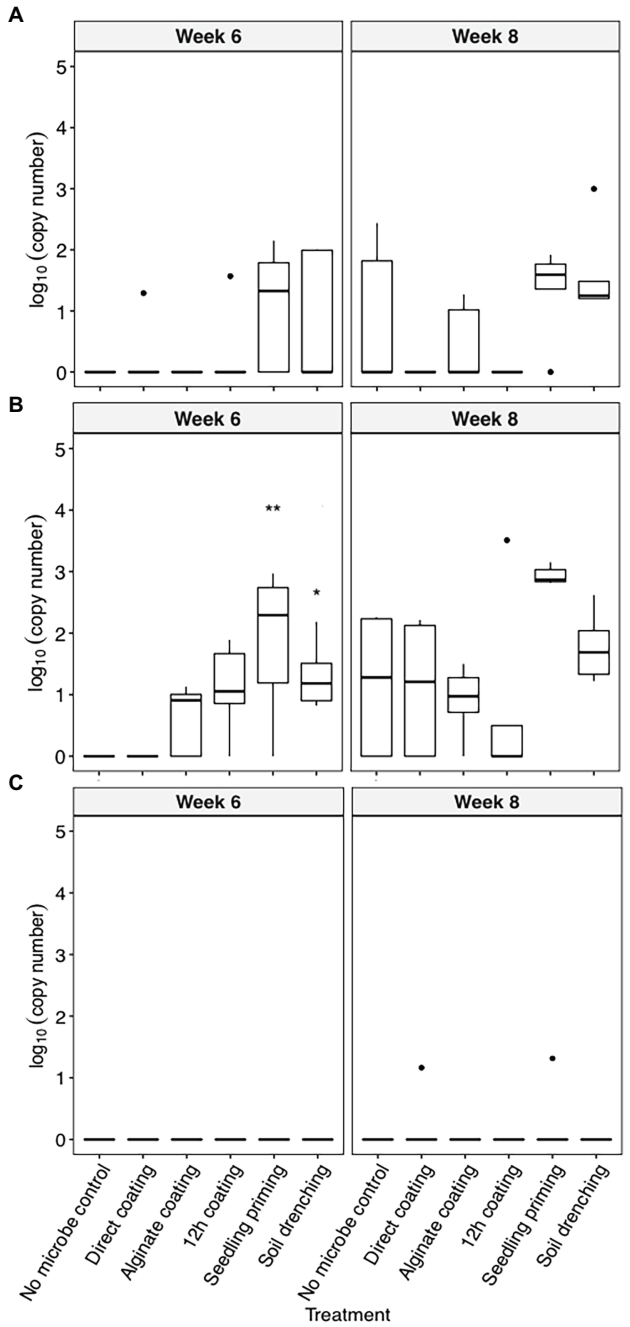

FIGURE 2 | The colonization [$\log_{10}$(bacterial DNA copy number)/ng of root endosphere DNA] of **(A)** *C. rhizosphaerae*, **(B)** *C. pinensis*, and **(C)** *Terrabacter* sp. in the root endosphere of *S. bicolor* inoculated using different methods at week 4, 6, and 8 after planting. ANOVA was performed with Tukey's HSD correction for multiple comparisons. Asterisks denote significant difference in the bacteria DNA copy number between inoculated samples and uninoculated controls. $^{*}p \leq 0.05$, $^{**}p \leq 0.01$.

and soil drench as compared to the seed coating methods at week 6 after planting (**Figure 2B**). *C. pinensis* was detected in the root endosphere of the uninoculated plants at week 8.

The Effect of Bacterial Isolate Inoculation on Plant Growth Under Sterile Greenhouse Condition

Linear models were used to determine the changes in sorghum root and shoot dry biomass for each combination of bacterial strain, inoculation method, sampling timepoint, and degree of colonization (log copy number). Overall, all three bacteria exhibited a certain amount of root growth promotion (**Figures 3A–C**), with *Terrabacter* sp. being particularly stronger than the other two at enhancing root growth on week 6 after planting (**Figure 3B**; **Table 3**). The degree of growth-promotion from these bacteria was affected by the inoculation methods. Although significant root growth-promotion was measured when inoculating *Terrabacter* sp. with all five inoculation methods, the degree of growth enhancement was greater when the three seed coating methods were used (**Figure 3**; **Table 3**). On the other hand, greater root growth-promotion was detected when inoculating *C. rhizosphaerae* and *C. pinensis* with the seedling priming compared to other inoculation methods (**Figure 3**). In fact, root growth-promotion from *C. rhizosphaerae* was only detectable with seedling priming despite this effect being marginally significant. For *C. pinensis*, significant root growth-promotion was also observed with alginate coating and marginally significant for 12 h coating. No significant root growth-promotion was measured when inoculating *C. rhizosphaerae* and *C. pinensis* with soil drench method.

Among the three bacteria used, only *C. pinensis* and *Terrabacter* sp. exhibited significant shoot growth enhancement (**Figures 4A–C**; **Table 4**). Significant shoot growth-promotion from *C. pinensis* was measured when inoculated with seedling priming, alginate, and 12 h coating methods. Significant shoot growth-promotion was also observed when *Terrabacter* sp. was inoculated with the same seed coating methods but not the seedling priming.

Quantification of Bacterial Colonization in Rhizosphere Under Field Condition

Alginate and 12 h coating method were further tested in the field to assess their efficacy for delivering the three bacterial inoculants to sorghum rhizosphere under non-sterile conditions in which there would be competition from the native microbial communities. While *C. rhizosphaerae* and *C. pinensis* were detected in the rhizosphere up to 12 weeks after inoculation in the field, DNA copy numbers in the rhizosphere of the inoculated plants were lower as compared to that of the greenhouse experiment and not significantly different from the uninoculated control (**Figures 5A,B**). *Terrabacter* sp. was not detected in either of the sampling timepoints (**Figure 5C**). No significant improvement in shoot dry weight was measured for all bacteria and inoculation treatment combinations at both sampling timepoints (**Figures 6A,B**). Bacterial colonization in the root endosphere was not quantified due to the lack of biomass difference between the inoculated plants and the uninoculated controls.

DISCUSSION

The application of plant growth-promoting bacteria has been adopted in many countries, especially Brazil to improve crop

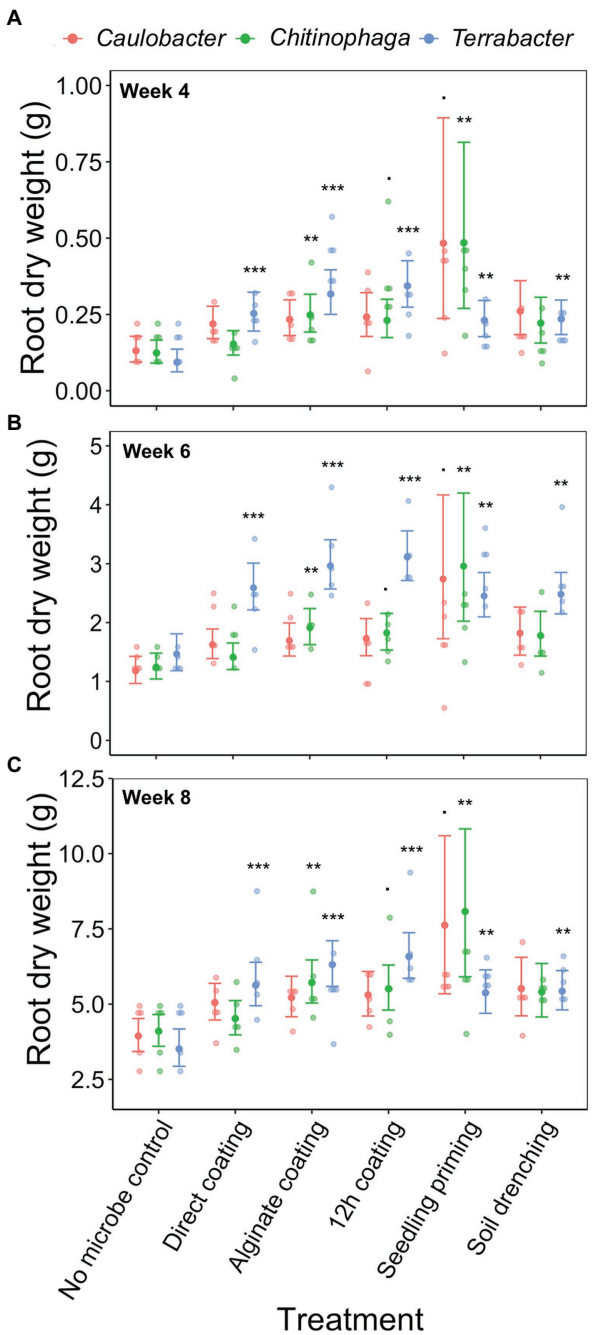

FIGURE 3 | Effects of bacterial inoculation using different inoculation methods on *S. bicolor* root dry weight at week **(A)** 4, **(B)** 6, and **(C)** 8 after planting. Root dry weight was fitted to linear model and Tukey's HSD correction was performed for multiple comparisons. Error bars and center points denote the 95% CIs and the marginal means for each strain and inoculation method combination, respectively, derived from the linear model. The distribution of raw data is represented by the dots. *$p \leq 0.1$, **$p \leq 0.01$, ***$p \leq 0.001$.

TABLE 3 | Linear model testing the effect of the degree of colonization (log copy number), bacterial strain, inoculation method, and their interactions on sorghum root dry weight.

	Estimate	Std. error	*t* value	*p* value
(Intercept)	0.663	0.020	32.826	<0.001
Log copy number	−0.010	0.007	−1.425	0.155
Chitinophaga	−0.008	0.028	−0.282	0.778
Terrabacter	−0.046	0.028	−1.655	0.099
Direct coating	0.038	0.038	0.991	0.323
Alginate coating	0.071	0.030	2.378	0.018
12 h coating	0.028	0.026	1.089	0.277
Seedling priming	0.298	0.120	2.478	0.014
Soil drench	0.117	0.055	2.132	0.034
Time Week 6	0.400	0.017	23.553	<0.001
Time Week 8	0.719	0.018	41.001	<0.001
Log copy number*Direct coating	0.016	0.014	1.133	0.258
Log copy number*Alginate coating	0.006	0.012	0.537	0.592
Log copy number*12 h coating	0.025	0.011	2.261	0.025
Log copy number*Seedling priming	−0.034	0.025	−1.367	0.173
Log copy number*Soil drench	−0.005	0.013	−0.37	0.712
*Chitinophaga**Direct coating	−0.047	0.034	−1.397	0.164
*Terrabacter**Direct coating	0.069	0.035	1.994	0.047
*Chitinophaga**Alginate coating	0.018	0.036	0.484	0.629
*Terrabacter**Alginate coating	0.097	0.034	2.848	0.005
*Chitinophaga**12 h coating	0.000	0.041	0.009	0.993
*Terrabacter**12 h coating	0.105	0.035	2.995	0.003
*Chitinophaga**Seedling priming	0.008	0.035	0.242	0.809
*Terrabacter**Seedling priming	−0.083	0.076	−1.09	0.277
*Chitinophaga**Soil drench	−0.019	0.034	−0.554	0.580
*Terrabacter**Soil drench	0.029	0.042	0.698	0.486
*Chitinophaga**Week 6	0.021	0.024	0.872	0.384
*Terrabacter**Week 6	0.098	0.024	4.143	<0.001
*Chitinophaga**Week 8	0.020	0.025	0.802	0.424
*Terrabacter**Week 8	0.012	0.024	0.483	0.630

*Backward selection was performed and the non-significant interactions (log copy number*strain, log copy number*sampling time, and treatment*sampling time) were removed from the model.*

yields and reduce the input of chemical fertilizer (Santos et al., 2019). However, there is a lack of publicly available literature that compares inoculation methods to determine which approach is more effective at delivering bacterial inoculants to the targeted plant to test their plant growth-promoting potential. To our knowledge, this is the first comprehensive study that evaluated the efficacy of multiple inoculation methods for delivering phylogenetically distinct inoculants to a cereal crop under sterile and non-sterile field conditions. We tested five inoculation methods and demonstrated that all the methods tested were successful at delivering at least one bacterial inoculant to sorghum under sterile conditions. However, the degree of plant growth-promotion from the inoculants was impacted by inoculation method. Two inoculation methods suitable for field planting, alginate and 12 h coating were tested under field condition but only a negligible amount of inoculated bacteria were detected in the rhizosphere. This may have been because the bacterial isolate concentration

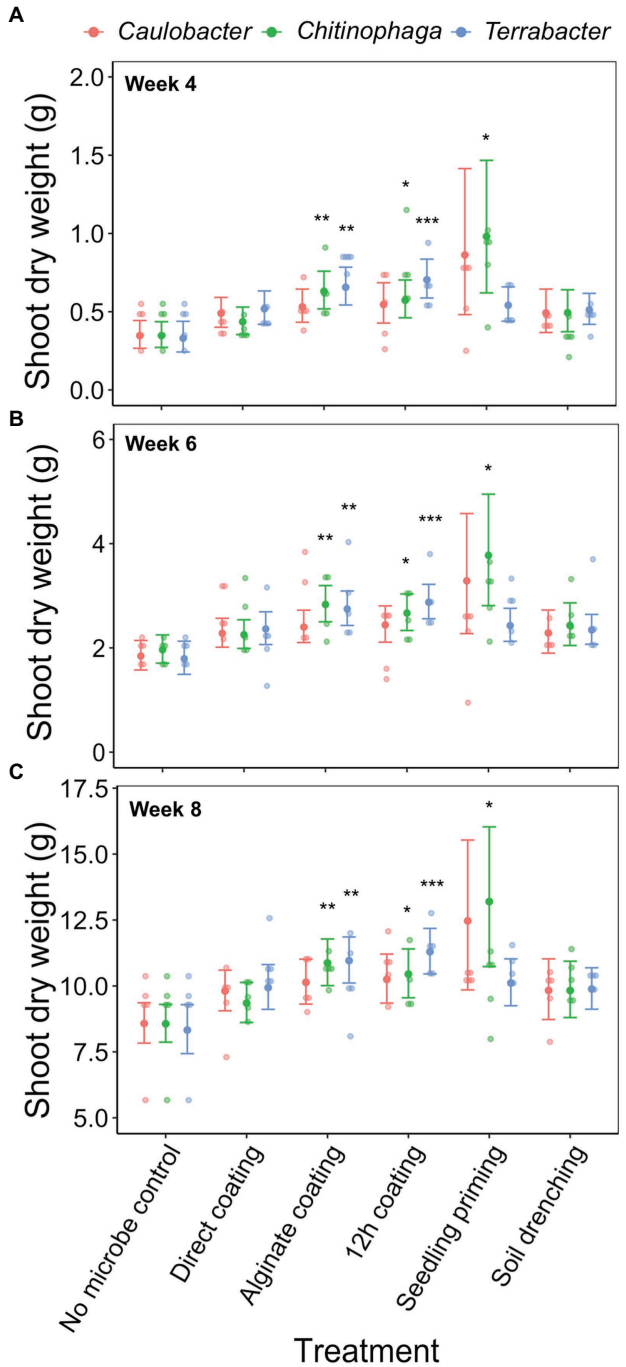

FIGURE 4 | Effects of bacterial inoculation using different inoculation methods on *S. bicolor* shoot dry weight at week **(A)** 4, **(B)** 6, and **(C)** 8 after planting. Shoot dry weight was fitted to linear model and Tukey's HSD correction was performed for multiple comparisons. Error bars and center points denote the 95% CIs and the marginal means for each strain and inoculation method combination, respectively, derived from the linear model. The distribution of raw data is represented by the dots. $^{*}p \leq 0.05$, $^{**}p \leq 0.01$, $^{***}p \leq 0.001$.

TABLE 4 | Linear model testing the effect of the degree of colonization (log copy number), bacterial strain, inoculation method, and their interactions on sorghum shoot dry weight.

	Estimate	Std. error	*t* value	*p* value
(Intercept)	0.760	0.025	30.299	<2e-16
Log copy number	−0.014	0.009	−1.541	0.125
Chitinophaga	0.000	0.034	0.002	0.998
Terrabacter	−0.011	0.035	−0.308	0.758
Direct coating	0.025	0.047	0.527	0.599
Alginate coating	0.107	0.037	2.885	0.004
12 h coating	0.042	0.032	1.295	0.197
Seedling priming	0.331	0.150	2.214	0.028
Soil drench	0.073	0.068	1.063	0.289
Week 6	0.478	0.021	22.660	<2e-16
Week 8	1.192	0.022	54.715	<2e-16
Log copy number*Direct coating	0.022	0.017	1.282	0.201
Log copy number*Alginate coating	−0.003	0.015	−0.181	0.857
Log copy number*12 h coating	0.026	0.014	1.842	0.067
Log copy number*Seedling priming	−0.040	0.031	−1.310	0.192
Log copy number*Soil drench	0.003	0.017	0.203	0.840
*Chitinophaga**Direct coating	−0.028	0.042	−0.671	0.503
*Terrabacter**Direct coating	0.025	0.043	0.575	0.566
*Chitinophaga**Alginate coating	0.044	0.045	0.974	0.331
*Terrabacter**Alginate coating	0.065	0.042	1.546	0.123
*Chitinophaga**12 h coating	0.012	0.050	0.248	0.805
*Terrabacter**12 h coating	0.077	0.044	1.773	0.077
*Chitinophaga**Seedling priming	0.038	0.043	0.882	0.379
*Terrabacter** Seedling priming	−0.115	0.094	−1.221	0.223
*Chitinophaga**Soil drench	0.001	0.042	0.014	0.989
*Terrabacter**Soil drench	0.020	0.052	0.388	0.699
*Chitinophaga**Week 6	0.023	0.030	0.790	0.431
*Terrabacter**Week 6	0.000	0.029	0.003	0.998
*Chitinophaga**Week 8	−0.001	0.030	−0.024	0.981
*Terrabacter**Week 8	−0.006	0.030	−0.210	0.834

*Backward selection was performed and the non-significant interactions (log copy number*strain, log copy number*sampling time, and treatment*sampling time) were removed from the model.*

used to coat the seeds (10^3–10^4 CFU per seed) was too low to facilitate their establishment in sorghum rhizosphere under non-sterile conditions where there is competition from the natural microbial communities (Mendoza-Suárez et al., 2021). Although a standard of 10^4 rhizobial cells per seed is widely used to inoculate legumes with medium-size seed (e.g., mung bean and pigeon pea) like sorghum (Lupwayi et al., 2000), this may not be applicable for the inoculation of non-rhizobia species and for non-legumes. On the other hand, successful colonization from inoculated bacteria was demonstrated in sorghum from a starting bacterial concentration as low as 10^2 CFU per seed under sterile conditions (Luna et al., 2010). Despite the fact that the inoculation methods used in the field study failed to facilitate higher than

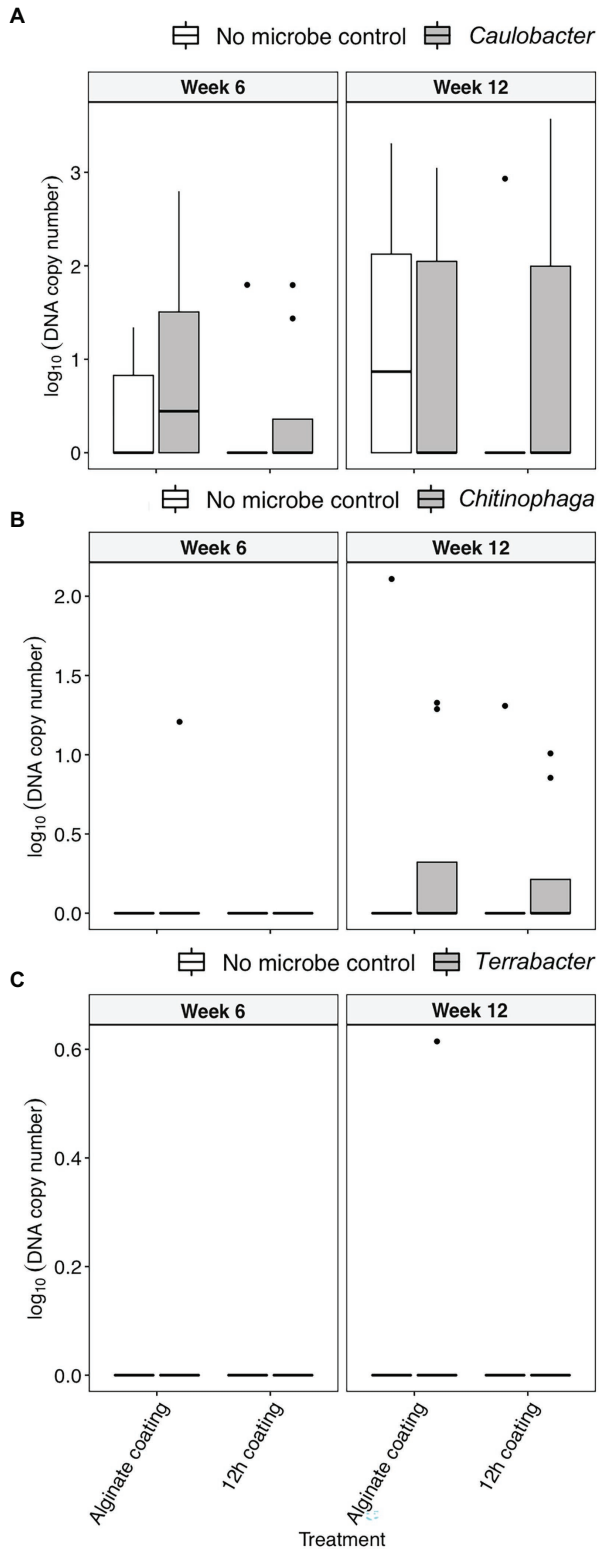

FIGURE 5 | The colonization [$\log_{10}$(bacterial DNA copy number)/ng of rhizosphere DNA] of **(A)** *C. rhizosphaerae*, **(B)** *C. pinensis*, and **(C)** *Terrabacter* sp. in the rhizosphere of *S. bicolor* inoculated with alginate and 12 h coating at week 6 and 12 after planting under field condition. ANOVA was performed with Tukey's HSD correction for multiple comparisons.

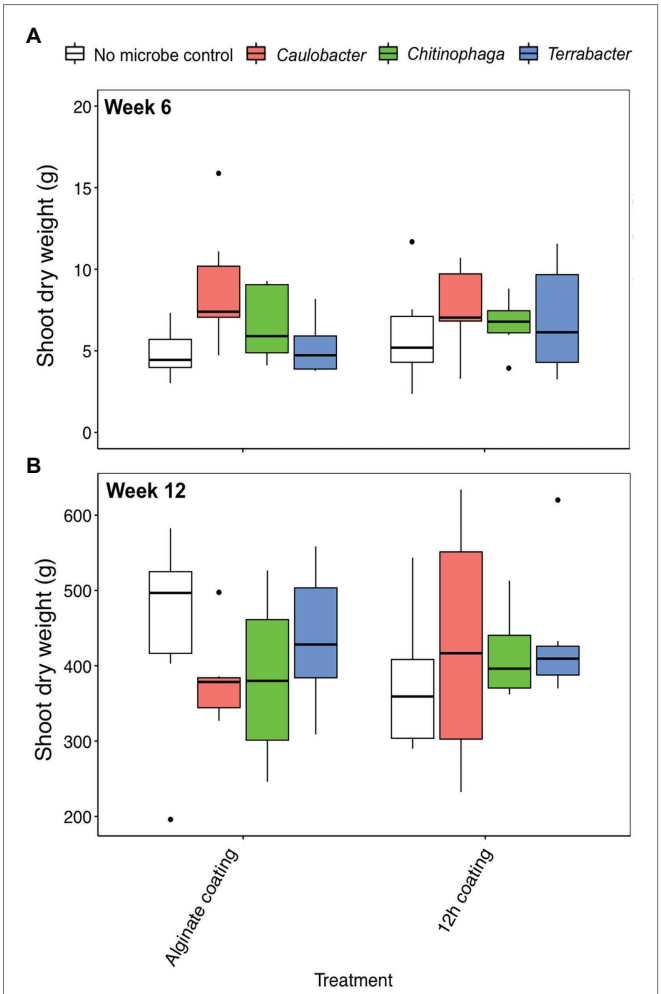

FIGURE 6 | Shoot dry weight of *Sorghum bicolor* inoculated with each bacterium using alginate and 12 h coating at **(A)** week 6 and **(B)** week 12 after planting in field. ANOVA was performed with Tukey's HSD correction for multiple comparisons. Asterisks denote significant difference in the shoot dry weight between inoculated plants and uninoculated controls.

background colonization levels or any growth promotion, our findings highlight the importance of testing inoculation methods under various conditions to ensure their efficacy under varying environments.

The results from the greenhouse study showed that all the bacterial inoculants used were able to persist in the sorghum rhizosphere or root until the end of the 8-week experiment. The persistence of bioinoculants over a targeted functional period is important so that their downstream impacts on plants could be sustained without needing to add another inoculant booster (Kaminsky et al., 2019). Although *C. rhizosphaerae* and *C. pinensis* were detected in the uninoculated plants on week 8, they were not observed in the controls from week 4 to week 6. We postulate that the detection of these two bacteria in the uninoculated plants may be attributed to cross-contamination between the uninoculated and inoculated samples collected at week 8. This may also be due to the amplification of closely related strains that survived the

soil sterilization and colonized sorghum later in the experiment since the genera *Caulobacter* and *Chitinophaga* are ubiquitous in soil (Fulthorpe et al., 2008; Wilhelm, 2018). Although we confirmed the specificity of each primer pairs by blasting the bacterial gene fragments used to design each primer pair against the NCBI database and also ensured that they do not amplify the similar isolates in our cultural collection that were in the same genera as the targeted bacteria, there may be more closely related strains that have not been discovered and sequenced. Our findings further demonstrated that two out of the three bacteria tested were effective in promoting sorghum root and shoot growth. To gain insight into why plant biomass was enhanced, we looked more closely at the bacterial genomic sequences which suggested genes underlying plant growth-promoting functions. For example, *C. pinensis* possesses 1-aminocyclopropane-1-carboxylate deaminase gene which is important for ameliorating plant stress (Glick, 2014) while *C. pinensis* and *C. rhizosphaerae* have genes encoding siderophore synthetase and transport system that may be important in solubilizing iron in soil (Kramer et al., 2020). A follow-up *in vivo* survey will be needed to confirm the mechanisms underpinning the plant growth-promoting properties of the bacteria used in this study.

Caulobacter rhizosphaerae and *Terrabacter* sp. Colonized the Rhizosphere While *Chitinophaga pinensis* Established in Both Rhizosphere and Root Endosphere

In this study, the compartmental specificity of the three inoculated bacterial isolates was demonstrated, with *C. pinensis* being the only strain that robustly colonized both the rhizosphere and root endosphere, whereas the other two were only able to colonize the rhizosphere. This result was in agreement with our expectations and other studies (Bai et al., 2015; Maggini et al., 2019) that show inoculated bacteria tend to colonize the plant compartments from which they are isolated. The degree of plant growth-promotion from *C. pinensis* was not greater than the other two bacterial isolates, although endophytic colonization could theoretically allow bacteria to interact directly with the host plant and potentially deliver the plant growth-promoting effects more efficient than the bacteria in the rhizosphere (Santoyo et al., 2016). Nonetheless, the compartmental specificity of inoculants may be crucial in determining their downstream impact on plants. For example, root nodule colonization of rhizobia is crucial for enhancing the nitrogen nutrition in the host plant because the root nodule restricts the entry of oxygen that can inhibit biological nitrogen fixation (Lindström and Mousavi, 2020).

Generalizations About Inoculation Methods for Bacteria

Seed inoculation is currently the most widely used approach for the introduction of bioinoculants because it is the most practical and cost-effective compared to other approaches (e.g., in-furrow inoculation; O'Callaghan, 2016). Nevertheless, we found that seed coating methods may not be suitable for the inoculation of Gram-negative bacteria, which may be due to their thinner cell wall structure that renders them vulnerable to desiccation in the seed coating process (Schimel et al., 2007). In accordance with our hypothesis, the seed coating methods were less effective in delivering the Gram-negative bacteria (*C. rhizosphaerae* and *C. pinensis*) to the sorghum rhizosphere compared to seedling priming and soil drench whereas the Gram-positive strain (*Terrabacter* sp.) could be delivered successfully with seed coating. Interestingly, we also observed increased colonization from *C. pinensis* but not *C. rhizosphaerae* with the 12 h seed coating method. Since *C. pinensis* is a root endophyte, we speculate that it may have colonized the seed endophytically during the longer seed coating process (Kandel et al., 2017), thereby enhancing its survival under desiccation. Similar results were also demonstrated in another study in which 12 h seed coating promoted the initial rhizosphere colonization of an endophytic biocontrol bacterium, *Serratia plymuthica* HRO-C48, on oilseed rape and enhanced the survival of this bacterium on seeds (Müller and Berg, 2007). Different inoculation methods may further affect the downstream impacts of inoculants on plants. For instance, seed inoculation of Gram-positive *Bacillus* strains on cowpea and mash bean has been shown to suppress root-infecting phytopathogens more effectively than soil drench (Dawar et al., 2010). The improved biocontrol abilities from these inoculants with seed inoculation may be attributed to the fact that seed inoculation allowed them to establish inside the root prior to pathogen infestation. On the other hand, soil drench has been shown to be more effective in delivering inoculants to Italian ryegrass growing on soil contaminated with diesel oil than the 12 h seed coating method, and improved plant growth-promotion and hydrocarbon degradation (Afzal et al., 2012). This was probably due to the greater density of inoculant being applied from the soil drench than the 12 h coating method in which the amount of bacteria applied to seeds was constrained by the seed size. These findings suggest that it may be important to tailor inoculation methods for inoculants with specific characteristics and functionalities.

Colonization Rates Are Not Linked to Growth Promotion

Although all the inoculation methods tested successfully delivered bacterial isolates to the sorghum rhizosphere in the greenhouse study, the impacts on sorghum growth were variable. Despite being equally effective at delivering *C. pinensis* to sorghum rhizosphere, no growth-promotion was observed with the soil drench method while both shoot and root growth promotions were detected with seedling priming. Similarly, *Burkholderia ambifaria* MCI 7 was reported to improve maize growth when coated on seed but was detrimental to growth when applied into the soil (Ciccillo et al., 2002). Although it was unclear why the same bacterium had contrasting effects on plant growth, the authors noted that the root adjacent to the stem was mainly colonized when the seed was coated whereas the entire root system was colonized with the soil drench method (Ciccillo et al., 2002). In our studies, *Terrabacter* sp. was in lower abundance in the rhizosphere but was still able to promote sorghum root

growth comparable to or better than the other two bacteria. This is in line with another study that observed similar biomass-promoting effects on banana from *Pseudomonas fluorescens* Ps006 and *Bacillus amyloliquefaciens* Bs006 despite *P. fluorescens* Ps006 being a less efficient root colonizer compared to *B. amyloliquefaciens* Bs006 (Gamez et al., 2019). These findings highlight that the degree of colonization by inoculated bacteria of host plants may not necessarily be directly related to the level of growth enhancement induced.

CONCLUSION

This study compared several different bacterial inoculation methods to determine the most suitable approach for studies of the impact of bacterial inoculation of plants grown in sterilized greenhouse soil experiments and in the field. Simply coating seeds with a bacterial suspension was suitable for the inoculation and successful colonization of Gram-positive bacteria in the greenhouse, whereas the field results were inconclusive. For Gram-negative bacteria direct inoculation using seedling priming or soil drench led to higher colonization efficiency than seed coating. The method of inoculation was critical in these types of experiments because the colonization rates and plant growth-promoting potential of inoculants were influenced by inoculation method. These findings show that the inoculation methods should be tailored to accommodate the characteristics of different bacterial inoculants to ensure successful colonization of the targeted plant species.

DATA AVAILABILITY STATEMENT

The datasets presented in this study can be found in online repositories. The names of the repository/repositories and accession number(s) can be found in the article/supplementary material.

AUTHOR CONTRIBUTIONS

DS contributed in conceptualization of experiment and revisions of the manuscript. YNC performed the experiment and statistical analyses and wrote the manuscript. SF helped with planting and maintaining the field, as well as sampling. All authors contributed to the article and approved the submitted version.

FUNDING

This research was funded by United States Department of Energy BER, Grant/Award Number: DE-SC0014395 and the University of Nebraska - Lincoln Agricultural Research Division.

ACKNOWLEDGMENTS

We thank Drew Tyre for the advice on the statistical analyses. This research was supported by the Office of Science (BER), U.S. Department of Energy (DE-SC0014395) and the University of Nebraska – Lincoln Agricultural Research Division.

SUPPLEMENTARY MATERIAL

The Supplementary Material for this article can be found online at: https://www.frontiersin.org/articles/10.3389/fmicb.2022.791110/full#supplementary-material

REFERENCES

Afzal, M., Yousaf, S., Reichenauer, T. G., and Sessitsch, A. (2012). The inoculation method affects colonization and performance of bacterial inoculant strains in the phytoremediation of soil contaminated with diesel oil. *Int. J. Phytoremediation* 14, 35–47. doi: 10.1080/15226514.2011.552928

Andrews, M., and Andrews, M. E. (2017). Specificity in legume-rhizobia symbioses. *Int. J. Mol. Sci.* 18:705. doi: 10.3390/ijms18040705

Bai, Y., Muller, D. B., Srinivas, G., Garrido-Oter, R., Potthoff, E., Rott, M., et al. (2015). Functional overlap of the *Arabidopsis* leaf and root microbiota. *Nature* 528, 364–369. doi: 10.1038/nature16192

Bhattacharyya, D., Duta, S., Yu, S.-M., Jeong, S. C., and Lee, Y. H. (2018). Taxonomic and functional changes of bacterial communities in the rhizosphere of kimchi cabbage after seed bacterization with *Proteus vulgaris* JBLS202. *Plant Pathol. J.* 34, 286–296. doi: 10.5423/PPJ.OA.03.2018.0047

Boyles, R. E., Brenton, Z. W., and Kresovich, S. (2019). Genetic and genomic resources of sorghum to connect genotype with phenotype in contrasting environments. *Plant J.* 97, 19–39. doi: 10.1111/tpj.14113

Campo, R. J., Araujo, R. S., Luís, F. M., and Hungria, M. (2010). In-furrow inoculation of soybean as alternative to fungicide and micronutrient seed treatment. *R. Bras. Ci. Solo* 34, 1103–1112. doi: 10.1590/S0100-06832010000400010

Carlstrom, C. I., Field, C. M., Bortfeld-Miller, M., Muller, B., Sunagawa, S., and Vorholt, J. A. (2019). Synthetic microbiota reveal priority effects and keystone strains in the *Arabidopsis* phyllosphere. *Nat. Ecol. Evol.* 3, 1445–1454. doi: 10.1038/s41559-019-0994-z

Chai, Y. N., Ge, Y., Stoerger, V., and Schachtman, D. P. (2021). High-resolution phenotyping of sorghum genotypic and phenotypic responses to low nitrogen and synthetic microbial communities. *Plant Cell Environ.* 44, 1611–1626. doi: 10.1111/pce.14004

Chiniquy, D., Barnes, E. M., Zhou, J., Hartman, K., Li, X., Sheflin, A., et al. (2021). Microbial community field surveys reveal abundant *pseudomonas* population in sorghum rhizosphere composed of many closely related phylotypes. *Front. Microbiol.* 12:598180. doi: 10.3389/fmicb.2021.598180

Chung, E. J., Park, T. S., Jeon, C. O., and Chung, Y. R. (2012). *Chitinophaga oryziterrae* sp. nov., isolated from the rhizosphere soil of rice (*Oryza sativa* L.). *Int. J. Syst. Evol. Microbiol.* 62, 3030–3035. doi: 10.1099/ijs.0.036442-0

Ciccillo, F., Fiore, A., Bevivino, A., Dalmastri, C., Tabacchioni, S., and Chiarini, L. (2002). Effects of two different application methods of *Burkholderia ambifaria* MCI 7 on plant growth and rhizospheric bacterial diversity. *Environ. Microbiol.* 4, 238–245. doi: 10.1046/j.1462-2920.2002.00291.x

Costanzo, M. C., Crawford, M. E., Hirschman, J. E., Kranz, J. E., Olsen, P., Robertson, L. S., et al. (2001). YPD, PombePD and WormPD: model organism volumes of the BioKnowledge library, an integrated resource for protein information. *Nucleic Acids Res.* 29, 75–79. doi: 10.1093/nar/29.1.75

Dawar, S., Wahab, S., Tariq, M., and Zaki, M. J. (2010). Application of *Bacillus* species in the control of root rot diseases of crop plants. *Arch. Phytopathol. Plant Protect.* 43, 412–418. doi: 10.1080/03235400701850870

Delaux, P.-M., and Schornack, S. (2021). Plant evolution driven by interactions with symbiotic and pathogenic microbes. *Science* 371:eaba6605. doi: 10.1126/science.aba6605

Dohrmann, A. B., Küting, M., Jünemann, S., Jaenicke, S., Schlüter, A., and Tebbe, C. C. (2013). Importance of rare taxa for bacterial diversity in the rhizosphere of Bt- and conventional maize varieties. *ISME J.* 7, 37–49. doi: 10.1038/ismej.2012.77

Egamberdieva, D., Wirth, S. J., Alqarawi, A. A., Abd_Allah, E. F., and Hashem, A. (2017). Phytohormones and beneficial microbes: essential components for plants to balance stress and fitness. *Front. Microbiol.* 8:2104. doi: 10.3389/fmicb.2017.02104

Fukami, J., Nogueira, M. A., Araujo, R. S., and Hungria, M. (2016). Accessing inoculation methods of maize and wheat with *Azospirillum brasilense*. *AMB Express* 6:3. doi: 10.1186/s13568-015-0171-y

Fulthorpe, R. R., Roesch, L. F. W., Riva, A., and Triplett, E. W. (2008). Distantly sampled soils carry few species in common. *ISME J.* 2, 901–910. doi: 10.1038/ismej.2008.55

Gamez, R., Cardinale, M., Montes, M., Ramirez, S., Schnell, S., and Rodriguez, F. (2019). Screening, plant growth promotion and root colonization pattern of two rhizobacteria (*Pseudomonas fluorescens* Ps006 and *Bacillus amyloliquefaciens* Bs006) on banana cv. Williams (*Musa acuminata* Colla). *Microbiol. Res.* 220, 12–20. doi: 10.1016/j.micres.2018.11.006

Gao, J. L., Sun, P., Sun, X. H., Tong, S., Yan, H., Han, M. L., et al. (2018). *Caulobacter zeae* sp. nov. and *Caulobacter radicis* sp. nov., novel endophytic bacteria isolated from maize root (*Zea mays* L.). *Syst. Appl. Microbiol.* 41, 604–610. doi: 10.1016/j.syapm.2018.08.010

García-Fraile, P., Carro, L., Robledo, M., Ramírez-Bahena, M.-H., Flores-Félix, J.-D., Fernández, M. T., et al. (2012). Rhizobium promotes non-legumes growth and quality in several production steps: towards a biofertilization of edible raw vegetables healthy for humans. *PLoS One* 7:e38122. doi: 10.1371/journal.pone.0038122

Glick, B. R. (2014). Bacteria with ACC deaminase can promote plant growth and help to feed the world. *Microbiol. Res.* 169, 30–39. doi: 10.1016/j.micres.2013.09.009

Harman, G. E., and Uphoff, N. (2019). Symbiotic root-endophytic soil microbes improve crop productivity and provide environmental benefits. *Scientifica* 2019:9106395. doi: 10.1155/2019/9106395

Hoagland, D. R., and Arnon, D. I. (1950). The water-culture method for growing plants without soil. *Calif. Agric. Exp. Stn. Circ.* 347, 1–32.

Hottes, A. K., Meewan, M., Yang, D., Arana, N., Romero, P., Mcadams, H. H., et al. (2004). Transcriptional profiling of *Caulobacter crescentus* during growth on complex and minimal media. *J. Bacteriol.* 186, 1448–1461. doi: 10.1128/JB.186.5.1448-1461.2004

Hungria, M., Nogueira, M. A., and Araujo, R. S. (2013). Co-inoculation of soybeans and common beans with rhizobia and azospirilla: strategies to improve sustainability. *Biol. Fertil. Soils* 49, 791–801. doi: 10.1007/s00374-012-0771-5

Kaminsky, L. M., Trexler, R. V., Malik, R. J., Hockett, K. L., and Bell, T. H. (2019). The inherent conflicts in developing soil microbial inoculants. *Trends Biotechnol.* 37, 140–151. doi: 10.1016/j.tibtech.2018.11.011

Kandel, S. L., Joubert, P. M., and Doty, S. L. (2017). Bacterial endophyte colonization and distribution within plants. *Microorganisms* 5:77. doi: 10.3390/microorganisms5040077

Kassambara, A. (2020). ggpubr: 'ggplot2' Based publication ready plots. R package version 0.4.0. Available at: https://CRAN.R-project.org/package=ggpubr (Accessed November 1, 2021).

Kramer, J., Özkaya, Ö., and Kümmerli, R. (2020). Bacterial siderophores in community and host interactions. *Nat. Rev. Microbiol.* 18, 152–163. doi: 10.1038/s41579-019-0284-4

Ledermann, R., Schulte, C. C. M., Poole, P. S., and Margolin, W. (2021). How rhizobia adapt to the nodule environment. *J. Bacteriol.* 203:e0053920. doi: 10.1128/JB.00539-20

Lenth, R. V. (2021). Emmeans: estimated marginal means, aka least-squares means. R package version 1.6.3.

Li, X., Rui, J., Mao, Y., Yannarell, A., and Mackie, R. (2014). Dynamics of the bacterial community structure in the rhizosphere of a maize cultivar. *Soil Biol. Biochem.* 68, 392–401. doi: 10.1016/j.soilbio.2013.10.017

Lindström, K., and Mousavi, S. A. (2020). Effectiveness of nitrogen fixation in rhizobia. *Microb. Biotechnol.* 13, 1314–1335. doi: 10.1111/1751-7915.13517

Lobo, C. B., Juárez Tomás, M. S., Viruel, E., Ferrero, M. A., and Lucca, M. E. (2019). Development of low-cost formulations of plant growth-promoting bacteria to be used as inoculants in beneficial agricultural technologies. *Microbiol. Res.* 219, 12–25. doi: 10.1016/j.micres.2018.10.012

Lopes, L. D., Chai, Y. N., Marsh, E. L., Rajewski, J. F., Dweikat, I., and Schachtman, D. P. (2021a). Sweet sorghum genotypes tolerant and sensitive to nitrogen stress select distinct root endosphere and rhizosphere bacterial communities. *Microorganisms* 9:1329. doi: 10.3390/microorganisms9061329

Lopes, M. J. D. S., Dias-Filho, M. B., and Gurgel, E. S. C. (2021b). Successful plant growth-promoting microbes: inoculation methods and abiotic factors. *Front. Sustain. Food Syst.* 5:606454. doi: 10.3389/fsufs.2021.606454

Luna, M. F., Galar, M. L., Aprea, J., Molinari, M. L., and Boiardi, J. L. (2010). Colonization of sorghum and wheat by seed inoculation with *Gluconacetobacter diazotrophicus*. *Biotechnol. Lett.* 32, 1071–1076. doi: 10.1007/s10529-010-0256-2

Lupwayi, N. Z., Olsen, P. E., Sande, E. S., Keyser, H. H., Collins, M. M., Singleton, P. W., et al. (2000). Inoculant quality and its evaluation. *Field Crop Res.* 65, 259–270. doi: 10.1016/S0378-4290(99)00091-X

Maggini, V., Mengoni, A., Gallo, E. R., Biffi, S., Fani, R., Firenzuoli, F., et al. (2019). Tissue specificity and differential effects on in vitro plant growth of single bacterial endophytes isolated from the roots, leaves and rhizospheric soil of *Echinacea purpurea*. *BMC Plant Biol.* 19:284. doi: 10.1186/s12870-019-1890-z

McPherson, M. R., Wang, P., Marsh, E. L., Mitchell, R. B., and Schachtman, D. P. (2018). Isolation and Analysis of Microbial Communities in Soil, Rhizosphere, and Roots in Perennial Grass Experiments. *J. Vis. Exp.* 137:57932. doi: 10.3791/57932

Mendes, R., Garbeva, P., and Raaijmakers, J. M. (2013). The rhizosphere microbiome: significance of plant beneficial, plant pathogenic, and human pathogenic microorganisms. *FEMS Microbiol. Rev.* 37, 634–663. doi: 10.1111/1574-6976.12028

Mendoza-Suárez, M., Andersen, S. U., Poole, P. S., and Sánchez-Cañizares, C. (2021). Competition, nodule occupancy, and persistence of inoculant strains: key factors in the *rhizobium*-legume symbioses. *Front. Plant Sci.* 12:690567. doi: 10.3389/fpls.2021.690567

Müller, H., and Berg, G. (2007). Impact of formulation procedures on the effect of the biocontrol agent *Serratia plymuthica* HRO-C48 on *Verticillium* wilt in oilseed rape. *BioControl* 53, 905–916. doi: 10.1007/s10526-007-9111-3

O'callaghan, M. (2016). Microbial inoculation of seed for improved crop performance: issues and opportunities. *Appl. Microbiol. Biotechnol.* 100, 5729–5746. doi: 10.1007/s00253-016-7590-9

Parniske, M. (2008). Arbuscular mycorrhiza: the mother of plant root endosymbioses. *Nat. Rev. Microbiol.* 6, 763–775. doi: 10.1038/nrmicro1987

Price, M. N., Dehal, P. S., and Arkin, A. P. (2010). FastTree 2-approximately maximum-likelihood trees for large alignments. *PLoS One* 5:e9490. doi: 10.1371/journal.pone.0009490

R Developmental Core Team (2018). R: A Language and Environment for Statistical Computing. R Foundation for Statistical Computing.

Reasoner, D. J., and Geldreich, E. E. (1985). A new medium for the enumeration and subculture of bacteria from potable water. *Appl. Environ. Microbiol.* 49, 1–7. doi: 10.1128/aem.49.1.1-7.1985

Rocha, I., Ma, Y., Souza-Alonso, P., Vosatka, M., Freitas, H., and Oliveira, R. S. (2019). Seed coating: a tool for delivering beneficial microbes to agricultural crops. *Front. Plant Sci.* 10:1357. doi: 10.3389/fpls.2019.01357

Santi, C., Bogusz, D., and Franche, C. (2013). Biological nitrogen fixation in non-legume plants. *Ann. Bot.* 111, 743–767. doi: 10.1093/aob/mct048

Santos, M. S., Nogueira, M. A., and Hungria, M. (2019). Microbial inoculants: reviewing the past, discussing the present and previewing an outstanding future for the use of beneficial bacteria in agriculture. *AMB Express* 9:205. doi: 10.1186/s13568-019-0932-0

Santoyo, G., Moreno-Hagelsieb, G., Del Carmen Orozco-Mosqueda, M., and Glick, B. R. (2016). Plant growth-promoting bacterial endophytes. *Microbiol. Res.* 183, 92–99. doi: 10.1016/j.micres.2015.11.008

Schimel, J., Balser, T. C., and Wallenstein, M. (2007). Microbial stress-response physiology and its implications for ecosystem function. *Ecology* 88, 1386–1394. doi: 10.1890/06-0219

Tonitto, C., and Ricker-Gilbert, J. E. (2016). Nutrient management in African sorghum cropping systems: applying meta-analysis to assess yield and profitability. *Agron. Sustain. Dev.* 36:10. doi: 10.1007/s13593-015-0336-8

Vassilev, N., Vassileva, M., Martos, V., Garcia Del Moral, L. F., Kowalska, J., Tylkowski, B., et al. (2020). Formulation of microbial inoculants by encapsulation in natural polysaccharides: focus on beneficial properties of carrier additives and derivatives. *Front. Plant Sci.* 11:270. doi: 10.3389/fpls.2020.00270

Venables, W. N., and Ripley, B. D. (2002). *Modern Applied Statistics with S. 4th Edn*. New York: Springer.

Viaene, T., Langendries, S., Beirinckx, S., Maes, M., and Goormachtig, S. (2016). *Streptomyces* as a plant's best friend? *FEMS Microbiol. Ecol.* 92:fiw119. doi: 10.1093/femsec/fiw119

Weller, D. M. (2007). *Pseudomonas* biocontrol agents of soilborne pathogens: looking back over 30 years. *Phytopathology* 97, 250–256. doi: 10.1094/PHYTO-97-2-0250

Wickham, H. (2016). *ggplot2: Elegant Graphics for Data Analysis*. New York: Springer-Verlag.

Wilhelm, R. C. (2018). Following the terrestrial tracks of *Caulobacter*—redefining the ecology of a reputed aquatic oligotroph. *ISME J.* 12, 3025–3037. doi: 10.1038/s41396-018-0257-z

Wippel, K., Tao, K., Niu, Y., Zgadzaj, R., Kiel, N., Guan, R., et al. (2021). Host preference and invasiveness of commensal bacteria in the *lotus* and *Arabidopsis* root microbiota. *Nat. Microbiol.* 6, 1150–1162. doi: 10.1038/s41564-021-00941-9

Xu, L., Naylor, D., Dong, Z., Simmons, T., Pierroz, G., Hixson, K. K., et al. (2018). Drought delays development of the sorghum root microbiome and enriches for monoderm bacteria. *Proc. Natl. Acad. Sci. U. S. A.* 115, E4284–E4293. doi: 10.1073/pnas.1717308115

Zaidi, A., Khan, M. S., Ahemad, M., and Oves, M. (2009). Plant growth promotion by phosphate solubilizing bacteria. *Acta Microbiol. Immunol. Hung.* 56, 263–284. doi: 10.1556/AMicr.56.2009.3.6

Conflict of Interest: The authors declare that the research was conducted in the absence of any commercial or financial relationships that could be construed as a potential conflict of interest.

Publisher's Note: All claims expressed in this article are solely those of the authors and do not necessarily represent those of their affiliated organizations, or those of the publisher, the editors and the reviewers. Any product that may be evaluated in this article, or claim that may be made by its manufacturer, is not guaranteed or endorsed by the publisher.

Copyright © 2022 Chai, Futrell and Schachtman. This is an open-access article distributed under the terms of the Creative Commons Attribution License (CC BY). The use, distribution or reproduction in other forums is permitted, provided the original author(s) and the copyright owner(s) are credited and that the original publication in this journal is cited, in accordance with accepted academic practice. No use, distribution or reproduction is permitted which does not comply with these terms.

frontiers in Microbiology

ORIGINAL RESEARCH
published: 18 February 2022
doi: 10.3389/fmicb.2022.833313

Newly Isolated *Paenibacillus monticola* sp. nov., a Novel Plant Growth-Promoting Rhizobacteria Strain From High-Altitude Spruce Forests in the Qilian Mountains, China

Hui-Ping Li[1,2], Ya-Nan Gan[1,2], Li-Jun Yue[1,2], Qing-Qing Han[1,2], Jia Chen[1,2], Qiong-Mei Liu[1,2], Qi Zhao[1,2] and Jin-Lin Zhang[1,2]**

[1] Key Laboratory of Grassland Livestock Industry Innovation, Ministry of Agriculture and Rural Affairs, College of Pastoral Agriculture Science and Technology, Lanzhou University, Lanzhou, China, [2] Center for Grassland Microbiome, State Key Laboratory of Grassland Agro-Ecosystems, Lanzhou University, Lanzhou, China

OPEN ACCESS

Edited by:
Clara Ivette Rincón Molina, Instituto Tecnológico de Tuxtla Gutiérrez/TecNM, Mexico

Reviewed by:
Anandham Rangasamy, Tamil Nadu Agricultural University, India
Maher Gtari, Carthage University, Tunisia

***Correspondence:**
Qi Zhao
qzhao@lzu.edu.cn
Jin-Lin Zhang
jlzhang@lzu.edu.cn

Specialty section:
This article was submitted to Microbe and Virus Interactions with Plants, a section of the journal Frontiers in Microbiology

Received: 11 December 2021
Accepted: 11 January 2022
Published: 18 February 2022

Citation:
Li H-P, Gan Y-N, Yue L-J, Han Q-Q, Chen J, Liu Q-M, Zhao Q and Zhang J-L (2022) Newly Isolated Paenibacillus monticola sp. nov., a Novel Plant Growth-Promoting Rhizobacteria Strain From High-Altitude Spruce Forests in the Qilian Mountains, China. Front. Microbiol. 13:833313. doi: 10.3389/fmicb.2022.833313

Species in the genus *Paenibacillus* from special habitats have attracted great attention due to their plant growth-promoting traits. A novel plant growth-promoting rhizobacteria (PGPR) species in the genus *Paenibacillus* was isolated from spruce forest at the height of 3,150 m in the Qilian Mountains, Gansu province, China. The phylogenetic analysis based on 16S rRNA, *rpoB*, and *nifH* gene sequences demonstrated that strain LC-T2^T was affiliated in the genus *Paenibacillus* and exhibited the highest sequence similarity with *Paenibacillus donghaensis* KCTC 13049^T (97.4%). Average nucleotide identity (ANIb and ANIm) and digital DNA–DNA hybridization (dDDH) between strain LC-T2^T and *P. donghaensis* KCTC 13049^T were 72.6, 83.3, and 21.2%, respectively, indicating their genetic differences at the species level. These differences were further verified by polar lipids profiles, major fatty acid contents, and several distinct physiological characteristics. Meanwhile, the draft genome analysis provided insight into the genetic features to support its plant-associated lifestyle and habitat adaptation. Subsequently, the effects of volatile organic compound (VOC) emitted from strain LC-T2^T on the growth of *Arabidopsis* were evaluated. Application of strain LC-T2^T significantly improved root surface area, root projection area, and root fork numbers by 158.3, 158.3, and 241.2%, respectively, compared to control. Also, the effects of LC-T2^T on the growth of white clover (*Trifolium repens* L.) were further assessed by pot experiment. Application of LC-T2^T also significantly improved the growth of white clover with root fresh weight increased over three-folds compared to control. Furthermore, the viable bacterial genera of rhizosphere soil were detected in each treatment. The number of genera from LC-T2^T-inoculated rhizosphere soil was 1.7-fold higher than that of control, and some isolates were similar to strain LC-T2^T, indicating that LC-T2^T inoculation was effective in the rhizosphere soil of white clover. Overall, strain LC-T2^T should be attributed to a

novel PGPR species within the genus *Paenibacillus* based on phylogenetic relatedness, genotypic features, and phenotypic and inoculation experiment, for which the name *Paenibacillus monticola* sp. nov. is proposed.

Keywords: *Paenibacillus*, PGPR, novel species, qilian mountains, spruce

INTRODUCTION

Plant growth-promoting rhizobacteria (PGPR) enhance growth and health of host plants through various mechanisms, including phosphate solubilization, nitrogen fixation, siderophore production, synthesis of phytohormone, and emission of volatile organic compounds (VOCs) (Ryu et al., 2003; Fürnkranz et al., 2012; Grady et al., 2016; He et al., 2021). Many PGPRs also prevent rhizosphere colonization of pathogenic or parasitic organisms by secreting antagonistic compounds and inducing plant defenses and/or competition for nutrients (Backer et al., 2018; Woo and Pepe, 2018; Naamala and Smith, 2021). These valuable characteristics can help to reduce the dependence of agricultural production on chemical fertilizers and insecticides, maximize the ecological benefits, and accelerate the emergence of their applications in biotechnological processes (Backer et al., 2018; Woo and Pepe, 2018; Rani et al., 2021). Globally, species of the genus *Paenibacillus* rank the top among PGPRs in agriculture and horticulture (Kiran et al., 2017; Daud et al., 2019; Liu et al., 2021). Many studies showed that some species in the genus *Paenibacillus* can promote the growth of host plants (Fürnkranz et al., 2012; Ker et al., 2012; Grady et al., 2016; Kumari and Thakur, 2018; Liu et al., 2021). In addition, inoculation of plants with *Paenibacillus* sp. strains also produce novel bioactive metabolites for biological control and industrial applications (Daud et al., 2019). Khan et al. (2007) and Aw et al. (2016) highlighted that *Paenibacillus* species effectively improved the growth of tomato (*Lycopersicon esculentum*) and had antibacterial activity against a wide spectrum of pathogens. Therefore, species of the genus *Paenibacillus* has enormous potential as PGPR. However, only a few species of *Paenibacillus* have been explored in detail concerning their effects on the growth of forage crops.

White clover (*Trifolium repens* L.) is a considerable legume forage crop with strong adaptability, wide distribution, and easy cultivation (Ballhorn and Elias, 2014). It is suitable for silaging, haying, and grazing for livestock due to its high quality (Acharya et al., 2011). Meanwhile, white clover can also maintain soil fertility by providing nitrogen from its symbiotic interactions with rhizobia (Shamseldin et al., 2021). Additionally, it has well-developed and numerous stolons and/or shoots that are beneficial for water and soil conservation (Ballhorn and Elias, 2014; Zhang et al., 2020). A previous study showed that inoculation with *Bacillus amyloliquefaciens* GB03 significantly increased plant growth and biomass of white clover under both non-saline and saline conditions (Han et al., 2014). However, the effects of PGPR strains of *Paenibacillus* on the growth of white clover are unknown.

The Qilian Mountains are hydrologically and ecologically vital unit, as it functions as the water source for the irrigation agriculture in the Hexi Corridor and also maintains the ecological viability in the northern Alxa Highland (Zhao et al., 2009). The Qilian Mountains cover a large area with a complex topography, changeable climate types, and large numbers of plant species with obvious differences in spatial distribution (Liu et al., 2004; Zhao et al., 2009). The altitude ranges from 1,173 to 5,546 m (Wu and Jiang, 1998; Liu et al., 2004). Spruce is the dominant tree species and generally distributed at 2,400–3,400 m (Zhao et al., 2009). The Qilian Mountains are one of the most challenging habitats and abundant ecosystems and have been attracting tremendous attention in the fields of agriculture, ecology, and biotechnology. Recently, extensive research focused on soil nutrient characteristics, community structure, and microbial diversity in the Qilian Mountains (Zhao et al., 2015; Zhu et al., 2017; Jian et al., 2020; Lan et al., 2020). The bacterial genus *Paenibacillus* was detected in the microbiomes of different moss species in the Qilian Mountains with plant-promoting traits (Lan et al., 2020), indicating that strains of the genus *Paenibacillus* with plant growth-promoting traits existed in the Qilian Mountains.

The genus *Paenibacillus* was classified by Ash et al. (1991, 1993) by distinguishing members of the "16S rRNA group 3" bacilli from other lineages in the genus *Bacillus*. Subsequently, taxonomic characteristics of the genus *Paenibacillus* were further revised by Shida et al. (1997) and Padda et al. (2017). Until now, 337 species have been identified in the genus *Paenibacillus*, and the type species of this genus is *Paenibacillus polymyxa*.[1] The DNA G + C content of species in *Paenibacillus* ranges from 39 to 54 mol% (Kiran et al., 2017). Anteiso-$C_{15:0}$ is the predominant cellular fatty acid, and menaquinone-7 (MK-7) is the major respiratory quinone (Ashraf et al., 2017; Padda et al., 2017). Several species of the genus were also found to produce chitinases (Fu et al., 2014; Loni et al., 2014). Members of the genus have been isolated from various habitats, including desert (Lim et al., 2006a,b), agricultural soil (Kim et al., 2015), rhizosphere (Son et al., 2014), honeybee larvae (Genersch et al., 2006), human feces (Clermont et al., 2015), milk (Scheldeman et al., 2004), fresh water (Baik et al., 2001; Bae et al., 2010), warm springs (Chou et al., 2007), and eutrophic lake and glacier (Montes et al., 2004; Kishore et al., 2010), etc.

Thus, this study was aimed to explore PGPR resources of the genus *Paenibacillus* from spruce forests in Qilian Mountains. A bacterium strain, designated as LC-T2^T, was isolated from high-altitude spruce forests in the Qilian Mountains. The taxonomic status of strain LC-T2^T was evaluated based on phenotypic, phylogenetic, genotypic, and chemotaxonomic data. Furthermore, the plant growth-promotion effects of strain LC-T2^T was assessed in *Arabidopsis* and white clover (*T. repens* L.). Our work indicated that novel

[1] http://www.bacterio.net/paenibacillus.html

species in *Paenibacillus* isolated from spruce forests in Qilian Mountains have potential application values in cultivation of legume crops.

MATERIALS AND METHODS

Sample Collection and Microorganisms Isolation

Soil samples were collected from forests of the Qilian Mountains, Gansu province, China (38°25′32″N, 99°55′40″E, 3,150 m). Spruce was the dominant tree species at the altitude of 3,150 m in the Qilian Mountains. The soil sample was serially diluted with sterile 0.9% NaCl (*w*/*v*) solution, and dilutions were spread on tryptone soya agar (TSA). All plates were incubated aerobically at 25°C for 7 days. Morphologically different single colonies were randomly picked and further purified. Finally, the purified isolates were preserved as a glycerol suspension (20%, *v*/*v*) at −80°C.

Phylogenetic Analysis

The genomic DNA of the isolate was extracted by Bacterial Genomic DNA Extraction kit (TianGen Biotech Co., Ltd., Beijing, China) according to manufacturer's instructions. The 16S rRNA gene was amplified by PCR using a pair of universal primers, 27F and 1492R, as previous described (Li et al., 2020). The RNA polymerase β-subunit (*rpoB*) gene, an iconic housekeeping gene of the genus *Paenibacillus*, was amplified with primers *rpoB* 1698F (5′-AACATCGGTTTGATCAAC-3′) and *rpoB* 2041R (5′-CGTTGCATGTTGGTACCCAT-3′) (Yang Y.J. et al., 2018). The nitrogenase reductase (*nif*H) gene was amplified using the primers POLF (5′-TGCGAYCCSARRGCBGGYATCGG-3′) and POLR (5′-ATSGCCATCATYTCRCCGGA-3′) (Menéndez et al., 2017). The PCR product was purified by PCR purification kit (Sangon Biotech Co., Ltd., Shanghai, China) according to the manufacturer's instructions. Cloning of the 16S rRNA gene was executed using a pMD 19-T Vector Cloning kit (Takara Bio., Inc., Otsu, Japan). Sequencing was performed by the Sanger method (Beijing AUGCT DNA-SYN Biotechnology Co., Ltd, Beijing, China). Then, the almost-complete 16S rRNA, *rpoB*, and *nifH* gene sequences were compiled with the program DNAMAN (version 8.0; Lynnon Biosoft, San Ramon, CA, United States) (Saitou and Nei, 1987). The EzTaxon-e server[2] (Yoon et al., 2017) was used to calculate the levels of sequence similarity between strain LC-T2^T and related type strains available in GenBank[3] (Sayers et al., 2020). The phylogeny of 16S rRNA, *rpoB*, and *nifH* sequences was reconstructed by the neighbor-joining (NJ) (Saitou and Nei, 1987), maximum-likelihood (ML) (Felsenstein, 1981), and maximum-parsimony (MP) methods (Fitch, 1971) with MEGA 7.0 program (Kumar et al., 2016). Evolutionary distances were calculated using the Kimura's two-parameter model, and bootstrap analysis was used to evaluate the tree topology by performing 1,000 replications (Felsenstein, 1985).

Draft Genome Sequencing, Assembly, and Annotation

The draft genome shotgun project was sequenced using paired-end sequencing technology with the Illumina NovoSeq-PE150 platform (Novogene Biotech Co., Ltd., Tianjin, China). High-quality genomic DNA was carried out using Bacterial Genomic DNA Extraction kit (TianGen Biotech Co., Ltd., Beijing, China) according to standard protocol. The sequencing generated 1-Gb clean data. A *de novo* assembly of the reads was carried out using SOAPdenovo (version 2.04). The completeness of microbial genomes was assessed using the bioinformatics tool CheckM (Parks et al., 2015). The complete 16S rRNA gene sequence of strain LC-T2^T was annotated *via* the RNAmmer 1.2 server (Lagesen et al., 2007) from the genome. The draft genome was annotated using the NCBI Prokaryotic Genome Annotation Pipeline (PGAP) (Tatusova et al., 2016; Haft et al., 2018). The predicted coding sequences (CDSs) and functional annotation were generated from the National Center for Biotechnology Information (NCBI) non-redundant database, Kyoto Encyclopedia of Genes and Genomes (KEGG), Cluster of Orthologous Groups of proteins (COG), and Gene Ontology (GO) databases. DNA G + C content was calculated from the draft genome sequence. BLAST algorithm (ANIb) and the MUMmer ultra-rapid aligning tool (ANIm) were used to calculate average nucleotide identity (ANI) by the JSpecies software tool available at the webpage.[4] The digital DNA–DNA hybridization (dDDH) between strain LC-T2^T and related reference strains was calculated by Genome-to-Genome Distance Calculator 2.1 (GGDC).[5]

Morphological, Physiological, and Biochemical Taxonomic Analysis

The morphological, physiological, and biochemical characterizations such as growth in different bacteriological media, temperature, pH and NaCl concentrations, the Gram reaction, motility, oxidase, catalase, hydrolysis of Tween 80, DNA, casein, starch, and cellulase were carried out according to Li et al. (2020). Biochemical features were performed using the API 20NE, API ZYM, and API 50CH systems (bioMérieux). GENIII MicroPlates (Biolog) were used to check the utilization of 71 carbon sources as described by the manufacturer's instructions. *Paenibacillus donghaensis* KCTC 13049^T, a Xylan-degrading bacterial strain isolated from east sea sediment, and *Paenibacillus odorifer* JCM 21743^T, a nitrogen-fixing strain isolated from wheat roots, were used as reference strains for comparative taxonomic characteristics (Berge et al., 2002; Choi et al., 2008). The two reference strains were obtained from the Korean Collection for Type Cultures (KCTC) and the Japan Collection of Microorganisms (JCM), respectively. Cells of strain LC-T2^T and the reference strains cultured on Reasoner's 2A (R2A) agar at 28°C were used for biochemical feature tests. For measurement of nitrogenase activity, strain LC-T2^T and reference strains were grown on nitrogen-free

[2]http://www.ezbiocloud.net/apps
[3]www.ncbi.nlm.nih.gov/genbank/
[4]http://www.imedea.uib.es/jspecies
[5]http://ggdc.dsmz.de/distcalc2.php

medium (Zhuang et al., 2017). After 48 h at 28°C, strains were incubated in culture bottles with 10% (*v*/*v*) acetylene in air for 2 h and then analyzed for ethylene production by 450-GC gas chromatography (Berge et al., 2002).

For chemotaxonomic analysis, cells of strain LC-T2^T and reference strains were routinely cultivated on R2A agar at 28°C and harvested at the mid-exponential growth phase. The fatty acid profiles were analyzed and identified by using the Microbial Identification System (Sherlock version 6.1; midi database, TSBA6) after saponification, methylation, and extraction, according to standard procedures (Sasser, 1990). The polar lipids were extracted and separated by a chloroform/methanol system and one- and two-dimensional thin-layer chromatography (TLC) as described previously (Minnikin et al., 1984; Kates, 1986). Total lipids were detected using molybdatophosphoric acid, aminolipids were detected using ninhydrin reagent, phospholipids were detected using molybdenum blue reagent, and glycolipids were detected using naphthol/sulfuric acid reagent (Minnikin et al., 1984; Kates, 1986). Respiratory quinones were extracted and purified from lyophilized cells, then analyzed by high performance liquid chromatography (HPLC) according to Collins' method (Collins, 1985).

Evaluation of Plant Growth-Promoting Abilities

Plate and pot experiments were used to evaluate plant growth-promoting capabilities of strain LC-T2^T. Double-sterile distilled water (DDW) served as control. *Escherichia coli* strain DH5α and commercial *B. amyloliquefaciens* strain GB03 served as positive control. *Arabidopsis* seeds were surface sterilized with 70% ethanol for 3 min, washed with DDW several times, followed by 1% sodium hypochlorite for 10 min, finally thoroughly washed with DDW for 8–10 times, and then planted on one side of specialized plastic Petri dishes (100 × 15 mm) that contained a center partition; both sides contain half-strength Murashige and Skoog (MS) solid medium with 0.8% (*w*/*v*) agar and 1.0% (*w*/*v*) sucrose. Seeds were vernalized for 2 days at 4°C in the absence of light. Bacterial suspensions were prepared according to previously described methods (He et al., 2018). Cells were harvested from R2A plates, put into DDW to yield 1.0×10^9 colony forming units (CFU) ml^{-1} as determined by optical density, and serially diluted with plate counts. Then, 10 μl of bacterial suspension was spotted at one side of the Petri dish and 2-day-old *Arabidopsis* seedlings were planted on the other side of the Petri dish. Seedlings were grown under growth chamber (Panasonic, Japan) with a 16/8-h light/dark cycle under 200 μmol m^{-2} s^{-1} total light intensity, a temperature of 22 ± 2°C, and a relative humidity of 50–55%. The root system was scanned by an EPSON scanner, and morphological parameters were analyzed using the root analysis system WinRHIZO (v5.0, Regent Instruments, Quebec, QC, Canada) after 14 days. In pot experiments, white clover (*T. repens* L.) seeds (presented by Wanhai Zhou at Gansu Agricultural University, China) were surface sterilized for 1 min in 70% ethanol followed by 10 min in 2% sodium hypochlorite; then, seeds were rinsed with sterile water for 10 times and germinated in filter paper for 3 days. The seedlings with uniform growth were transferred to a plastic pot (diameter 9 cm, depth 10 cm) containing autoclave-sterilized commercial vermiculite–soil mixture and watered with modified half-strength Hoagland's solution three times per week. White clover seedlings were inoculated with 2 ml of prepared bacterial suspension culture as bacterial treatments or the same volume of DDW as control. Thirty-day-old plants were harvested for plant growth and physiological index measurements. When sampling, the rhizosphere soil samples were collected from the surface of root, and the culturable bacteria in rhizosphere were isolated again by multiple-dilution method to verify the effective inoculation.

Data Analysis

Results of the growth and physiological parameters were showed as means with standard errors (n = 6). Statistical analysis was assessed by one-way analysis of variance (ANOVA) using SPSS statistical software (Ver. 19.0, SPSS Inc., Chicago, IL, United States). Duncan's multiple range test was executed to detect a difference between means at a significance level of $P < 0.05$.

RESULTS

Phylogenetic Analysis

The complete 16S rRNA gene sequence (1,546 bp) was obtained from draft genome (GenBank accession number: OK058271). Comparative analysis built on 16S rRNA gene sequence revealed that strain LC-T2^T was phylogenetically affiliated to the genus *Paenibacillus* in the family *Paenibacillaceae*. On the basis of phylogenetic analysis, the highest level of similarity was found between strain LC-T2^T and *P. donghaensis* KCTC 13049^T (97.4%), followed by *P. odorifer* JCM 21743^T (96.8%) and other recognized members of the genus *Paenibacillus* (<96.7%). In the neighbor-joining phylogenetic tree, strain LC-T2^T fell within the cluster comprising the *Paenibacillus* species and formed a distinct genetic lineage with *P. donghaensis* KCTC 13049^T (**Supplementary Figure 1**) and likewise in the tree based on the ML and MP methods (data not shown). The *rpoB* gene fragment of strain LC-T2^T (GenBank accession number: OK094314) shared 87.2% sequence identity with *P. donghaensis* KCTC 13049^T and less than 84.8% identity with other members of the genus *Paenibacillus* (**Figure 1**). These data further confirmed that target lineage was belonging to the genus *Paenibacillus* and closely clustered with *P. donghaensis* KCTC 13049^T. The comparison of the *nifH* gene sequence of strain LC-T2^T (GenBank accession number: OK094315) with those of the type strains also showed that *P. donghaensis* KCTC 13049^T was the most closely related living species, with a similarity value of 81.4%, followed by *P. odorifer* JCM 21743^T (80.1%). The remaining available *nifH* sequences of the type species of the genus *Paenibacillus* showed less than 80% similarity to strain LC-T2^T. The phylogenetic analysis of *nifH* indicated that strain LC-T2^T clustered with *P. donghaensis* KCTC 13049^T and was

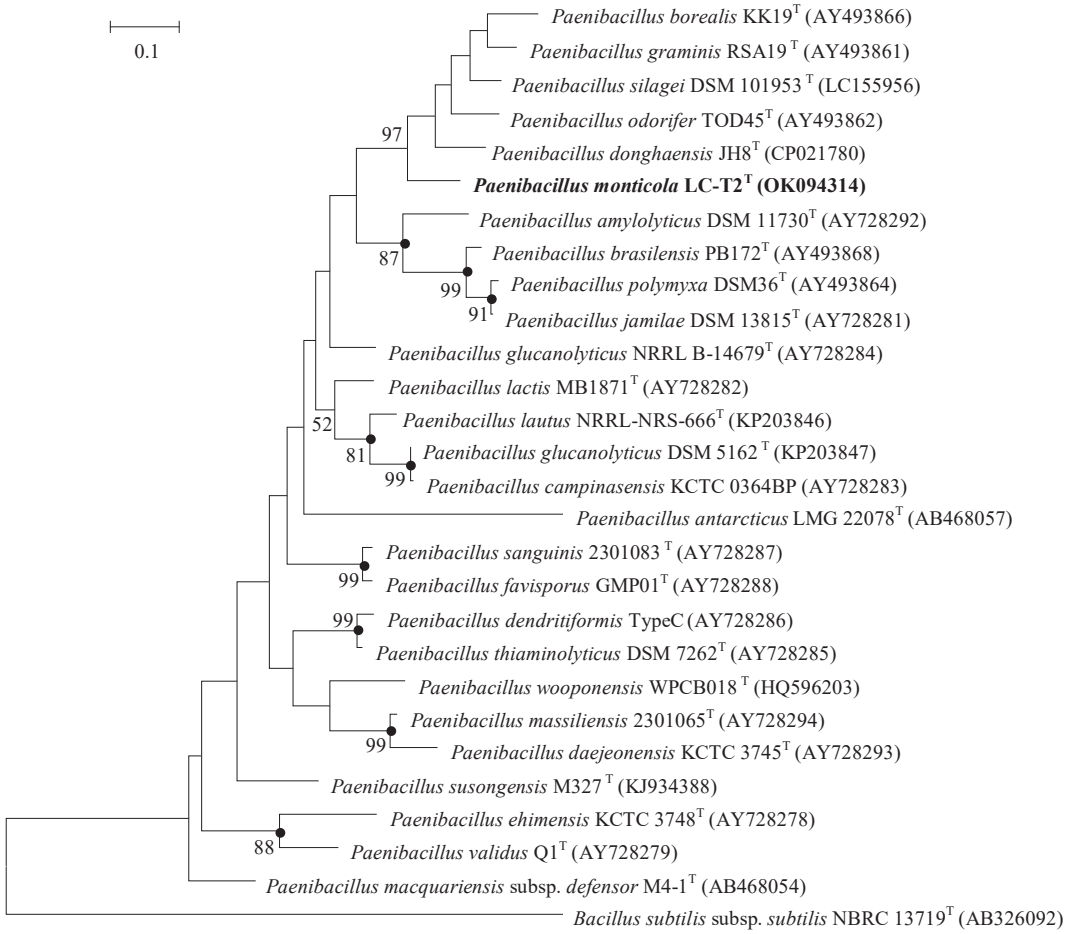

FIGURE 1 | Maximum Likelihood phylogenetic trees based on partial *rpoB* gene sequences showing the relationships between strain LC-T2^T and closely related species. *Bacillus subtilis subsp. subtilis* NBRC 13719^T was used as the outgroups. Numbers at branching points are bootstrap values > 50%. Bar, 0.1 substitutions per nucleotide position. Filled circles indicate that the corresponding nodes were also formed in neighbor-joining and maximum-parsimony trees. *rpoB* gene sequences of *Paenibacillus donghaensis* JH8^T was obtained from the genome sequence of strain *P. donghaensis* JH8^T.

phylogenetically divergent from the cluster of any recognized species of the genus *Paenibacillus* (**Supplementary Figure 2**).

Genome Characteristics of *Paenibacillus monticona* sp. nov. LC-T2^T

Draft genome sequencing of strain LC-T2^T (accession number: WJXB00000000) yielded a length of 7,082,651 bp with 35 contigs (total number > 500 bp) and N50 value of 657,675 after assembly. All contigs were larger than 536 bp, and the largest was 1,092,698 bp. The sequencing coverage was about ×200. A total of 6,236 genes were predicted, out of which 5,978 were protein-coding genes, 112 genes for RNA, and 146 pseudo genes (**Supplementary Table 1**). The DNA G + C content of strain LC-T2^T was 46.0 mol%, which fell within the range given for species of the genus *Paenibacillus* (Yang D. et al., 2018). The pairwise ANIb, ANIm, and dDDH values between the genome of LC-T2^T and four genomes of related species were 72.6–77.2, 83.3–84.3, and 20.4–23.0%, respectively. These values were obviously lower than the critical value of genomic species identification. The detailed results are displayed in **Table 1**.

Insights From the Genome Sequence

Strain LC-T2^T was isolated from high-altitude spruce forests in the Qilian Mountains. As shown in **Table 2**, the genome of strain LC-T2^T contained a large number of genes that were related to plant growth and habitat adaptation, such as

TABLE 1 | Average nucleotide identity (ANIb and ANIm) and DNA–DNA hybridization (DDH) values (%) of strain LC-T2^T with phylogenetically related species of the genus *Paenibacillus*.

Species name	ANIb	ANIm	DDH
Paenibacillus donghaensis KCTC 13049^T	72.6	83.3	21.2
Paenibacillus odorifer JCM 21743^T	77.2	84.3	23.0
Paenibacillus wynnii DSM 18334^T	75.1	83.7	20.4
Paenibacillus borealis DSM 13188^T	74.3	83.7	21.0

TABLE 2 | Putative gene identified in LC-T2^T genome related to plant associated lifestyle and habitat adaptation.

Categories	Gene annotation	Gene numbers
Plant growth promotion	Phosphate solubilization	
	Pyruvate kinase (*pyk*)	2
	Phosphoenolpyruvate carboxylase (*ppc*)	1
	Acetate kinase (*ackA*)	1
	Citrate kinase (*citA*/*citZ*)	2
	Shikimate kinase (*aroK*)	1
	L-lactate dehydrogenase (*ldh*)	1
	Alkaline phosphatase (*phoP*/*phoR*)	6
	Nicotinamide adenine dinucleotide (NADH) pyrophosphatase (*nudC*)	1
	Auxin biosynthesis	
	Tryptophan synthase α chain (*trpA*)	1
	Tryptophan synthase β chain (*trpB*)	1
	Indole-3-glycerol phosphate synthase (*trpC*)	1
	Tryptophan–tRNA ligase (*trpS*)	1
	Nitrogen fixation	
	Nitrogenase iron protein (*nifH*)	1
	Others related to plant promotion	
	Arginine decarboxylase (*speA*)	1
	Acetolactate synthase small/large subunit (*ilvH*/*ilvB*)	2
Habitat adaptation	Plant rhizosphere environments	
	Flagellar motility (*motA*/*motB*/*swrC*)	3
	Chemotaxis (*cheA*/*cheY*/*cheR*/*cheB*/*cheW*)	12
	Oxidative stress alleviation	
	Superoxide dismutase [Mn] (*sodA*)	1
	Superoxide dismutase [Fe] (*sodF*)	1
	Catalase (*katA*)	1
	Cold and heat shock protein	
	Cold shock protein (*cspA*)	2
	Heat shock protein (*Hsp*20)	1
	Transcriptional regulator of stress and heat shock response (*ctsR*)	1

10 genes coding for phosphate solubilization (*pyk*, *ppc*, *ackA*, *citA*, *citZ*, *aroK*, *ldh*, *phoP*, *phoR*, and *nudC*), four for auxin biosynthesis (*trpA*, *trpB*, *trpC*, and *trpS*), one for nitrogen fixation (*nifH*), and three for other processes of growth promotion (*speA*, *ilvH*, and *ilvB*), suggesting that strain LC-T2^T had the ability to promote plant growth. The genome of strain LC-T2^T contained several genes associated with secretion systems, biofilm formation, or motility. For instance, three genes responsible for flagellar motility (*motA*, *motB*, and *swrC*) and five genes responsible for chemotaxis (*cheA*, *cheY*, *cheR*, *cheB*, and *cheW*) indicated that strain LC-T2^T could get attracted to or move toward nutrients and interact with plants. Additionally, extreme conditions, such as low temperature, hypoxia, alpine, strong ultraviolet, erosive forces, and thaw–freezing cycles, prevailed in the Qilian Mountains at high altitudes and shaped abundant extreme microorganisms. The genome of strain LC-T2^T is well equipped with several genes that could alleviate the reactive oxygen species. Some genes responsible for superoxide dismutase [Mn] (*sodA*), superoxide dismutase [Fe] (*sodF*), and catalase (*katA*), demonstrated that strain LC-T2^T could cope with rhizosphere oxidative environments. Notably, several genes of strain LC-T2^T genome responded to extreme temperature at the height of 3,150 m in the Qilian Mountains. Genes coding for cold shock (*cspA*) and heat shock (*Hsp*20) showed that strain LC-T2^T was able to adapt the temperature variation. In accordance with the data presented above, the draft genome analysis provided insights into the genetic features to support its plant-associated lifestyle and habitat adaptation.

Phenotypic and Biochemical Characteristics

The cell of strain LC-T2^T was aerobic, Gram-negative (**Supplementary Figure 3A**), rod-shaped (4.2–4.5 × 0.6–0.7 μm) (**Supplementary Figure 3B**), and motile *via* peritrichous flagella (**Supplementary Figure 3C**). Colonies of strain LC-T2^T on R2A agar were white, round, and smooth with approximately 0.5–1.5 mm in diameter after culture at 28°C for 3 days. It was able to grow aerobically at 4–32°C (optimum at 25–28°C), at pH 6.0–11.5 (optimum at 8.0–8.5), and with 0–1.5% (*w*/*v*) NaCl (optimum at 0%). Strain LC-T2^T and the reference strains were positive for catalase and reduction of nitrate to nitrite, but they were negative for oxidase and hydrolysis of DNA, Tween 80, and cellulose. The detailed differential physiological and biochemical characteristics of strain LC-T2^T and its closest type strains of the genus *Paenibacillus* are given in **Table 3** and **Figure 2**. Strain LC-T2^T was distinguished from the reference strains in API 20NE test strips: assimilation of glucose, mannitol, and *N*-Acetyl-glucosamine. Strain LC-T2^T also differed from the closely related species in API ZYM test strips: cystine arylamidase, α-chymotrypsin, and acid phosphatase. Meanwhile, strain LC-T2^T also distinguished from the reference-type species in API 50CH test strips: D-ribose and methyl-α-D-glucopyranoside, *N*-acetyl-glucosamine, and inulin test. In the aspect of nitrogenase activity, the amount of strain LC-T2^T and reference strains, *P. donghaensis* KCTC 13049^T and *P. odorifer* JCM 21743^T, that could reduce acetylene to ethylene were 19.7, 15.5, and 25.4 (nmol C_2H_4) (mg protein)$^{-1}$ h^{-1}, respectively (**Table 3**).

The predominant cellular fatty acids (>10.0% of total fatty acids) of strain LC-T2^T was identified as anteiso-$C_{15:0}$ (56.5%) and $C_{16:0}$ (12.3%) (**Figure 2**). The fatty acid profile of strain LC-T2^T was similar to the reference strains, and all three species also contained anteiso-$C_{15:0}$ (40.3–56.5%) and $C_{16:0}$ (12.3–22.5%) as their major fatty acid. Moreover, the proportion of anteiso-$C_{15:0}$ of strain LC-T2^T was 2.4- and 1.2-fold higher than that of *P. donghaensis* KCTC 13049^T and *P. odorifer* JCM 21743^T, respectively, whereas the content of $C_{16:0}$ of strain LC-T2^T was nearly two-fold lower than that of the reference strains (**Figure 2**). The polar lipid pattern of strain LC-T2^T was dominated by the presence of large amounts of diphosphatidylglycerol (DPG)

TABLE 3 | Characteristics that differentiate the novel species LC-T2^T from phylogenetically related species of the genus *Paenibacillus*.

Characteristic	1	2	3
Habitat	Soil	Sediment	Rhizosphere
Temperature range (optimum) (oC)	4–32 (25–28)	4–30 (20–25)*	5–35 (30)#
pH range (optimum)	6–11.5 (8.0–8.5)	6–10 (ND)*	5.0–10.0 (ND)$
NaCl range (optimum)	0–1.5 (0%)	0–3.0 (ND)*	0–3.0 (ND)$
Assimilation of 20NE			
Glucose	−	w	+
Mannitol	+	−	−
N-Acetyl-glucosamine	−	−	+
Enzyme activity (API ZYM)			
Cystine arylamidase	−	w	−
α-chymotrypsin	−	−	w
Acid phosphatase	w	-	w
Acid production from API 50CH			
D-ribose	−	+	+
Methyl-α-D-glucopyranoside	+	−	+
D-mannose	+	w	w
N-acetyl-glucosamine	+	−	+
Inulin	−	−	+
Mannitol	+	+	−
D-melezitose	w	w	−
D-turanose	+	+	−
Nitrogenase activity [(nmol C_2H_4) (mg protein) $^{-1}$ h^{-1}]	19.7 ± 1.6ab	15.5 ± 2.4b	25.4 ± 1.7a
DNA G + C content (mol%)	46.0	53.1*	44.0#

Strains: 1, LC-T2^T; 2, Paenibacillus donghaensis KCTC 13049^T; 3, Paenibacillus odorifer JCM 21743^T. Data for those strains are from this study, except as labelled. All strains were positive for motility, reduction of nitrate to nitrite, catalase, alkaline phosphatase, esterase (C4), esterase lipase (C8), leucine arylamidase, valine arylamidase, naphthol-AS-BI-phosphohydrolase, α-galactosidase, β-galactosidase, α-glucosidase, and β-glucosidase activities. Hydrolysis of aesculin, assimilation of: maltose. All strains were negative for lipase (C14), trypsin, β-glucuronidase, N-acetyl-β-glucosaminidase, α-mannosidase, and α-fucosidase activities and oxidase, hydrolysis of: DNA, Tween 80, and cellulose, assimilation of: mannose, arabinose, gluconate, citrate, adipic acid, capric acid, and phenylacetic acid. +, positive; −, negative; w, weakly positive; ND, no data available.

**Data from Choi et al. (2008) and Jung et al. (2017).*

#*Data from Berge et al. (2002).*

$*Data from Liu et al. (2018).*

and phosphatidylethanolamine (PE) and small amounts of phosphatidylglycerol (PG) and several unidentified ingredients as follows: three unidentified phospholipids (PL1–3), two unidentified aminophospholipids (APL1–2), and one unidentified glycolipid (GL1) (**Supplementary Figure 4**). MK-7 was detected as the only respiratory quinone in strain LC-T2^T.

Growth Promotion of *Arabidopsis thaliana* Exposed to Strain LC-T2^T

The apparent growth differences of *Arabidopsis* were observed between LC-T2^T exposure and the other three treatments after 2 weeks of plant growth (**Figure 3A**). The significant differences were mainly observed on plant roots. Specifically, the total root length was significantly greater for LC-T2^T-exposed roots ($P < 0.05$) by 61.0, 50.4, and 36.7% compared to control, DH5α, and GB03 exposure, respectively (**Figure 3B**). The highest root surface area and root projection area were also observed from exposure to LC-T2^T VOCs. The root surface area was increased ($P < 0.05$) by 61.3, 53.1, and 28.8% (**Figure 3C**), and the root projection area was enhanced ($P < 0.05$) by 61.3, 53.1, and 28.7% (**Figure 3D**) compared to control, DH5α, and GB03 exposure, respectively. The root fork numbers was increased over 1.9-fold ($P < 0.05$) with LC-T2^T VOCs compared to control and DH5α exposure, respectively. However, the root fork numbers of LC-T2^T were little lower than GB03 exposure (**Figure 3E**).

The Effect of Strain LC-T2^T on the Growth of White Clover

The influence of strain LC-T2^T on the growth of white clover was further assessed. Shoot height was increased by 31.5 ($P < 0.05$), 42.7 ($P < 0.05$), and 7.3% compared to control, DH5α, and GB03 treatments, respectively (**Figure 4C**), and root length was increased by 24.4 ($P < 0.05$) and 10.9% compared to control and DH5α treatments, respectively (**Figure 4D**).

Plants inoculated with LC-T2^T had a higher biomass than that of control, DH5α, and GB03. Shoot fresh weight was raised with the LC-T2^T group by 147.5 ($P < 0.05$), 117.6 ($P < 0.05$), and 2.0% (**Figure 4E**) and shoot dry weight was increased with the LC-T2^T group by 128.6 ($P < 0.05$), 127.1 ($P < 0.05$), and 10.8% compared to control, DH5α, and GB03 treatments, respectively (**Figure 4F**). Likewise, the root fresh weight of LC-T2^T-inoculated plants was about 216.2 and 89.8% (**Figure 4G**) and the root dry weight of LC-T2^T-inoculated plants was about 104.7 and 86.5% (**Figure 4H**) higher than those of the control and DH5α treatments, respectively ($P < 0.05$). However, the root fresh weight and root dry weight of LC-T2^T were a little lower compared to GB03 exposure (**Figures 4G,H**).

Strain LC-T2^T can also enhance the accumulation of plant biomass by root activity and chlorophyll content. Root activity was improved with the LC-T2^T group by 57.7 and 60.2% compared to control and DH5α treatments, respectively ($P < 0.05$; **Supplementary Figure 5A**). The content of chlorophyll a of LC-T2^T-inoculated plants was increased by 25.9 ($P < 0.05$), 27.1 ($P < 0.05$), and 1.8% compared to control, DH5α, and GB03 treatments, respectively (**Supplementary Figure 5B**), and the content of chlorophyll b was improved by 2.1- ($P < 0.05$), 1.2- ($P < 0.05$), and 1.0-fold with LC-T2^T treatment compared to control, DH5α, and GB03 treatments, respectively (**Supplementary Figure 5B**).

In addition, the photosynthetic rate was enhanced with the LC-T2^T group by 13.7 and 26.5% compared to control and DH5α treatments, respectively (**Supplementary Figure 5C**). The transpiration rate was raised by 1.2- and 1.5-fold ($P < 0.05$) with LC-T2^T-inoculated plants (**Supplementary Figure 5D**), and the stomatal conductance was increased by 17.4 and 39.1% (**Supplementary Figure 5E**) compared to control and DH5α treatments, respectively. The photosynthetic rate, transpiration rate, and stomatal conductance of LC-T2^T-inoculated plants were slightly lower than those of GB03 treatment, and differences were not statistically significant (**Supplementary Figures 5C–E**). The water-use efficiency was improved by

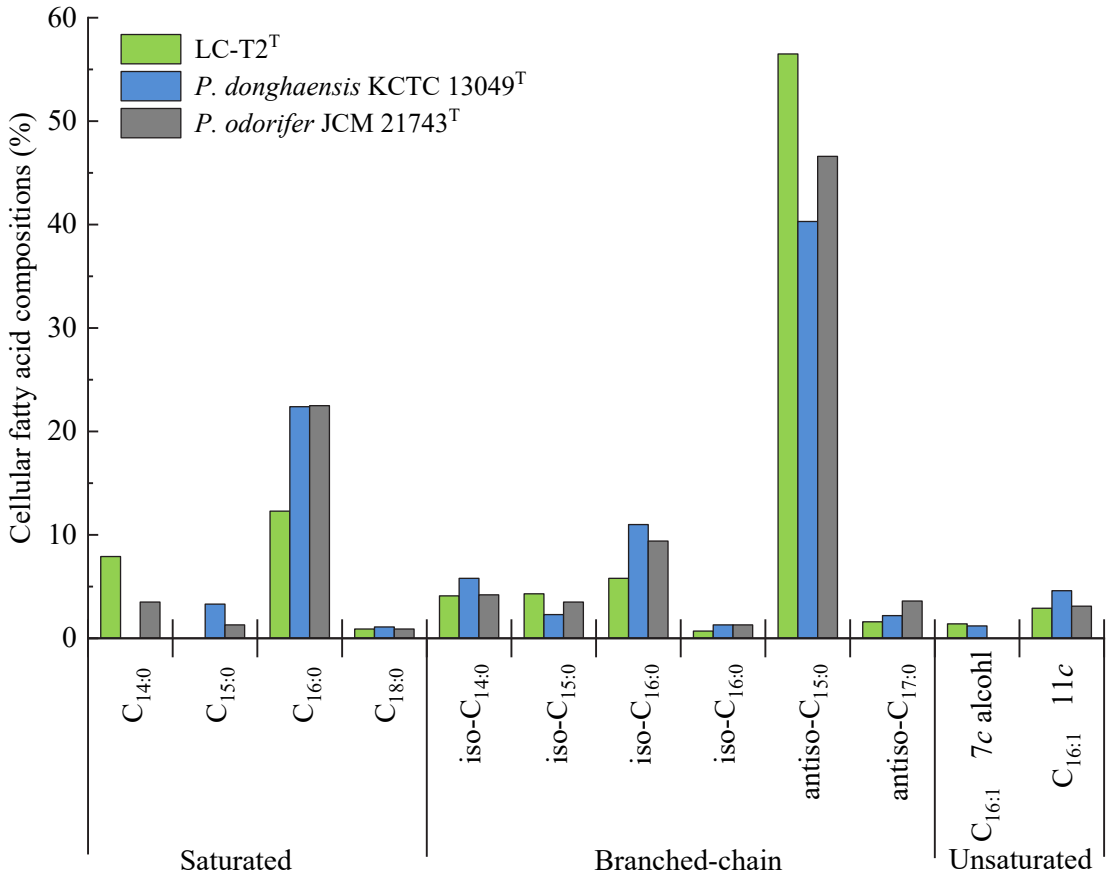

FIGURE 2 | Cellular fatty acid compositions (%) of strain LC-T2^T and the type strains of phylogenetically related species of the genus *Paenibacillus*.

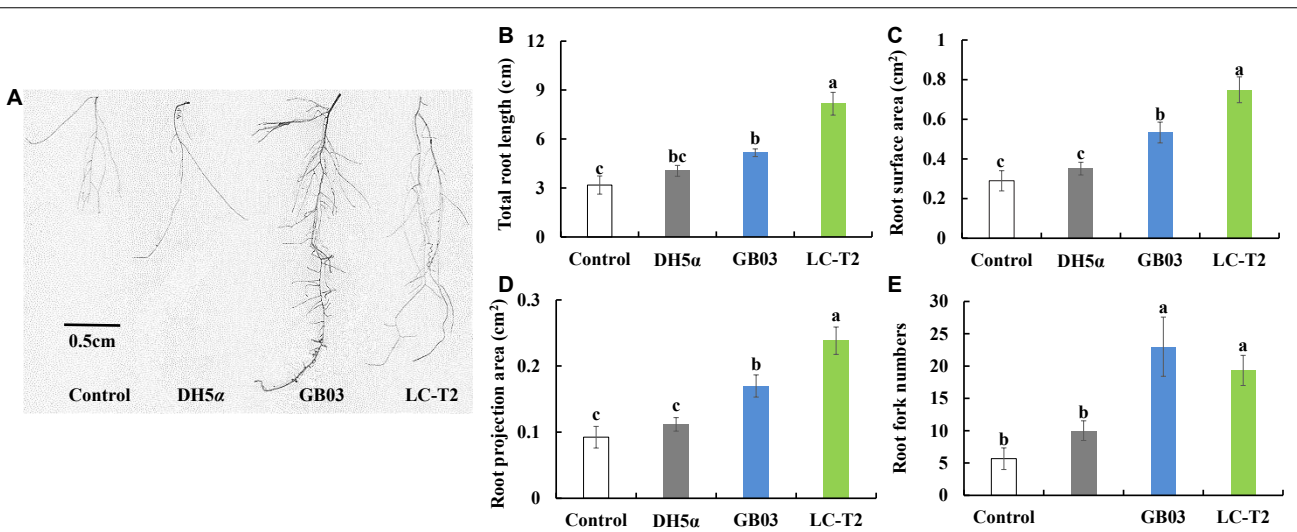

FIGURE 3 | Effects of roots growth of *Arabidopsis* exposure to LC-T2^T volatile organic compounds (VOCs). *Escherichia coli* (DH5α) and *Bacillus amyloliquefaciens* (GB03) as positive control I. **(A)** plant root image, **(B)** total root length, **(C)** root surface area, **(D)** root projection area, and **(E)** root fork numbers. Seedlings were taken image and root growth index were measured after 2 weeks exposure to *E. coli* (DH5α), *B. amyloliquefaciens* (GB03), and *Paenibacillus monticola* LC-T2^T, respectively. Values are means and bars indicate SDs (n = 6). Columns with different letters indicate significant difference at $P < 0.05$ (Duncan test).

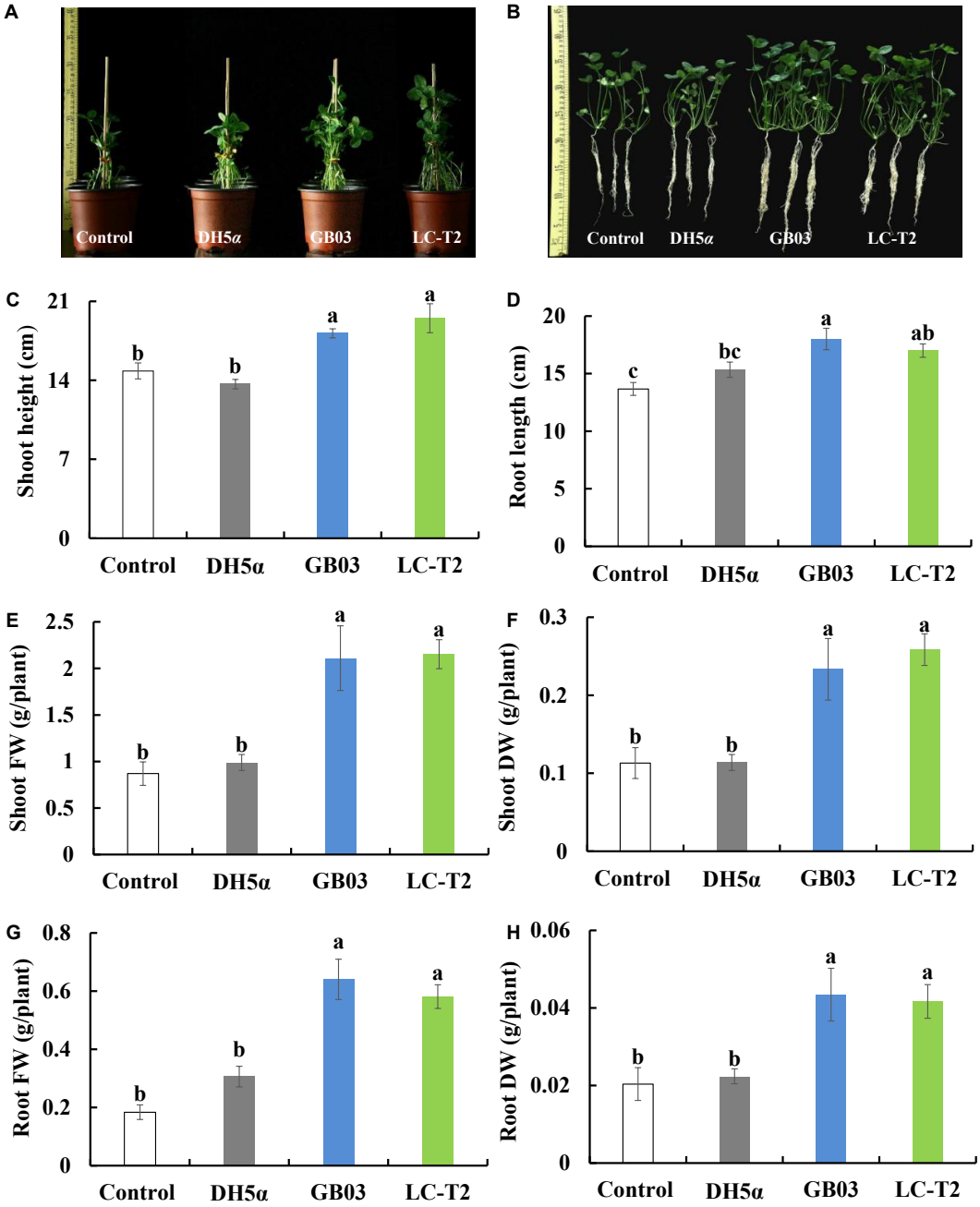

FIGURE 4 | Effects of LC-T2^T inoculation on seedling growth of white clover. *Escherichia coli* (DH5α) and *Bacillus amyloliquefaciens* (GB03) as positive control. **(A,B)** whole plant image, **(C)** shoot height, **(D)** root length, **(E)** shoot fresh weight, **(F)** shoot dry weight, **(G)** root fresh weight, and **(H)** root dry weight. Seedlings were taken image and biomass were measured after 30 days inoculate to bacterials suspension and double-sterile distilled water (DDW), respectively. Values are means and bars indicate SDs (n = 6). Columns with different letters indicate significant difference at $P < 0.05$ (Duncan test).

1.8- ($P < 0.05$), 1. 2-, and 1.2-fold with LC-T2^T treatment compared to control, DH5α, and GB03 treatments, respectively (**Supplementary Figure 5F**).

Effectiveness of LC-T2^T Inoculation

Culturable bacterial strains have been isolated from the rhizosphere after 20 days of inoculation to verify the existence of inoculated strains. The number of genera from LC-T2^T-inoculated rhizosphere soil was 1.7-fold higher than that of control and DH5α, respectively. In the diversity and number of species, LC-T2^T-inoculated soil was also superior to control and DH5α-inoculated soil (**Table 4**). Some isolates were similar to strain LC-T2^T and GB03, respectively, except for DH5α treatment (**Supplementary Tables 2**, **3**). The species in the genus

Bacillus and *Pseudomonas* were also isolated from all inoculated soils, whereas a higher abundance of *Rhodococcus qingshengii* was found in control and DH5α-inoculated soils.

DISCUSSION

Researchers have always sought to isolate novel species of the genus *Paenibacillus* from different habitats. As an important ecological security barrier in western China, the Qilian Mountains possess abundant glacier, water, forest, grassland, and animal resources (Zhao et al., 2009). The rich and diverse natural eco-environments of the Qilian Mountains harbor unique and great diversity of microbial resources. In the current work, a novel *Paenibacillus* species from spruce forest at a high altitude of 3,150 m in the Qilian Mountains was isolated and characterized. A phylogenetic analysis of 16S rRNA gene sequence, one of the most powerful and frequently used methods for identification of bacteria (Busse et al., 1996), revealed that strain LC-T2^T was a member of the genus *Paenibacillus* with the highest similarity to *P. donghaensis* KCTC 13049^T (97.4%). To further define the phylogenetic affinity of strain LC-T2^T, we also analyzed *rpoB* gene sequence, which was more discriminative than 16S rRNA gene sequence in distinguishing members of the genus *Paenibacillus* (da Mota et al., 2004). Nitrogen fixation-related genes are widely used as marker genes to analyze the phylogenetic relationship of nitrogen-fixing bacteria and archaea (Jacobson et al., 1989; Choo et al., 2003; Brigle et al., 2011; Gaby and Buckley, 2014). Most members of the genus *Paenibacillus* have been found to possess nitrogenase activity. Therefore, *nifH* gene sequence was also used to distinguish members of the genus *Paenibacillus*. In all phylogenetic trees (**Figure 1** and **Supplementary Figures 1**, **2**), strain LC-T2^T was obviously different from all known taxa. In brief, the phylogenetic analysis based on 16S rRNA, *rpoB*, and *nifH* gene sequences highlighted that strain LC-T2^T was assigned to a novel species in the genus *Paenibacillus*.

At the genomic level, this study provided more robust evidence to support the taxonomic status of strain LC-T2^T. The dDDH value and ANI value between strain LC-T2^T and its closest phylogenetic relatives were lower than 23.0 and 84.3%, respectively. Studies have shown that the cut-off of 70% genomic relatedness with dDDH was generally recommended for species delineation and has been found to correlate to 95–96% ANI (Richter and Rosselló-Móra, 2009; Meier-Kolthoff et al., 2013, 2014a,b). In the current work, both dDDH value and ANI value were significantly below the threshold for species circumscriptions. These data demonstrated that strain LC-T2^T should be considered as the representative of a novel species of the genus *Paenibacillus*. Meanwhile, *rpoB* gene sequence similarity can provide efficient supplement to dDDH and ANI measurements to delineate bacterial species and genera, especially for *Paenibacillus* (Adékambi et al., 2008). On the basis of previous research, 97.7% sequence similarity of *rpoB* gene was, as a threshold for species delineation, correlated with a dDDH value < 70% and an ANI value < 94.3% (Adékambi et al., 2008). Here, we found that *rpoB* gene sequence identity of strain LC-T2^T with the other *Paenibacillus* species was lower than 87.2%. In summary, the values of ANIb, ANIm, and dDDH between strain LC-T2^T and the typical strains for the closest *Paenibacillus* species were obviously lower than the acceptable threshold for bacterial species definition (**Table 1**), indicating that strain LC-T2^T represented a novel *Paenibacillus* species.

A classification of strain LC-T2^T at species level was greatly supported by phenotypic, physiological, and chemotaxonomic data. As shown in **Table 3**, **Figure 2**, and **Supplementary Figures 3**, **4**, the similarities and differences of strain LC-T2^T and its closest typical strains in the genus *Paenibacillus* are presented. Members of *Paenibacillus* were known to be Gram-positive, variable, and negative (Aw et al., 2016). Strain LC-T2^T was found Gram-negative during the whole culture period, which was significantly different from the two reference strains (Berge et al., 2002; Choi et al., 2008). The dominant fatty acids, polar lipid profiles, and respiratory quinone of strain LC-T2^T were in accordance with those found in members of the genus *Paenibacillus* (Ash et al., 1993; Shida et al., 1997; Lim et al., 2006a,b; Priest, 2009; Huang et al., 2016; Ashraf et al., 2017; Yang D. et al., 2018; Yang Y.J. et al., 2018). However, differences were observed in proportion of these components, which enabled strain LC-T2^T to be clearly distinguished. Additionally, the nitrogenase activity of strain LC-T2^T was about 27.1% higher than that of *P. donghaensis* KCTC 13049^T and 22.4% lower than that of *P. odorifer* JCM 21743^T (**Table 3**). Previous studies suggested that *P. donghaensis* KCTC 13049^T and *P. odorifer* JCM 21743^T exhibited a weak nitrogenase activity (Berge et al., 2002; Jin et al., 2011; Xie et al., 2012; Zhuang et al., 2017). In the current work, nitrogenase activities of reference strains were in good agreement with the results of previous studies (Berge et al., 2002; Jin et al., 2011; Xie et al., 2012; Zhuang et al., 2017). Therefore, strain LC-T2^T could also be classified as bacterial strains with a weak nitrogenase activity.

Previous models of rhizobacterial-stimulated plant growth promotion suggested that soil microbes can drive plant growth promotion *via* emission of volatile chemicals (Timmusk et al., 1999; Ryu et al., 2003; Zhang et al., 2007; Luo et al., 2020). In *Arabidopsis*, volatile emissions from GB03 can regulate auxin homeostasis, transport, and cell expansion (Ryu et al., 2003; Zhang et al., 2007). In this work, strain LC-T2^T conferred an increased total root length, root surface area, root project area, and root fork numbers in Petri dish-grown Arabidopsis seedlings *via* emission of volatile chemicals (**Figure 3**). Interestingly, the root length of seedlings inoculated with LC-T2^T was longer than that inoculated with GB03, but the number of root fork was less than that inoculated with GB03, which might be attributed to GB03 VOCs that could increase the root auxin content and auxin accumulation at the lateral root initiation sites (Zhang et al., 2007; Xie et al., 2009; Zamioudis et al., 2013). Studies showed that GB03 VOCs specifically regulated plant auxin homeostasis to accelerate leaf expansion. Conveniently, adventitious roots seemed to successfully offer such a balance (Zhang et al., 2007). However, in the present study, LC-T2^T VOCs mainly promoted the plant growth through increasing root length rather than the

TABLE 4 | The number of genera counted from isolates in the white clover rhizosphere soil.

Treatments	Control	DH5α	GB03	LC-T2
Number of genus	6	6	10	10
Genus	*Bacillus* *Flavobacterium Microbacterium* *Paenarthrobacter Rhodococcus* *Sphingobacterium*	*Microbacterium* *Paenarthrobacter* *Paracoccus* *Pseudomonas Rhodococcus* *Sphingomonas*	*Arthrobacter* Bacillus *Curvibacter* *Flavobacterium* *Leifsonia* *Paracoccus* *Paenarthrobacter* *Pseudomonas* *Pseudarthrobacter Rhodococcus*	*Arthrobacter* *Asticcacaulis* *Bacillus* *Exiguobacterium* *Flavobacterium Microbacterium* *Paenibacillus* *Pseudomonas* *Rhodococcus* *Sphingopyxis*

number of adventitious roots in *Arabidopsis*. Combined with the data of LC-T2^T genome, genes coding for the production of auxins were identified (**Table 2**). Therefore, it was inferred that a different mechanism existed in the regulation patterns of hormone-related genes between strain LC-T2^T and GB03, which requires to be further verified. In addition, volatile metabolites from some species of the genus *Paenibacillus* could also activate induced systemic resistance (ISR) against pathogenic microorganisms (Timmusk et al., 2005; Kiran et al., 2017; Daud et al., 2019). However, whether the VOCs from strain LC-T2^T could also prevent pathogenic microorganisms remains to be investigated.

The beneficial effects of PGPR arouse interests and have been studied in various plants over the past decades worldwide (Zhao et al., 2016; Brito et al., 2017; Backer et al., 2018; Kumari and Thakur, 2018). Various studies demonstrated that soil inoculation with PGPR can promote plant growth, increase crop yields, enhance plant stress tolerance, and augment reproductive success (Han et al., 2014; Niu et al., 2016; Ke et al., 2019). The interest in *Paenibacillus* has mounted up since many strains have been found to possess potential agronomic value (e.g., *Paenibacillus ehimensis*, *Paenibacillus alvei*, *P. polymyxa*, and *Paenibacillus riograndensis*) (Antonopoulos et al., 2008; Naing et al., 2014; Brito et al., 2017). Kumari and Thakur (2018) demonstrated that treatment with *Paenibacillus* sp. ISTP10 significantly improved root fresh weight (131%), shoot fresh weight (105.14%), and total chlorophyll content (77.85%) of cotton in Cd-contaminated soil. White clover (*T. repens* L.), as a kind of high-quality forage in northwest China, has been gradually recognized of its advantages (Zhang et al., 2020). Therefore, its yield and quality have attracted considerable attention. However, available studies involved in the interaction of white clover with *Paenibacillus* sp. were rarely reported. Here, the substantial effects of the novel species of *Paenibacillus* LC-T2^T on the growth of white clover were further assessed after it was found to have a positive response on the roots of *A. thaliana*. The plant appearance became larger, and all physiological parameters showed rising tendency in varying degrees with LC-T2^T treatment compared to the control and DH5α treatments (**Figure 4** and **Supplementary Figure 5**). Noticeably, shoot weight and root weight of samples inoculated with LC-T2^T were almost twice as higher compared to control and DH5α treatments (**Figures 4E–H**). Interestingly, shoot height and shoot weight of LC-T2^T-inoculated plants were slightly higher than those of GB03-inoculated plants. However, root length and root weight of LC-T2^T were slightly lower than GB03, which was similar to results from plate experiment. Kim et al. (2011) found that among the selected 20 representative PGPR, most of the recognized genera were *Paenibacillus*, *Bacillus*, and *Pseudomonas*, which could remarkably enhance plant height, stem diameter, and fresh weight of cucumber. However, there was no obvious correlation between different isolates on the growth of cucumber based on PGPR genetic diversity, which suggested that there were differences in the regulation mechanism of different strains on cucumber growth. Therefore, it was supposed that strain LC-T2^T and GB03 had different regulation patterns on the shoot and root of plant growth promotion, which needs to be further explored.

The success of colonization in the rhizosphere was one of the prerequisites for microbial inoculants to exhibit their plant growth-promotion characteristics (Mosimann et al., 2017; Mawarda et al., 2020). In this work, numerous bacterial strains were found from the rhizosphere soil after 20-day inoculation, and the number of genera of the isolates from LC-T2^T-inoculated soil was almost twice that of control and DH5α-inoculated soil (**Table 4**). Some isolates were found to be similar to strain LC-T2^T (**Supplementary Table 2**). These results suggested that rhizosphere inoculation with LC-T2^T was effective. Strain LC-T2^T had the capability of rapidly adapting to the environment, recruiting more rhizobacteria, and inhibiting pathogenic bacteria, which were vital for host plant growth promotion (Schreiter et al., 2014; Ke et al., 2019). In addition, species belonging to the genus *Bacillus* and *Pseudomonas* were also found in all inoculated rhizosphere soils, indicating that the genus *Bacillus* and *Pseudomonas* were the dominant genera in the soil (Zaidi et al., 2009). Also, a kind of carbendazim-degrading bacterium species, *R. qingshengii*, were obtained from DH5α-inoculated rhizosphere soil that probably inhibited or inactivated other microorganisms while degrading carbendazim (Xu et al., 2007). These results demonstrated that strain DH5α had poor survival and colonization ability in the rhizosphere and was at a competitive disadvantage (Majidzadeh and Fatahi-Bafghi, 2018; Chen et al., 2019). In light of the above research results, we supposed that both LC-T2^T VOCs and soil inoculation of LC-T2^T could improve plant growth, and LC-T2^T could be qualified as a kind of PGPR candidate for agricultural crop production.

CONCLUSION

Sequence analysis of housekeeping genes (16S rRNA and *rpoB*) and *nif*H gene demonstrated that strain LC-T2^T could be representative of a new species within the genus *Paenibacillus*. The dDDH, ANIb, and ANIm analyses confirmed this presumption with their values less than 23.0, 77.2, and 84.3%, respectively. The distinctness and potential beneficial functions of strain LC-T2^T at the species level was also supported by genomic data. The taxonomic status of strain LC-T2^T was further clarified according to the content of anteiso-$C_{15:0}$ and $C_{16:0}$ and the profiles of DPG, PE, and PG. The above results clearly located that strain LC-T2^T is a novel species within *Paenibacillus*. This work also established that rhizosphere inoculation with strain LC-T2^T could significantly increase plant growth of legume crops like white clover, which made strain LC-T2^T a potential excellent PGPR strain for practical application in legume crops.

Description of *Paenibacillus monticola* sp. nov.

Paenibacillus monticola (mon.ti'co.la. L. n. *mons*, *-ntis* mountain; L. suff. *-cola*, inhabitant; N.L. masc. n. *monticola*, living in the mountains).

Cells are Gram-stain-negative, rod-shaped (4.2–4.5 × 0.6–0.7 μm) and motile by means of peritrichous flagella. Colonies of strain LC-T2^T were white, round, and smooth with approximately 0.5–1.5 mm in diameter after culture at 28°C for 3 days on R2A agar. The isolate grew well on R2A agar, ISP 2 agar, PYG agar, and TY agar and weakly on NA and TSA, but no growth occurs on MA, LB agar, and MacConkey agar. Growth of strain LC-T2^T occurred at 4–32°C (optimum, 25–28°C), at pH 6.0–11.5 (optimum, 8.0–8.5), and with 0–1.5% (*w*/*v*) NaCl (optimum, 0%). Strain LC-T2^T was positive for catalase, the reduction of nitrate to nitrite, and the assimilation of mannitol, but it was negative for oxidase and hydrolysis of cellulose, Tween 80, and DNA. In API ZYM test strips, strain LC-T2^T was as follows: positive for alkaline phosphatase, acid phosphatase, esterase (C4), esterase lipase (C8), leucine arylamidase, valine arylamidase, naphthol-AS-BI-phosphohydrolase, α-galactosidase, β-galactosidase, α-glucosidase, and β-glucosidase activities and negative for lipase (C14), trypsin, β-glucuronidase, *N*-acetyl-β-glucosaminidase, α-mannosidase, cystine arylamidase, α-chymotrypsin, and α-fucosidase activities. Acid is produced from methyl-β-D-xylopyranoside, D-mannose, *N*-acetyl-glucosamine, mannitol, D-turanose, L-arabinose, D-cellobiose, D-lactose, D-raffinose, D-turanose, D-sucrose, arbutin, and esculin. The following compounds are utilized as sole carbon sources in the GENIII microplates: Dextrin, D-maltose, D-trehalose, D-cellobiose, gentiobiose, sucrose, D-turanose, stachyose, D-raffinose, α-D-lactose, D-melibiose, *N*-acetyl-D-glucosamine, α-D-glucose, D-mannose, D-fructose, D-galactose, D-sorbitol, and D-mannitol. The predominant cellular fatty acids (> 10.0% of total fatty acids) of strain LC-T2^T were anteiso-$C_{15:0}$ and $C_{16:0}$. The major polar lipids of strain LC-T2^T were established as DPG, PE, PG, and several unidentified ingredient as follows: three unidentified phospholipids (PL1–3), two unidentified aminophospholipids (APL1–2), and one unidentified glycolipid (GL1). Menaquinone-7 (MK-7) was detected as the only respiratory quinone. The DNA G + C content is 46.0 mol%.

The type strain is LC-T2^T (=CCTCC AB 2019254^T = KCTC 43175^T), isolated from spruce forest in the Qilian Mountains, Gansu province, China (38°25′32″N, 99°55′40″E). The GenBank/EMBL/DDBJ accession number for 16S rRNA, *rpoB*, and *nifH* gene sequence and the whole-genome sequence of strain LC-T2^T can be found at: https://www.ncbi.nlm.nih.gov/genbank/, OK058271, OK094314, OK094315, and WJXB00000000, respectively.

DATA AVAILABILITY STATEMENT

The datasets presented in this study can be found in online repositories. The names of the repositories and accession numbers can be found below: https://www.ncbi.nlm.nih.gov/genbank/, OK058271 https://www.ncbi.nlm.nih.gov/genbank/, OK094314 https://www.ncbi.nlm.nih.gov/genbank/, OK094315 https://www.ncbi.nlm.nih.gov/genbank/, WJXB00000000.

AUTHOR CONTRIBUTIONS

H-PL and QZ designed the experiments. L-JY provided the soil samples. H-PL performed most work on isolating and identifying bacterial strains, being assisted by Y-NG, JC, and Q-ML and wrote the first draft of the manuscript. Y-NG and JC assisted in the completion of the plant inoculation experiment. Q-QH did the proofreading of the first version. QZ and J-LZ provided guidance in scientific knowledge and correction of grammatical errors. All authors contributed to the article and approved the submitted version.

FUNDING

This work was financially supported by the National Natural Science Foundation of China (Grant No. 31801944), the National Key Research and Development Program of China (Grant No. 2019YFC0507703), the Natural Science Foundation of Gansu Province, China (Grant No. 17JR5RA211), and the Fundamental Research Funds for the Central Universities (Grant No. lzujbky-2021-ct16).

ACKNOWLEDGMENTS

We thank Songzhen Yang at Guangdong Culture Collection Center of China for providing related technical supports.

SUPPLEMENTARY MATERIAL

The Supplementary Material for this article can be found online at: https://www.frontiersin.org/articles/10.3389/fmicb.2022.833313/full#supplementary-material

REFERENCES

Acharya, A. R., Wofford, D. S., Kenworthy, K., and Quesenberry, K. H. (2011). Combining ability analysis of resistance in white clover to southern root-knot nematode. *Crop. Sci.* 51, 1928–1934. doi: 10.2135/cropsci2010.12.0695

Adékambi, T., Shinnick, T. M., Raoult, D., and Drancourt, M. (2008). Complete rpoB gene sequencing as a suitable supplement to DNA–DNA hybridization for bacterial species and genus delineation. *Int. J. Syst. Evol. Microbiol.* 58, 1807–1814. doi: 10.1099/ijs.0.65440-0

Antonopoulos, D. F., Tjamos, S. E., Antoniou, P. P., Rafeletos, P., and Tjamos, E. C. (2008). Effect of *Paenibacillus alvei*, strain K165, on the germination of *Verticillium dahliae* microsclerotia in planta. *Biol. Control* 46, 166–170. doi: 10.1016/j.biocontrol.2008.05.003

Ash, C., Farrow, J. A. E., Wallbanks, S., and Collins, M. D. (1991). Phylogenetic heterogeneity of the genus *Bacillus* revealed by comparative analysis of small-subunit-ribosomal RNA sequences. *Lett. Appl. Microbiol.* 13, 202–206. doi: 10.1111/j.1472-765X.1991.tb00608.x

Ash, C., Priest, F. G., and Collins, M. D. (1993). Molecular identification of rRNA group 3 bacilli (Ash, Farrow, Wallbanks and Collins) using a PCR probe test. *Anton. Leeuw. Int. J. G.* 64, 253–260. doi: 10.1007/BF00873085

Ashraf, S., Soudi, M. R., Amoozegar, M. A., Nikou, M. M., and Spröer, C. (2017). *Paenibacillus xanthanilyticus* sp. nov. a xanthan-degrading bacterium isolated from soil. *Int. J. Syst. Evol. Microbiol.* 68, 76–80. doi: 10.1099/ijsem.0.002453

Aw, Y. K., Ong, K. S., Lee, L. H., Cheow, Y. L., Yule, C. M., and Lee, S. M. (2016). Newly isolated *Paenibacillus tyrfis* sp. nov., from Malaysian tropical peat swamp soil with broad spectrum antimicrobial activity. *Front. Microbiol.* 7:219. doi: 10.3389/fmicb.2016.00219

Backer, R., Rokem, J. S., Ilangumaran, G., Lamont, J., Praslickova, D., Ricci, E., et al. (2018). Plant growth-promoting rhizobacteria: context, mechanisms of action, and roadmap to commercialization of biostimulants for sustainable agriculture. *Front. Plant Sci.* 9:1473. doi: 10.3389/fpls.2018.01473

Bae, J. Y., Kim, K. Y., Kim, J. H., Lee, K., Cho, J. C., and Cha, C. J. (2010). *Paenibacillus aestuarii* sp. nov., isolated from an estuarine wetland. *Int. J. Syst. Evol. Microbiol.* 60, 644–647. doi: 10.1099/ijs.0.011544-0

Baik, K. S., Choe, H. N., Park, S. C., Kim, E. M., and Seong, C. N. (2001). *Paenibacillus wooponensis* sp. nov., isolated from wetland freshwater. *Int. J. Syst. Evol. Microbiol.* 61, 2763–2768. doi: 10.1099/ijs.0.000187

Ballhorn, D. J., and Elias, J. D. (2014). Salinity-mediated cyanogenesis in white clover (*Trifolium repens*) affects trophic interactions. *Ann. Bot.* 114, 357–366. doi: 10.1093/aob/mcu141

Berge, O., Guinebretière, M. H., Achouak, W., Normand, P., and Heulin, T. (2002). *Paenibacillus graminis* sp. nov. and *Paenibacillus odorifer* sp. nov., isolated from plant roots, soil and food. *Int. J. Syst. Evol. Microbiol.* 52, 607–616. doi: 10.1099/00207713-52-2-607

Brigle, K. E., Newton, W. E., and Dean, D. R. (2011). Complete nucleotide sequence of the *Azotobacter vinelandii* nitrogenase structural gene cluster. *Gene* 37, 37–44. doi: 10.1016/0378-1119(85)90255-0

Brito, L. F., Irla, M., Kalinowski, J., and Wendisch, V. F. (2017). Detailed transcriptome analysis of the plant growth promoting *Paenibacillus riograndensis* SBR5 by using RNA-seq technology. *BMC Genomics* 18:846. doi: 10.1186/s12864-017-4235-z

Busse, H. J., Denner, E. B. M., and Lubitz, W. (1996). Classification and identification of bacteria: current approaches to an old problem. Overview of methods used in bacterial systematics. *J. Biotechnol.* 47, 3–38. doi: 10.1016/0168-1656(96)01379-x

Chen, L., Chang, Q., Yan, Q., Yang, G., Zhang, Y., and Feng, Y. (2019). Structure of an endogalactosylceramidase from *Rhodococcus hoagii* 103S reveals the molecular basis of its substrate specificity. *J. Struct. Biol.* 208:107393. doi: 10.1016/j.jsb.2019.09.010

Choi, J. H., Im, W. T., Yoo, J. S., Lee, S. M., Moon, D. S., Kim, H. J., et al. (2008). *Paenibacillus donghaensis* sp. nov., a xylan-degrading and nitrogen-fixing bacterium isolated from East Sea sediment. *J. Microbiol. Biotechnol.* 18, 189–193. doi: 10.1007/s12275-007-0217-1

Choo, Q. C., Samian, M. R., and Najimudin, N. (2003). Phylogeny and characterization of three nifH-homologous genes from *Paenibacillus azotofixans*. *Appl. Environ. Microbiol.* 69, 3658–3662. doi: 10.1128/AEM.69.6.3658-3662.2003

Chou, J. H., Chou, Y. J., Lin, K. Y., Sheu, S. Y., Sheu, D. S., Arun, A. B., et al. (2007). *Paenibacillus fonticola* sp. nov., isolated from a warm spring. *Int. J. Syst. Evol. Microbiol.* 57, 1346–1350. doi: 10.1099/ijs.0.64872-0

Clermont, D., Gomard, M., Hamon, S., Bonne, I., Fernandez, J. C., Wheeler, R., et al. (2015). *Paenibacillus faecis* sp. nov., isolated from human faeces. *Int. J. Syst. Evol. Microbiol.* 65, 4621–4626. doi: 10.1099/ijsem.0.001977

Collins, M. (1985). "Isoprenoid quinone analysis in classification and identification," in *Chemical Methods in Bacterial Systematics*, eds M. Goodfellow and D. E. Minnikin (London: Academic Press), 267–287.

da Mota, F. F., Gomes, E. A., Paiva, E., Rosado, A. S., and Seldin, L. (2004). Use of rpoB gene analysis for identification of nitrogen-fixing *Paenibacillus* species as an alternative to the 16S rRNA gene. *Lett. Appl. Microbiol.* 39, 34–40. doi: 10.1111/j.1472-765X.2004.01536.x

Daud, N. S., Mohd Din, A. R. J., Rosli, M. A., Azam, Z. M., Othman, N. Z., and Sarmidi, M. R. (2019). *Paenibacillus polymyxa* bioactive compounds for agricultural and biotechnological applications. *Biocatal. Agric. Biotechnol.* 18:101092. doi: 10.1016/j.bcab.2019.101092

Felsenstein, J. (1981). Evolutionary trees from DNA sequences: a maximum likelihood approach. *J. Mol. Evol.* 17, 368–376. doi: 10.1007/bf01734359

Felsenstein, J. (1985). Confidence limits on phylogenies: an approach using the bootstrap. *Evolution* 39, 783–791. doi: 10.1111/j.1558-5646.1985.tb00420.x

Fitch, W. M. (1971). Toward defining the course of evolution: minimum change for a specific tree topology. *Syst. Biol.* 20, 406–416. doi: 10.2307/2412116

Fu, X., Yan, Q., Yang, S., Yang, X., Guo, Y., and Jiang, Z. (2014). An acidic, thermostable exochitinase with β-N-acetylglucosaminidase activity from *Paenibacillus barengoltzii* converting chitin to N-acetyl glucosamine. *Biotechnol. Biofuels* 7:174. doi: 10.1186/s13068-014-0174-y

Fürnkranz, M., Adam, E., Müller, H., Grube, M., Huss, H., Winkler, J., et al. (2012). Promotion of growth, health and stress tolerance of styrian oil pumpkins by bacterial endophytes. *Eur. J. Plant Pathol.* 13, 509–519. doi: 10.1007/s10658-012-0033-2

Gaby, J. C., and Buckley, D. H. (2014). A comprehensive aligned nifH gene database: a multipurpose tool for studies of nitrogen-fixing bacteria. *Database (Oxford)* 2014:bau001. doi: 10.1093/database/bau001

Genersch, E., Forsgren, E., Pentikäinen, J., Ashiralieva, A., Rauch, S., Kilwinski, J., et al. (2006). Reclassification of *Paenibacillus larvae* subsp. *pulvifaciens* and *Paenibacillus larvae* subsp. larvae as *Paenibacillus larvae* without subspecies differentiation. *Int. J. Syst. Evol. Microbiol.* 56, 501–511. doi: 10.1099/ijs.0.63928-0

Grady, E. N., Macdonald, J., Liu, L., Richman, A., and Yuan, Z. C. (2016). Current knowledge and perspectives of *Paenibacillus*: a review. *Microb. Cell Fact.* 15:203. doi: 10.1186/s12934-016-0603-7

Haft, D. H., DiCuccio, M., Badretdin, A., Brover, V., Chetvernin, V., O'Neill, K., et al. (2018). RefSeq: an update on prokaryotic genome annotation and curation. *Nucleic Acids Res.* 46, D851–D860. doi: 10.1093/nar/gkx1068

Han, Q. Q., Lü, X. P., Bai, J. P., Qiao, Y., Paré, P. W., Wang, S. M., et al. (2014). Beneficial soil bacterium *Bacillus subtilis* (GB03) augments salt tolerance of white clover. *Front. Plant Sci.* 5:525. doi: 10.3389/fpls.2014.00525

He, A. L., Niu, S. Q., Zhao, Q., Li, Y. S., Gou, J. Y., Gao, H. J., et al. (2018). Induced salt tolerance of perennial ryegrass by a novel bacterium strain from the rhizosphere of a desert shrub *Haloxylon ammodendron*. *Int. J. Mol. Sci.* 19:469. doi: 10.3390/ijms19020469

He, A., Niu, S., Yang, D., Ren, W., Zhao, L., Sun, Y., et al. (2021). Two PGPR strains from the rhizosphere of *Haloxylon ammodendron* promoted growth and enhanced drought tolerance of ryegrass. *Plant Physiol. Biochem.* 161, 74–85. doi: 10.1016/j.plaphy.2021.02.003

Huang, H., Zhang, F., Liu, M., Cui, Y., Sun, Q., Zhu, J., et al. (2016). *Paenibacillus silvae* sp. nov. isolated from tropical rainforest soil. *Int. J. Syst. Evol. Microbiol.* 67, 795–799. doi: 10.1099/ijsem.0.001608

Jacobson, M. R., Brigle, K. E., Bennett, L. T., Setterquist, R. A., Wilson, M. S., Cash, V. L., et al. (1989). Physical and genetic map of the major nif gene cluster from *Azotobacter vinelandii*. *J. Bacteriol.* 171, 1017–1027. doi: 10.1128/jb.171.2.1017-1027.1989

Jian, M. A., Xian, D. L., Guang, L., Wei, J. Z., Shun, L. W., Wen, M. J., et al. (2020). Spatial and temporal variations of soil moisture and temperature of *Picea Crassifolia* forest in north piedmont of central Qilian Mountains. *Arid. Land Geogr.* 43, 1033–1040. doi: 10.12118/j.issn.1000-6060.2020.04.18

Jin, H. J., Lv, J., and Chen, S. F. (2011). *Paenibacillus sophorae* sp. nov. a nitrogen-fixing species isolated from the rhizosphere of *Sophora japonica*. *Int. J. Syst. Evol. Microbiol.* 61, 767–771. doi: 10.1099/ijs.0.021709-0

Jung, B. K., Hong, S. J., Jo, H. W., Jung, Y. G., Park, Y. J., Park, C. E., et al. (2017). Genome sequencing to develop *Paenibacillus donghaensis* strain JH8T (KCTC 13049T= LMG 23780T) as a microbial fertilizer and correlation to its plant growth-promoting phenotype. *Mar. Genomics* 37, 39–42. doi: 10.1016/j.margen.2017.11.006

Kates, M. (1986). *Techniques of Lipidology*, 2nd Edn. Amsterdam: Elsevier, 106–107, 241–246.

Ke, X., Feng, S., Wang, J., Lu, W., Zhang, W., Chen, M., et al. (2019). Effect of inoculation with nitrogen-fixing bacterium *Pseudomonas* stutzeri A1501 on maize plant growth and the microbiome indigenous to the rhizosphere. *Syst. Appl. Microbiol.* 42, 248–260. doi: 10.1016/j.syapm.2018.10.010

Ker, K., Seguin, P., Driscoll, B. T., Fyles, J. W., and Smith, D. L. (2012). Switchgrass establishment and seeding year production can be improved by inoculation with rhizosphere endophytes. *Biomass. Bioenerg.* 47, 295–301. doi: 10.1016/j.biombioe.2012.09.031

Khan, Z., Kim, S. G., Jeon, Y. H., Khan, H. U., Son, S. H., and Kim, Y. H. (2007). A plant growth promoting rhizobacterium, *Paenibacillus polymyxa* strain GBR-1, suppresses root-knot nematode. *Bioresour. Technol.* 99, 3016–3023. doi: 10.1016/j.biortech.2007.06.031

Kim, D. U., Kim, S. G., Lee, H., Chun, J., Cho, J. C., and Ka, J. O. (2015). *Paenibacillus xanthinilyticus* sp. nov., isolated from agricultural soil. *Int. J. Syst. Evol. Microbiol.* 65, 2937–2942. doi: 10.1099/ijs.0.000359

Kim, W. I., Cho, W. K., Kim, S. N., Chu, H., Ryu, K. Y., Yun, J. C., et al. (2011). Genetic diversity of cultivable plant growth-promoting rhizobacteria in Korea. *J. Microbiol. Biotechnol.* 21, 777–790. doi: 10.4014/jmb.1101.01031

Kiran, S., Swarnkar, M. K., Mayilraj, S., Tewari, R., and Gulati, A. (2017). *Paenibacillus ihbetae* sp. nov., a cold-adapted antimicrobial producing bacterium isolated from high altitude Suraj Tal Lake in the Indian trans-Himalayas. *Syst. Appl. Microbiol.* 40, 430–439. doi: 10.1016/j.syapm.2017.07.005

Kishore, K., Begum, Z., Pathan, A. A. A., and Shivaji, S. (2010). *Paenibacillus glacialis* sp. nov., isolated from the Kafni glacier of the Himalayas, India. *Int. J. Syst. Evol. Microbiol.* 60, 1909–1913. doi: 10.1034/j.1399-3011.2000.00698.x

Kumar, S., Stecher, G., and Tamura, K. (2016). MEGA7: molecular evolutionary genetics analysis version 7.0 for bigger datasets. *Mol. Biol. Evol.* 33, 1870–1874. doi: 10.1093/molbev/msw054

Kumari, M., and Thakur, I. S. (2018). Biochemical and proteomic characterization of *Paenibacillus* sp. ISTP10 for its role in plant growth promotion and in rhizostabilization of cadmium. *Bioresource Technol. Rep.* 3, 59–66. doi: 10.1016/0165-1218(75)90120-2

Lagesen, K., Hallin, P., Rødland, E. A., Stærfeldt, H. H., Rognes, T., and Ussery, D. W. (2007). RNAmmer: consistent and rapid annotation of ribosomal RNA genes. *Nucleic Acids Res.* 35, 3100–3108. doi: 10.1093/nar/gkm160

Lan, X. J., Zhou, H., Yao, T., Dong, W. Q., Zhang, J. G., and Han, D. R. (2020). Community structure and function of cultivable endophytic bacteria isolated from four moss species in Qilian Mountain. *Symbiosis* 80, 257–267. doi: 10.1007/s13199-020-00669-w

Li, H. P., Yao, D., Shao, K. Z., Han, Q. Q., Gou, J. Y., Zhao, Q., et al. (2020). *Altererythrobacter rhizovicinus* sp. nov., isolated from rhizosphere soil of *Haloxylon ammodendron*. *Int. J. Syst. Evol. Microbiol.* 70, 680–686. doi: 10.1099/ijsem.0.003817

Lim, J. M., Jeon, C. O., Lee, J. C., Xu, L. H., Jiang, C. L., and Kim, C. J. (2006a). *Paenibacillus gansuensis* sp. nov., isolated from desert soil of Gansu Province in China. *Int. J. Syst. Evol. Microbiol.* 56, 2131–2134. doi: 10.1099/ijs.0.64210-0

Lim, J. M., Jeon, C. O., Park, D. J., Xu, L. H., Jiang, C. L., and Kim, C. J. (2006b). *Paenibacillus xinjiangensis* sp. nov., isolated from Xinjiang province in China. *Int. J. Syst. Evol. Microbiol.* 56, 2579–2582. doi: 10.1099/ijs.0.64465-0

Liu, H., Li, Y., Ge, K., Du, B., Liu, K., Wang, C., et al. (2021). Interactional mechanisms of *Paenibacillus polymyxa* SC2 and pepper (*Capsicum annuum* L.) suggested by transcriptomics. *BMC Microbiol.* 21:70. doi: 10.1186/s12866-021-02132-2

Liu, L. H., Yuan, T., Yang, F., Liu, Z. W., Yang, M. Y., Peng, G. X., et al. (2018). *Paenibacillus bryophyllum* sp. nov. a nitrogen-fixing species isolated from *Bryophyllum pinnatum*. *Anton. Leeuwenhoek* 111, 2267–2273. doi: 10.1007/s10482-018-1117-6

Liu, Y., Zou, S. B., and Chen, F. H. (2004). "Bioclimatic modeling the spatial distribution of mountain forests in the Qilian Mountains, Northwest of China, using down-scaled climatic models," in *Proceedings of the 2004 IEEE International Geoscience and Remote Sensing Symposium*, Vol. 7, (Piscataway, NJ: IEEE), 4625–4628. doi: 10.1109/IGARSS.2004.1370187

Loni, P. P., Patil, J. U., Phugare, S. S., and Bajekal, S. S. (2014). Purification and characterization of alkaline chitinase from *Paenibacillus pasadenensis* NCIM 5434. *J. Basic Microbiol.* 54, 1080–1089. doi: 10.1002/jobm.201300533

Luo, Y., Zhou, M., Zhao, Q., Wang, F., Gao, J., Sheng, H., et al. (2020). Complete genome sequence of *Sphingomonas* sp. Cra20, a drought resistant and plant growth promoting rhizobacteria. *Genomics* 112, 3648–3657. doi: 10.1016/j.ygeno.2020.04.013

Majidzadeh, M., and Fatahi-Bafghi, M. (2018). Current taxonomy of *Rhodococcus* species and their role in infections. *Eur. J. Clin. Microbiol.* 37, 2045–2062. doi: 10.1007/s10096-018-3364-x

Mawarda, P. C., Roux, X. L., van Elsas, J. D., and Salles, J. F. (2020). Deliberate introduction of invisible invaders: a critical appraisal of the impact of microbial inoculants on soil microbial communities. *Soil Biol. Biochem.* 148:107874. doi: 10.1016/j.soilbio.2020.107874

Meier-Kolthoff, J. P., Auch, A. F., Klenk, H. P., and Göker, M. (2013). Genome sequence-based species delimitation with confidence intervals and improved distance functions. *BMC Bioinformatics* 14:60. doi: 10.1186/1471-2105-14-60

Meier-Kolthoff, J. P., Hahnke, R. L., Petersen, J., Scheuner, C., Michael, V., Fiebig, A., et al. (2014a). Complete genome sequence of DSM 30083(T), the type strain (U5/41(T)) of *Escherichia coli*, and a proposal for delineating subspecies in microbial taxonomy. *Stand. Genomic Sci.* 9:2. doi: 10.1186/1944-3277-9-2

Meier-Kolthoff, J. P., Klenk, H. P., and Göker, M. (2014b). Taxonomic use of DNA G+C content and DNA-DNA hybridization in the genomic age. *Int. J. Syst. Evol. Microbiol.* 264, 352–356. doi: 10.1099/ijs.0.056994-0

Menéndez, E., Flores-félix, J. D., Mulas, R., Andrés, F. G., Fernández-Pascual, M., Peix, A., et al. (2017). *Paenibacillus tritici* sp. nov. isolated from wheat roots. *Int. J. Syst. Evol. Microbiol.* 67, 2312–2316. doi: 10.1099/ijsem.0.001949

Minnikin, D. E., O'donnell, A. G., Goodfellow, M., Alderson, G., Athalye, M., Schaal, A., et al. (1984). An integrated procedure for the extraction of bacterial isoprenoid quinones and polar lipids. *J. Microbiol. Methods* 2, 233–241. doi: 10.1016/0167-7012(84)90018-6

Montes, M. J., Mercadé, E., Bozal, N., and Guinea, J. (2004). *Paenibacillus antarcticus* sp. nov., a novel psychrotolerant organism from the Antarctic environment. *Int. J. Syst. Evol. Microbiol.* 54, 1521–1526. doi: 10.1099/ijs.0.63078-0

Mosimann, C., Oberhänsli, T., Ziegler, D., Nassal, D., Kandeler, E., Boller, T., et al. (2017). Tracing of two *Pseudomonas* strains in the root and rhizoplane of maize, as related to their plant growth-promoting effect in contrasting soils. *Front. Microbiol.* 7:2150. doi: 10.3389/fmicb.2016.02150

Naamala, J., and Smith, D. L. (2021). Microbial derived compounds, a step toward enhancing microbial inoculants technology for sustainable agriculture. *Front. Microbiol.* 12:634807. doi: 10.3389/fmicb.2021.634807

Naing, K. W., Anees, M., Kim, S. J., Nam, Y., Kim, Y. C., and Kim, K. Y. (2014). Characterization of antifungal activity of *Paenibacillus ehimensis* KWN38 against soilborne phytopathogenic fungi belonging to various taxonomic groups. *Ann. Microbiol.* 64, 55–63. doi: 10.1007/s13213-013-0632-y

Niu, S. Q., Li, H. R., Paré, P. W., Aziz, M., Wang, S. M., Shi, H. Z., et al. (2016). Induced growth promotion and higher salt tolerance in the halophyte grass *Puccinellia tenuiflora* by beneficial rhizobacteria. *Plant Soil* 407, 217–230. doi: 10.1007/s11104-015-2767-z

Padda, K. P., Puri, A., and Chanway, C. P. (2017). "*Paenibacillus polymyxa*: a prominent biofertilizer and biocontrol agent for sustainable agriculture," in *Agriculturally Important Microbes for Sustainable Agriculture*, eds V. Meena, P. Mishra, J. Bisht, and A. Pattanayak (Singapore: Springer), 165–191. doi: 10.1007/978-98-10-5343-6_6

Parks, D. H., Imelfort, M., Skennerton, C. T., Hugenholtz, P., and Tyson, G. W. (2015). CheckM: assessing the quality of microbial genomes recovered from isolates, single cells, and metagenomes. *Genome Res.* 25, 1043–1055. doi: 10.1101/gr.186072.114

Priest, F. G. (2009). "Genus I. *Paenibacillus*," in *Bergey's Manual of Systematic Bacteriology*, Vol. 3, eds P. de Vos, G. Garrity, D. Jones, N. R. Krieg, W. Ludwig, et al. (New York, NY: Springer), 269–327.

Rani, R., Kumar, V., Gupta, P., and Chandra, A. (2021). Potential use of *Solanum lycopersicum* and plant growth promoting rhizobacterial (PGPR) strains for the phytoremediation of endosulfan stressed soil. *Chemosphere* 279:130589. doi: 10.1016/j.chemosphere.2021.130589

Richter, M., and Rosselló-Móra, R. (2009). Shifting the genomic gold standard for the prokaryotic species definition. *Proc. Natl. Acad. Sci. U.S.A.* 106, 19126–19131. doi: 10.1073/pnas.0906412106

Ryu, C. M., Farag, M. A., Hu, C. H., Reddy, M. S., Wei, H. X., Paré, P. W., et al. (2003). Bacterial volatiles promote growth in *Arabidopsis*. *Proc. Natl. Acad. Sci. U.S.A.* 100, 4927–4932. doi: 10.1073/pnas.0730845100

Saitou, N., and Nei, M. (1987). The neighbor-joining method: a new method for reconstructing phylogenetic trees. *Mol. Biol. Evol.* 4, 406–425. doi: 10.1093/oxfordjournals.molbev.a040454

Sasser, M. (1990). *Identification of Bacteria by Gas Chromatography of Cellular Fatty Acids. Midi. Technical. Note. 101*. Newark, NJ: Springer.

Sayers, E. W., Cavanaugh, M., Clark, K., Ostell, J., Pruitt, K. D., and Karsch-Mizrachi, I. (2020). GenBank. *Nucleic Acids Res.* 48, D84–D86. doi: 10.1093/nar/gkz956

Scheldeman, P., Goossens, K., Rodriguez-Diaz, M., Pil, A., Goris, J., Herman, L., et al. (2004). *Paenibacillus lactis* sp. nov., isolated from raw and heat-treated milk. *Int. J. Syst. Evol. Microbiol.* 54, 885–891. doi: 10.1099/ijs.0.02822-0

Schreiter, S., Ding, G. C., Heuer, H., Neumann, G., Sandmann, M., Grosch, R., et al. (2014). Effect of the soil type on the microbiome in the rhizosphere of field-grown lettuce. *Front. Microbiol.* 5:144. doi: 10.3389/fmicb.2014.00144

Shamseldin, A., Epstein, B., Sadowsky, M. J., and Zhang, Q. (2021). Comparative genomic analysis of diverse rhizobia and effective nitrogen-fixing clover-nodulating rhizobium strains adapted to Egyptian dry ecosystems. *Symbiosis* 84, 39–47. doi: 10.1007/s13199-021-00764-6

Shida, O., Takagi, H., Kadowaki, K., Nakamura, L. K., and Komagata, K. (1997). Transfer of *Bacillus alginolyticus*, *Bacillus chondroitinus, Bacillus curdlanolyticus, Bacillus glucanolyticus, Bacillus kobensis,* and *Bacillus thiaminolyticus* to the genus *Paenibacillus* and emended description of the genus *Paenibacillus*. *Int. J. Syst. Bacteriol.* 47, 289–298. doi: 10.1099/00207713-47-2-289

Son, J. S., Kang, H. U., and Ghim, S. Y. (2014). *Paenibacillus dongdonensis* sp. nov., isolated from rhizospheric soil of *Elymus tsukushiensis*. *Int. J. Syst. Evol. Microbiol.* 64, 2865–2870. doi: 10.1099/ijs.0.061077-0

Tatusova, T., DiCuccio, M., Badretdin, A., Chetvernin, V., Nawrocki, E. P., Zaslavsky, L., et al. (2016). NCBI prokaryotic genome annotation pipeline. *Nucleic Acids Res.* 44, 6614–6624. doi: 10.1089/cmb.2017.0066

Timmusk, S., Grantcharova, N., and Wagner, E. G. H. (2005). *Paenibacillus polymyxa* invades plant roots and forms biofilms. *Appl. Environ. Microbiol.* 71, 7292–7300. doi: 10.1128/AEM.71.11.7292-7300.2005

Timmusk, S., Nicander, B., Granhall, U., and Tillberg, E. (1999). Cytokinin production by *Paenibacillus polymyxa*. *Soil Biol. Biochem.* 31, 1847–1852. doi: 10.1016/s0038-0717(99)00113-3

Woo, S. L., and Pepe, O. (2018). Microbial consortia: promising probiotics as plant biostimulants for sustainable agriculture. *Front. Plant Sci.* 9:1801. doi: 10.3389/fpls.2018.01801

Wu, G., and Jiang, C. (1998). *Physical Division of Gansu Province (in Chinese)*. Gansu: Scientific and Technology Press of Gansu, 226–228.

Xie, J. B., Zhang, L. H., Zhou, Y. G., Liu, H. C., and Chen, S. F. (2012). *Paenibacillus taohuashanense* sp. nov. a nitrogen-fixing species isolated from rhizosphere soil of the root of *Caragana kansuensis* Pojark. *Anton. Leeuwenhoek* 102, 735–741. doi: 10.1007/s10482-012-9773-4

Xie, X., Zhang, H., and Paré, P. W. (2009). Sustained growth promotion in *Arabidopsis* with long-term exposure to the beneficial soil bacterium *Bacillus subtilis* (GB03). *Plant Signal. Behav.* 4, 948–953. doi: 10.4161/psb.4.10.9709

Xu, J. L., He, J., Wang, Z. C., Wang, K., Li, W. J., Tang, S. K., et al. (2007). *Rhodococcus qingshengii* sp. nov., a carbendazim-degrading bacterium. *Int. J. Syst. Evol. Microbiol.* 57, 2754–2757. doi: 10.1099/ijs.0.65095-0

Yang, D., Cha, S., Choi, J., and Seo, T. (2018). *Paenibacillus mobilis* sp. nov., a Gram-stain-negative bacterium isolated from soil. *Int. J. Syst. Evol. Microbiol.* 68, 1140–1145. doi: 10.1099/ijsem.0.002643

Yang, Y. J., Zhang, Y. T., Chen, G. Q., Cheng, D., Qiu, J. G., He, Q., et al. (2018). *Paenibacillus shunpengii* sp. nov., isolated from farmland soil. *Int. J. Syst. Evol. Microbiol.* 68, 211–216. doi: 10.1099/ijsem.0.002484

Yoon, S. H., Ha, S. M., Kwon, S., Lim, J., Kim, Y., Seo, H., et al. (2017). Introducing EzBioCloud: a taxonomically united database of 16S rRNA gene sequences and whole-genome assemblies. *Int. J. Syst. Evol. Microbiol.* 67, 1613–1617. doi: 10.1099/ijsem.0.001755

Zaidi, A., Khan, M. S., Ahemad, M., and Oves, M. (2009). Plant growth promotion by phosphate solubilizing bacteria. *Acta Microbiol. Immunol. Hung.* 56, 263–284. doi: 10.1016/s0734-9750(99)00014-2

Zamioudis, C., Mastranesti, P., Dhonukshe, P., Blilou, I., and Pieterse, C. M. J. (2013). Unraveling root developmental programs initiated by beneficial *Pseudomonas* spp. bacteria. *Plant Physiol.* 162, 304–318. doi: 10.1104/pp.112.212597

Zhang, H., Kim, M. S., Krishnamachari, V., Payton, P., Sun, Y., and Grimson, M. (2007). Rhizobacterial volatile emissions regulate auxin homeostasis and cell expansion in *Arabidopsis*. *Planta* 226, 839–851. doi: 10.1007/s00425-007-0530-2

Zhang, Y. Z., Li, Y. P., Hassan, M. J., Li, Z., and Peng, Y. (2020). Indole-3-acetic acid improves drought tolerance of white clover via activating auxin, abscisic acid and jasmonic acid related genes and inhibiting senescence genes. *BMC Plant Biol.* 20:150. doi: 10.1186/s12870-020-02354-y

Zhao, C. Y., Qi, P. C., and Feng, Z. D. (2009). Spatial modelling of the variability of the soil moisture regime at the landscape scale in the southern Qilian Mountains, China. *Hydrol. Earth Syst. Sci.* 6, 6335–6358. doi: 10.5194/hessd-6-6335-2009

Zhao, S., Wei, H., Lin, C. Y., Zeng, Y., Tucker, M. P., Himmel, M. E., et al. (2016). *Burkholderia phytofirmans* inoculation-induced changes on the shoot cell anatomy and iron accumulation reveal novel components of *Arabidopsis*-endophyte interaction that can benefit downstream biomass deconstruction. *Front. Plant Sci.* 7:24. doi: 10.3389/fpls.2016.00024

Zhao, W. J., Liu, X. D., Jing, W. M., Xu, L. H., Niu, Y., Qi, P., et al. (2015). Spatial heterogeneity of community structure of Picea Crassifolia forest in Qilian Mountains, China. *Chin. J. Appl. Ecol.* 26, 2591–2599.

Zhu, P., Chen, R. S., Song, Y. X., Han, C. T., Liu, G. X., Chen, T., et al. (2017). Soil bacterial community composition and diversity of four representative vegetation types in the middle section of the Qilian Mountains, China. *Acta Ecol. Sin.* 37, 3505–3514. doi: 10.5846/stxb201602290348

Zhuang, J., Xin, D., Zhang, Y. Q., Guo, J., and Zhang, J. (2017). *Paenibacillus albidus* sp. nov. isolated from grassland soil. *Int. J. Syst. Evol. Microbiol.* 67, 4685–4691. doi: 10.1099/ijsem.0.002356

Conflict of Interest: The authors declare that the research was conducted in the absence of any commercial or financial relationships that could be construed as a potential conflict of interest.

Publisher's Note: All claims expressed in this article are solely those of the authors and do not necessarily represent those of their affiliated organizations, or those of the publisher, the editors and the reviewers. Any product that may be evaluated in this article, or claim that may be made by its manufacturer, is not guaranteed or endorsed by the publisher.

Copyright © 2022 Li, Gan, Yue, Han, Chen, Liu, Zhao and Zhang. This is an open-access article distributed under the terms of the Creative Commons Attribution License (CC BY). The use, distribution or reproduction in other forums is permitted, provided the original author(s) and the copyright owner(s) are credited and that the original publication in this journal is cited, in accordance with accepted academic practice. No use, distribution or reproduction is permitted which does not comply with these terms.

frontiers | Frontiers in Microbiology

ORIGINAL RESEARCH
published: 29 April 2022
doi: 10.3389/fmicb.2022.892533

Identification of the Phosphorus-Solubilizing Bacteria Strain JP233 and Its Effects on Soil Phosphorus Leaching Loss and Crop Growth

Haiyang Yu[1†], Xiaoqing Wu[1†], Guangzhi Zhang[1], Fangyuan Zhou[1], Paul R. Harvey[1,2], Leilei Wang[1], Susu Fan[1], Xueying Xie[1], Feng Li[1], Hongzi Zhou[1], Xiaoyan Zhao[1] and Xinjian Zhang[1]*

[1] Shandong Provincial Key Laboratory of Applied Microbiology, Ecology Institute, Qilu University of Technology (Shandong Academy of Sciences), Ji'nan, China, [2] CSIRO Agriculture and Food, Glen Osmond, SA, Australia

OPEN ACCESS

Edited by:
José David Flores Félix, Universidade da Beira Interior, Portugal

Reviewed by:
Sumera Yasmin, National Institute for Biotechnology and Genetic Engineering, Pakistan
Riyazali Zafarali Sayyed, P.S.G.V.P.M's Arts, Science and Commerce College, India

***Correspondence:**
Xinjian Zhang
zhangxj@sdas.org

[†] These authors have contributed equally to this work

Specialty section:
This article was submitted to Microbe and Virus Interactions with Plants, a section of the journal Frontiers in Microbiology

Received: 09 March 2022
Accepted: 11 April 2022
Published: 29 April 2022

Citation:
Yu H, Wu X, Zhang G, Zhou F, Harvey PR, Wang L, Fan S, Xie X, Li F, Zhou H, Zhao X and Zhang X (2022) Identification of the Phosphorus-Solubilizing Bacteria Strain JP233 and Its Effects on Soil Phosphorus Leaching Loss and Crop Growth. Front. Microbiol. 13:892533. doi: 10.3389/fmicb.2022.892533

Phosphorus (P) is one of the most limiting nutrients in global agricultural ecosystems, and phosphorus-solubilizing bacteria (PSB) can convert insoluble P into soluble P, thereby improving the absorption and use of soil P by plants. Increasing leaching loss of soil P due to PSB that could lead to water eutrophication is a major concern, although no direct experimental evidence is available to evaluate these effects. In this study, a highly efficient PSB strain, *Pseudomonas* sp. JP233, was isolated from soil and its P-solubilizing agent was identified by metabolomics and HPLC analyses. The effects of JP233 on P contents in soil leachates were also analyzed by microcosm leaching experiments in the absence and presence of maize. JP233 could solubilize insoluble P into soluble forms, and the molybdate reactive phosphorus (MRP) content reached 258.07 mg/L in NBRIP medium containing 5 g/L $Ca_3(PO_4)_2$ within 48 h. Metabolomics analysis demonstrated that the organic acid involved in JP233 P solubilization was primarily 2-keto gluconic acid (2KGA). Further, HPLC analysis revealed that 2KGA contents rapidly accumulated to 19.33 mg/mL within 48 h. Microcosm leaching experiments showed that MRP and total phosphorus (TP) contents in soil leaching solutions were not significantly higher after JP233 inoculation. However, inoculation with JP233 into maize plant soils significantly decreased MRP and TP contents in the soil leaching solutions on days 14 ($P < 0.01$), 21 ($P < 0.01$), and 28 ($P < 0.05$). Inoculation with strain JP233 also significantly increased the biomass of maize aerial components and that of whole plants ($P < 0.05$). Thus, strain JP233 exhibited a significant plant-growth-promoting effect on maize development. In conclusion, the application of PSB into soils does not significantly increase P leachate loss. Rather, the application of PSB can help reduce P leachate loss, while significantly promoting plant absorption and use of soil P.

Keywords: *Pseudomonas* sp., P-solubilizing bacteria (PSB), 2-keto gluconic acid (2KGA), soil P leaching test, plant growth promotion

INTRODUCTION

Phosphorus (P) is an essential nutrient for plants that is involved in diverse biochemical processes including lipid metabolism and the biosynthesis of nucleic acids and cell membranes (Ha and Tran, 2014). However, P is one of the most limiting nutrients in global agricultural ecosystems (Lin et al., 2016). P that is applied to soils can accumulate in non-labile forms due to its high-affinity chemical reactions and its occlusion to soil minerals and organic matter, leading to the prevalence of "legacy P." The accumulation of legacy P in soils and potential transfer to water bodies ultimately leads to environmental concerns of eutrophication (Gatiboni et al., 2020). Therefore, the development of methods to improve the bioavailability of immobilized P in agricultural soils are critical (Yu et al., 2019) to mitigate the continued application of P beyond that which required by plants.

The use of phosphorus-solubilizing bacteria (PSB) could represent promising management strategies for improving P use efficiency. PSB are capable of converting insoluble P into soluble forms that are bioavailable for plant uptake (Sharma et al., 2013; Paulucci et al., 2015; Khan et al., 2021). Isolates have been obtained from numerous environments including agricultural soils, rhizosphere soils, sewage sludges, with *Pseudomonas* and *Bacillus* species most represented among cultures (Sharma et al., 2013; Yu et al., 2019; Chawngthu et al., 2020; Kaur and Kaur, 2020). The addition of PSB to agricultural settings have led to growth enhancement effects on maize, wheat, soybean, barley, sesame, century plant, and wild mint (Afzal et al., 2010; Pereira and Castro, 2014; Bautista-Cruz et al., 2019; Prakash and Arora, 2019; Chouyia et al., 2020; Kusale et al., 2021; Nithyapriya et al., 2021). Further, previous studies have shown that PSB can reduce soil legacy P by increasing use efficiency from fertilizers and improving long-term efficiency of agricultural production (Gatiboni et al., 2020).

The reported mechanisms of P solubilization by PSB in soils involve the release of complexes or mineral dissolving compounds (e.g., organic acid anions and extracellular enzymes) into the environment, or alternatively, through the direct release of P during substrate degradation. Organic acids are the basis of inorganic P solubilization in PSB *via* their lowering of soil pH, enhancing chelation of cations bound to P, competing with P for adsorption sites on soils, and forming soluble complexes with metal ions that are associated with insoluble P (Sharma et al., 2013).

Phosphorus-solubilizing bacteria are capable of converting insoluble P into soluble forms, although concerns have been raised regarding increased leaching-loss of soil P by PSB. However, PSB can help improve plant absorption and use of soil P, thereby helping reduce leaching-loss of P. Nevertheless, the association between P solubilizing effects of PSB and risks of P leaching-loss has not been studied. The aims of the present study were to: (1) isolate highly efficient PSB from agricultural ecosystems, (2) identify mechanisms of P solubilization by the PSB, (3) investigate the direct influence of PSB on P leaching without plants, and (4) analyze the influence of PSB on P leaching with plants, in addition to assessing their influence on plant development. This study provides a foundation for informing PSB application to agricultural ecosystems.

MATERIALS AND METHODS

Isolation of Phosphorus-Solubilizing Bacteria From Agriculture Soils

Soil samples were collected from the vegetable greenhouse facility of the Research and Development Base at the Shouguang Facility Agriculture Center, Chinese Academy of Sciences (118°86′82″ E, 36°90′99″ N). Soil physicochemical properties included a pH = 7.81, available N = 84 mg/kg, available P = 109.85 mg/kg, available K = 224.97 mg/kg, total P = 2,754.87 mg/kg, total K = 5,639.67 mg/kg, and organic matter content = 1.93%. The soil particle size distribution included 8.39% clay (<2 μm), 69.89% silt (2–50 μm), and 21.72% sand (50–2,000 μm).

About 10 g of soil samples were mixed with 90 mL of sterilized ddH_2O (dd'H_2O) and homogenized by shaking for 30 min in a conical flask. After serial dilution (10^{-2}–10^{-6}) with dd'H_2O, a 100 μL aliquot of each suspension was plated on National Botanical Research Institute's phosphate growth medium (NBRIP) agar plates [including per liter: 10 g glucose, 5.0 g $MgCl_2.6H_2O$, 0.25 g $MgSO_4.7H_2O$, 0.1 g $(NH_4)_2SO_4$, 0.2 g KCl, 5.0 g $Ca_3(PO_4)_2$, and 15 g agar, with pH adjusted to 7.5–8.0] (Nautiyal, 1999). Cultures were incubated at 28°C for 7 days. Bacterial colonies were subsequently selected from plates based on the appearance of a clear halo. Bacterial colonies, which can produce a clear halo zone on a plate, indicate the production of organic acids into the surrounding medium. The isolated strains were purified over five times, and each isolate following purification was stored in a glycerol stock at −20°C.

Determination of Phosphorus Contents in Soils and Soil Leachates

Molybdate reactive phosphorus (MRP) was measured to directly analyze the P contents of samples using the molybdenum-antimony colorimetric method and by filtering soil leachate with a 0.45 μm microporous filter membrane (Heckrath et al., 1995). Total phosphorus (TP) was determined by adding 4 mL of 50 g/L potassium persulfate to leachate without filtration treatment, digestion at 120°C for 30 min in an autoclave sterilizer and measuring P concentrations of the digested P with molybdenum blue colorimetry (Huang, 2019).

Total phosphorus was determined using the potassium persulfate digestion method (Su and Chen, 2010). Soil samples were first air-dried, ground, and sieved, followed by mixing with 5 mL of hot potassium persulfate solution. The mixture was heated in an autoclave sterilizer until the pressure reached 1.1 kg/cm and the temperature was 120°C, where it was maintained for 30 min. The solution was then cooled to room temperature, transferred to a 100 mL volumetric flask to a constant volume, and filtered with phosphorus-free filter paper. An aliquot (2 mL) of the filtered sample was pipetted into a 50 mL volumetric flask, two drops of a dinitrophenol indicator were added, and the pH was adjusted with sodium carbonate solution

and sulfuric acid solution until a yellowish color was observed. Subsequently, 5 mL of a molybdenum-antimony stock solution (13 g ammonium molybdate, 0.35 g antimony potassium tartrate, 150 mL concentrated sulfuric acid, and dd'H_2O to 500 mL) was added along with 1 mL of a 10% ascorbic acid solution. The mixture was maintained at room temperature for 30 min, and the absorbance at a wavelength of 700 nm was determined. Available phosphorus (AP) was determined using the Olsen method (Bao, 2000). Briefly, samples were passed through a 2 mm sieve after air drying and sodium bicarbonate was added prior to oscillating filtration for 30 min. Then, 5 mL of filtrate was mixed with the molybdenum-antimony chromogenic agent, followed by addition of water up to 50 mL, maintenance at room temperature for 30 min, and measurement of absorbance at a 700 nm wavelength.

Determination of Phosphorus Solubilizing Capacity for Selected Strains

Each isolated PSB colony was inoculated into NBRIP liquid medium and incubated on a rotary shaker at 180 r/min and 30°C for 48 h, followed by measurement of soluble P contents in each fermentation culture. To measure P content, a small amount of fermentation broth was centrifuged at 10,000 r/min for 10 min and 1 mL of supernatant was removed and diluted, if necessary. Then, 1 mL of molybdenum-antimony antibody solution and 0.5 mL of ascorbic acid solution was added in turn, mixed well, and reacted at room temperature for 15 min. The samples without P were used as blank controls. The MRP contents were then determined as described in section "Determination of P Contents in Soils and Soil Leachates." Strains with strong P solubilizing ability were stored in glycerol in a −20°C freezer until later use.

Amplification and Molecular Identification of 16S rRNA Genes of the Phosphorus-Solubilizing Bacteria Strain JP233

Strain JP233 exhibited relatively strong P solubilizing ability and was further identified using 16S rRNA gene sequencing. Genomic DNA of the strain was extracted (using Bacterial DNA Kit, OMEGA Bio-Tek, Suite 450400 Pinnacle Way, Norcross, GA, United States) and 16S rRNA genes of the strain were amplified by PCR using universal primers for bacteria: 27F (5′-AGAGTTTGATCCTGGCTCAG-3′) and 1492R (5′-GGGTTACCTTGTTACGACTTC-3′). PCR reaction program included pre-denaturation at 95°C for 5 min, followed by 35 cycles of denaturation at 94°C for 40 s, annealing at 52°C for 30 s and extension at 72°C for 90 s, and all followed by a final extension at 72°C for 10 min. The PCR amplification products were submitted to Sangon Biotech (Shanghai) Co., Ltd. (Shanghai, China) for DNA sequencing. The resulting 16S rRNA gene sequences were aligned and compared with references in the NCBI GenBank database.

Metabolome Analysis

Treatment group samples were inoculated with the stable JP233 strain in NBRIP liquid medium, while the control group was NBRIP liquid medium without strain inoculation. Each group comprised six independent biological replicates. Cultivation was conducted at 150 r/min for 48 h at 28°C. A total of 1 mL of bacterial suspension was removed from each treatment, centrifuged at 3,000 r/min at 4°C for 10 min, and 800 μL of the supernatant was transferred to a cryovial and placed in a −80°C freezer for preservation. The samples were then subjected to non-targeted metabolomics analysis at LC-Bio Co., Ltd. (Hangzhou, China).

The samples were thawed on ice and metabolites were extracted from 20 μL of each sample using 120 μL of pre-cooled 50% methanol buffer, followed by vortexing for 1 min and incubating for 10 min at room temperature and then storage at −20°C overnight. The mixture was then centrifuged at 4,000 *g* for 20 min and the supernatant was subsequently transferred to 96 well plates. Pooled quality control (QC) samples were also prepared by combining 10 μL of each extraction mixture. All samples were analyzed using a TripleTOF 5600 Plus high-resolution tandem mass spectrometer (SCIEX, Warrington, United Kingdom) in both positive and negative ion modes. Chromatographic separation was performed with an ultra-performance liquid chromatography (UPLC) system (SCIEX, Warrington, United Kingdom). An ACQUITY UPLC T3 column (100 mm × 2.1 mm, 1.8 μm, Water, United Kingdom) was used for reversed-phase separation. The mobile phase consisted of solvent A (water, 0.1% formic acid) and solvent B (acetonitrile, 0.1% formic acid), while the column temperature was maintained at 35°C. The TripleTOF 5600 Plus system was used to detect metabolites eluted from the column. The ion spray floating voltage was set at 5 kV for the positive-ion mode and at −4.5 kV for the negative-ion mode. A QC sample was analyzed every 10 samples to evaluate LC-MS stability. The acquired LC-MS data pretreatment was conducted with the XCMS software program. Raw data files were converted into the mzXML format and processed using the XCMS, CAMERA, and metaX toolboxes for the R software environment. Each ion was identified using comprehensive retention time and m/z information and these data were matched to both in-house and public databases. The open access databases KEGG[1] and HMDB[2] were used to annotate metabolites by matching exact molecular mass data (m/z) to those from the databases, when considering a threshold of 10 ppm. Peak intensity data was further pre-processed using the metaX program. Features that were detected in <50% of the QC samples or <80% of the test samples were removed and values for missing peaks were extrapolated using the k-nearest neighbor algorithm to further improve data quality. The relative standard deviations of metabolic features were calculated across all QC samples and those with standard deviations >30% were removed. Data normalization was performed on all samples using the probabilistic quotient normalization algorithm. The QC-robust spline batch correction was then used for QC samples. *p* values were calculated with student *t*-tests that were adjusted for multiple tests using a false discovery rate (FDR) (Benjamini-Hochberg) for different metabolite selection.

[1]https://www.kegg.jp/

[2]https://hmdb.ca/

A variable importance for the projection (VIP) cut-off value of 1.0 was used to identify important features.

Determination of 2-Keto Gluconic Acid Production Capacity of JP233

The 2-keto gluconic acid (2KGA) standard solution was prepared by precisely weighing 0.1000 g of the 2KGA standard and dissolving it with distilled water, followed by bringing it to a constant volume in a 50 mL volumetric flask to prepare a 2 mg/mL stock solution. The stock solution was diluted with distilled water to achieve 2KGA standard solutions with concentrations of 2 mg/mL, 1.5 mg/mL, 1 mg/mL, 0.8 mg/mL, 0.5 mg/mL, and 0.1 mg/mL, mixed well and then filtered with 0.22 μm aqueous microporous filter membranes. The solutions were then subjected to degassing treatments using an ultrasonic cleaner for 15 min and subsequent high-performance liquid chromatography (HPLC) determination (Wang et al., 2014).

Pretreatment of samples for testing included first inoculating strain JP233 into NBRIP liquid medium and culturing with shaking at 180 r/min for 6 days at 30°C. The fermentation broth was sampled every 12 h and filtered with a disposable sterile filter (0.22 μm pore diameter) and the filtrate was collected to directly determine the pH and 2KGA contents. The pH of the fermentation broth was measured with a pH meter and 2KGA contents were determined with HPLC (Niu et al., 2012). HPLC was used to characterize the samples using an Agilent 1200 system with an Aminex HPX-87H (300 mm × 7.8 mm, 9 μm) column, 5 mM H_2SO_4 as the mobile phase, a column temperature of 55°C, a flow rate of 0.6 mL/min, a detection wavelength of 210 nm, and 20 μL sample sizes, while using a DAD detector. Peak areas were determined from chromatograms and standard curves were constructed with the peak areas as the ordinate and the concentrations of the standard working solution as the abscissa. The standard curve equation was $y = 913.15x + 12.353$ ($R^2 = 0.9998$).

Effects of Phosphorus-Solubilizing Bacteria Strain JP233 on Phosphorus Leaching From Soils

Microcosm experiments were designed to investigate the effects of JP233 on P leaching. Specifically, a PVC tube with an inner diameter of 7 cm and a length of 40 cm was placed in the soil column (as described in section "Isolation of Phosphorus-Solubilizing Bacteria From Agriculture Soils") (Xie et al., 2019). Petrolatum was first evenly applied to the inner wall of the tube and a layer of 300 mesh nylon mesh was placed on the bottom of the column, followed by layering of about 60 g of quartz sand (about 1 cm thickness), and then a layer of 300 mesh nylon mesh that was placed to prevent soil infiltration. Finally, 1,800 g of test soil was loaded into the upper portion of the nylon mesh based on the actual soil bulk density in the field. KH_2PO_4 (0.44 g) was mixed into the surface soil and the loaded soil column was placed above a beaker to collect leachate. Three soil columns were established in the treatment and control groups, and 600 mL of deionized water was added to each column to achieve the maximum water holding capacity and ensure consistency of soil conditions in each column. Activated JP233 was inoculated into 250 mL of nutrient broth medium and placed in a shaker at 180 rpm and at 28°C for 24 h. The bacterial solutions were centrifuged twice and 150 mL of dd'H_2O was used to resuspend cells, followed by application to the soil columns. In place of cultures, 150 mL of dd'H_2O only was applied to soil columns in the control group. After inoculation, 100 mL of water was added to the soil columns every 3 days to replenish soil water, while leached fluid was collected into a beaker and TP and MRP contents in the leachate fluids were measured (as described in section "Determination of P Contents in Soils and Soil Leachates") on the same day. The experiments lasted 30 days, and the total phosphorus loss was calculated from the measurements. The calculation formulae used were:

$$\text{MRP mass}_n = \text{MRP concentration}_n \times \text{Leachate volumen}_n \quad (1)$$

$$\text{Total MRP mass} = \sum_{i=1}^{n} \text{MRPmass}_i \quad (2)$$

$$\text{TP mass}_n = \text{TP concentration}_n \times \text{Leachate volume}_n \quad (3)$$

$$\text{Total TP mass} = \sum_{i=1}^{n} \text{TPmass}_i \quad (4)$$

where n indicates the nth watering. At the end of the experiment, soil samples were removed in layers (0–10 cm, 10–20 cm, 20–30 cm, and 30–40 cm layers), and the soil samples were air-dried and sieved to determine TP and AP mass concentrations in each layer of soil samples (as described in section "Determination of P Contents in Soils and Soil Leachates").

Effects of Phosphorus-Solubilizing Bacteria Strain JP233 on Soil Phosphorus Leaching and Maize Growth

Maize seeds with full grains were selected and pre-germinated on moist filter paper for 24 h before sowing. Two experimental groups were established in the experiment, with the treatment group being inoculated with JP233 cultures and the control group without bacterial inoculation. Three independent biological replicates were used for each group. The soil column leaching device used for the experiment was the same as described in section "Determination of 2-Keto Gluconic Acid Production Capacity of JP233." Activated JP233 was inoculated into 3 mL of nutrient broth medium, individually inoculated into three tubes, and placed in a shaker for cultivation over 48 h. Bacterial solutions were then centrifuged twice (5,000 r/min), supernatants were discarded, and the bacterial solutions were resuspended with sterile water to an OD_{600} of 1.0. Six pre-germinated seeds per treatment were soaked in the resuspended bacterial solutions for 30 min, and two were sown in each treatment soil column after soaking. Six pre-germinated seeds per control were soaked in sterile water for 30 min and two were placed in each control soil column after soaking.

After sowing, each soil column was watered every 7 days over 28 days (i.e., at days 7, 14, 21, and 28) based on maize growth water requirements, with watering volumes of 150, 300, 550, and 400 mL, respectively. Soil leachates were collected after each watering to determine TP and MRP contents (as described in sections "Determination of P Contents in Soils and Soil Leachates" and "Effects of Phosphorus-Solubilizing Bacteria Strain JP233 on P Leaching From Soils"). At the end of the pot culture experiments, the soil columns were divided into two layers comprising the 0–20 cm and 20–40 cm layers, and their rhizosphere and non-rhizosphere soils were retrieved. The soil samples were air-dried and sieved to determine TP and AP mass concentrations (as described in section "Determination of P Contents in Soils and Soil Leachates"). At the end of the leaching experiment, the maize plants were removed intact and oven-dried to a constant weight at 80°C. The dry matter mass of the aerial components and roots of the maize were separately weighed.

Statistical Analyses

All experimental data were collated using Microsoft Excel 2016 and plotted using SigmaPlot 12.5. One-way analysis of variance (one-way ANOVA) was performed using the SPSS 24.0 statistical software program with all test data and using a significance level threshold of 0.05 or 0.01.

RESULTS

Isolation of an Efficient Phosphorus-Solubilizing Bacteria Strain, JP233

Three PSB strains (identified as JP233, JP236, and J221) were screened based on the appearance of a clear halo on NBRIP agar plates. Soluble P content measurements in liquid culture demonstrated that strains JP233 (**Figures 1A,B**), JP236, and J221 released 258.07 ± 0.74, 110.11 ± 0.42, and 62.7 ± 0.35 mg/L soluble P from 5 g/L $Ca_3(PO_4)_2$ within 48 h, respectively. Strain JP233 achieved the best P solubilization and was thus used for follow-up studies. 16S rRNA gene sequencing (GenBank ID: MW990045) analyses indicated that JP233 was highly related to some *Pseudomonas* species, such as *P. putida*, *P. plecoglossicida*, *P. moteilii*, *P. asiatica*, showing sequence identity bigger than 99.72%.

Identification of the Critical Metabolite Involved in Phosphorus-Solubilization by JP233

Untargeted metabolomics was used to evaluate the metabolites that differed between the JP233 treatment (JP) and the blank control (CK) groups cultured in NBRIP liquid medium for 48 h. Differential metabolites were identified as significantly different based on the ratio (JP/CK) >2, a *q* value (Benjamini-Hochberg's adjustment) <0.05, and a VIP > 1. A total of 660 and 618 significantly upregulated metabolites were identified in negative- and positive-ion mode, respectively. Annotation of the metabolites was conducted using in-house and public databases (included KEGG and HMDB databases). Eleven upregulated metabolites were classified as organic acids including 2KGA (ratio = 567.60, *q* value = 1.87E-05, VIP = 3.17), (2-methoxyethoxy)propanoic acid (ratio = 1158.55, *q* value = 1.16E-07, VIP = 3.34), 2-oxopentanedioic acid (ratio = 977.61, *q* value = 1.75E-06, VIP = 3.31), D-(+)-pantothenic acid (ratio = 536.42, *q* value = 6.15E-07, VIP = 3.17), N-acetyl-L-glutamic acid (ratio = 38.17, *q* value = 2.86E-05, VIP = 2.46), *trans*-aconitic acid (ratio = 26.38, *q* value = 4.45E-06, VIP = 2.35), succinic acid (ratio = 23.05, *q* value = 2.43E-10, VIP = 2.25), 3-oxopentanoic acid (ratio = 8.45, *q* value = 1.09E-09, VIP = 1.87), maleic acid (ratio = 4.66, *q* value = 1.83E-09, VIP = 1.61), pantothenic acid (ratio = 106.80, *q* value = 3.19E-12, VIP = 2.83), and 2-ketohexanoic acid (ratio = 8.74, *q* value = 4.36E-07, VIP = 1.93). Moreover, the relative peak areas of the above organic acids exhibited large differences, with the largest being 2KGA, which was an order of magnitude larger than the organic acid with the second largest normalized intensity (**Figures 2A,B**).

High-performance liquid chromatography analysis was conducted to validate 2KGA production by strain JP233 in NBRIP liquid medium. 2KGA could be detected in the fermentation liquor of JP233 and concentrations rapidly rose within 48 h (**Figure 2C**), followed by fluctuations in concentrations in the range of 13.62–19.33 mg/mL until 156 h. Over the same experimental period, the fermentation liquor pH significantly dropped from an initial value of 7.66 to 4.43 within 24 h, followed by stabilization in the range of 4.43–4.53 until 156 h. The above results consequently indicated that JP233 could produce considerable concentrations of 2KGA in NBRIP medium and acidification occurred when 2KGA was produced. The preliminary conclusion was drawn that acidification caused by 2KGA production played an important role in P solubilization by JP233. It is noteworthy that a drastic drop in pH is observed within the first 12 h while production of 2KGA was afterward, which means the other organic acids also played roles in early acidification.

Influence on Phosphorus Leaching by Direct Application of JP233 to Soils

Microcosmic experiments were conducted to analyze the influence of JP233 on P leaching from soils. MRP and TP levels were determined from soil leachates every 3 days from the 6th day until the 30th day in both treatment and control groups. On the first measurement time point (6 days post inoculation, dpi), MRP (P = 0.017, α = 0.05) and TP (P = 0.003, α = 0.01) levels in soil leachates were significantly higher in the JP233 treatment group than in the CK group. However, significant differences in MRP or TP loss between the treatment and the CK groups were not observed in subsequent leachate measurements, with the sole exception of TP loss (P = 0.049, α = 0.05) at 30 dpi (**Figures 3A,B**). After the leaching tests, the cumulative leaching loss of MRP and TP contents in soil leachates were calculated. The amounts of MRP and TP lost in the treatment group were 0.363 ± 0.027 mg and 2.16 ± 0.220 mg, respectively, while those in the control group were 0.345 ± 0.028 mg and 1.940 ± 0.130 mg, respectively. Thus, significant differences

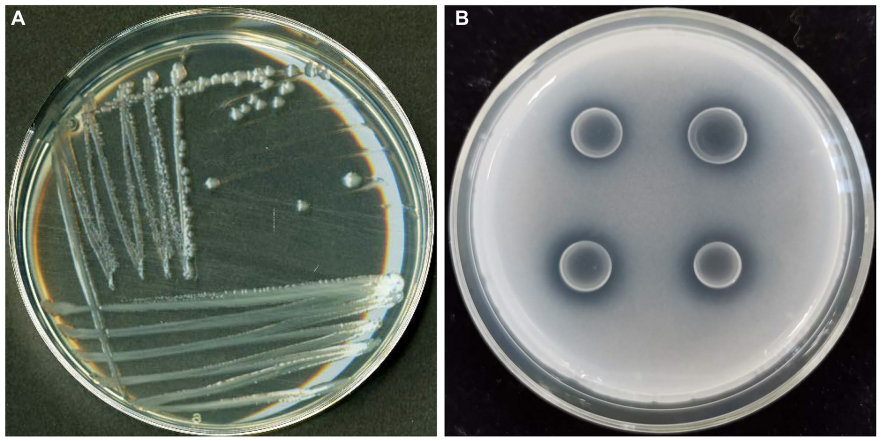

FIGURE 1 | Colony morphology of PSB strain JP233 on an LB plate **(A)** and its characteristic P solubilizing halo on an NBRIP plate **(B)**.

in total leaching loss of MRP (P = 0.448, α = 0.05) or TP (P = 0.209, α = 0.05) were not observed between the treatment and control groups.

The concentrations of TP and AP in the 0–10, 10–20, 20–30, and 30–40 cm soil layers were also measured after leaching experiments. AP and TP concentrations in the 0–10 cm soil layer were the highest, while P levels in the other soil layers were relatively similar. Further, statistically significant differences in the concentrations of AP or TP between the treatment and control groups were not apparent for each soil layer (**Figures 3C,D**).

The above results indicated that insoluble phosphorus was converted into soluble phosphorus after the PSB strain JP233 was applied to the soils, resulting in increased leaching of MRP and TP, although these differences were not statistically significant. Thus, the MRP and TP contents retained in the soils were essentially not different from those in the control.

Influence on Phosphorus Leaching by Inoculation of JP233 Cultures to Maize Plant Soils

Maize was planted in the same microcosm leaching devices described above and watered every 7 days according to maize seedling water requirements, followed by collecting leaching solution after each watering to measure MRP and TP. The treatment group was inoculated with JP233, while the control group was not inoculated with cultures. The MRP content of the treatment group was lower than that of the control group in each leaching test, with no significant difference in levels on day 7, but statistically significant differences on days 14 (P = 0.008, α = 0.01), 21 (P = 0.000, α = 0.01), and 28 (P = 0.026, α = 0.05) (**Figure 4A**). TP differences exhibited similar trends, with lower TP content in the treatment group than in the control group and without significant differences in levels on day 7, but statistically significant differences on days 14 (P = 0.000, α = 0.01), 21 (P = 0.002, α = 0.01), and 28 (P = 0.056, α = 0.05) (**Figure 4B**). After leaching tests, cumulative leaching loss of MRP and TP in soil leachates were calculated. MRP and TP concentrations in the treatment group were 0.747 ± 0.139 mg and 2.489 ± 0.232 mg, respectively, while these values in the control group were 2.384 ± 0.214 mg and 4.290 ± 0257 mg, respectively. Significant differences were observed in both total leaching loss of MRP (P = 0.000, α = 0.01) and TP (P = 0.001, α = 0.01) when comparing the treatment and control groups.

The mass concentrations of residual AP and total TP in rhizosphere and non-rhizosphere soils were determined after the leaching experiments. AP contents in the rhizosphere and non-rhizosphere soils at a depth of 0–20 cm in the treatment group were significantly lower than in the control group and significant differences were not observed in AP contents when compared between rhizosphere and non-rhizosphere soils at a depth of 20–40 cm between the two groups (**Figure 4C**). However, significant differences in TP content were not observed between rhizosphere and non-rhizosphere soils at both depths when comparing the two groups (**Figure 4D**).

Maize biomass accumulation was also evaluated after the leaching experiments. JP233 inoculation significantly increased the dry matter mass of aerial maize components (P = 0.023, α = 0.05) (**Figures 5A,C**) and also increased the mass of root dry matter, although not significantly (**Figures 5B,C**), but did significantly increase the dry matter of the entire plant (P = 0.037, α = 0.05) (**Figure 5C**).

The above results indicated that MRP and TP contents of soil leachate after inoculation with strain JP233 into maize plant soils were significantly lower than in controls without inoculation. AP content retained in inoculated soils decreased compared to controls, while TP contents in soils were not different from controls. In addition, JP233 inoculation significantly increased dry matter quality and promoted maize growth.

DISCUSSION

Phosphorus-solubilizing bacteria are commonly used plant probiotics that promote plant development by converting

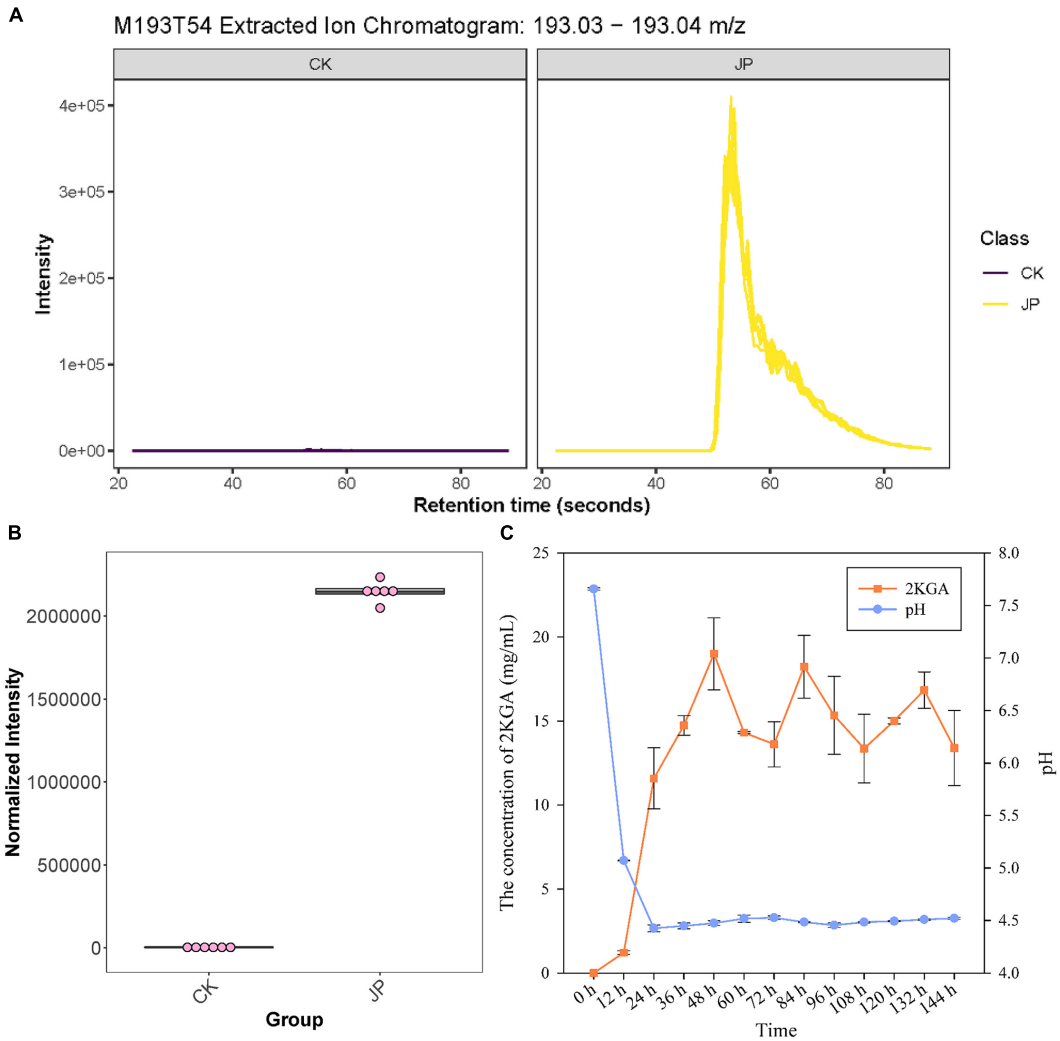

FIGURE 2 | Metabolomic and HPLC identification and analysis of 2KGA. **(A)** The extracted ion chromatogram of compound M193T54 (identified as 2KGA *via* database alignment) from the JP233 treatment and CK. The yellow chromatogram indicates treatment and the purple one indicates CK. **(B)** Normalized intensity boxplot of M193T54 (2KGA) in the JP233 treatment and CK. **(C)** Changes of 2KGA concentration and the pH of JP233 fermentation broths. Results represent means ± SD (n = 6).

insoluble P into soluble P that is easily absorbed and used by roots (Hamid et al., 2021). The mechanism of P solubilization by PSB is relatively clear and occurs primarily through the secretion of organic acids that dissolve inorganic phosphorus or *via* the secretion of phosphatases that degrade organophosphorus. P solubilizing bacteria are an important type of microbial fertilizer and many efficient strains have been developed into agents for application (Sarkar et al., 2021). However, it has remained unclear whether the solubilization of soil P by PSB will result in additional phosphorus migration into groundwater, thereby contributing to eutrophication of water bodies.

In this study, a highly efficient PSB strain, *Pseudomonas* sp. JP233, was isolated from agricultural soils that could release 258.07 mg/L MRP from 5 g/L $Ca_3(PO_4)_2$ within 48 h, representing a P conversion efficiency of 25.81%. *Pseudomonas* strains have been demonstrated to vary in their ability to dissolve P, for example with the PSB strains *Pseudomonas* sp. P34, *P. fluorescens* MS-01, *P. putida* PSE3, *Pseudomonas* sp. RT5RP2, *Pseudomonas* sp. RT6RP, *P. lurida* M2RH3, and *P. putida* PSRB6 dissolving 101.60, 29.80, 319.00, 38.33, 35.40, 340.00, and 100.00 mg/L of soluble P, respectively (Hariprasad and Niranjana, 2009; Selvakumar et al., 2011, 2013; Ahmad et al., 2013; Kadmiri et al., 2018; Liu et al., 2019).

Metabolome analysis and HPLC determination identified 2KGA as the primary P solubilizing organic acid that is secreted by JP233. 2KGA is converted from gluconic acid in the periplasm by an FAD-dependent gluconate dehydrogenase that is encoded by the gad operon (Yum et al., 1997; Toyama et al., 2007; Saichana et al., 2009). Indeed, expression of the gad operon of *P. putida* KT 2440 in *Enterobacter asburiae* PSI3 improves mineral phosphate solubilization (Kumar et al., 2013). In addition, *Gluconobacter*, *Pseudogluconobacter*, *Pseudomonas*,

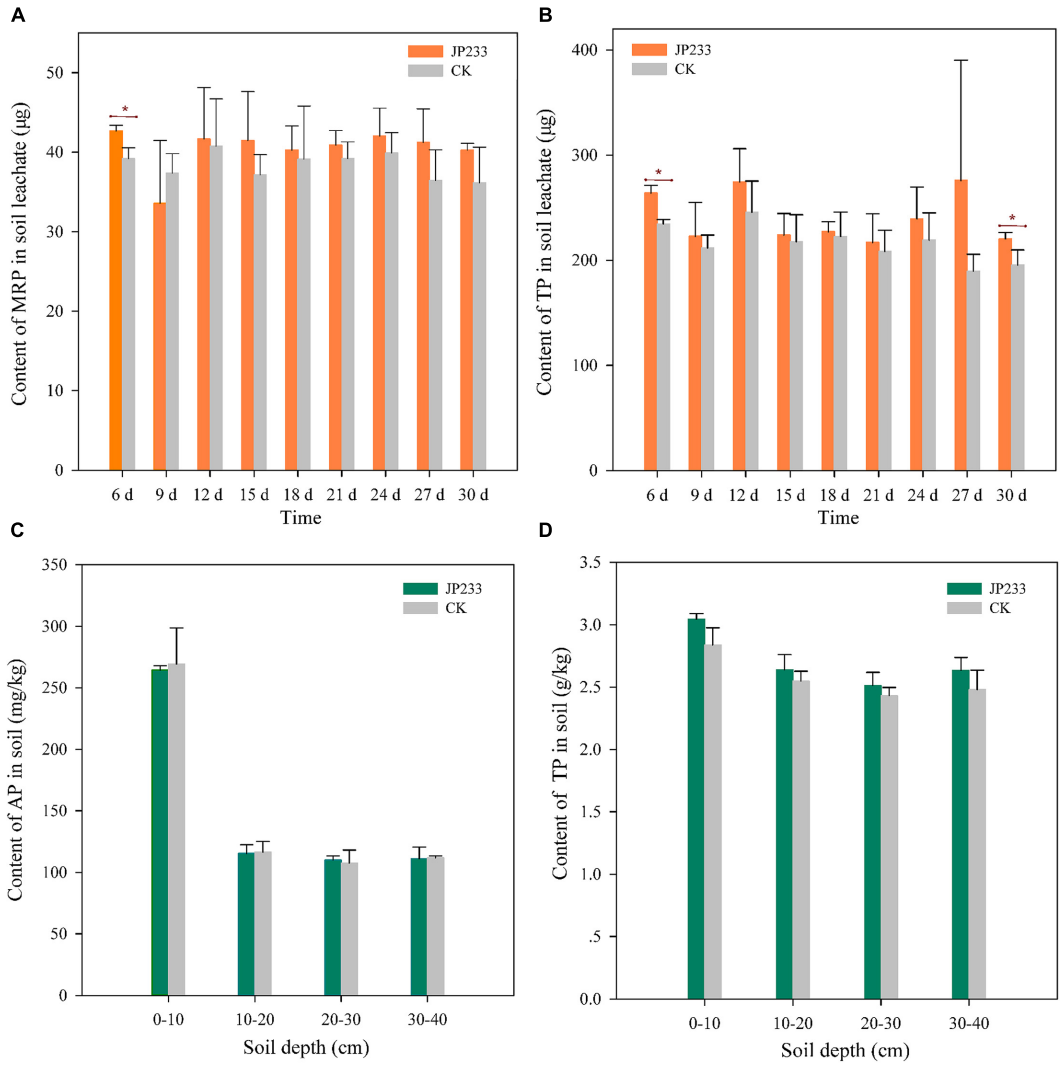

FIGURE 3 | P contents in soil leachates and soils after JP233 treatment. **(A,B)** Show differences in MRP and TP contents in soil leachate. **(C,D)** Show differences of AP and TP contents in the soil column. Results represent means ± SD. One-way ANOVA was performed for each time or soil depth. *Statistically significant at $P < 0.05$.

Serratia, *Klebsiella*, and *Enterobacter* spp. have all been shown to produce 2KGA (Hwangbo et al., 2003; Li et al., 2016). 2KGA-producing *Pseudomonas* species include *P. corrugate*, *P. fluorescens*, *P. plecoglossicida*, and *P. aureofaciens* (Trivedi and Sa, 2008; Sun et al., 2013; Umezawa et al., 2015; Wang et al., 2019).

Other organic acids were also produced by JP233 including (2-methoxyethoxy) propanoic acid, 2-oxopentanedioic acid, D-(+)-pantothenic acid, N-acetyl-L-glutamic acid, *trans*-aconitic acid, succinic acid, 3-oxopentanoic acid, maleic acid, pantothenic acid, and 2-ketohexanoic acid. Acids released by PSB that have been shown to be involved in P solubilization include citric acid, formic acid, gluconic acid, 2-keto gluconic acid, lactic acid, malic acid, oxalic acid, propionic acid, and succinic acid (Khan et al., 2007; Sharma et al., 2013; Alori et al., 2017; Chakdar et al., 2018; Su et al., 2019; Monroy Miguel et al., 2020; Spohn et al., 2020). It should be noted that organic acids produced by strains of the genus are not identical. For example, the organic acids produced by *P. poae* BIHB 751 are gluconic acid, ketogluconic acid, citric acid and malic acid, while those by *P. trivialis* BIHB 769 are gluconic acid, ketogluconic acid, lactic acid, fumaric acid, malic acid, and succinic acid, and those by *Pseudomonas* sp. AZ15 are oxalic acid, gluconic acid, acetic acid, lactic acid, and citric acid (Vyas and Gulati, 2009; Zaheer et al., 2019; Rawat et al., 2021). Comparison against other strains revealed that strain JP233 exhibited a high capacity for P solubilization and produced a wide variety of organic acids.

The MRP and TP contents in soil leachate increased (albeit overall insignificantly) in microcosm leaching experiments when JP233 was applied to soils, although a significant increase was observed in the first leaching measurement at 7 days. The MRP and TP contents in surface soil layers were higher than those in deeper layers after 30 days, although statistically significant

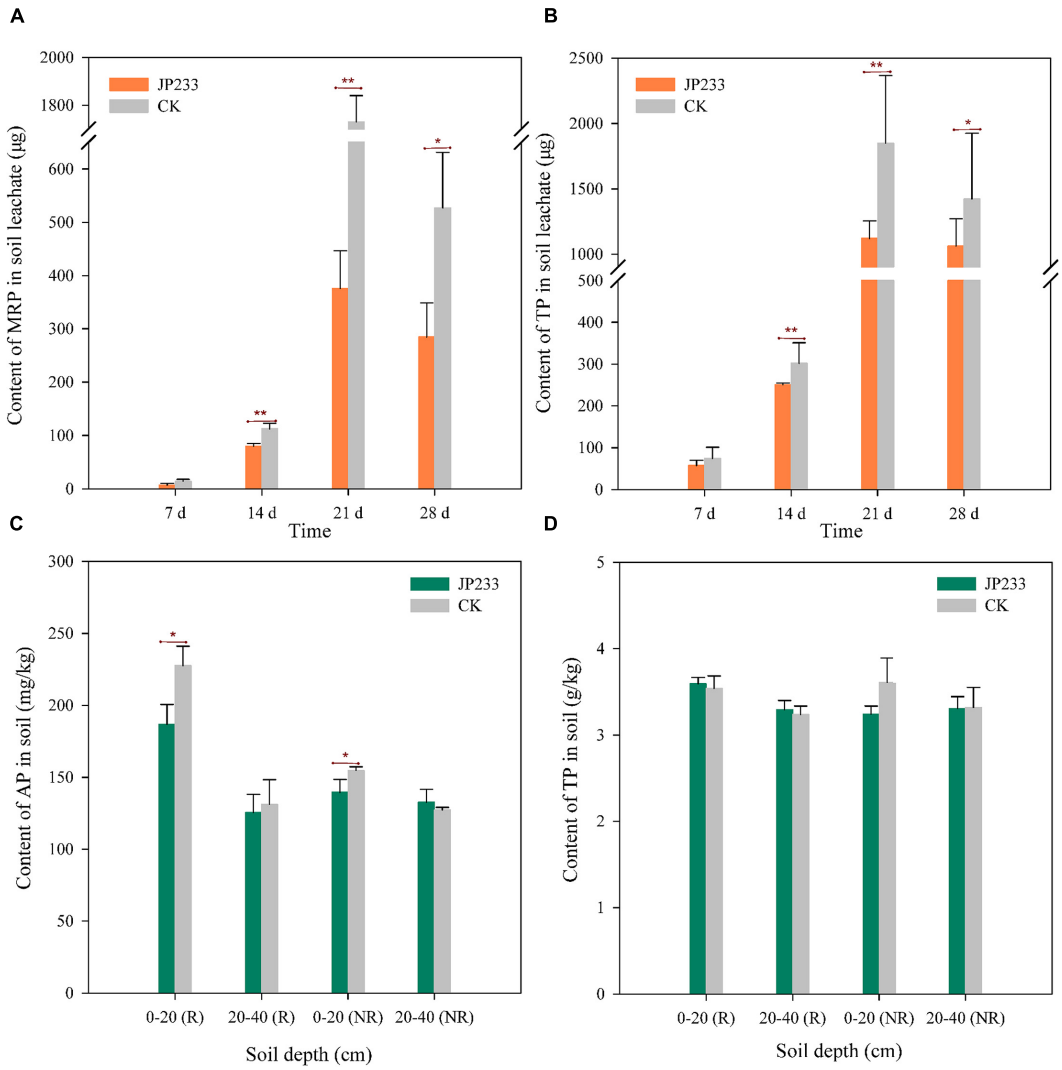

FIGURE 4 | P contents in soil leachates and soils after JP233 treatment in maize plant soils. **(A,B)** Show differences in MRP and TP contents in soil leachate. **(C,D)** Show differences of AP and TP contents in the soil column. Results represent means ± SD. One-way ANOVA was performed for each time or soil depth. *Statistically significant at $P < 0.05$, **statistically significant $P < 0.01$.

differences were not observed between the JP233 treatment and control soils. Thus, the application of PSB strain JP233 to soil could not alone improve the solubility of soil P, although a non-significant increase in P leaching loss was observed. This result could be due to the existence of abundant P-fixing compounds in the soils, in addition to the P-solubilizing effects of PSB being relatively limited. These results are also consistent with those previously reported (Yu et al., 2019), wherein strain PSB *P. prosekii* YLYP6 could produce 716 mg/L of AP under optimized conditions. This study also only observed a significant difference between treatment and control groups on the 10th day when measuring at days 4, 10, and 30.

When PSB JP233 was inoculated into maize plant soils, leaching loss of P significantly decreased. After watering on days 14, 21, and 28, the concentrations of MRP and TP lost to leakage in the treatment group were significantly lower than in the control group. Further, the amount of MRP and TP lost to leakage in the treatment group was lower than in the control group on day 7, albeit not significantly. Moreover, AP remaining in the rhizosphere and non-rhizosphere soils were also significantly lower than in the control at 0–20 cm depth, but not significantly different at 20–40 cm depth, nor were TP contents significantly different among different soil zones. In the results of this current study, P solubilization by PSB JP233 led to less P loss from pot experiments with plants compared to controls. A previous study hypothesized that organic acids in root exudates (e.g., oxalic acid) were involved in the mobilization of P within the rhizosphere (Ström, 1997), which may explain why maize itself resulted in excessive P loss. Regarding why the effect was minimized when PSB JP233 was present, possible explanations could be that the activation of P by PSB produced an active state of P that is more readily absorbed, or that PSB promoted

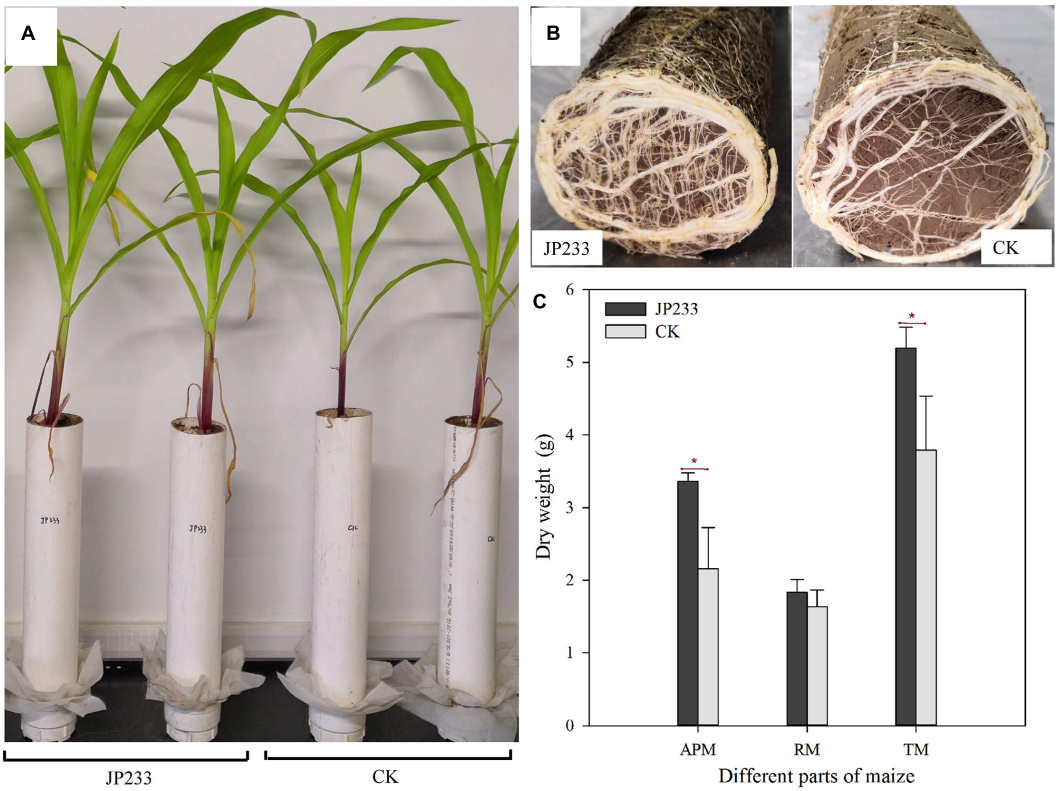

FIGURE 5 | Effects of JP233 treatment on maize seedling biomass. **(A)** Aerial plant component growth status of JP233 treatment and CK group plants. **(B)** Root growth status at the bottom of the soil column of the JP233 treatment and CK group plants. **(C)** Differences in masses of JP233 treatment and CK dry matter. APM, aerial part mass; RM, root mass; TM, total mass. Results represent means ± SD. One-way ANOVA was performed for each time or soil depth. *Statistically significant at $P < 0.05$.

the uptake of P by plants through unknown mechanisms; these mechanisms require further investigation. Concomitantly, the aerial component and whole dry matter weight of maize plants treated with JP233 were significantly larger compared to non-treated ones. Thus, JP233 inoculation promoted maize plant growth. These results suggest that the growing plant roots can absorb more soluble P from soil into plant tissues, while organic acids like 2KGA produced by JP233 dissolve more soluble P in soils. These results can be explained by the absorption of P by maize roots, rather than leaving soluble P in soils or accumulating it within leachate, thereby leading to significantly reduced leachate loss of P and concomitant significant increases of maize plant biomass of maize.

CONCLUSION

In this study, the roles of PSB were investigated from an environmental perspective, focusing on the growth promotion effects of PSB on plants, while also analyzing the risk of PSB application on the transfer of soil soluble P to groundwater. These data were used to provide a foundation for the rational use of PSB. An efficient PSB strain, *Pseudomonas* sp. JP233, was isolated and identified from soils. Metabolomics and HPLC analyses revealed that its primary P solubilizing organic acid was 2KGA. Microcosm leaching tests indicated that JP233 alone did not significantly increase leaching loss of MRP and TP. When inoculated into maize plant soils, JP233 significantly reduced MRP and TP loss compared to controls. Moreover, inoculation with JP233 significantly increased the biomass of maize aerial components and for the whole plant.

DATA AVAILABILITY STATEMENT

The raw data supporting the conclusions of this article will be made available by the authors, without undue reservation.

AUTHOR CONTRIBUTIONS

HY: methodology, investigation, writing-original draft, data curation, and formal analysis. XW: conceptualization, writing-original draft, visualization, data curation, and formal analysis. GZ: resources and investigation. FZ: software and resources. PH: conceptualization and writing-review and editing. LW: methodology. SF, XX, and FL: investigation. HZ and XiaZ: validation. XinZ: conceptualization, supervision, project administration, funding acquisition, and writing-review and

editing. All authors contributed to the article and approved the submitted version.

FUNDING

This work was supported by the Major Science and Technology Innovation Engineering Project of Shandong Province (grant numbers 2019JZZY020610 and 2021TZXD002), National Key Research and Development Project of China (grant numbers 2018YFD0200604 and 2017YFD0800402), and National Natural Science Foundation of China (grant number 31901928).

ACKNOWLEDGMENTS

We thank LetPub (www.letpub.com) for linguistic assistance and pre-submission expert review.

SUPPLEMENTARY MATERIAL

The Supplementary Material for this article can be found online at: https://www.frontiersin.org/articles/10.3389/fmicb.2022.892533/full#supplementary-material

REFERENCES

Afzal, A., Bano, A., and Fatima, M. (2010). Higher soybean yield by inoculation with N-fixing and P-solubilizing bacteria. *Agron. Sustain. Dev.* 30, 487–495. doi: 10.1051/agro/2009041

Ahmad, E., Khan, M. S., and Zaidi, A. (2013). ACC deaminase producing *Pseudomonas putida* strain PSE3 and *Rhizobium leguminosarum* strain RP2 in synergism improves growth, nodulation and yield of pea grown in alluvial soils. *Symbiosis* 61, 93–104. doi: 10.1007/s13199-013-0259-6

Alori, E. T., Glick, B. R., and Babalola, O. O. (2017). Microbial phosphorus solubilization and its potential for use in sustainable agriculture. *Front. Microbiol.* 8:971. doi: 10.3389/fmicb.2017.00971

Bao, S. (2000). *Soil Agrochemical Analysis*. Beijing: China Agriculture Press.

Bautista-Cruz, A., Antonio-Revuelta, B., Del Carmen Martínez Gallegos, V., and Báez-Pérez, A. (2019). Phosphate-solubilizing bacteria improve *Agave angustifolia* Haw. Growth under field conditions. *J. Sci. Food Agr.* 99, 6601–6607. doi: 10.1002/jsfa.9946

Chakdar, H., Dastager, S. G., Khire, J. M., Rane, D., and Dharne, M. S. (2018). Characterization of mineral phosphate solubilizing and plant growth promoting bacteria from termite soil of arid region. *3 Biotech* 8:463. doi: 10.1007/s13205-018-1488-4

Chawngthu, L., Hnamte, R., and Lalfakzuala, R. (2020). Isolation and characterization of rhizospheric phosphate solubilizing bacteria from wetland paddy field of Mizoram, India. *Geomicrobiol. J.* 37, 1–10. doi: 10.1080/01490451.2019.1709108

Chouyia, F. E., Romano, I., Fechtali, T., Fagnano, M., Fiorentino, N., Visconti, D., et al. (2020). P-solubilizing *Streptomyces roseocinereus* MS1B15 with multiple plant growth-promoting traits enhance barley development and regulate rhizosphere microbial population. *Front. Plant Sci.* 11:1137. doi: 10.3389/fpls.2020.01137

Gatiboni, L., Brunetto, G., Pavinato, P. S., and George, T. S. (2020). Editorial: legacy phosphorus in agriculture: role of past management and perspectives for the future. *Front. Earth Sci.* 8:619935. doi: 10.3389/feart.2020.619935

Ha, S., and Tran, L. S. (2014). Understanding plant responses to phosphorus starvation for improvement of plant tolerance to phosphorus deficiency by biotechnological approaches. *Crit. Rev. Biotechnol.* 34, 16–30. doi: 10.3109/07388551.2013.783549

Hamid, B., Zaman, M., Farooq, S., Fatima, S., Sayyed, R. Z., Ahmad Baba, Z., et al. (2021). Bacterial plant biostimulants: a sustainable way towards improving growth, productivity, and health of crops. *Sustainability* 13:2856. doi: 10.3390/su13052856

Hariprasad, P., and Niranjana, S. R. (2009). Isolation and characterization of phosphate solubilizing rhizobacteria to improve plant health of tomato. *Plant Soil* 316, 13–24. doi: 10.1007/s11104-008-9754-6

Heckrath, G., Brookes, P. C., Poulton, P. R., and Goulding, K. W. T. (1995). Phosphorus leaching from soils containing different phosphorus concentrations in the broadbalk experiment. *J. Environ. Qual.* 24, 904–910. doi: 10.2134/jeq1995.00472425002400050018x

Huang, Y. (2019). Study on the analysis of total phosphorus by molybdate spectrophotometric determination. *Biol. Chem. Eng.* 5, 98–101. doi: 10.3969/j.issn.2096-0387.2019.06.029

Hwangbo, H., Park, R. D., Kim, Y. W., Rim, Y. S., Park, K. H., Kim, T. H., et al. (2003). 2-ketogluconic acid production and phosphate solubilization by *Enterobacter intermedium*. *Curr. Microbiol.* 47, 0087–0092. doi: 10.1007/s00284-002-3951-y

Kadmiri, I. M., Chaouqui, L., Azaroual, S. E., Sijilmassi, B., Yaakoubi, K., and Wahby, I. (2018). Phosphate-solubilizing and auxin-producing rhizobacteria promote plant growth under saline conditions. *Arab. J. Sci. Eng.* 43, 3403–3415. doi: 10.1007/s13369-017-3042-9

Kaur, R., and Kaur, S. (2020). Variation in the phosphate solubilizing bacteria from virgin and the agricultural soils of Punjab. *Curr. Microbiol.* 77, 2118–2127. doi: 10.1007/s00284-020-02080-6

Khan, M. S., Zaidi, A., and Wani, P. A. (2007). Role of phosphate-solubilizing microorganisms in sustainable agriculture-a review. *Agron. Sustain. Dev.* 27, 29–43. doi: 10.1007/978-90-481-2666-8_34

Khan, N., Ali, S., Shahid, M. A., Mustafa, A., Sayyed, R. Z., and Curá, J. A. (2021). Insights into the interactions among roots, rhizosphere, and rhizobacteria for improving plant growth and tolerance to abiotic stresses: a review. *Cells* 10:1551. doi: 10.3390/cells10061551

Kumar, C., Yadav, K., Archana, G., and Naresh Kumar, G. (2013). 2-ketogluconic acid secretion by incorporation of *Pseudomonas putida* KT 2440 gluconate dehydrogenase (gad) operon in *enterobacter asburiae* PSI3 improves mineral phosphate solubilization. *Curr. Microbiol.* 67, 388–394. doi: 10.1007/s00284-013-0372-z

Kusale, S. P., Attar, Y. C., Sayyed, R. Z., Malek, R. A., Ilyas, N., Suriani, N. L., et al. (2021). Production of plant beneficial and antioxidants metabolites by *Klebsiella variicola* under salinity stress. *Molecules* 26:1894. doi: 10.3390/molecules26071894

Li, K., Mao, X., Liu, L., Lin, J., Sun, M., Wei, D., et al. (2016). Overexpression of membrane-bound gluconate-2-dehydrogenase to enhance the production of 2-keto-d-gluconic acid by *Gluconobacter oxydans*. *Microbial Cell Fact.* 15:121. doi: 10.1186/s12934-016-0521-8

Lin, S., Litaker, R. W., and Sunda, W. G. (2016). Phosphorus physiological ecology and molecular mechanisms in marine phytoplankton. *J. Phycol.* 52, 10–36. doi: 10.1111/jpy.12365

Liu, X., Jiang, X., He, X., Zhao, W., Cao, Y., Guo, T., et al. (2019). Phosphate-solubilizing *Pseudomonas* sp. Strain P34-L promotes wheat growth by colonizing the wheat rhizosphere and improving the wheat root system and soil phosphorus nutritional status. *J. Plant Growth Regul.* 38, 1314–1324. doi: 10.1007/s00344-019-09935-8

Monroy Miguel, R., Carrillo González, R., Rios Leal, E., and González-Chávez, M. D. C. A. (2020). Screening bacterial phosphate solubilization with bulk-tricalcium phosphate and hydroxyapatite nanoparticles. *Anton. Leeuw.* 113, 1033–1047. doi: 10.1007/s10482-020-01409-2

Nautiyal, C. S. (1999). An efficient microbiological growth medium for screening phosphate solubilizing microorganisms. *Fems Microbiol. Lett.* 170, 265–270. doi: 10.1111/j.1574-6968.1999.tb13383.x

Nithyapriya, S., Lalitha, S., Sayyed, R. Z., Reddy, M. S., Dailin, D. J., Enshasy, H. A. E., et al. (2021). Production, purification, and characterization of *Bacillibactin siderophore* of *Bacillus subtilis* and its application for improvement in plant growth and oil content in sesame. *Sustainability* 13:5394. doi: 10.3390/su13105394

Niu, P. Q., Yang, A. H., Yang, S. X., Liu, L. M., and Chen, J. (2012). Screening and identification of 2-keto-d-gluconic acid-producing strain. *Chinese J. Process Eng.* 6, 1008–1013.

Paulucci, N. S., Gallarato, L. A., Reguera, Y. B., Vicario, J. C., Cesari, A. B., de Lema, M. B. G., et al. (2015). Arachis hypogaea PGPR isolated from Argentine soil modifies its lipids components in response to temperature and salinity. *Microbiol. Res.* 173, 1–9. doi: 10.1016/j.micres.2014.12.012

Pereira, S. I. A., and Castro, P. M. L. (2014). Phosphate-solubilizing rhizobacteria enhance *Zea mays* growth in agricultural P-deficient soils. *Ecol. Eng.* 73, 526–535. doi: 10.1016/j.ecoleng.2014.09.060

Prakash, J., and Arora, N. K. (2019). Phosphate-solubilizing *Bacillus* sp. enhances growth, phosphorus uptake and oil yield of *Mentha arvensis* L. *3 Biotech* 9:126. doi: 10.1007/s13205-019-1660-5

Rawat, P., Das, S., Shankhdhar, D., and Shankhdhar, S. C. (2021). Phosphate-solubilizing microorganisms: mechanism and their role in phosphate solubilization and uptake. *J. Soil Sci. Plant Nut.* 21, 49–68. doi: 10.1007/s42729-020-00342-7

Saichana, I., Moonmangmee, D., Adachi, O., Matsushita, K., and Toyama, H. (2009). Screening of thermotolerant Gluconobacter strains for production of 5-keto-D-gluconic acid and disruption of flavin adenine dinucleotide-containing D-gluconate dehydrogenase. *Appl. Environ. Microbiol.* 75, 4240–4247. doi: 10.1128/AEM.00640-09

Sarkar, D., Sankar, A., Devika, O. S., Singh, S., Shikha, Parihar, M., et al. (2021). Optimizing nutrient use efficiency, productivity, energetics, and economics of red cabbage following mineral fertilization and biopriming with compatible rhizosphere microbes. *Sci. Rep.* 11:15680. doi: 10.1038/s41598-021-95092-6

Selvakumar, G., Joshi, P., Suyal, P., Mishra, P. K., Joshi, G. K., Bisht, J. K., et al. (2011). *Pseudomonas lurida* M2RH3 (MTCC 9245), a psychrotolerant bacterium from the Uttarakhand Himalayas, solubilizes phosphate and promotes wheat seedling growth. *World J. Microb. Biot.* 27, 1129–1135. doi: 10.1007/s11274-010-0559-4

Selvakumar, G., Joshi, P., Suyal, P., Mishra, P. K., Joshi, G. K., Venugopalan, R., et al. (2013). Rock phosphate solubilization by psychrotolerant *Pseudomonas* spp. and their effect on lentil growth and nutrient uptake under polyhouse conditions. *Ann. Microbiol.* 63, 1353–1362. doi: 10.1007/s13213-012-0594-5

Sharma, S. B., Sayyed, R. Z., Trivedi, M. H., and Gobi, T. A. (2013). Phosphate solubilizing microbes: sustainable approach for managing phosphorus deficiency in agricultural soils. *SpringerPlus* 2:587. doi: 10.1186/2193-1801-2-587

Spohn, M., Zeißig, I., Brucker, E., Widdig, M., Lacher, U., and Aburto, F. (2020). Phosphorus solubilization in the rhizosphere in two saprolites with contrasting phosphorus fractions. *Geoderma* 366:114245. doi: 10.1016/j.geoderma.2020.114245

Ström, L. (1997). Root exudation of organic acids: importance to nutrient availability and the calcifuge and calcicole behaviour of plants. *Oikos* 80, 459–466. doi: 10.2307/3546618

Su, M., Han, F., Wu, Y., Yan, Z., Lv, Z., Tian, D., et al. (2019). Effects of phosphate-solubilizing bacteria on phosphorous release and sorption on montmorillonite. *Appl. Clay Sci.* 181:105227. doi: 10.1016/j.clay.2019.105227

Su, W. H., and Chen, Y. R. (2010). Determination of total phosphorus in soil by potassium persulfate digestion. *Light Text. Ind. Fujian* 6, 43–45. doi: 10.3969/j.issn.1007-550X.2010.06.00

Sun, W. J., Yun, Q. Q., Zhou, Y. Z., Cui, F. J., Yu, S. L., Zhou, Q., et al. (2013). Continuous 2-keto-gluconic acid (2KGA) production from corn starch hydrolysate by *Pseudomonas fluorescens* AR4. *Biochem. Eng. J.* 77, 97–102. doi: 10.1016/j.bej.2013.05.010

Toyama, H., Furuya, N., Saichana, I., Ano, Y., Adachi, O., and Matsushita, K. (2007). Membrane-Bound, 2-Keto-D-gluconate-yielding D-gluconate dehydrogenase from "Gluconobacter dioxyacetonicus" IFO 3271: molecular properties and gene disruption. *Appl. Environ. Microbiol.* 73, 6551–6556. doi: 10.1128/AEM.00493-07

Trivedi, P., and Sa, T. (2008). *Pseudomonas corrugata* (NRRL B-30409) mutants increased phosphate solubilization, organic acid production, and plant growth at lower temperatures. *Curr. Microbiol.* 56, 140–144. doi: 10.1007/s00284-007-9058-8

Umezawa, K., Takeda, K., Ishida, T., Sunagawa, N., Makabe, A., Isobe, K., et al. (2015). A novel pyrroloquinoline quinone-dependent 2-keto-D-glucose dehydrogenase from *Pseudomonas aureofaciens*. *J. Bacteriol.* 197, 1322–1329. doi: 10.1128/JB.02376-14

Vyas, P., and Gulati, A. (2009). Organic acid production *in vitro* and plant growth promotion in maize under controlled environment by phosphate-solubilizing fluorescent *Pseudomonas*. *BMC Microbiol.* 9:174. doi: 10.1186/1471-2180-9-174

Wang, D. M., Sun, L., Sun, W. J., Cui, F. J., Gong, J. S., Zhang, X. M., et al. (2019). A membrane-bound gluconate dehydrogenase from 2-keto-d-gluconic acid industrial producing strain *Pseudomonas plecoglossicida* JUIM01: purification, characterization, and gene identification. *Appl. Biochem. Biotech.* 188, 897–913. doi: 10.1007/s12010-019-02951-0

Wang, X. J., Cheng, X. Z., Feng, C. L., and Wang, L. L. (2014). Study on fermentation conditions of 2-keto-D-gluconic acid by P. putida KD-1. *China Food Addit.* 3, 109–114. doi: 10.3969/j.issn.1006-2513.2014.03.011

Xie, Z. J., Li, S. Y., Tang, S. C., Huang, L. J., Wang, G. X., Sun, X. L., et al. (2019). Phosphorus leaching from soil profiles in agricultural and forest lands measured by a cascade extraction method. *J. Environ. Qual.* 48, 568–578. doi: 10.2134/jeq2018.07.0285

Yu, L. Y., Huang, H. B., Wang, X. H., Li, S., Feng, N. X., Zhao, H. M., et al. (2019). Novel phosphate-solubilising bacteria isolated from sewage sludge and the mechanism of phosphate solubilisation. *Sci. Total Environ.* 658, 474–484. doi: 10.1016/j.scitotenv.2018.12.166

Yum, D. Y., Lee, Y. P., and Pan, J. G. (1997). Cloning and expression of a gene cluster encoding three subunits of membrane-bound gluconate dehydrogenase from *Erwinia cypripedii* ATCC 29267 in *Escherichia coli*. *J. Bacteriol.* 179, 6566–6572. doi: 10.1128/jb.179.21.6566-6572.1997

Zaheer, A., Malik, A., Sher, A., Mansoor Qaisrani, M., Mehmood, A., Ullah Khan, S., et al. (2019). Isolation, characterization, and effect of phosphate-zinc-solubilizing bacterial strains on chickpea (*Cicer arietinum* L.) growth. *Saudi J. Biol. Sci.* 26, 1061–1067. doi: 10.1016/j.sjbs.2019.04.004

Conflict of Interest: The authors declare that the research was conducted in the absence of any commercial or financial relationships that could be construed as a potential conflict of interest.

Publisher's Note: All claims expressed in this article are solely those of the authors and do not necessarily represent those of their affiliated organizations, or those of the publisher, the editors and the reviewers. Any product that may be evaluated in this article, or claim that may be made by its manufacturer, is not guaranteed or endorsed by the publisher.

Copyright © 2022 Yu, Wu, Zhang, Zhou, Harvey, Wang, Fan, Xie, Li, Zhou, Zhao and Zhang. This is an open-access article distributed under the terms of the Creative Commons Attribution License (CC BY). The use, distribution or reproduction in other forums is permitted, provided the original author(s) and the copyright owner(s) are credited and that the original publication in this journal is cited, in accordance with accepted academic practice. No use, distribution or reproduction is permitted which does not comply with these terms.

frontiers | Frontiers in Microbiology

ORIGINAL RESEARCH
published: 20 May 2022
doi: 10.3389/fmicb.2022.891245

Volatile Organic Compounds of *Streptomyces* sp. TOR3209 Stimulated Tobacco Growth by Up-Regulating the Expression of Genes Related to Plant Growth and Development

Yuxi He[1], Wenyu Guo[1,2], Jieli Peng[1], Jinying Guo[2], Jia Ma[1], Xu Wang[1], Cuimian Zhang[1], Nan Jia[1], Entao Wang[3], Dong Hu[1] and Zhanwu Wang[1]**

[1] Institute of Agro-Resources and Environment/Hebei Fertilizer Technology Innovation Center, Hebei Academy of Agriculture and Forestry Sciences, Shijiazhuang, China, [2] School of Landscape and Ecological Engineering, Hebei University of Engineering, Handan, China, [3] Departamento de Microbiología, Escuela Nacional de Ciencias Biológicas, Instituto Politécnico Nacional, Mexico City, Mexico

OPEN ACCESS

Edited by:
Reiner Rincón Rosales, Tuxtla Gutierrez Institute of Technology, Mexico

Reviewed by:
Laith Khalil Tawfeeq Al-Ani, Universiti Sains Malaysia, Malaysia
Mohsen Mohamed Elsharkawy, Kafrelsheikh University, Egypt

***Correspondence:**
Dong Hu
donghu1983@163.com
Zhanwu Wang
zhanwuw@126.com

Specialty section:
This article was submitted to Microbe and Virus Interactions with Plants, a section of the journal Frontiers in Microbiology

Received: *07 March 2022*
Accepted: *08 April 2022*
Published: *20 May 2022*

Citation:
He Y, Guo W, Peng J, Guo J, Ma J, Wang X, Zhang C, Jia N, Wang E, Hu D and Wang Z (2022) Volatile Organic Compounds of Streptomyces sp. TOR3209 Stimulated Tobacco Growth by Up-Regulating the Expression of Genes Related to Plant Growth and Development. Front. Microbiol. 13:891245. doi: 10.3389/fmicb.2022.891245

To investigate the mechanism underlying the plant growth-promoting (PGP) effects of strain *Streptomyces* sp. TOR3209, PGP traits responsible for indoleacetic acid production, siderophore production, and phosphate solubilization were tested by culturing the strain TOR3209 in the corresponding media. The effects of volatile organic compounds (VOCs) produced by the strain TOR3209 on plant growth were observed by co-culturing this strain with tobacco seedlings in I-plates. Meanwhile, the effects of VOCs on tobacco gene expression were estimated by performing a transcriptome analysis, and VOCs were identified by the solid-phase micro-extraction (SPME) method. The results showed positive reactions for the three tested PGP traits in the culture of strain TOR3209, while the tobacco seedlings co-cultured with strain TOR3209 revealed an increase in the fresh weight by up to 100% when compared to that of the control plants, demonstrating that the production VOCs was also a PGP trait. In transcriptome analysis, plants co-cultured with strain TOR3209 presented the highest up-regulated expression of the genes involved in plant growth and development processes, implying that the bacterial VOCs played a role as a regulator of plant gene expression. Among the VOCs produced by the strain TOR3209, two antifungal molecules, 2,4-bis(1,1-dimethylethyl)-phenol and hexanedioic acid dibutyl ester, were found as the main compounds. Conclusively, up-regulation in the expression of growth- and development-related genes via VOCs production is an important PGP mechanism in strain TOR3209. Further efforts to explore the effective VOCs and investigate the effects of the two main VOCs in the future are recommended.

Keywords: RNA sequencing, SPME, *Streptomyces*, plant growth-promoting rhizobacteria (PGPR), volatile organic compounds (VOCs)

INTRODUCTION

In the context of population growth and rapid economic development, chemical fertilizers/pesticides have been used in agriculture to increase production, while the excessive use of these chemicals has caused serious negative impacts on the agricultural ecosystems (Vejan et al., 2016). To reduce the application of chemical fertilizers/pesticides while maintaining high production, environment-friendly biofertilizers and biopesticides have been explored (Parewa et al., 2021). In the development of biofertilizers and biopesticides, microorganisms and their metabolites have received a lot of attention, since their interactions with the plants could improve the growth and production (Saharan and Nehra, 2011; Bhattacharyya and Jha, 2012) by various mechanisms, as mentioned in the following sections. In general, all the microbes with plant growth-promoting (PGP) abilities are called PGP microorganisms; among them, the bacteria colonized in the rhizosphere, so-called PGP rhizobacteria (PGPR), have been studied extensively and applied widely (Basu et al., 2021; Mohanty et al., 2021).

Many studies on PGPR have been focused on the capacities of the bacteria to promote plant health, such as growth-enhancing potential, stress tolerance, and the production of useful biologically active secondary metabolites (Spaepen and Vanderleyden, 2011). PGPR can stimulate plant growth by various mechanisms, such as nitrogen fixation (Nassar et al., 2005), phosphate dissolution, siderophore production, antibiotic secretion, and production of plant beneficial volatile organic compounds (VOCs) (Oleńska et al., 2020). They can also promote nutrient availability, nutrient uptake (Pailan et al., 2015), and produce plant hormones, such as auxins (Lee et al., 2012), cytokinins (Lugtenberg and Kamilova, 2009), abscisic acid (Sgroy et al., 2009), and gibberellins (Khan et al., 2014). These abilities can significantly help and improve the growth of their host plants. Therefore, the PGP microorganisms, such as *Rhizobium*, *Bacillus*, *Pseudomonas*, *Streptomyces,* and *Trichoderma,* and their metabolites have attracted increasing attention in the production of biological fertilizers and/or biopesticides (Atieno et al., 2020).

The members of the genus *Streptomyces* are Gram-positive, spore-forming bacteria that are widely distributed in the soil and other habitats, and they are well known for their ability to produce a large number of bioactive secondary metabolites (antibiotics) (Quinn et al., 2020), but rarely act as phytopathogens (Li et al., 2019). Recently, *Streptomyces* strains have been utilized as PGPR for several crops, including wheat (Akbari et al., 2020), tomato (Hu et al., 2020), chickpea (Gopalakrishnan et al., 2015), sorghum (Gopalakrishnan et al., 2013), and rice (Suárez-Moreno et al., 2019). The PGP effects of these *Streptomyces* strains have been attributed to their production of siderophores and indole-3-acetic acid, nitrogen fixation, and phosphate solubilization, which make them potential biofertilizers (Romano-Armada et al., 2020). In addition, some of the *Streptomyces* strains could improve plant growth and production by increasing the plant resistance to phytopathogens and to the abiotic stresses, which is related to their production of chitinolytic enzymes (inhibiting insects and fungi), induction of non-specific plant resistance, production of bioactive compounds (VOCs), and antibiotic/siderophore production (Romano-Armada et al., 2020). From *Streptomyces* species, more than 120 volatile substances belonging to alkenes, esters, alcohols, and ketones have been detected (Schöller et al., 2002), and various functions of these VOCs have been reported in agriculture, including PGP effects and phytopathogen control (Olanrewaju and Babalola, 2019). However, the mechanism by which the VOCs produced by *Streptomyces* promote plant growth and development is unclear.

Volatile organic compounds are secondary metabolites produced by many fungi and bacteria (Korpi et al., 2009), which are believed to act as signal molecules in interspecific and intraspecific interactions and in intercellular communication (Schmidt et al., 2015). Therefore, the in-depth study on the effects of VOCs on plant gene expression might provide some insight into the interactions between microbes and plants, as well as into the exploration of biofertilizers/biopesticides. Previously, *Streptomyces* sp. TOR3209 was isolated from the rhizosphere of tomato as a PGP bacterium (Hu et al., 2012), and the inoculation of this strain could significantly promote the growth and enhance the yield of tomato and other crops by changing the structure of the microbial community in the rhizosphere (Hu et al., 2020). However, its capacity to produce VOCs and whether the VOCs play a role in inducing the PGP effects have not been revealed. To check if the VOC production is one of the mechanisms of PGP effects in the strain TOR3209 and to estimate the effects of plant metabolism, we evaluated the PGP ability of VOCs produced by *Streptomyces* sp. TOR3209 and investigated the molecular composition of these VOCs. We also identify the important molecular events involved in the rhizosphere bacteria–plant interaction by transcriptome analysis.

MATERIALS AND METHODS

Incubation of Bacteria and Inoculant Preparation

The strain *Streptomyces* sp. TOR3209 originally isolated from the rhizosphere of tomato plants (Hu et al., 2012) was used in this study, considering its role in the promotion of growth in tomatoes and other plants (Hu et al., 2020). To prepare the inoculant, the strain TOR3209 was massively inoculated on plates containing the Gause's No.1 medium (soluble starch 20 g, KNO_3 1.0 g, K_2PO_4 0.5 g, $MgSO_4{\cdot}7H_2O$ 0.5 g, NaCl 0.5 g, $FeSO_4{\cdot}7H_2O$ 0.01 g, Agar 20 g, in 1 L of distilled water, pH 7.2–7.4) and incubated at 30°C for 24 h. Then the bacterial biomass was scraped off the plate, suspended in sterilized 10 mM $MgCl_2$, and adjusted to 10^8–10^9 CFU/ml based on both optical density ($OD_{600} = 1.0$) and plate count. To test the effects of VOCs, strain TOR3209 was cultured overnight in Gause's No.1 liquid medium at 30°C with shaking at 180 rpm.

Plant Growth-Promoting Test

To estimate the PGP effects of strain TOR3209 or its VOCs, tobacco (*Nicotiana benthamiana* Domin) was used as a model plant, which showed a positive response to inoculation of strain TOR3209 in our previous study. The seeds of tobacco were purchased from Huayueyang Biotechnology (Beijing) Co., Ltd.

Growth Promotion of Plants by Inoculation

The seeds were surface sterilized with 95% ethanol for 30 s, 2% (v/v) sodium hypochlorite for 5 min, and then washed with sterile distilled water (SDW) three times as described previously (Hu et al., 2020). The surface-sterilized seeds were germinated on 0.5× Murashige and Skoog (MS) medium (PhytoTechnology, United States) supplemented with 1.5% (w/v) sucrose and 1.8% agar (w/v). The MS agar plates with seeds were kept at 4°C for 12 h for vernalization and then kept in a plant growth chamber for germination at 25°C under a long-day photoperiod (day/night: 16/8 h) with a light intensity of 100 μmol m^{-2} s^{-1}. After 5 days of incubation, the seedlings were transferred to a 24-well plate containing the MS agar and incubated in the plant growth chamber with 16 h light/8 h dark conditions. Five days later, tobacco plants in the plate were inoculated with 20 μl of inoculant (10^{8-9} CFU/ml) around the root, and the negative control plants were inoculated with 20 μl of sterilized 10 mM $MgCl_2$ solution. The tobacco seedlings were harvested 5 days after the inoculation, and total fresh weight was measured. The experiment was repeated three times, and 10 replications (seedlings) for each treatment were included each time.

Growth Promotion of Plants by VOCs of Strain TOR3209

Previously, the VOCs of bacteria have been reported as novel agents in promoting plant growth (Audrain et al., 2015). To evaluate the growth-promoting effect of VOCs on the tobacco plants, specialized plastic Petri dishes (I-plates with 9 cm in diameter) were used, which were divided by a partition into two equal chambers. In these I-plates, *Streptomyces* sp. TOR3209 and tobacco plants could be co-cultivated without direct contact. One chamber of the I-plate contained half-strength MS agar, and the other chamber contained Gause's No.1 medium with a sterile filter paper disk (8 mm in diameter) on its surface. After 5 days of germination as mentioned earlier, five seedlings were transferred to the chamber containing MS agar. After 3 days of plant growth, 20 μl of overnight incubated strain TOR3209 (see section Incubation of Bacteria and Inoculant Preparation) or sterilized distilled water (SDW) for treatment and control (CK), respectively, were applied drop-wise onto the filter paper disk in the chamber containing Gause's No.1 medium. Then, the I-plates were sealed with parafilm and cultured in the growth chamber under the day/night cycle of 16/8 h, with a light intensity of 100 μmol m^{-2} s^{-1} at 25°C. The fresh weight of each plant was measured after 1 week of growth. The experiment was repeated independently for three times, and 10 replications (seedlings) per treatment were included each time.

Characterization of Plant Growth-Promoting Traits

To estimate the possible PGP mechanism of strain TOR3209, the PGP traits mentioned by Romano-Armada et al. (2020), such as the formation of indole-3-acetic acid (IAA), production of siderophores, and solubilization of phosphate, were measured for this strain.

Auxin Production Assay

The production of IAA was quantified by the colorimetric method using the Salkowski reagent (50 ml of 35% $HClO_4$ and 1 ml of 0.5 M $FeCl_3$) (Glickmann and Dessaux, 1995). The strain TOR3209 was activated in LB (Difco) broth for 24 h, and then a full loop of the culture was inoculated in 5 ml of the LB broth for culturing at 30°C with shaking at 180 rpm for 16 h. Then, 20 μl of bacterial suspension was transferred to 5 ml of LB broth supplemented with 0.1% L-tryptophan. After 16 h of incubation, 1 ml of the bacterial culture was centrifuged at 8,000 rpm for 10 min to remove the cells, and 300 μl of the supernatant was mixed with 600 μl of Salkowski reagent. The mixture was left in the dark for 30 min to develop the color (Phi et al., 2010). After the reaction, the absorbance of the mixture was measured at 540 nm using a UV–visible spectrophotometer (MAPADA, China). The concentration of IAA in the culture was calculated (Sigma, USA) based on the standard curve of IAA (serial dilutions from 0 to 50 μg/ml). The experiment was repeated three times, and 10 replications were included for each treatment each time.

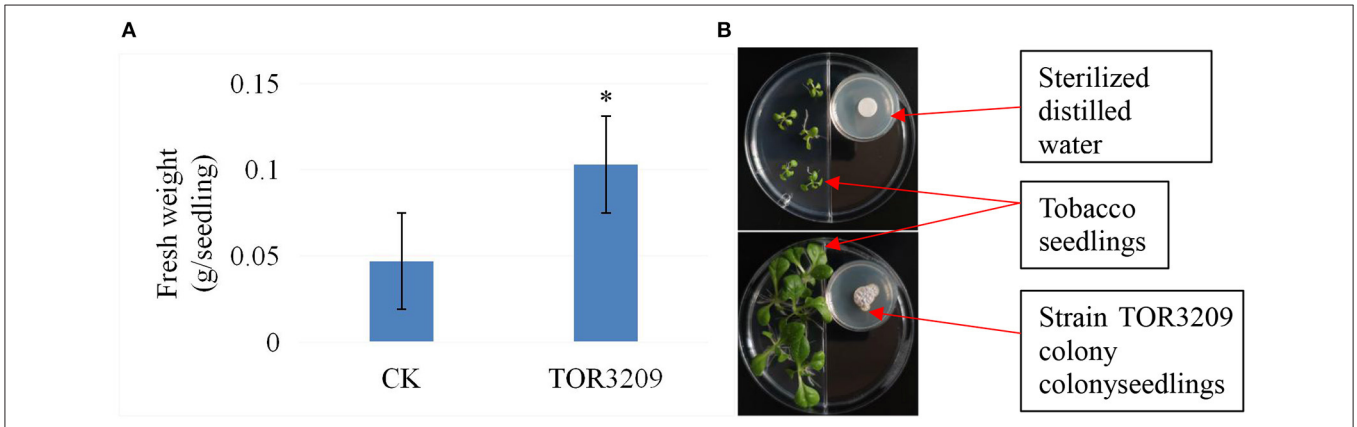

FIGURE 1 | Comparison of effects of strain TOR3209 VOCs on tobacco growth. **(A)** Comparison of fresh weight between the CK seedlings and treatment seedlings; **(B)** Photographs showing the growth promotion on growth of tomato seedlings by strain TOR3209 co-culture (bellow) in comparison with CK control (upper). * The same letter followed the values in the same column means no significant difference based on the least significant difference (LSD) test ($p < 0.05$).

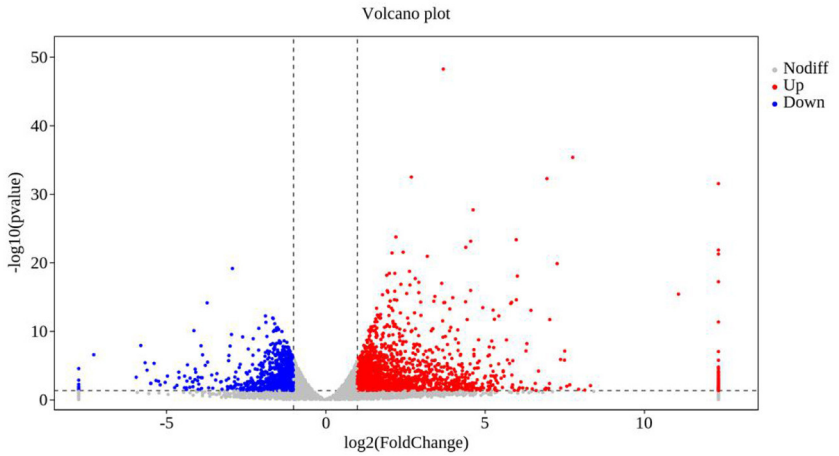

FIGURE 2 | Volcanic diagrams of differential expression genes. The horizontal coordinates are log2 (fold change) and the ordinates are -log10 (*p*-value). The two vertical dashed lines are 2 times the difference threshold, and the horizontal dashed lines are *p*-value 0.05 thresholds. A red dot indicates the upregulated genes group, a blue dot indicates the downregulated genes group, and a gray dot represents a non-significant difference in the expression of the genes group. The scale was fixed considering the minimum and maximum log2 values (between −7.74 and 12.33) included in the **Supplementary Tables 1, 2**.

Siderophore Production

In this analysis, siderophore production was checked as described previously (Neilands, 1987). Briefly, the strain TOR3209 was cultured on Chrome Azurol S (CAS) agar (Pérez-Miranda et al., 2007) and incubated at 30°C for 7 days. The formation of a yellow ring around the colony indicates the production of siderophore. To determine the siderophore type, a $FeCl_3$ test was performed (Chowdappa et al., 2020). Briefly, the strain was cultured in 5 ml of CAS broth at 30°C with rotation for 5 days, and 1 ml of supernatant of the culture obtained by centrifugation (12,000 rpm for 1 min) was mixed with 2 ml of $FeCl_3$ solution (2%, w/v). Then the absorption was scanned from 300 to 600 nm with a spectrophotometer (MAPADA, China). The occurrence of a peak between 420 and 450 nm and a peak at 495 nm demonstrate the presence of hydroxamate and catecholate types of siderophores, respectively. The CAS broth without inoculation was used as a blank to detect the siderophore type. The experiment was repeated three times, and 10 replications were included for each treatment each time.

Phosphate Solubilization

A single colony of strain TOR3209 grown on Gause's No. 1 medium at 30°C for 3 days was inoculated in an organic phosphorus medium (Jiwen et al., 2011) and an inorganic phosphorus (PKO) medium (Nautiyal, 1999), respectively, to measure the phosphorus solubilization. The inoculated plates were cultured at 30°C for 12 days, and the formation of a transparent ring surrounding the colony demonstrated the dissolution of phosphorus. Since the organophosphorus component in the medium is prepared using egg yolk (lecithin), it may undergo denaturation during long-term culture. Therefore, a control plate was set up for the organophosphorus solubilization to avoid false-positive results. The experiment was repeated three times, and 10 replications were included for each treatment each time.

Expression of Plant Genes Responding to the VOCs

After 7 days of exposure to VOCs (co-cultured with strain TOR3209 in I-plates), as mentioned in Section Growth Promotion of Plants by VOCs of Strain TOR3209, the aerial parts (leaves and stems) of tobacco seedlings were collected from three I-plates of treatment or control in triplicate (15 plants in total for treatment or control). Experiments for treatments and controls were repeated three times per group. Total RNA was extracted from the plant samples using the TIANGEN Magnetic Tissue/Cell/Blood Total RNA Kit (DP762- T1A), according to the manufacturer's guidelines. The concentration of RNA in the extracts was determined using a NanoDrop spectrophotometer (Thermo Scientific), and the quality and integrity of RNA in the extracts were tested by agarose gel electrophoresis (Laila et al., 2017). For each extract, 3 μg of RNA was used as input material to construct the sequencing library using the NEBNext Ultra II RNA Library Prep Kit for Illumina (#E7775). The procedure described by Laila et al. (2017) was followed. Briefly, mRNAs were purified from total RNAs using poly-T oligo-attached magnetic beads. Fragmentation was carried out using divalent cations under elevated temperature in an Illumina proprietary fragmentation buffer. The first strand of cDNA was synthesized using random oligonucleotides and SuperScript II. Synthesis of the second strand of cDNA was subsequently performed using DNA polymerase I and RNase H. Remaining overhangs were converted into blunt ends via exonuclease/polymerase activities, and the enzymes were later removed. After adenylation of the 3′ ends of the DNA fragments, Illumina PE adapter oligonucleotides were ligated to prepare for hybridization. To select the cDNA fragments of the preferred size (200 bp), the

TABLE 1 | Most important differentially expressed genes in tobacco plants inoculated with TOR3209.

Gene ID	Log2 fold change	Gene description
Up-regulated genes		
Niben101Scf00107g03008	12.33288866	Cysteine-rich venom protein
Niben101Scf02349g03003	11.07906488	Peroxidase 4
Niben101Scf00661g00002	8.319303503	UDP-glycosyltransferase 74 F1 LENGTH = 449
Niben101Scf08670g00020	8.139389486	Glutamate receptor 2.9
Niben101Scf07123g01015	7.759232431	Leucine-rich repeat receptor-like protein kinase family protein LENGTH = 1,045
Niben101Scf01463g08009	7.667222902	Calmodulin binding protein-like LENGTH = 494
Niben101Scf01942g04001	7.576358542	WRKY transcription factor 44
Niben101Scf02188g00002	7.509948729	WRKY transcription factor 1
Niben101Scf08526g02006	7.503570319	WRKY transcription factor 1
Niben101Scf12084g00003	7.382594655	WRKY transcription factor 1
Niben101Scf01400g00014	7.377702267	Thaumatin-like protein
Niben101Scf02115g04004	7.269910522	Eukaryotic aspartyl protease family protein LENGTH = 474
Niben101Scf12266g09001	7.039494994	Tetratricopeptide repeat (TPR)-like superfamily protein LENGTH=305
Niben101Scf02406g00002	7.031384344	GDSL esterase/lipase
Niben101Scf07589g01006	7.006395689	conserved hypothetical protein (*Ricinus communis*) gb|EEF44100.1| conserved hypothetical protein (*Ricinus communis*)
Niben101Scf06916g01011	6.949992145	NAC domain-containing protein 2
Niben101Scf13429g04019	6.919290018	L-lactate dehydrogenase A-like 6B
Niben101Scf05057g04016	6.905727119	WRKY transcription factor 1
Niben101Scf00892g00003	6.885022202	VQ motif protein (*Medicago truncatula*)
Niben101Scf06301g01003	6.687192872	Aspartic proteinase A1
Niben101Scf00096g00004	6.612642405	Myb family transcription factor APL
Niben101Scf04894g00006	6.58495066	UDP-glucose 4-epimerase
Niben101Scf08351g01002	6.490137969	Tumor susceptibility gene 101 protein
Niben101Scf02041g00002	6.447680321	Chitinase 8
Niben101Scf15327g00001	6.323748925	Calcium-binding protein CML39
Niben101Scf08921g02023	6.32181607	Cathepsin B-like cysteine proteinase 6
Niben101Scf11071g04005	6.293992449	Calmodulin binding protein-like LENGTH = 451
Niben101Scf00332g06012	6.191447348	Pyrophosphate-energized vacuolar membrane proton pump
Niben101Scf04944g05002	6.134053016	WRKY transcription factor 18
Niben101Scf02411g00015	6.088949822	Receptor kinase 3 LENGTH = 850
Niben101Scf02175g06008	6.068739476	Alkaline/neutral invertase LENGTH = 617
Niben101Scf11182g00003	6.021299925	Endonuclease 2
Niben101Scf00149g12021	5.991619157	Pyruvate decarboxylase 4
Niben101Scf04869g03002	5.988250289	Glucan endo-1,3-beta-glucosidase
Niben101Scf02264g06032	5.929532592	receptor kinase 2 LENGTH = 847
Niben101Scf07058g04002	5.880166829	P-loop containing nucleoside triphosphate hydrolases superfamily protein LENGTH = 500
Niben101Scf05099g01002	5.873047764	Mitochondrial import inner membrane translocase subunit Tim17/Tim22/Tim23 family protein LENGTH = 178
Niben101Scf06603g03002	5.867685439	WRKY transcription factor 55
Niben101Scf01444g00001	5.851494959	Inositol-1,4,5-trisphosphate 5-phosphatase 1
Niben101Scf02132g02012	5.848879214	2-aminoethanethiol dioxygenase-like protein (*Medicago truncatula*)
Niben101Scf01001g00003	5.843684467	Glucan endo-1,3-beta-glucosidase
Niben101Scf00526g00018	5.814028502	NAC domain-containing protein 86
Niben101Scf03374g06002	5.777012957	Non-specific lipid transfer protein-like 1
Niben101Scf00870g16006	5.709724282	ATP-dependent RNA helicase eIF4A
Niben101Scf02877g02005	5.681180326	Strictosidine synthase 1
Niben101Scf16244g02026	5.609478878	30S ribosomal protein S19
Niben101Scf03773g00009	5.57985346	Ethylene-responsive transcription factor 9
Niben101Scf10126g00007	5.515465694	Arogenate dehydrogenase LENGTH = 640
Niben101Scf12102g01006	5.441617826	VQ motif protein (*Medicago truncatula*)

(Continued)

TABLE 1 | Continued

Gene ID	Log2 fold change	Gene description
Niben101Scf03595g10007	5.436938026	60S acidic ribosomal protein P1
Niben101Scf13920g00005	5.405652462	Acyl-CoA N-acyltransferases (NAT) superfamily protein (*Arabidopsis thaliana*) putative alanine acetyl transferase (*Arabidopsis thaliana*) gb|AAD15401.1| putative alanine acetyl transferase (*Arabidopsis thaliana*) gb|ABD60717.1| (*Arabidopsis thaliana*) gb|AEC08624.1| GCN5-related N-acetyltransferase-like protein (*Arabidopsis thaliana*)
Niben101Scf01094g03014	5.380529892	Ethylene-responsive transcription factor 1B
Down-regulated genes		
Niben101Scf00495g00003	−7.742771091	Chaperone protein ClpB
Niben101Scf04889g00020	−7.269929829	myb-like transcription factor family protein LENGTH = 233
Niben101Scf04040g08015	−5.793913087	17.3 kDa class II heat shock protein
Niben101Scf06977g00014	−5.659566414	Chaperone protein ClpB
Niben101Scf04040g09011	−5.597721532	17.3 kDa class II heat shock protein
Niben101Scf10384g00015	−5.479676566	17.6 kDa class I heat shock protein
Niben101Scf08675g00002	−5.47869793	BAG family molecular chaperone regulator 6
Niben101Scf03114g03011	−5.377817272	Chaperone protein HtpG
Niben101Scf00298g00001	−5.316649482	Ethylene-responsive transcription factor 1
Niben101Scf05378g03025	−5.236085551	ATP-dependent zinc metalloprotease FtsH
Niben101Scf02175g06018	−5.185219051	BAG family molecular chaperone regulator 6
Niben101Scf04040g09016	−5.028860367	17.3 kDa class II heat shock protein
Niben101Scf10306g00005	−4.958344447	17.3 kDa class II heat shock protein
Niben101Scf02552g00013	−4.659113231	Subtilisin-like serine protease 2 LENGTH = 764
Niben101Scf10384g00016	−4.602974453	17.6 kDa class I heat shock protein
Niben101Scf02124g01003	−4.593158829	Heat shock 70 kDa protein
Niben101Scf07790g00006	−4.426069226	COBRA-like protein 10
Niben101Scf04410g09016	−4.419070922	Chaperone protein ClpB
Niben101Scf02267g00013	−4.344794817	17.3 kDa class II heat shock protein
Niben101Scf01412g00015	−4.328983756	17.7 kDa class II heat shock protein
Niben101Scf02913g00028	−4.256421593	Alpha-galactosidase
Niben101Scf09552g01024	−4.24630503	Protein kinase superfamily protein with octicosapeptide/Phox/Bem1p domain LENGTH = 1,054
Niben101Scf00117g02017	−4.1759724	Octic, putative isoform 1 (*Theobroma cacao*)

library fragments were purified using the AMPure XP system (Beckman Coulter, Beverly, CA, USA). DNA fragments with ligated adaptor molecules on both ends were selectively enriched using Illumina PCR Primer Cocktail in a 15-cycle PCR reaction. Products were purified (AMPure XP system) and quantified by performing the Agilent High Sensitivity DNA assay on a Bioanalyzer 2100 system (Agilent). The sequencing library was then sequenced commercially on a Novaseq platform (Illumina) by Shanghai Personal Biotechnology Cp. Ltd. Filtration of high-quality reads by eliminating low-quality reads ($Q < 20$), removal of adapter, assembling of the transcriptome, and quantification of transcript abundances were performed as described by Howlader et al. (2020).

The gene expression levels between the samples subjected to VOC treatment and the control were estimated by using fragments per kilobase of transcript per million fragments mapped (FPKM) values, as described by Howlader et al. (2020). In the transcription group, we generally took into account FPKM > 1 when the gene was expressed. Pearson correlation coefficients were used to determine the level of correlation between the expression of genes in the samples to test the reliability of the experiments and whether sample selection was reasonable (van Ruissen et al., 2005). The log2 fold change was calculated by dividing the FPKM values of the treatment groups by the values of the control group. High-quality reads were processed using the Perl script, and the differentially expressed genes (DEGs) were identified using the edgeR package (Boscari et al., 2013), taking a fold change ≥ 2 as the threshold value.

The cluster analysis of FPKM-normalized expression values was carried out, as mentioned by Howlader et al. (2020), to differentiate the up- and down-regulated transcripts between the VOC treatment and the control samples, by using the cluster software version 3.0 and the Java TreeView to visualize the dendrogram. For GSEA, the KEGG pathway collection (Homo sapiens (human) Release 53.0) (Kanehisa and Goto, 2000) was used to define the gene sets using the GSEABase package in Bioconductor/R version 2.9.2 (Gentleman, 2004). Gene ontology (GO) and the Kyoto Encyclopedia of Genes and Genomes (KEGG) pathway enrichment analysis were used to characterize the differentially expressed genes, and GO functional annotations were obtained from the non-redundant annotation results using the Blast2GO software (Conesa et al., 2005).

Extraction and Identification of VOCs

The strain TOR3209 was activated by culturing in Luria-Bertani (LB) broth (NaCl 10 g, tryptone 10 g, yeast extract 5 g, distilled water 1 L, pH 6.8–7.2) for 16 h at 30°C with shaking at 180 rpm. Then 40 μl of the culture was dropped on the LB agar in bottles ($18 \times 18 \times 3$ cm^3) and cultured for 3 days at 30°C. The VOCs produced in the bottles were extracted and detected commercially by the solid-phase micro-extraction (SPME) method (Agilent, 6890N-5975B MSD, USA) (Gu et al., 2007). Briefly, SPME fibers were introduced into the atmosphere of the bottle to absorb the VOCs. Then, the SPME fibers with VOCs were incubated at 70°C for 20 min and were desorbed at 250°C for 5 min in the injection port using a DB-WAX column (30 m × 0.25 mm × 0.25 μm - polar, J&W Scientific, Folsom, CA). The initial oven temperature

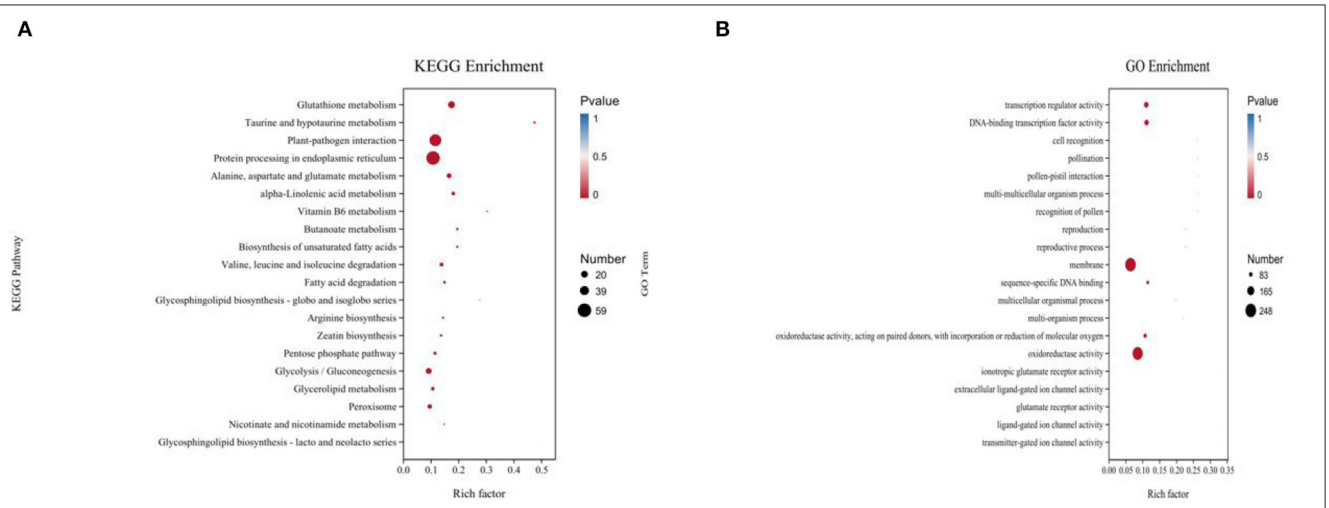

FIGURE 3 | Gene ontology (GO) **(A)** and KEGG pathway-rich analysis **(B)**. Based on the GO-rich and KEGG results, the extent of richness is measured by the rich factor, false discovery rate (FDR) values, and the number of genes that were collected into this GO term or KEGG pathway. Rich factor refers to the ratio of the number of different genes collected in the GO term or KEGG pathway to the number of genes annotated.

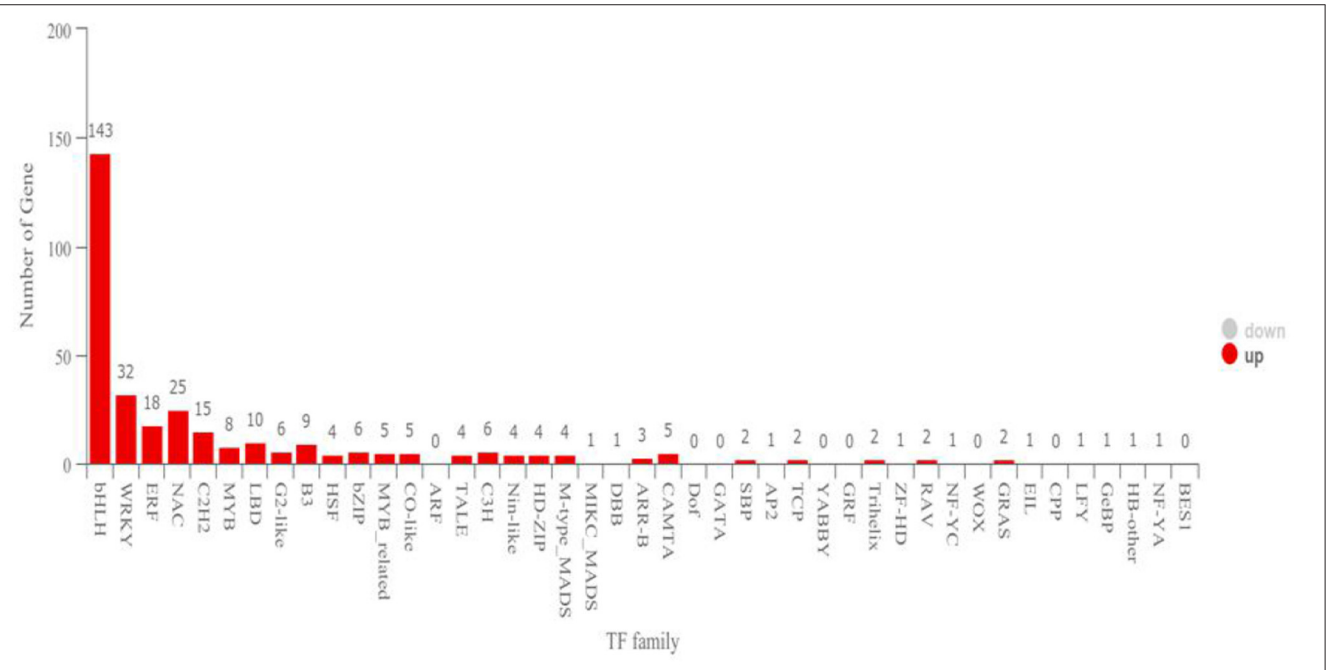

FIGURE 4 | Transcription factor family. The horizontal coordinates are different transcription factor families, and the ordinates are the number of genes that fall into that transcription factor family.

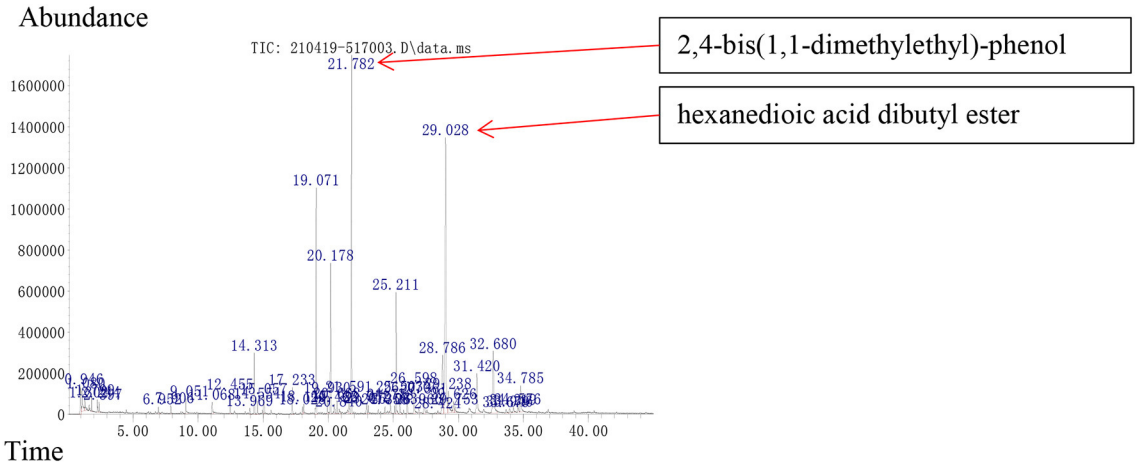

FIGURE 5 | Volatile organic compounds of strain TOR3209 using GC-MS. The samples were incubated in bottle containing LB agar for 3 days. 2,4-bis(1,1-dimethylethyl)-phenol and hexanedioic acid dibutyl ester were detected.

was 40°C (held for 2 min), ramped at 2°C/min to 220°C, and finally ramped at 20°C/min to 240°C (held for 10 min). GC–MS runs were performed for a total of 103 min. Compounds were identified by comparing their retention indices (RI) determined relatively to a homologous series of pure n-alkane standards or values reported in the literature (Jennings and Shibamoto, 1980). Fragmentation patterns in the mass spectra were also compared with those available in the Library of the National Institute of Standards and Technology (NIST05). The effective compounds were identified and estimated according to the methods described in the literature (Li et al., 2018; Chowdhary and Sharma, 2020). Experiments for treatments and controls were repeated three times per group.

Statistical Analysis

The data obtained from the plant growth promotion test were statistically analyzed by ANOVA, and the mean values of the treated samples were separated by the least significant difference (LSD) test at $p < 0.05$ using SPSS version 19.0 (SPSS Inc., USA). Experiments were done in 10 replicates, and each experiment was repeated for three times. The results of repeated trials of each experiment were similar. Therefore, one representative trial for each experiment is reported in the Section Results.

RESULTS

Effects of Strain TOR3209 Inoculation and VOCs on the Growth of Plant

In the growth tests (**Supplementary Table 1**), a tendency toward the promotion of growth was observed in the tobacco seedlings. The seedlings grown in MS medium inoculated with strain TOR3209 showed a 20% increase in their total fresh weight after 5 days of inoculation, in comparison with the controls. However, the increase in growth was not significant according to the LSD test. In I-plates, the total fresh weight of tobacco seedlings co-incubated with strain TOR3209 was significantly elevated up to 100% (**Figure 1**).

PGP Traits of *Streptomyces* sp. TOR3209

The analysis of IAA production showed that strain TOR3209 produced 12.06 μg/ml of IAA in the culture. In the P solubilization test, the strain TOR3209 grew slowly and weakly on the PKO medium. After 2–7 days of incubation, the colonies gradually expanded, and the phosphate solubilizing ring gradually appeared, but the ring was not clear and remained unchanged after 7 days. On organophosphorus medium, strain TOR3209 presented a more obvious dissolving effect. After 5 days of incubation, the solubilization ring was very obvious (SI = 1.6), and it continuously expanded until the entire plate became almost transparent. On CAS medium, colonies of strain TOR3209 began to grow after 1 week of incubation with the appearance of yellow circles, indicating the production of siderophores. Based on the result of the $FeCl_3$ test, the siderophores produced by the strain TOR3209 were hydroxamate type. Detailed results for PGP traits of *Streptomyces* sp. TOR3209 are available in **Supplementary Figure 1**.

Transcriptomal Analysis of Tobacco Plants Responding to VOCs

In transcriptomal analysis, 38,254 genes were detected in the plants co-cultured with strain TOR3209, and 37,636 genes were detected in the control plants. Analysis of RNAseq data revealed that 3,191 differentially expressed transcripts (DEGs) were induced by the VOCs of strain TOR3209, including 2,155 up-regulated and 1,036 down-regulated transcripts (**Figure 2**). The most important (Log2 fold change >5 or <-4) up-regulated (52) and down-regulated (23) transcripts are listed in **Table 1**. Among them, UDP-glycosyltransferase, glutamate

receptor, RING/U-box protein with C6HC-type zinc finger, and leucine-rich repeat receptor-like protein kinase family protein were the highest up-regulated DEGs in the VOC-treated tobacco seedlings. Chaperone protein ClpB, MYB-like transcription factor family protein, and 17.3 kDa class II heat shock proteins were significantly repressed by the VOC treatment.

In the functional annotation, DEGs with the largest increase in expression were those related to cell recognition, pollination, pollen–pistil interaction, multi-multicellular organism process, and recognition of pollen based upon the GO enrichment analyses (**Figure 3**; **Table 1**). Based on the KEGG pathway, the most significant up-regulated transcripts by VOCs were categorized as those related to glutathione metabolism, taurine and hypotaurine metabolism, and glycosphingolipid biosynthesis pathways (**Figure 3**). The expression profile of TF genes displays the upcoming transcription actions regulated by these genes. The largest TF families detected in our study were basic helix-loop-helix (bHLH) DNA-binding superfamily protein, WRKY, NAC domain-containing protein (NAC), ethylene-responsive factor (ERF), and zinc finger protein genes (C2H2) (**Figure 4**).

Analysis of VOCs Produced by *Streptomyces* sp. TOR3209

In GC–MS analysis, 48 compounds were detected, among which eight (accounting for 15.22% of the total VOCs) were reported as PGP effective VOCs, and 14 (accounting for 37.36% of the total VOCs) had the potential to increase the resistance of the plant to phytopathogens (**Supplementary Table 2**). According to their relative abundances, seven compounds could be identified as the main components, each contributing to more than 5% of the total: the pathogen-inhibiting compounds like trans-1,10-dimethyl-trans-9-decalol (9.43%), 1,4,5,6,7,8,9,9a-octahydro-1,1,7-trimethyl-[3aR-(3a.alpha.,7.alpha.,9a.beta.)]-3a,7-methano-3aH-cyclopentacyclooctene (6.29%), and 2,4-bis(1,1-dimethylethyl)- phenol (13.61%); the growth-promoting compounds like n-hexadecanoic acid (6.53%) (Chowdhary and Sharma, 2020); and the compounds of an unknown function like (-)-.alpha.-Panasinsen (5.12%), pentadecanoic acid (5.58%), and hexanedioic acid dibutyl ester (25.58%). Among these compounds, 2,4-di-tert-butylphenol [o 2,4-bis(1,1-dimethylethyl)- phenol] and dibutyl adipate (o hexanedioic acid dibutyl ester) were the most abundant VOCs produced by the strain TOR3209 (**Figure 5**).

DISCUSSION

It is well known that some microorganisms have the potential to promote plant growth through direct and/or indirect effects. The direct effects include the production of molecules that promote plant growth (Goswami et al., 2016). In this study, the growth (total fresh weight) of tobacco seedlings was significantly increased (100%) by co-culturing with the strain *Streptomyces* sp. TOR3209 (**Figure 1**; **Supplementary Table 1**), demonstrating that this strain produced VOCs as PGP agents, consistent with the previous reports for other microbial VOCs (Kanchiswamy et al., 2015). These results suggest an alternative mechanism for the PGP effects of strain TOR3209, other than the previously described regulation of the rhizosphere microbial community (Hu et al., 2020).

As reported previously, the VOCs mainly react with the aerial parts of the plants (Asari et al., 2016). Considering the low amount of VOCs, it could be hypothesized that they cannot function as nutrients, but can serve as signals to regulate the production of plant genes related to growth. Indeed, the transcriptome analysis based upon the KEGG analysis (Kanehisa and Goto, 2000) in the present study revealed that VOCs of strain TOR3209 up-regulated the expression of multiple genes to improve plant growth. The highest increase in the expression was noted for the genes of UDP-glycosyltransferase, glutamate receptor, RING/U-box protein with C6HC-type zinc finger, and leucine-rich repeat receptor-like protein kinase family protein in the VOC treatment samples, which indicated the possible relationships between these genes and the increased growth. The expression of UDP-glucuronosyltransferase (UGT) in meristematic cells is correlated with mitosis and is required for the normal development of plants (Woo et al., 1999). So, the VOCs of strain TOR3209 might increase plant growth by promoting cell division. Also, glycosylation is a universally important mechanism in certain organisms to control the impact of a wide range of hydrophobic compounds that can directly derange cellular metabolism (Nebert, 1991). Therefore, VOCs of strain TOR3209 might also promote plant growth by regulating the UGT-mediated glycosylation in plants. Plant glutamate receptor-like genes (GLRs) coded amino acid receptors related to plant defense and innate immune response (Forde and Roberts, 2014). Recently, the role of GLRs in controlling the plant height has also been established (Kaur, 2020), which further explained the PGP effects of VOCs produced by strain TOR3209. U-box proteins play important myriad functions in plants, such as in growth and development, cell cycle regulation, morphogenesis, stress resistance, and regulating the innate immune response of plants to biotic stress factors. Therefore, strain TOR3209 was capable of promoting growth through VOCs that induce the expression of genes coding U-box proteins and LRR-RLKs (Liu et al., 2017), which further regulate the expression of other genes related to the plant growth and development, including the synthesis of proteins and enzymes.

Transcription factors (TFs) play essential roles in plants, as well as in all other living organisms, by controlling the expression of genes involved in various cellular processes (Han et al., 2014). Numerous processes, such as brassinosteroid signaling, ABA signaling, and axillary meristem formation, are regulated by the members of the bHLH family of TFs during the seedling development (Zhao et al., 2012). A total of 143 transcripts were identified as bHLH TF proteins in the present study, which have been identified as phytochrome-interacting factors (Toledo-Ortiz et al., 2003) and constitute the largest TF family proteins that are produced during the interaction of tobacco plants with the VOCs of strain TOR3209. These results further indicated that the VOCs produced by strain TOR3209 were capable of promoting plant growth by regulating a serial synthesis of TFs. Another large NAC TF family was involved in inducing diverse developmental events in *Arabidopsis* and soybean (Shamimuzzaman and Vodkin,

2013). This NAC TF family has the capacity to permit crosstalk between different pathways (Olsen et al., 2005). In our present study, 25 putative NAC genes were detected during plant growth. Furthermore, genes encoding C_2H_2 zinc finger protein play a significant role in the development and differentiation (Razin et al., 2012). During the interaction, 15 putative C_2H_2 zinc finger genes were identified. In addition, ethylene-responsive factor (ERF) TFs belonging to the Apetala2/ERF TF family were also found to be involved in plant growth. The WRKY genes coding TFs were involved in a broad range of biological processes, including diverse biotic/abiotic stress responses, and developmental and physiological processes (Birkenbihl et al., 2017). A total of 18 putative ERF and 32 putative WRKY genes were detected during plant development in the present study. So, it is clear that the VOCs of *Streptomyces* sp. TOR3209 could regulate diverse metabolism pathways, which further improved the growth of tobacco plants.

The significantly down-regulated genes in the samples subjected to VOC treatment were chaperone protein ClpB, MYB-like transcription factor family protein, and 17.3 kDa class II heat shock proteins. These three genes and most of the other down-regulated genes are genes that confer adaptation to environmental stress. ClpB (caseinlytic proteinase) is related to the disaggregation of protein complexes and cell adaptation to heat stress (HS) (Mishra and Grover, 2016). A MYB-like transcription factor is involved in plant abiotic stress (like salt) tolerance and phytohormone signal transduction (Zhang et al., 2018). Furthermore, the 17.3 kDa class II heat shock proteins are also stress tolerance proteins related to heat shock (Kang et al., 2021). The reason why the expression of these genes was elevated by VOC treatment is not very clear, but it is possible that the VOCs shuttled down the expression of genes related to some unnecessary cell functions, while stimulating the expression of other genes essential for plant growth.

Previously, more than 120 VOCs have been detected in *Streptomyces*, which have been classified into different chemical groups, such as alkanes, alkenes, esters, alcohols, and ketones (Schöller et al., 2002). According to the literature, 15.22% (eight) of the VOC molecules detected in the present study presented PGP effects, which might be the potential compounds directly responsible for the growth promotion of tobacco seedlings in the I-plates co-cultured with strain TOR3209. Meanwhile, more VOCs (37.36%, 14 molecules) were related to the resistance to phytopathogens; however, it is not clear whether these VOCs can also promote the growth of plants. As the most abundant compound (25.58%) in the VOCs of strain TOR3209, the effects of hexanedioic acid dibutyl ester on the plant has not been reported and its function in regulating plant growth deserves further study.

In the PGP trait analysis, 12.06 μg/ml of IAA production by strain TOR3209 was recorded, which is relatively a high level since values around 5 to 10 μg/ml are commonly reported. However, some actinobacterial strains capable of producing more than 40 μg/ml have been isolated (Vasconcellos et al., 2010). In addition, the IAA production efficiency of strain TOR3209 might be increased by optimizing the culture conditions, because the production of IAA by a *Streptomyces* strain was increased from 20.46 to 82.36 μg/ml by modifying the medium components (Myo et al., 2019). Therefore, strain TOR3209 could be a good stimulator of plant growth via the production of IAA, as described for other *Streptomyces* strains and other bacteria (Hayat et al., 2010). Another PGP trait of strain TOR3209 is to dissolve phosphate, particularly the organic phosphate, which could subsequently promote plant growth (Spaepen et al., 2007). In this study, we also proved the ability of strain TOR3209 to produce siderophore, a low-molecular-weight iron-binding compound that could help the plant chelate iron in the Fe^{3+} restricted soil (Bottini et al., 2004) and inhibit plant pathogens due to their competitive role (Otieno et al., 2015). Currently, many siderophore molecules, with diverse chemical structures and different bioactivities against a wide spectrum of pathogenic bacteria, have been isolated from *Streptomyces* species (Terra et al., 2021). Different from the previous reports that the *Strteptomyces tendae* Tü 901/8c and *Streptomyces* sp. Tü 6125 isolated from soils produced the catecholate siderophore (Fiedler et al., 2001), the strain TOR3209 produced the hydroxamate siderophore, indicating that different *Streptomyces* species might have distinct pathways for the synthesis of siderophore. Although the PGP features of strain TOR3209 were detected in the present study, they might not contribute to the growth of tobacco seedlings in the inoculation test in the present study, since they are not necessary for the plants grown in the sterilized medium, which is different from the situation in soils (Hu et al., 2020). However, the capacity of *Streptomyces* species to produce IAA and siderophore deserves further study to explore their biofertilizer and biopesticide properties.

In our present study, the promotion of plant growth was not statistically significant following the direct inoculation of strain TOR3209, but it was significant in VOC treatments (**Supplementary Table 1**). This was inconsistent with the previous results that inoculation with strain TOR3209 significantly promoted the growth of tomato plants (Hu et al., 2020). This discrepancy might be related to the differences in the culture conditions because the inoculated plants were cultured in soil (Hu et al., 2020), while the experiments in our study were carried out in medium or artificial substrate. In the medium, the rhizosphere microbiome is absent and the nutrients are not limited, which might also explain why the direct inoculation with the strain could not significantly improve the growth of tobacco seedlings in the present study. Furthermore, plant genotypes (Schwachtje et al., 2012) and environmental conditions (Martínez et al., 2011) also affect the inoculation effects of PGPR, and even the PGP effects of microbial siderophore could be different for distinct tobacco varieties (Robin et al., 2006).

CONCLUSION

The VOCs of strain TOR3209 could improve the growth of the tested plants and induce the up-regulated expression of a key group of genes associated with plant growth and development and the down-regulation of some adaptation genes. Remarkably, our results suggest that the genes related

to UDP-glycosyltransferase, glutamate receptor, RING/U-box protein with C6HC-type zinc finger, and leucine-rich repeat receptor-like protein kinase family protein presented greatly up-regulated expression in the tobacco seedlings in response to the VOCs of strain TOR3209, and all these genes were involved in the plant growth and development processes. In addition, the important VOCs of strain TOR3209 were found to be 2,4-bis(1,1-dimethylethyl)-phenol and hexanedioic acid dibutyl ester (with two compounds exhibiting antifungal functions), and their other PGP effects need to be further investigated. In the long term, these new findings would facilitate the development of biofertilizers and biopesticides.

DATA AVAILABILITY STATEMENT

The datasets presented in this study can be found in online repositories. The names of the repository/repositories and accession number(s) can be found at: National Center for Biotechnology Information (NCBI) BioProject database under accession number PRJNA814410.

AUTHOR CONTRIBUTIONS

YH conceived the study and wrote the manuscript. YH and ZW designed the experiments. YH, WG, JP, JG, JM, XW, CZ, NJ, EW, DH, and ZW did the experiments. YH and WG assisted in the data analysis. YH, EW, and JG edited the article. All authors contributed to the article and approved the submitted version.

FUNDING

This work was supported by the National Key Research and Development Program of China (2021YFD1901004-4), the HAAFS Science and Technology Innovation Special Project (2022KJCXZX-ZHS-3), and the Project of Natural Science Foundation of Hebei Province (C2020301047). EW was supported by the Project of Sabbatical Year and SIP20200726 authorized by IPN, Mexico.

ACKNOWLEDGMENTS

Sequencing services were provided by Personal Biotechnology Co., Ltd. Shanghai, China. The data were analyzed by using the free online platform Personalbio GenesCloud (http://www.genescloud.cn).

SUPPLEMENTARY MATERIAL

The Supplementary Material for this article can be found online at: https://www.frontiersin.org/articles/10.3389/fmicb.2022.891245/full#supplementary-material

REFERENCES

Akbari, A., Gharanjik, S., Koobaz, P., and Sadeghi, A. (2020). Plant growth promoting *Streptomyces* strains are selectively interacting with the wheat cultivars especially in saline conditions. *Heliyon* 6, e03445. doi: 10.1016/j.heliyon.2020.e03445

Asari, S., Matzén, S., Petersen, M. A., Bejai, S., and Meijer, J. (2016). Multiple effects of *Bacillus amyloliquefaciens* volatile compounds: plant growth promotion and growth inhibition of phytopathogens. *FEMS Microbiol. Ecol.* 92, fiw070. doi: 10.1093/femsec/fiw070

Atieno, M., Herrmann, L., Nguyen, H. T., Phan, H. T., Nguyen, N. K., Srean, P., et al. (2020). Assessment of biofertilizer use for sustainable agriculture in the Great Mekong Region. *J. Environ. Manage.* 275, 111300. doi: 10.1016/j.jenvman.2020.111300

Audrain, B., Farag, M. A., Ryu, C.-M., and Ghigo, J.-M. (2015). Role of bacterial volatile compounds in bacterial biology. *FEMS Microbiol. Rev.* 39, 222–233. doi: 10.1093/femsre/fuu013

Basu, A., Prasad, P., Das, S. N., Kalam, S., Sayyed, R. Z., Reddy, M. S., et al. (2021). Plant growth promoting rhizobacteria (PGPR) as green bioinoculants: recent developments, constraints, and prospects. *Sustainability* 13, 1140. doi: 10.3390/su13031140

Bhattacharyya, P. N., and Jha, D. K. (2012). Plant growth-promoting rhizobacteria (PGPR): emergence in agriculture. *World J. Microbiol. Biotechnol.* 28, 1327–1350. doi: 10.1007/s11274-011-0979-9

Birkenbihl, R. P., Kracher, B., Roccaro, M., and Somssich, I. E. (2017). Induced genome-wide binding of three Arabidopsis WRKY transcription factors during early MAMP-triggered immunity. *Plant Cell* 29, 20–38. doi: 10.1105/tpc.16.00681

Boscari, A., Ferrarini, A., Giudice, J., d., Venturini, L., Delledone, M., et al. (2013). Mapping and analysis of illumina reads for transcriptome of medicago truncatula during the early organogenesis of the nodule. *Bioprotocol* 3, e966. doi: 10.21769/BioProtoc.966

Bottini, R., Cassán, F., and Piccoli, P. (2004). Gibberellin production by bacteria and its involvement in plant growth promotion and yield increase. *Appl. Microbiol. Biotechnol.* 65, 497–503. doi: 10.1007/s00253-004-1696-1

Chowdappa, S., Jagannath, S., Konappa, N., Udayashankar, A. C., and Jogaiah, S. (2020). Detection and characterization of antibacterial siderophores secreted by endophytic fungi from *Cymbidium aloifolium*. *Biomolecules* 10, 1412. doi: 10.3390/biom10101412

Chowdhary, K., and Sharma, S. (2020). Plant growth promotion and biocontrol potential of fungal endophytes in the inflorescence of *Aloe vera* L. *Proc. Natl. Acad. Sci. India Section B Biol. Sci.* 90, 1045–1055. doi: 10.1007/s40011-020-01173-3

Conesa, A., Götz, S., García-Gómez, J. M., Terol, J., Talón, M., and Robles, M. (2005). Blast2GO: a universal tool for annotation, visualization and analysis in functional genomics research. *Bioinformatics* 21, 3674–3676. doi: 10.1093/bioinformatics/bti610

Fiedler, H.-P., Krastel, P., Müller, J., Gebhardt, K., and Zeeck, A. (2001). Enterobactin: the characteristic catecholate siderophore of Enterobacteriaceae is produced by *Streptomyces* species. *FEMS Microbiol. Lett.* 196, 147–151. doi: 10.1111/j.1574-6968.2001.tb10556.x

Forde, B. G., and Roberts, M. R. (2014). Glutamate receptor-like channels in plants: a role as amino acid sensors in plant defence? *F1000Prime Rep.* 6, 37–37. doi: 10.12703/P6-37

Gentleman, R. C., Carey, V. J., Bates, D. M., Bolstad, B., Dettling, M., Dudoit, S., et al. (2004). Bioconductor: open software development for computational biology and bioinformatics. *Genome Biol.* 5, R80. doi: 10.1186/gb-2004-5-10-r80

Glickmann, E., and Dessaux, Y. (1995). A critical examination of the specificity of the salkowski reagent for indolic compounds produced by phytopathogenic bacteria. *Appl. Environ. Microbiol.* 61, 793–796. doi: 10.1128/aem.61.2.793-796.1995

Gopalakrishnan, S., Srinivas, V., Alekhya, G., Prakash, B., Kudapa, H., Rathore, A., et al. (2015). The extent of grain yield and plant growth enhancement by plant

growth-promoting broad-spectrum *Streptomyces* sp. *in chickpea. SpringerPlus* 4, 1–10. doi: 10.1186/s40064-015-0811-3

Gopalakrishnan, S., Srinivas, V., Sree Vidya, M., and Rathore, A. (2013). Plant growth-promoting activities of *Streptomyces* spp. in sorghum and rice. *SpringerPlus* 2, 1–8. doi: 10.1186/2193-1801-2-574

Goswami, D., Thakker, J. N., and Dhandhukia, P. C. (2016). Portraying mechanics of plant growth promoting rhizobacteria (PGPR): a review. *Cogent Food Agric.* 2, 1127500. doi: 10.1080/23311932.2015.1127500

Gu, Y.-Q., Mo, M.-H., Zhou, J.-P., Zou, C.-S., and Zhang, K.-Q. (2007). Evaluation and identification of potential organic nematicidal volatiles from soil bacteria. *Soil Biol. Biochem.* 39, 2567–2575. doi: 10.1016/j.soilbio.2007.05.011

Han, X., Kumar, D., Chen, H., Wu, S., and Kim, J.-Y. (2014). Transcription factor-mediated cell-to-cell signalling in plants. *J. Exp. Bot.* 65, 1737–1749. doi: 10.1093/jxb/ert422

Hayat, R., Ali, S., Amara, U., Khalid, R., and Ahmed, I. (2010). Soil beneficial bacteria and their role in plant growth promotion: a review. *Ann. Microbiol.* 60, 579–598. doi: 10.1007/s13213-010-0117-1

Howlader, J., Robin, A. H. K., Natarajan, S., Biswas, M. K., Sumi, K. R., Song, C. Y., et al. (2020). Transcriptome analysis by rna–seq reveals genes related to plant height in two sets of parent-hybrid combinations in easter lily (*Lilium longiflorum*). *Sci. Rep.* 10, 1–15. doi: 10.1038/s41598-020-65909-x

Hu, D., Li, S., Li, Y., Peng, J., Wei, X., Ma, J., et al. (2020). *Streptomyces* sp. strain TOR3209: a rhizosphere bacterium promoting growth of tomato by affecting the rhizosphere microbial community. *Sci. Rep.* 10, 20132. doi: 10.1038/s41598-020-76887-5

Hu, D., Li, X., Chang, Y., He, H., Zhang, C., Jia, N., et al. (2012). Genome sequence of *Streptomyces* sp. strain TOR3209, a rhizosphere microecology regulator isolated from tomato rhizosphere. *J. Bacteriol.* 194, 1627–1627. doi: 10.1128/JB.06684-11

Jennings, W., and Shibamoto, T. (1980). "Part A - analytical considerations," in *Qualitative Analysis of Flavor and Fragrance Volatiles by Glass Capillary Gas Chromatography,* eds W. Jennings and T. Shibamoto (New York, NY: Academic Press), 1–27.

Jiwen, W., Jing, Z., Baoen, X., Yingying, L., and Guanjie, L. (2011). Isolation and screening of organic phosphorus-solubilizing bacterium and its initial identification. *Henan Sci.* 29, 31–34. doi: 10.13537/j.issn.1004-3918.2011.01.016

Kanchiswamy, C. N., Malnoy, M., and Maffei, M. E. (2015). Bioprospecting bacterial and fungal volatiles for sustainable agriculture. *Trends Plant Sci.* 20, 206–211. doi: 10.1016/j.tplants.2015.01.004

Kanehisa, M., and Goto, S. (2000). KEGG: kyoto encyclopedia of genes and genomes. *Nucleic Acids Res.* 28, 27–30. doi: 10.1093/nar/28.1.27

Kang, Y., Jang, S.-W., Lee, H. J., Barchenger, D. W., and Jang, S. (2021). Expression profiling of heat shock protein genes as putative early heat-responsive members in lettuce. *Horticulturae* 7, 312. doi: 10.3390/horticulturae7090312

Kaur, A. (2020). *A Novel Maize Dwarf Resulting From a Gain-of-Function Mutation in a Glutamate Receptor Gene*. West Lafayette: Purdue University Graduate School.

Khan, A. L., Waqas, M., Kang, S.-M., Al-Harrasi, A., Hussain, J., Al-Rawahi, A., et al. (2014). Bacterial endophyte *Sphingomonas* sp. LK11 produces gibberellins and IAA and promotes tomato plant growth. *J. Microbiol.* 52, 689-695. doi: 10.1007/s12275-014-4002-7

Korpi, A., Järnberg, J., and Pasanen, A.-L. (2009). Microbial volatile organic compounds. *Crit. Rev. Toxicol.* 39, 139–193. doi: 10.1080/10408440802291497

Laila, R., Robin, A. H. K., Yang, K., Park, J.-I., Suh, M. C., Kim, J., et al. (2017). Developmental and genotypic variation in leaf wax content and composition, and in expression of wax biosynthetic genes in Brassica oleracea var. capitata. *Front. Plant Sci.* 7, 1972. doi: 10.3389/fpls.2016.01972

Lee, S., Ka, J.-O., and Song, H.-G. (2012). Growth promotion of *Xanthium italicum* by application of rhizobacterial isolates of *Bacillus aryabhattai* in microcosm soil. *J. Microbiol.* 50, 45–49. doi: 10.1007/s12275-012-1415-z

Li, C., Zhang, J., Zhao, C., Jiang, H., Ren, X., Su, W., et al. (2018). Effects of 3-methyl-1-butanol on seed germination and seedling growth of maize and wheat. *Bull. Botanical Res.* 38, 785–789. doi: 10.7525/j.issn.1673-5102.2018.05.019

Li, Y., Liu, J., Díaz-Cruz, G., Cheng, Z., and Bignell, D. R. (2019). Virulence mechanisms of plant-pathogenic *Streptomyces* species: an updated review. *Microbiology* 165, 1025–1040. doi: 10.1099/mic.0.000818

Liu, P.-L., Du, L., Huang, Y., Gao, S.-M., and Yu, M. (2017). Origin and diversification of leucine-rich repeat receptor-like protein kinase (LRR-RLK) genes in plants. *BMC Evol. Biol.* 17, 47. doi: 10.1186/s12862-017-0891-5

Lugtenberg, B., and Kamilova, F. (2009). Plant-growth-promoting rhizobacteria. *Annu. Rev. Microbiol.* 63, 541–556. doi: 10.1146/annurev.micro.62.081307.162918

Martínez, O. A., Jorquera, M. A., Crowley, D. E., and de la Luz Mora, M. (2011). Influence of nitrogen fertilisation on pasture culturable rhizobacteria occurrence and the role of environmental factors on their potential PGPR activities. *Biol. Fertil. Soils* 47, 875–885. doi: 10.1007/s00374-011-0593-x

Mishra, R. C., and Grover, A. (2016). ClpB/Hsp100 proteins and heat stress tolerance in plants. *Crit. Rev. Biotechnol.* 36, 862–874. doi: 10.3109/07388551.2015.1051942

Mohanty, P., Singh, P. K., Chakraborty, D., Mishra, S., and Pattnaik, R. (2021). Insight into the role of PGPR in sustainable agriculture and environment. *Front. Sustain. Food Syst* 5, 667150. doi: 10.3389/fsufs.2021.667150

Myo, E. M., Ge, B., Ma, J., Cui, H., Liu, B., Shi, L., et al. (2019). Indole-3-acetic acid production by *Streptomyces* fradiae NKZ-259 and its formulation to enhance plant growth. *BMC Microbiol.* 19, 155. doi: 10.1186/s12866-019-1528-1

Nassar, A. H., El-Tarabily, K. A., and Sivasithamparam, K. (2005). Promotion of plant growth by an auxin-producing isolate of the yeast *Williopsis saturnus* endophytic in maize (Zea mays L.) roots. *Biol. Fertil. Soils* 42, 97–108. doi: 10.1007/s00374-005-0008-y

Nautiyal, C. S. (1999). An efficient microbiological growth medium for screening phosphate solubilizing microorganisms. *FEMS Microbiol. Lett.* 170, 265–270. doi: 10.1111/j.1574-6968.1999.tb13383.x

Nebert, D. W. (1991). MINIREVIEW: proposed role of drug-metabolizing enzymes: regulation of steady state levels of the ligands that effect growth, homeostasis, differentiation, and neuroendocrine functions. *Mol. Endocrinol.* 5, 1203–1214. doi: 10.1210/mend-5-9-1203

Neilands, J. (1987). "Comparative biochemistry of microbial iron assimilation," in *Iron Transport in Microbes, Plants and Animals* (Weinheim: Federal Republic of Germany), 3–34.

Olanrewaju, O. S., and Babalola, O. O. (2019). *Streptomyces*: implications and interactions in plant growth promotion. *Appl. Microbiol. Biotechnol.* 103, 1179–1188. doi: 10.1007/s00253-018-09577-y

Oleńska, E., Małek, W., Wójcik, M., Swiecicka, I., Thijs, S., and Vangronsveld, J. (2020). Beneficial features of plant growth-promoting rhizobacteria for improving plant growth and health in challenging conditions: a methodical review. *Sci. Total Environ.* 743, 140682. doi: 10.1016/j.scitotenv.2020.140682

Olsen, A. N., Ernst, H. A., Leggio, L. L., and Skriver, K. (2005). NAC transcription factors: structurally distinct, functionally diverse. *Trends Plant Sci.* 10, 79–87. doi: 10.1016/j.tplants.2004.12.010

Otieno, N., Lally, R., Kiwanuka, S., Lloyd, A., Ryan, D., Germaine, K., et al. (2015). Plant growth promotion induced by phosphate solubilizing endophytic *Pseudomonas* isolates. *Front. Microbiol.* 6, 745. doi: 10.3389/fmicb.2015.00745

Pailan, S., Gupta, D., Apte, S., Krishnamurthi, S., and Saha, P. (2015). Degradation of organophosphate insecticide by a novel *Bacillus aryabhattai* strain SanPS1, isolated from soil of agricultural field in Burdwan, West Bengal, India. *Int. Biodeterior. Biodegradation* 103, 191–195. doi: 10.1016/j.ibiod.2015.05.006

Parewa, H. P., Joshi, N., Meena, V. S., Joshi, S., Choudhary, A., Ram, M., et al. (2021). "Chapter 9 - Role of biofertilizers and biopesticides in organic farming," in *Advances in Organic Farming,* eds V. S. Meena, S. K. Meena, A. Rakshit, J. Stanley, and C. Srinivasarao (Woodhead Publishing), 133–159.

Pérez-Miranda, S., Cabirol, N., George-Téllez, R., Zamudio-Rivera, L. S., and Fernández, F. J. (2007). O-CAS, a fast and universal method for siderophore detection. *J. Microbiol. Methods* 70, 127–131. doi: 10.1016/j.mimet.2007.03.023

Phi, Q.-T., Park, Y.-M., Seul, K.-J., Ryu, C.-M., Park, S.-H., Kim, J.-G., et al. (2010). Assessment of root-associated *Paenibacillus polymyxa* groups on growth promotion and induced systemic resistance in pepper. *J. Microbiol. Biotechnol.* 20, 1605–1613. doi: 10.4014/jmb.1007.07014

Quinn, G. A., Banat, A. M., Abdelhameed, A. M., and Banat, I. M. (2020). *Streptomyces* from traditional medicine: sources of new innovations in antibiotic discovery. *J. Med. Microbiol.* 69, 1040. doi: 10.1099/jmm.0.001232

Razin, S. V., Borunova, V. V., Maksimenko, O. G., and Kantidze, O. L. (2012). Cys2His2 zinc finger protein family: classification, functions, and major members. *Biochemistry* 77, 217–226. doi: 10.1134/S0006297912030017

Robin, A., Mougel, C., Siblot, S., Vansuyt, G., Mazurier, S., and Lemanceau, P. (2006). Effect of ferritin overexpression in tobacco on the structure of bacterial and pseudomonad communities associated with the roots. *FEMS Microbiol. Ecol.* 58, 492–502. doi: 10.1111/j.1574-6941.2006.00174.x

Romano-Armada, N., Yañez-Yazlle, M. F., Irazusta, V. P., Rajal, V. B., and Moraga, N. B. (2020). Potential of bioremediation and PGP traits in *Streptomyces* as strategies for bio-reclamation of salt-affected soils for agriculture. *Pathogens* 9, 117. doi: 10.3390/pathogens9020117

Saharan, B., and Nehra, V. (2011). Plant growth promoting rhizobacteria: a critical review. *Life Sci. Med. Res.* 21, 30. Available online at: https://www.researchgate.net/publication/284340739

Schmidt, R., Cordovez, V., de Boer, W., Raaijmakers, J., and Garbeva, P. (2015). Volatile affairs in microbial interactions. *ISME J.* 9, 2329–2335. doi: 10.1038/ismej.2015.42

Schöller, C. E. G., Gürtler, H., Pedersen, R., Molin, S., and Wilkins, K. (2002). Volatile metabolites from *Actinomycetes*. *J. Agric. Food Chem.* 50, 2615–2621. doi: 10.1021/jf0116754

Schwachtje, J., Karojet, S., Kunz, S., Brouwer, S., and van Dongen, J. T. (2012). Plant-growth promoting effect of newly isolated rhizobacteria varies between two Arabidopsis ecotypes. *Plant Signal. Behav.* 7, 623–627. doi: 10.4161/psb.20176

Sgroy, V., Cassán, F., Masciarelli, O., Del Papa, M. F., Lagares, A., and Luna, V. (2009). Isolation and characterization of endophytic plant growth-promoting (PGPB) or stress homeostasis-regulating (PSHB) bacteria associated to the halophyte Prosopis strombulifera. *Appl. Microbiol. Biotechnol.* 85, 371–381. doi: 10.1007/s00253-009-2116-3

Shamimuzzaman, M., and Vodkin, L. (2013). Genome-wide identification of binding sites for NAC and YABBY transcription factors and co-regulated genes during soybean seedling development by ChIP-Seq and RNA-Seq. *BMC Genomics* 14, 477. doi: 10.1186/1471-2164-14-477

Spaepen, S., and Vanderleyden, J. (2011). Auxin and plant-microbe interactions. *Cold Spring Harb. Perspect. Biol.* 3, a001438. doi: 10.1101/cshperspect.a001438

Spaepen, S., Vanderleyden, J., and Remans, R. (2007). Indole-3-acetic acid in microbial and microorganism-plant signaling. *FEMS Microbiol. Rev.* 31, 425–448. doi: 10.1111/j.1574-6976.2007.00072.x

Suárez-Moreno, Z. R., Vinchira-Villarraga, D. M., Vergara-Morales, D. I., Castellanos, L., Ramos, F. A., Guarnaccia, C., et al. (2019). Plant-growth promotion and biocontrol properties of three *Streptomyces* spp. isolates to control bacterial rice pathogens. *Front. Microbiol.* 10, 290. doi: 10.3389/fmicb.2019.00290

Terra, L., Ratcliffe, N., Castro, H. C., Vicente, A. C. P., and Dyson, P. (2021). Biotechnological potential of *Streptomyces* siderophores as new antibiotics. *Curr. Med. Chem.* 28, 1407–1421. doi: 10.2174/0929867327666200510235512

Toledo-Ortiz, G., Huq, E., and Quail, P. H. (2003). The arabidopsis basic/helix-loop-helix transcription factor family. *Plant Cell* 15, 1749–1770. doi: 10.1105/tpc.013839

van Ruissen, F., Ruijter, J. M., Schaaf, G. J., Asgharnegad, L., Zwijnenburg, D. A., Kool, M., et al. (2005). Evaluation of the similarity of gene expression data estimated with SAGE and Affymetrix GeneChips. *BMC Genomics* 6, 91. doi: 10.1186/1471-2164-6-91

Vasconcellos, R. L. F.,d., Silva, M. C. P.,d., Ribeiro, C. M., and Cardoso, E. J. B. N. (2010). Isolation and screening for plant growth-promoting (PGP) *actinobacteria* from Araucaria angustifolia rhizosphere soil. *Sci. Agric.* 67, 743–746. doi: 10.1590/S0103-90162010000600019

Vejan, P., Abdullah, R., Khadiran, T., Ismail, S., and Nasrulhaq Boyce, A. (2016). Role of plant growth promoting rhizobacteria in agricultural sustainability—a review. *Molecules* 21, 573. doi: 10.3390/molecules21050573

Woo, H.-H., Orbach, M. J., Hirsch, A. M., and Hawes, M. C. (1999). Meristem-localized inducible expression of a UDP-glycosyltransferase gene is essential for growth and development in pea and alfalfa. *Plant Cell* 11, 2303–2315. doi: 10.1105/tpc.11.12.2303

Zhang, T., Zhao, Y., Wang, Y., Liu, Z., and Gao, C. (2018). Comprehensive analysis of MYB gene family and their expressions under abiotic stresses and hormone treatments in Tamarix hispida. *Front. Plant Sci.* 9, 1303. doi: 10.3389/fpls.2018.01303

Zhao, H., Li, X., and Ma, L. (2012). Basic helix-loop-helix transcription factors and epidermal cell fate determination in Arabidopsis. *Plant Signal. Behav.* 7, 1556–1560. doi: 10.4161/psb.22404

Conflict of Interest: The authors declare that the research was conducted in the absence of any commercial or financial relationships that could be construed as a potential conflict of interest.

Publisher's Note: All claims expressed in this article are solely those of the authors and do not necessarily represent those of their affiliated organizations, or those of the publisher, the editors and the reviewers. Any product that may be evaluated in this article, or claim that may be made by its manufacturer, is not guaranteed or endorsed by the publisher.

Copyright © 2022 He, Guo, Peng, Guo, Ma, Wang, Zhang, Jia, Wang, Hu and Wang. This is an open-access article distributed under the terms of the Creative Commons Attribution License (CC BY). The use, distribution or reproduction in other forums is permitted, provided the original author(s) and the copyright owner(s) are credited and that the original publication in this journal is cited, in accordance with accepted academic practice. No use, distribution or reproduction is permitted which does not comply with these terms.

frontiers | Frontiers in Microbiology

ORIGINAL RESEARCH
published: 07 July 2022
doi: 10.3389/fmicb.2022.903467

Melatonin Attenuates the Urea-Induced Yields Improvement Through Remodeling Transcriptome and Rhizosphere Microbial Community Structure in Soybean

Renhao Xiao[1†], Qin Han[1†], Yu Liu[1], Xuehai Zhang[1], Qingnan Hao[2], Qingqing Chai[1], Yongfang Hao[1], Junbo Deng[2], Xia Li[1] and Hongtao Ji[1]*

[1] National Key Laboratory of Crop Genetic Improvement, Hubei Hongshan Laboratory, College of Plant Science and Technology, Huazhong Agricultural University, Wuhan, China, [2] Oil Crops Research Institute, Chinese Academy of Agricultural Sciences, Wuhan, China

OPEN ACCESS

Edited by:
Víctor Manuel Ruíz-Valdiviezo, Tecnológico Nacional de México/Instituto Tecnológico de Tuxtla Gutiérrez, Mexico

Reviewed by:
Hayssam M. Ali, King Saud University, Saudi Arabia
Tahir Naqqash, Bahauddin Zakariya University, Pakistan

***Correspondence:**
Hongtao Ji
htji@mail.hzau.edu.cn

[†] These authors share first authorship

Specialty section:
This article was submitted to Microbe and Virus Interactions with Plants, a section of the journal Frontiers in Microbiology

Received: 24 March 2022
Accepted: 06 June 2022
Published: 07 July 2022

Citation:
Xiao R, Han Q, Liu Y, Zhang X, Hao Q, Chai Q, Hao Y, Deng J, Li X and Ji H (2022) Melatonin Attenuates the Urea-Induced Yields Improvement Through Remodeling Transcriptome and Rhizosphere Microbial Community Structure in Soybean. Front. Microbiol. 13:903467. doi: 10.3389/fmicb.2022.903467

Foliar application of nitrogen to enhance crop productivity has been widely used. Melatonin is an effective regulator in promoting plant growth. However, the effects of melatonin and the combination of melatonin and nitrogen on soybeans yields production remain largely unknown. In this study, a field experiment was conducted to evaluate the effects and mechanisms of spraying leaves with melatonin and urea on soybeans. Foliar application of urea significantly increased soybean yields and melatonin did not affect the yields, while combination of melatonin and urea significantly reduced the yields compared to the application of urea alone. A leaf transcriptional profile was then carried out to reveal the underlying mechanism and found that foliar spraying of urea specifically induced the expression of genes related to amino acid transport and nitrogen metabolism. However, foliar application of melatonin significantly changed the transcriptional pattern established by urea application and increased the expression of genes related to abiotic stress signaling pathways. The effects of melatonin and urea treatment on soil microbiome were also investigated. Neither melatonin nor urea application altered the soil microbial alpha diversity, but melatonin application changed rhizosphere microbial community structure, whereas the combination of melatonin and urea did not. Melatonin or urea application altered the abundance of certain taxa. The number of taxa changed by melatonin treatment was higher than urea treatment. Collectively, our results provide new and valuable insights into the effects of foliar application of melatonin to urea and further show that melatonin exerts strong antagonistic effects on urea-induced soybean yields, gene expression and certain soil microorganisms.

Keywords: soybean yields, foliar application, gene expression, nitrogen metabolism, microbiome

INTRODUCTION

Nitrogen fertilizers are used to increase global crop yields in the last half century (Lassaletta et al., 2014; Garnett et al., 2015), whereas excessive nitrogen fertilization does not further promote crop productivity but lead to environmental pollution. In China, the overuse of nitrogen fertilizer has become one of the major issues in recent years. Thus, it is necessary to explore new strategies for improving nitrogen utilization efficiency without increasing nitrogen fertilizers application. Melatonin (*N*-acetyl-5-methoxytryptamine) is a crucial plant growth regulator and regulates plant growth and development, response to various abiotic stresses, nitrogen uptake and metabolism (Arnao and Hernández-Ruiz, 2014, 2019). However, whether melatonin could promote plant nitrogen utilization efficiency and crop yields remain large unknown.

Melatonin (*N*-acetyl-5-methoxytryptamine) was first discovered in the bovine pineal gland of animals, and it was also shown to be present in higher plants and involved in plant growth and development regulation (Lerner et al., 1958; Hattori et al., 1995). Plant melatonin not only regulates many physiological processes but also acts as a protective agent against multiple stresses. It was reported that melatonin regulated seed germination, root growth, flowering, photosynthesis and leaf senescence (Zhang et al., 2012; Byeon and Back, 2014; Wei et al., 2015). Melatonin could also protect plants against multiple biotic and abiotic stresses (Arnao and Hernández-Ruiz, 2015; Tiwari et al., 2021). Treatment with exogenous melatonin significantly improves the resistance of plants to salt stress (Zheng et al., 2017), heat stress (Zhang J. et al., 2017), chilling (Balabusta et al., 2016), and drought stress (Cao et al., 2020) through remodeling a series of physiological and transcriptomic profiles. More important, melatonin has been shown to promote plant nutrient uptake and metabolism under various stresses condition. Melatonin application promotes nitrogen metabolism in alfalfa exposed to drought stress (Antoniou et al., 2017). Zhang R. et al. (2017) also found that melatonin improved the tolerance of cucumber seedlings to high nitrate levels by enhancing the activities of nitrogen metabolism-related enzymes. Melatonin also significantly decreases the melon leaf NH_4^+ content by improving the activities of enzymes involved in nitrogen metabolism under chilling stress (Gao et al., 2016). Recently, Qiao et al. (2019) reported that melatonin promotes winter wheat growth and yield by increasing the activities of nitrogen uptake and metabolism-related enzymes under nitrogen-deficient conditions. These studies emphasized the role of melatonin in promoting plant nutrient uptake and metabolism under stresses condition, whereas the effects of melatonin on crop plant nitrogen uptake and metabolism under normal nitrogen condition remain elusive.

Soil nitrogen fertilization is commonly used to enhance crop productivity, but soil nitrogen fertilization not only affects soil properties but also directly affects the abundance of members of the soil microbial community, including bacteria, fungi and other microorganisms (Chu et al., 2007; Wang et al., 2017). The impact of soil nitrogen fertilization on soil bacterial diversity has been studied in maize (Rodríguez-Blanco et al., 2015), rice (Zhang et al., 2019), wheat (Chen et al., 2019), and soybean (Liu et al., 2019). In addition, the foliar application of urea is another method of nitrogen fertilization to enhance crop productivity (Wagan et al., 2017). Foliar urea application has some advantages compared to soil application especially for the legume crops; crops can absorb foliar-applied urea even in dry weather conditions, and the absorption of urea can reduce the loss of nitrogen to soil (Gooding and Davies, 1992). For legume crops, foliar application could reduce the inhibition role of nitrogen to root nodule development and symbiotic nitrogen fixation (Lin et al., 2018; Nishida et al., 2018). Thus, foliar application of nitrogen fertilizer has become more popular, and the physiological effects of foliar urea application on crop plants have been explored extensively in recent years (Hassanein et al., 2019; Cassim et al., 2020; Lyu et al., 2021). In wheat, foliar urea application altered storage protein distribution of grain by promoting the expression of the majority of storage protein-encoding genes (Rossmann et al., 2019), but the global transcriptional profile of soybean after foliar urea application has rarely been reported.

The changes in leaf transcription patterns that occur after foliar urea treatment also induce changes in the rhizosphere microbiome. Using culture-independent methods, González-Arenzana et al. (2017) found that foliar application of urea significantly alters the microbial diversity and population structure of the must, but did not affect grape microbiota. Foliar application of urea to the aerial parts of wheat increased the abundance of bacteria and decreased the abundance of some fungal genera on the roots of plants grown in uncontaminated soil and soil contaminated with the noxious fungus *Fusarium* spp. (Vran, 1972). In soybean, the effects of foliar nitrogen application on the root and soil microbiomes have rarely been explored, and the role of foliar melatonin application on the rhizosphere microbiome community of soybeans is also unreported.

Soybean, an important legume worldwide, is a major source of oil and protein for people and livestock (Gaonkar and Rosentrater, 2019). Effective agroecosystem practices to enhance nitrogen use efficiency, increase the yields and explore the underlying mechanism remain challenges. In this study, we tried to figure out whether melatonin could further promote soybean yields under urea condition and investigate the underlying mechanism. Through a field experiment by spraying soybean with melatonin and/or urea in two places, we confirmed that additional melatonin application resulted a significant decrease of soybean yields, altered the leaf gene expression pattern, and changed certain soil microorganisms compared with urea application alone.

MATERIALS AND METHODS

Plant Materials and Treatments

Experiments were conducted at Jingmen (latitude 30°52′29″, longitude 112°11′31″) and Yangluo (latitude 30°43′8″, longitude 114°30′27″) experimental base of the Chinese Academy of Agricultural Sciences, Hubei, China. The soil physicochemical properties of both fields are clay with medium soil fertility and

flat terrain. In Jingmen base, the soil pH is 5.53, organic matters are 21.39 g·kg^{-1}, soil available potassium is 183 mg·kg^{-1}, soil available phosphorus is 44.5 mg·kg^{-1} and soil total nitrogen is 1.06 g·kg^{-1}. In Yangluo station, the soil pH is 8.11, organic matters are 15.94 g·kg^{-1}, soil available potassium is 136.29 mg·kg^{-1}, soil available phosphorus is 11.68 mg·kg^{-1} and alkali-hydrolyzable nitrogen is 87.41 mg·kg^{-1}. The two soybean cultivars (ZD63, Zhongdou 63; and WD28, Wandou 28) were sowed on 9th June, 2020 with a plant-spacing of 10 cm and row spacing of 50 cm, respectively. To ensure the germination rate, more seeds were sowed in the field and the plants were thinned to a final stand of 200,000 plants ha^{-1} within 3 weeks to meet space requirement. When soybean grown at R1 (beginning of the flowering stage, fifth unrolled trifoliate leaf) stages on 22th July, and R3 [Beginning pod—pods are 3/16 inch (5 mm) at one of the four uppermost nodes] on 24th August, the experimental plants were divided into four groups as follows: (i) the control group, which was treated with water; (ii) the urea group, which was treated with 3 kg ha^{-1} urea by leaf spraying (on the top and bottom sides of all leaves until water dripped). (iii) the melatonin group, which was treated with 100 μmol·L^{-1} melatonin by leaf spraying. (iv) the urea + melatonin group, which was treated with 3 kg·ha^{-1} urea plus 100 μmol·L^{-1} melatonin by leaf spraying. The urea was bought from Sinopharm Chemical Reagent Co., Ltd., company (CAS: 57-13-6), the melatonin was diluted into distilled water (without surfactant) to make 100 μmol·L^{-1} melatonin solution. The plants were treated for a total of two times (at R1 and R3 growth stage). Each treatment was repeated in three plots of 7.5 m^2 each (3 × 2.5 m^2). Soil samples from root rhizosphere were then collected at 12th August and 2nd September, the trifoliate leaves were also harvested simultaneously. The soil and leaves samples were stored at −80°C for microbiome analysis and transcriptomic analysis.

Transcriptomic Analysis RNA Extraction

Total RNA was extracted from 100 mg trifoliate leaves (samples were collected on 2nd September from Yangluo base) using TRIzol® Reagent (Plant RNA Purification Reagent for plant tissue) according the manufacturer's instructions (Invitrogen). The genomic DNA was removed using DNase I (TaKara). The RNA quality was determined by 2100 Bioanalyser (Agilent) and quantified using the ND-2000 (NanoDrop Technologies). Only high-quality RNA sample (OD260/280 = 1.8∼2.2, OD260/230 ≥ 2.0, RIN ≥ 6.5, 28S:18S ≥ 1.0, > 1 μg) was used to construct sequencing library.

Library Preparation, and Illumina Hiseq xten/Nova seq 6000 Sequencing

RNA-seq transcriptome libraries were prepared following TruSeqTM RNA sample preparation Kit from Illumina (San Diego, CA, United States) using 1 μg of total RNA. Firstly, messenger RNA was isolated according to polyA selection method by oligo(dT) beads and then fragmented by fragmentation buffer. Secondly, double-stranded cDNA was synthesized using a SuperScript double-stranded cDNA synthesis kit (Invitrogen, CA, United States) with random hexamer primers (Illumina). Then the synthesized cDNA was subjected to end-repair, phosphorylation and "A" base addition according to Illumina's library construction protocol. Libraries were size selected for cDNA target fragments of 300 bp on 2% Low Range Ultra Agarose followed by PCR amplified using Phusion DNA polymerase (NEB) for 15 PCR cycles. After quantified by TBS380, paired-end RNA-seq sequencing library was sequenced with the Illumina HiSeq xten/NovaSeq 6000 sequencer (2 × 150 bp read length). Statistical methods were used to calculate the base distribution and quality fluctuation of each cycle of all sequenced reads, which could intuitively reflect the library construction quality and measurement of sequenced samples from a macro-perspective.

Read Mapping

The raw paired end reads were trimmed and quality controlled by SeqPrep[1] and Sickle[2] with default parameters. During this step, clean data (clean reads) were obtained by removing reads containing adapters or poly-N sequences as well as low-quality reads. Additionally, Q20 and Q30 values and the GC content of the clean data were calculated. Then clean reads were separately aligned to reference genome with orientation mode using HISAT2[3] software (Kim et al., 2015). The mapped reads of each sample were assembled by StringTie[4] in a reference-based approach (Pertea et al., 2015).

Differential Expression Analysis and Functional Enrichment

To identify differential expression genes between two different samples, the expression level of each transcript was calculated according to the transcripts per million reads (TPM) method. RNA-Seq by Expectation Maximization (RSEM)[5] was used to quantify gene abundances (Dewey and Li, 2011). DESeq2 (Love et al., 2014) provides statistical routines for detecting differential expression in digital gene expression data, which uses a model based on the negative binomial distribution. The resulting *P* values were adjusted using the Benjamini and Hochberg approach for controlling the false-discovery rate (FDR). Genes with P adjust < 0.05 found by DESeq2 and log2 (fold change) ≥ 1 were assigned as differentially expressed. Functional-enrichment analysis including GO was performed to identify which DEGs were significantly enriched in GO terms at Bonferroni-corrected *P*-value ≤ 0.05 compared with the whole-transcriptome background. GO functional enrichment was carried out by Goatools[6]. We then explored the molecular functions of 234,966 genes in each cluster using GO annotations, 174,190 genes for cellular component and 639,419 genes for biological process GO annotations.

[1]https://github.com/jstjohn/SeqPrep
[2]https://github.com/najoshi/sickle
[3]http://ccb.jhu.edu/software/hisat2/index.shtml
[4]https://ccb.jhu.edu/software/stringtie/index.shtml?t=example
[5]http://deweylab.biostat.wisc.edu/rsem/
[6]https://github.com/tanghaibao/Goatools

Quantitative RT-PCR

To validate the RNA-seq results, the total RNA used for RNA-seq was also reverse-transcribed into cDNA with Hifair® II 1st Strand cDNA Synthesis SuperMix (YEASEN, CA, United States). Different expression genes were selected and verified by RT-qPCR using SYBR Green PCR Master Mix (YEASEN, CA, United States) and the Bio-Rad CFX384 PCR detection system. The relative mRNA level of each target gene was evaluated against soybean elongation factor 1-beta (*GmELF1b*) (Glyma.02G276600). The primers were shown in **Supplementary Table 4**. Three technical replicates were performed and the relative levels of transcript abundance were calculated using the $2^{-\Delta\Delta CT}$ method.

16S rRNA Gene Sample Preparation, Sequencing and Analysis

In total, 48 rhizosphere soil (24 samples were collected on 12th August and 24 samples were collected on 2nd September) and 4 bulk soil samples (mixed samples collected on 12th August and 2nd September) from Yangluo base were used for sequencing according to standard protocols at Personal Biotechnology Co., Ltd., (Shanghai, China). Total genomic DNA samples were extracted using the OMEGA Soil DNA Kit (D5625-01) (Omega Bio-Tek, Norcross, GA, United States) following the manufacturer's instructions. The quantity and quality of extracted DNAs were measured using a NanoDrop ND-1000 spectrophotometer (Thermo Fisher Scientific, Waltham, MA, United States) and agarose gel electrophoresis, respectively. The V3-V4 target region of 16S rRNA gene fragments were amplification and sequenced on an Illumina Novaseq PE250 sequencing platform (Illumina, San Diego, United States).

Sequence data analyses were mainly performed using QIIME2 2019.4 (Bolyen et al., 2018) and R packages (v3.2.0). Alpha diversity indices, such as Chao1, Observed species, and Shannon were calculated using the non-singleton amplicon sequence variants (ASV) table in QIIME2, and visualized as box plots. Beta-diversity (between-sample diversity) was estimated by Bray-Curtis distance and the differentiation of microbiota structure among groups was assessed by PERMANOVA (Permutational multivariate analysis of variance) in QIIME2. LEfSe (Linear discriminant analysis effect size) was performed to detect differentially abundant taxa across groups using the default parameters (Segata et al., 2011). Quantitative real-time PCR amplifications (qPCR) were used to determine the abundances of total bacteria (the primers Eub338F/Eub518R) in the bulk soil and rhizosphere according to Nadkarni et al. (2002) and Fierer et al. (2005). Standard curves were generated using 10-fold serial dilutions of *Escherichia coli* DNA sample.

Soybean Yields Evaluation

Five square meters plot containing 100 plants were used for yield evaluation. The seeds from three plots were weighted individually, and the variance analysis was performed by using GraphPad prism 8.0 software. The data are reported as the mean and standard error (SE) values of three biological replicates. Ordinary one-way analysis of variance (ANOVA) and Tukey's multiple comparisons tests were used to determine the significance of the differences among samples.

RESULTS

Melatonin Reduces the Effect of Urea on Increasing Soybean Yields

Nitrogen is an important macronutrient required for plant growth and crop productivity. Melatonin is reported to be one of the most widely used plant growth-promoting reagent. To investigate whether melatonin application could further promote soybean yields under urea fertilization conditions, we sprayed soybean leaves with both melatonin (M treatment, 100 $\mu mol \cdot L^{-1}$) and urea (N treatment, 3 $kg \cdot ha^{-1}$). Our yields evaluation results showed that foliar application of urea (N treatment, 3 $kg \cdot ha^{-1}$) to two cultivars of Chinese soybean (Zhongdou 63, ZD63; Wandou 28, WD28) significantly increased their yields when compared with the yields of seedlings exposed to control conditions in two fields (**Figures 1A,B**). However, spraying exogenous melatonin alone could not further improve soybean yields. On the contrary, foliar application of both melatonin and urea (MN treatment) resulted in a lower production than the urea treatment (**Figures 1A,B**). In the two experimental fields, the yields of the two cultivars showed the same trend in response to melatonin and urea fertilizer treatment (**Figures 1A,B**). These results indicated that spraying leaves with melatonin significantly reduced the effect of urea on increasing soybean yields.

Identification of Differentially Expressed Genes in Response to Melatonin and Urea Treatments

To further study the molecular mechanism underlying the effects of melatonin and nitrogen on soybean yields, we performed RNA-seq analysis. Eleven ZD63 leaf samples treated with urea (N), melatonin (M) and MN (melatonin and urea together) were collected for transcriptome analysis. A total of 491,611,474 raw reads were generated from these samples, and the average number of raw reads for each sample was 44,691,952. An average of 97.89% of the raw reads had a quality score of Q30 (an error probability for base calling of less than 0.1%). After filtering and trimming the raw reads, 486,975,816 high-quality reads were used for further analysis and an average of 93.71% of the raw reads had a quality score of Q30 (**Supplementary Table 1**). The clean data from each sample were mapped to the *Glycine max* Wm82.a4 reference genome sequence with TopHat2 HISAT2 software. The proportion of total mapped reads ranged from 90.92 to 96.22% (**Supplementary Table 2**). Based on Pearson's correlation analysis, there were significant differences between the control and different treatments. The controls and MN samples are high correlated between biological replicates ($R^2 > 0.89$). The correlation of two urea samples is 0.85. The correlations among three melatonin samples are 0.77, 0.80 and 0.95, respectively (**Supplementary Figure 1**).

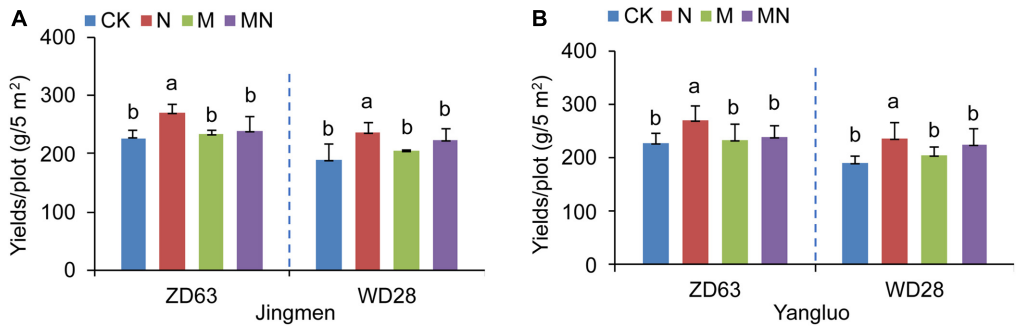

FIGURE 1 | The yields of two soybean cultivars under different treatments. **(A,B)** The yields of Zhongdou 63 (ZD63) and Wandou 28 (WD28) after foliar application of melatonin and/or urea at Jingmen **(A)** and Yangluo **(B)** field station. CK, Control; N, foliar application of urea alone; M, foliar application of melatonin alone; MN, foliar application of both melatonin and urea. Data indicates means ± SE with One-way ANOVA analysis. Different letters indicate significant differences.

We then identified the differentially expressed genes (DEGs) from different foliar spray treatments. The number of DEGs was calculated compared with the control group (the threshold for all the comparisons was DEGs $\geq$ 2-fold change; P adjust $<$ 0.05). Compared with the control, the urea treatment produced 4,222 DEGs in total, with 2,254 DEGs being upregulated and 1,968 DEGs being downregulated. A total of 7,170 DEGs were identified in response to melatonin treatment, including 4,287 upregulated and 2,883 downregulated DEGs. MN treatment resulted in a maximum amount of 8,773 DEGs, including 4,807 upregulated and 3,966 downregulated DEGs (**Figure 2A** and **Supplementary Table 3**). Venn diagram analysis of these DEGs among the different treatment groups revealed 1,847 upregulated and 1,278 downregulated DEGs as shared DEGs among the N, M and MN treatment groups (**Figure 2B**). However, when the transcriptome profiles induced by the three different treatments were compared, each treatment was found to induce unique differences in gene expression; 115 upregulated DEGs and 176 downregulated DEGs were uniquely associated with urea treatment, 925 upregulated DEGs and 590 downregulated DEGs were only observed after melatonin treatment, and 1,567 upregulated DEGs and 1,483 downregulated DEGs were specifically observed in response to MN treatment. We then performed qRT-PCR to validate the RNA-seq results. As shown in **Figures 2C–K**, the nine selected genes displayed the similar expression pattern with RNA-seq data. These results indicated that the RNA-seq data is convincing. All these DEGs might be responsive to respective treatments and subsequently affect plant growth and yield production.

Foliar Application of Melatonin and Urea Influence Multiple Biological Processes

To understand the possible biological processes in which these DEGs are involved, we then performed gene ontology (GO) term[7] enrichment analysis of all 11,005 DEGs (**Supplementary Table 5**). The top 20 enrichments in urea treatment groups are shown in **Figure 3**. We found that the upregulated DEGs were involved in "regulation of salicylic acid biosynthetic and metabolic process, response to chitin, response to nitrogen compound, response to organonitrogen compound, cell recognition, recognition of pollen," and "organic acid transport," and the downregulated DEGs were involved in "protein-chromophore linkage, photosynthesis," and "light harvesting in photosystem I"; The above-listed GO items were also found in melatonin and MN treatment (**Supplementary Figures 2, 3**), which indicated that melatonin and/or urea treatment regulated some common biological processes. In the individual urea treatment group, the GO term "amino acid transport" was specifically upregulated, which suggested that urea might be catalyzed by urease and reutilized through amino acid transport biological processes (**Figure 3A**). We also found that urea treatment downregulated genes associated with "photosynthetic electron transport chain, fatty acid biosynthetic process and auxin-activated signaling pathway." The decrease in the carbon fixation/metabolism and auxin signaling pathway might be explained by the reduction of plant growth and promotion the seed filling (**Figure 3B**). However, the DEGs associated melatonin treatment involved in different biological processes compared with those associated with urea treatment. Upregulated DEGs under melatonin treatment involved in the biological processes of "response to hydrogen peroxide, second-messenger-mediated signaling, calcium-mediated signaling, response to wounding," and "response to heat" (**Supplementary Figure 2**). All these processes represent the reported roles of melatonin in regulating plant growth and responses to various abiotic stresses. When the melatonin and urea treatments were combined, we found that the addition of the melatonin significantly altered the urea-induced changes in gene expression and biological processes (**Supplementary Figure 3**); in addition to the above-listed common biological processes which existed in all three treatments, the "response to wounding" biological processes was found in melatonin treatment and MN treatment, but not in the urea treatment, indicating that the addition of melatonin induces genes expression related to abiotic stress pathway. We also found that under MN treatment, the specifically upregulated GO terms were "cell death, xyloglucan metabolic process, cell wall macromolecule metabolic process," and "protein ubiquitination" (**Supplementary Figure 3A**), which further indicated that

[7]http://geneontology.org/

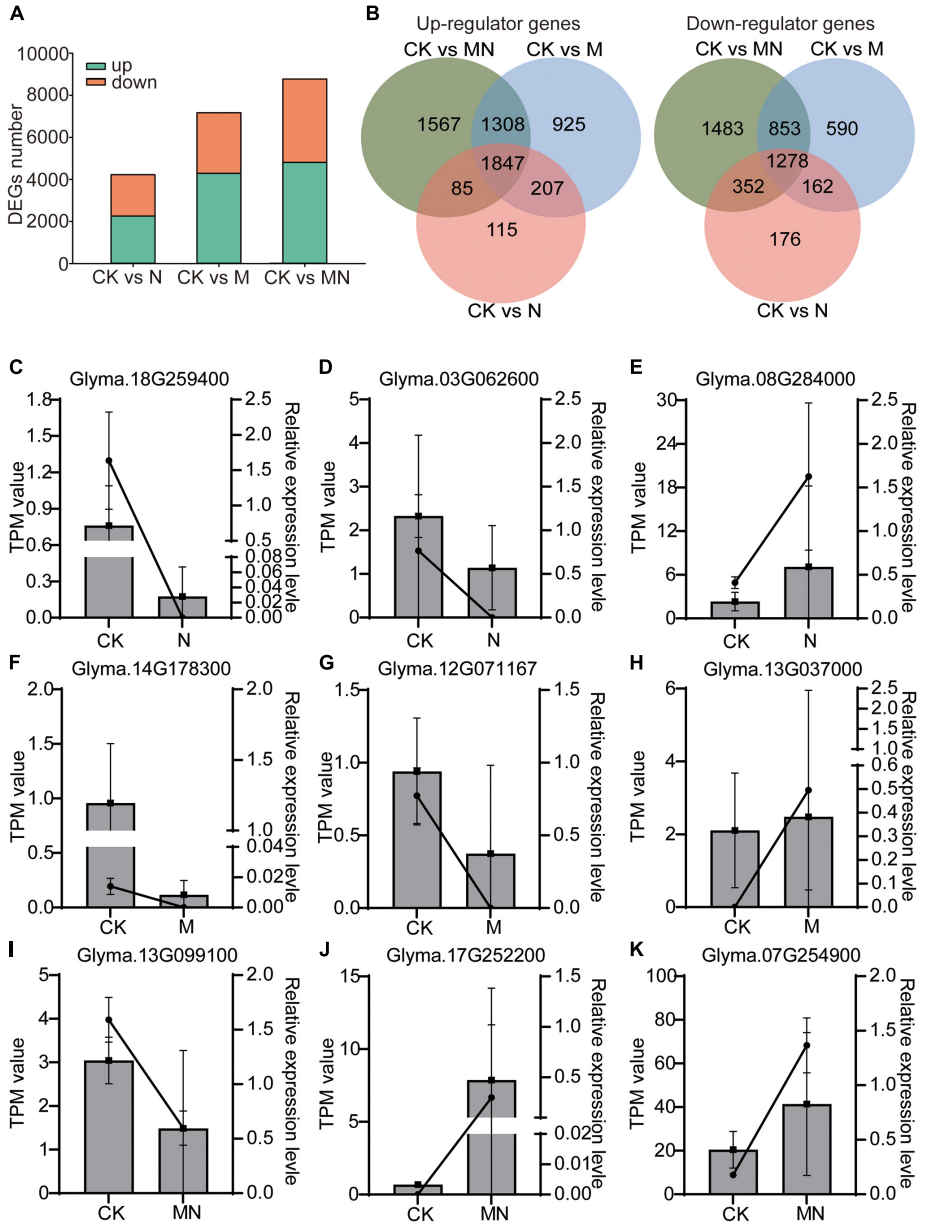

FIGURE 2 | Differentially expressed genes in responsive to different treatments. **(A)** Total number of upregulated (green) and downregulated (orange) DEGs identified for N, M, and MN treatments compared with the control. **(B)** Venn diagram depicting the number of upregulated and downregulated DEGs. **(C–K)** The mRNA abundance of nine DEGs using qRT-PCR assay. Lines represent the results of the transcriptome data (TPM value); column charts represent the results of qRT-PCR. Data shown means ± SD (n = 3 replicates/group).

the addition of melatonin might trigger a stress response and subsequently affect crop growth and yield production.

Melatonin Alters Nitrogen Uptake or Metabolic Biological Processes

Urea notably increased the expression of genes related to amino acid transport, whereas melatonin induced the expression of genes related to hydrogen peroxide, second messenger-mediated signaling, and abiotic stress processes. These results led us to hypothesize that melatonin might play an antagonistic role in the context of urea application. To further understand the different effects of the melatonin and urea treatments, we performed hierarchical clustering using silhouette plots to assess the expression patterns of all 11,005 DEGs associated with all the treatments (**Figure 4A**). The heat maps were then created on Majorbio Cloud Platform[8]. Top twenty clusters were formed, and the clusters in the control treatment groups were significantly

[8]www.majorbio.com

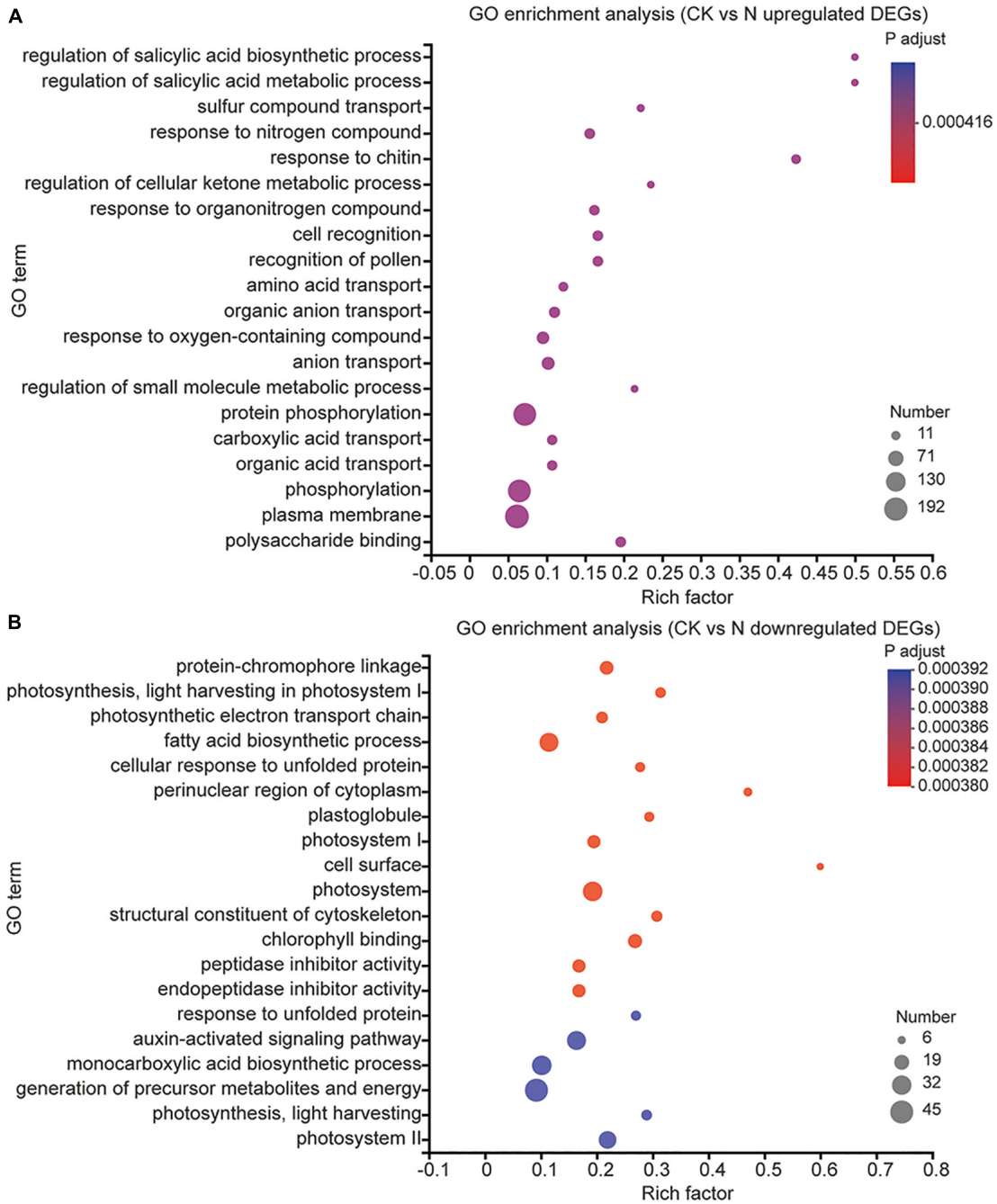

FIGURE 3 | GO enrichment analysis of DEGs under urea treatments. **(A)** The GO terms were enriched from upregulated DEGs. **(B)** The GO terms were enriched from downregulated DEGs.

different from those in the melatonin, urea and MN treatment groups (**Figure 4A** and **Supplementary Table 6**). MN treatment has more differences than melatonin or urea treatment, which demonstrated that additional melatonin treatment significantly altered the transcriptional patterns induced by urea treatment. For example, we found that the DEGs in three clusters (Cluster 9, Cluster 19 and Cluster 18) had similar expression patterns in response to the melatonin and MN treatments compared with urea treatment. A total of 289 DEGs in Cluster 9 were downregulated in response to the melatonin and MN treatments, and these DEGs were not affected by the urea treatment (**Figure 4B**). In Cluster 19, 80 DEGs that were downregulated in response to urea treatment were highly expressed in response to the melatonin and MN treatments (**Figure 4C**). Cluster 18 contained 37 DEGs that were upregulated in response to the urea treatment, while these DEGs were downregulated in response to

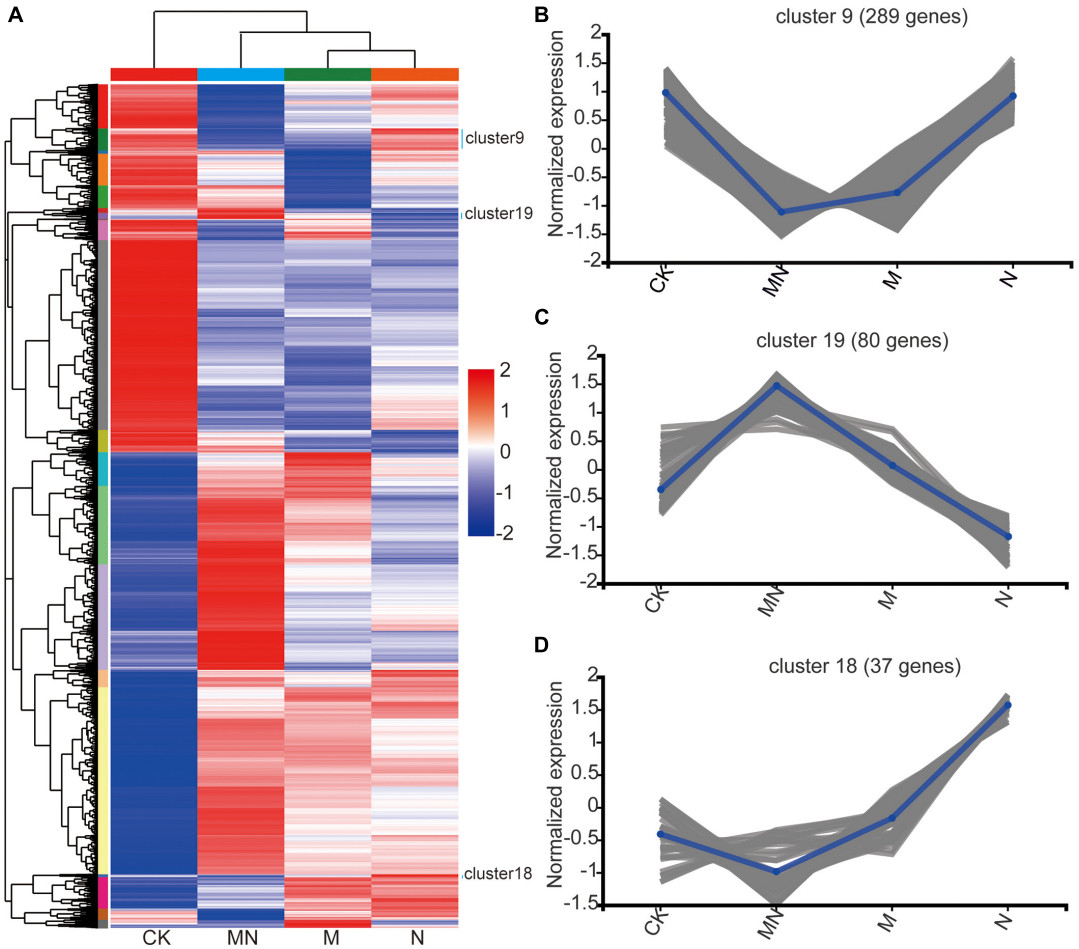

FIGURE 4 | The expression pattern of DEGs among different treatments. **(A)** All DEGs were clustered and shown in a heat map. **(B–D)** Normalized expression pattern of DEGs from cluster 9, 19 and 18. CK, Control; N, foliar application of urea alone; M, foliar application of melatonin alone; MN, foliar application of both melatonin and urea.

the melatonin and MN treatments (**Figure 4D**). These results indicated that the melatonin and urea treatments induced different DEGs and affect different physiological pathways.

We also utilized the GO enrichment tool to examine the functions of these DEGs in Clusters 9, 18 and 19. In Cluster 9, all genes displayed lower expression level under melatonin and MN treatment than urea treatment (**Figure 4B**), and these genes were involved in "starch biosynthetic process (GO:0019252)," "amine transport (GO:0015837)," "methylammonium transport (GO:0015843)" and "glycogen biosynthetic process (GO:0005978)" (**Figure 5A**), indicating that repression of these biological processes by melatonin and MN treatment might reduce the growth of soybean and yields production; In Cluster 18, all genes showed highest expression level in response to urea treatment (**Figure 4D**). The genes were involved in "lignin metabolic process," "flavone biosynthetic process (GO:0051554)" and several transporters activity-related processes (**Figure 5B**), indicating that these genes might be beneficial for soybean development in response to urea treatment. In Cluster 19, all genes showed highest expression level in response to both melatonin and MN treatment (**Figure 4C**). We found that "heat shock protein binding (GO:0031072)," "misfolded protein binding (GO:0051787)" and unfolded protein binding related biological processes were highly enriched in Cluster 19 (**Figure 5C**). These highly expressed genes in response to melatonin and MN treatment might repress soybean growth and reduce yields.

Melatonin Affects the Microbial Community Diversity in Soybean Rhizosphere

Rhizosphere microbe play an important role in plant growth and yield. Firstly, we quantified bacterial numbers in rhizosphere samples using a general bacterial primer pair targeted at the *16S rRNA* gene. We found four treatments (ZD28N, ZD63N, ZD63M and ZD63NM) significantly reduced bacterial target numbers in rhizosphere samples compared to the bulk soil, but there was no significant difference among other treatments (**Supplementary Figure 4**). This result indicated that urea and

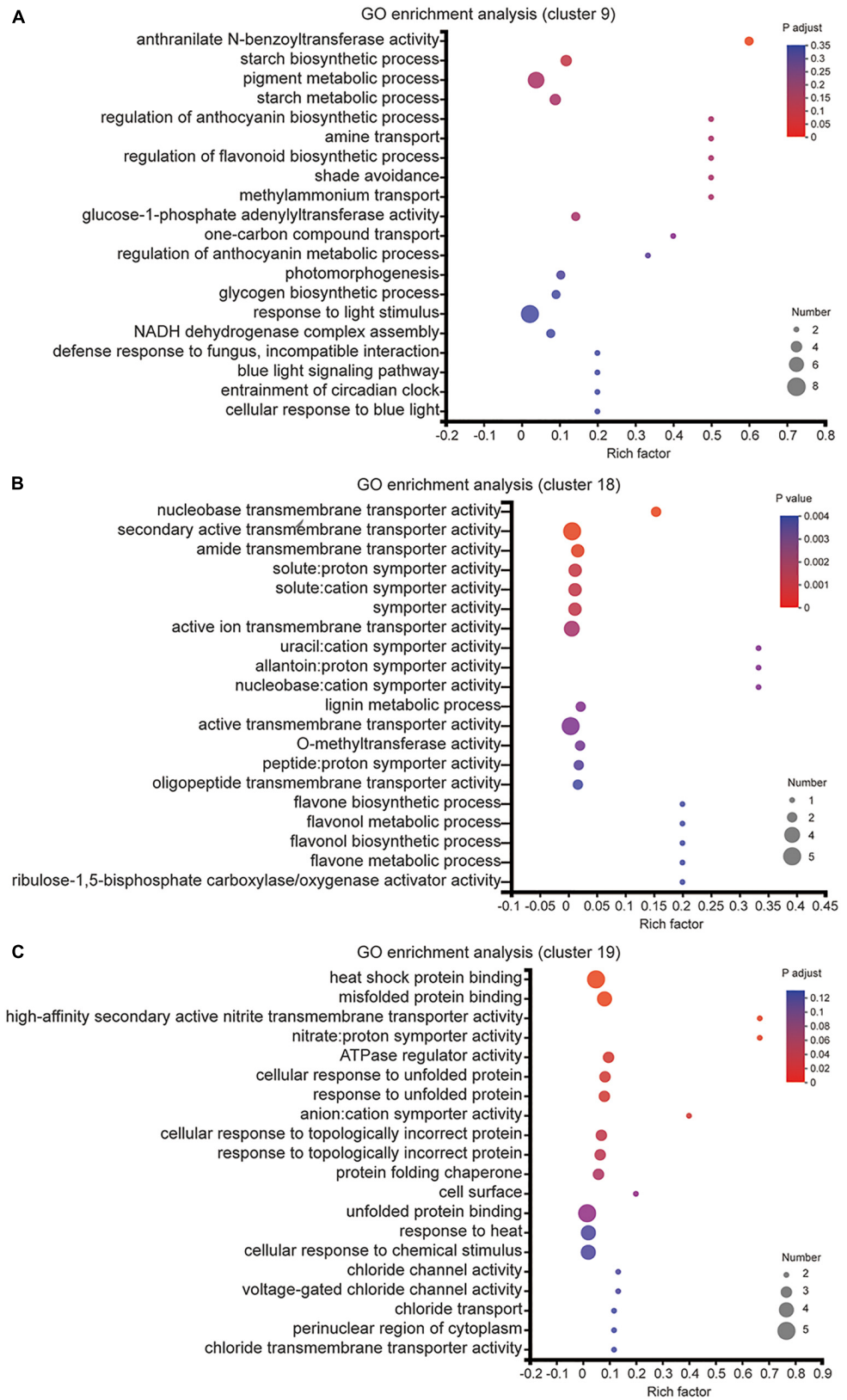

FIGURE 5 | GO enrichment analysis of DEGs from cluster 9, cluster 18 and cluster 19. **(A–C)** The enriched GO terms of cluster 9 **(A)**, cluster 18 **(B)** and cluster 19 **(C)** DEGs.

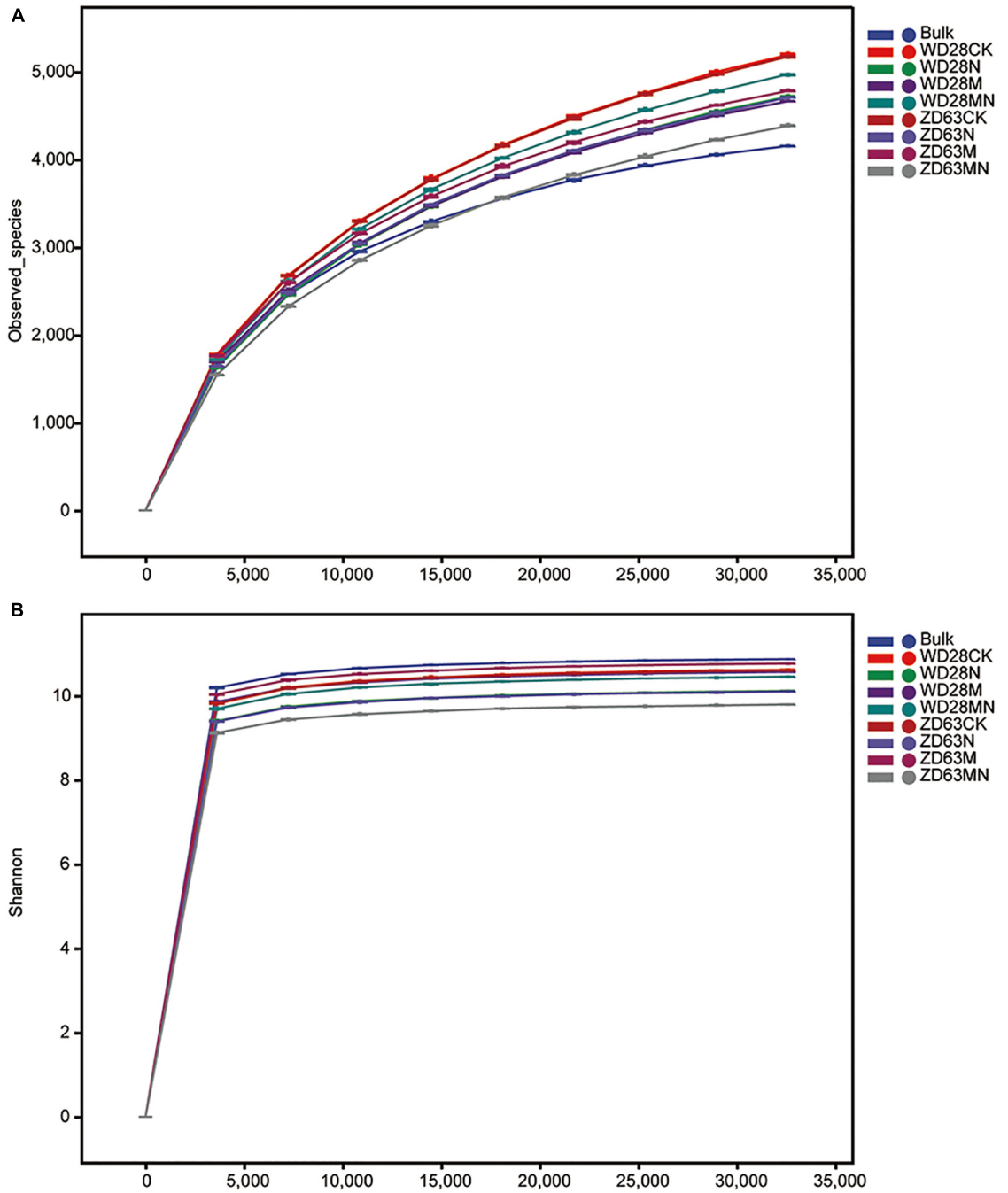

FIGURE 6 | Rarefaction curves of rhizosphere samples with different treatments. **(A,B)** The rhizosphere samples were collected from Yangluo **(A)** and Jinmen **(B)** field station, where two cultivars WD28 and ZD63 were planted. WD28CK or ZD63CK indicates normal growth WD28 or ZD63 without treatment; WD28M or ZD63M indicates foliar application of melatonin to WD28 or ZD63; WD28N or ZD63N indicates foliar application of urea to WD28 or ZD63; WD28MN or ZD63MN indicates foliar application of both melatonin and urea to WD28 or ZD63.

melatonin treatment did not affect the total number of bacteria in rhizosphere soil. To further evaluate whether the effects of urea and melatonin on the yield of were related to rhizosphere microbe, we detected the microbial community diversity and structure of rhizosphere samples collected from Yangluo base by 16S rRNA sequencing. In total, 5,273,449 (average of 101,412) high-quality 16S rRNA gene (V3-V4) reads were obtained from 52 samples, and 3,136,811 (average of 60,323) ASVs were obtained. Rarefaction curves based on species richness (observed species and Shannon index) showed clear asymptotes and plateau levels for the different samples (**Figures 6A,B**); these results indicated that the sampling depth was adequate. Across all

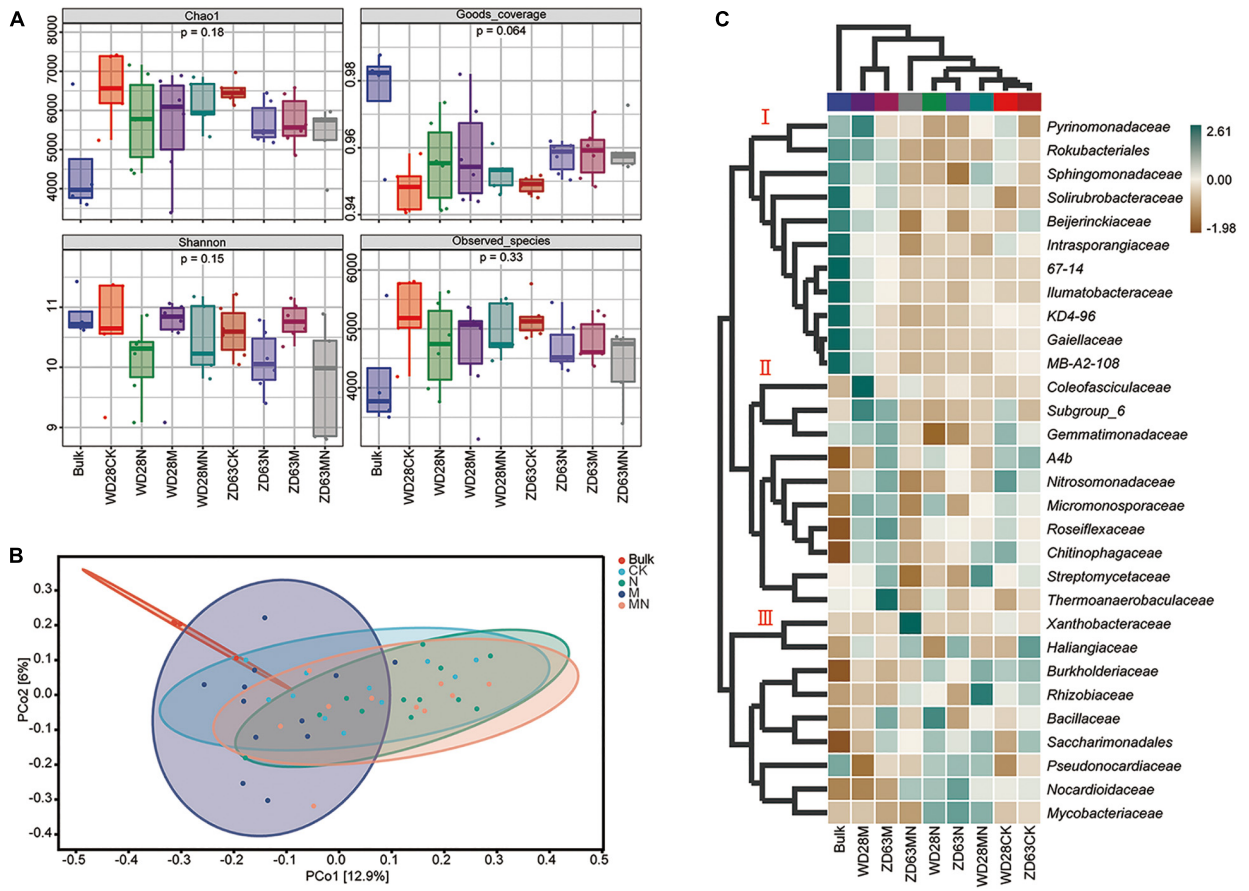

FIGURE 7 | Effects of urea and melatonin on microbial diversity and composition in soybean rhizosphere. **(A)** The alpha diversity (Chao1, Goods_coverage, Shannon, Observed_species) analysis of samples. **(B)** PCoA analysis based on Bray-Curtis distances of the different treatment of rhizosphere sample; Clustering significance by treatment was determined by Adonis [Pr (> F) = 0.001]. **(C)** Composition and clustering of bacterial microorganisms from different rhizosphere samples on the Family level.

the samples, we detected approximately 27 phyla, 78 classes, 156 orders, 246 families and 391 genera. The top ten phyla were Acidobacteria, Proteobacteria, Acidobacteria, Chloroflexi, Cyanobacteria, Firmicutes, Bacteroidetes, Gemmatimonadetes, Patescibacteria and Rokubacteria.

Combining two sampling times, we found that the alpha diversity indexes including Chao1, Goods_coverage, Shannon and Observed_species were not significantly different among the different treatment groups (**Figure 7A**), which indicated that the foliar urea and melatonin treatments did not affect rhizosphere microbial alpha diversity. We then conducted beta-diversity (PCoA) analysis to detect differences in structure among samples. The PCoA showed that the rhizosphere samples from the bulk soil and treatment groups were clearly separated (**Figure 7B**), indicating that planting soybean plants can affect the microbial community structure of soil. However, the rhizosphere samples from the control and urea treatment groups were not clearly separated (**Figure 7B**), and PERMANOVA based on the Bray-Curtis distances showed that the differences were not significant (**Table 1**); these results suggested that foliar urea treatments did also not affect the rhizosphere microbial community structure. For the melatonin treated samples, the rhizosphere samples were significantly separated from the control, urea treatment and urea plus melatonin treatment. The PERMANOVA based on the Bray-Curtis distances showed that the differences between melatonin and other three treatments were significant (**Table 1**); these results suggested that foliar urea treatments did not affect the rhizosphere microbial community structure, but melatonin did. For the urea and melatonin treatment, we found that the microbial community structure was similar to that treated with urea alone, but significantly different from that treated with melatonin (**Table 1**). It suggested that the effect of melatonin on rhizosphere microbial structure began to weaken when urea was added.

The Effect of Melatonin on Rhizosphere Microbial Species Was Greater Than That of Urea

To further determine the trends of the changes in microbial abundance among the various treatment groups, we conducted a cluster analysis at the family level. The result showed that samples

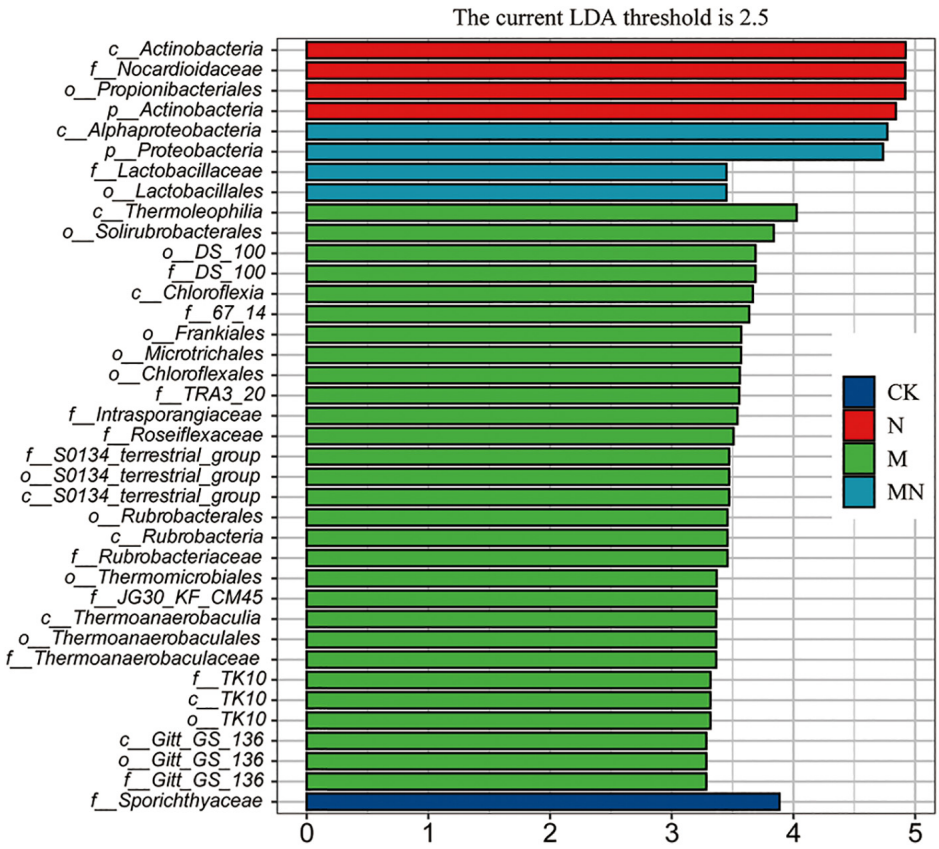

FIGURE 8 | Effects of nitrogen and melatonin on microbe species in soybean rhizosphere. Linear discriminant analysis (LDA) coupled with the effect size measurements identifies the significant abundance of data in different treatment. Only taxa with LDA values greater than 2.5 ($P < 0.05$) were shown.

exposed to the same treatment obviously clustered together, and the top 30 families could be divided into three main clusters, which hosted distinct bacterial assemblages (**Figure 7C**). Among them, the abundance of cluster 1 was higher in the bulk soil, the abundance of taxa in cluster 2 was higher in melatonin treatment groups, and the abundance of taxa in cluster 3 was the highest in the urea and melatonin plus urea treatment groups. The taxa enriched in the control samples include cluster 2 and cluster 3. Finally, through linear discriminant analysis (LEfSe, LDA log score threshold > 2.5, abundance > 0.001 and $P < 0.05$), we found that the *f__Nocardioidaceae* abundance increased after urea treatment. Nevertheless, the abundance of a large number of taxa was altered after melatonin treatment. For example, the relative abundances of *f__DS_100*, *f__67_14*, *f__TRA3_20*, *f__Intrasporangiaceae*, *f__Roseiflexaceae*, *f__*S0134_terrestrial_group, *f__Rubrobacteriaceae*, *f__JG30_KF_CM45*, *f__Thermoanaerobaculaceae*, *f__TK10* and *f__Gitt_GS_136* were altered. When urea and melatonin were treated together, the changed microorganisms became less (**Figure 8**). These results indicated that the effect of urea on rhizosphere microorganisms was less than that of melatonin, urea treatment only changed the abundance of a few microorganisms which led to little effect on microbial community structure; while melatonin treatment increased the abundance of microorganisms, which led to significant changes in microbial community structure. The abundance of microorganisms decreased when urea plus melatonin treatment was applied, but the yield did not increase (**Figure 1**). It suggested that the response of underground microbial community to foliar urea and melatonin treatment was independent of yield.

DISCUSSION

Nitrogen is an essential nutrient for plant growth and crop yields. Melatonin has been reported to promote nitrogen uptake and assimilation and increase plant growth (Qiao et al., 2019), but few studies have explored the possible effects of melatonin and nitrogen treatment on soybean with detailed transcriptomic and microbiome analyses. In this study, a combination of transcriptomic and microbiome analyses was performed to highlight the effect of exogenous melatonin and urea on field growth soybean. Field experiments revealed that foliar application of both melatonin and urea decreased soybean yields compared with application of urea alone (**Figure 1**). Our transcriptome analysis revealed that urea treatment induced genes expression related to amino acid transport and nitrogen compound response processes, while melatonin

TABLE 1 | PERMANOVA analysis of the rhizosphere microbial community in different group based on Bray–Curtis.

Group 1	Group 2	Sample size	Permutations	Pseudo F	*P*-value	*Q*-value
All	–	49	999	1.932	0.001	–
Bulk	CK	15	999	2.830	0.003	0.005
Bulk	N	16	999	3.684	0.001	0.005
Bulk	M	16	999	2.038	0.003	0.005
Bulk	NM	14	999	3.332	0.002	0.005
CK	N	23	999	1.165	0.128	0.160
CK	M	23	999	1.462	0.016	0.023
CK	NM	21	999	1.096	0.215	0.239
N	M	24	999	2.279	0.001	0.005
N	NM	22	999	1.029	0.329	0.329
M	NM	22	999	1.803	0.002	0.005

application may exert its opposite effects mainly through regulation the genes expression related to signal transduction and stress response pathways (**Figure 3** and **Supplementary Figures 2**, **3**). The combined application of melatonin and urea significantly altered the gene expression pattern compared with the urea treatment (**Figure 4**). The microbiome analysis also demonstrated that melatonin not urea treatments affected the rhizosphere microbial community structure, and the combined application of melatonin and urea showed similar microbial community structure to that treated with urea alone. Both melatonin and urea treatment changed the abundance of several microorganisms (**Figures 7**, **8**). This study highlighted the possible antagonistic effects of melatonin application on the transcriptomic and soil microorganisms compared with urea treatment in soybean.

A transcriptional approach was first used to explain the antagonistic effects between melatonin and urea treatment. Foliar application of melatonin or urea could induce some similar and different changes at the transcriptional level in soybean (**Figure 3**). Urea or melatonin treatment affected several common biological processes, such as responsive to salicylic acid biosynthetic and metabolic process, chitin, nitrogen compound and organonitrogen compound, indicating overlapping functions of these two chemical compounds. However, a significant difference was also observed. Our Venn diagram sorting, hierarchical clustering, and GO enrichment analysis revealed some specific DEGs were induced upon different treatments. It is noteworthy that urea treatment affected amino acid transport biological process specifically, which was different from melatonin treatment. We found some DEGs under melatonin and MN treatments displayed similar expression pattern compared with urea treatment (**Figures 4C,D**), for example, DEGs in two clusters (Cluster 9 and Cluster 18) decreased expression in response to the melatonin and MN treatments compared with urea treatment (**Figure 4**). We then took a close look at the gene expression under melatonin and urea treatment and found that the expression levels of the *GmNRT2.5* (*Glyma.08G284000* and *Glyma.18G141900*) genes which involved in nitrate transport were upregulated in the urea treated samples (**Figure 2E**). While under melatonin treatment, the genes involved in abiotic stresses were mainly induced. For example, the expression of genes related to wounding responses *GmJAR6* (*Glyma.06G243500*), heat responses *GmHSF18* (*Glyma.09G143200* and *Glyma.16G196200*), and *GmHSP20* (*Glyma.20G015900, Glyma.07G043600* and *Glyma.16G012000*) were highly induced in RNA-seq data (**Figure 4A** and **Supplementary Table 3**). When melatonin and urea were both applied to soybean, obviously different transcription patterns were observed. Additional melatonin application induced the expression of genes related to salt stress response (*Glyma.10G253000*) and cell death (*GmTIR2*; *Glyma.06G268700, Glyma.08G301200* and *Glyma.09G075500*). These transcriptional differences between melatonin and urea treatment might partially explain the reduced soybean yields by additional application melatonin to urea treatment, implying that melatonin was not beneficial for soybean growth and yields production when foliar application it at grain filling stage. In addition, it was clearly demonstrated that urea is converted to amino acids in leaves after foliar application, and root nitrogen uptake is enhanced by the application of urea to leaves of apple trees (Dong et al., 2015), we speculated that foliar melatonin application might also affect the leaf nitrogen metabolism and root nitrogen uptake. Based on the transcriptomic results and soybean yields production under melatonin treatment, we might carefully choose an appropriate growth stage of soybean for melatonin foliar application, and the melatonin concentration should also be considered.

Rhizosphere or root microorganisms play an important role in the soil nitrogen cycle and are beneficial to the absorption of nitrogen by plants (Hacquard et al., 2015). In turn, nitrogen in the soil also affects the microbial community structure in the soil (Zeng et al., 2016), but the response of the microbial structure in the rhizosphere or root to different forms or concentrations of nitrogen [nitrate (NO_3^--N, NH_4^+-N) and organic nitrogen] varies in soil and water environments (Gallart et al., 2018; Zhao et al., 2020). Generally, nitrogen levels in the soil mainly increased the abundance of *Proteobacteria* and *Bacteroidetes* but decreased the abundance of *Acidobacteria* and *Planctomycetes* (Kavamura et al., 2018; Liu et al., 2019; Zhou et al., 2021). In wheat, high levels of inorganic nitrogen in soil were found to have a significantly negative effect on bacterial richness and diversity, leading to a less stable bacterial community structure over time (Kavamura et al., 2018). In

leguminous plants, application of excessive levels of nitrogen compounds to soil strongly inhibits nodule formation and changes the rhizosphere microbial community structure. Foliar nitrogen application can enhance crop yields; but it can alleviate the effect of nitrogen on soil properties. In our study, we found that the abundance of only a few taxa (such as *Nocardioidaceae*) were altered after nitrogen treatment through linear discriminant analysis (**Figure 7**). At the community level, we found that foliar application of urea reduced the abundance and diversity of rhizosphere microorganisms, but the difference was not significant (**Figure 7A**). In addition, foliar application of urea had no effect on the structure of rhizosphere microorganisms (**Figure 8**). These results suggested that compared to soil nitrogen application, aboveground nitrogen application has little effect on underground rhizosphere microorganisms. Altogether, our findings addressed the interesting question about whether the benefits associated with foliar urea application can be attributed to meeting the nutritional demand of the crop plant for nitrogen without restructuring the soil microbial community assemblage.

However, the effect of melatonin treatment on rhizosphere microorganisms was obviously different from that of urea treatment. Melatonin treatment did not change the soil microbial alpha diversity, but it did alter rhizosphere microbial community structure and the abundance of a larger number of taxa than urea treatment (**Figure 8**). Melatonin inhibited the abundance of *Nocardioidaceae* but increased the abundance of *f__DS_100*, *f__67_14*, *f__*TRA3_20, *f__Intrasporangiaceae*, *f__*Roseiflexaceae, *f__S0134_terrestrial_group*, *f__Rubrobacteriaceae*, *f__JG30_KF_CM45*, *f__Thermoanaerobaculaceae*, *f__TK10* and *f__Gitt_GS_136*, resulting in significant changes in the community structure of rhizosphere microorganisms. Interestingly, melatonin did not change the structure of rhizosphere microbial community when urea was applied at the same time, but it could affect the promotion role of urea on yield. Melatonin had been shown to reprogram gut microbiota communities in animals and humans (Ghareghani et al., 2018; Ren et al., 2018). In mice, melatonin can reverse high-fat diet-induced lipid accumulation and gut microbiota alterations (Yin et al., 2018). The effect of melatonin on rhizosphere microbial community structure has not been reported in soybean, and the mechanism is unknown. We speculated that melatonin may affect the structure of rhizosphere microorganisms by affecting plant physiological metabolism.

In conclusion, we proved that melatonin could not further promote soybean yields under urea treatment, and revealed the possible mechanism by transcriptomic and microbiome analyses. Foliar application of melatonin induced the expression of a set of genes in soybean leaves and changed rhizosphere microbial community structure which different from urea treatment, which might influence the soybean yields. Thus, to develop melatonin as a plant growth regulator that can be practically used in crop production, optimized agricultural practices including the crop performance, application method and plant growth stage still required further exploration.

DATA AVAILABILITY STATEMENT

The data presented in this study are deposited in the National Genomics Data Center repository, accession number: PRJCA009060 (https://ngdc.cncb.ac.cn/bioproject/).

AUTHOR CONTRIBUTIONS

HJ conceived and designed the project. RX, QH, YL, XZ, QGH, QC, YH, and JD performed the experiments. RX and QH analyzed the data. RX, QH, and HJ wrote the manuscript. All authors read and approved the final manuscript.

FUNDING

This work was funded by the National Key Research and Development Program of China (2018YFD10009002). The funder was not involved in the design of the study, analysis of data, and manuscript writing.

SUPPLEMENTARY MATERIAL

The Supplementary Material for this article can be found online at: https://www.frontiersin.org/articles/10.3389/fmicb.2022.903467/full#supplementary-material

Supplementary Figure 1 | Correlation analysis between samples. CK, Control; N, foliar application of urea alone; M, foliar application of melatonin alone; MN, foliar application of both melatonin and urea. The colors represent the correlation coefficient (red color indicates higher correlation and blue color indicates lower correlation).

Supplementary Figure 2 | GO enrichment analysis of DEGs under melatonin treatments. **(A)** The GO terms were enriched from upregulated DEGs. **(B)** The GO terms were enriched from downregulated DEGs.

Supplementary Figure 3 | GO enrichment analysis of DEGs under urea and melatonin treatments. **(A)** The GO terms were enriched from upregulated DEGs. **(B)** The GO terms were enriched from downregulated DEGs.

Supplementary Figure 4 | The quantification of total bacteria in rhizosphere samples. The quantification of total bacteria in rhizosphere samples. qPCR results of the different treatments were analyzed with Newman-Keuls Multiple Comparison Test tests ($n = 3$, * indicates $P < 0.05$). WD28CK or ZD63CK indicates normal growth WD28 or ZD63 without treatment; WD28M or ZD63M indicates foliar application of melatonin to WD28 or ZD63; WD28N or ZD63N indicates foliar application of urea to WD28 or ZD63; WD28MN or ZD63MN indicates foliar application of both melatonin and urea to WD28 or ZD63.

Supplementary Table 1 | Raw data statistics.

Supplementary Table 2 | Quality control data statistics.

Supplementary Table 3 | Differentially expressed genes.

Supplementary Table 4 | qRT-PCR primers.

Supplementary Table 5 | GO enrichment analysis of CK compared with each differern treatment.

Supplementary Table 6 | GO enrichment analysis of different clusters.

REFERENCES

Antoniou, C., Chatzimichail, G., Xenofontos, R., Pavlou, J. J., Panagiotou, E., Christou, A., et al. (2017). Melatonin systemically ameliorates drought stress-induced damage in *Medicago sativa* plants by modulating nitro-oxidative homeostasis and proline metabolism. *J. Pineal Res.* 62:e12401. doi: 10.1111/jpi.12401

Arnao, M. B., and Hernández-Ruiz, J. (2014). Melatonin: plant growth regulator and/or biostimulator during stress? *Trends Plant Sci.* 19, 789–797. doi: 10.1016/j.tplants.2014.07.006

Arnao, M. B., and Hernández-Ruiz, J. (2015). Functions of melatonin in plants: a review. *J. Pineal Res.* 59, 133–150. doi: 10.1111/jpi.12253

Arnao, M. B., and Hernández-Ruiz, J. (2019). Melatonin: a new plant hormone and/or a plant master regulator? *Trends Plant Sci.* 24, 38–48. doi: 10.1016/j.tplants.2018.10.010

Balabusta, M., Katarzyna, S., and Posmyk, M. M. (2016). Exogenous melatonin improves antioxidant defense in cucumber seeds (*Cucumis sativus* L.) germinated under chilling stress. *Front. Plant Sci.* 7:575. doi: 10.3389/fpls.2016.00575

Bolyen, E., Rideout, J. R., Dillon, M. R., Bokulich, N. A., and Caporaso, J. G. (2018). QIIME 2: reproducible, interactive, scalable, and extensible microbiome data science. *PeerJ Prepr.* 6:e27295v2. doi: 10.7287/peerj.preprints.27295v2

Byeon, Y., and Back, K. (2014). An increase in melatonin in transgenic rice causes pleiotropic phenotypes, including enhanced seedling growth, delayed flowering, and low grain yield. *J. Pineal Res.* 56, 408–414. doi: 10.1111/jpi.12129

Cao, L., Jin, X., Zhang, Y., Zhang, M., and Wang, Y. (2020). Transcriptomic and metabolomic profiling of melatonin treated soybean (*Glycine max* L.) under drought stress during grain filling period through regulation of secondary metabolite biosynthesis pathways. *PLoS One* 15:e0239701. doi: 10.1371/journal.pone.0239701

Cassim, B. M. A. R., Machado, A. P. M., Fortune, D., Moreira, F. R., Zampar, É. J. D. O., and Batista, M. A. (2020). Effects of foliar application of urea and urea-formaldehyde/triazone on soybean and corn crops. *Agronomy* 10:1549. doi: 10.3390/agronomy10101549

Chen, S., Waghmode, T. R., Sun, R., Kuramae, E. E., Hu, C., and Liu, B. (2019). Root-associated microbiomes of wheat under the combined effect of plant development and nitrogen fertilization. *Microbiome* 7:136. doi: 10.1186/s40168-019-0750-2

Chu, H., Lin, X., Fujii, T., Morimoto, S., Yagi, K., Hu, J., et al. (2007). Soil microbial biomass, dehydrogenase activity, bacterial community structure in response to long-term fertilizer management. *Soil Biol. Biochem.* 39, 2971–2976. doi: 10.1016/j.soilbio.2007.05.031

Dewey, C. N., and Li, B. (2011). RSEM: accurate transcript quantification from RNA-Seq data with or without a reference genome. *BMC Bioinformatics* 12:323. doi: 10.1186/1471-2105-12-323

Dong, S., Cheng, L., Scagel, C., and Fuchigami, L. (2015). Timing of urea application affects leaf and root N uptake in young Fuji/M.9 apple trees. *J. Hortic. Sci. Biotechnol.* 80, 116–120. doi: 10.1080/14620316.2005.11511901

Fierer, N., Jackson, J. A., Vilgalys, R., and Jackson, R. B. (2005). Assessment of soil microbial community structure by use of taxon-specific quantitative PCR assays. *Appl. Environ. Microbiol.* 71, 4117–4120. doi: 10.1128/AEM.71.7.4117-4120.2005

Gallart, M., Adair, K. L., Love, J., Meason, D. F., Clinton, P. W., and Xue, J. M. (2018). Host genotype and nitrogen form shape the root microbiome of *Pinus radiata*. *Microb. Ecol.* 75, 419–433. doi: 10.1007/s00248-017-1055-2

Gao, Q. H., Jia, S. S., Miao, Y. M., Xiao-Min, L. U., and Hui-Min, L. I. (2016). Effects of exogenous melatonin on nitrogen metabolism and osmotic adjustment substances of melon seedlings under sub-low temperature. *Ying Yong Sheng Tai Xue Bao* 27, 519–524. doi: 10.13287/j.1001-9332.201602.016

Gaonkar, V., and Rosentrater, K. A. (2019). *Integrated Processing Technologies for Food and Agricultural By-Products*. Cambridge, MA: Academic Press, 73–104. doi: 10.1016/b978-0-12-814138-0.00004-6

Garnett, T., Plett, D., Heuer, S., and Okamoto, M. (2015). Genetic approaches to enhancing nitrogen-use efficiency (NUE) in cereals: challenges and future directions. *Funct. Plant Biol.* 42, 921–941. doi: 10.1071/FP15025

Ghareghani, M., Reiter, R. J., Zibara, K., and Farhadi, N. (2018). Latitude, vitamin D, melatonin, and gut microbiota act in concert to initiate multiple sclerosis: a new mechanistic pathway. *Front. Immunol.* 9:2484. doi: 10.3389/fimmu.2018.02484

González-Arenzana, L., Portu, J., Lopez, R., Garijo, P., Garde-Cerdan, T., and Lopez-Alfaro, I. (2017). Phenylalanine and urea foliar application: effect on grape and must microbiota. *Int. J. Food Microbiol.* 245, 88–97. doi: 10.1016/j.ijfoodmicro.2017.01.017

Gooding, M. J., and Davies, W. P. (1992). Foliar urea fertilization of cereals: a review. *Fertilizer Res.* 32, 209–222. doi: 10.1007/BF01048783

Hacquard, S., Garrido-Oter, R., Gonzalez, A., Spaepen, S., Ackermann, G., Lebeis, S., et al. (2015). Microbiota and host nutrition across plant and animal kingdoms. *Cell Host Microbe* 17, 603–616. doi: 10.1016/j.chom.2015.04.009

Hassanein, A., Mesbah, E., Soliman, F., and El-Aidy, T. (2019). Effect of nitrogen rates, biofertilizers and foliar urea application on yield and yield components of maize (*Zea mays*, L.). *J. Plant Prod.* 10, 53–58. doi: 10.21608/jpp.2019.36203

Hattori, A., Migitaka, H., Iigo, M., Itoh, M., and Reiter, R. J. (1995). Identification of melatonin in plants and its effects on plasma melatonin levels and binding to melatonin receptors in vertebrates. *Biochem. Mol. Biol. Int.* 35, 627–634.

Kavamura, V. N., Rifat, H., Clark, I. M., Maike, R., Rodrigo, M., Hirsch, P. R., et al. (2018). Inorganic nitrogen application affects both taxonomical and predicted functional structure of wheat rhizosphere bacterial communities. *Front. Microbiol.* 9:1074. doi: 10.3389/fmicb.2018.01074

Kim, D., Langmead, B., and Salzberg, S. L. (2015). HISAT: a fast spliced aligner with low memory requirements. *Nat. Methods* 12, 357–360. doi: 10.1038/nmeth.3317

Lassaletta, L., Billen, G., Grizzetti, B., Anglade, J., and Garnier, J. (2014). 50 year trends in nitrogen use efficiency of world cropping systems: the relationship between yield and nitrogen input to cropland. *Environ. Res. Lett.* 9:105011. doi: 10.1088/1748-9326/9/10/105011

Lerner, A. B., Case, J. D., Takahashi, Y., Lee, T. H., and Mori, W. (1958). Isolation of melatonin, the pineal gland factor that lightens melanocytes1. *J. Am. Chem. Soc.* 80, 2587–2587. doi: 10.1021/ja01543a060

Lin, J. S., Li, X., Luo, Z., Mysore, K. S., Wen, J., and Xie, F. (2018). NIN interacts with NLPs to mediate nitrate inhibition of nodulation in *Medicago truncatula*. *Nat. Plants* 4, 942–952. doi: 10.1038/s41477-018-0261-3

Liu, F., Hewezi, T., Lebeis, S. L., Pantalone, V., Grewal, P. S., and Staton, M. E. (2019). Soil indigenous microbiome and plant genotypes cooperatively modify soybean rhizosphere microbiome assembly. *BMC Microbiol.* 19:201. doi: 10.1186/s12866-019-1572-x

Love, M. I., Huber, W., and Anders, S. (2014). Moderated estimation of fold change and dispersion for RNA-seq data with DESeq2. *Genome Biol.* 15:550. doi: 10.1186/s13059-014-0550-8

Lyu, X., Liu, Y., Li, N., Ku, L., Hou, Y., and Wen, X. (2021). Foliar applications of various nitrogen (N) forms to winter wheat affect grain protein accumulation and quality *via* N metabolism and remobilization. *Crop J.* doi: 10.1016/j.cj.2021.10.009 [Epub ahead of print].

Nadkarni, M. A., Martin, F. E., Jacques, N. A., and Hunter, N. (2002). Determination of bacterial load by real-time PCR using a broad-range (universal) probe and primers set. *Microbiology* 148, 257–266. doi: 10.1099/00221287-148-1-257

Nishida, H., Tanaka, S., Handa, Y., Ito, M., Sakamoto, Y., Matsunaga, S., et al. (2018). A NIN-LIKE PROTEIN mediates nitrate-induced control of root nodule symbiosis in *Lotus japonicus*. *Nat. Commun.* 9:499. doi: 10.1038/s41467-018-02831-x

Pertea, M., Pertea, G. M., Antonescu, C. M., Chang, T. C., Mendell, J. T., and Salzberg, S. L. (2015). StringTie enables improved reconstruction of a transcriptome from RNA-seq reads. *Nat. Biotechnol.* 33, 290–295. doi: 10.1038/nbt.3122

Qiao, Y., Yin, L., Wang, B., Ke, Q., Deng, X., and Wang, S. (2019). Melatonin promotes plant growth by increasing nitrogen uptake and assimilation under nitrogen deficient condition in winter wheat. *Plant Physiol. Biochem.* 139, 342–349. doi: 10.1016/j.plaphy.2019.03.037

Ren, W., Peng, W., Yan, J., Gang, L., and Yin, Y. (2018). Melatonin alleviates weanling stress in mice: involvement of intestinal microbiota. *J. Pineal Res.* 64:e12448. doi: 10.1111/jpi.12448

Rodríguez-Blanco, A., Sicardi, M., and Frioni, L. (2015). Plant genotype and nitrogen fertilization effects on abundance and diversity of diazotrophic

bacteria associated with maize (*Zea mays* L.). *Biol. Fertil. Soils* 51, 391–402. doi: 10.1007/s00374-014-0986-8

Rossmann, A., Buchner, P., Savill, G. P., Powers, S. J., Hawkesford, M. J., and Muhling, K. H. (2019). Foliar N application at anthesis stimulates gene expression of grain protein fractions and alters protein body distribution in winter wheat (*Triticum aestivum* L.). *J. Agric. Food Chem.* 67, 12709–12719. doi: 10.1021/acs.jafc.9b04634

Segata, N., Izard, J., Waldron, L., Gevers, D., Miropolsky, L., and Huttenhower, G. C. (2011). Metagenomic biomarker discovery and explanation. *Genome Biol.* 12:R60. doi: 10.1186/gb-2011-12-6-r60

Tiwari, R. K., Lal, M. K., Kumar, R., Chourasia, K. N., Naga, K. C., Kumar, D., et al. (2021). Mechanistic insights on melatonin-mediated drought stress mitigation in plants. *Physiol. Plant.* 172, 1212–1226. doi: 10.1111/ppl.13307

Vran, J. (1972). The effect of foliar application of urea on the root fungi of wheat growing in soil artificially contaminated with *Fusarium* spp. *Folia Microbiol.* 17, 500–504. doi: 10.1007/BF02872735

Wagan, Z. A., Buriro, M., Wagan, T. A., Wagan, Z. A., Jamro, S. A., Memon, Q. U. A., et al. (2017). Effect of foliar applied urea on growth and yield of wheat (*Triticum aestivum* L.). *Int. J. Bioorganic Chem.* 2, 185–191. doi: 10.11648/j.ijbc.20170204.15

Wang, J., Song, Y., Ma, T., Raza, W., Li, J., Howland, J. G., et al. (2017). Impacts of inorganic and organic fertilization treatments on bacterial and fungal communities in a paddy soil. *Appl. Soil Ecol.* 112, 42–50. doi: 10.1016/j.apsoil.2017.01.005

Wei, W., Li, Q. T., Chu, Y. N., Reiter, R. J., Yu, X. M., Zhu, D. H., et al. (2015). Melatonin enhances plant growth and abiotic stress tolerance in soybean plants. *J. Exp. Bot.* 66, 695–707. doi: 10.1093/jxb/eru392

Yin, J., Li, Y., Han, H., Chen, S., Gao, J., Liu, G., et al. (2018). Melatonin reprogramming of gut microbiota improves lipid dysmetabolism in high-fat diet-fed mice. *J. Pineal Res.* 65:e12524. doi: 10.1111/jpi.12524

Zeng, J., Liu, X., Song, L., Lin, X., Zhang, H., Shen, C., et al. (2016). Nitrogen fertilization directly affects soil bacterial diversity and indirectly affects bacterial community composition. *Soil Biol. Biochem.* 92, 41–49. doi: 10.1016/j.soilbio.2015.09.018

Zhang, J., Liu, Y. X., Zhang, N., Hu, B., Jin, T., Xu, H., et al. (2019). NRT1.1B is associated with root microbiota composition and nitrogen use in field-grown rice. *Nat. Biotechnol.* 37, 676–684. doi: 10.1038/s41587-019-0104-4

Zhang, J., Shi, Y., Zhang, X., Du, H., Xu, B., and Huang, B. (2017). Melatonin suppression of heat-induced leaf senescence involves changes in abscisic acid and cytokinin biosynthesis and signaling pathways in perennial ryegrass (*Lolium perenne* L.). *Environ. Exp. Bot.* 138, 36–45. doi: 10.1016/j.envexpbot.2017.02.012

Zhang, N., Zhao, B., Zhang, H. J., Weeda, S., Yang, C., Yang, Z. C., et al. (2012). Melatonin promotes water-stress tolerance, lateral root formation, and seed germination in cucumber (*Cucumis sativus* L.). *J. Pineal Res.* 54, 15–23. doi: 10.1111/j.1600-079x.2012.01015.x

Zhang, R., Sun, Y., Liu, Z., Jin, W., and Sun, Y. (2017). Effects of melatonin on seedling growth, mineral nutrition, and nitrogen metabolism in cucumber under nitrate stress. *J. Pineal Res.* 62:e12403. doi: 10.1111/jpi.12403

Zhao, C., Ni, H., Zhao, L., Zhou, L., Borras-Hidalgo, O., and Cui, R. (2020). High nitrogen concentration alter microbial community in *Allium fistulosum* rhizosphere. *PLoS One* 15:e0241371. doi: 10.1371/journal.pone.0241371

Zheng, X., Tan, D. X., Allan, A. C., Zuo, B., Zhao, Y., Reiter, R. J., et al. (2017). Chloroplastic biosynthesis of melatonin and its involvement in protection of plants from salt stress. *Sci. Rep.* 7:41236. doi: 10.1038/srep41236

Zhou, W., Dong, J., Ding, D., Long, L., Suo, A., Lin, X., et al. (2021). Rhizosphere microbiome dynamics in tropical seagrass under short-term inorganic nitrogen fertilization. *Environ. Sci. Pollut. Res. Int.* 28, 19021–19033. doi: 10.1007/s11356-020-12048-5

Conflict of Interest: The authors declare that the research was conducted in the absence of any commercial or financial relationships that could be construed as a potential conflict of interest.

Publisher's Note: All claims expressed in this article are solely those of the authors and do not necessarily represent those of their affiliated organizations, or those of the publisher, the editors and the reviewers. Any product that may be evaluated in this article, or claim that may be made by its manufacturer, is not guaranteed or endorsed by the publisher.

Copyright © 2022 Xiao, Han, Liu, Zhang, Hao, Chai, Hao, Deng, Li and Ji. This is an open-access article distributed under the terms of the Creative Commons Attribution License (CC BY). The use, distribution or reproduction in other forums is permitted, provided the original author(s) and the copyright owner(s) are credited and that the original publication in this journal is cited, in accordance with accepted academic practice. No use, distribution or reproduction is permitted which does not comply with these terms.

frontiers | Frontiers in Microbiology

TYPE Original Research
PUBLISHED 04 October 2022
DOI 10.3389/fmicb.2022.974473

Check for updates

OPEN ACCESS

EDITED BY
José David Flores Félix,
Universidade da Beira Interior, Portugal

REVIEWED BY
Orlando Borras-Hidalgo,
Qilu University of Technology, China
Chunhao Jiang,
Nanjing Agricultural University, China

*CORRESPONDENCE
Zhaolin Ji
zhlji@yzu.edu.cn

SPECIALTY SECTION
This article was submitted to Microbe and Virus Interactions with Plants, a section of the journal Frontiers in Microbiology

RECEIVED 21 June 2022
ACCEPTED 29 August 2022
PUBLISHED 04 October 2022

CITATION
Yang L, Yan C, Peng S, Chen L, Guo J, Lu Y, Li L and Ji Z (2022) Broad-spectrum resistance mechanism of serine protease Sp1 in *Bacillus licheniformis* W10 *via* dual comparative transcriptome analysis. *Front. Microbiol.* 13:974473. doi: 10.3389/fmicb.2022.974473

COPYRIGHT
© 2022 Yang, Yan, Peng, Chen, Guo, Lu, Li and Ji. This is an open-access article distributed under the terms of the Creative Commons Attribution License (CC BY). The use, distribution or reproduction in other forums is permitted, provided the original author(s) and the copyright owner(s) are credited and that the original publication in this journal is cited, in accordance with accepted academic practice. No use, distribution or reproduction is permitted which does not comply with these terms.

Broad-spectrum resistance mechanism of serine protease Sp1 in *Bacillus licheniformis* W10 *via* dual comparative transcriptome analysis

Lina Yang[1], Chun Yan[1], Shuai Peng[1], Lili Chen[1], Junjie Guo[1], Yihe Lu[1], Lianwei Li[2] and Zhaolin Ji[1]*

[1]College of Horticulture and Plant Protection, Yangzhou University, Yangzhou, China, [2]The Key Laboratory of Biotechnology for Medicinal Plants of Jiangsu Province, School of Life Sciences, Jiangsu Normal University, Xuzhou, China

Antagonistic microorganisms are considered to be the most promising biological controls for plant disease. However, they are still not as popular as chemical pesticides due to complex environmental factors in the field. It is urgent to exploit their potential genetic characteristics and excellent properties to develop biopesticides with antimicrobial substances as the main components. Here, the serine protease Sp1 isolated from the *Bacillus licheniformis* W10 strain was confirmed to have a broad antifungal and antibacterial spectrum. Sp1 treatment significantly inhibited fungal vegetative growth and damaged the structure of hyphae, in accordance with that caused by W10 strain. Furthermore, Sp1 could activate the systemic resistance of peach twigs, fruits and tobacco. Dual comparative transcriptome analysis uncovered how Sp1 resisted the plant pathogenic fungus *Phomopsis amygdali* and the potential molecular resistance mechanisms of tobacco. In PSp1 vs. *P. amygdali*, RNA-seq identified 150 differentially expressed genes (DEGs) that were upregulated and 209 DEGs that were downregulated. Further analysis found that Sp1 might act on the energy supply and cell wall structure to inhibit the development of *P. amygdali*. In TSp1 vs. Xanthi tobacco, RNA-seq identified that 5937 DEGs were upregulated and 2929 DEGs were downregulated. DEGs were enriched in the metabolic biosynthesis pathways of secondary metabolites, plant hormone signal transduction, plant–pathogen interactions, and MAPK signaling pathway–plant and further found that the genes of salicylic acid (SA) and jasmonic acid (JA) signaling pathways were highly expressed and the contents of SA and JA increased significantly, suggesting that systemic resistance induced by Sp1 shares

features of SAR and ISR. In addition, Sp1 might induce the plant defense responses of tobacco. This study provides insights into the broad-spectrum resistance molecular mechanism of Sp1, which could be used as a potential biocontrol product.

KEYWORDS

***Bacillus licheniformis* W10, Sp1 protein, broad-spectrum resistance mechanism, transcriptome analysis, disease resistance**

Introduction

The United Nations Food and Agriculture Organization estimates that the global economic damages due to plant diseases are more than 22 billion dollars and that reduced agricultural production is exacerbating global hunger and endangering livelihoods. Chemical pesticides are widely used in disease prevention and control due to their quick effects. However, long-term, unreasonable application could easily produce pesticide residue, pathogen resistance, and adverse effects on human and animal health and the environment. Therefore, biological control is one of the most promising methods to control plant diseases from a security perspective (Aktuganov et al., 2014; Syed Ab Rahman et al., 2018; He et al., 2021). *Bacillus* spp. widely distributed in various ecological environments, such as plants and soil, and could colonize plant environments, inhibit pathogen infection, induce plant resistance, be compatible with chemical pesticides and produce endospores with strong stress resistance. *Bacillus* spp. are widely used biocontrol bacteria, among which *B. licheniformis* is a member (Fira et al., 2018; Won et al., 2021). There have been many reports on the biocontrol mechanism of *B. licheniformis*, including antagonism, competition, lysozyme, induced disease resistance, and growth promotion (Pérez-García et al., 2011; Muslim et al., 2016; Jeong et al., 2017; Won et al., 2019; Ji et al., 2020a). Studies have confirmed that *B. licheniformis* has certain control effects on plant diseases caused by fungi, oomycetes, bacteria, viruses and nematodes (Asraful Islam et al., 2010; Slimene et al., 2015; Bhai et al., 2019; Abdelkhalek et al., 2020; Panichikkal et al., 2021; Upadhyay and Mohan, 2021).

Biocontrol strains have excellent effects on research conditions, and various biopesticides have been developed. However, they were still not as popular as chemical pesticides in a survey covering nearly two decades. Complex environmental factors in the field easily affect their development and metabolism, such as temperature, light, humidity, nutrients, chemical substances, and various stress conditions (Someya, 2008). Therefore, it is urgent to explore their potential genetic characteristics and excellent properties, and developing biopesticides with antimicrobe substances as the main components, transferring these substances into plants to obtain resistant transgenic plants, or constructing efficient biocontrol engineering bacteria are important directions for the biological control of diseases.

The most prominent feature of *Bacillus* is their abundant metabolic system and ability to produce various extracellular proteins, including chitinase, glucanase, peptide, lipopeptide and other types of antifungal proteins (Leelasuphakul et al., 2006; Gomaa, 2012; Fira et al., 2018). Chitinase and glucanase were reported to be major mucolytic enzymes that dissolve fungal cell walls (Ji et al., 2020b). Lipopeptides such as iturins and surfactin from *Bacillus* are widely known for targeting the host cell wall that causes its collapse and the membrane through pore formation, ultimately leading to cell death and inhibiting fungal growth (Someya, 2008; Tian et al., 2021). Wang et al. (2014) identified a 55 kDa antifungal protein produced by the *B. licheniformis* HS10 strain that was a carboxypeptidase and had significant inhibitory effects on eight different plant pathogenic fungi. The 31 kDa antifungal protein with hydrolyzing activity on casein in *B. licheniformis* BS-3 inhibited the growth of *Aspergillus niger*, *Magnaporthe oryzae*, and *Rhizoctonia solani* (Cui et al., 2012). The 48 kDa serine protease MG-3A purified from the *B. amyloliquefaciens* MG-3 strain exhibited promising antifungal activity against four kinds of fungi and effectively extended the shelf life of loquat fruit (Yan et al., 2021). *B. licheniformis* W10 strains were isolated from the tomato rhizosphere by our lab and have significant inhibitory effects on *Botrytis cinerea*, *Monilinia fructicola*, and *Sclerotinia sclerotiorum*. Studies have shown that treatment with W10 can cause malformed mycelium, extravasation of protoplasm, and changes in cell membrane permeability, and can inhibit vegetative growth and conidial germination (Ji et al., 2015, 2020a). Furthermore, an approximately 48 kDa extracellular antifungal protein that encoded serine proteases (named the Sp1 protein) was purified from *B. licheniformis* W10 strain, and it was found that Sp1 had a strong inhibitory effect on *B. cinerea*, good thermal stability and pH tolerance, demonstrating that the Sp1 protein could be a potential biocontrol enzyme of plant pathogenic fungi (Ji et al., 2020b). However, the underlying molecular regulatory mechanism of the antifungal protein of *Bacillus* is still not clear.

Serine proteases depend on their serine residue for catalytic activity are widespread and numerous. Most of them were grouped into about six clans due to protein three-dimensional

structures and the order of catalytic residues in the polypeptide chain, including SA, SB (subtilisin), SC, SE, SF, and SG family (Rawlings and Barrett, 1994). W10-Sp1 protein had a conserved S8 domain which belongs to subtilisin family. The subtilisin family that first observed in *B. subtilis* is the second largest family of serine proteases, present in many organisms, however, mostly found in plant, such as in tomato, potato, *Arabidopsis*, grape, soybean and tobacco (Figueiredo et al., 2018). Plant subtilases play important roles in its development functions, including the growth of seeds and fruits and cell wall modification, besides that, they have got more attention in the plant response to the biotic and abiotic stress (Schaller et al., 2012). Studies have been reported that they mainly response to drought and salt stress (Liu and Howell, 2010; Budič et al., 2013). Accumulation of the subtilases were found after infection with the pathogens in tomato, grapevine and cotton (Vera et al., 1989; Monteiro et al., 2013; Duan et al., 2016), and further some substrates were identified such as systemin and the leucine-rich repeat (LRP), initiated defense signaling pathway and activated the expression of defense-related genes (Bergey et al., 1996; Tornero et al., 1996; Ryan, 2000). In addition, studies have showed that some specific subtilases are involved in plant programmed cell death (PCD) (Fernández et al., 2015). Besides that, subtilases are also found in pathogens as one of the virulence factors to disrupt host cell membrane during infection process, or degraded host PR protein, or as an avirulent to trigger a strong plant defense reaction (Olivieri et al., 1998; Walter et al., 2010; Chalfoun et al., 2013). Above all, subtilases perform multiple functions whether in plants or in pathogens. However, the specific mechanisms in biocontrol microorganism need to be further studied.

In this study, we found that W10-Sp1 had a broad antifungal effect, further inhibiting the growth of some bacteria and activating the systemic resistance of peach twigs, fruits and tobacco. Then, the broad-spectrum resistance molecular mechanism of the Sp1 protein was explored through dual comparative transcriptome analysis.

Materials and methods

Strains, culture conditions and purification of the W10-Sp1 protein

Strains of bacteria, including *Bacillus licheniformis* W10 (CGMCC No. 14859), *Xanthomonas arboricola* pv. *pruni*, *Pseudomonas cichorii*, *Pseudomonas syringae* pv. *tomato*, *Acidovorax avenae* subsp. *citrulli* and *Pectobacterium carotovorum* subsp. *carotovorum*, and fungi, including *Botrytis cinerea, Phomopsis amygdali*, *Rhizoctonia solani*, *Monilinia fructicola*, *Sclerotina sclerotiorum*, *Glomerella cingulata*, *Rhizopus stolonifer*, *Fusarium moniliforme*, *Alternaria cerasi* and *Gaeumannomyces graminis,* were preserved at the Peach Disease Research Laboratory, College of Horticulture and Plant Protection, Yangzhou University, China. Fungal strains were cultured at 25°C in potato dextrose agar (PDA) medium. Bacterial strains were cultured at 28°C in nutrient agar (NA) medium. The W10-Sp1 protein was purified according to our previous work (**Supplementary Figure S1**; Ji et al., 2020b). Peach [*Prunus persica* (L.) Batsch] ("Liutiaobaifeng") twigs were used within 1- to 2-year old in this study. Peach fruits were from peach experimental and demonstration bases at Yangshan, Wuxi, China. Xanthi tobacco (*Nicotiana tabacum* L. "Xanthi") plants were potted at 25°C with 80% relative humidity for 6–8 leaf stage.

Antagonism assay of the W10-Sp1 protein against different fungal/bacterial strains

In confrontation assays against fungus, the different plant pathogenic fungal blocks (6 mm) were separately inoculated on the center of PDA plates (diameter was 9 cm). Then, the sterilized paper disks were symmetrically placed on both sides of the fungal blocks, one side was dropped with 10 μl of sterile water, and the other side was placed in 10 μl of purified W10-Sp1 protein solution at a concentration of 20 mg/L. The plates were cultured at 25°C until the vegetative mycelium overgrew, and the inhibitory diameters were measured.

In confrontation assays against bacteria, overnight cultures of plant pathogenic bacteria (OD_{600} = 0.8) were mixed with NA agar medium and poured into plates with a diameter of 9 cm. Then, the sterilized paper disks were symmetrically placed on both sides of the center, one side was dropped with 10 μl of sterile water, and the other side was placed in 10 μl of purified W10-Sp1 protein solution at a concentration of 20 mg/L. After culturing at 28°C for 24 h, the inhibitory diameters were measured. All treatments were replicated three times.

EC_{50} measurement

W10-Sp1 protein was separately added to PDA medium at concentrations of 25, 50, 100, 250, and 500 μg/ml, and sterile water was used as a control. Then, the hyphal blocks were inoculated in the center of the plates and cultured at 25°C in the dark until the control strains overgrew on the PDA medium. When the EC_{50} of Sp1 protein to *G. graminis* was measured, the concentrations of W10-Sp1 protein were 0.25, 0.5, 1.0, 5.0, and 25 mg/L. The inhibitory rate (%) = [(control growth diameter-treated growth diameter)/(control growth diameter − 6)] × 100%. The concentrations of W10-Sp1 protein were logarithmically transformed to 10 as the abscissa, and the probability value corresponding to the inhibitory rate was used as the ordinate to obtain the regression equation. When the inhibitory rate was 50%, the corresponding concentration value was the EC_{50} value.

RNA extraction and RNA sequencing

To explore the mechanism of how the W10-Sp1 protein resisted the plant pathogenic fungus, *P. amygdali* was used as an example in this study. Hyphal blocks of *P. amygdali* were cultured in liquid PDA medium at 25°C for 36 h, and then W10-Sp1 protein solution was added at a concentration of 100 mg/L for another 36 h (PSp1). Equal amounts of sterile water were used as a control (PCK). To explore the systemic resistance mechanism of the W10-Sp1 protein, W10-Sp1 protein at a concentration of 100 mg/L was injected into the lower leaf of Xanthi tobacco, and sterile water was injected into the control. Then, the upper leaf was used for further research. Three biological replicates were performed, and RNA was extracted from 12 samples with an RNA kit (Cat no. 12183018A, Invitrogen, United States). The DNA library was constructed and sequenced. The adapter reads were removed from the raw sequencing data, along with the reads that could not be used to determine the base information and low-quality reads; thus, clean reads were obtained. The clean reads were aligned to the reference genomes of *P. amygdali* and Xanthi tobacco using HISAT2 software. The FPKM values were used to estimate the sequencing depth and gene length.

Differentially expressed genes analysis

Differentially expressed genes (DEGs) in treated samples vs. CK were determined by DESeq2 software. GO (Gene Ontology) terms and KEGG (Kyoto Encyclopedia of Genes and Genomes) pathway enrichment of DEGs were analyzed by clusterProfile, and the PPI (protein–protein interaction) networks of DEGs were predicted according to STRING software.

Quantitative reverse transcription PCR analysis

Differentially expressed genes were randomly selected for reverse transcription PCR (qRT-PCR) to verify the accuracy of the dual transcriptome data. RNA was extracted from the same samples and reverse transcribed into cDNA as the templates for qRT-PCR. qRT-PCR was performed on a Bio-Rad CFX96 instrument (Bio-Rad, United States) according to the manufacturer's instructions. All experiments were performed for three independent replicates. The primers used are listed in **Supplementary Table S5**.

Conductivity measurement

The same amount of hyphal blocks were put into 40 ml of liquid PDA medium and cultured at 25°C and 180 r/min for 48 h. The plates were filtrated and washed with sterile water three times to remove the medium. Then, the hyphal blocks were placed into 5 ml of W10-Sp1 protein solution with EC_{50} or $2EC_{50}$ concentrations and cultured at 25°C and 180 r/min, and the conductivity was detected after 2, 4, 6, 12, and 24 h of culturing within a DDS-307 conductivity meter. Finally, the samples were boiled for 0.5 h, and the conductivity was detected after cooling. Relative conductivity = (conductivity before water bath/conductivity after water bath) × 100%. All treatments were replicated three times.

Salicylic acid and jasmonic acid content measurement with high-performance liquid chromatography–tandem mass spectrometry method

Xanthi tobacco at the 8–10 leaf stage was selected for injection with 50 μl of W10-Sp1 at a concentration of 100 mg/L or the same amount of sterile water. The upper leaves were taken at 12 hpi and used for the extraction of plant hormones and content measurement which were referred to the reference (Pan et al., 2010). Samples were quantified by high-performance liquid chromatography–tandem mass spectrometry (HPLC-MS/MS) analysis using Poroshell 120 SB-C18 (2.1 × 150, 2.7 μm). The gradient elution program: 20% A (0.1% formic acid-methyl alcohol) at 0∼1 min; 20% A∼80% A at 1∼9 min; 80% A at 9∼10 min; 80% A∼20% A at 10∼10.1 min; 20% A at 10.1∼15 min. The peak flow of the standard of SA was at ∼5.61 min; of the standard of JA was at ∼6.22 min.

Results

Inhibitory effects of purified W10-Sp1 protein on 10 kinds of plant pathogenic fungi

Our previous work demonstrated that strains of *B. licheniformis* W10 and its extracellular antifungal crude protein had a better biocontrol effect to inhibit gray mold caused by *B. cinerea* and peach brown rot caused by *M. fructicola* (Ji et al., 2015, 2020a) and purified a protein, Sp1, which encoded a serine protease from the extracellular crude protein and significantly inhibited the mycelial growth of *B. cinerea* (Ji et al., 2020b). Therefore, we wondered whether the Sp1 protein could be a broad-spectrum antifungal protein. Purified W10-Sp1 protein was used to explore its effects on 10 kinds of different plant pathogenic fungi, including *B. cinerea, P. amygdali*, *R. solani*, *M. fructicola*, *S. sclerotiorum*, *G. cingulata*, *R. stolonifer*, *F. moniliforme*, *A. cerasi* and *G. graminis*. The

10.3389/fmicb.2022.974473

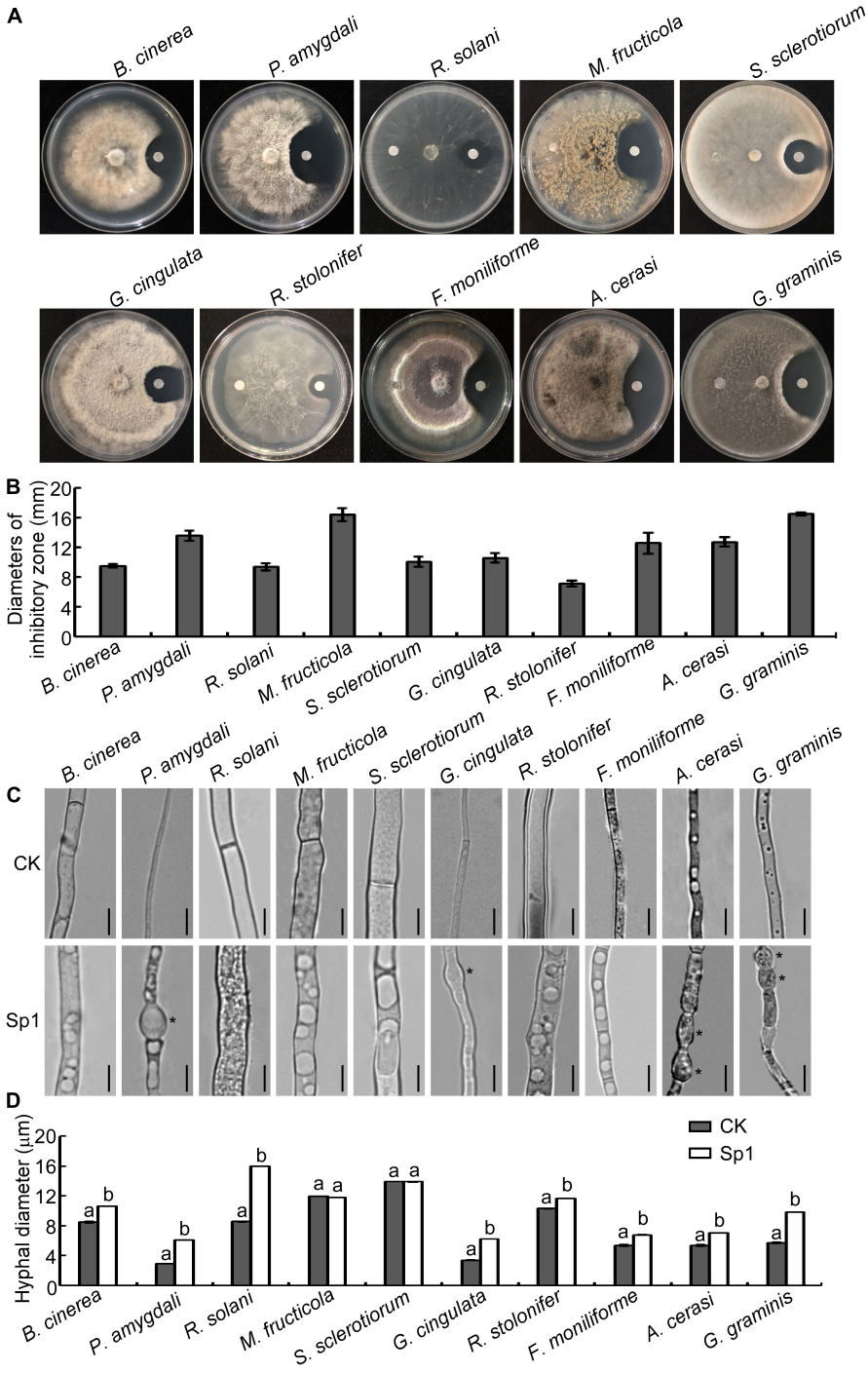

FIGURE 1
W10-Sp1 protein significantly affected the mycelial growth and the hyphal morphology of 10 kinds of fungi. **(A)** Hyphal cakes with diameters of 6 mm of 10 kinds of fungi were inoculated in the center of PDA plates. Sterilized paper disks were placed equidistant on both sides of the hyphal block. The left side was treated with sterile water, and the right side was treated with purified W10-Sp1 protein. Photographs were taken to observe the inhibition effect of W10-Sp1 after fungi overgrew the plate. **(B)** Measurement of the diameters of the inhibitory zone. Experiments were repeated three times with similar results. **(C)** Hyphal blocks of 10 kinds of fungi were separately placed into liquid PDA medium and shaken at 25°C and 160 rpm for 48 h. Then, they were treated with the purified W10-Sp1 protein in PDA medium and shaken under the same conditions for another 24 h. Sterile water was used as a CK (control). The morphology of single hyphae was separately observed under the microscope at 40×. Asterisks indicate malformed positions. Bar = 20 μm. **(D)** Measurement of hyphal diameter with different treatments under the microscope. Letters represent significant differences. Experiments were repeated three times with similar results (Duncan's new multiple range test, $p < 0.05$).

inhibitory effects of W10-Sp1 on the vegetative mycelia of these fungi were observed by confrontation culture on PDA medium at 25°C. The results showed that W10-Sp1 had the most obvious inhibitory effects on *G. graminis* and *M. fructicola*, and the diameters of the inhibitory zones were 16.5 mm and 16.4 mm, respectively. This was followed by *P. amygdali* (13.6 mm), *A. cerasi* (12.7 mm), *F. moniliforme* (12.6 mm), *G. cingulata* (10.6 mm), *S. sclerotiorum* (10.0 mm), *B. cinerea* (9.5 mm), *R. solani* (9.4 mm), and *R. stolonifer* (7.2 mm) (Figures 1A,B).

Then, the hyphal blocks of these fungi were separately cultured in liquid PDA medium for 48 h at 25°C and then treated with W10-Sp1 protein or sterile water for another 24 h, and the single hyphal morphology was observed under a microscope. The results showed that the W10-Sp1 protein affected hyphal morphology in three ways: some were malformed and swollen in *P. amygdali*, *G. cingulata*, *A. cerasi* and *G. graminis* (Figure 1C); hyphal diameter increased in *B. cinerea, P. amygdali*, *R. solani*, *G. cingulata*, *R. stolonifer*, *F. moniliforme*, *A. cerasi*, and *G. graminis* (Figures 1C,D); and large or more vesicle-like structures occurred in the hyphae in nearly all 10 kinds of fungi (Figure 1C).

In addition, a certain amount of spore suspension was treated with W10-Sp1 protein at a final concentration of 50 mg/L, and the germination rate was observed at 12 hours post-inoculation (hpi) in hollow glasses, respectively. The results found that W10-Sp1 significantly inhibited the spore germination of those fungi compared with that of the untreated fungi; the inhibitory rates were between 58.6∼72.9%, and the highest was that of *M. fructicola* (Table 1). Overall, the results indicated that W10-Sp1 has a stronger inhibitory effect on these 10 kinds of plant pathogenic fungi.

The W10-Sp1 protein had significant differences in EC_{50} value among different plant pathogenic fungi

The antifungal effects of the W10-Sp1 protein on these 10 kinds of plant pathogenic fungi became much stronger with increasing concentrations. However, there were certain differences in inhibitory effects among the different fungi (Supplementary Figure S2). EC_{50} represents concentrations required for a half maximal effect. Linear regression analysis and EC_{50} values were calculated in different fungi treated with Sp1 protein at different concentrations. The results showed that the W10-Sp1 protein had the best anti-*G. graminis* effect, with an EC_{50} value of 4.2 mg/L, followed by *P. amygdali* (82.8 mg/L), *G. cingulata* (106.6 mg/L), *A. cerasi* (133.8 mg/L), *R. solani* (183.8 mg/L), *M. fructicola* (185.6 mg/L), *R. stolonifer* (204.9 mg/L), *S. sclerotiorum* (244.9 mg/L), *F. moniliforme* (298.8 mg/L) and *B. cinerea* (398.2 mg/L) (Table 2). These results indicated that the W10-Sp1 protein could be used as a broad-spectrum antifungal drug in the future.

Inhibitory effects of W10-Sp1 protein on four kinds of plant pathogenic bacteria

We were then determined whether the W10-Sp1 protein had an inhibitory effect on plant pathogenic bacteria. Strains of *X. arboricola* pv. *pruni*, *P. cichorii*, *P. syringae* pv. *tomato*, *A. avenae* subsp. *citrulli* and *P. carotovorum* subsp. *carotovorum* were mixed with NA medium with treated paper disks with or without W10-Sp1 solution (20 mg/L) and cultured at 28°C for 48 h. The W10-Sp1 protein had significant inhibitory effects on *X. arboricola* (19.8 mm), *P. cichorii* (16.7 mm), *P. syringae* (15.7 mm), and *A. avenae* (12.7 mm), but had no effect on *P. carotovorum* (Figures 2A,B). These results suggested that W10-Sp1 also had- antibacterial effects.

TABLE 1 Effects of purified W10-Sp1 protein on spore germination rates of different plant pathogenic fungi.

Strains	Spore germination rates (%)†		Inhibitory rates (%)‡
	CK	W10-Sp1	
B. cinerea	59.7 ± 3.5^a	24.7 ± 2.9^b	58.6 ± 5.0
P. amygdali	52.7 ± 4.8^a	18.8 ± 1.8^b	64.3 ± 3.4
M. fructicola	50.7 ± 2.9^a	13.7 ± 3.1^b	72.9 ± 6.0
G. cingulata	54.3 ± 3.8^a	17.3 ± 2.4^b	68.1 ± 4.4
R. stolonifer	62.0 ± 4.6^a	22.0 ± 3.2^b	64.5 ± 5.1

†Spore suspensions with the concentration of 1.0×10^5 spores/ml of different fungi were treated with sterile water (CK) or W10-Sp1 protein with a final concentration of 50 mg/L, separately. Inoculated 40 μl on the concavity slides, and spore germination rates were observed at 12 hours post-inoculation (hpi). Germination rates = (number of spore germination observed/number of total spores observed) × 100%. Lowercase represents significant difference. Experiments were repeated three times with similar results. Duncan's new multiple range test, $p < 0.05$.
‡Inhibitory rates = [(spore germination rates of control − spore germination rates of treatment with Sp1 protein)/spore germination rates of control] × 100%.

TABLE 2 EC_{50} values of purified W10-Sp1 against different plant pathogenic fungi.

Strains	Linear regression equation	R^2	EC_{50}
B. cinerea	$y = 0.8943 + 1.5791x$	0.9560	398.2
P. amygdali	$y = -0.3619 + 2.7956x$	0.9941	82.8
R. solani	$y = 0.6318 + 1.9291x$	0.9976	183.8
M. fructicola	$y = 3.0350 + 0.8662x$	0.9955	185.6
S. sclerotiorum	$y = 1.8022 + 1.3928x$	0.9303	244.9
G. cingulata	$y = 0.0607 + 2.4360x$	0.9570	106.6
R. stolonifer	$y = 1.9864 + 1.3038x$	0.9994	204.9
F. moniliforme	$y = 0.9520 + 1.6353x$	0.9072	298.8
A. cerasi	$y = 3.6248 + 0.6467x$	0.9908	133.8
G. graminis	$y = 4.1025 + 1.4408x$	0.9242	4.2

Logarithm of 10 of concentrations of W10-Sp1 protein was used as abscissa and probability values corresponding to inhibitory rate were used as ordinate to obtain regression equation. When inhibitory rate was 50%, the corresponding concentration value was EC_{50} value.

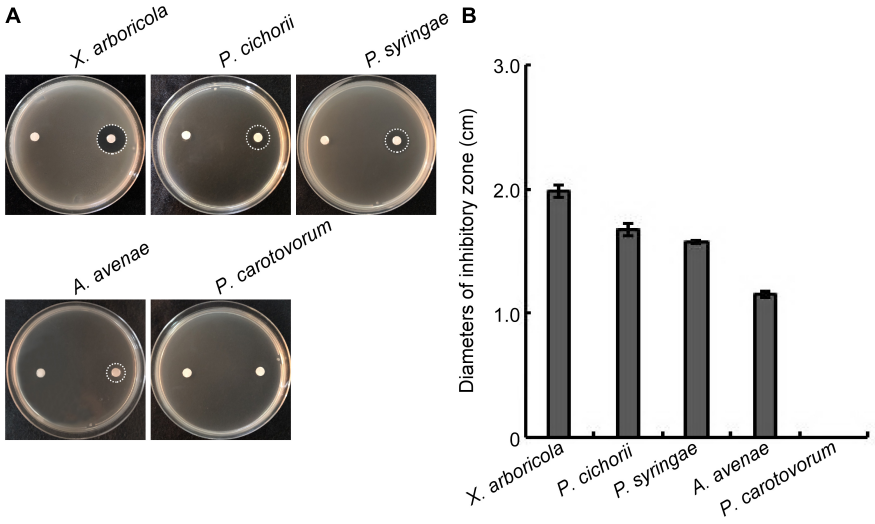

FIGURE 2
Effects of the W10-Sp1 protein on different plant pathogenic bacteria. **(A)** Bacterial suspensions (OD_{600} = 0.8) of different strains were mixed with NA medium. Two disinfected paper disks were separately placed on both sides of the plates. Sterilized water was used to treat the left sides; W10-Sp1 protein was used to treat the right sides. Photographs were taken at 2 days post-inoculation (dpi). **(B)** Measurement of the diameters of the inhibitory zone. Experiments were repeated three times with similar results.

Transcriptome analysis of W10-Sp1 protein anti-fungal mechanism

Based on the better inhibitory effect of the W10-Sp1 protein on *P. amygdali*, it was selected in this study to further explore its anti-fungal mechanism. Hyphal blocks of *P. amygdali* were cultured in liquid PDA medium for 48 h, and then 100 mg/L W10-Sp1 protein solution was added and shaken at 25°C for another 24 h (PSp1). Medium without W10-Sp1 protein was used as a control (PCK). RNA was extracted to analyze the differentially expressed genes (DEGs) in the whole genome of *P. amygdali,* which was obtained by our lab (in preparation). The average total numbers of clean reads were 45.38 Mb and 42.48 Mb; the Q20 values were 99.02% and 99.04%; the Q30 values were 97.86% and 97.89%; and the total mapping ratios were 97.94% and 98.07% in the three PCK (PCK-1, PCK-2, PCK-3) samples and the three PSp1 (PSp1-1, PSp1-2, PSp1-3) samples, respectively (**Supplementary Table S1**). Eight genes were selected at random to verify the accuracy of RNA-seq by qRT-PCR under similar treatments. The qRT-PCR results showed that the expression levels of GME1740_g, GME8443_g, and GME8738_g were upregulated, and the expression levels of the other five genes were downregulated, which was consistent with the RNA-seq results (**Supplementary Figure S3**), indicating that the RNA-seq data were reliable. A total of 11,677 transcripts were obtained, among which 10,721 were present in both conditions. However, 364 and 592 transcripts were specifically expressed in PSp1 and PCK samples, respectively (**Figure 3A**). DEG analysis found that 150 transcripts were upregulated, 209 transcripts were downregulated, and most genes (14562 transcripts) had no differential expression (| log2 fold change (FC)| > 0, padj < 0.05) (**Figure 3B**). Furthermore, GO and KEGG pathway enrichments were analyzed. The top 10 GO enrichments were coenzyme binding, carbohydrate metabolic process, flavin adenine dinucleotide binding, NAD binding, oxidoreductase activity, peptidase activity, proteolysis, endopeptidase activity, external encapsulating structure and hydrolase activity (**Figure 3C**). The top 10 KEGG enrichments were biosynthesis of secondary metabolites, valine, leucine and isoleucine degradation, carbon metabolism, starch and sucrose metabolism, propanoate metabolism, glutathione metabolism, glyoxylate and dicarboxylate metabolism, fatty acid metabolism, biosynthesis of amino acids and pentose phosphate pathway (**Figure 3D**).

W10-Sp1 treatment might affect the energy supply and the cell wall structure of *Phomopsis amygdali*

Differentially expressed genes in coenzyme binding included 12 upregulated and 10 downregulated genes under W10-Sp1 treatment of the hyphae of *P. amygdali* compared with untreated hyphae. In carbohydrate metabolic processes, five DEGs were upregulated, and eight DEGs were downregulated. There were three upregulated and seven downregulated DEGs in hydrolase activity and six DEGs in valine, leucine and isoleucine degradation processes that were all upregulated (**Figure 4**). In addition, we found that genes expressing glycosyl hydrolase

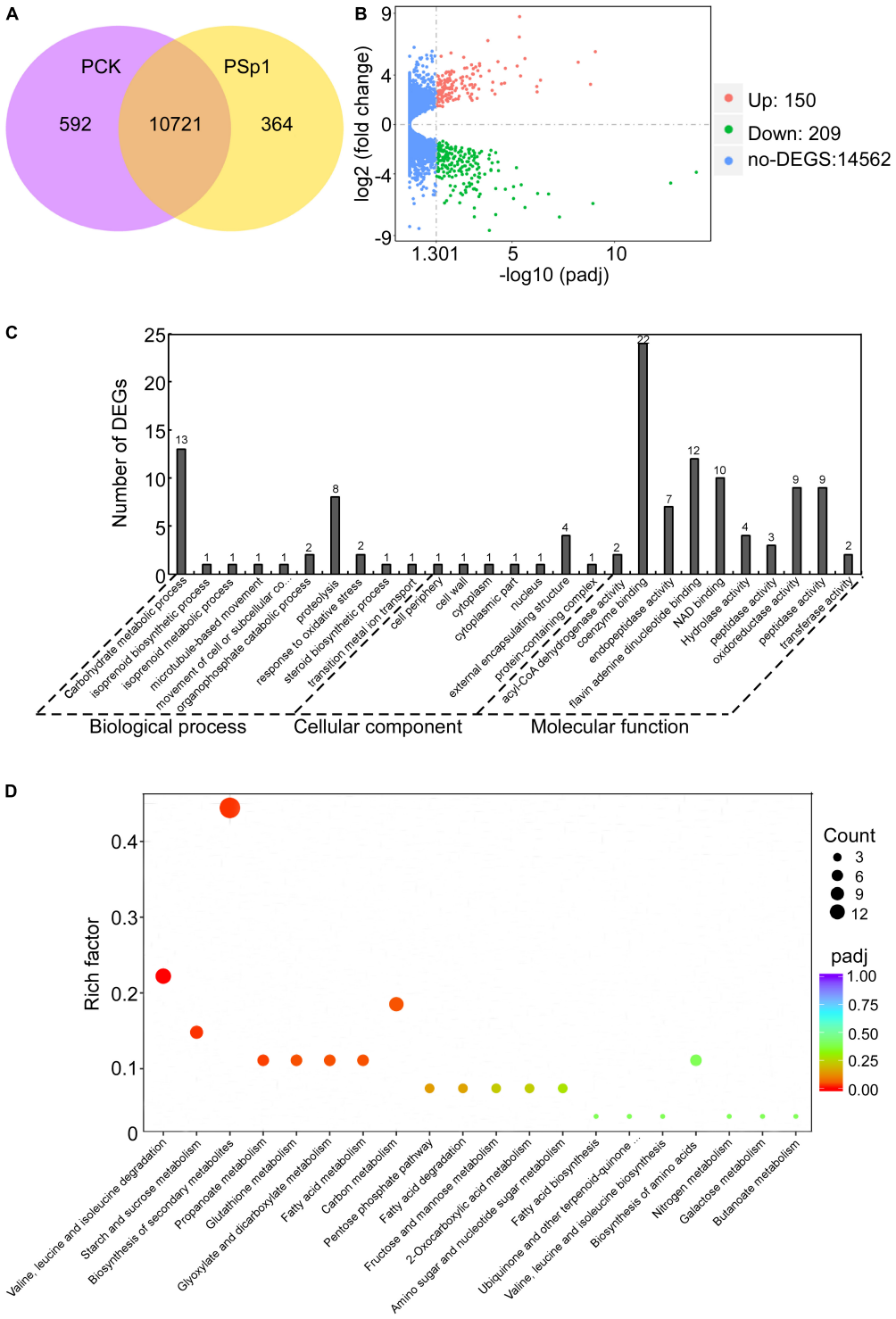

FIGURE 3
Transcriptome analysis of W10-Sp1 treating the *P. amygdali* ZN32 strain (PSp1) vs. the ZN32 strain (PCK). **(A)** Venn diagram presenting the overlap of expressed genes between PCK and PSp1. Purple represents the number of expressed genes of PCK; yellow represents the number of expressed genes of PSp1; orange represents the overlapping expressed genes of PSp1 and PCK. **(B)** Volcano plot of DEGs between PSp1 and PCK. Splashes represent different genes, where red shows significantly upregulated genes after purified Sp1 protein was used to treat hyphae of *P. amygdali* ZN32, green shows downregulated genes, and blue shows no significant difference between the samples of PSp1 and PCK. **(C)** GO analysis of DEGs. The X-axis represents the analysis categories, including biological process, molecular function and cellular component. The *Y*-axis represents the number of DEGs. **(D)** Bubble diagram of the KEGG pathway analysis of DEGs. The *X*-axis represents the top 20 KEGG signaling pathways. The *Y*-axis represents enriched factors. The closer the color was to red, the smaller the padj value and the higher the significance level.

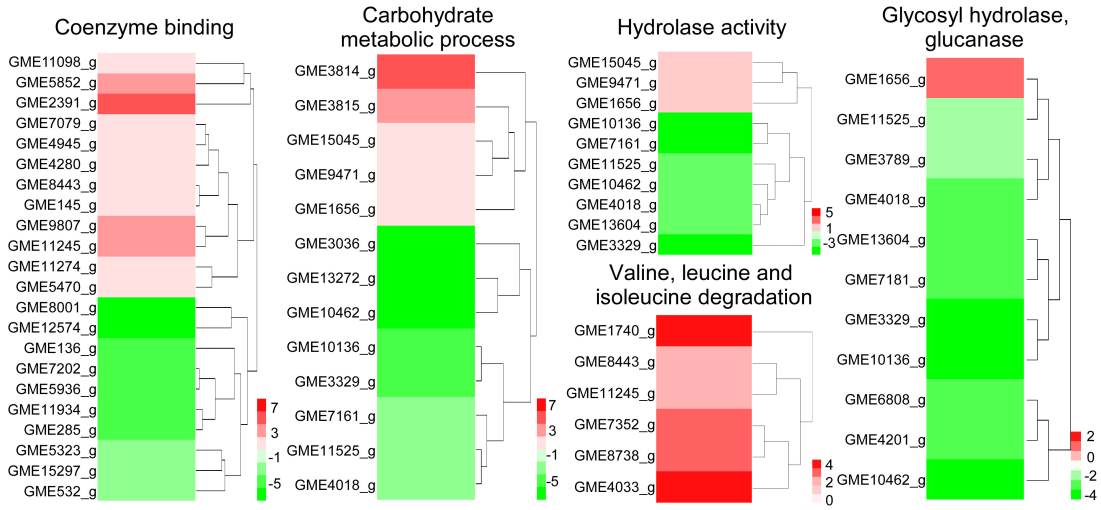

FIGURE 4
Heatmap analysis of DEGs related to key enzymes of the TCA cycle, glycosyl hydrolase and glucanase. The red color represents DEGs with upregulation, and the green color represents DEGs with downregulation.

(an important energy production enzyme) and glucanase (cell wall glucan hydrolase) were notably downregulated (Figure 4). These results indicated that W10-Sp1 treatment might affect the energy supply and the cell wall structure of *P. amygdali*.

The W10-Sp1 protein caused cell damage in nine kinds of plant pathogenic fungi

The above studies showed that the W10-Sp1 protein significantly affected the hyphal morphology of the fungi and DEGs of cell wall related-genes which might be due to the damage of cell structure. Ten different kinds of fungi were cultured in liquid PDA medium for 48 h and then washed three times to remove the medium. The relative conductivity (RC) of liquid-culture hyphae under the treatment of W10-Sp1 protein (two different concentrations were used) or sterile water was measured at 2, 4, 6, 12, and 24 hpi. Treatment of W10-Sp1 protein with nine kinds of fungi significantly increased the conductivity in the solutions in addition to *G. graminis*; the higher the Sp1 protein concentration was used, the higher the value of RC (Figures 5A–H). The results indicated that cell structure of the fungi was damaged under W10-Sp1 protein treatment.

W10-Sp1 protein was involved in activating systemic resistance

Based on the significant antifungal effect of the W10-Sp1 protein, we wanted to explore its effect on disease control. Hyphal cakes of *P. amygdali* were inoculated onto disinfected and wounded peach twigs and then dipped into 50 mg/L or 200 mg/L W10-Sp1 protein for 30 min at 24 hpi. Inoculated PDA cakes or hyphal cakes without Sp1 treatment were used as negative or positive controls, respectively, and disease symptoms were observed at 7 dpi. The length of lesions were reduced by 36.8∼46.1% compared with no treatment with W10-Sp1 protein (Figures 6A,B). Furthermore, disinfected peach twigs were first dipped into the same concentration of W10-Sp1 protein for 30 min and then inoculated with hyphal cakes of *P. amygdali*. Symptoms were observed at 7 dpi. Amazingly, the length of lesions were reduced by 40.9∼55.5%, and the peach shoot blight-control effect was better than that of treatment with W10-Sp1 solution after inoculation (Figures 6A,B). In addition, hyphal cakes of *M. fructicola* were inoculated on peach fruits after spraying different concentrations of W10-Sp1 protein solution and cultured at 28°C with 90% relative humidity for 7 days. PDA-treated peach fruits and only-inoculated hyphal cakes were used as controls. The results showed that the peach brown rot-control rate was reduced by 52.4% under the treatment of 50 mg/L W10-Sp1 protein and 93.5% under the treatment of 200 mg/L W10-Sp1 protein (Figures 6C,D).

Furthermore, 10 mg/L W10-Sp1 protein was injected into the lower leaves of Xanthi tobacco, and hyphal cakes of *B. cinerea* were inoculated onto the upper leaves at different induction times from 0∼36 hpi. The results showed that the best induced gray mold resistance time by the W10-Sp1 protein was at 12 hpi, and the lesion diameters were approximately 2.5 mm (Figures 6E,F). Furthermore, different concentrations of 1, 10 or 100 mg/L W10-Sp1 protein were applied to the lower leaves of Xanthi tobacco for 12 h, after which *B. cinerea* was inoculated onto the upper leaves, and symptoms were observed

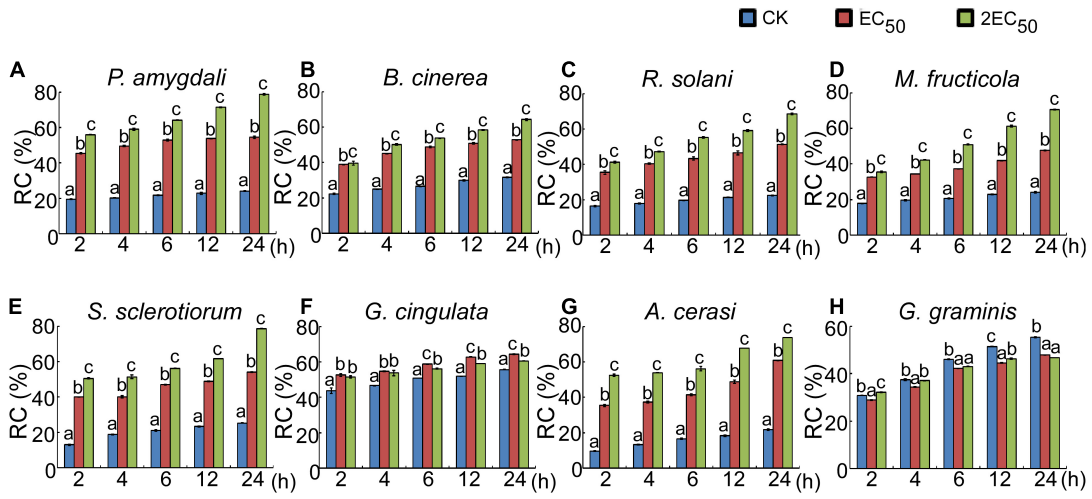

FIGURE 5
Effects of the W10-Sp1 protein on cell damage of different plant pathogenic fungi. The hyphal blocks of each fungal strain were shaken in liquid PDA medium at 25°C and 160 r/min for 48 h and washed repeatedly with sterile water, and the surface medium of mycelium pellets was removed. Then, they were placed in purified W10-Sp1 solution at EC_{50} and $2EC_{50}$ concentration, and the conductivity of the solution was measured after coculture for 2, 4, 6, 12, and 24 h. Finally, the cocultures were heated in boiling water for 30 min, and the final conductivity was measured after cooling **(A–H)**. Relative conductivity = (conductivity before the water bath/conductivity after the water bath) × 100%. Experiments were repeated three times with similar results (Duncan's new multiple range test, $p < 0.05$).

at 24 hpi, separately. The results showed that the diameters of the lesions were 1.62, 0.28 and 0.23 mm at different inducing concentrations. There was no significant differences among the three concentrations (**Figures 6G,H**). Overall, the results revealed that the W10-Sp1 protein activated systemic resistance independent of its concentration.

Transcriptome analysis of W10-Sp1 protein activation systemic resistance mechanism

W10-Sp1 protein-treated Xanthi tobacco (TCK) was used to further explore its mechanism of systemic resistance through transcriptome analysis due to the complete genome information of tobacco. The RNA of sterile water-treated Xanthi tobacco (TSp1) was used as a control group. RNA-seq was verified by qRT-PCR by selecting 16 genes involved in auxin synthesis, SA metabolism, JA metabolism and phenylpropanoid biosynthesis. The expression trends of qRT-PCR were consistent with those of RNA-seq in addition to that of *CCOAOMT2*. Thus, the RNA-seq had approximately 93.8% accuracy (**Supplementary Figure S4**). A total of 51,708 transcripts were obtained, among which 47,881 were present in both conditions. However, 1473 and 2354 transcripts were specifically expressed in TCK or TSp1 samples, respectively (**Figure 7A**). DEG analysis found that 5937 transcripts were upregulated (FC ≥ -2, q-value ≤ 0.001), 2925 transcripts were downregulated (FC ≤ -2, q-value ≤ 0.001), and most of the genes (39,710 transcripts) had no differential expression (FC < 2 or q-value > 0.001) (**Figure 7B**). The average total numbers of clean reads were 44.91 Mb and 44.74 Mb; the Q20 values were 99.02% and 99.04%; the Q30 values were 96.89% and 96.95%; and the total mapping ratios were 85.06% and 85.18% in the three TCK and TSp1 samples, respectively (**Supplementary Table S2**). The top 10 GO enrichments were metabolic process, cellular process, binding, catalytic activity, cell, cell part, membrane, organelle, membrane part and response to stimulus (**Table 3**). The top 10 KEGG pathways enriched were metabolic pathway, biosynthesis of secondary metabolites, plant hormone signal transduction, plant–pathogen interaction, MAPK signaling pathway-plant, protein processing in endoplasmic reticulum, starch and sucrose metabolism, biosynthesis of amino acids, phenylpropanoid biosynthesis, and endocytosis (**Table 4**).

The W10-Sp1 protein significantly affected plant hormones, especially increasing the intracellular contents of salicylic acid and jasmonic acid

Plant hormones play important roles in various stress conditions, including biotic or abiotic stress (Coolen et al., 2016). RNA-seq in the samples of W10-Sp1 protein-treated Xanthi tobacco also significantly induced plant hormone signal transduction, and approximately two-thirds were upregulated. Nearly all genes that regulated auxin (IAA), cytokinin (CTK), gibberellin (GA), abscisic acid (ABA), and salicylic acid (SA)

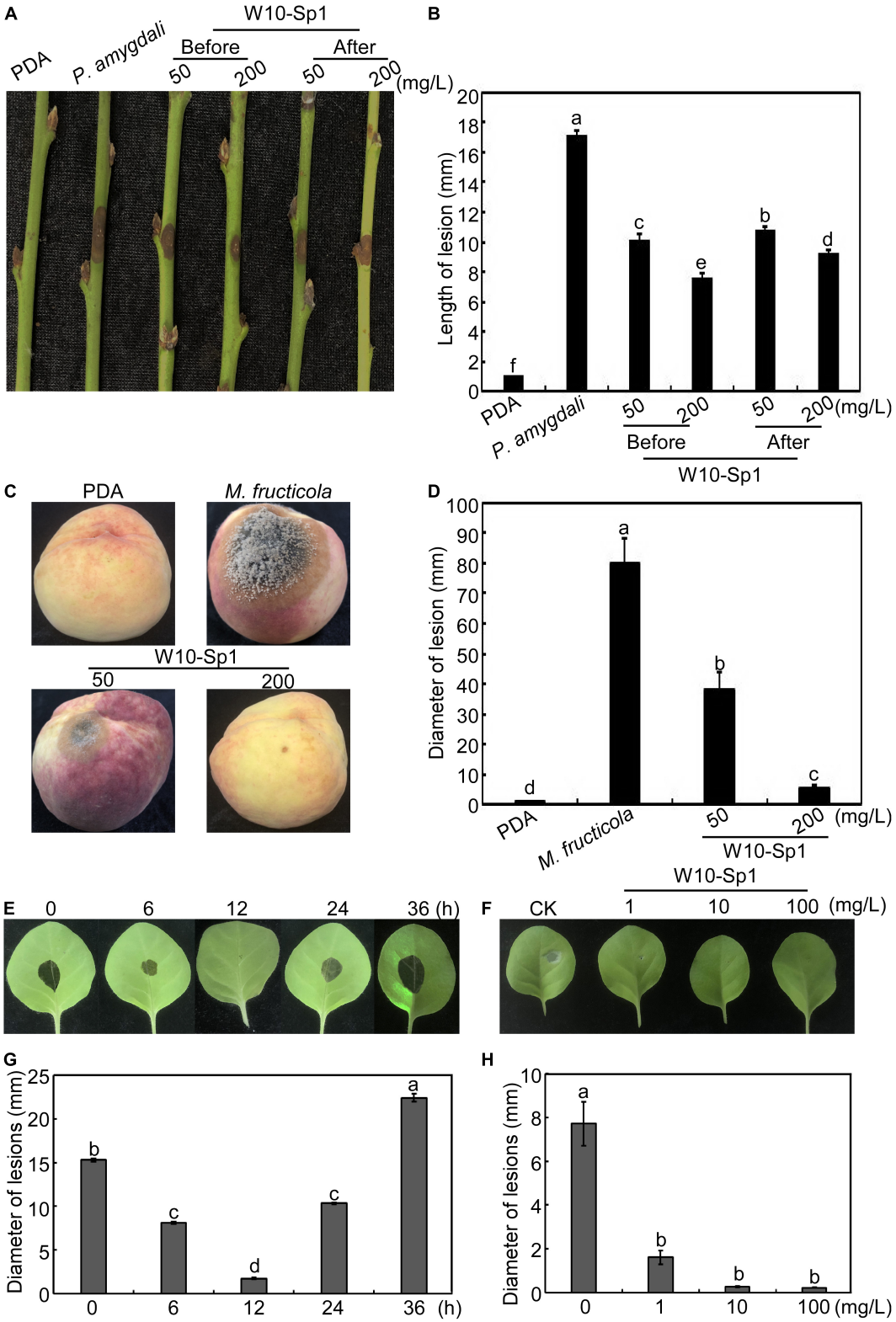

FIGURE 6
W10-Sp1 activated systemic resistance of the host. **(A)** Two treatments for control of peach shoot blight: hyphal cakes of *P. amygdali* were inoculated on the wounded peach twigs for 24 h, after which the hyphal cakes were removed and the twigs were dipped in the W10-Sp1 protein solution for 30 min (after); another treatment used W10-Sp1 protein solution to dip the disinfected twigs for 30 min, and then the hyphal cakes of *P. amygdali* were inoculated (before). The results of both treatments were observed at 7 dpi. **(B)** Measurement of lesion length at 7 dpi
(Continued)

FIGURE 6 (Continued)
for peach shoot blight-control effect. **(C)** W10-Sp1 protein solution was sprayed onto disinfected peach fruits for 30 min at different concentrations, and then the hyphal cakes of *M. fructicola* were inoculated, and the results were observed at 7 dpi. **(D)** Measurement of lesion diameters at 7 dpi for peach brown rot-control effect. Direct inoculation of hyphal cakes was used as a positive control; equal solid PDA media inoculation was used as a negative control. **(E)** W10-Sp1 protein was injected into the leaves of Xanthi tobacco and inoculated with hyphal cakes of *B. cinerea* on upper leaves at 0, 6, 12, 24, and 36 h post-injection (hpi), and disease symptoms were observed at another 24 hpi. **(F)** Measurement of lesion diameters at 24 hpi of different incubation time treatments of Sp1 protein. **(G)** Different concentrations of purified Sp1 protein were injected into Xanthi tobacco and then inoculated into hyphal cakes of *B. cinerea* at 12 h post-injection. CK was treated with equal amounts of sterile water. **(H)** Measurement of lesion diameters at 24 hpi after treatment with different concentrations of Sp1 protein.

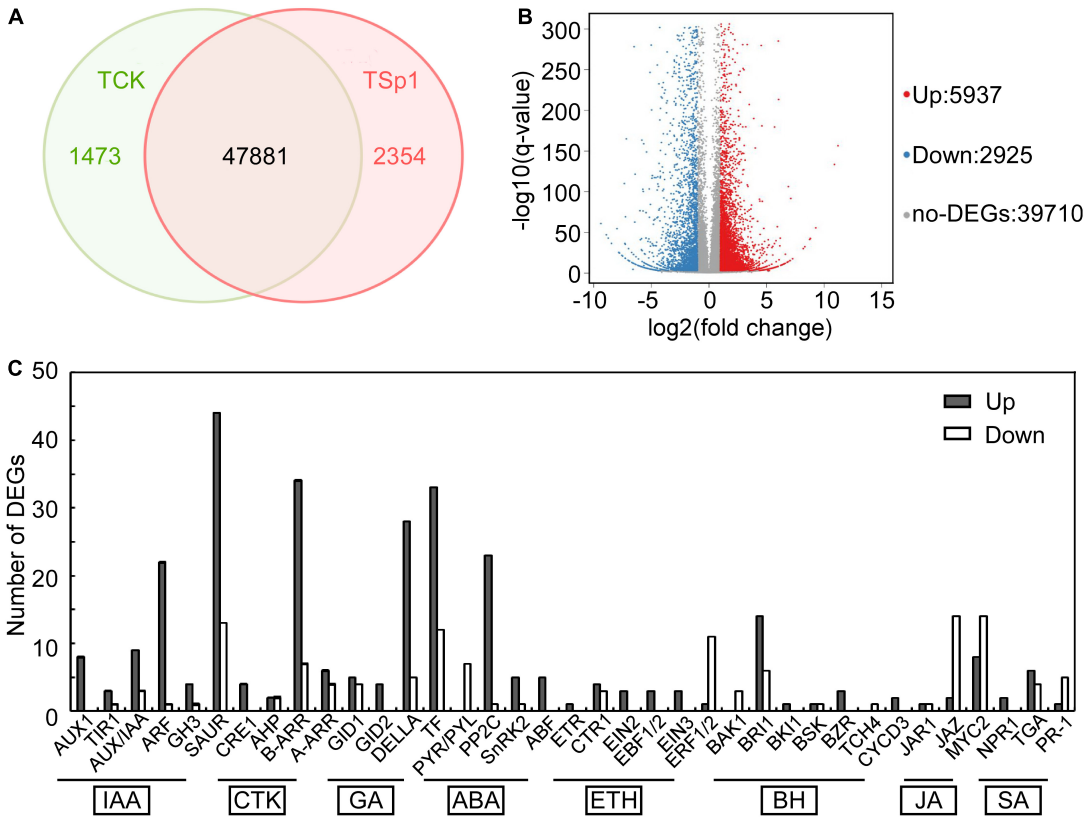

FIGURE 7
Transcriptome analysis between the samples of W10-Sp1 treating Xanthi tobacco (TSp1) to Xanthi tobacco (TCK). **(A)** Venn diagram presenting the overlap of expressed genes between TSp1 and TCK. Green represents the number of expressed genes of TCK; red represents the number of expressed genes of TSp1. **(B)** Volcano plot of DEGs between TCK and TSp1. Splashes represent different genes, where red indicates significantly upregulated genes after Sp1 protein was used to treat Xanthi tobacco, blue indicates downregulated genes, and gray indicates no significant difference. **(C)** Analysis of DEGs focusing on the plant hormone signaling pathway of TSp1 vs. TCK. The gray box represents upregulated DEGs of TSp1 vs. TCK, and the white box represents downregulated DEGs.

signal transduction were differentially expressed. In total, 96 DEGs were upregulated and 34 DEGs were downregulated in IAA signal transduction; 46 DEGs were upregulated and 13 DEGs were downregulated in CTK signal transduction; 70 DEGs were upregulated and 21 DEGs were downregulated in GA signal transduction; and 33 DEGs were upregulated and 9 DEGs were downregulated in ABA signal transduction (Figure 7C).

In addition, plant hormones such as SA and JA are important regulators of activating systemic resistance; therefore, DEGs in the SA and JA signal transduction pathways were further analyzed by RNA-seq. NPR1, a positive regulator of the SA signaling pathway, was upregulated by two genes. There were six upregulated and four downregulated *TGA* genes. However, the disease resistance-related gene *PR1* was upregulated by one gene and downregulated by five genes, which showed more significant differences. In the JA signaling pathway, the negative regulatory factor *JAZ* was upregulated by 2 genes and downregulated by 14 genes with more significant differences. There were 8 upregulated and 14 downregulated genes in the transcription factor *MYC2* that regulated JA signal termination,

TABLE 3 The top 10 GO enrichment list of 5618 DEGs of Sp1 protein vs. control tobacco.

Ontology	GO term	Number of genes
biological_process	Metabolic process	805
biological_process	Cellular process	721
molecular_function	Binding	700
molecular_function	Catalytic activity	689
cellular_component	Cell	597
cellular_component	Cell part	590
cellular_component	Membrane	454
cellular_component	Organelle	411
cellular_component	Membrane part	388
biological_process	Response to stimulus	263

and downregulated genes showed more significant differences, suggesting that W10-Sp1 might enhance the JA signaling pathway in Xanthi tobacco by inhibiting the expression of its negative regulatory genes (**Supplementary Table S3**). These results indicated that the SA and JA signaling pathways were induced by the W10-Sp1 protein. Furthermore, the contents of SA and JA were detected in different treated samples with HPLC-MS/MS method. The content of SA increased 7.2-fold and that of JA increased 4.8-fold compared W10-Sp1-treated Xanthi tobacco for 12 h to untreated tobacco in the upper leaves of Xanthi tobacco (**Figure 8** and **Table 5**). The results suggested that W10-Sp1 treatment activated the intracellular SA and JA signaling pathways.

Impact of W10-Sp1 protein on the plant–pathogen interaction pathway of tobacco

A total of 426 DEGs were identified in the plant–pathogen interaction pathway under W10-Sp1 treatment, including Ca^{2+}/CaM signal pathway-related genes (*NOS*, *CML*), the transcription factor WRKY, serine/threonine-protein kinases (*PTO*, *PBS1*), and a disease resistance protein (*RPS4*) (**Figure 9** and **Supplementary Table S4**). Furthermore, the plant–pathogen interaction pathway that was potentially regulated by W10-Sp1 was described according to the number of DEGs. We found that family genes of *RPM1,* which recognized bacterial effectors, included 81 upregulated DEGs and 8 downregulated DEGs; LRR receptor-like serine/threonine-protein kinase *FLS2,* which recognized bacterial flagellin signaling transduction pathways, was upregulated by 66 genes and downregulated by 18 genes. In addition, recognition of bacterial effector signal transduction pathway disease resistance protein Prf family genes showed 44 upregulated genes and 2 downregulated genes, and other genes in these pathways were also differentially upregulated or downregulated (**Figure 9**). Further, the expressions of receptor-genes were significantly up-regulated or down-regulated by qRT-PCR (**Supplementary Figure S5**). These results indicated that W10-Sp1 treatment might induce the plant defense response to control pathogen infection by significantly stimulating the expression of these three signaling pathways.

TABLE 4 The top 10 KEGG pathway functional enrichment results of Sp1 protein –vs.- control tobacco.

Pathway	DEGs genes with pathway annotation (6880)	All genes with pathway annotation (51507)	*P*-value	*Q*-value	Pathway ID
Metabolic pathways	1709 (24.84%)	13255 (25.73%)	0.967253	1.0	ko01110
Biosynthesis of secondary metabolites	995 (14.46%)	7021 (13.63%)	0.01668	0.09789	ko01110
Plant hormone signal transduction	407 (5.92%)	1965 (3.82%)	0	0	ko04075
Plant–pathogen interaction	364 (5.29%)	2921 (5.67%)	0.93336	1.0	ko04626
MAPK signaling pathway–plant	308 (4.48%)	2117 (4.11%)	0.05460	0.26321	ko04016
Protein processing in endoplasmic reticulum	261 (3.79%)	2313 (4.49%)	0.99901	1.0	ko04141
Starch and sucrose metabolism	235 (3.42%)	1487 (2.89%)	0.00326	0.02591	ko00500
RNA transport	213 (3.1%)	1853 (3.6%)	0.99337	1.0	Ko03013
Phenylpropanoid biosynthesis	205 (2.98%)	1762 (3.42%)	0.98720	1.0	ko00940
Endocytosis	181 (2.63%)	1845 (3.58%)	1.0	1.0	ko04144

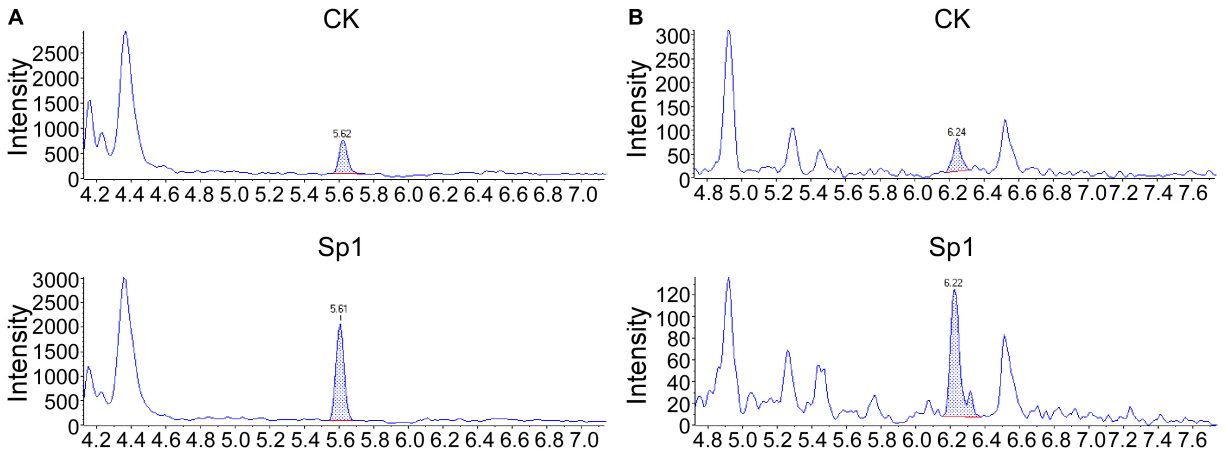

FIGURE 8
MS/MS spectra of MRM chromatograms of detected the contents of SA and JA in 50 mg of the Xanthi tobacco samples treated with W10-Sp1 protein or control. **(A)** MS/MS spectra of detected SA from 50 mg of upper leaves of Xanthi tobacco under different treatments. The peak flow of the standard of SA was at ∼5.61 min. **(B)** MS/MS spectra of detected JA from 50 mg of upper leaves of Xanthi tobacco under different treatments. The peak flow of the standard of JA was at ∼6.22 min.

Discussion

Our previous work purified and identified a serine protease, Sp1, from *B. licheniformis* W10 strains, which significantly inhibited the growth of *B. cinerea* and had higher temperature and pH tolerance, suggesting that the protein could be a potential biopesticide (Ji et al., 2020b). To explore its applicability, here, the purified W10-Sp1 protein notably inhibited the growth of ten kinds of plant pathogenic fungi (*B. cinerea, P. amygdali*, *R. solani*, *M. fructicola*, *S. sclerotiorum*, *G. cingulata*, *R. stolonifer*, *F. moniliforme*, *A. cerasi* and *G. graminis*) and four kinds of bacteria (*X. arboricola*, *P. cichorii*, *P. syringae*, *A. avenae*), indicating that the W10-Sp1 protein has a broad antimicrobial spectrum. Most of the literature have reported that proteins secreted by *Bacillus* have antifungal activity; however, little is known about their antibacterial activity (Li et al., 2009; Cui et al., 2012; Wang et al., 2014; Slimene et al., 2015; Yan et al., 2021). It was not clear whether the antimicrobial spectra of different antifungal proteins were consistent, and some pathogenic fungi were not detected.

TABLE 5 The contents of SA and JA in the samples of W10-Sp1-treated Xanthi tobacco for 12 h and untreated tobacco with HPLC-MS/MS method.

Hormone	TCK (ng/g)	TSp1 (ng/g)
SA	0.3106 ± 0.0148	2.2312 ± 0.0990**
JA	0.0183 ± 0.0049	0.0879 ± 0.0192**

The content of each hormone component in the sample (ng/g) = The concentration of each component in the test solution (ng/ml) × Sample extraction liquid volume (ml)/The sample quality (g). Asterisks represent a significant differences. Experiments were repeated three times with similar results. Duncan's new multiple range test, $p < 0.01$.

In this work, the antifungal activity of the W10-Sp1 protein might be the reason for its affecting hyphal structure (including increasing hyphal diameter, leading to swollen hyphae and producing vesicular-like structures) and inhibiting spore germination. The characteristics were in accordance with those of the treatment of *B. licheniformis* W10 strains (Tang et al., 2005; Sun et al., 2007), which indicated that the W10-Sp1 protein was an important extracellular secreted substance for the biocontrol function of *B. licheniformis*. Furthermore, the EC_{50} values of its antifungal activity were 4.2–398.2 mg/L with 10 different plant pathogenic fungi; among them, the W10-Sp1 protein had a much better biocontrol effect on *G. graminis*, and that of *B. cinerea* was the worst. The EC_{50} values provide an important experimental basis for the applicability of the products of the W10-Sp1 protein as the main ingredients in the future.

In addition, *P. amygdali,* which causes peach shoot blight to seriously affect peach production (Yang et al., 2022), was used as an example in the present work to explore the underlying molecular regulatory mechanism of the W10-Sp1 protein in plant pathogenic fungi through transcriptome analysis. RNA-seq identified 359 DEGs, 150 of which were upregulated and 209 of which were downregulated in the whole genome of *P. amygdali* treated with the W10-Sp1 protein when compared with untreated hyphae of *P. amygdali* (PCK). The top 10 GO enrichment and KEGG pathway enrichment analyses showed that treatment of *P. amygdali* with the W10-Sp1 protein significantly affected coenzyme binding, carbohydrate metabolic processes, amino acid metabolism, fatty acid metabolism, glyoxylate and dicarboxylate metabolism, and propanote metabolism. Interestingly, those pathways and biological processes had a common intersection, which was

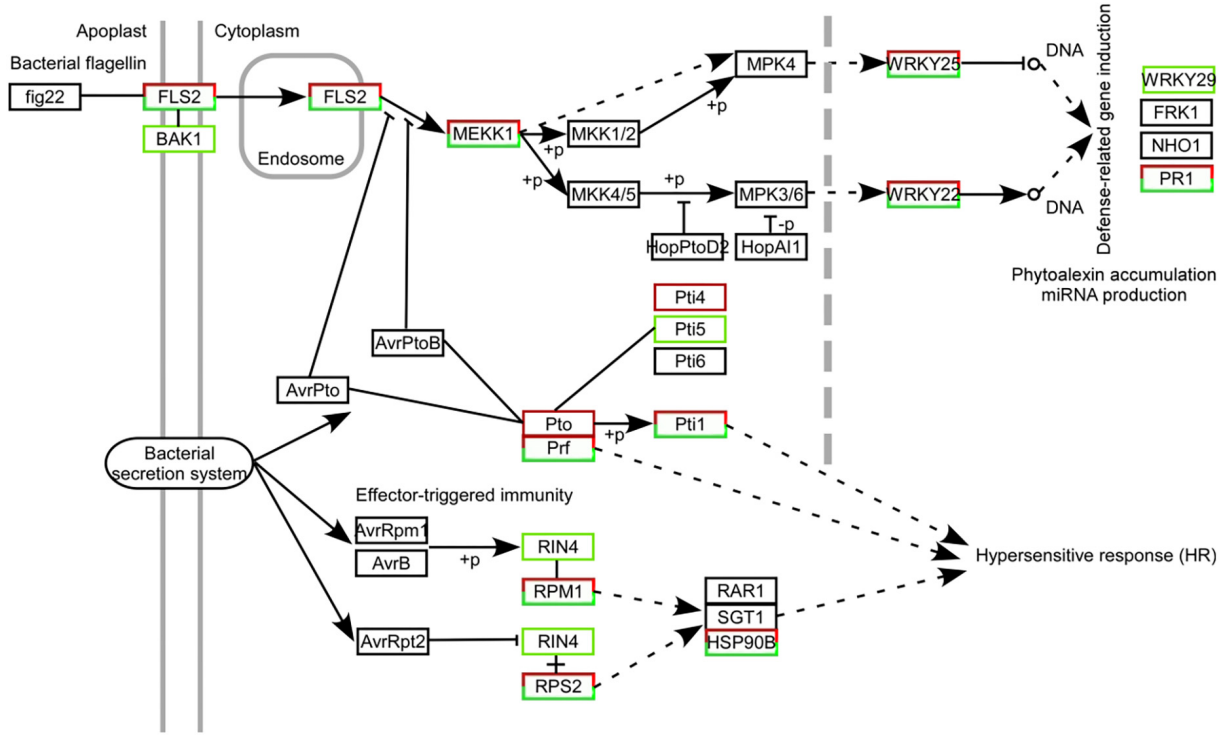

FIGURE 9
Statistical map of DEGs in the immune signaling pathways mediated by Fls2, Prf, and Rpm1 strongly induced in Xanthi tobacco treated with the W10-Sp1 protein. The black box represents no differential expression; the red box represents DEGs with upregulation; the green box represents DEGs with downregulation; and the red and green combined box represents both upregulated and downregulated DEGs.

the TCA cycle. DEGs in the molecular function category of coenzyme binding, such as acetyl-CoA, which is a key regulator of the TCA cycle, were highly active. Amino acids are indispensable components in the formation of cell structures and various enzymes. The degradation of valine, leucine and isoleucine might be related to propanoate metabolism, which enters the TCA cycle (Tian et al., 2021). DEGs of valine, leucine and isoleucine degradation were all upregulated in this work, indicating that some cell structures and enzymatic activities might be damaged, similar to the hyphal morphological changes in *P. amygdali*. The results suggested that W10-Sp1 treatment affected the energy supply and amino acid metabolism of *P. amygdali*. In addition, genes expressing glycosyl hydrolase (GME11525_g, GME3789_g, GME4018_g, GME13604_g, GME7161_g, GME3329_g, GME10136_g) and glucanase (GME6808_g, GME4201_g, GME10462_g) were notably downregulated. Protein glycosylation is one of the most common and highly conserved posttranslational modifications in eukaryotes and plays important roles in protein structure and function (Willer et al., 2005). It has been reported that glycosylation is closely related to the virulence of plant pathogens and affects biological processes such as pathogen adhesion, signal transduction, immune response and colonization (Li et al., 2013; Rempe et al., 2016; Liu et al., 2021). Among them, glycosyl hydrolase and glycosyltransferase drive essential functions. Glycosylated proteins play important roles in composition of fungal cell wall structure. Moreover, glycolysis and the TCA cycle are both important energy supply processes, and there is crosstalk between the two processes (Payne et al., 2010). Besides that, previous work has reported that cyclic lipopeptides isolated from *Bacillus* inhibited the activity of (1,3)-beta-D-glucan synthase in fungi and caused abnormal cell walls (Kurtz and Douglas, 1997). They all affected the composition of the cell wall. Therefore, we suspect that the W10-Sp1 protein might affect the energy supply and cell wall structure, to inhibit the development of *P. amygdali* (**Figure 10**). Conductivity analysis confirmed the results that W10-Sp1 treatment surely damaged the cell wall of nine fungi. To our knowledge, this is the first study to uncover how biocontrol antifungal proteins protect against plant pathogens.

Furthermore, we found that the W10-Sp1 protein has a better disease control effect, especially when pre-spraying the host, than when the protein was sprayed after inoculation with the pathogen. Furthermore, injection into the lower leaf of Xanthi tobacco within Sp1 protein for 12 h significantly inhibited the infection of *B. cinerea*, indicating that W10-Sp1 activated systemic resistance of the host, including peach twigs, fruits and Xanthi tobacco. Transcriptome analysis in

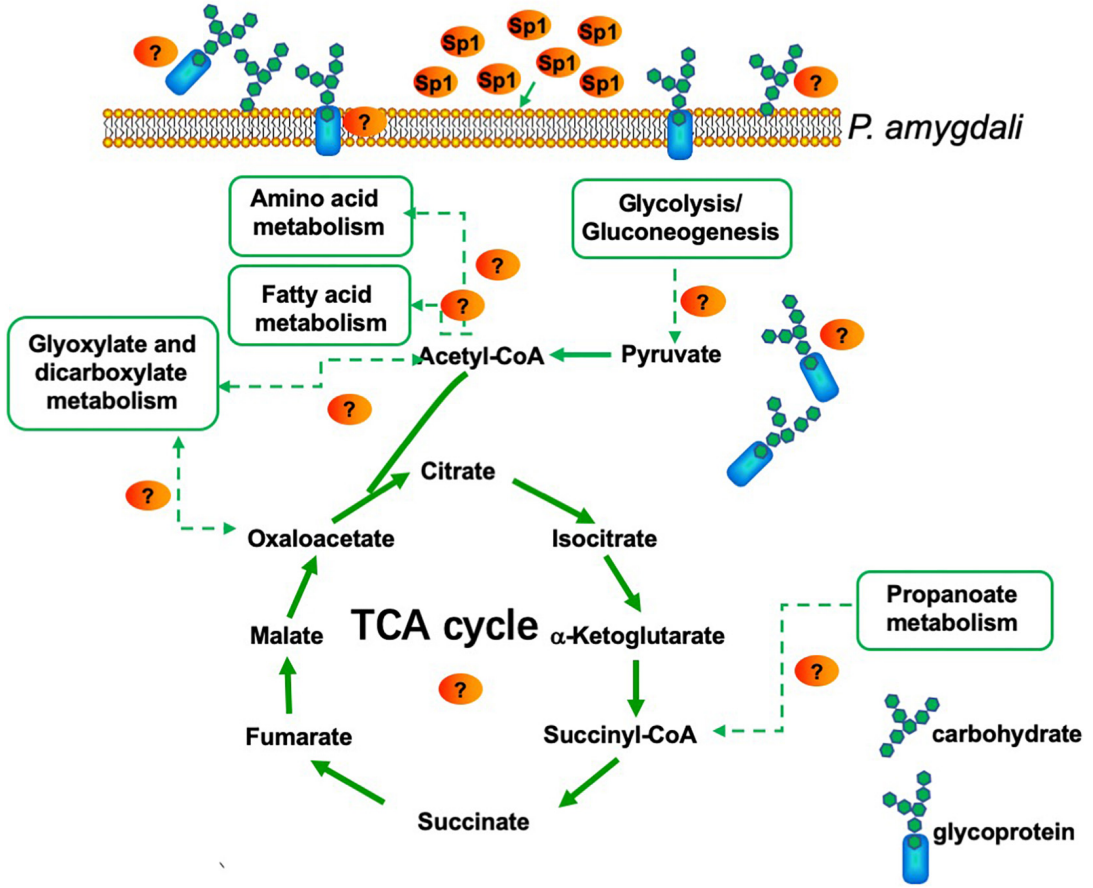

FIGURE 10
Model for *P. amygdali* inducing energy supply and cell wall structure by purified W10-Sp1 protein.

Xanthi tobacco treated or not treated with the W10-Sp1 protein was used to explore the underlying mechanism of systemic resistance. There were 8862 DEGs treated with W10-Sp1 protein for 12 h compared with sterile water-treated Xanthi tobacco, 5937 of which were upregulated and 2925 of which were downregulated. The DEGs were mainly enriched in five pathways, including metabolic pathways, biosynthesis of secondary metabolites, plant hormone signal transduction, plant–pathogen interaction and MAPK signaling pathway–plant. The pathogenesis of plant–pathogen interactions and plant hormone signal transduction were also induced by hosts infected with pathogens such as sunflower/tomato infected with *Verticillium dahlia* (Tan et al., 2015; Guo et al., 2017) or biocontrol bacteria pre-treated with hosts and then infected with pathogens, such as cotton inoculated with *Chaetomium globosum* CEF-082 and *V. dahlia* (Zhang et al., 2020).

Plants encounter a variety of microorganisms, including both beneficial and pathogenic microorganisms, which establish an interaction relationship with each other through their sophisticated innate immune response (Rodriguez et al., 2019). In general, beneficial microorganisms can activate induced systemic resistance (ISR) of plants to suppress plant disease in uninoculated plant organs, and pathogenic microorganisms activate systemic acquired resistance (SAR) of plants, thus relieving plant disease in uninoculated plant organs (Nishad et al., 2020). Plant hormones, including SA and JA/ET, are well known to activate plant defense response (Robert-Seilaniantz et al., 2011; Pieterse et al., 2012); among them, SA signaling is vital for SAR (Bernsdorff et al., 2016); however, JA/ET signaling plays important roles in ISR independent of the SA signaling pathway (Ahn et al., 2007). Most work has demonstrated that antagonistic microorganisms or their secondary metabolites can activate ISR (Shoresh et al., 2010; Elsharkawy et al., 2013; Mejri et al., 2018). In the present study, transcriptome analysis found that DEGs in the SA and JA signaling pathways were highly active, and the contents of intracellular SA and JA were measured, which both significantly increased with W10-Sp1 treatment of Xanthi tobacco, implying that the Sp1 protein activated SAR and ISR in tobacco by simultaneously activating the SA and JA signaling pathways. The results were in agreement with the study that showed that *B. cereus* AR156 activated SA and JA signaling to activate systemic resistance in *Arabidopsis thaliana*, and similar results were obtained in *P. fluorescens* WCS417 in tomato against *P. syringae* pv. *tomato*

and *B. amyloliquefaciens* I3 in the seeds of *A. thaliana* (Van Wees et al., 1997; Niu et al., 2011; Ilham et al., 2019). This might be the first report indicating that systemic resistance induced by antifungal proteins shares features of SAR and ISR.

In addition, RNA-seq in this study identified that DEGs were also enriched in the plant–pathogen interaction pathway and found that certain genes, including *CDPK, RBOH, CNGCS, FLS2, PTO, PRF, NOS, PR-1, PBS1* and *CML,* were significantly upregulated or downregulated. A further statistical map of DEGs indicated that the W10-Sp1 protein strongly activated the Fls2-, Prf- and Rpm1-mediated immune response pathways, which might trigger the defense response of Xanthi tobacco, thus producing disease resistance. The immune responses mediated by Fls2, Rboh, CNGC and CaM/CML were activated after plants were infected by pathogens or plants were treated with biocontrol bacteria or exposed to various stresses in previous work (Zhang et al., 2014, 2020; Singh and Bhatla, 2016).

There is a close relationship between plant development and disease resistance. RNA-seq of TSp1 to TCK identified that DEGs were enriched in photosystem, protein chromophore, chlorophyll and defense response in the GO lineage DAG graph (**Supplementary Figure S6**), indicating that W10-Sp1 protein might promote the growth of Xanthi tobacco by strengthening its photosynthesis. In addition, the plant hormones IAA, GA, and CTK were differentially expressed, which also affected the development of Xanthi tobacco treated with the W10-Sp1 protein. It is worth mentioning that *B. licheniformis* W10 is a plant growth-promoting rhizobacterium (PGPR). These results indicated that the Sp1 protein was surely an important antimicrobial protein of the W10 strain.

In summary, in the present work, we found that serine protease Sp1 secreted by *B. licheniformis* W10 has a broad antifungal spectrum by inhibiting its vegetative growth, changing its hyphal structure and reducing the spore germination. In addition, the W10-Sp1 protein also has an inhibitory effect on some plant pathogenic bacteria. Furthermore, dual transcriptome analysis indicated its potential molecular mechanism of anti-fungal resistance, activated systemic resistance and induced plant defense responses. The W10-Sp1 protein might perform similar functions in a variety of plant pathogenic fungi and plants. This study supplies a solid foundation for the applicability of the Sp1 protein.

Data availability statement

The raw data of RNA-seq in this work has successfully submitted to Sequence Read Archive (SRA) database at National Center for Biotechnology Information (NCBI). The BioProject ID was PRJNA852429 (https://www.ncbi.nlm.nih.gov/search/all/?term=%20PRJNA852429) and PRJNA853397 (https://www.ncbi.nlm.nih.gov/search/all/?term=+PRJNA853397).

Author contributions

LY, LL, and ZJ designed, supervised, and wrote the manuscript. CY, JG, and YL performed the experiments and analyzed the data. SP and LC supplied the transcriptome analysis. All authors have read and approved the manuscript.

Funding

This work was supported by the Natural Science Foundation of Jiangsu Province of China (BK20200929), China Agriculture Research System of MOF and MARA (Grant No. CARS-30-3-02), Yangzhou University Research Foundation for Advanced Talents (Grant No. 5018/137011834), and Suzhou Local Rural Talents Training Funding Project.

Conflict of interest

The authors declare that the research was conducted in the absence of any commercial or financial relationships that could be construed as a potential conflict of interest.

Publisher's note

All claims expressed in this article are solely those of the authors and do not necessarily represent those of their affiliated organizations, or those of the publisher, the editors and the reviewers. Any product that may be evaluated in this article, or claim that may be made by its manufacturer, is not guaranteed or endorsed by the publisher.

Supplementary material

The Supplementary Material for this article can be found online at: https://www.frontiersin.org/articles/10.3389/fmicb.2022.974473/full#supplementary-material

SUPPLEMENTARY FIGURE S1
Identification of purified W10-Sp1 protein by SDS-PAGE.

SUPPLEMENTARY FIGURE S2
Effects of different concentrations of W10-Sp1 protein to the mycelium of 10 kinds of plant pathogenic fungi.

SUPPLEMENTARY FIGURE S3
Verification of RNA-Seq of PSp1-vs.- PCK by qRT-PCR.

SUPPLEMENTARY FIGURE S4
Verification of RNA-Seq of TSp1-vs.- TCK by qRT-PCR.

SUPPLEMENTARY FIGURE S5
Directed acyclic graph (DAG) of GO enrichment of DEGs in Xanthi tobacco treated by W10-Sp1 protein.

References

Abdelkhalek, A., Al-Askar, A. A., and Behiry, S. I. (2020). *Bacillus licheniformis* strain POT1 mediated polyphenol biosynthetic pathways genes activation and systemic resistance in potato plants against Alfalfa mosaic virus. *Sci. Rep.* 10:16120. doi: 10.1038/s41598-020-72676-2

Ahn, I. P., Lee, S. W., and Suh, S. C. (2007). Rhizobacteria-induced priming in *Arabidopsis* is dependent on ethylene, jasmonic acid, and NPR1. *Mol. Plant Microbe Interact.* 20, 759–768. doi: 10.1094/MPMI-20-7-0759

Aktuganov, G., Jokela, J., Kivelä, H., Khalikova, E., Melentjev, A., Galimzianova, N., et al. (2014). Isolation and identification of cyclic lipopeptides from *Paenibacillus ehimensis*, strain IB-X-b. *J. Chromatogr. B Analyt. Technol. Biomed. Life Sci.* 973c, 9–16. doi: 10.1016/j.jchromb.2014.09.042

Asraful Islam, S. M., Math, R. K., Kim, J. M., Yun, M. G., Cho, J. J., Kim, E. J., et al. (2010). Effect of plant age on endophytic bacterial diversity of balloon flower (*Platycodon grandiflorum*) root and their antimicrobial activities. *Curr. Microbiol.* 61, 346–356. doi: 10.1007/s00284-010-9618-1

Bergey, D. R., Howe, G. A., and Ryan, C. A. (1996). Polypeptide signaling for plant defensive genes exhibits analogies to defense signaling in animals. *Proc. Natl. Acad. Sci. U.S.A.* 93, 12053–12058.

Bernsdorff, F., Döring, A. C., Gruner, K., Schuck, S., Bräutigam, A., and Zeier, J. (2016). Pipecolic acid orchestrates plant systemic acquired resistance and defense priming via salicylic acid-dependent and –independent pathways. *Plant Cell* 28, 102–129. doi: 10.1105/tpc.15.00496

Bhai, R. S., Prameela, T. P., Vincy, K., Biju, C. N., Srinivasan, V., and Babu, K. N. (2019). Soil solarization and amelioration with calcium chloride or *Bacillus licheniformis* – An effective integrated strategy for the management of bacterial wilt of ginger incited by *Ralstonia pseudosolanacearum*. *Eur. J. Plant Pathol.* 154, 903–917.

Budič, M., Sabotič, J., Meglič, V., Kos, J., and Kidrič, M. (2013). Characterization of two novel subtilases from common bean (*Phaseolus vulgaris* L.) and their responses to drought. *Plant Physiol. Biochem.* 62, 79–87. doi: 10.1016/j.plaphy.2012.10.022

Chalfoun, N. R., Grellet-Bournonville, C. F., Martínez-Zamora, M. G., Díaz-Perales, A., Castagnaro, A. P., and Díaz-Ricci, J. C. (2013). Purification and characterization of AsES protein: A subtilisin secreted by *Acremonium strictum* is a novel plant defense elicitor. *J. Biol. Chem.* 288, 14098–14113. doi: 10.1074/jbc.M112.429423

Coolen, S., Proietti, S., Hickman, R., Davila Olivas, N. H., Huang, P. P., Van Verk, M. C., et al. (2016). Transcriptome dynamics of *Arabidopsis* during sequential biotic and abiotic stresses. *Plant J.* 86, 249–267. doi: 10.1111/tpj.13167

Cui, T. B., Chai, H. Y., and Jiang, L. X. (2012). Isolation and partial characterization of an antifungal protein produced by *Bacillus licheniformis* BS-3. *Molecules* 17, 7336–7347. doi: 10.3390/molecules17067336

Duan, X., Zhang, Z., Wang, J., and Zuo, K. (2016). Characterization of a novel cotton subtilase gene GbSBT1 in response to extracellular stimulations and its role in *Verticillium* resistance. *PLoS One* 11:e0153988. doi: 10.1371/journal.pone.0153988

Elsharkawy, M. M., Shimizu, M., Takahashi, H., Ozaki, K., and Hyakumachi, M. (2013). Induction of systemic resistance against cucumber mosaic virus in *Arabidopsis thaliana* by *Trichoderma asperellum* SKT-1. *Plant Pathol. J.* 29, 193–200. doi: 10.5423/PPJ.SI.07.2012.01

Fernández, M. B., Daleo, G. R., and Guevara, M. G. (2015). Isolation and characterization of a *Solanum tuberosum* subtilisin-like protein with caspase-3 activity (StSBTc-3). *Plant Physiol. Biochem.* 86, 137–146. doi: 10.1016/j.plaphy.2014.12.001

Figueiredo, J., Sousa Silva, M., and Figueiredo, A. (2018). Subtilisin-like proteases in plant defence: The past, the present and beyond. *Mol. Plant Pathol.* 19, 1017–1028. doi: 10.1111/mpp.12567

Fira, D., Dimkić, I., Berić, T., Lozo, J., and Stanković, S. (2018). Biological control of plant pathogens by *Bacillus* species. *J. Biotechnol.* 285, 44–55.

Gomaa, E. Z. (2012). Chitinase production by *Bacillus thuringiensis* and *Bacillus licheniformis*: Their potential in antifungal biocontrol. *J. Microbiol.* 50, 103–111. doi: 10.1007/s12275-012-1343-y

Guo, S., Zuo, Y., Zhang, Y., Wu, C., Su, W., Jin, W., et al. (2017). Large-scale transcriptome comparison of sunflower genes responsive to *Verticillium dahliae*. *BMC Genomics* 18:42. doi: 10.1186/s12864-016-3386-7

He, D. C., He, M. H., Amalin, D. M., Liu, W., Alvindia, D. G., and Zhan, J. (2021). Biological control of plant diseases: An evolutionary and eco-economic consideration. *Pathogens* 10:1311. doi: 10.3390/pathogens10101311

Ilham, B., Noureddine, C., Philippe, G., Mohammed, E. G., Brahim, E., Sophie, A., et al. (2019). Induced systemic resistance (ISR) in *Arabidopsis thaliana* by *Bacillus amyloliquefaciens* and *Trichoderma harzianum* used as seed treatments. *Agriculture* 9:166.

Jeong, M. H., Lee, Y. S., Cho, J. Y., Ahn, Y. S., Moon, J. H., Hyun, H. N., et al. (2017). Isolation and characterization of metabolites from *Bacillus licheniformis* MH48 with antifungal activity against plant pathogens. *Microb. Pathog.* 110, 645–653. doi: 10.1016/j.micpath.2017.07.027

Ji, Z. L., He, H. W., Zhou, H. J., Han, F., Tong, Y. H., Ye, Z. W., et al. (2015). The biocontrol effects of the *Bacillus licheniformis* W10 strain and its antifungal protein against brown rot in peach. *Hortic. Plant J.* 1, 131–138.

Ji, Z. L., Peng, S., Zhu, W., Dong, J. P., and Zhu, F. (2020a). Induced resistance in nectarine fruit by *Bacillus licheniformis* W10 for the control of brown rot caused by *Monilinia fructicola*. *Food Microbiol.* 92:103558. doi: 10.1016/j.fm.2020.103558

Ji, Z. L., Peng, S., Chen, L. L., Liu, Y., Yan, C., and Zhu, F. (2020b). Identification and characterization of a serine protease from *Bacillus licheniformis* W10: A potential antifungal agent. *Int. J. Biol. Macromol.* 145, 594–603. doi: 10.1016/j.ijbiomac.2019.12.216

Kurtz, M. B., and Douglas, C. M. (1997). Lipopeptide inhibitors of fungal glucan synthase. *J. Med. Vet. Mycol.* 35, 79–86.

Leelasuphakul, W., Sivanunsakul, P., and Phongpaichit, S. (2006). Purification, characterization and synergistic activity of β-1,3-glucanase and antibiotic extract from an antagonistic *Bacillus subtilis* NSRS 89-24 against rice blast and sheath blight. *Enzyme Microbial Technol.* 38, 990–997.

Li, J., Yang, Q., Zhao, L. H., Zhang, S. M., Wang, Y. X., and Zhao, X. Y. (2009). Purification and characterization of a novel antifungal protein from *Bacillus subtilis* strain B29. *J. Zhejiang Univ. Sci. B* 10, 264–272. doi: 10.1631/jzus.B0820341

Li, S., Zhang, L., Yao, Q., Li, L., Dong, N., Rong, J., et al. (2013). Pathogen blocks host death receptor signalling by arginine GlcNAcylation of death domains. *Nature* 501, 242–246.

Liu, C., Talbot, N. J., and Chen, X. L. (2021). Protein glycosylation during infection by plant pathogenic fungi. *New Phytol.* 230, 1329–1335.

Liu, J. X., and Howell, S. H. (2010). bZIP28 and NF-Y transcription factors are activated by ER stress and assemble into a transcriptional complex to regulate stress response genes in *Arabidopsis*. *Plant Cell* 22, 782–796. doi: 10.1105/tpc.109.072173

Mejri, S., Siah, A., Coutte, F., Magnin-Robert, M., Randoux, B., Tisserant, B., et al. (2018). Biocontrol of the wheat pathogen *Zymoseptoria tritici* using cyclic lipopeptides from *Bacillus subtilis*. *Environ. Sci. Pollut. Res. Int.* 25, 29822–29833. doi: 10.1007/s11356-017-9241-9

Monteiro, F., Sebastiana, M., Pais, M. S., and Figueiredo, A. (2013). Reference gene selection and validation for the early responses to downy mildew infection in susceptible and resistant *Vitis vinifera* cultivars. *PLoS One* 8:e72998. doi: 10.1371/journal.pone.0072998

Muslim, S. N., Al-Kadmy, I. M. S., Hussein, N. H., Mohammed Ali, A. N., Taha, B. M., Aziz, S. N., et al. (2016). Chitosanase purified from bacterial isolate *Bacillus licheniformis* of ruined vegetables displays broad spectrum biofilm inhibition. *Microb. Pathog.* 100, 257–262. doi: 10.1016/j.micpath.2016.10.001

Nishad, R., Ahmed, T., Rahman, V. J., and Kareem, A. (2020). Modulation of plant defense system in response to microbial interactions. *Front. Microbiol.* 11:1298. doi: 10.3389/fmicb.2020.01298

Niu, D. D., Liu, H. X., Jiang, C. H., Wang, Y. P., Wang, Q. Y., Jin, H. L., et al. (2011). The plant growth-promoting rhizobacterium *Bacillus cereus* AR156 induces systemic resistance in *Arabidopsis thaliana* by simultaneously activating salicylate- and jasmonate/ethylene-dependent signaling pathways. *Mol. Plant Microbe Interact.* 24, 533–542. doi: 10.1094/MPMI-09-10-0213

Olivieri, F., Godoy, A. V., Escande, A., and Casalongue, C. A. (1998). Analysis of intercellular washing fluids of potato tubers and detection of increased proteolytic activity upon fungal infection. *Physiol. Plant* 104, 232–238.

Pan, X. Q., Welti, R., and Wang, X. M. (2010). Quantitative analysis of major plant hormones in crude plant extracts by high-performance liquid chromatography–mass spectrometry. *Nat. Protoc.* 5, 986–992. doi: 10.1038/nprot.2010.37

Panichikkal, J., Puthiyattil, N., Raveendran, A., Nair, R. A., and Krishnankutty, R. E. (2021). Application of encapsulated *Bacillus licheniformis* supplemented with chitosan nanoparticles and rice starch for the control of *Sclerotium rolfsii* in *Capsicum annuum* (L.) seedlings. *Curr. Microbiol.* 78, 911–919. doi: 10.1007/s00284-021-02361-8

Payne, K. A., Hough, D. W., and Danson, M. J. (2010). Discovery of a putative acetoin dehydrogenase complex in the hyperthermophilic archaeon *Sulfolobus solfataricus*. *FEBS Lett.* 584, 1231–1234. doi: 10.1016/j.febslet.2010.02.037

Pérez-García, A., Romero, D., and de Vicente, A. (2011). Plant protection and growth stimulation by microorganisms: Biotechnological applications of bacilli in agriculture. *Curr. Opin. Biotechnol.* 22, 187–193. doi: 10.1016/j.copbio.2010.12.003

Pieterse, C. M., Van der Does, D., Zamioudis, C., Leon-Reyes, A., and Van Wees, S. C. (2012). Hormonal modulation of plant immunity. *Annu. Rev. Cell Dev. Biol.* 28, 489–521.

Rawlings, N. D., and Barrett, A. J. (1994). Families of serine peptidases. *Methods Enzymol.* 244, 19–61.

Rempe, K. A., Porsch, E. A., Wilson, J. M., and St Geme, J. W. III (2016). The HMW1 and HMW2 adhesins enhance the ability of nontypeable *Haemophilus influenzae* to colonize the upper respiratory tract of rhesus macaques. *Infect. Immun.* 84, 2771–2778. doi: 10.1128/IAI.00153-16

Robert-Seilaniantz, A., Grant, M., and Jones, J. D. (2011). Hormone crosstalk in plant disease and defense: More than just jasmonate-salicylate antagonism. *Annu. Rev. Phytopathol.* 49, 317–343. doi: 10.1146/annurev-phyto-073009-114447

Rodriguez, P. A., Rothballer, M., Chowdhury, S. P., Nussbaumer, T., Gutjahr, C., and Falter-Braun, P. (2019). Systems biology of plant-microbiome interactions. *Mol. Plant* 12, 804–821.

Ryan, C. A. (2000). The systemin signaling pathway: Differential activation of plant defensive genes. *Biochim. Biophys. Acta* 1477, 112–121. doi: 10.1016/s0167-4838(99)00269-1

Schaller, A., Stintzi, A., and Graff, L. (2012). Subtilases – Versatile tools for protein turnover, plant development, and interactions with the environment. *Physiol. Plant* 145, 52–66. doi: 10.1111/j.1399-3054.2011.01529.x

Shoresh, M., Harman, G. E., and Mastouri, F. (2010). Induced systemic resistance and plant responses to fungal biocontrol agents. *Annu. Rev. Phytopathol.* 48, 21–43.

Singh, N., and Bhatla, S. C. (2016). Nitric oxide and iron modulate heme oxygenase activity as a long distance signaling response to salt stress in sunflower seedling cotyledons. *Nitric Oxide* 53, 54–64. doi: 10.1016/j.niox.2016.01.003

Slimene, I. B., Tabbene, O., Gharbi, D., Mnasri, B., Schmitter, J. M., Urdaci, M. C., et al. (2015). Isolation of a chitinolytic *Bacillus licheniformis* S213 strain exerting a biological control against Phoma medicaginis infection. *Appl. Biochem. Biotechnol.* 175, 3494–3506. doi: 10.1007/s12010-015-1520-7

Someya, N. (2008). Biological control of fungal plant diseases using antagonistic bacteria. *J. Gen. Plant Pathol.* 74, 459–460.

Sun, Q. L., Chen, X. J., Tong, Y. H., Ji, Z. L., Li, H. D., and Xu, J. Y. (2007). Inhibition of antifungal protein produced by *Bacillus iicheniformis* W10 to *Sclerotinia sclerotiorum* and control of rape stem rot by the protein. *J. Yangzhou Univ.* 28, 82–86.

Syed Ab Rahman, S. F., Singh, E., Pieterse, C. M. J., and Schenk, P. M. (2018). Emerging microbial biocontrol strategies for plant pathogens. *Plant Sci.* 267, 102–111.

Tan, G., Liu, K., Kang, J., Xu, K., Zhang, Y., Hu, L., et al. (2015). Transcriptome analysis of the compatible interaction of tomato with *Verticillium dahliae* using RNA-sequencing. *Front. Plant Sci.* 6:428. doi: 10.3389/fpls.2015.00428

Tang, L. J., Ji, Z. L., Xu, J. Y., Chen, X. J., and Tong, Y. H. (2005). Mechanisms of action to *Botrytis cinerea* and antimicrobial substance of *Bacillus licheniformis* W10. *Chin. J. Biol. Control* 21, 203–205.

Tian, D., Song, X., Li, C., Zhou, W., Qin, L., Wei, L., et al. (2021). Antifungal mechanism of *Bacillus amyloliquefaciens* strain GKT04 against *Fusarium wilt* revealed using genomic and transcriptomic analyses. *Microbiologyopen* 10:e1192. doi: 10.1002/mbo3.1192

Tornero, P., Mayda, E., Gómez, M. D., Cañas, L., Conejero, V., and Vera, P. (1996). Characterization of LRP, a leucine-rich repeat (LRR) protein from tomato plants that is processed during pathogenesis. *Plant J.* 10, 315–330. doi: 10.1046/j.1365-313x.1996.10020315.x

Upadhyay, A., and Mohan, S. (2021). *Bacillus subtilis* and *B. licheniformis* isolated from *Heterorhabditis indica* infected apple root borer (*Dorysthenes huegelii*) suppresses nematode production in *Galleria mellonella*. *Acta Parasitol.* 66, 989–996. doi: 10.1007/s11686-021-00366-8

Van Wees, S. C., Pieterse, C. M., Trijssenaar, A., Van 't Westende, Y. A., Hartog, F., and Van Loon, L. C. (1997). Differential induction of systemic resistance in *Arabidopsis* by biocontrol bacteria. *Mol. Plant Microbe Interact.* 10, 716–724. doi: 10.1094/MPMI.1997.10.6.716

Vera, P., Yago, J. H., and Conejero, V. (1989). Immunogold localization of the Citrus exocortis viroid-induced pathogenesis-related proteinase p69 in tomato leaves. *Plant Physiol.* 91, 119–123. doi: 10.1104/pp.91.1.119

Walter, S., Nicholson, P., and Doohan, F. M. (2010). Action and reaction of host and pathogen during *Fusarium* head blight disease. *New Phytol.* 185, 54–66. doi: 10.1111/j.1469-8137.2009.03041.x

Wang, Z., Wang, Y., Zheng, L., Yang, X., Liu, H., and Guo, J. (2014). Isolation and characterization of an antifungal protein from *Bacillus licheniformis* HS10. *Biochem. Biophys. Res. Commun.* 454, 48–52. doi: 10.1016/j.bbrc.2014.10.031

Willer, T., Brandl, M., Sipiczki, M., and Strahl, S. (2005). Protein O-mannosylation is crucial for cell wall integrity, septation and viability in fission yeast. *Mol. Microbiol.* 57, 156–170. doi: 10.1111/j.1365-2958.2005.04692.x

Won, S. J., Kwon, J. H., Kim, D. H., and Ahn, Y. S. (2019). The effect of *Bacillus licheniformis* MH48 on control of foliar fungal diseases and growth promotion of *Camellia oleifera* seedlings in the coastal reclaimed land of Korea. *Pathogens* 8:6. doi: 10.3390/pathogens8010006

Won, S. J., Moon, J. H., Ajuna, H. B., Choi, S. I., Maung, C. E. H., Lee, S., et al. (2021). Biological control of leaf blight disease caused by *Pestalotiopsis maculans* and growth promotion of *Quercus acutissima* Carruth container seedlings using *Bacillus velezensis* CE 100. *Int. J. Mol. Sci.* 22:11296. doi: 10.3390/ijms222011296

Yan, F., Ye, X., Li, C., Wang, P., Chen, S., and Lin, H. (2021). Isolation, purification, gene cloning and expression of antifungal protein from *Bacillus amyloliquefaciens* MG-3. *Food Chem.* 349:129130. doi: 10.1016/j.foodchem.2021.129130

Yang, L., Zhang, L., Cao, J., Wang, L., Shi, H., Zhu, F., et al. (2022). Rapid detection of peach shoot blight caused by *Phomopsis amygdali* utilizing a new target gene identified from denome sequences within loop-mediated isothermal amplification. *Plant Dis.* 106, 669–675. doi: 10.1094/PDIS-08-21-1645-RE

Zhang, H., Yang, Y., Wang, C., Liu, M., Li, H., Fu, Y., et al. (2014). Large-scale transcriptome comparison reveals distinct gene activations in wheat responding to stripe rust and powdery mildew. *BMC Genomics* 15:898. doi: 10.1186/1471-2164-15-898

Zhang, Y., Yang, N., Zhao, L., Zhu, H., and Tang, C. (2020). Transcriptome analysis reveals the defense mechanism of cotton against *Verticillium dahliae* in the presence of the biocontrol fungus *Chaetomium globosum* CEF-082. *BMC Plant Biol.* 20:89. doi: 10.1186/s12870-019-2221-0

frontiers | Frontiers in Microbiology

TYPE Original Research
PUBLISHED 13 October 2022
DOI 10.3389/fmicb.2022.947678

Check for updates

OPEN ACCESS

EDITED BY
Reiner Rincón Rosales,
Tuxtla Gutierrez Institute of Technology, Mexico

REVIEWED BY
Luyao Wang,
Chinese Academy of Agricultural Sciences, China
Betsy Peña-Ocaña,
Instituto Nacional de Cardiologia Ignacio Chavez, Mexico
Clara Ivette Rincón Molina,
Instituto Tecnológico de Tuxtla Gutiérrez/TecNM, Mexico

*CORRESPONDENCE
Sergio Encarnacion Guevara
encarnacion@ccg.unam.mx

SPECIALTY SECTION
This article was submitted to Microbe and Virus Interactions With Plants, a section of the journal Frontiers in Microbiology

RECEIVED 19 May 2022
ACCEPTED 05 September 2022
PUBLISHED 13 October 2022

CITATION
Taboada-Castro H, Gil J, Gómez-Caudillo L, Escorcia-Rodríguez JM, Freyre-González JA and Encarnación-Guevara S (2022) *Rhizobium etli* CFN42 proteomes showed isoenzymes in free-living and symbiosis with a different transcriptional regulation inferred from a transcriptional regulatory network. *Front. Microbiol.* 13:947678. doi: 10.3389/fmicb.2022.947678

COPYRIGHT
© 2022 Taboada-Castro, Gil, Gómez-Caudillo, Escorcia-Rodríguez, Freyre-González and Encarnación-Guevara. This is an open-access article distributed under the terms of the Creative Commons Attribution License (CC BY). The use, distribution or reproduction in other forums is permitted, provided the original author(s) and the copyright owner(s) are credited and that the original publication in this journal is cited, in accordance with accepted academic practice. No use, distribution or reproduction is permitted which does not comply with these terms.

Rhizobium etli CFN42 proteomes showed isoenzymes in free-living and symbiosis with a different transcriptional regulation inferred from a transcriptional regulatory network

Hermenegildo Taboada-Castro[1], Jeovanis Gil[2], Leopoldo Gómez-Caudillo[1], Juan Miguel Escorcia-Rodríguez[3], Julio Augusto Freyre-González[3] and Sergio Encarnación-Guevara[1]*

[1]Proteomics Laboratory, Program of Functional Genomics of Prokaryotes, Center for Genomic Sciences, National Autonomous University of Mexico, Cuernavaca, Morelos, Mexico, [2]Division of Oncology, Section for Clinical Chemistry, Department of Translational Medicine, Lund University, Lund, Sweden, [3]Regulatory Systems Biology Research Group, Program of Systems Biology, Center for Genomic Sciences, National Autonomous University of Mexico, Mexico City, Mexico

A comparative proteomic study at 6h of growth in minimal medium (MM) and bacteroids at 18days of symbiosis of *Rhizobium etli* CFN42 with the *Phaseolus vulgaris* leguminous plant was performed. A gene ontology classification of proteins in MM and bacteroid, showed 31 and 10 pathways with higher or equal than 30 and 20% of proteins with respect to genome content per pathway, respectively. These pathways were for energy and environmental compound metabolism, contributing to understand how *Rhizobium* is adapted to the different conditions. Metabolic maps based on orthology of the protein profiles, showed 101 and 74 functional homologous proteins in the MM and bacteroid profiles, respectively, which were grouped in 34 different isoenzymes showing a great impact in metabolism by covering 60 metabolic pathways in MM and symbiosis. Taking advantage of co-expression of transcriptional regulators (TF's) in the profiles, by selection of genes whose matrices were clustered with matrices of TF's, Transcriptional Regulatory networks (TRN´s) were deduced by the first time for these metabolic stages. In these clustered TF-MM and clustered TF-bacteroid networks, containing 654 and 246 proteins, including 93 and 46 TFs, respectively, showing valuable information of the TF's and their regulated genes with high stringency. Isoenzymes were specific for adaptation to the different conditions and a different transcriptional regulation for MM and bacteroid was deduced. The parameters of the TRNs of these expected biological networks and biological networks of *E. coli* and *B. subtilis* segregate from the random theoretical networks. These are useful data to design experiments on TF gene–target relationships for bases to construct a TRN.

KEYWORDS

transcriptional regulatory network, *Rhizobium etli*, nitrogen fixation, *Phaseolus vulgaris*, free life, proteomics, Isoenzymes

Introduction

Rhizobium etli CFN42 is a soil bacterium classified as an alpha-proteobacterium able to establish a symbiotic relationship with leguminous plants, and this faculty is shared with some members of the beta-proteobacterium group (Andrews and Andrews 2017; Lardi and Pessi 2018; Dicenzo et al. 2019). When the seeds of the bean plant *Phaseolus vulgaris* germinate with *R. etli* CFN42 in a tropical soil, chemical communication starts in the roots to establish a symbiotic relationship. In this process, the root of the plant develops an infection thread through which the bacteria are internalized and travel with some duplications, while the root cortex gives rise to the nodule primordium. When the infection thread reaches the nodule cells, the bacteria are released into organelle-like membranes derived from the host cell plasmalemma called the symbiosome in the nodule. In this stage, *Rhizobium* has some additional duplications, but very soon they stop growing and become pleomorphic, and symbiotic biological nitrogen fixation (SNF) starts (Rascio and La Rocca 2013; Dicenzo et al. 2019). These pleomorphic bacteria, called bacteroids, carry out the expensive reduction of atmospheric N_2 to ammonium, which is exported to the plant cell, in an exchange of carbon compounds supplied from the photosynthesis of the plant cells. This photosynthate is metabolized by the bacteroid to sustain the SNF (Rascio and La Rocca 2013). Rhizobial inoculants are inexpensive alternatives to environmentally polluting industrial nitrogen fertilizers, with significant impacts on the livelihood of the community. Replacing the use of chemical fertilizers with SNF is a relevant strategy against global warming, favoring sustainable agriculture for the production of grains for human consumption, feed and pasture species (Oldroyd et al. 2011; Ferguson et al. 2019). Proteomic studies on symbiosis have been reported (Larrainzar and Wienkoop 2017; Lardi and Pessi 2018; Liu et al. 2018; Khatabi et al. 2019) and a search for binding sites (motifs) of transcriptional regulators (TFs; Fischer 1994; Tsoy et al. 2016; Rutten and Poole 2019). Now, the first study on O_2-dependent regulation of the SNF by extending known motifs by bioinformatic methods was performed to establish a regulatory network of proteins and global TFs considering 50 genomes of the Alphaproteobacteria by extending known motifs recognized by the TFs based on a phylogenetic footprinting approach, i.e., the *nifA-rpoN* regulon of nitrogen fixation in the Alphaproteobacteria group was searched, and the deduced matrix from the motifs of the TFs inferred with a strict *p*-value was used to scan with the Run profile tool in the Regpredict site (Novichkov et al. 2010). Using the same *p*-value to search for additional regulon members, 95 operons with potential NifA-binding sites comprising 280 genes were found in Alphaproteobacteria (Tsoy et al. 2016). The NifA-RpoN regulon of *R. etli* CFN42 was determined experimentally and with bioinformatic methods; it consisted of 120 genes, which indicates that the aforementioned study of the NifA regulon in Alphaproteobacteria is highly conservative, highlighting that genes not directly related to nitrogen fixation were found (Salazar et al. 2010), as was also observed (Tsoy et al. 2016). Based on the biological functions resulting from protein interactions, the symbiosis interactome of *Sinorhizobium meliloti* with its host plants was proposed by computational methods, which is composed of 440 proteins involved in 1041 unique interactions (Rodriguez-Llorente et al. 2009).

These data show that the symbiotic nitrogen fixation regulatory circuitry is suspected to be complex. Most of the symbiotic stage protein profiles in the cited literature include TFs (see above), but efforts are needed to infer the genetic circuitry between TFs and the proteins for each profile. We need to take advantage of the co-expression of TFs with potential target proteins in a proteomic profile due to the enrichment of common motif sites involved in the transcriptional regulation of these genes (Van Helden et al. 1998; McGuire et al. 2000; Aerts et al. 2003; Ihuegbu et al. 2012), considering autoregulation of the TFs and that they are involved in the transcriptional regulation of proteins of their respective profile.

We recently constructed the RhizoBindingSites database[1] (Taboada-Castro et al. 2020), a DNA-motif site collection based on the inferred motifs from each gene recognizing a site in its own promoter region, covering nine representative genomes of the taxon Rhizobiales. This algorithm aligns all the upstream regions of the orthologous genes per gene per genome to search for pairs or conserved position-specific trinucleotides (dyads) to define the motifs (Defrance et al. 2008). These dyads represented in a position-specific scoring matrix (PSSM; Hertz et al. 1990) were used to scan all the genes of a respective genome. These output data per gene per genome were fractionated at low, medium, and high stringency of *p*-value ranges. These data are used to match protein profiles from experimental or theoretical data to predict transcriptional regulatory networks at the desired *p*-value, or using the "auto" option, in which in each round the algorithm selects the data with the lowest *p*-value (high stringency) by searching from the highly strict to low strict data in the proper genome, assuring the output data are with the highly strict *p*-value as possible (Taboada-Castro et al. 2020). This database contains from one to five conserved motifs represented in matrices per

1 http://rhizobindingsites.ccg.unam.mx/ (accessed September 8, 2022).

gene that have different significance. At the moment, it is not clear which motifs conserved in a gene are directly involved in the recognition of the ARN polymerase and which *p*-value corresponds to the biological action of the TF. The lowest *p*-values are generally used (Tsoy et al. 2016). Inferred data on transcriptional regulation in the SNF are important to accelerate experiments on transcriptional regulation to define TF gene targets, which are basic components of a regulatory network (Resendis-Antonio et al. 2005, 2012; Tsoy et al. 2016).

For *R. etli* CFN42, a systems biology of the metabolic activity during SNF integrating proteome and transcriptome data was used, i.e., 415 proteins and 689 upregulated genes, respectively. From this, 292 unique proteins were identified. This constraint-based model was used to simulate metabolic activity during SNF, and 76.83% of enzymes were justified. The metabolic pathways sustaining SNF activity were discussed compared with aerobic growth in succinate ammonium minimal medium (MM; Resendis-Antonio et al. 2011).

In this work, the study of the SNF proteome of *R. etli* CFN42 was revised with the same experimental conditions (Resendis-Antonio et al. 2011), comparing the aerobic growth at 6 h in MM and the symbiosis at 18 days post-inoculation (dpi). A total of 1730 proteins were identified in MM and 730 in bacteroids; compared to the first report (Resendis-Antonio et al. 2011), it contains 2.5 times more proteins identified in symbiosis. Similar pathways supporting the SNF and a role of the different genome compartments were identified, and new pathways related to adaptation to environmental conditions were described. A new study of the vicinity of the genes expressed in the genome of *R. etli* CFN42 showed specific zones for growth in MM and bacteroid. The chromosome has more genes for growth in MM than in bacteroid, which were more scattered, while for the SNF, the symbiotic plasmid d (p42d) has more genes than for growth in MM. The MM and bacteroid proteome profiles included 127 and 62 TFs, respectively. A potential transcriptional regulatory network for MM and bacteroid was constructed using the RhizoBindingSites database and the prediction of regulatory network approach with the auto option, proposing on average 87% of TF gen-target relationships with *p*-values ranging from 1.0e-5 to 1.0e-20, which represents a strict criterion.

Assuming that the TFs in MM and bacteroid profiles are involved in the transcription of their corresponding protein profile, a bioinformatic study with conserved motifs of TFs was used to establish a TF gen-target relationship, and a transcriptional regulatory network for MM and bacteroid was proposed.

Materials and methods

Culture of *Rhizobium etli* CFN42 strain

The *R. etli* CFN42 strain was grown in minimal medium with ammonium chloride and succinic acid as previously reported (Taboada et al. 2018), it was cultured for 6 h, and the cells were pelleted by centrifugation at 7,500 × *g* at 5°C, for 5 min.

Plant inoculation with *Rhizobium etli* CFN42

The *Phaseolus vulgaris* bean seeds were surface sterilized and placed on 0.8% agar in Petri dishes (Wacek and Brill 1976). Each seed was inoculated with 10^5 *R. etli* cells previously washed with sterilized distilled water after growing in a peptone-yeast-rich medium as described (Encarnación et al. 1995); after 18 days post-inoculation, the bacteroid were extracted on a percoll gradient as described (Romanov et al. 1994).

Sample preparation

The cell pellets from both free-living bacteria and bacteroid were lysed in a solution containing 7 M urea, 2% CHAPS, 1 mM DTT in 50 mM Tris–HCl pH 8. Cells were resuspended in the lysis buffer and sonicated on the ice for 15 microns. Samples were incubated with an additional 20 mM DTT for 30 min at 40°C to completely reduce disulfide bridges. Cysteine residues were alkylated with 50 mM IAA for 30 min at room temperature in darkness. After centrifugation, the proteins were collected in the supernatant. Proteins were precipitated overnight with cold ethanol (9 volumes) and washed with a 90% ethanol solution.

The precipitate was dissolved in sodium deoxycholate SDC 0.5%, SDS 0.5%, in 100 mM triethylammonium bicarbonate buffer (TEAB). Proteins were submitted to a chemical acetylation reaction of all lysine residues as previously described (Gil et al. 2017; Gil and Encarnación-Guevara 2022). Fully acetylated proteins were dissolved in AmBiC 50 mM, SDC 0.5%, and digested by adding trypsin to a ratio of 1:50 (enzyme:protein), and the reaction was incubated for 16 h at 37°C. SDC was removed with ethyl acetate acidified with trifluoroacetic acid (TFA) as previously reported (Gil et al. 2017; Gil and Encarnación-Guevara 2022). The peptide mixture was dried on a Speed-Vac and stored at −80°C until MS analysis.

LC–MS/MS and data analysis

Peptides were dissolved in 0.1% TFA in water and loaded on an RSLC nano UPLC system (Ultimate 3000, Dionex) coupled to a Q-Exactive high-resolution mass spectrometer (Thermo Fischer Scientific). The chromatographic conditions, as well as the MS acquisition parameters, were as previously described (Gil et al. 2017). The analysis was performed at the Proteomics Core Facility, Ecole Polytechnique Fédérale de Lausanne in Switzerland. The data presented in the study are deposited in the ProteomeXchange Consortium via the PRIDE repository

(Perez-Riverol et al. 2022), accession numbers PXD035204 and 10.6019/PXD035204.

Raw data were processed for peptide and protein identification/quantification using the MaxQuant platform. The database search parameters were as follows: Trypsin/R was selected as the digestion enzyme, up to two missed cleavages were allowed, carbamidomethylcysteine and acetylated lysine were set as fix modifications, and oxidized methionine was considered variable. The database used for protein identification was released in 2006 (González et al. 2006) and is publicly available through the UniProt repository. Three biological replicates of each condition were included in the study. Proteins and peptides were identified with an FDR of 1% based on the target-decoy strategy integrated in the software.

Statistical analysis

Only proteins identified with at least two peptides and one of these unique peptides and at least two intensity values in each condition were used for statistical analysis. The protein abundance was normalized, and missing values were imputed with the Random Forest method (missForest, R package; Stekhoven and Bühlmann 2012). The PCA was carried out on the protein intensity correlation matrix (FactoMiner, R package; Lê et al. 2008) to generate a protein abundance pattern for the cell lines. To determine whether any component could distinguish between the cell lines, the sample scores for each component were plotted. After finding the component, we identified the more correlated proteins in that component with discriminatory capacity using the square cosine of the correlation matrix between the components and the proteins (Abdi and Williams 2010). It is observed in the graphic, MM and bacteroid conditions were clustered separately but grouped by condition, recovering a great diversity of data, 64.8 and 19.3% of data for one and two dimensions, respectively, giving a total of 84.1% (Figure 1). A total of 1,730 and 735 proteins were significantly identified in the minimal medium and bacteroid, respectively. In addition, 322 proteins were without change in their expression.

Metabolic pathways analysis

Overrepresentation of pathways was performed online employing the Gene List Analysis tool on the PANTHER Classification System site.[2] Only proteins with an absolute value of association with a *p*-value equal or greater than 0.5 with data of the first two components (Abdi and Williams 2010) were selected for comparative overrepresentation analysis based on Gene Ontology (Ashburner et al. 2000). To obtain the GO terms significantly overrepresented in this experiment we used the hypergeometric test and only processes with a *p*-value less than 0.05 were selected. The presence of genes for each metabolic pathway was compared as percent respect of the background number of genes per pathway in MM and bacteroid profiles (Figures 3, 4).

Metabolic maps construction

For analysis of metabolic pathways in MM and bacteroid, and genes without changes in their expression, the Kegg mapper[3] was used (Kanehisa 2017). This mapper uses the KO Kegg Orthology, which is based on the function of the ortholog genes. The K identifiers for *R. etli* CFN42 were obtained for the entire genome with the application blastKOALA[4] (Kanehisa et al. 2016), the input was the sequences in FASTA format of the genes from *R. etli* CFN42 genome divided into two parts, then the *R. etli* CFN42 locus tag identifier was associated to the K identifiers, and a list including MM, bacteroid and with no change expression proteins was used in the Kegg mapper (Supplementery Table 2). Obtention of the EC number was from the KO Orthology application from Kegg[5] (Kanehisa et al. 2016).

Design of a regulatory network

The protein profiles of *R. etli* CFN42 grown in minimal medium (MM) at 6 h and of bacteroid isolated from nodules at 18 days post-inoculation of the bean plant *Phaseolus vulgaris*, were used to construct a transcriptional regulatory network with the application "Prediction of transcriptional regulatory networks" of the RhizoBindingSites database (Taboada-Castro et al. 2020). Briefly, this database contains predicted matrices deduced from conserved dyads (Defrance et al. 2008), composed of position-specific di or tri-nucleotides in the orthologs genes of each gene in members of the Rhizobiales taxon. These position-specific nucleotides were converted into a matrix format, which describes the conserved motifs for each gene (Hertz et al. 1990), the dyad analysis of the footprinting discovery algorithm deduced from one to five matrices per gene. The matrices of the TF's were used to scan with a matrix-scan RSAT analysis (Nguyen et al. 2018), all the upstream regulatory sequences of the genes, establishing TF gene-target relationships data, which is in the motif information window of the RhizoBindingSites database (Taboada-Castro et al. 2020; RhizoBindingSites database user guide), this information is used in the "Prediction of a transcriptional regulatory network" application.

2 http://www.pantherdb.org/ (accessed September 8, 2022).

3 https://www.genome.jp/kegg/tool/map_pathway.html (accessed September 8, 2022).

4 https://www.kegg.jp/blastkoala/ (accessed September 8, 2022).

5 https://www.genome.jp/kegg/ko.html (accessed September 8, 2022).

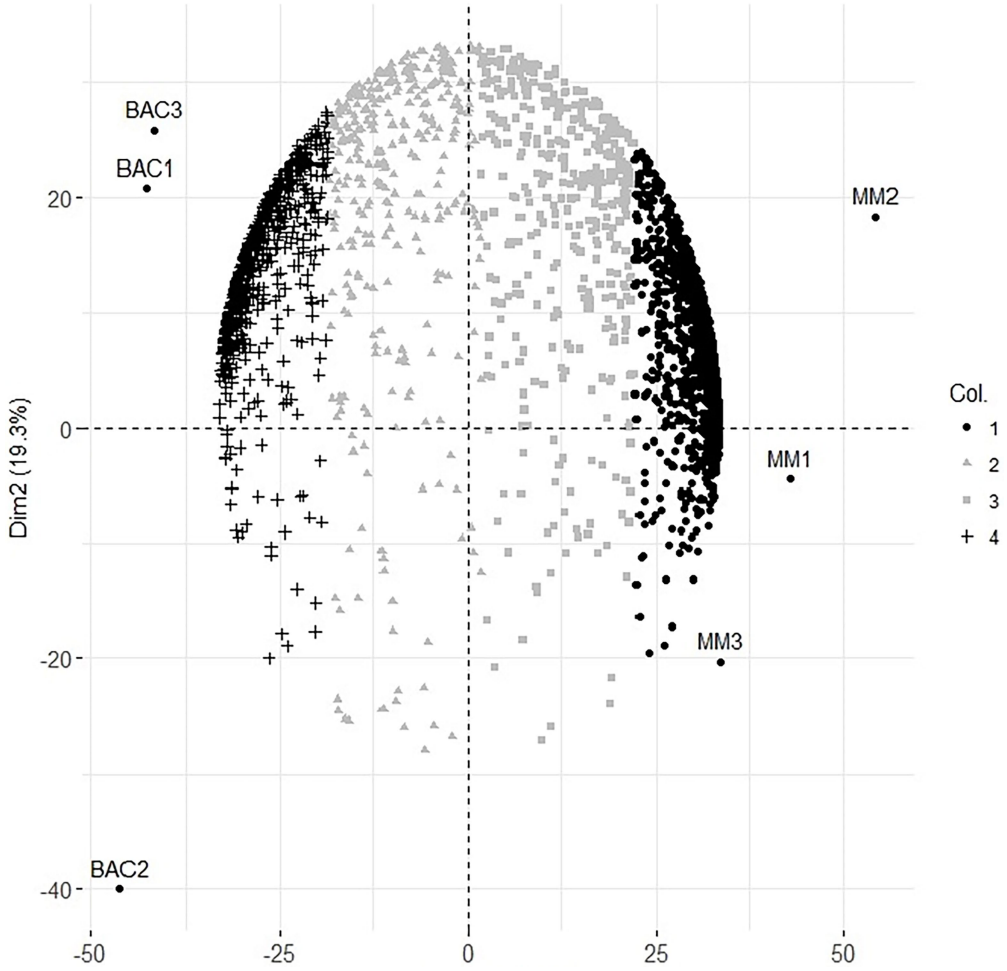

FIGURE 1
Principal component analysis of protein expression at 6 h of minimal medium growth MM1, MM2, MM3 and 18days post inoculation Bacteroids of the symbiosis from *Rhizobium etli* CFN42 with the plant Phaseolus vulgaris Bac1, Bac2, Bac3 biological replicates.

For the prediction of transcriptional regulatory networks, a three-step method was implemented. The first step consisted in to construct networks with the MM protein profile including the 127 co-expressed TF´s. As well as, the bacteroid protein profile with the 62 co-expressed TFs, with the application "Prediction of the transcriptional regulatory network" from the RhizoBindingSites database, with the "auto" option. This step, is to eliminate the genes of the proteins not recognized by any TF, and TF's whose matrices had no homology with any upstream regulatory sequences of potential target genes. With the option "auto". With this option, the application searches for TF gene-target relationships for each of the TF's co-expressed with the entered genes by looking into the motif information data from the RhizoBindingSites database. Only 1,336 genes, including 107 TF's genes from MM (Supplementary Table 1A) and 583 genes including, 50 TF's co-expressed bacteroid genes (Supplementary Table 1B), respectively, were found with a relationship, giving rise to hypothetical regulons available (Supplementary Tables 1A, B). The TF-matrices may have homology with the upstream regulatory sequences of target genes three levels of stringency, low stringency (*p*-value from 1.0e-4 to 9.9e-4), medium stringency level (*p*-value 1.0e-5 to 9.9e-5) or highly strict (from the *p*-value 1.0e-6 to lower *p*-values). In the second step, a matrix- clustering analysis for each condition, with the matrices of the 1336 genes of MM, as well as, the matrices of the 583 bacteroid genes including their respective TF´s was done (Castro-Mondragon et al. 2017). This step is to eliminate false-positive data as possibly, since the motifs are short conserved functionally compromised sequences (Ihuegbu et al. 2012), to avoid possible TF gene-target relationships by chance. In this analysis, the matrix of a TF should be grouped by homology with the nucleotide sequence of matrices of the potential target genes. Matrix-clustering algorithm creates the file clusters_motif_names.tab, which is edited to obtain all the genes whose matrices were clustered containing at least two different genes. Only the clusters, including matrices of a TF or TFs (Clustered-TF) were selected from MM (Supplementary Table 1C) and bacteroid profiles (Supplementary Table 1D), the NCBI genomic information of the

genes was added to these tables as well as the Clustered-TF for each cluster (column headed "Clustered-TF" Supplementary Tables 1C, D). An alignment of MM and bacteroid matrices from matrix-clustering showed how much conserved are motifs in the clusters (Supplementary Tables 1E, F, respectively). The matrices were grouped into 207 and 92 clusters for MM and bacteroid, respectively. In this second step, additional depuration of genes after a matrix-clustering analysis was observed since only 655 genes, including 93 TF's genes from MM, and 247 genes, including 46 TF's genes, were clustered. A TF gen-target relationship with only genes of a clusters was confirmed (Results and discussion, Appendix G and H). In the third step, second networks were constructed (as in the first step) only with clustered-TF genes, called "Clustered-TF-MM" and "Clustered-TF-BACTEROID" (Figure 5). and cluster_97 and cluster_112 from bacteroid were chosen. For cluster_34, all the genes had a TF gene-target relationship. For cluster_195, 22 out of 27 genes were connected (Supplementary Table 1G). For cluster_97, 21 of 26 genes were connected and for cluster_112, 21 from 22 genes were connected (Supplementary Table 1H). It is worth noticing that, after the matrix-clustering grouping genes, all the genes for each condition had one or more relationships. Quality of MM, bacteroid, clustered-TF-MM and Clustered-TF-BACTEROID networks were analyzed (Results and discussion, Figure 5). Then, the transcriptional regulatory networks of MM and bacteroid protein profiles are constructed with motifs interspecies conserved.

These data confirmed that clustered matrices of genes are strongly related to the structure of a network, and these genes probably represent hubs.

To search for expected transcriptional regulation for isoenzymes in MM and bacteroids, the tables of the transcriptional regulatory networks described above were ordered in decreasing order by the column headed "*p*-value" (Supplementary Tables 1A, B). These tables were identified in the right column with the condition they pertain giving rise to new files ordered from MM and bacteroid and Clustered-TF-MM and Clustered-TF-BACTEROID separately. A Supplementary Table 1I containing the "K" number with a *R. etli* CFN42 locus tag identifier and the pertaining physiological condition per row was constructed. Then, the table from Supplementary Table 1I was paired with new files from the MM and bacteroid and Clustered-TF-MM and Clustered-TF-BACTEROID aforementioned. A new file with three groups of columns was produced; the first group contains information on the expected regulation with information from MM and bacteroid networks (with columns; Condition, Locus tag, K number, Upstream_region, Matrix_ID, Chain, End_motif, Start_motif, Site, Weight, *p*-value, and Significance). The second group of columns contains information of the expected transcriptional regulation with information from the Clustered-TF-MM and Clustered-TF-BACTEROID with columns headed as the MM and bacteroid data. The third group of columns contains information of the enzymatic function of the K numbers headed as; Condition, Locus tag, K number, Compartment, locus name, COG number, COG group, Function from KO orthology, and Function from NBCI. To look for the expected transcriptional regulation for the same K number with different locus tag in MM and bacteroid, it was located in the column "Matrix_ID" with a format "RHE_RS13345_m5," which means the TF is RHE_RS13345 and "_m5" means the matrix number "5" of the TF (as was mentioned, a TF has one to five matrices; Supplementary Table 4).

Properties of networks

The most recent *E. coli* and *B. subtilis* "strong" evidence networks were retrieved from Abasy Atlas v2.2 (Escorcia-Rodríguez et al. 2020). Both networks only include regulatory interactions supported by experiments showing a direct interaction between the transcription factor and the upstream region of the target gene. We contrasted the inferred networks with the *E. coli* and *B. subtilis* curated networks as a positive control, and 1000 Erdös-Rényi random networks parametrized having the same number of nodes and edges as the corresponding biological networks as a negative control.

We computed several global structural properties for regulatory networks. Namely, regulators ($k_{out} > 0$), self-regulations, maximum out-connectivity, giant component size, network density, feedforward circuits, complex feedforward circuits, 3-Feedback loops, average shortest path length, network diameter, average clustering coefficient, adjusted coefficient of determination (R^2_{adj}) of $P(k)$, and R^2_{adj} of $C(k)$. Regulators, self-regulations, maximum out-connectivity, and giant component size were normalized by the number of nodes in the network. The density was included as the product of the network density and the fraction of regulators. Network diameter was normalized by (number of nodes – 2; as if no shortcuts would exist). 3-feedback loops, feedforward loops, and complex feedforward loops were normalized by the number of potential motifs in the network, defined as:

$$\frac{n!}{(n-r)!}\left(\frac{TF_n}{n}\right)^{TF_m}$$

Where n is the number of nodes in the network, r is the number of nodes in the motif ($r = 3$), TF_n is the number of TFs in the network, and TF_m is the number of TFs required for each motif type ($TF_m = 3$ for 3-feedback loops, and $TF_m = 2$ for feedforward and complex feedforward loops). We scaled the values of each property vector across networks to the range between 0 and 1, inclusively. Then, we clustered networks and properties using Ward's method. Further, we used pairwise Pearson correlation for the network property profiles and clustered the networks according to the Euclidean distance using Ward's method.

Hierarchy reconstruction of networks

First, we removed all the structural genes (nodes having $k_{out} = 0$) and their interactions from the network. Next, we classified each network edge (a, b) as 'top-down' if $k_a^{out} > k_b^{out}$ (where k_n^{out} is the out-connectivity of node *n*), otherwise, it was classified as 'bottom-up'. Then, we removed all the 'bottom-up' edges from the network. This step removed the feedback circuits present in the network, transforming it into a directed acyclic graph. Then we applied a modified topological sorting algorithm that returned the list of layers composing the hierarchy, where each node in a layer only can regulate nodes in lower layers. As the number of 'bottom-up' edges is low (<5% in average), our strategy maintains the global structure of the network to reveal the hierarchy. Besides structural nodes, no other nodes are removed, and 'bottom-up' edges can be added back to the hierarchy to reveal the feedback among layers and reconstruct the original network.

Results and discussion

In a previous study, we identified 292 proteins of the symbiotic state at 18 days post-inoculation (Resendis-Antonio et al. 2011); now, we discuss new data covering 2.5 times more proteins from symbiosis in this work. Principal components (one and two) covered 84.1% of the total initial data (Figure 1). The update of the *R. etli* CFN42-*Phaseolus vulgaris* bean plant symbiosis is with 1,730, 738, and 323 protein profiles for MM, bacteroid, and without no change in their expression, respectively (see below). There were 39.7% of common proteins in the bacteroid between the previous report (Resendis-Antonio et al. 2011) and this study. The low coverage observed in the new data may be due to the great diversity of different experiments collected for the last study. While in the new data, the variation in the experimental condition was from only two biological replicates, because our interest was to take advantage of the TF and non-TF protein co-expression (Galán-Vásquez and Perez-Rueda 2019), under the assumption that these TFs were involved in the transcriptional regulation of these proteins, to establish a TF gene–target relationship, only new data are considered in this analysis, and our previous data are considered only for discussion.

Compartmentation of proteins in MM and bacteroid

Rhizobium etli CFN42 contains six plasmids and a chromosome (González et al. 2003). An analysis of gene location from MM and bacteroid showed that for MM proteins, most of the genes are codified in the chromosome, while for bacteroid proteins, higher participation was found for plasmids p42b, p42d, p42e, p42f than in MM (Figure 2). Of note, the symbiotic plasmid (p42d) had a 5.3% higher participation in bacteroids than in MM, in line with a wide transcription rate of the symbiotic plasmid (psym) genes of *R. etli* CFN42 under microaerobic conditions (as in symbiosis) or in aerobic conditions in the presence of genistein (Valderrama et al. 1996). Additionally, many of the genes expressed in MM (78.7%) and bacteroid (67.1%) were from the chromosome, while 21 and 32% of the expressed genes were from plasmids, respectively. The higher number of genes expressed from the chromosome agrees with the finding that exponential growth in MM and nitrogen fixation activity have in common a great demand for energy synthesis, and most of the metabolic pathways for this process are similar (see below). One of the exceptional differences is that in symbiosis, the high-affinity *cbb3* cytochrome oxidase terminal is expressed (Delgado et al. 1998; Lopez et al. 2001). *Rhizobium leguminosarum* bv. *viciae* UMP791 contain five plasmids and a chromosome, similar to *R. etli* CFN42, which contains six plasmids. A proteome analysis of *R. leguminosarum* bacteroid with its host plant *Pisum sativum* showed that most of the bacteroid proteins were from the chromosome (81.6%), showing a lower participation of the plasmids than with the *R. etli* CFN42 strain (Durán et al. 2020).

The plasmids contain essential genes for growth in MM, such as p42e (*minCDE*; Landeta et al. 2011) and plasmid p42f (*panCB*; Villaseñor et al. 2011). Moreover, a cured *R. etli* CFN42 of p42f complemented with the *panCB* genes did not restore wild-type growth, meaning that p42f has unidentified genes that are important for growth in MM (Villaseñor et al. 2011).

Metabolic pathways

A detailed view of the pathways that operate in exponential growth in MM (ammonium-succinate) and bacteroid, a non-growing state in symbiosis at 18 days post-inoculation, with a maximal peak of nitrogen fixation, showed 105 pathways according to the KEEG program with Gen Ontology (GO) gene off classification (see "Materials and Methods" section; Maere et al. 2005; Figure 3). In MM, 31 representative metabolic pathways with greater or equal to 30% of genes, and in bacteroid, 10 pathways with greater or equal to 20% of genes per pathway with respect to the genome content were found (Figure 3), which is related to the high demand for the synthesis of metabolites to sustain growth in a minimal medium compared to the non-growing bacteroid state. In contrast, in symbiosis, most of the energy for the synthesis of metabolites is dedicated to nitrogen fixation. In agreement with this, carbon metabolism, including synthesis of amino acids, sugars, purine and pyrimidine, sulfur metabolism, glycolysis-gluconeogenesis, pyruvate metabolism, TCA cycle, oxidative phosphorylation, nitrogen metabolism, fatty acid metabolism, nicotinate and nicotinamide, vitamin synthesis, DNA replication, aminoacyl-tRNA biosynthesis, ribosome synthesis, protein export, and flagellar assembly, had a higher percentage of genes in MM than in bacteroids (Resendis-Antonio et al. 2011), as was shown in a comparative proteomic study of a free-living aerobic condition and the symbiosis of the *Bradyrhizobium japonicum* USDA110 strain (Sarma and Emerich

2005, 2006). Some other pathways, such as histidine metabolism, glutathione metabolism, pentose phosphate pathway, beta-alanine, starch, and sucrose metabolism, were similar in MM and bacteroids; likely, histidine metabolism is necessary for the synthesis of inosine monophosphate, a precursor for the synthesis of purines and subsequently for the synthesis of allantoin and allantoic acids. These nitrogen compounds from nitrogen fixation are exported to the bean plant *Phaseolus vulgaris* by the *R. etli* CFN42 bacteroid (Alamillo et al. 2010; Collier and Tegeder 2012). Glutathione plays a crucial role against oxidative damage during the establishment of symbiosis (Hérouart et al. 2002); it is a precursor for cysteine synthesis, a sulfur donor for the synthesis of the Fe-S centers involved in defense against oxidative stress and in the prosthetic groups of sensory proteins. The pentose phosphate pathway is essential for the synthesis of phosphoribosyl pyrophosphate (PRPP), a precursor for purine synthesis during symbiosis (Newman et al. 1994; Miranda-Ríos et al. 1997). Beta-alanine is a precursor for the synthesis of pantothenate, which is essential for the ubiquitous compound coenzyme A (coA), subsequently used for many metabolic reactions, including phospholipid synthesis, fatty acid synthesis and degradation, and the tricarboxylic acid cycle. The *panCB* genes for the synthesis of pantothenate codified in p42f from the *R. etli* CFN42 strain were characterized (Villaseñor et al. 2011). Starch and sucrose synthesis was not detected in free-living or symbiotic conditions of *R. etli* CFN42. For the synthesis and degradation of ketone bodies, phosphonate and phosphinate metabolism were higher in bacteroids than in MM. *R. etli* CFN42 synthesizes poly-β-hydroxybutyrate granules during symbiosis with *P. vulgaris*; because this polymer is a reserve of carbon and reducing power, its accumulation is greater in symbiosis than in MM, where the energy is for supporting growth (Cevallos et al. 1996). Additionally, there is a high demand for phosphate in nitrogen-fixing nodules; it is an essential macronutrient necessary for the synthesis of proteins and nucleic acids (Liu et al. 2018), and phosphate is probably limited during symbiosis. As a response, the transcription of this pathway is raised, as was shown for bacteroids harvested from soybeans grown under field conditions (Delmotte et al. 2010). A detailed study with transcriptomic and proteomic technologies of the symbiosis compared with the aerobic growth showed 3,587 genes/proteins, expressing 43% of the predicted genome from *B. japonicum* (Delmotte et al. 2010), 807 proteins were identified in symbiosis; while in this study, 738 proteins were identified; i.e., in this study, there is a great proteomic coverage of the symbiosis *R. etli* CFN42-*Phaseolus vulgaris* bean plant considering that the *B japonicum* genome size is bigger than the *R. etli* genome. Although *R. etli* is a fast grower and *B. japonicum* is a slow grower in minimal medium, they elicit determinate nodules. In contrast to the symbiont *S. meliloti* with their host *Medicago sativa* alfalfa plant that induces indeterminate nodules, there are notable differences between the structure and composition of the symbiont in determinate and indeterminate nodules, reviewed in (Rascio and La Rocca 2013). Although *B. japonicum* and *R. etli* symbiosis occur in temperate and tropical

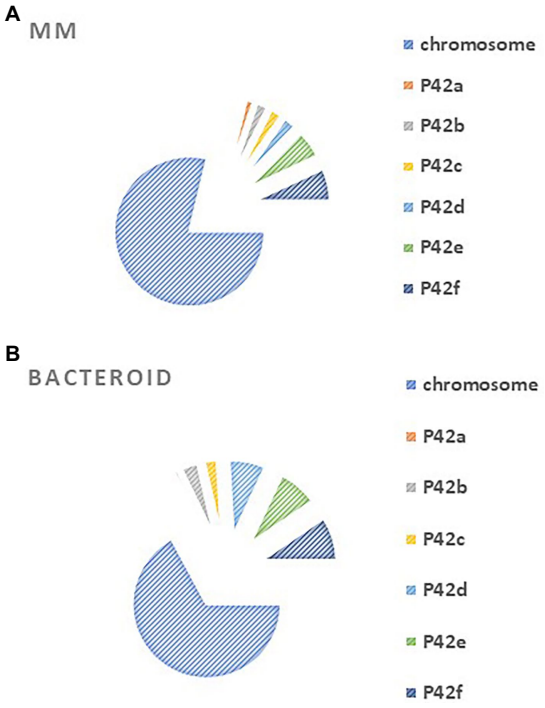

FIGURE 2
Compartmentation of **(A)** minimal medium protein profile expressed at six hours of growth in minimal medium and **(B)** 18 days post inoculation of bacteroid protein profile from *Rhizobium etli* CFN42.

weather, respectively, despite these differences, *R. etli* and *B. japonicum* symbiosis is more similar than *S. meliloti* symbiosis. A proteomic comparison of free-living and symbiosis from *B. japonicum* showed a greater number of proteases in free life than in symbiosis (Sarma and Emerich 2006). Similarly, in this study, 27 and two proteases were expressed. Most likely, the recycling of metabolites may be one of the factors that impacts the spending of energy in free life and symbiosis. It was suggested that bacteroids expend their energy judiciously between protein synthesis and nitrogen fixation by altering protein turnover (Sarma and Emerich 2006).

Environmental metabolism

Moreover, some GO genes classified for the metabolism of environmental compounds were mapped; in MM, these genes covered approximately 39% of genes, while in bacteroids, they covered 14% with respect to the genome content (microbial metabolism in diverse environments, Figure 4). For some pathways, there is a low representation with respect to the total content of the *R. etli* CFN42 genome. The pathways for the degradation of benzoate, caprolactam, and naphthalene were more highly expressed in MM than in bacteroids. For chloroalkane and chloroalkene degradation and novobiocin biosynthesis, the

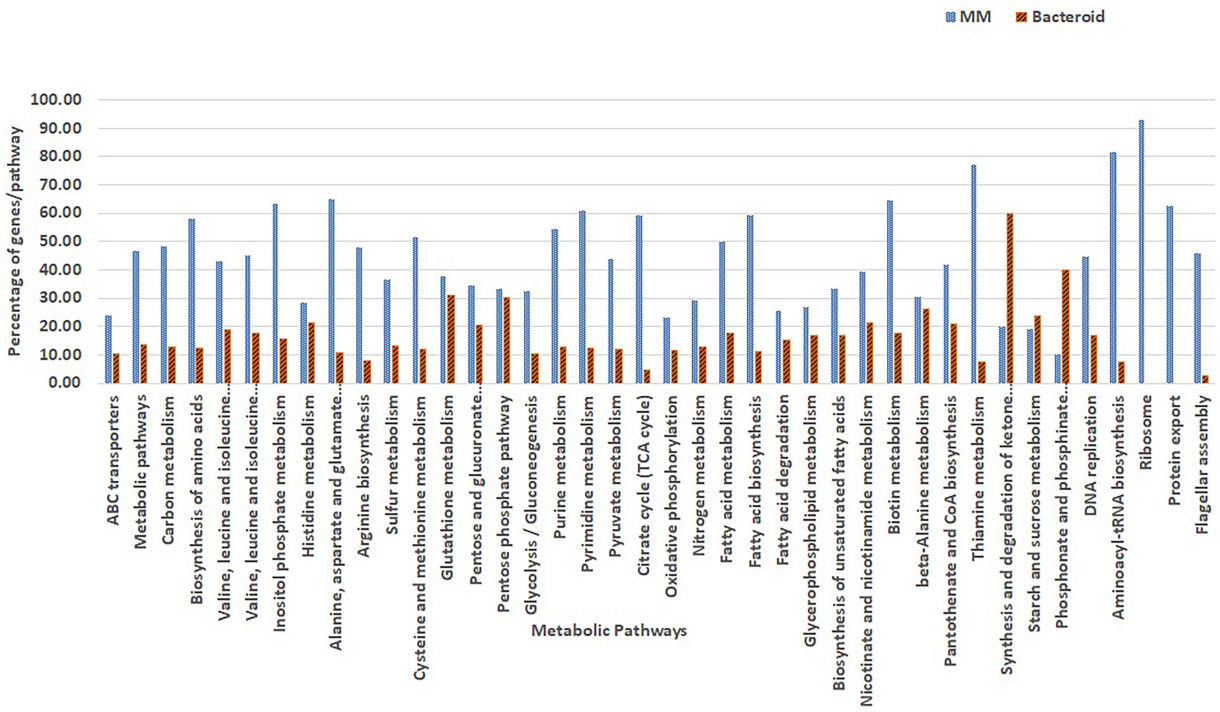

FIGURE 3
Comparison of GO classified proteins expressed per metabolic pathway in minimal medium and bacteroids from *Rhizobium etli* CFN42.

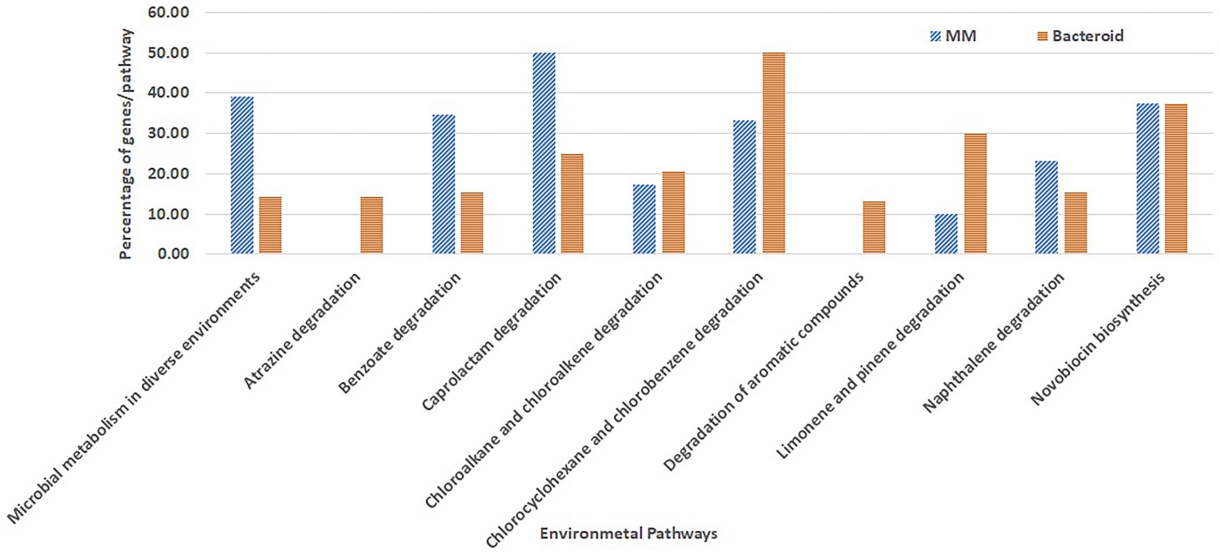

FIGURE 4
Metabolic pathways for biosynthesis and degradation of organic compounds environment related from *Rhizobium etli* CFN42.

number of proteins expressed was similar (Figure 4). Proteins for the degradation of chloroalkane and chloroalkene were also identified in a metagenomic analysis in the rhizosphere soil of a constructed wetland (Bai et al. 2014). Novobiocin is a very potent inhibitor of DNA gyrase, which works by targeting the GyrB subunit of the enzyme for energy transduction, and resistance to novobiocin of *Lotus rhizobia* was related to the effectiveness of the symbiosis with *Lotus pedunculatus* (Pankhurst 1977). For the degradation of atrazine, chlorocyclohexane and chlorobenzene, and aromatic compounds limonene and pinene, the number of

genes was higher in bacteroid than in MM. Atrazine is an herbicide that may inhibit the growth of *Rhizobium* species, *P. vulgaris-Rhizobium* sp. Consortium symbiosis has been used for the bioremediation of soil contaminated with atrazine (Madariaga-Navarrete et al. 2017). Genes for the degradation of the aromatic compounds chlorocyclohexane and chlorobenzene were also reported in the genome of *Burkholderia phenoliruptrix* BR3459a, a symbiont of the *Mimosa flocculosa* leguminous plant (Zuleta et al. 2014). It was observed that for the *Rhizobium leguminosarum* E20-8 strain, limonene and pinene have antioxidant activity promoting growth under stress provoked by cadmium (Sá et al. 2020) and antibacterial activity (Ghaffari et al. 2019). In the *B. japonicum* bacteroid proteome, the NrgC protein and a gene for phenazine biosynthesis were identified for a response against microbial attack (Sarma and Emerich 2005, 2006). These genes in MM and bacteroid for degradation of metabolites of the environment are used for a fast response, competence, and better adaptation in soil conditions. Unlike *B. japonicum* (Sarma and Emerich 2006), *R. etli* bacteroid showed a wide strategy to withstand environmental stresses.

Isoenzymes in MM and bacteroid

The KEEG mapper for visualization of the metabolic maps was used (see "Materials and Methods" section). This mapper uses the "K" number to identify the function of the gene, and it is assigned based on the orthology of the genes (Kanehisa et al. 2016). For an integral view of the metabolism in MM, bacteroid, and proteins present in both conditions with "no change" (Nch), genes were mapped (Supplementary Tables 2 and 3A). Discussion of the central metabolism involved 37 representative pathways. Analysis of mapped genes showed that for some enzymatic reactions, different genes for the same enzymatic step in MM and bacteroid were found, e.g., for the pentose phosphate pathway there were two genes for the conversion of D-ribulose phosphate to D-ribose-5P by the 6-phosphogluconate dehydrogenase enzyme; one is expressed in MM RHE_RS12615, and a different one was expressed in the bacteroid RHE_RS17825 (Table 1), suggesting the presence of a condition-dependent isoform (Supplementary Table 2 pathway 15, and Supplementary Table 3A). From here on, we will call it "multiplicity." The Fructose and mannose metabolism pathway (Supplementary Table 2 pathway 10, and Supplementary Table 3A), for the catalysis of L-fucose to L-fucolactone by the enzyme D-threo-aldose 1-dehydrogenase; the proteins in MM RHE_RS02500 and bacteroid RHE_RS28605 were expressed (Table 1), showing multiplicity. For the galactose metabolism pathway (Supplementary Table 2 pathway 11, and Supplementary Table 3A), the conversion of UDP-glucose to UDP-galactose, UDP-glucose 4-epimerase was synthesized in MM RHE_RS03845 and in bacteroid RHE_RS17845 was expressed. As well as, for the enzyme *dgoD*, galactonate dehydratase [EC:4.2.1.6] for catalysis of D-galactonate to 2-dehydro-3-deoxy-D-galactonate in MM the RHE_RS18905 and in bacteroid RHE_RS24515 proteins were expressed (Table 1), showing multiplicity for two different enzymes of the same pathway. These data showed that the same enzymatic reactions are performed in MM and bacteroids with distinct proteins, suggesting that some alternative proteins are specific for free-living aerobic conditions and others for symbiosis for the same metabolic step. The pyruvate metabolism pathway (Supplementary Table 2 pathway 18, and Supplementary Table 3A), for the conversion of acetyl-CoA to acetoacetyl-CoA in MM, RHE_RS23190 was expressed, while in bacteroid, two different genes were expressed; RHE_RS02820 and RHE_RS20545 which showed differences in metabolism from MM and in bacteroid (Table 1), and since distinct TFs were identified in MM and bacteroid, a different transcriptional regulation for isoenzymes was analyzed (see below). Moreover, for the inositol phosphate pathway (Supplementary Table 2 pathway 2, and Supplementary Table 3A), for the myo-inositol-1(or 4)-monophosphatase enzyme in MM was identified the RHE_RS10865, RHE_RS17960, and RHE_RS22570 enzymes, and in bacteroid RHE_RS22680 and RHE_RS04240 were found (Table 1), again showing that the metabolism in symbiosis compared with MM has some differences. For valine, leucine, and isoleucine biosynthesis pathway (Supplementary Table 2 pathway 6, and Supplementary Table 3A), the enzyme *ilvD*, dihydroxy-acid dehydratase [EC:4.2.1.9], and the RHE_RS08720 and RHE_RS23070 proteins were expressed in MM and bacteroid, respectively, supporting multiplicity (Table 1). Similarly, for valine, leucine, and isoleucine degradation (Supplementary Table 2 pathway 7, and Supplementary Table 3A), the enzyme *acd* acyl-CoA dehydrogenase [EC:1.3.8.7] RHE_RS20670 was expressed in MM and in bacteroid, the isoenzyme RHE_RS04555 was identified (Table 1). Additionally, for the enzyme *atoB*, acetyl-CoA C-acetyltransferase [EC:2.3.1.9] in MM the RHE_RS23190 was present, and in bacteroids, the isoenzymes RHE_RS02820 and RHE_RS20545 were found (Table 1), showing a multigenic strategy for the degradation of branched-chain amino acids. For the synthesis of the poly-β-hydroxybutyrate polymer, the enzyme β-ketothiolase (acetyl-CoA C-acetyltransferase) converts two molecules of acetyl-CoA to acetoacetyl-CoA. In MM, the enzyme RHE_RS23190 was detected, and in bacteroid, two enzymes, RHE_RS02820 and RHE_RS20545, were identified (Table 1).

The ABC components of the sugar transporters were present in MM and bacteroid; i.e., maltose/maltodextrin, galactose, raffinose/stachyose/melibiose, lactose/L-arabinose, sorbitol/mannitol, trehalose/maltose, cellobiose, chitobiose, arabinooligosaccharide. In bacteroids, for monosaccharide transporters, glucose, ribose, galactofuranose, and myo-inositol 1-phosphate were identified, while D-xylose, fructose, rhamnose, myo-inositol, and glycerol were identified in MM (Supplementary Table 2 pathway 37).

The multiplicity of ABC transporters was for seven K numbers (Supplementary Table 3A); for *afuA*, *fbpA*; iron(III) transport system substrate-binding protein; in MM,

TABLE 1 Isoenzymes in MM and bacteroid from *Rhizobium etli* CFN42.

K number	Physiological condition	Locus tag	Annotation from BlastKoala*
K02035	MM	RHE_RS10550	ABC.PE.S; peptide/nickel transport system substrate-binding protein
K02035	MM	RHE_RS20405	ABC.PE.S; peptide/nickel transport system substrate-binding protein
K02035	MM	RHE_RS22160	ABC.PE.S; peptide/nickel transport system substrate-binding protein
K02035	MM	RHE_RS23500	ABC.PE.S; peptide/nickel transport system substrate-binding protein
K02035	MM	RHE_RS23525	ABC.PE.S; peptide/nickel transport system substrate-binding protein
K02035	MM	RHE_RS24485	ABC.PE.S; peptide/nickel transport system substrate-binding protein
K02035	MM	RHE_RS27640	ABC.PE.S; peptide/nickel transport system substrate-binding protein
K02035	MM	RHE_RS27665	ABC.PE.S; peptide/nickel transport system substrate-binding protein
K02035	MM	RHE_RS03080	ABC.PE.S; peptide/nickel transport system substrate-binding protein
K02035	Bacteroid	RHE_RS10750	ABC.PE.S; peptide/nickel transport system substrate-binding protein
K02035	Bacteroid	RHE_RS22645	ABC.PE.S; peptide/nickel transport system substrate-binding protein
K02035	Bacteroid	RHE_RS28255	ABC.PE.S; peptide/nickel transport system substrate-binding protein
K02035	Bacteroid	RHE_RS01120	ABC.PE.S; peptide/nickel transport system substrate-binding protein
K02052	MM	RHE_RS17470	ABC.SP.A; putative spermidine/putrescine transport system ATP-binding protein
K02052	Bacteroid	RHE_RS14790	ABC.SP.A; putative spermidine/putrescine transport system ATP-binding protein
K02052	Bacteroid	RHE_RS14870	ABC.SP.A; putative spermidine/putrescine transport system ATP-binding protein
K00249	MM	RHE_RS20670	ACADM, acd; acyl-CoA dehydrogenase [EC:1.3.8.7]
K00249	Bacteroid	RHE_RS04555	ACADM, acd; acyl-CoA dehydrogenase [EC:1.3.8.7]
K00626	MM	RHE_RS23190	ACAT, atoB; acetyl-CoA C-acetyltransferase [EC:2.3.1.9]
K00626	Bacteroid	RHE_RS20545	ACAT, atoB; acetyl-CoA C-acetyltransferase [EC:2.3.1.9]
K00626	Bacteroid	RHE_RS02820	ACAT, atoB; acetyl-CoA C-acetyltransferase [EC:2.3.1.9]
K01486	MM	RHE_RS17480	ade; adenine deaminase [EC:3.5.4.2]
K01486	Bacteroid	RHE_RS15825	ade; adenine deaminase [EC:3.5.4.2]
K02012	MM	RHE_RS10880	afuA, fbpA; iron(III) transport system substrate-binding protein
K02012	Bacteroid	RHE_RS13955	afuA, fbpA; iron(III) transport system substrate-binding protein
K00759	MM	RHE_RS15525	APRT, apt; adenine phosphoribosyltransferase [EC:2.4.2.7]
K00759	Bacteroid	RHE_RS31115	APRT, apt; adenine phosphoribosyltransferase [EC:2.4.2.7]
K05349	MM	RHE_RS28885	bglX; beta-glucosidase [EC:3.2.1.21]
K05349	Bacteroid	RHE_RS29645	bglX; beta-glucosidase [EC:3.2.1.21]
K01255	MM	RHE_RS01080	CARP, pepA; leucyl aminopeptidase [EC:3.4.11.1]
K01255	Bacteroid	RHE_RS07430	CARP, pepA; leucyl aminopeptidase [EC:3.4.11.1]
K00405	MM	RHE_RS29065	ccoO; cytochrome c oxidase cbb3-type subunit II
K00405	Bacteroid	RHE_RS30885	ccoO; cytochrome c oxidase cbb3-type subunit II
K03412	MM	RHE_RS03250	cheB; two-component system, chemotaxis family, protein-glutamate methylesterase/glutaminase [EC:3.1.1.61 3.5.1.44]
K03412	Bacteroid	RHE_RS26805	cheB; two-component system, chemotaxis family, protein-glutamate methylesterase/glutaminase [EC:3.1.1.61 3.5.1.44]
K03412	Bacteroid	RHE_RS17965	cheB; two-component system, chemotaxis family, protein-glutamate methylesterase/glutaminase [EC:3.1.1.61 3.5.1.44]
K00390	MM	RHE_RS05785	cysH; phosphoadenosine phosphosulfate reductase [EC:1.8.4.8 1.8.4.10]
K00390	Bacteroid	RHE_RS05785	cysH; phosphoadenosine phosphosulfate reductase [EC:1.8.4.8 1.8.4.10]
K00285	MM	RHE_RS28700	dadA; D-amino-acid dehydrogenase [EC:1.4.5.1]
K00285	Bacteroid	RHE_RS03755	dadA; D-amino-acid dehydrogenase [EC:1.4.5.1]
K01714	MM	RHE_RS26910	dapA; 4-hydroxy-tetrahydrodipicolinate synthase [EC:4.3.3.7]
K01714	MM	RHE_RS27660	dapA; 4-hydroxy-tetrahydrodipicolinate synthase [EC:4.3.3.7]
K01714	MM	RHE_RS03065	dapA; 4-hydroxy-tetrahydrodipicolinate synthase [EC:4.3.3.7]
K01714	Bacteroid	RHE_RS07055	dapA; 4-hydroxy-tetrahydrodipicolinate synthase [EC:4.3.3.7]
K01714	Bacteroid	RHE_RS19830	dapA; 4-hydroxy-tetrahydrodipicolinate synthase [EC:4.3.3.7]
K01714	Bacteroid	RHE_RS22155	dapA; 4-hydroxy-tetrahydrodipicolinate synthase [EC:4.3.3.7]

(Continued)

TABLE 1 (Continued)

K number	Physiological condition	Locus tag	Annotation from BlastKoala*
K01714	Bacteroid	RHE_RS14280	dapA; 4-hydroxy-tetrahydrodipicolinate synthase [EC:4.3.3.7]
K02031	MM	RHE_RS24230	ddpD; peptide/nickel transport system ATP-binding protein
K02031	MM	RHE_RS24500	ddpD; peptide/nickel transport system ATP-binding protein
K02031	MM	RHE_RS25825	ddpD; peptide/nickel transport system ATP-binding protein
K02031	MM	RHE_RS27625	ddpD; peptide/nickel transport system ATP-binding protein
K02031	MM	RHE_RS20420	ddpD; peptide/nickel transport system ATP-binding protein
K02031	Bacteroid	RHE_RS28270	ddpD; peptide/nickel transport system ATP-binding protein
K01684	MM	RHE_RS18905	dgoD; galactonate dehydratase [EC:4.2.1.6]
K01684	Bacteroid	RHE_RS24515	dgoD; galactonate dehydratase [EC:4.2.1.6]
K00064	MM	RHE_RS02500	E1.1.1.122; D-threo-aldose 1-dehydrogenase [EC:1.1.1.122]
K00064	Bacteroid	RHE_RS28605	E1.1.1.122; D-threo-aldose 1-dehydrogenase [EC:1.1.1.122]
K01092	MM	RHE_RS17960	E3.1.3.25, IMPA, suhB; myo-inositol-1(or 4)-monophosphatase [EC:3.1.3.25]
K01092	MM	RHE_RS22570	E3.1.3.25, IMPA, suhB; myo-inositol-1(or 4)-monophosphatase [EC:3.1.3.25]
K01092	MM	RHE_RS10865	E3.1.3.25, IMPA, suhB; myo-inositol-1(or 4)-monophosphatase [EC:3.1.3.25]
K01092	Bacteroid	RHE_RS04240	E3.1.3.25, IMPA, suhB; myo-inositol-1(or 4)-monophosphatase [EC:3.1.3.25]
K01092	Bacteroid	RHE_RS22680	E3.1.3.25, IMPA, suhB; myo-inositol-1(or 4)-monophosphatase [EC:3.1.3.25]
K01560	MM	RHE_RS05045	E3.8.1.2; 2-haloacid dehalogenase [EC:3.8.1.2]
K01560	Bacteroid	RHE_RS28210	E3.8.1.2; 2-haloacid dehalogenase [EC:3.8.1.2]
K01768	MM	RHE_RS18990	E4.6.1.1; adenylate cyclase [EC:4.6.1.1]
K01768	MM	RHE_RS24270	E4.6.1.1; adenylate cyclase [EC:4.6.1.1]
K01768	MM	RHE_RS18920	E4.6.1.1; adenylate cyclase [EC:4.6.1.1]
K01768	Bacteroid	RHE_RS11150	E4.6.1.1; adenylate cyclase [EC:4.6.1.1]
K01768	Bacteroid	RHE_RS12750	E4.6.1.1; adenylate cyclase [EC:4.6.1.1]
K01768	Bacteroid	RHE_RS13090	E4.6.1.1; adenylate cyclase [EC:4.6.1.1]
K01768	Bacteroid	RHE_RS13735	E4.6.1.1; adenylate cyclase [EC:4.6.1.1]
K01768	Bacteroid	RHE_RS14395	E4.6.1.1; adenylate cyclase [EC:4.6.1.1]
K01768	Bacteroid	RHE_RS18920	E4.6.1.1; adenylate cyclase [EC:4.6.1.1]
K01768	Bacteroid	RHE_RS24935	E4.6.1.1; adenylate cyclase [EC:4.6.1.1]
K09458	MM	RHE_RS12650	fabF, OXSM, CEM1; 3-oxoacyl-[acyl-carrier-protein] synthase II [EC:2.3.1.179]
K09458	MM	RHE_RS12655	fabF, OXSM, CEM1; 3-oxoacyl-[acyl-carrier-protein] synthase II [EC:2.3.1.179]
K09458	MM	RHE_RS07375	fabF, OXSM, CEM1; 3-oxoacyl-[acyl-carrier-protein] synthase II [EC:2.3.1.179]
K09458	Bacteroid	RHE_RS10850	fabF, OXSM, CEM1; 3-oxoacyl-[acyl-carrier-protein] synthase II [EC:2.3.1.179]
K00059	MM	RHE_RS06685	fabG, OAR1; 3-oxoacyl-[acyl-carrier protein] reductase [EC:1.1.1.100]
K00059	MM	RHE_RS07365	fabG, OAR1; 3-oxoacyl-[acyl-carrier protein] reductase [EC:1.1.1.100]
K00059	MM	RHE_RS05335	fabG, OAR1; 3-oxoacyl-[acyl-carrier protein] reductase [EC:1.1.1.100]
K00059	Bacteroid	RHE_RS25095	fabG, OAR1; 3-oxoacyl-[acyl-carrier protein] reductase [EC:1.1.1.100]
K00059	Bacteroid	RHE_RS19755	fabG, OAR1; 3-oxoacyl-[acyl-carrier protein] reductase [EC:1.1.1.100]
K00135	MM	RHE_RS00470	gabD; succinate-semialdehyde dehydrogenase / glutarate-semialdehyde dehydrogenase [EC:1.2.1.16 1.2.1.79 1.2.1.20]
K00135	Bacteroid	RHE_RS28200	gabD; succinate-semialdehyde dehydrogenase / glutarate-semialdehyde dehydrogenase [EC:1.2.1.16 1.2.1.79 1.2.1.20]
K00135	Bacteroid	RHE_RS29885	gabD; succinate-semialdehyde dehydrogenase / glutarate-semialdehyde dehydrogenase [EC:1.2.1.16 1.2.1.79 1.2.1.20]
K02433	MM	RHE_RS09475	gatA, QRSL1; aspartyl-tRNA(Asn)/glutamyl-tRNA(Gln) amidotransferase subunit A [EC:6.3.5.6 6.3.5.7]
K02433	Bacteroid	RHE_RS25710	gatA, QRSL1; aspartyl-tRNA(Asn)/glutamyl-tRNA(Gln) amidotransferase subunit A [EC:6.3.5.6 6.3.5.7]
K02433	Bacteroid	RHE_RS01105	gatA, QRSL1; aspartyl-tRNA(Asn)/glutamyl-tRNA(Gln) amidotransferase subunit A [EC:6.3.5.6 6.3.5.7]

(Continued)

TABLE 1 (Continued)

K number	Physiological condition	Locus tag	Annotation from BlastKoala*
K00605	MM	RHE_RS11460	gcvT, AMT; aminomethyltransferase [EC:2.1.2.10]
K00605	Bacteroid	RHE_RS26150	gcvT, AMT; aminomethyltransferase [EC:2.1.2.10]
K00605	Bacteroid	RHE_RS26195	gcvT, AMT; aminomethyltransferase [EC:2.1.2.10]
K16147	MM	RHE_RS27870	glgE; starch synthase (maltosyl-transferring) [EC:2.4.99.16]
K16147	Bacteroid	RHE_RS27870	glgE; starch synthase (maltosyl-transferring) [EC:2.4.99.16]
K00799	MM	RHE_RS05865	GST, gst; glutathione S-transferase [EC:2.5.1.18]
K00799	MM	RHE_RS06130	GST, gst; glutathione S-transferase [EC:2.5.1.18]
K00799	MM	RHE_RS06230	GST, gst; glutathione S-transferase [EC:2.5.1.18]
K00799	MM	RHE_RS11855	GST, gst; glutathione S-transferase [EC:2.5.1.18]
K00799	MM	RHE_RS01425	GST, gst; glutathione S-transferase [EC:2.5.1.18]
K00799	Bacteroid	RHE_RS07560	GST, gst; glutathione S-transferase [EC:2.5.1.18]
K00799	Bacteroid	RHE_RS12380	GST, gst; glutathione S-transferase [EC:2.5.1.18]
K00799	Bacteroid	RHE_RS25110	GST, gst; glutathione S-transferase [EC:2.5.1.18]
K00799	Bacteroid	RHE_RS05070	GST, gst; glutathione S-transferase [EC:2.5.1.18]
K02495	MM	RHE_RS30905	hemN, hemZ; oxygen-independent coproporphyrinogen III oxidase [EC:1.3.98.3]
K02495	MM	RHE_RS29140	hemN, hemZ; oxygen-independent coproporphyrinogen III oxidase [EC:1.3.98.3]
K02495	Bacteroid	RHE_RS30730	hemN, hemZ; oxygen-independent coproporphyrinogen III oxidase [EC:1.3.98.3]
K00817	MM	RHE_RS19480	hisC; histidinol-phosphate aminotransferase [EC:2.6.1.9]
K00817	Bacteroid	RHE_RS30550	hisC; histidinol-phosphate aminotransferase [EC:2.6.1.9]
K00817	Bacteroid	RHE_RS06810	hisC; histidinol-phosphate aminotransferase [EC:2.6.1.9]
K00457	MM	RHE_RS23940	HPD, hppD; 4-hydroxyphenylpyruvate dioxygenase [EC:1.13.11.27]
K00457	Bacteroid	RHE_RS08930	HPD, hppD; 4-hydroxyphenylpyruvate dioxygenase [EC:1.13.11.27]
K01745	MM	RHE_RS24440	hutH, HAL; histidine ammonia-lyase [EC:4.3.1.3]
K01745	Bacteroid	RHE_RS01780	hutH, HAL; histidine ammonia-lyase [EC:4.3.1.3]
K10191	MM	RHE_RS22750	lacK; lactose/L-arabinose transport system ATP-binding protein
K10191	Bacteroid	RHE_RS19645	lacK; lactose/L-arabinose transport system ATP-binding protein
K10111	MM	RHE_RS14795	malK, mtlK, thuK; multiple sugar transport system ATP-binding protein [EC:7.5.2.-]
K10111	MM	RHE_RS27505	malK, mtlK, thuK; multiple sugar transport system ATP-binding protein [EC:7.5.2.-]
K10111	MM	RHE_RS10605	malK, mtlK, thuK; multiple sugar transport system ATP-binding protein [EC:7.5.2.-]
K10111	Bacteroid	RHE_RS25965	malK, mtlK, thuK; multiple sugar transport system ATP-binding protein [EC:7.5.2.-]
K03406	MM	RHE_RS02080	mcp; methyl-accepting chemotaxis protein
K03406	MM	RHE_RS02690	mcp; methyl-accepting chemotaxis protein
K03406	MM	RHE_RS03220	mcp; methyl-accepting chemotaxis protein
K03406	MM	RHE_RS03580	mcp; methyl-accepting chemotaxis protein
K03406	MM	RHE_RS03585	mcp; methyl-accepting chemotaxis protein
K03406	MM	RHE_RS04470	mcp; methyl-accepting chemotaxis protein
K03406	MM	RHE_RS04590	mcp; methyl-accepting chemotaxis protein
K03406	MM	RHE_RS04920	mcp; methyl-accepting chemotaxis protein
K03406	MM	RHE_RS05950	mcp; methyl-accepting chemotaxis protein
K03406	MM	RHE_RS06430	mcp; methyl-accepting chemotaxis protein
K03406	MM	RHE_RS17765	mcp; methyl-accepting chemotaxis protein
K03406	MM	RHE_RS17980	mcp; methyl-accepting chemotaxis protein
K03406	MM	RHE_RS17990	mcp; methyl-accepting chemotaxis protein
K03406	MM	RHE_RS27980	mcp; methyl-accepting chemotaxis protein
K03406	MM	RHE_RS02065	mcp; methyl-accepting chemotaxis protein
K03406	Bacteroid	RHE_RS27360	mcp; methyl-accepting chemotaxis protein
K10112	MM	RHE_RS18950	msmX, msmK, malK, sugC, ggtA, msiK; multiple sugar transport system ATP-binding protein
K10112	MM	RHE_RS22575	msmX, msmK, malK, sugC, ggtA, msiK; multiple sugar transport system ATP-binding protein
K10112	MM	RHE_RS23370	msmX, msmK, malK, sugC, ggtA, msiK; multiple sugar transport system ATP-binding protein

(Continued)

TABLE 1 (Continued)

K number	Physiological condition	Locus tag	Annotation from BlastKoala*
K10112	MM	RHE_RS26890	msmX, msmK, malK, sugC, ggtA, msiK; multiple sugar transport system ATP-binding protein
K10112	MM	RHE_RS28085	msmX, msmK, malK, sugC, ggtA, msiK; multiple sugar transport system ATP-binding protein
K10112	MM	RHE_RS29410	msmX, msmK, malK, sugC, ggtA, msiK; multiple sugar transport system ATP-binding protein
K10112	MM	RHE_RS12565	msmX, msmK, malK, sugC, ggtA, msiK; multiple sugar transport system ATP-binding protein
K10112	Bacteroid	RHE_RS24950	msmX, msmK, malK, sugC, ggtA, msiK; multiple sugar transport system ATP-binding protein
K10112	Bacteroid	RHE_RS28400	msmX, msmK, malK, sugC, ggtA, msiK; multiple sugar transport system ATP-binding protein
K10112	Bacteroid	RHE_RS24520	msmX, msmK, malK, sugC, ggtA, msiK; multiple sugar transport system ATP-binding protein
K01916	MM	RHE_RS06125	nadE; NAD+ synthase [EC:6.3.1.5]
K01916	Bacteroid	RHE_RS06125	nadE; NAD+ synthase [EC:6.3.1.5]
K00459	MM	RHE_RS29235	ncd2, npd; nitronate monooxygenase [EC:1.13.12.16]
K00459	Bacteroid	RHE_RS02555	ncd2, npd; nitronate monooxygenase [EC:1.13.12.16]
K23537	MM	RHE_RS10660	nupA; general nucleoside transport system ATP-binding protein
K23537	Bacteroid	RHE_RS00955	nupA; general nucleoside transport system ATP-binding protein
K10018	MM	RHE_RS24420	occT, nocT; octopine/nopaline transport system substrate-binding protein
K10018	Bacteroid	RHE_RS30295	occT, nocT; octopine/nopaline transport system substrate-binding protein
K00033	MM	RHE_RS12615	PGD, gnd, gntZ; 6-phosphogluconate dehydrogenase [EC:1.1.1.44 1.1.1.343]
K00033	Bacteroid	RHE_RS17825	PGD, gnd, gntZ; 6-phosphogluconate dehydrogenase [EC:1.1.1.44 1.1.1.343]
K22468	MM	RHE_RS02565	ppk2; polyphosphate kinase [EC:2.7.4.1]
K22468	Bacteroid	RHE_RS23870	ppk2; polyphosphate kinase [EC:2.7.4.1]
K00286	MM	RHE_RS15425	proC; pyrroline-5-carboxylate reductase [EC:1.5.1.2]
K00286	Bacteroid	RHE_RS28670	proC; pyrroline-5-carboxylate reductase [EC:1.5.1.2]
K10439	MM	RHE_RS22400	rbsB; ribose transport system substrate-binding protein
K10439	MM	RHE_RS27555	rbsB; ribose transport system substrate-binding protein
K10439	MM	RHE_RS30010	rbsB; ribose transport system substrate-binding protein
K10439	MM	RHE_RS30060	rbsB; ribose transport system substrate-binding protein
K10439	MM	RHE_RS09135	rbsB; ribose transport system substrate-binding protein
K10439	Bacteroid	RHE_RS29865	rbsB; ribose transport system substrate-binding protein
K02968	MM	RHE_RS01805	RP-S20, rpsT; small subunit ribosomal protein S20
K02968	Bacteroid	RHE_RS01805	RP-S20, rpsT; small subunit ribosomal protein S20
K01609	MM	RHE_RS11125	trpC; indole-3-glycerol phosphate synthase [EC:4.1.1.48]
K01609	Bacteroid	RHE_RS11125	trpC; indole-3-glycerol phosphate synthase [EC:4.1.1.48]

*Annotation of genes in the program BlastKoala (Kanehisa et al. 2016), based on the orthology assigns a *K* number.

RHE_RS10880 was identified, and RHE_RS13955 in bacteroid (Table 1). For *occT*, *nocT*, octopine/nopaline transport system substrate-binding protein; in MM, RHE_RS24420 was identified and RHE_RS30295 was expressed in bacteroid (Table 1). The *malK*, *mtlK*, *thuK*; multiple sugar transport system ATP-binding protein [EC:3.6.3.-]; in MM, the proteins RHE_RS10605, RHE_RS14795, RHE_RS27505 were identified, and RHE_RS25965 was expressed in bacteroid (Table 1). The *msmX*, *msmK*, *malK*, *sugC*, *ggtA*, *msiK*; multiple sugar transport system ATP-binding protein, in MM represented by RHE_RS12565, RHE_RS18950, RHE_RS22575, RHE_RS23370, RHE_RS26890, RHE_RS28085, RHE_RS29410 were found, while the RHE_RS24520, RHE_RS24950 and RHE_RS28400 were identified in bacteroid (Table 1). For the *lacK*; lactose/L-arabinose transport system ATP-binding protein, sn-glycerol-3-phosphate ABC transporter, the ATP-binding protein UgpC in MM RHE_RS22750 and in bacteroid RHE_RS19645 were identified (Table 1). The *rbsB*; ribose transport system substrate-binding protein is represented by the isoenzymes RHE_RS09135, RHE_RS22400, RHE_RS27555, RHE_RS30010, RHE_RS30060 in MM, and RHE_RS29865 was expressed in bacteroid (Table 1). For the *nupA*, general nucleoside transport system ATP-binding protein in MM RHE_RS10660 and in bacteroid RHE_RS00955 were identified (Table 1; Supplementary Table 2, pathway 37 and Supplementary Table 3A). Once multiplicity was detected in MM and bacteroid, a wide search for multiplicity in data was performed. Interestingly, from the 101 proteins representing 48 unique K numbers (a K number may have more than one protein), 34 isoenzymes were identified that cover 60 metabolic pathways (Table 1; Supplementary Table 3A). In synthesis, multiplicity in only one enzyme was equally found for other metabolic processes such as for peptidases, inhibitors, amino acids and related enzymes, messenger ARN biogenesis, ribosome, ribosome biogenesis, transfer ARN biogenesis,

translation factors, chaperones and folding catalysis, DNA replication proteins, DNA repair, and recombination proteins. While other pathways had multiplicity in two different enzymes, e.g., lipid biosynthesis proteins, mitochondrial biogenesis, two-component system, and bacterial motility proteins. Furthermore, multiplicity for three enzymes in a pathway was also detected, e.g., glutathione metabolism (Supplementary Table 2 pathway 3, and Supplementary Table 3A), for *pepA*, leucyl aminopeptidase [EC:3.4.11.1] enzyme, the RHE_RS01080 was expressed in MM, while in bacteroid the RHE_RS07430 was identified (Table 1). For the *gst*, glutathione S-transferase [EC:2.5.1.18] in MM RHE_RS01425, RHE_RS05865, RHE_RS06130, RHE_RS06230, and RHE_RS11855 were identified and in bacteroids, RHE_RS05070, RHE_RS07560, RHE_RS25110, and RHE_RS12380 were identified (Table 1). As well as, the *gntZ*, 6-phosphogluconate dehydrogenase [EC:1.1.1.44 1.1.1.343] in MM RHE_RS12615 and in the bacteroid RHE_RS17825 were expressed (Table 1). Multiplicity was also found in 5 transcription regulators and 16 transporters (Supplementary Table 3A).

From this data, there are some relevant points; it has been shown that during symbiosis of *R. leguminosarum*, bacteroids become auxotrophic for branched-chain amino acids, and their supply depends on the leguminous pea plant (Prell et al. 2009). In contrast, in *R. etli* CFN42, for valine, leucine, and isoleucine biosynthesis, 9, 3, and 3 enzymes were detected in MM, bacteroid, and Nch, respectively (Supplementary Table 2 pathway 6, and Supplementary Table 3A), suggesting a functional pathway in *R. etli* CFN42. Multiplicity was also found for the β-hydroxybutyrate dehydrogenase enzyme in *B. japonicum* USDA110, two isoforms were exclusively expressed in free-living conditions and a new isoform was expressed in nodule proteomes (Sarma and Emerich 2006). Another difference between the symbiosis of *R. etli* CFN42 is the expression of a great number of ABC sugars transporters which does not seem to be expressed in the symbiosis of *B. japonicum* and *S. meliloti*, reviewed in (Sarma and Emerich 2006). Also, this data confirmed two different systems for defense against oxidative stress for *R. etli* CFN42 (Resendis-Antonio et al. 2011), which is also observed in *S. meliloti* 1021 (see below), one prevailing in free-living conditions and the other in symbiosis. As shown, the multiplicity of genes for an enzyme is a generality in the cellular functioning of *R. etli* CFN42 in free-living conditions and symbiosis, clearly showing a greater genetic redundancy for enzymes expressed in MM than in symbiosis that may or may not be paralogous genes (Supplementary Table 3A). Additionally, a contrasting analysis of function assigned to the genes between the KO Orthology database (Kanehisa et al. 2016; Kanehisa 2017) and the NCBI database[6] was performed from the 48 unique K numbers covering 101 and 74 proteins for MM and bacteroid, respectively (Table 1); only four K numbers from *R. etli* CFN42; K01684, K02433, K00459, and K10439 were different, showing a great coincidence between the two methods (see shaded green rows; Supplementary Table 3A). When genes with the same annotated function exist, phenotypic change of a bacterium is not present by loss of function of a gene copy; it is called "Robustness," which is the ability to maintain the function when there is a change, as it was from free life to symbiosis (González et al. 2006; Diss et al. 2014), and they are maintained by context-dependent differences (Putty et al. 2013). These data suggest that when *R. etli* CFN42 is in free life and under symbiotic conditions, there is a metabolic adaptation, implying distinct transcriptional regulation for these genes.

Isoenzymes in *Sinorhizobium meliloti* 1021

An identical analysis was performed with a peptone yeast-rich medium and bacteroid transcriptome data from *S. meliloti* 1021 to search for isoenzymes. Significant data were selected with two parameters, log ≥0.96 and with software with $p \geq 0.05$ (Barnett et al. 2004). In contrast to *R. etli* CFN42, *S. meliloti* only showed 7K genes for isoenzymes; SMc03978 *tkt2* for transketolase was expressed in TY, while in bacteroids, SMc00270 was expressed (Supplementary Table 3B). The protein SMc03994 for the 30S ribosomal protein S21 was present in TY medium, while SMc04320 for the 30S ribosomal protein was present in bacteroids. The SMa0744 protein GroEL was translated in TY and was substituted by the SMa0124 GroEL protein in bacteroids. Moreover, SMc02897 for the cytochrome C transmembrane protein was expressed in TY medium, and the equivalent activity was substituted by the SMc01981 cytochrome C protein in the bacteroid. Moreover, as shown for *R. etli* CFN42 for defense against oxidative stress in MM and bacteroids, *S. meliloti* 1,021 in TY medium expressed five glutathione-S transferases, SMc00097 (gst2), SMc00383 (gst3), SMc00407 (gst4), SMc03082 (gst8), and SMc00036 (gst1). This activity was performed by the SMc01443 (gst6) glutathione-S transferase protein in bacteroids (Supplementary Table 3B). These data suggest that an alternative system for defense against oxidative stress also exists in *S. meliloti* 1021 bacteroids. There were contrasting low K numbers in *S. meliloti* 1021 compared with the *R. etli* CFN42 genome, and these data probably have a bias from a different method for the selection of significant data between these bacteria.

Transcriptional regulatory network

Taking advantage of the RhizoBindingSites database[7] (Taboada-Castro et al. 2020), networks were constructed for MM and bacteroid protein profiles with the application "Prediction of regulatory network" (see "Materials and Methods" section). A

6 https://www.ncbi.nlm.nih.gov/genome/browse/#!/proteins/827/383937%7CRhizobium%20etli/ (accessed September 8, 2022).

7 http://rhizobindingsites.ccg.unam.mx/ (accessed September 8, 2022).

three-step method to build a network was implemented (see "Materials and Methods" section). In the second step (see methods), Clustered-TF genes obtained with the matrix-clustering analysis, were used as input in the application of RhizoBindingSites database "Prediction of regulatory networks" with the option "auto", to corroborated potential TF gen-target relationships. The cluster_34 and cluster_195 from MM, and cluster_97 and cluster_112 from bacteroid were chosen. For cluster_34, all the genes had a TF gene-target relationship. Indeed, for cluster_195, 22 out of 27 genes were connected (Supplementary Table 1G). For cluster_97, 21 of 26 genes were connected and for cluster_112, 21 from 22 genes were connected (Supplementary Table 1H). These data showed that the matrix of a clustered-TF, has homology to a matrix of the target gene. In consequence, the matrices from both, the TF´s and the gene-target are conserved in their respective orthologs genes, because upstream regulatory regions of the orthologs genes were used to deduce the matrices (Taboada-Castro et al. 2020). Suggesting, this conservation is by a compromised function of the motifs for the TF and the target genes and not by chance. Then, the transcriptional regulatory networks of MM and bacteroid protein profiles are constructed with motifs interspecies conserved. The quality of the MM, bacteroid, clustered-TF-MM and clustered-TF-BACTEROID networks, which are data of the three-step method, was compared by analyzing the number of interactions per p-value range. The number of interactions of p-values with low stringency decreased, and those with a higher stringency in the network from clustered-TF-MM and clustered-TF-BACTEROID increased, meaning that there was an enrichment of interactions with high stringency p-value levels (see "Materials and Methods" section, Figure 5), emphasizing that most of the TF gene–target interactions eliminated from clustered-TF-MM and clustered-TF-BACTEROID had low stringency p-values. These data confirmed that clustered matrices of genes are strongly related to the structure of a network, and these genes probably represent hubs. We expect this new method will be helpful for the depuration of regulons from any potential TF gene-target data, since it provides data with the highest level of restriction as possible, based on coexpression of the TF´s, instead of arbitrarily imposing a threshold to determine the significance of data. The number of clusters per network was 654 and 92 for Clustered-TF-MM and Clustered-TF-BACTEROID, respectively. Moreover, 654 proteins, including 93 TFs for Clustered-TF-MM, and 246 TFs for Clustered-TF-BACTEROID, including 46 TF proteins, were identified (Supplementary Tables 4A-B). These expected regulatory networks had 5,091 and 1,114 TF gene–target relationships for MM and bacteroid, respectively, the hypothetical regulons are available (Supplementary Tables 4 A-B). Additionally, to determine whether the matrices of these networks detect motifs in the upstream regulatory region of their corresponding orthologous genes in the order Rhizobiales, an analysis with a footprint-scan method was conducted (Nguyen et al. 2018). These data showed a great number of motifs detected with these matrices even for phylogenetically distant species of *R. etli* CFN42 (data not shown), suggesting that this conservation of motifs occurs by a functional compromise.

We wondered how our inferred networks assess against known curated networks. As no curated network is available for *R. etli*, inspired by recent work showing that assessing using network structural properties provides results consistent with using a gold-standard (Zorro-Aranda et al. 2022), we performed a pairwise comparison *via* correlation of the normalized structural profiles of two well-curated regulatory networks, *E. coli* and *B. subtilis*, as positive control and a background of Erdös-Rényi parametrized random networks as a negative control (Figure 6A; "Materials and Methods" section).

Comparing these properties showed that negative control networks were clearly segregated from the experimental and

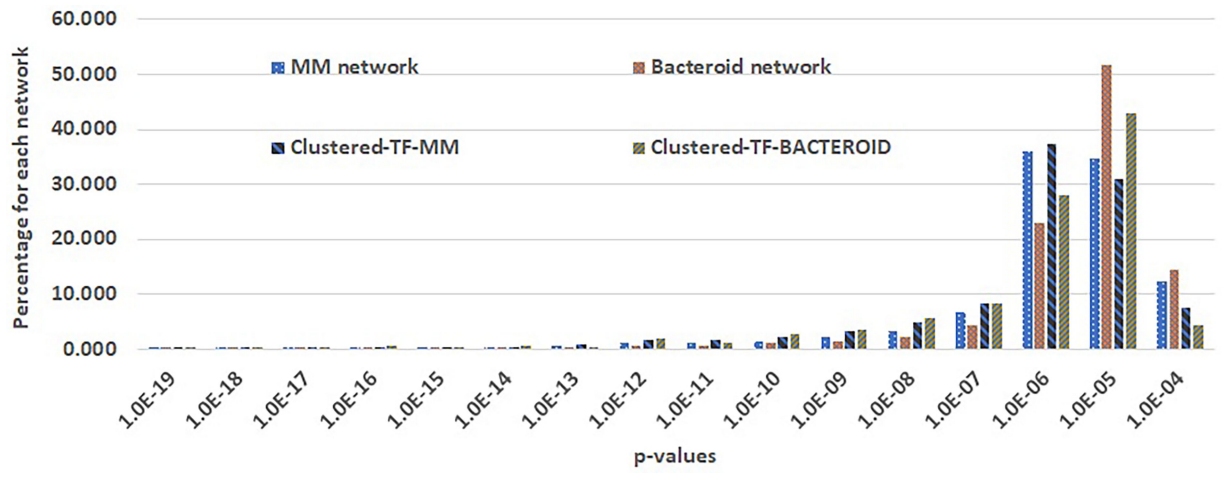

FIGURE 5
Comparison of genes per p-value range of the first and second transcriptional regulatory networks of minimal medium and bacteroid from *Rhizobium etli* CFN42.

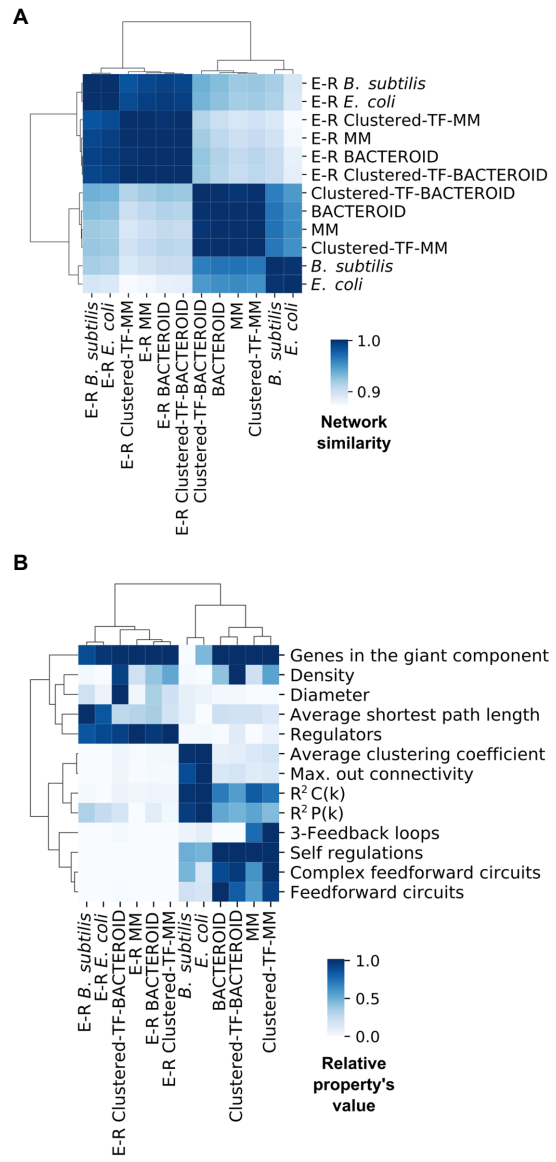

FIGURE 6
(A) Network similarity and **(B)** Symmetric properties of experimental networks from *Escherichia coli*, *Bacillus subtilis* and predicted networks from *Rhizobium etli* CFN42; MM, Clustered-TF-MM, BACTEROID and Clustered-TF-BACTEROID compared with 1000 Erdös-Rényi random networks.

inferred biological networks, showing that experimental and inferred biological networks were more similar (Figure 6A). Consequently, the inferred biological networks were not random. We then analyzed these structural property profiles of the networks using mix-max scaling across networks to maximize the differences (Figure 6B). We confirmed the segregation of the negative controls from the biological and experimental networks, which means that our networks are not random and that the experimental and inferred networks were more similar. The density was higher for the inferred networks than for the experimental networks. Between the inferred networks, the density of bacteroid and clustered-TF-BACTEROID was higher than that of the MM and clustered-TF-MM networks. The density of Clustered-TF-MM and Clustered-TF-BACTEROID could be increased due to grouping the matrices with the aforementioned matrix-clustering strategy (Figure 6B; "Materials and Methods" section).

The scale-free properties of the inferred networks were contrasted to the experimental networks of *E. coli* and *B. subtilis* by two alternative methods: robust linear regression and maximum likelihood estimation. Currently, the transcriptional regulatory network of a *Rhizobium* strain is unknown. A bioinformatic study based on functional relationships from the PROLINKS and STRING databases showed a scale-free interaction network and modularity for *Sinorhizobium meliloti* (Rodriguez-Llorente et al. 2009). However, they considered greater, more significant proteins than this study. Consistently, many genes showed a modular organization in a metabolic network of *R. etli* CFN42 with proteomic, transcriptomic, and metabolomic data (Resendis-Antonio et al. 2012). Additionally, there are more 3-feedback loops in the MM and Clustered-TF-MM networks than in the bacteroid, Clustered-TF-BACTEROID, *E. coli*, and *B. subtilis* networks. The self-regulation, complex feed-forward circuits, and feed-forward circuits from inferred networks were higher than the experimental ones (Figure 6B). Self-regulation is higher for inferred networks than experimental networks because the RhizoBindingSites database was built only with genes whose matrices could recognize a motif in their upstream promoter region.

The average clustering coefficient, maximum out connectivity, cluster coefficient R^2 C(k), and connectivity distribution R^2 P(k) were higher for the experimental than for inferred biological networks, implying that the inferred networks have an atypical very low modularity. As previously shown in several organisms (Freyre-González et al. 2008; 2012; Freyre-González and Tauch 2017; Escorcia-Rodríguez et al. 2021), the Natural Decomposition Approach (NDA) reveals that bacterial regulatory networks shape a diamond-like, three-tier, hierarchy where global TFs govern modules, and the local response of these modules is integrated at the promoter level by intermodular genes, whereas modules are shaped by local TFs and structural genes (Freyre-González et al. 2022). An analysis of our predicted networks using the NDA showed a hierarchy only composed of global TF and basal machinery, where neither modules nor intermodular genes could be identified (data not shown). These could be a consequence of the atypical high density of the inferred network, as this causes the networks to be more interconnected than usual.

As we found that in our networks the integrative layer composed of the intermodular genes is absent, we leverage that it has been previously shown that regulatory networks are mainly descendent (Ma et al. 2004) but there are still some feedback circuits (Freyre-González et al. 2008, 2012). We unveil a hierarchy of the inferred networks by removing the top-down edges, thus eliminating feedback, and applying a topological

sorting algorithm to the predicted network (Figure 7; Supplementary Table 5 and "Materials and Methods" section). Our strategy maintains the global structure of the network to reveal the hierarchy. Besides structural nodes, no other nodes are removed, and 'bottom-up' edges can be added back to the hierarchy to reveal the feedback among layers and reconstruct the original network.

The hierarchy of the MM network showed that RHE_RS06405 (MucR family) is at the top. Under the top, there are four genes: RHE_RS25725 (LysR family), RHE_RS16230 (ROK family), RHE_RS05945 (LuxR family), and RHE_RS02355 (ROK family; Figure 7A; Supplementary Table 5). In contrast, for the Clustered-TF-MM network (Figure 7B; Supplementary Table 5), RHE_RS06405 (MucR family) and RHE_RS05945 (LuxR family) were at the top, and under the top seven TFs identified, RHE_RS25725 (LysR family) and RHE_RS20575 (*carD* family), a CarD protein, pertaining to the CarD_CdnL_TRCF family of TFs described in *Mycobacterium tuberculosis* 2018, binds to RNA polymerase and activates transcription by stabilizing the transcription initiation complex, elongation or termination steps, and deletion of N-terminal residues hampers amyloid formation (Kaur et al. 2018). It was shown that the interaction of CarD with the RNAP beta-subunit is responsible for mediating *M. tuberculosis* viability, rifampicin resistance, and pathogenesis. It is a highly expressed protein, also induced by multiple stresses. Transient depletion of CarD makes *M. tuberculosis* more sensitive to being killed by reactive oxygen species, and its mutation abolishes persistence in mice (Weiss et al. 2012). In addition, RHE_RS16230 (ROK family), RHE_RS02355 (ROK family), RHE_RS17050 (response regulator), RHE_RS01875 (helix-turn-helix transcriptional regulator), and RHE_RS00415 (TetR family) were identified. For bacteroid and clustered TF-BACTEROID, the hierarchy of transcriptional regulatory networks showed the same three TFs at the top; RHE_RS23775 (NAC, nitrogen assimilation transcriptional regulator). In *Escherichia coli,* the *nac* and *glnK* promoters were strongly activated when cells stopped growing, and ammonium became scarce (Atkinson et al., 2002), as well as RHE_RS03515 (substrate-binding domain) and RHE_RS10580 (LacI family DNA-binding transcriptional regulator; Figures 7C,D; Supplementary Table 5). For MM and clustered-TF-MM transcriptional regulatory networks, seven and six different levels of regulation are shown, respectively (Figures 7A,B; Supplementary Table 5). In contrast, for bacteroid and clustered-TF_BACTEROID, only three and four levels of regulation were shown, respectively (Figures 7C,D; Supplementary Table 5).

Inferred transcriptional regulation of isoenzymes in MM and bacteroids

TF gene–target relationships for genes coding for isoenzymes in the MM, Clustered-TF-MM and bacteroid, Clustered-TF-BACTEROID networks were inferred (Supplementary Table 6). The transcriptional regulator per locus tag is found in the column E headed "Matrix_ID" with the RHE_RS13345_m5 format (Supplementary Table 6), see "Materials and Methods" section. It is shown by the enzyme PGD, *gnd*, *gntZ*; 6-phosphogluconate dehydrogenase [EC:1.1.1.44 1.1.1.343] (Supplementary Table 6, column AK), the isoenzymes RHE_RS12615 and RHE_RS17825 were expressed in MM and in the bacteroid (Supplementary Table 6, column B), respectively. In MM, the transcriptional regulator is RHE_RS13345_m5 (Supplementary Table 6, column E) with a *p*-value of 1.7e-5 (Supplementary Table 6, column K), and in the bacteroid, it is RHE_RS27925_m4 (Supplementary Table 6, column E) with a *p*-value of 0.18e-4 (Supplementary Table 6, column K). However, there are no data with respect to the Clustered-TF-MM and Clustered-TF-BACTEROID networks (Supplementary Table 6, columns S–Z) due to a reduction of TF's by the matrix-clustering analysis. Therefore, *fabG*, OAR1; 3-oxoacyl-[acyl-carrier protein] reductase [EC:1.1.1.100] (Supplementary Table 6, columns A–K) enzyme for fatty acid biosynthesis, we identified RHE_RS05335 and RHE_RS06685 in MM, and RHE_RS19755 in bacteroid (Supplementary Table 6, column B), which are potentially regulated by the TFs RHE_17755_m2, RHE_RS30790_m1 and RHE_RS23180_m2 (Supplementary Table 6, columns E and S), with *p*-value of 7.30E-07, 1.20E-06 and 2.60E-06 (Supplementary Table 6, columns K and Y), respectively, for MM, bacteroid and Clustered-TF-MM and Clustered-TF-BACTEROID networks, showing for this enzymatic step that the multiplicity also corresponds with a different TF involved in transcriptional regulation. Note that each network contains its own *p*-value (see Supplementary Table 6, columns K and Y). For a better choice of a TF gene-target, data from a clustered-TF network and a low *p*-value as possible is desirable. From here on, in this discussion, the *p*-value located in Supplementary Table 6, column K, for not clustered networks and Supplementary Table 6, column Y, for clustered networks will be omitted. Concerning the enzyme D-threo-aldose 1-dehydrogenase [EC:1.1.1.122], in MM and bacteroid, the isoenzymes RHE_RS02500 and RHE_RS28605 were expressed, and the inferred TFs were RHE_RS22090_m3 and RHE_RS03515_m5, respectively, showing a potentially distinct TF-dependent physiological condition, but incomplete data were obtained for Clustered-TF networks (Supplementary Table 6, columns S–Z). In the case of *gcvT* and AMT, aminomethyltransferase enzyme [EC:2.1.2.10] in MM expressed RHE_RS28340 and two isoenzymes in bacteroid; RHE_RS26195 and RHE_RS26150 were expressed, and their corresponding TFs RHE_RS28340_m3, RHE_RS00285_m4, and RHE_RS05730_m3 were deduced, respectively, for both non and clustered-TF networks, supporting the suggestion of distinct regulation of these genes in MM and bacteroid (Supplementary Table 6).

Most likely, the microaerobic conditions and the metabolic functions prevailing in the bacteroid (fixing nitrogen), in comparison with the bacteria cultivated in MM (free life), induce specific strategies against oxidative stress, e.g., for the case of the enzyme GST, *gst*; glutathione S-transferase

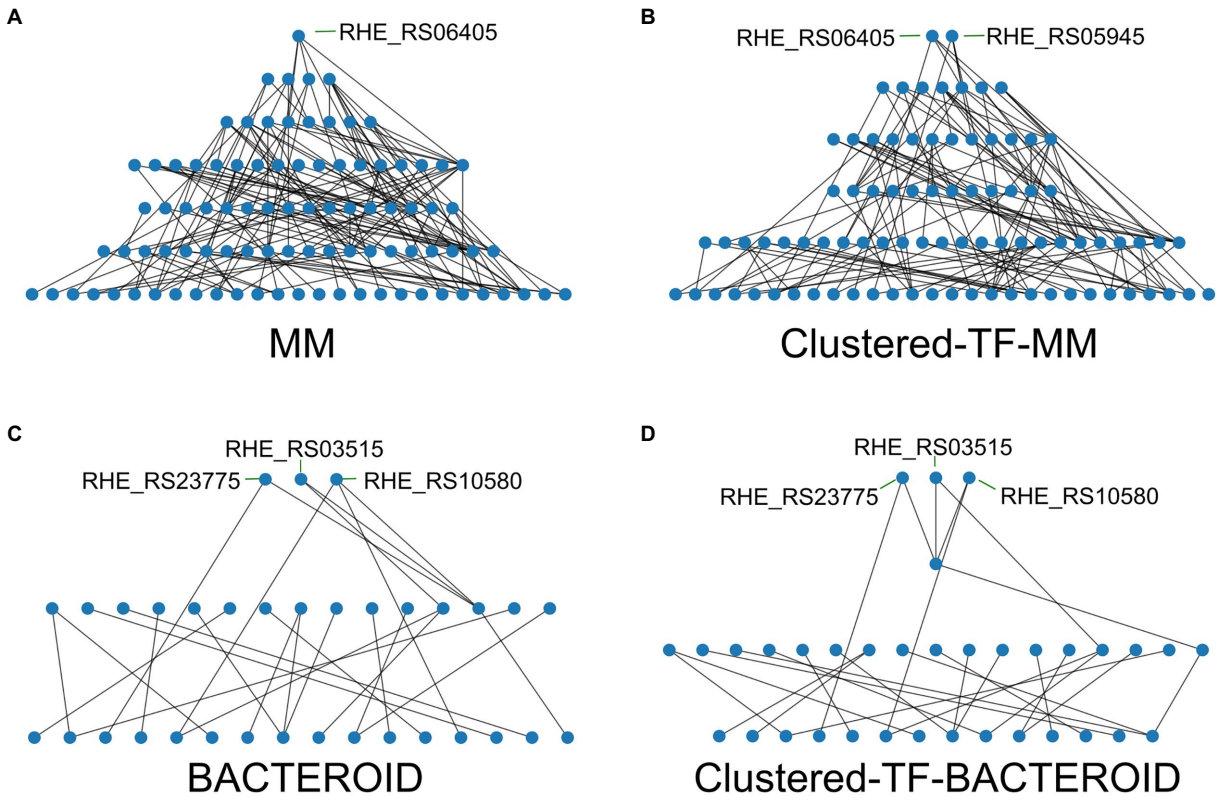

FIGURE 7
Hierarchy of the transcriptional regulators (TF's) of the networks; **(A)** Minimal medium, **(B)** Clustered-TF-MM, **(C)** BACTEROID, and **(D)** Clustered-TF-BACTEROID from *Rhizobium etli* CFN42.

[EC:2.5.1.18], in MM RHE_RS0630 and RHE_RS11855 proteins were expressed for the MM network, while in bacteroid, the RHE_RS12380 was identified with a Clustered-TF network, with the TFs RHE_RS06135_m4, RHE_RS27645_m3 in MM and RHE_RS08350_m3 in the bacteroid (Supplementary Table 6). Regarding *yghU* and *yfcG*, GSH-dependent disulfide-bond oxidoreductase [EC:1.8.4.-] in MM and bacteroid isoenzymes RHE_RS22490 and RHE_RS04155, respectively, were expressed, potentially under the transcriptional control of TFs RHE_RS12670_m4 and RHE_RS12205_m4, respectively (Supplementary Table 6). For these proteins involved in the repair of oxidized proteins, a different transcriptional regulation is suggested in MM and bacteroid and clustered-TF-MM and clustered-TF-BACTEROID networks. Iron transport is relevant for metabolism regarding *afuA* and *fbpA*, which encode the iron(III) transport system substrate-binding protein and express the isoenzymes RHE_RS10880 and RHE_RS13955 in MM and bacteroid, respectively, with the TFs RHE_RS28340_m4 and RHE_RS16205_m5, respectively, for MM and bacteroid networks (Supplementary Table 6), our data suggest two distinct metabolic strategies for transport of iron in MM (free life) and bacteroid (nitrogen fixing) conditions. It has been discussed that transport is specific for these metabolic stages (Sarma and Emerich 2006); indeed, this was supported for amino acid transport regarding ABC.PA. S; the polar amino acid transport system substrate-binding protein, in MM RHE_RS02695, RHE_RS11720, and RHE_RS27400, and in bacteroid RHE_RS07475 and RHE_RS27430 were expressed, potentially regulated by the TFs RHE_RS30745_m3, RHE_RS24110_m2, RHE_RS14135_m3 and RHE_RS18525_m2, RHE_RS26505_m5, respectively. All these data were clustering TF-associated, showing distinct TFs for each metabolic condition (Supplementary Table 6). Concerning transcriptional regulators, *lacI* and *galR* belonging to the LacI family in Clustered-TF-MM RHE_RS03090, RHE_RS12585, RHE_RS17450, RHE_RS23055, RHE_RS23350, and RHE_RS27560 were expressed in comparison with Clustered-TF-BACTEROID, where the following proteins were identified: RHE_RS03515, RHE_RS15245, and RHE_RS27525. Probably some genes are expressed because they respond to different physiological conditions with the aim of regulating different groups of genes. The inferred TFs for these genes were RHE_RS03090_m2, RHE_RS12585_m4, RHE_RS17450_m4, RHE_RS23055_m3, RHE_RS23350_m1, RHE_RS27560_m3, and RHE_RS03515_m5 for cluster-TF-MM, as well as, RHE_RS24095_m3 for bacteroid network, and RHE_RS03515_m5, RHE_RS27525_m2 for clustered-TF-BACTEROID, respectively (Supplementary Table 6). These data support the idea that

isoenzymes have distinct regulations. For the ABCB-BAC ATP-binding cassette, subfamily B, bacterial beta-(1 –> 2) glucan export ATP-binding/permease NdvA protein, the proteins RHE_RS20455 and RHE_RS10390 were expressed in MM and bacteroid, respectively, with the TFs RHE_RS23325_m5 and RHE_RS26875_m3, for both not and clustered-TF were inferred, respectively, supporting a differential transcriptional regulation (Supplementary Table 6). Multiple *rbsB*; ribose transport system substrate-binding protein transporters, RHE_RS09135, RHE_RS22400, RHE_RS27555, RHE_RS30060, and RHE_RS30060 were expressed in MM, while RHE_RS29865 was identified in bacteroid; the data suggested that they were under the Clustered-TF transcriptional control of RHE_RS22090_m2, RHE_11740_m2, RHE_RS27560_m3, RHE_RS04690_m3 and RHE_RS02355_m4 and the not clustering TF associated RHE_RS10580_m1, respectively (Supplementary Table 6). Currently, it is not clear whether the plant supplies sugar to the bacteroid. A metabolome study showed that GDP-mannose and GDP-galactose were identified to be 7.4 times higher in bacteroids than in bacteria grown in MM (data not shown); in the opposite sense, proteins for these pathways were significantly higher in MM than in bacteroids (Supplementary Table 2, pathway 10). The two-component system, OmpR family response regulator proteins RHE_RS06580, RHE_RS10890, RHE_RS12325, and RHE_RS21355, were detected in MM and RHE_RS29195 in bacteroid, with TFs RHE_RS06580_m4, RHE_RS05790_m3, RHE_RS12325_m2, and RHE_RS21355_m3, for the proteins expressed in MM and RHE_RS29195_m2 for bacteroid, respectively (Supplementary Table 6), for non and clustered-TF networks, showing that multiplicity has a distinct potentially transcriptional regulation. The *nodD* LysR family transcriptional regulator recognizes a *nod-box* for transcriptional activation (Mao et al. 1994). We have demonstrated the function of the *nodD* transcriptional regulators by supplementation of MM with the flavonoid naringenin, which induced the synthesis of the nodulation factor (Meneses et al. 2017). The *nodD* genes RHE_RS30790, RHE_RS31010, and RHE_RS31005 proteins were expressed in Clustered-TF-MM and Clustered-TF-BACTEROID, respectively, probably under the transcriptional control of the inferred TFs RHE_RS30790_m2, RHE_RS12670_m4 Clustered-TF and RHE_RS20460_m2, not Clustered-TF, respectively (Supplementary Table 6). It was demonstrated that lysR *nodD* genes were autoregulated (Hu et al. 2000), as was *in silico* shown for the NodD RHE_RS30790 (Taboada-Castro et al. 2020); in addition, the *nodD* genes may be regulated by other TFs (Barnett and Long 2015), as was inferred for *nodD* RHE_RS31005 (Taboada-Castro et al. 2020). Altogether, these data suggested that in addition to specific isoenzymes expressed in a condition-dependent manner, they are potentially under specific transcriptional regulatory control. This data suggested how *R. etli* CFN42 re-program its transcriptional regulatory network to be metabolically adapted for growth in MM or in the symbiosis with the leguminous plant.

Conclusion

A free-living and symbiotic proteomic study from *R. etli* CFN42 were performed. A lower number of proteins per pathway in bacteroids than in MM was found, and approximately 30 and 20% of proteins for some metabolic pathways were detected in MM and bacteroids with respect to the genomic content, respectively. A mapping of classified proteins based on orthology allowed us to discover the presence of isoenzymes specific for growth in minimal medium and symbiosis with deduced specific transcriptional regulation. In addition to the metabolic pathways identified, genes for the degradation of environmental compounds were detected in MM and symbiotic proteomes. In contrast, a low number of isoenzymes were found in the *S. meliloti* transcriptome data. Taking advantage of the RhizoBindingSites database, which contains inferred TF gene–target relationships of *R. etli* CFN42 and eight additional symbiotic species, a method was implemented to construct transcriptional regulatory networks for these metabolic conditions. An inferred clustered TF gene network was constructed with motifs highly conserved in the upstream regulatory regions of the genes that are also conserved in the orthologous genes from each gene.

This pioneer bioinformatic framework is an important reference to obtain basic information on the genetic circuitry to increase knowledge about an experimental transcriptional regulatory network. Given the changing climate conditions, experimental validation of these genetic circuits for remodeling the metabolic pathways to optimize the SNF of *R. etli* CFN42 is the next step.

Data availability statement

The authors acknowledge that the data presented in this study must be deposited and made publicly available in an acceptable repository, prior to publication. Frontiers cannot accept a manuscript that does not adhere to our open data policies.

Author contributions

HT-C, JG, and SE-G conceived the idea. JG, HT-C, JF-G, JE-R, LG-C, and SE-G designed the analysis. HT-C, JG, JF-G, and SE-G analyzed the results and drafted the manuscript. SE-G revised the manuscript. All authors contributed to the article and approved the submitted version.

Funding

Part of this work was supported by the Programa de Apoyo a Proyectos de Investigación e Innovación Tecnológica

(PAPIIT-UNAM), grants IN 213522 to SE-G and IN202421 to JF-G. JE-R is a doctoral student from Programa de Doctorado en Ciencias Biomédicas, Universidad Nacional Autónoma de México (UNAM); he received fellowship 959406 from CONACYT.

Acknowledgments

The authors wish to thank María del Carmen Vargas-Lagunas and Yolanda Mora for their technical support.

Conflict of interest

The authors declare that the research was conducted in the absence of any commercial or financial relationships that could be construed as a potential conflict of interest.

Publisher's note

All claims expressed in this article are solely those of the authors and do not necessarily represent those of their affiliated organizations, or those of the publisher, the editors and the reviewers. Any product that may be evaluated in this article, or claim that may be made by its manufacturer, is not guaranteed or endorsed by the publisher.

Supplementary material

The Supplementary material for this article can be found online at: https://www.frontiersin.org/articles/10.3389/fmicb.2022.947678/full#supplementary-material

SUPPLEMENTARY TABLE 1
Method for network construction A-I.

SUPPLEMENTARY TABLE 2
Metabolic pathways of the proteins expressed in Minimal medium, bacteroid and present in both conditions from *Rhizobium etli* CFN42.

SUPPLEMENTARY TABLE 3
Isoenzymes from *Rhizobium etli* CFN42 and *Sinorhizobium meliloti* 1021.

SUPPLEMENTARY TABLE 4
Predicted second transcriptional regulatory network with matrix-clustering of MM and Bacteroid profiles from *Rhizobium etli* CFN42.

SUPPLEMENTARY TABLE 5
Predicted Transcription Factor hierarchy in networks of MM, Clustered-TF-MM, BACTEROID and Clustered-TF-BACTEROID from *Rhizobium etli* CFN42.

SUPPLEMENTARY TABLE 6
Isoenzymes with inferred Transcriptional regulation of non-clustered and clustered networks from *Rhizobium etli* CFN42.

References

Abdi, H., and Williams, L. J. (2010). Principal component analysis. *Wiley Interdiscip. Rev. Comput. Stat.* 2, 433–459. doi: 10.1002/WICS.101

Aerts, S., Thijs, G., Coessens, B., Staes, M., Moreau, Y., and De Moor, B. (2003). Toucan: deciphering the cis-regulatory logic of coregulated genes. *Nucleic Acids Res.* 31, 1753–1764. doi: 10.1093/nar/gkg268

Alamillo, J. M., Dí Az-Leal, J. L., Sánchez-Moran, M. A. V., and Pineda, M. (2010). Molecular analysis of ureide accumulation under drought stress in *Phaseolus vulgaris* L. *Plant Cell Environ.* 33, 1828–1837. doi: 10.1111/j.1365-3040.2010.02187.x

Andrews, M. E. M., and Andrews, M. E. M. (2017). Specificity in legume-rhizobia symbioses. *Int. J. Mol. Sci.* 18. doi: 10.3390/ijms18040705

Ashburner, M., Ball, C. A., Blake, J. A., Botstein, D., Butler, H., Cherry, J. M., et al. (2000). Gene ontology: tool for the unification of biology. The gene ontology consortium. *Nat. Genet.* 25, 25–29. doi: 10.1038/75556

Atkinson, M. R., Blauwkamp, T. A., Bondarenko, V., Studitsky, V., and Ninfa, A. J. (2002). Activation of the glnA, glnK, and nac promoters as Escherichia coli undergoes the transition from nitrogen excess growth to nitrogen starvation. *J. Bacteriol.* 184, 5358–5363. doi: 10.1128/JB.184.19.5358-5363.2002

Bai, Y., Liang, J., Liu, R., Hu, C., and Qu, J. (2014). Metagenomic analysis reveals microbial diversity and function in the rhizosphere soil of a constructed wetland. *Environ. Technol.* 35, 2521–2527. doi: 10.1080/09593330.2014.911361

Barnett, M. J., and Long, S. R. (2015). The *sinorhizobium meliloti* SyrM Regulon: effects on global gene expression are mediated by *syrA* and *nodD3*. *J. Bacteriol.* 197, 1792–1806. doi: 10.1128/JB.02626-14

Barnett, M. J., Toman, C. J., Fisher, R. F., and Long, S. R. (2004). A dual-genome Symbiosis Chip for coordinate study of signal exchange and development in a prokaryote-host interaction. *Proc. Natl. Acad. Sci. U. S. A.* 101, 16636–16641. doi: 10.1073/pnas.0407269101

Castro-Mondragon, J. A., Jaeger, S., Thieffry, D., Thomas-Chollier, M., and van Helden, J. (2017). RSAT matrix-clustering: dynamic exploration and redundancy reduction of transcription factor binding motif collections. *Nucleic Acids Res.* 45:e119. doi: 10.1093/nar/gkx314

Cevallos, M. A., Encarnación, S., Leija, A., Mora, Y., and Mora, J. (1996). Genetic and physiological characterization of a *rhizobium etli* mutant strain unable to synthesize poly-beta-hydroxybutyrate. *J. Bacteriol.* 178, 1646–1654. Available at: http://www.ncbi.nlm.nih.gov/pubmed/8626293 [], doi: 10.1128/jb.178.6.1646-1654.1996

Collier, R., and Tegeder, M. (2012). Soybean ureide transporters play a critical role in nodule development, function and nitrogen export. *Plant J.* 72, 355–367. doi: 10.1111/j.1365-313X.2012.05086.x

Defrance, M., Janky, R., Sand, O., and van Helden, J. (2008). Using RSAT oligo-analysis and dyad-analysis tools to discover regulatory signals in nucleic sequences. *Nat. Protoc.* 3, 1589–1603. doi: 10.1038/nprot.2008.98

Delgado, M. J., Bedmar, E. J., and Downie, J. A. (1998). Genes involved in the formation and assembly of rhizobial cytochromes and their role in symbiotic nitrogen fixation. *Adv. Microb. Physiol.* 40, 191–231. doi: 10.1016/s0065-2911(08)60132-0

Delmotte, N., Ahrens, C. H., Knief, C., Qeli, E., Koch, M., Fischer, H. M., et al. (2010). An integrated proteomics and transcriptomics reference data set provides new insights into the *Bradyrhizobium japonicum* bacteroid metabolism in soybean root nodules. *Proteomics* 10, 1391–1400. doi: 10.1002/pmic.200900710

Dicenzo, G. C., Zamani, M., Checcucci, A., Fondi, M., Griffitts, J. S., Finan, T. M., et al. (2019). Multidisciplinary approaches for studying rhizobium–legume symbioses. *Can. J. Microbiol.* 65, 1–33. doi: 10.1139/cjm-2018-0377

Diss, G., Ascencio, D., Deluna, A., and Landry, C. R. (2014). Molecular mechanisms of paralogous compensation and the robustness of cellular networks. J. *Exp. Zool. Part B Mol. Dev. Evol.* 322, 488–499. doi: 10.1002/jez.b.22555

Durán, D., Albareda, M., Marina, A., García, C., Ruiz-Argüeso, T., and Palacios, J. (2020). Proteome analysis reveals a significant host-specific response in *rhizobium leguminosarum* bv *viciae* endosymbiotic cells. *Mol. Cell. Proteomics* 20:100009. doi: 10.1074/mcp.RA120.002276

Encarnación, S., Dunn, M., Willms, K., Mora, J., Dunn, M., Willms, K., et al. (1995). Fermentative and aerobic metabolism in *rhizobium etli*. *J. Bacteriol.* 177, 3058–3066. doi: 10.1128/jb.177.11.3058-3066.1995

Escorcia-Rodríguez, J. M., Tauch, A., and Freyre-González, J. A. (2020). Abasy atlas v2.2: the most comprehensive and up-to-date inventory of meta-curated, historical, bacterial regulatory networks, their completeness and system-level characterization. *Comput. Struct. Biotechnol. J.* 18, 1228–1237. doi: 10.1016/j.csbj.2020.05.015

Escorcia-Rodríguez, J. M., Tauch, A., and Freyre-González, J. A. (2021). *Corynebacterium glutamicum* regulation beyond transcription: organizing principles

and reconstruction of an extended regulatory network incorporating regulations mediated by small RNA and protein-protein interactions. *Microorganisms* 9. doi: 10.3390/microorganisms9071395

Ferguson, B. J., Mens, C., Hastwell, A. H., Zhang, M., Su, H., Jones, C. H., et al. (2019). Legume nodulation: the host controls the party. *Blackwell Publishing Ltd* 42, 41–51. doi: 10.1111/pce.13348

Fischer, H. M. (1994). Genetic regulation of nitrogen fixation in rhizobia. *Microbiol. Rev.* 58, 352–386. doi: 10.1128/mr.58.3.352-386.1994

Freyre-González, J. A., Alonso-Pavón, J. A., Treviño-Quintanilla, L. G., and Collado-Vides, J. (2008). Functional architecture of *Escherichia coli*: new insights provided by a natural decomposition approach. *Genome Biol.* 9:R154. doi: 10.1186/gb-2008-9-10-r154

Freyre-González, J. A., Escorcia-Rodríguez, J. M., Gutiérrez-Mondragón, L. F., Martí-Vértiz, J., Torres-Franco, C. N., and Zorro-Aranda, A. (2022). System principles governing the organization, architecture, dynamics, and evolution of gene regulatory networks. *Front. Bioeng. Biotechnol.* 10:888732. doi: 10.3389/FBIOE.2022.888732

Freyre-González, J. A., and Tauch, A. (2017). Functional architecture and global properties of the Corynebacterium glutamicum regulatory network: novel insights from a dataset with a high genomic coverage. *J. Biotechnol.* 257, 199–210. doi: 10.1016/j.jbiotec.2016.10.025

Freyre-González, J. A., Treviño-Quintanilla, L. G., Valtierra-Gutiérrez, I. A., Gutiérrez-Ríos, R. M., and Alonso-Pavón, J. A. (2012). Prokaryotic regulatory systems biology: common principles governing the functional architectures of *Bacillus subtilis* and *Escherichia coli* unveiled by the natural decomposition approach. *J. Biotechnol.* 161, 278–286. doi: 10.1016/j.jbiotec.2012.03.028

Galán-Vásquez, E., and Perez-Rueda, E. (2019). Identification of modules with similar gene regulation and metabolic functions based on co-expression data. *Front. Mol. Biosci.* 6:139. doi: 10.3389/fmolb.2019.00139

Ghaffari, T., Kafil, H. S., Asnaashari, S., Farajnia, S., Delazar, A., Baek, S. C., et al. (2019). Chemical composition and antimicrobial activity of essential oils from the aerial parts of *Pinus eldarica* grown in northwestern Iran. *Molecules* 24:3203. doi: 10.3390/molecules24173203

Gil, J., and Encarnación-Guevara, S. (2022). "Lysine acetylation stoichiometry analysis at the proteome level", in *Clinical Proteomics. Methods in Molecular Biology. Vol. 2420*. eds. F. J. Corrales, A. Paradela and A. Marcilla New York, NY: Humana.

Gil, J., Ramírez-Torres, A., Chiappe, D., Luna-Penãloza, J., Fernandez-Reyes, F. C., Arcos-Encarnación, B., et al. (2017). Lysine acetylation stoichiometry and proteomics analyses reveal pathways regulated by sirtuin 1 in human cells. *J. Biol. Chem.* 292, 18129–18144. doi: 10.1074/jbc.M117.784546

González, V., Bustos, P., Ramírez-Romero, M., Medrano-Soto, A., Salgado, H., Hernández-González, I., et al. (2003). The mosaic structure of the symbiotic plasmid of *Rhizobium etli* CFN42 and its relation to other symbiotic genome compartments. *Genome Biol.* 4:R36. doi: 10.1186/gb-2003-4-6-r36

González, V., Santamaría, R. I., Bustos, P., Hernández-González, I., Medrano-Soto, A., Moreno-Hagelsieb, G., et al. (2006). The partitioned *Rhizobium etli* genome: genetic and metabolic redundancy in seven interacting replicons. *Proc. Natl. Acad. Sci. U. S. A.* 103, 3834–3839. doi: 10.1073/pnas.0508502103

Hérouart, D., Baudouin, E., Frendo, P., Harrison, J., Santos, R., Jamet, A., et al. (2002). Reactive oxygen species, nitric oxide and glutathione: a key role in the establishment of the legume-rhizobium symbiosis? *Plant Physiol. Biochem.* 40, 40, 619–624. doi: 10.1016/S0981-9428(02)01415-8

Hertz, G. Z., Hartzell, G. W., and Stormo, G. D. (1990). Identification of consensus patterns in unaligned DNA sequences known to be functionally related. *Comput. Appl. Biosci.* 6, 81–92. Available at: http://www.ncbi.nlm.nih.gov/pubmed/2193692 (Accessed March 14, 2017).

Hu, H., Liu, S., Yang, Y., Chang, W., and Hong, G. (2000). In *Rhizobium leguminosarum*, NodD represses its own transcription by competing with RNA polymerase for binding sites. *Nucleic Acids Res.* 28, 2784–2793. doi: 10.1093/nar/28.14.2784

Ihuegbu, N. E., Stormo, G. D., and Buhler, J. (2012). Fast, sensitive discovery of conserved genome-wide motifs. *J. Comput. Biol.* 19, 139–147. doi: 10.1089/cmb.2011.0249

Kanehisa, M. (2017). "Enzyme annotation and metabolic reconstruction using KEGG," in *Protein Function Prediction. Methods in Molecular Biology. Vol. 1611*. ed. Kihara, D. (New York, NY: Humana Press).

Kanehisa, M., Sato, Y., and Morishima, K. (2016). BlastKOALA and GhostKOALA: KEGG tools for functional characterization of genome and metagenome sequences. *J. Mol. Biol.* 428, 726–731. doi: 10.1016/j.jmb.2015.11.006

Kaur, G., Kaundal, S., Kapoor, S., Grimes, J. M., Huiskonen, J. T., and Thakur, K. G. (2018). *Mycobacterium tuberculosis* CarD, an essential global transcriptional regulator forms amyloid-like fibrils. *Sci. Rep.* 8:10124. doi: 10.1038/s41598-018-28290-4

Khatabi, B., Gharechahi, J., Ghaffari, M. R., Liu, D., Haynes, P. A., McKay, M. J., et al. (2019). Plant–microbe symbiosis: what has proteomics taught us? *Proteomics* 19:1800105. doi: 10.1002/pmic.201800105

Landeta, C., Dávalos, A., Cevallos, M. Á., Geiger, O., Brom, S., and Romero, D. (2011). Plasmids with a chromosome-like role in rhizobia. *J. Bacteriol.* 193, 1317–1326. doi: 10.1128/JB.01184-10

Lardi, M., and Pessi, G. (2018). Functional genomics approaches to studying symbioses between legumes and nitrogen-fixing rhizobia. *High Throughput* 7:15. doi: 10.3390/ht7020015

Larrainzar, E., and Wienkoop, S. (2017). A proteomic view on the role of legume symbiotic interactions. *Front. Plant Sci.* 8:1267. doi: 10.3389/fpls.2017.01267

Lê, S., Josse, J., Rennes, A., and Husson, F. (2008). FactoMineR: an R package for multivariate analysis. *J. Stat. Softw.* 25, 1–18. doi: 10.18637/jss.v025.i01

Liu, A., Contador, C. A., Fan, K., and Lam, H.-M. (2018). Interaction and regulation of carbon, nitrogen, and phosphorus metabolisms in root nodules of legumes. *Front. Plant Sci.* 9:1860. doi: 10.3389/fpls.2018.01860

Lopez, O., Morera, C., Miranda-Rios, J., Girard, L., Romero, D., and Soberon, M. (2001). Regulation of gene expression in response to oxygen in *Rhizobium etli*: role of FnrN in *fixNOQP* expression and in symbiotic nitrogen fixation. *J. Bacteriol.* 183, 6999–7006. doi: 10.1128/JB.183.24.6999-7006.2001

Ma, H. W., Buer, J., and Zeng, A. P. (2004). Hierarchical structure and modules in the *Escherichia coli* transcriptional regulatory network revealed by a new top-down approach. *BMC Bioinform.* 5, 1–10. doi: 10.1186/1471-2105-5-199

Madariaga-Navarrete, A., Rodríguez-Pastrana, B. R., Villagómez-Ibarra, J. R., Acevedo-Sandoval, O. A., Perry, G., and Islas-Pelcastre, M. (2017). Bioremediation model for atrazine contaminated agricultural soils using phytoremediation (using *Phaseolus vulgaris* L.) and a locally adapted microbial consortium. *J. Environ. Sci. Heal. Part B Pestic. Food Contam. Agric. Wastes* 52, 367–375. doi: 10.1080/03601234.2017.1292092

Maere, S., Heymans, K., and Kuiper, M. (2005). BiNGO: a Cytoscape plugin to assess overrepresentation of gene ontology categories in biological networks. *Bioinformatics* 21, 3448–3449. doi: 10.1093/bioinformatics/bti551

Mao, C., Downie, J. A., and Hong, G. (1994). Two inverted repeats in the *nodD* promoter region are involved in *nodD* regulation in *Rhizobium leguminosarum*. *Gene* 145, 87–90. doi: 10.1016/0378-1119(94)90327-1

McGuire, A. M., Hughes, J. D., and Church, G. M. (2000). Conservation of DNA regulatory motifs and discovery of new motifs in microbial genomes. *Genome Res.* 10, 744–757. doi: 10.1101/GR.10.6.744

Meneses, N., Taboada, H., Dunn, M. F. M. F., Vargas, M., Del, C. M. C., Buchs, N., et al. (2017). The naringenin-induced exoproteome of *Rhizobium etli* CE3. *Arch. Microbiol.* 199, 737–755. doi: 10.1007/s00203-017-1351-8

Miranda-Ríos, J., Morera, C., Taboada, H., Dávalos, A., Encarnación, S., Mora, J., et al. (1997). Expression of thiamin biosynthetic genes (*thiCOGE*) and production of symbiotic terminal oxidase *cbb3* in *Rhizobium etli*. *J. Bacteriol.* 179, 6887–6893. doi: 10.1128/jb.179.22.6887-6893.1997

Newman, J. D., Diebold, R. J., Schultz, B. W., and Noel, K. D. (1994). Infection of soybean and pea nodules by *Rhizobium* spp. purine auxotrophs in the presence of 5-aminoimidazole-4-carboxamide riboside. *J. Bacteriol.* 176, 3286–3294. doi: 10.1128/jb.176.11.3286-3294.1994

Nguyen, N. T. T., Contreras-Moreira, B., Castro-Mondragon, J. A., Santana-Garcia, W., Ossio, R., Robles-Espinoza, C. D. D. D., et al. (2018). RSAT 2018: regulatory sequence analysis tools 20th anniversary. *Nucleic Acids Res.* 46, W209–W214. doi: 10.1093/nar/gky317

Novichkov, P. S., Rodionov, D. A., Stavrovskaya, E. D., Novichkova, E. S., Kazakov, A. E., Gelfand, M. S., et al. (2010). RegPredict: an integrated system for regulon inference in prokaryotes by comparative genomics approach. *Nucleic Acids Res.* 38, W299–W307. doi: 10.1093/nar/gkq531

Oldroyd, G. E. D., Murray, J. D., Poole, P. S., and Downie, J. A. (2011). The rules of engagement in the legume-rhizobial symbiosis. *Annu. Rev. Genet.* 45, 119–144. doi: 10.1146/annurev-genet-110410-132549

Pankhurst, C. E. (1977). Symbiotic effectiveness of antibiotic-resistant mutants of fast-and slow-growing strains of *Rhizobium* nodulating lotus species. *Can. J. Microbiol.* 23, 1026–1033. doi: 10.1139/m77-152

Perez-Riverol, Y., Bai, J., Bandla, C., Hewapathirana, S., García-Seisdedos, D., Kamatchinathan, S., et al. (2022). The PRIDE database resources in 2022: a hub for mass spectrometry-based proteomics evidences. *Nucleic Acids Res.* 50, D543–D552. doi: 10.1093/nar/gkab1038

Prell, J., White, J. P., Bourdes, A., Bunnewell, S., Bongaerts, R. J., and Poole, P. S. (2009). Legumes regulate *rhizobium* bacteroid development and persistence by the supply of branched-chain amino acids. *Proc. Natl. Acad. Sci. U. S. A.* 106, 12477–12482. doi: 10.1073/pnas.0903653106

Putty, K., Marcus, S. A., Mittl, P. R. E., Bogadi, L. E., Hunter, A. M., Arur, S., et al. (2013). Robustness of *Helicobacter pylori* infection conferred by context-variable

redundancy among cysteine-rich paralogs. *PLoS One* 8:e59560. doi: 10.1371/journal.pone.0059560

Rascio, N., and La Rocca, N. (2013). *Biological Nitrogen Fixation. Reference Module in Earth Systems and Environmental Sciences* (New, York: Elsevier). doi:10.1016/B978-0-12-409548-9.00685-0.

Resendis-Antonio, O., Freyre-González, J. A., Menchaca-Méndez, R., Gutiérrez-Ríos, R. M., Martínez-Antonio, A., Ávila-Sánchez, C., et al. (2005). Modular analysis of the transcriptional regulatory network of *E. coli*. *Trends Genet.* 21, 16–20. doi: 10.1016/j.tig.2004.11.010

Resendis-Antonio, O., Hernández, M., Mora, Y., and Encarnación, S. (2012). Functional modules, structural topology, and optimal activity in metabolic networks. *PLoS Comput. Biol.* 8:e1002720. doi: 10.1371/journal.pcbi.1002720

Resendis-Antonio, O., Hernández, M., Salazar, E., Contreras, S., Batallar, G. M., Mora, Y., et al. (2011). Systems biology of bacterial nitrogen fixation: high-throughput technology and its integrative description with constraint-based modeling. *BMC Syst. Biol.* 5:120. doi: 10.1186/1752-0509-5-120

Rodriguez-Llorente, I., Caviedes, M. A., Dary, M., Palomares, A. J., Cánovas, F. M., and Peregrín-Alvarez, J. M. (2009). The Symbiosis Interactome: a computational approach reveals novel components, functional interactions and modules in *Sinorhizobium meliloti*. *BMC Syst. Biol.* 3, 1–18. doi: 10.1186/1752-0509-3-63

Romanov, V. I., Hernandez-Lucas, I., and Martinez-Romero, E. (1994). Carbon metabolism enzymes of *Rhizobium tropici* cultures and bacteroids. *Appl. Environ. Microbiol.* 60, 2339–2342. doi: 10.1128/aem.60.7.2339-2342.1994

Rutten, P. J., and Poole, P. S. (2019). Oxygen regulatory mechanisms of nitrogen fixation in rhizobia. *Adv. Microb. Physiol.* 75, 325–389. doi: 10.1016/bs.ampbs.2019.08.001

Sá, C., Matos, D., Pires, A., Cardoso, P., and Figueira, E. (2020). Airborne exposure of *Rhizobium leguminosarum* strain E20-8 to volatile monoterpenes: effects on cells challenged by cadmium. *J. Hazard. Mater.* 388:121783. doi: 10.1016/j.jhazmat.2019.121783

Salazar, E., Javier Díaz-Mejía, J., Moreno-Hagelsieb, G., Martínez-Batallar, G., Mora, Y., Mora, J., et al. (2010). Characterization of the Nif A-RpoN regulon in *Rhizobium etli* in free life and in symbiosis with *Phaseolus vulgaris*. *Appl. Environ. Microbiol.* 76, 4510–4520. doi: 10.1128/AEM.02007-09

Sarma, A. D., and Emerich, D. W. (2005). Global protein expression pattern of *Bradyrhizobium japonicum* bacteroids: a prelude to functional proteomics. *Proteomics* 5, 4170–4184. doi: 10.1002/pmic.200401296

Sarma, A. D., and Emerich, D. W. (2006). A comparative proteomic evaluation of culture grown vs nodule isolated *Bradyrhizobium japonicum*. *Proteomics* 6, 3008–3028. doi: 10.1002/pmic.200500783

Stekhoven, D. J., and Bühlmann, P. (2012). MissForest: non-parametric missing value imputation for mixed-type data. *Bioinformatics* 28, 112–118. doi: 10.1093/BIOINFORMATICS/BTR597

Taboada, H., Meneses, N., Dunn, M. F., Vargas-Lagunas, C., Buchs, N., Castro-Mondragon, J. A., et al. (2018). Proteins in the periplasmic space and outer membrane vesicles of *Rhizobium etli* CE3 grown in minimal medium are largely distinct and change with growth phase. *Microbiology* 165, 638–650. doi: 10.1099/mic.0.000720

Taboada-Castro, H., Castro-Mondragón, J. A., Aguilar-Vera, A., Hernández-Álvarez, A. J., van Helden, J., and Encarnación-Guevara, S. (2020). RhizoBindingSites, a database of DNA-binding motifs in nitrogen-fixing bacteria inferred using a footprint discovery approach. *Front. Microbiol.* 11:567471. doi: 10.3389/fmicb.2020.567471

Tsoy, O. V., Ravcheev, D. A., Cuklina, J., and Gelfand, M. S. (2016). Nitrogen fixation and molecular oxygen: comparative genomic reconstruction of transcription regulation in Alphaproteobacteria. *Front. Microbiol.* 7:1343. doi: 10.3389/fmicb.2016.01343

Valderrama, B., Dávalos, A., Girard, L., Morett, E., Mora, J., Valderrama, B., et al. (1996). Regulatory proteins and cis-acting elements involved in the transcriptional control of *Rhizobium etli* reiterated *nifH* genes. *J. Bacteriol.* 178, 3119–3126. doi: 10.1128/jb.178.11.3119-3126.1996

Van Helden, J., André, B., and Collado-Vides, J. (1998). Extracting regulatory sites from the upstream region of yeast genes by computational analysis of oligonucleotide frequencies. *J. Mol. Biol.* 281, 827–842. doi: 10.1006/jmbi.1998.1947

Villaseñor, T., Brom, S., Dávalos, A., Lozano, L., Romero, D., Los Santos, A. G., et al. (2011). Housekeeping genes essential for pantothenate biosynthesis are plasmid-encoded in *Rhizobium etli* and *rhizobium leguminosarum*. *BMC Microbiol.* 11:66. doi: 10.1186/1471-2180-11-66

Wacek, T. J., and Brill, W. J. (1976). Simple, rapid assay for screening nitrogen-fixing ability in soybean1. *Crop Sci.* 16, 519–523. doi: 10.2135/cropsci1976.0011183X001600040020x

Weiss, L. A., Harrison, P. G., Nickels, B. E., Glickman, M. S., Campbell, E. A., Darst, S. A., et al. (2012). Interaction of CarD with RNA polymerase mediates *Mycobacterium tuberculosis* viability, rifampin resistance, and pathogenesis. *J. Bacteriol.* 194, 5621–5631. doi: 10.1128/JB.00879-12

Zorro-Aranda, A., Escorcia-Rodríguez, J. M., González-Kise, J. K., and Freyre-González, J. A. (2022). Curation, inference, and assessment of a globally reconstructed gene regulatory network for *Streptomyces coelicolor*. *Sci. Rep.* 12:2840. doi: 10.1038/S41598-022-06658-X

Zuleta, L. F. G., Cunha, C. D. O., de Carvalho, F. M., Ciapina, L. P., Souza, R. C., Mercante, F. M., et al. (2014). The complete genome of *Burkholderia phenoliruptrix* strain BR3459a, a symbiont of *Mimosa flocculosa*: highlighting the coexistence of symbiotic and pathogenic genes. *BMC Genomics* 15, 1–19. doi: 10.1186/1471-2164-15-535

frontiers | Frontiers in Microbiology

TYPE Original Research
PUBLISHED 24 October 2022
DOI 10.3389/fmicb.2022.917382

Check for updates

OPEN ACCESS

EDITED BY
Víctor Manuel Ruíz-Valdiviezo,
Tecnológico Nacional de México/Instituto Tecnológico de Tuxtla Gutiérrez, Mexico

REVIEWED BY
Jesús Muñoz-Rojas,
Meritorious Autonomous University of Puebla, Mexico
Pradeep Kumar Rai,
Indian Farmers Fertilizer Cooperative Limited, India

*CORRESPONDENCE
Bingxue Li
libingxue@syau.edu.cn
Ning Zhang
zhangning@syau.edu.cn

†These authors have contributed equally to this work

SPECIALTY SECTION
This article was submitted to Microbe and Virus Interactions With Plants, a section of the journal Frontiers in Microbiology

RECEIVED 11 April 2022
ACCEPTED 10 October 2022
PUBLISHED 24 October 2022

CITATION
Deng C, Liang X, Zhang N, Li B, Wang X and Zeng N (2022) Molecular mechanisms of plant growth promotion for methylotrophic *Bacillus aryabhattai* LAD. *Front. Microbiol.* 13:917382. doi: 10.3389/fmicb.2022.917382

COPYRIGHT
© 2022 Deng, Liang, Zhang, Li, Wang and Zeng. This is an open-access article distributed under the terms of the Creative Commons Attribution License (CC BY). The use, distribution or reproduction in other forums is permitted, provided the original author(s) and the copyright owner(s) are credited and that the original publication in this journal is cited, in accordance with accepted academic practice. No use, distribution or reproduction is permitted which does not comply with these terms.

Molecular mechanisms of plant growth promotion for methylotrophic *Bacillus aryabhattai* LAD

Chao Deng[1†], Xiaolong Liang[2†], Ning Zhang[3*], Bingxue Li[1*], Xiaoyu Wang[1] and Nan Zeng[1]

[1]College of Land and Environment, Shenyang Agricultural University, Shenyang, China, [2]Key Laboratory of Pollution Ecology and Environmental Engineering, Institute of Applied Ecology, Chinese Academy of Sciences, Shenyang, China, [3]College of Bioscience and Biotechnology, Shenyang Agricultural University, Shenyang, China

Plant growth-promoting rhizobacteria (PGPR) can produce hormone-like substances, promote plant nutrient uptake, enhance plant resistance, inhibit the growth of pathogenic bacteria, and induce plant resistance to biotic and abiotic stresses. *Bacillus* is one of the most studied genera that promote plant root development. Since its discovery in 2009, *B. aryabhattai* has shown promising properties such as promoting plant growth and improving crop yield. However, the mechanisms of *B. aryabhattai* promoting plant growth remain to be investigated. In this study, the chromosome of *B. aryabhattai* strain LAD and five plasmids within the cell were sequenced and annotated. The genome, with a length of 5,194,589bp and 38.12% GC content, contains 5,288 putative protein-coding genes, 39 rRNA, and 112 tRNA. The length of the five plasmids ranged from 116,519 to 212,484bp, and a total of 810 putative protein-coding genes, 4 rRNA, and 32 tRNA were predicted in the plasmids. Functional annotation of the predicted genes revealed numerous genes associated with indole-3 acetic acid (IAA) and exopolysaccharides (EPSs) biosynthesis, membrane transport, nitrogen cycle metabolism, signal transduction, cell mobility, stress response, and antibiotic resistance on the genome which benefits the plants. Genes of carbohydrate-active enzymes were detected in both the genome and plasmids suggesting that LAD has the capacity of synthesizing saccharides and utilizing organic materials like root exudates. LAD can utilize different carbon sources of varied carbon chain length, i.e., methanol, acetate, glycerol, glucose, sucrose, and starch for growth and temperature adaptation suggesting a high versatility of LAD for thriving in fluctuating environments. LAD produced the most EPSs with sucrose as sole carbon source, and high concentration of IAA was produced when the maize plant was cultivated with LAD, which may enhance plant growth. LAD significantly stimulated the development of the maize root. The genome-based information and experimental evidence demonstrated that LAD with diverse metabolic capabilities and positive interactions with plants has tremendous potential for adaptation to the dynamic soil environments and promoting plant growth.

KEYWORDS

carbohydrate-active enzymes, sequencing, rhizosphere, growth promoting, indole acetic acid

Introduction

Plant growth and development is highly dependent on the interactions with other living organisms that habitat the soil ecosystem. These interactions are very complex and critical for maintaining the biodiversity in the below-ground system (Lau and Lennon, 2011; Bever et al., 2013; Shao et al., 2018). Microbes are the most abundant and diverse entities in soil and can directly participate in ecological processes and nutrient cycling. The role of soil microbial community in soil ecosystem functioning and plant production has been widely investigated *via* isolation of culturable microbes and culture-independent techniques (Liu et al., 2019; Roy et al., 2020). However, the soil environment is extremely heterogeneous imposing great challenges on studies of soil microbial ecology.

Roots harbor a rich abundance of biomass and are the crucial organ of the plant to absorb water and nutrients for the plant. Rhizosphere the narrow region immediately adjacent to the root is the plant root-soil interface and is the hot spot for microbial interactions and cross-kingdom interactions between plants and microbes (Chaparro et al., 2014; Korenblum et al., 2020). Rhizosphere microbes and the plant may form symbiotic relationships in which the root microbiome utilizes root exudates and secretes compounds benefiting plant growth (Berendsen et al., 2012). Rhizosphere microbes may synthesize antibiotics as required by the plant for suppression of soil-borne pathogens and ultimately enhance the plant health (Mendes et al., 2013; Lazcano et al., 2021). Other rhizosphere microbiome-plant mutualistic interactions include microbiome fixing and providing essential elements (e.g., nitrogen) for plant growth (Moreau et al., 2019). Rhizosphere microbiome may also induce systemic root exudation of metabolites and mediate root-root signaling promoting soil conditioning (Korenblum et al., 2020). Meanwhile, many environmental and biotic factors can influence rhizosphere microbiome-plant interactions making it more complicated to study the mechanism of different rhizosphere microbes promoting plant growth.

Rhizospheric microorganisms could produce hormone-like substances, then promote plant growth and nutrient uptake, inhibit the growth of pathogenic bacteria and induce plant resistance to biotic and abiotic stresses (Ahmed and Hasnain, 2014). For example, inoculation with typical beneficial microbial mycorrhizal fungi not only promotes the secretion of organic acids and phosphatases from the roots of symbiotic plants, but also enhances the ability of plant to activate insoluble phosphates in the soil and promotes the uptake of water and minerals, especially phosphate (Berta, 2000; Erik et al., 2000; Philippe, 2001; Maria, 2005). *Bacillus amylolyticus* strain B3 harbors functional genes capable of directly promoting crop growth, like *yhcX* and *ysnE*, key genes for plant growth hormone (IAA) synthesis; and *AlsS*, *AlsD*, and *AlsR*, synthase genes related to the volatile disease-promoting substance 2,3-butanediol. The phytase synthesis gene *phy* is present intact in the B3 genome, and phytase can catalyze the degradation of phytic acid into inositol, facilitating plant uptake and utilization of nutrients from soil (Idriss et al., 2002; Zhang et al., 2010). The exocrine secretion of *Bacillus subtilis* BS-2 promotes rice growth, increases chlorophyll content in the crop, slows membrane lipid peroxidation in rice, and promotes indoleacetic acid production in the plant (Ma et al., 2018). Bacterial colonization can trigger plant immune reaction, and the interaction between beneficial bacteria and plant immune system is essential for efficient bacterial colonization, survival, and plant growth promoting hormone production (Tzipilevich et al., 2021).

Bacillus is the one of the most studied genera among the plant growth promoting rhizobacteria and shows tremendous potential in promoting plant growth (Chen et al., 2007; Tahir et al., 2017; Backer et al., 2018). *Bacillus aryabhattai* are widely distributed in nature but were only discovered in 2009 (Shivaji et al., 2009). More strains of *B. aryabhattai* were isolated from various environments including plant roots, and evaluations of this rhizosphere bacteria have revealed promising properties of this *Bacillus* species for promoting plant growth and improving crop yields thus having attracted plenty of attention from researchers (Bhattacharyya et al., 2017; Park et al., 2017; Ghosh et al., 2018). Mehmood et al. (2021) found that *B. aryabhattai* promoted wheat growth and reduced the effects of salt stress on wheat. However, the mechanism of this rhizobacteria species promoting plant growth remains to be investigated. With the development of sequencing technology, whole genome sequencing of the isolated microbial strains has been widely used to reveal the potential functions of the microbes in enhancing the plant performance (Chu et al., 2020; Chen et al., 2022).

In a recent study, an excellent plant inter-rhizosphere strain, *B. aryabhattai* LAD, was isolated from maize rhizosphere, and the impact of LAD on rhizosphere microbial structure was also explored in the previous study (Deng et al., 2022). LAD showed promising plant growth promoting properties, including nitrogen fixation and phosphorus solubilization and IAA production. Here, we aimed to reveal the genes related to plant growth-promoting functions of this strain through whole genome sequencing and investigate the genetic differences between this strain and similar plant growth promoting rhizobacterial strains *via* comparative genomics. The metabolic and phenotypic traits and habitat-specific adaptations of this strain to maize root promotion were also investigated.

Materials and methods

Total DNA extraction and whole genome sequencing

The strain LAD was isolated from maize rhizosphere in our lab, and initial characterization of the newly isolated bacterial strain was performed and the effects of LAD on corn seedlings were also evaluated. In this study, LAD was grown in its optimum

growth medium containing 20 g L^{-1} sucrose, 2 g L^{-1} beef extract, 0.4 g L^{-1} KH_2PO_4, 0.4 g L^{-1} $MgSO_4 \cdot 7H_2O$, 0.4 g L^{-1} NaCl, 0.4 g L^{-1} $CaSO_4 \cdot 2H_2O$, and 2 g L^{-1} $CaCO_3$ at 180 rpm and 37°C. The bacterial cells were harvested at the late exponential phase (around 22 h) for total DNA extraction with the extraction kit. The extracted DNA was quantified with Nanodrop 2000 spectrophotometer (Thermo Fisher Scientific, Waltham, MA, United States) and sent out to Shanghai Personal Biotechnology Co., Ltd. for next-generation sequencing of the total DNA. Whole genome sequencing of LAD was performed using on PacBio Sequel (Pacific Biosciences of California, Inc., Menlo Park, CA, United States) and Illumina NovaSeq (Illumina, Inc., San Diego, CA, United States) sequencing platforms, respectively.

Whole genome annotation

The obtained sequence reads from PacBio platform were assembled into contigs using HGAP4 WGS-Assembler 8.2 and CANU (Chin et al., 2016; Koren et al., 2017). The Illunima reads were employed for correction of the assembled contigs with Pilon 1.22 to get the final complete genome (Walker et al., 2014). GeneMarkS was used for finding protein-coding genes *via* GeneMark.hmm program (Besemer et al., 2001). Transfer RNAs (tRNAs) were predicted using tRNAscan-SE, and the prediction of other non-coding RNAs was performed in Rfam (Lowe and Eddy, 1997; Kalvari et al., 2018). Clustered regularly interspaced short palindromic repeats (CRISPRs) were predicted using CRISPRFinder program (Grissa et al., 2007). PHASTER (Phage Search Tool Enhanced Release) was used for detection of prophages on the genome (Arndt et al., 2016).

Genomic comparisons

Reference genome sequences of other *Bacillus* strains were retrieved from NCBI GenBank database for comparative genomic analysis of *B. aryabhattai* LAD (Table 1). *B. aryabhattai* is a homotypic synonym of *Priestia aryabhattai*. Pairwise genome comparisons were performed on JSpeciesWS which evaluates whole genome homologies *via* BLAST alignments for determination of the average nucleotide identity (ANI) between genome sequences (Richter et al., 2016). The bacterial pan genome analysis (BPGA) pipeline was used to identify the orthologous pan genome profile among the genomes of the *B. aryabhattai* strains (Chaudhari et al., 2016). Core genome (the set of shared genes by all strains), accessory genome (genes shared by different strains but not by all strains), and unique genes (exclusively belonging to one strain), and pan genome (non-homologous genes) were identified with BPGA. Carbohydrate-active enzymes (CAZy) were characterized based on the CAZy database (Lombard et al., 2014). The whole genomic sequence data of *B. aryabhattai* LAD was deposited to NCBI GenBank, with the accession number of GCA_017743055.1.

TABLE 1 Genome information of 19 strains used in this study.

Organism	GenBank accession	Level	Size (Mb)	Gene
B. aryabhattai B8W22	GCF_000956595.1	Contig	1.72	5,135
B. cereus group sp. N11	GCF_016483605.1	Contig	1.99	4,923
B. cereus group sp. N6	GCF_016483705.1	Contig	1.95	5,104
B. megaterium DSM319	GCF_000025805.1	Complete	1.7	4,987
B. megaterium NCT-2	GCF_000334875.3	Complete	1.91	4,640
B. megaterium ATCC 14581	GCF_006094495.1	Complete	1.9	4,908
Bacillus sp. AM1(2019)	GCF_009906915.1	Complete	1.5	5,179
B. aryabhattai K13	GCF_002688605.1	Complete	1.8	4,844
B. aryabhattai LAD	GCA_017743055.1	Complete	1.64	5,198
B. aryabhattai AB211	GCF_001858395.1	Scaffold	1.85	4,682
B. aryabhattai AFS075785	GCF_002569785.1	Scaffold	1.78	4,386
B. aryabhattai FJ-6	GCF_013372535.1	Contig	1.78	4,153
B. aryabhattai B14	GCF_002167185.1	Contig	1.6	5,006
B. megaterium BIM B-1314D	GCF_013389435.1	Complete	2	4,822
B. aryabhattai S00060	GCF_014138775.1	Scaffold	2.02	5,346
B. aryabhattai G25-109	GCF_015845475.1	Contig	1.8	5,378
B. megaterium CDC 2008724142	GCF_017086565.1	Complete	1.99	5,274
B. aryabhattai ME39	GCF_903971025.1	Contig	1.9	5,611
B. megaterium H2	GCF_017352315.1	Complete	2.12	5,322

Bacillus aryabhattai LAD growth under different temperatures and carbon sources

The growth of LAD on different carbon sources and at different temperatures was evaluated with Epoch 2 microplate spectrophotometer (BioTek Instruments Inc., Winooski, VT, United States). LAD cells were inoculated in LB medium and grown at 37°C overnight. The LAD culture was used as inoculum (1%) for growth in the optimum growth medium, but the carbon source in the medium was the same concentration (2%, m v^{-1}) of sodium acetate, glycerol, glucose, sucrose, or starch. The growth of LAD on methanol was also examined in the optimum medium but with the carbon source replaced with 0.5% (v v^{-1}) methanol. The growth curves of LAD populations on different carbon sources and at different temperatures (20°C and 37°C) were obtained by culturing the cells in 24-well plates and analyzed at a 1-h interval in the Epoch 2 microplate spectrophotometer. Each treatment included three replicates, and the mean cell density was used to plot the growth curves.

Indole-3-acetic acid production by *Bacillus aryabhattai* LAD

The maize seeds (Dongdan 1,331) were immersed in 10^5 CFU ml^{-1} LAD cell suspensions and cultivated in the artificial climate room for 8 days. As the control treatment, the maize seeds were immersed in sterilized water and cultured for 8 days under

the same conditions. Each treatment included three replicates, and *t*-test was used to reveal the statistical differences between LAD treatment and control. The plant was removed after cultivation, and the liquid culture was concentrated by rotary evaporation and was archived for later use. Liquid chromatography system of Waters ACQUITY UPLC (Milford, MA, USA) with a liquid chromatography column (182.1 mm × 50 mm i.d., 1.7 μm) was used to determine the amount of the produced IAA (Fu et al., 2012). IAA was isolated in a mobile phase consisting of methanol solution (mobile phase A) and 0.1% formic acid aqueous solution (mobile phase B). The gradient elusion was run at a flow rate of 0.2 ml min^{-1} with initial 20% mobile phase A which was increased to 80% in the next 12 min. The volume fraction of mobile phase A was reduced from 80 to 20% in the time range of 12 to 16 min. The injection volume for all samples was 3 μl and the column temperature was 40°C. The mass spectrometer that affiliated with the UPLC system used an electrospray ion source, with a capillary voltage of 0.8 KV in positive ion mode (ESI+), a taper voltage of 25 V, a dissolvent temperature of 650°C, a dissolvent gas flow rate of 1,000 l h^{-1}, and a conical hole back blow 51 h^{-1}. The collision voltage was set 30 V at 176 > 103 and 15 V at 176 > 130.

Production of exopolysaccharides

LAD cells were grown in LB medium at 37°C for 24 h before the cells were transferred into the optimum growth medium with different carbon sources, i.e., methanol (0.5, v v^{-1}), sodium acetate (2%, m v^{-1}), glycerol (2%, m v^{-1}), glucose (2%, m v^{-1}), sucrose (2%, m v^{-1}), and starch (2%, m v^{-1}), respectively. The bacterial cells were cultivated at 37°C with the EPSs production being evaluated at 24 and 72 h of the cultivation. For EPSs extraction, 10 ml bacterial culture was centrifuged at 5,000 rpm for 20 min, and the supernatant was transferred to a clean 50 ml centrifuge tube with 2-fold volume of 95% ethanol. The mixture was stirred using a glass rod until clear flocculent precipitation appeared. The mixture was stored at 4°C for 24 h before centrifugation at 10,000 rpm for 15 min. The extracted products, crude EPSs, were air dried at room temperature and weighed for determination of the EPSs production on different carbon sources.

Impacts of LAD on maize root development

LAD was cultivated in selective nutrient broth at 37°C for 72 h (until OD_{600nm} reached 1.4). The LAD cells were harvested by centrifugation and resuspended in sterile water, and the cell suspension was diluted to a final concentration of 10^5 CFU ml^{-1} using sterile water. The maize seeds were immersed in the diluted bacterial suspension for 24 h, after which the maize seeds were cultivated in laboratory hydroponics and in the field, respectively. In the control treatment, the maize seeds were soaked in the sterile water for 24 h before being cultivated in laboratory hydroponics and field. The root development of the maize seedlings in hydroponics was measured by a root system analyzer after 14 days, while measurement of the root development of each maize plant grown in field was performed after 60 days (Bucksch et al., 2014). The hydroponic and field cultivation for each treatment included 10 maize plants, respectively. Each treatment was repeated three times. Student's *t*-test was used to compare the root development under LAD treatment with that of the control to show the statistical differences.

Results

Functional annotation of *Bacillus aryabhattai* LAD whole genome

A total of 184,213 sequence reads was obtained in the next-generation sequencing. The *de novo* genome assembly using HGAP revealed a single circular chromosome genome and five circular plasmids in *B. aryabhattai* LAD. The newly sequenced genome was composed of 5,194,589 bp with a GC content of 38.12% (Figure 1). The five plasmids contained 212,484, 168,720, 137,532, 126,990, and 116,519 bp, respectively, with GC content ranging from 33.71 to 35.18%. The properties of the chromosome genome and plasmids are shown in Table 2. The genome contained 5,390 predicted genes, and the total length of the predicted genes was 4,303,422 genes accounting for 82.8% of the genome length. The five plasmids contained 246, 181, 165, 129, and 141 genes, respectively, with the coding percentage ranging from 66.7 to 73%. There were 112 tRNA genes and 39 rRNA genes on the chromosome genome. Fifteen genome islands (GIs), 4 CRISPRs, and 2 incomplete prophages were predicted on the genome of *B. aryabhattai* LAD. There were 13 5S rRNA genes (with an average length of 110 bp), 13 16S rRNA genes (average length of 1,549 bp), and 13 23S rRNA genes (average length of 2,932 bp) on the genome. The genomic annotation also revealed rRNA genes on plasmid1 and plasmid4. Specifically, one 5S rRNA gene of 108 bp was present on plasmid1, and there were one 5S rRNA gene (111 bp), one 16S rRNA gene (1,549 bp), and one 23S rRNA gene (2,932 bp) on plasmid4.

There were 148 CAZymes, including 35 glycosyltransferases (GTs), 1 polysaccharide lyases (PLs), 34 carbohydrate esterases (CEs), 12 auxiliary activities (AAs), 17 carbohydrate binding modules (CBMs), and 49 glycoside hydrolases (GHs) identified in the *B. aryabhattai* LAD chromosome genome *via* the CAZy annotation pipeline (Figure 2A). CAZymes were also present in two plasmids, with 1 GTs, 2 CEs, 2AAs, and 2GHs identified on plasmid 1, and 1 GTs and 1 GHs identified on plasmid 2. The eggNOG (evolutionary genealogy of genes: Non-supervised Orthologous Groups) annotation revealed an abundance of genes for basic cellular functions including amino acid transport and metabolism (381 genes, accounting for 7.07% of

the total gene abundance), carbohydrate transport and metabolism (305, 5.7%), inorganic ion transport and metabolism (268, 5%), energy production and conversion (249, 4.6%), cell wall/membrane/envelope biogenesis (202, 3.7%), signal transduction mechanisms (188, 3.5%), and replication, recombination and repair (166, 3.1%; Figure 2B). The Gene Ontology (GO) classification revealed that ion binding, oxidoreductase activity, and DNA binding were very active molecular functions, and cellular nitrogen compound metabolic process, biosynthetic process, small molecule metabolic process, and transport were major biological processes (Figure 2B). The analysis against the Comprehensive Antibiotic Resistance Database (CARD) identified 28 antibiotic resistance genes and 4 antibiotic biosynthesis genes on the genome and 3 more antibiotic resistance genes on the plasmids.

Dig of promoting growth genes

In the whole genome of LAD strain, there were many genes related to the promotion of plant growth, some of which are shown in the Table 3. Ten related genes were found to be involved in the Nitrogen metabolism pathway in LAD strains, and the *NifF* gene was found at chr_4496 and *NifU* gene at chr_5091. In the KEGG pathway of Tryptophan metabolism, 25 genes related to IAA synthesis were identified, including amidase *(amiE)*, which hydrolyzes indole-3-acetamide to indoleacetic acid, and aldehyde dehydrogenase *(ALDH)*, which hydrolyzes indole-3-acetaldehyde to indoleacetic acid. We identified 20 genes related to biofilm formation. Four genes encoding related proteins in LAD strains mapped to the KEGG pathway of phosphonate and phosphinate metabolism, including phosphoenolpyruvate phosphomutase *(pepM)*, phosphonopyruvate decarboxylase,

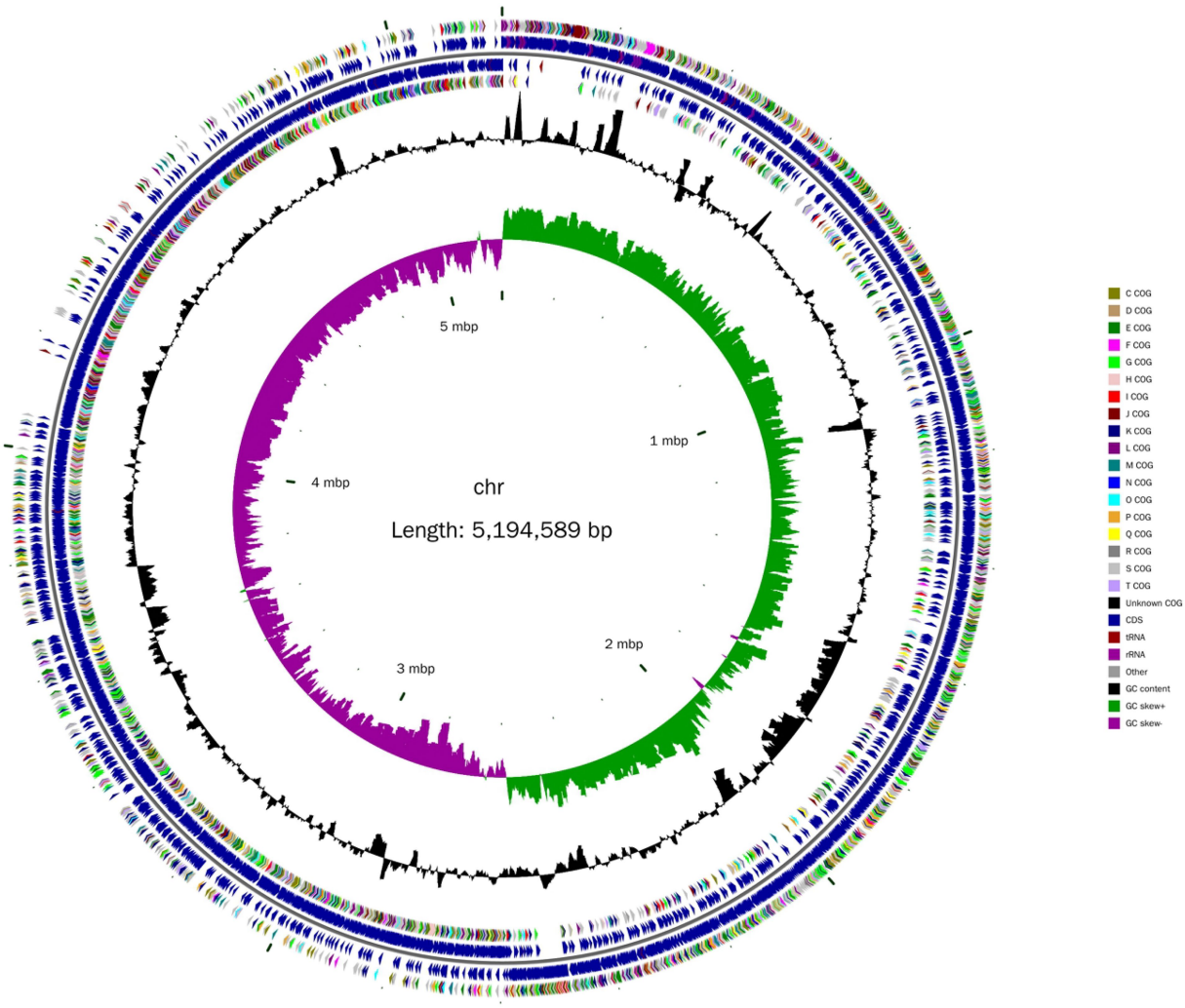

FIGURE 1
Circular chromosome diagram of *B. aryabhattai* LAD. From the inner circle to the outer circle, the information on each of the seven circles shows genome position, GC skew, GC content, coding sequence on the positive and strands (classified by Cluster of Orthologous Groups of protein), and the position of the coding sequence, tRNA and rRNA on the genome.

TABLE 2 Basic features of *B. aryabhattai* LAD chromosome genome and plasmids.

	Chromosome genome	Plasmid1	Plasmid2	Plasmid3	Plasmid4	Plasmid5
Length (bp)	5,194,589	212,484	168,720	137,532	126,990	116,519
GC content (%)	38.13	33.73	34.03	33.97	35.18	33.71
Gene number	5,390	246	181	165	129	141
Gene total length (bp)	4,303,422	141,816	123,078	96,090	88,983	79,167
Gene density (genes per kb)	1.038	1.158	1.073	1.2	1.016	1.21
Longest gene length (bp)	8,088	1,926	1,833	2,502	2,649	2,208
Gene average length (bp)	798.41	576.49	679.99	582.36	689.79	561.47
Gene length/genome (%)	82.84	66.74	72.95	69.87	70.07	67.94
GC content in gene region (%)	39.03	35.83	35.85	35.71	35.75	35.57
tRNA number	112	9	0	0	23	0
rRNA number	39	1	0	0	3	0

phosphoribosyl 1,2-cyclic phosphate phosphodiesterase (*phnP*) and phosphinothricin acetyltransferase (*pat*, *bar*), and a total of 53 phosphatase genes were identified in the LAD genome, mapping to 34 KEGG metabolic pathways. The extracellular polysaccharide production by LAD strains is closely related to carbohydrate metabolism, a total of 315 carbohydrate related genes were found for carbohydrate metabolism. The two-component regulatory system is a major mechanism for biotransduction and response to external environmental changes, which can sense environmental changes, regulate internal gene expression and play an important role in the survival and adaptation of microorganisms to different environments, and help microorganisms preserve their competitive advantage in the environment. A total of 98 KEGG pathways of two-component system were identified in LAD strains, including phosphate limitation, oxygen limitation, and temperature limitation system. A total of 106 genes related to the ABC transporters metabolic pathway were identified in LAD strains, including mineral and organic ion transporters, phosphate and amino acid transporters, peptide and nickel transporters, monoasccharide transporters, oligosaccharide, polyol, lipid transporters, metallic cation and iron-siderop hore and vitamin B12 transporters.

Comparative genomics analyses

The ANI between the whole genome sequences was measured by pairwise genome comparisons using JSpeciesWS Online Service to evaluate the homologies of the whole genomes and determine if the strains belong to the same species. The matrix of nucleotide identities between the whole genomes of the *Bacillus* strains was shown in Table 4. The ANI value of *B. aryabhattai* LAD based on BLAST against other *Bacillus* strains ranged from 67.7 to 95.6%, and the aligned percentage of the genome sequence ranged from 24.2 to 82.4%. The ANI values of *B. aryabhattai* LAD compared with other *B. aryabhattai* strains and *B. megaterium* strains were higher than 95%, which was the threshold identity for species boundaries.

PGAP pipeline was used to determine the pan-genome for *B. aryabhattai* LAD and 18 other *Bacillus* strains. The 19 compared *Bacillus* strains had a total pan-genome consisted of 94,898 putative protein-coding genes, and 1,111 of them (accounting for 1.17% the pan-genome) were core conserved genes across the genomes of the 19 strains (Figure 3). The number of strain-specific genes for each train ranged from 0 to 288, and *Priestia aryabhattai* FJ-16 had 288 strain-specific genes which was the highest among the 20 strains. The isolate in this study, *B. aryabhattai* LAD, had 1 strain-specific gene.

Highly reliable pan-genome analysis can be obtained by mathematical extrapolation with more than five genomes (Vernikos et al., 2015). The analysis *via* BPGA showed that the pan-genome of the 19 *Bacillus* genomes had a parameter γ of 0.4 in the reduced power-fit curve equation [f(x) = 4175n0.4] suggesting that the pan-genome was open (Figure 4). The exponential curve equation of core genome [f1(x) = 4228.01e-0.07] had a steep slope and reached a minimum of 1,111 gene families.

Bacillusaryabhattai LAD growth and production of IAA and EPSs

The growth of *B. aryabhattai* LAD on different carbon sources was evaluated with Epoch 2 microplate spectrophotometer at 20°C and 37°C. The results showed that LAD can utilize all the six carbon sources, including acetate, glycerol, glucose, sucrose, starch, and methanol, under appropriate temperatures (Figure 5). LAD had the best growth on sucrose at 37°C, and the bacterial density reached the highest OD_{600} value (as high as 1.9). Glucose and glycerol supported good LAD growth both at 20°C and 37°C, with the OD_{600} value of glucose reaching 1.4 at 20°C and 1.5 at 37°C, and the OD_{600} value of glycerol reaching 1.1 at 20°C and 1.8 at 37°C. Interestingly, LAD can efficiently utilize methanol as carbon source for growth with the ability to reach a high bacterial density (an OD_{600} value of 0.4 at 20°C and 0.2 at 37°C) which demonstrates that *B. aryabhattai* LAD belongs to methylotrophic bacteria. Acetate also supported the growth of LAD with the

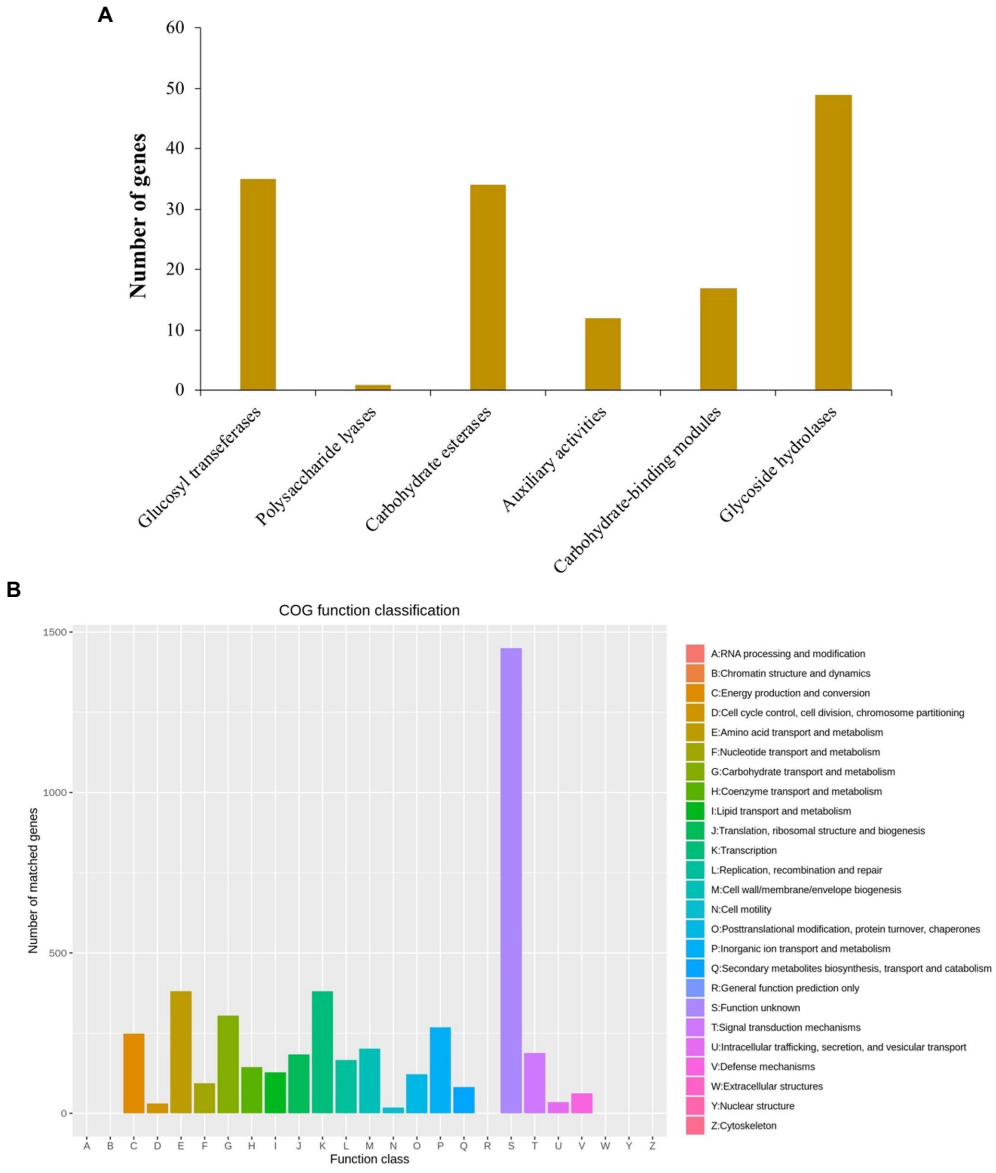

FIGURE 2
(A) Annotation of carbohydrate active enzymes (CAZymes) genes on *B. aryabhattai* LAD genome. The hmmscan program was used for estimation of the CAZy genes (alignment length>80 amino acids, *E*-value <1e-5; alignment length<80 amino acids, *E*-value <1e-3). **(B)** eggNOG annotation. The protein-coding gene sequences were compared to COG database using DIAMOND blastp (cutoff at 1e-6).

bacterial cell density reaching an OD_{600} of 0.4 at 37°C. LAD was able to utilize starch, but the bacterial growth rate and final cell density were both lower than using other carbon sources.

To examine the IAA-producing capacity of LAD, maize seedlings were cultivated with LAD cell suspensions (10^5 CFU ml^{-1}) and with the same volume of sterile water, respectively, for 8 days. The concentrations of IAA in the bacterial suspensions and water were measured with UPLC. The concentration of IAA in the LAD suspension was 0.191 ± 0.014 μg ml^{-1}, which was significantly higher than that in the hydroponic system without LAD (0.036 ± 0.0096 μg ml^{-1}; *t*-test, $p < 0.001$; Figure 6). The results showed that LAD can produce IAA or promote IAA secretion from maize roots. The test of EPSs in the LAD cultures showed that stable production of EPSs by LAD was only detected in medium with sucrose as the sole carbon source. The EPSs production in sucrose supplemented medium was 3.18 ± 0.0198 g L^{-1} at 24 h and 0.63 ± 0.0041 g L^{-1} at 72 h.

Impacts on maize root development

To investigate how LAD affects the maize root development, the maize seeds were treated with 10^5 CFU ml^{-1} LAD cell suspensions and grown in laboratory and filed soils, respectively.

TABLE 3 Genes related to the promotion of plant growth(partial).

KEGG pathway_ ID	Gene_ ID	Annotation information
K03839	chr_4996	*fldA*,*nifF*,*isiB*;flavodoxin I
K04488	chr_5091	*iscU*,*nifU*;nitrogen fixation protein *NifU* and related proteins
K01426	chr_999	E3.5.1.4, *amiE*; amidase
K00128	chr_2221	*ALDH*; aldehyde dehydrogenase (NAD+)
K01841	chr_754	*pepM*; phosphoenolpyruvate phosphomutase
K09459	chr_755	E4.1.1.82; phosphonopyruvate decarboxylase
K06167	chr_2553	*phnP*; phosphoribosyl 1,2-cyclic phosphate phosphodiesterase
K03823	chr_2685	*pat*; phosphinothricin acetyltransferase
K07658	chr_3082	*phoB1*, *phoP*; two-component system, *OmpR* family, alkaline phosphatase synthesis response regulator *PhoP*
K07658	chr_4881	*phoB1*, *phoP*; two-component system, *OmpR* family, alkaline phosphatase synthesis response regulator *PhoP*
K01113	chr_5,198	*phoD*; alkaline phosphatase D

TABLE 4 Average nucleotide identities (ANI) analysis for pairwise genome comparison between *B. aryabhattai* LAD and other *Bacillus* strains.

	B8W22	DSM 319	NCT-2	AB 211	B14	AFS075,785	N11	ATCC 14581	AM1 (2019)	FJ-6	BIM B-1314D	S00 060	G25-109	N11	LAD
B. aryabhattai B8W22	*	99.94	99.81	99.96	99.92	99.94	99.92	99.84	79.19	99.95	99.8	99.79	99.93	85.11	99.77
B. megaterium DSM319	99.94	*	99.88	99.93	99.87	99.92	99.95	99.9	79.09	99.93	99.86	99.81	99.94	85.39	99.83
B. megaterium NCT-2	99.81	99.88	*	99.86	99.64	99.77	99.85	99.96	79.6	99.78	99.95	99.91	99.9	86.24	99.91
B. aryabhattai AB211	99.96	99.93	99.86	*	99.89	99.93	99.91	99.87	79.34	99.93	99.84	99.83	99.93	85.21	99.82
B. aryabhattai B14	99.92	99.87	99.64	99.89	*	99.93	99.89	99.68	79.18	99.93	99.59	99.55	99.82	84.43	99.56
B. aryabhattai AFS075785	99.94	99.92	99.77	99.93	99.93	*	99.93	99.78	79.35	99.98	99.73	99.71	99.89	84.85	99.69
B. cereus group sp. N11	99.92	99.95	99.85	99.91	99.89	99.93	*	99.87	79.07	99.94	99.82	99.768	99.92	85.39	99.78
B. megaterium ATCC 14581	99.84	99.9	99.96	99.87	99.68	99.78	99.87	*	79.27	99.81	99.95	99.901	99.91	86.43	99.91
Bacillus sp. AM1(2019)	79.19	79.09	79.6	79.34	79.18	79.35	79.07	79.27	*	79.17	79.19	79.159	78.95	67.27	78.89
B. aryabhattai FJ-6	99.95	99.93	99.78	99.93	99.93	99.98	99.94	99.81	79.17	*	99.74	99.717	99.89	85	99.71
B. megaterium BIM B-1314D	99.8	99.86	99.95	99.84	99.59	99.73	99.82	99.95	79.19	99.74	*	99.96	99.91	86.29	99.95
B. aryabhattai S00060	99.79	99.81	99.91	99.83	99.55	99.71	99.77	99.9	79.16	99.72	99.96	*	99.91	86.17	99.93
B. aryabhattai G25-109	99.93	99.94	99.9	99.93	99.82	99.89	99.92	99.91	78.945	99.89	99.91	99.91	*	85.47	99.87
B. cereus group sp. N11	85.11	85.39	86.24	85.21	84.43	84.85	85.39	86.43	67.27	85	86.29	86.17	85.47	*	86.49
B. aryabhattai LAD	99.77	99.83	99.91	99.82	99.56	99.69	99.78	99.91	78.89	99.71	99.95	99.93	99.87	86.49	*

Asterisk indicates the same strain.

The roots were collected and analyzed with root analyzer. The laboratory cultivation results showed that the total root length, total root surface area and total root volume of the LAD treatment group is 97.0, 90.1, and 75.6% higher than that of the control, respectively (*t*-test, $p < 0.001$; Figure 7). Like the laboratory cultivation, the results of field experiments revealed an increase of

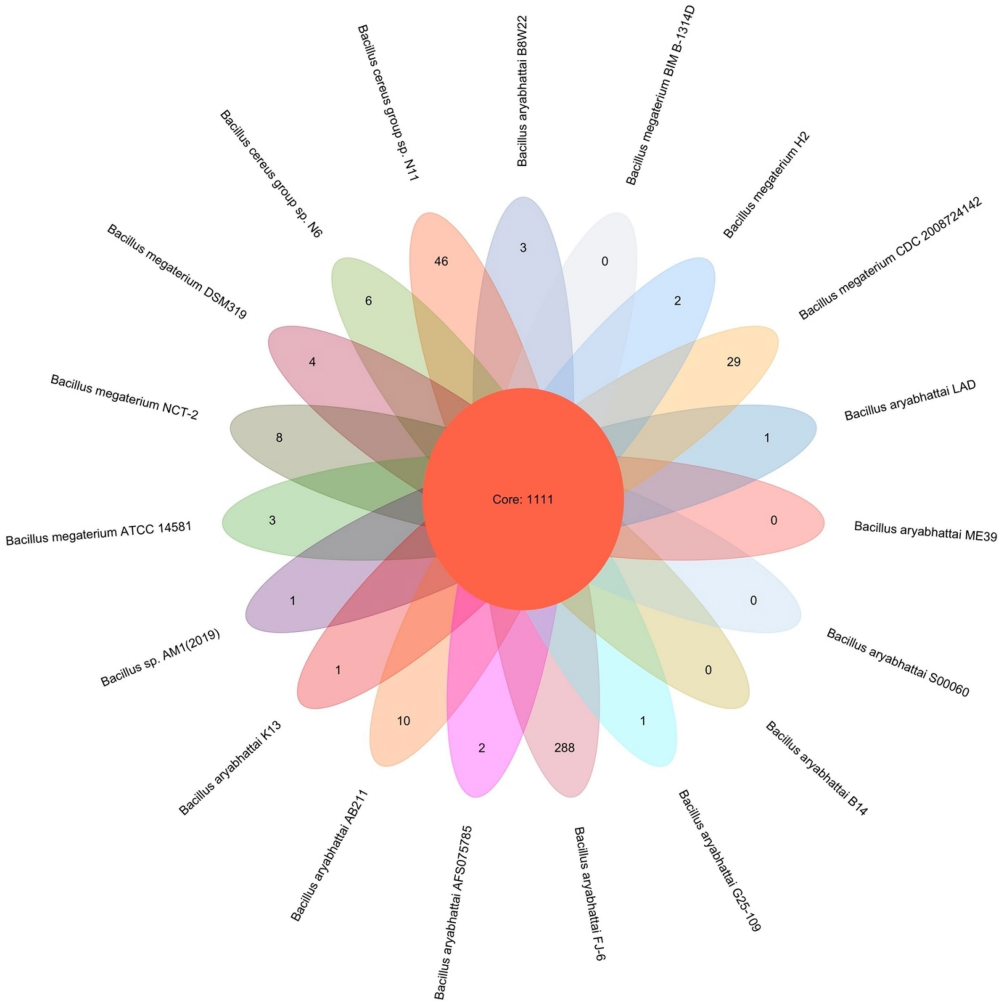

FIGURE 3
Pan-genome analysis of 19 *Bacillus* strains. The number in the overlapping center represents the number of orthologous coding sequences (core genome) shared by all analyzed strains. The number of coding sequences specific to each strain was shown in the non-overlapping portion of the oval.

47.6, 43.1, and 42.9% in the total root length, surface area, and volume in the LAD treatment compared with the control (*t*-test, $p < 0.001$). The longest root in the LAD treatment was 197% longer than the longest root in the control. The experiments demonstrated that LAD treatment significantly increased the maize root length, surface area, and volume ($p < 0.001$).

Discussion

Plant-microbiome interactions are critical for plant health and growth. Rhizosphere microbes reside near or on the plant root and have direct contact and intense interactions with the plant tissue, therefore the root microbiome can utilize root exudates and secrete compounds that remarkably influence plant growth (Haney et al., 2015; Pascale et al., 2020). The interactions between plant and rhizosphere microbes are extremely complex, and the mechanism, ecological significance, and potential for application remain to be clarified. The data in this study shed light on the mechanism of *B. aryabhattai* LAD promoting plant growth based on both genomic analysis and experimental evidence. Whole genome sequencing of *B. aryabhattai* LAD showed that the rhizobacteria had diverse pathways for carbohydrate metabolism and mechanisms for environmental adaptations. The growth experiments of *B. aryabhattai* LAD demonstrated that LAD cells can utilize different types of carbons sources ranging from one-carbon methanol to polymeric carbohydrate starch, and the LAD cells can also grow well in a wide range of temperatures (20°C to 37°C). These properties are important for LAD to adapt to the fluctuating conditions in soil environments and further forming possible symbiosis with plant hosts, as plant root secretion of different carbon chain length may serve as nutrient supply for the root-associated bacteria while the bacterial activities may facilitate plant performance (Blom et al., 2011; Cheng et al., 2019; Lucke et al., 2020).

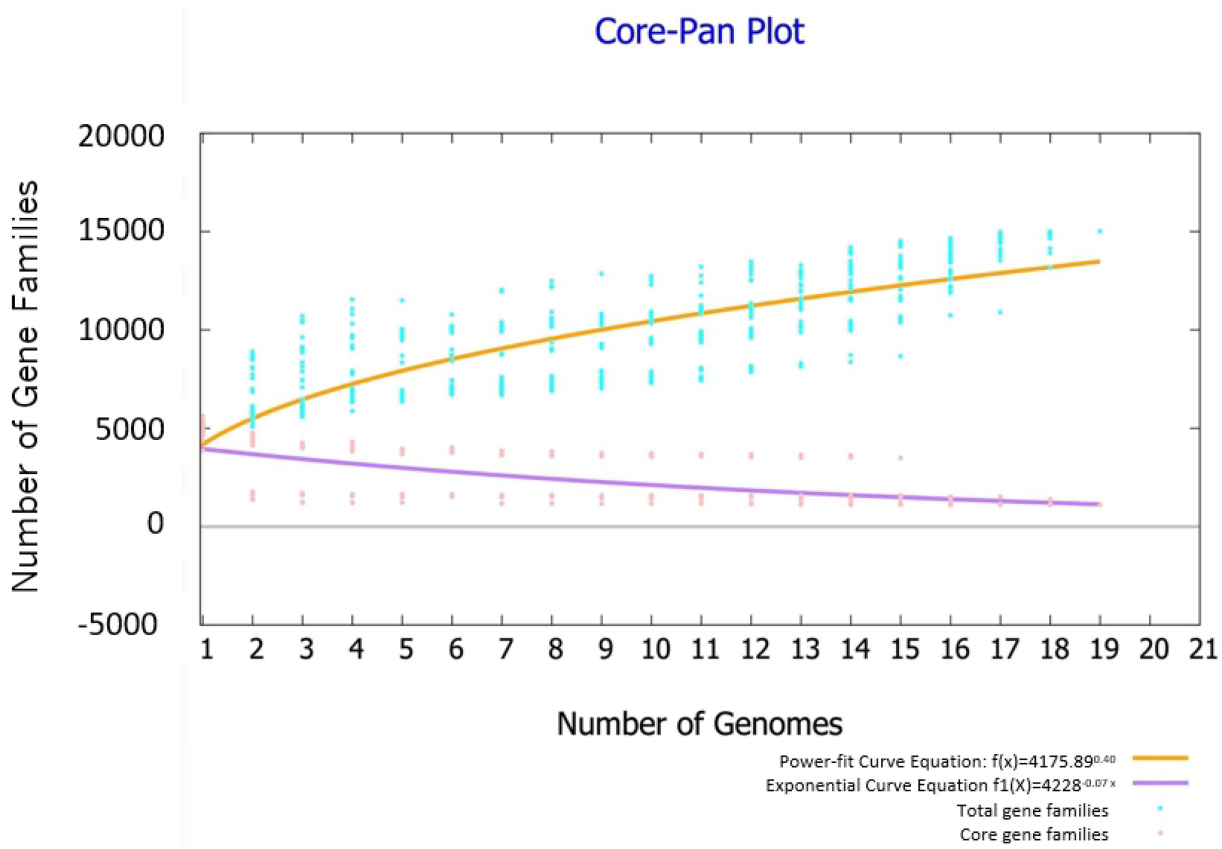

FIGURE 4
Pan genome and core genome profile plot of 19 *Bacillus* strains. The analysis was performed through the Bacterial Pan Genome Analysis (BPGA) software package.

IAA, one of the most common and physiologically active plant hormones in nature, can induce cell elongation and division and is important for plant development and growth. Bacterial production of IAA as plant growth promoting strategy has been demonstrated in previous studies (Mohite, 2013; Wagi and Ahmed, 2019). For example, the IAA production by *B. cereus* So3II and *B. subtilis* Mt3b was shown by, and the growth conditions of the two *Bacillus* strains could be optimized to enhance optimum bacterial growth and production of IAA which ultimately may be used for plant growth stimulation. *B. aryabhattai* LAD in the present study produced high yield of IAA when cultivated with maize plant suggesting the symbiosis of the rhizobacteria with maize plant. Besides IAA production, *B. aryabhattai* LAD can also produce EPSs which is another plant growth-promoting trait (Wagi and Ahmed, 2019). A recent study by showed that EPS-producing bacteria stimulated the salt tolerance of plant because the bacterial produced EPSs can bind cations significantly decreasing the Na^+ content in the environment (Upadhyay et al., 2011). Interestingly, the EPSs production decreased from 3.18 g L^{-1} at 24 h to 0.63 g L^{-1} at 72 h, suggesting that the produced EPSs might be utilized by LAD cells when available nutrients are depleted.

Microbial metabolisms associated with one-carbon compound conversion were prevalent in rhizosphere, and the methanol metabolism by *B. aryabhattai* LAD may contribute to the rhizosphere nutrient cycling (Knief et al., 2012; Li et al., 2019). The genome annotation revealed that *B. aryabhattai* LAD genome contains genes of alcohol dehydrogenases, and the alcohol dehydrogenases enzymes can facilitate the conversion of alcohols to aldehydes with production of NADH. Aldehyde dehydrogenase genes were also detected on *B. aryabhattai* LAD genome, and the products of the genes catalyze the oxidation of the aldehydes generated from methanol. The other possible pathway for methanol metabolism in *B. aryabhattai* LAD was through alcohol oxidase (AOX), catalyzing the oxidation of methanol to formaldehyde with production of hydrogen peroxide, and catalase, breaking down hydrogen peroxide, as genes for AOX and peroxidase were detected on *B. aryabhattai* LAD genome. Plant roots secrete a variety of carbon-containing compounds which significantly influence rhizobacterial activities and community structure (O'Neal et al., 2020; Okutani et al., 2020; Liang et al., 2021). The root exudates of varied molecular weight and complexity may serve as organic carbon sources for microbial growth, and the ability for rhizobacteria utilizing root exudates is critical for both the bacterial populations and the host plant (Mark et al., 2005; Fethel et al., 2014; Olanrewaju et al., 2019). The CAZymes annotation of *B. aryabhattai* LAD genome revealed an

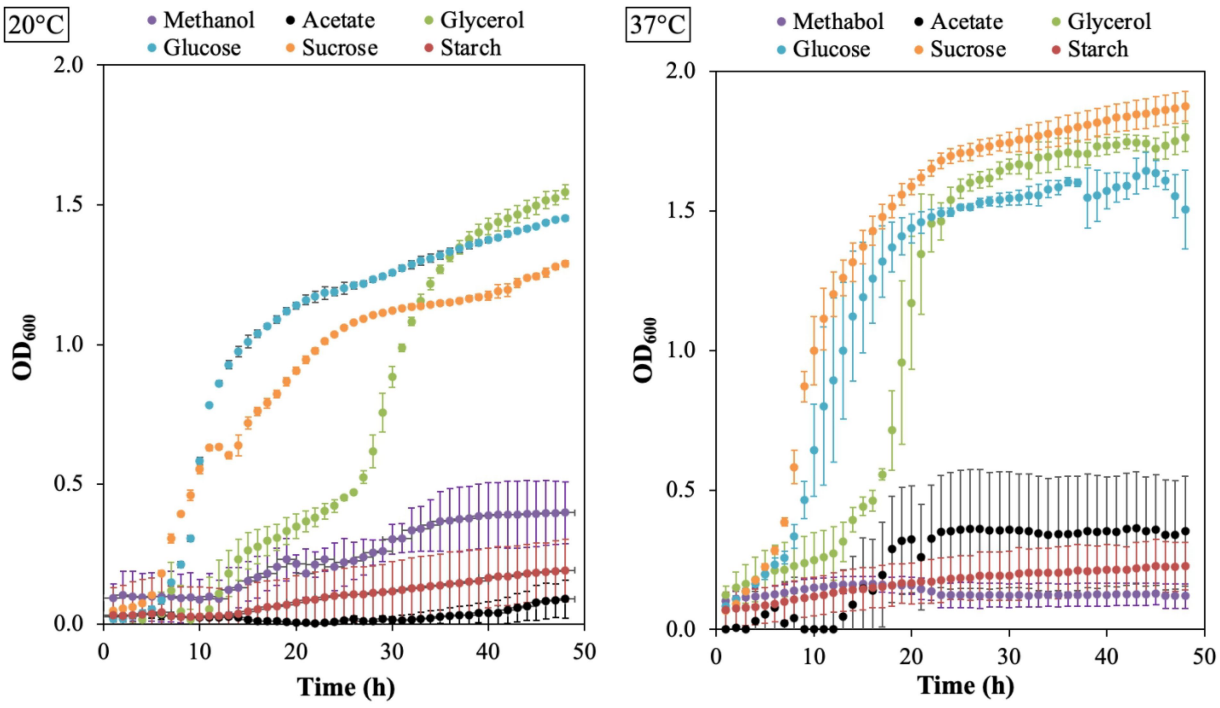

FIGURE 5
The growth plots for *B. aryabhattai* LAD. LAD cells were cultivated in the optimum growth medium with different carbon sources, i.e., methanol (0.5, v v^{-1}), sodium acetate (2%), glycerol (2%), glucose (2%), sucrose (2%), and starch (2%), respectively. The temperature for LAD growth included 20°C and 37°C. Each data point represents the mean value of three replicates.

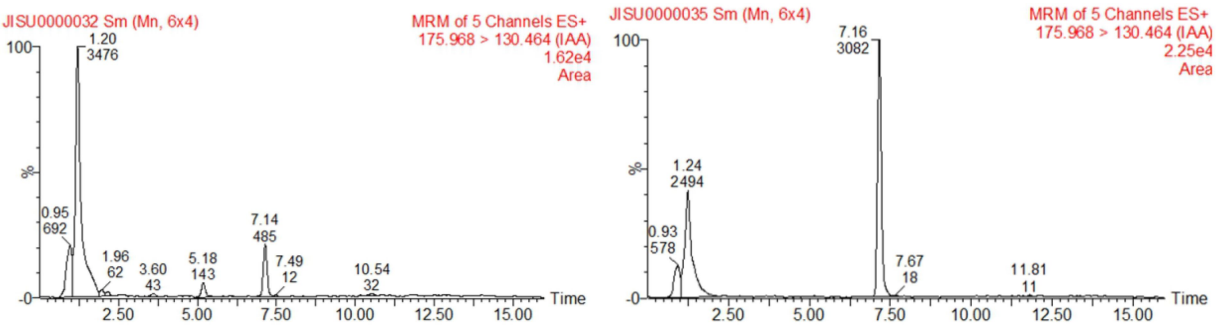

FIGURE 6
Detection of IAA production by UPLC. The left figure shows the sample of the control, and the right shows the sample of *B. aryabhattai* LAD culture cultivated with maize seedlings.

abundance of genes associated with the assimilation, modification, and decomposition of carbohydrates.

The whole genome of *B. aryabhattai* LAD was obtained *via* next-generation sequencing, and the comparative analysis showed that *B. aryabhattai* LAD had high similarities to other *B. aryabhattai* strains and strains in *B. megaterium*. For genomic characterization of *B. aryabhattai* LAD, the pan and core genome analysis were performed to cluster the genes in all the examined genomes. The eggNOG annotation and GO annotation revealed large groups of genes associated with carbohydrate transport and metabolism, oxidoreductase activity, cellular nitrogen compound metabolic process, and biosynthetic process, all of which are important for the symbiotic relationship between bacterial populations and plants and were also found in other plant growth promoting bacterial strains (Taghavi et al., 2010; Han et al., 2011; Bhattacharyya et al., 2017). The CARD analysis identified 31 antibiotic resistance genes and 4 antibiotic biosynthesis genes on the genome and plasmids of *B. aryabhattai* LAD, suggesting that *B. aryabhattai* LAD can be resistant to various antibiotics and have potential for synthesizing antibiotics. Antibiotics production were

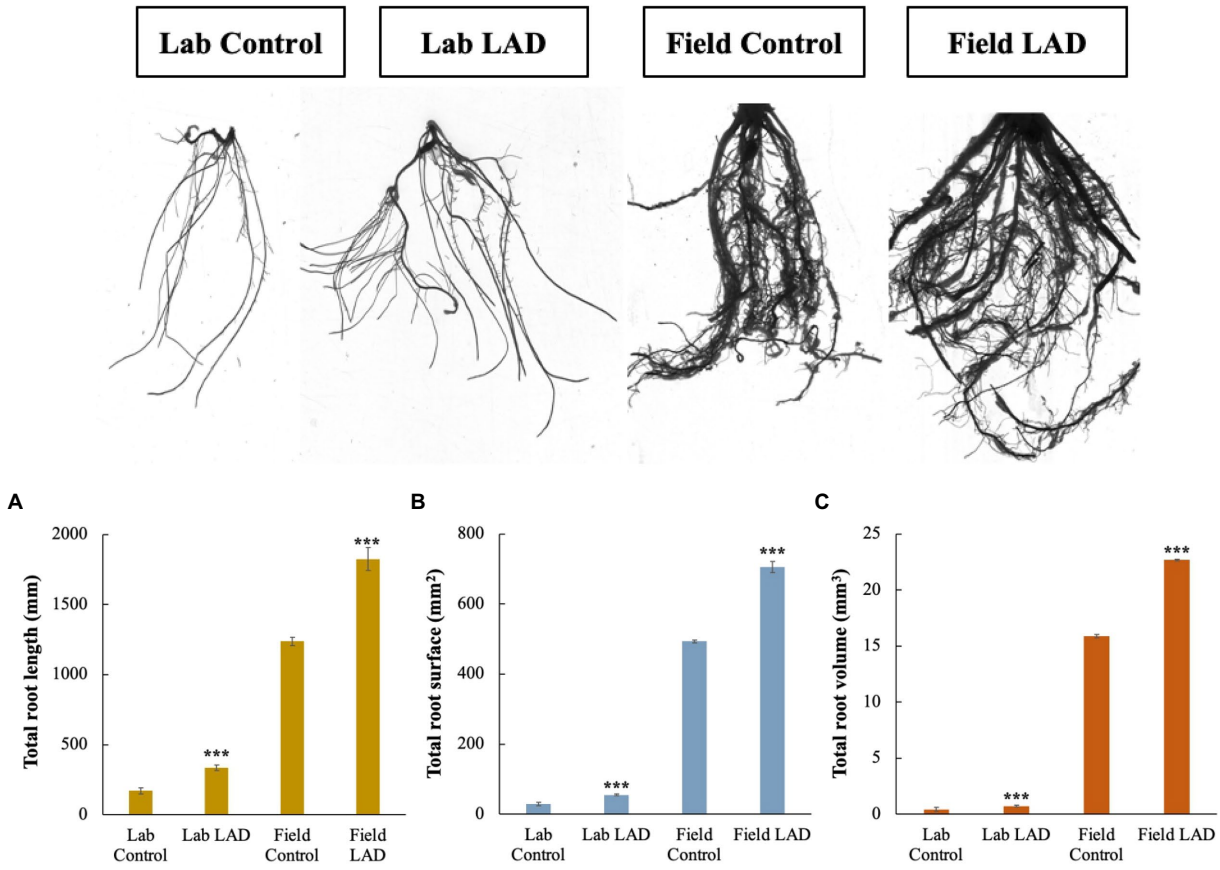

FIGURE 7
Maize root development in laboratory and field soils impacted by *B. aryabhattai* LAD. **(A)** The impacts of LAD on the maize root length. **(B)** The impacts of LAD on the maize root surface area. **(C)** The impacts of LAD on the maize root volume. Lab control: the root of the maize seedlings treated with water and cultivated in laboratory soil for 14 d; Lab LAD: the root of the maize seedlings treated with LAD and cultivated in laboratory soil for 14 d; Field control: the root of the maize seedlings treated with water and cultivated in laboratory soil for 60 d; Field LAD: the root of the maize seedlings treated with LAD and cultivated in laboratory soil for 60 d. Each treatment had 10 maize plants and was repeated three times. Student's *t*-test was used to compare the root development under LAD treatment with that of the control. Statistical differences were shown with asterisks (i.e., *** representing $p < 0.001$).

also reported in other *Bacillus* strains which has a major role for rhizobacteria to suppress plant diseases. For example, the whole genome sequencing of *B. amyloliquefaciens* FZB42 showed a high potential for production of polyketides bacillaene and difficidin, and over 8.5% of the genome is committed antibiotics and siderophores biosynthesis (Chen et al., 2007). Kinsella et al. (2008) also showed a high yield of antibiotics (i.e., surfactin and iturin) by *Bacillus subtilis* on cucumber roots (Kinsella et al., 2008).

Conclusion

Plant roots harbor a diverse microbial community, and the complicated interactions between plant and rhizosphere microbes have major ecological importance and critical implications for agricultural practices. The whole genome sequencing of methylotrophic *B. aryabhattai* LAD revealed many signature genes that are functionally associated with plant growth promotion. Genome analyses revealed the ability of *B. aryabhattai* LAD to adapt to the environments with antibiotics, oxidative, cold temperature, and heavy metal stresses. Our experiments confirmed that *B. aryabhattai* LAD has versatile metabolism and can utilize a wide range of carbon sources. *B. aryabhattai* LAD is also capable of synthesizing IAA and EPSs that are beneficial for plant growth and bacterial colonization. The genomics analysis and experimental studies collectively demonstrated the plant growth promoting capacities of *B. aryabhattai* LAD making it an exceptional bacterial strain for application in agricultural practices. The impacts of *B. aryabhattai* LAD on maize root development was directly evaluated, and the results demonstrated the root development stimulation and plant growth promoting capacities of the *Bacillus* strain. Future efforts are needed for studying the molecular mechanisms of *B. aryabhattai* LAD in promoting plant growth and evaluating the ecological impacts of bioaugmentation with LAD on soil microbial community.

Data availability statement

The datasets presented in this study can be found in online repositories. The names of the repository/repositories and accession number(s) can be found in the article/supplementary material.

Ethics statement

Study protocols of plant materials comply with the IUCN Policy Statement on Research Involving Species at Risk of Extinction and the Convention on the Trade in Endangered Species of Wild Fauna and Flora.

Author contributions

NZh and BL conceived and designed the study. CD conducted the experiments. CD, XW, NZe, and XL performed data analysis and prepared the figures. XL wrote the main manuscript. All authors contributed to the article and approved the submitted version.

Funding

This work was supported by the National Key Research and Development Program of China (2017YFD0200807), the Liaoning Province Rural Science and Technology Special Action Project (2022-09), and Shenyang Science and Technology Project (20-207-3-35).

Conflict of interest

The authors declare that the research was conducted in the absence of any commercial or financial relationships that could be construed as a potential conflict of interest.

Publisher's note

All claims expressed in this article are solely those of the authors and do not necessarily represent those of their affiliated organizations, or those of the publisher, the editors and the reviewers. Any product that may be evaluated in this article, or claim that may be made by its manufacturer, is not guaranteed or endorsed by the publisher.

References

Ahmed, A., and Hasnain, S. (2014). Auxins as one of the factors of plant growth improvement by plant growth promoting rhizobacteria. *Pol. J. Microbiol.* 63, 261–266. doi: 10.33073/pjm-2014-035

Arndt, D., Grant, J. R., Marcu, A., Sajed, T., Pon, A., Liang, Y., et al. (2016). PHASTER: a better, faster version of the PHAST phage search tool. *Nucleic Acids Res.* 44, W16–W21. doi: 10.1093/nar/gkw387

Backer, R., Rokem, J. S., Ilangumaran, G., Lamont, J., Praslickova, D., Ricci, E., et al. (2018). Plant growth-promoting rhizobacteria: context, mechanisms of action, and roadmap to commercialization of biostimulants for sustainable agriculture. *Front. Plant Sci.* 9:1473. doi: 10.3389/fpls.2018.01473

Berendsen, R. L., Pieterse, C. M., and Bakker, P. A. (2012). The rhizosphere microbiome and plant health. *Trends Plant Sci.* 17, 478–486. doi: 10.1016/j.tplants.2012.04.001

Berta, B. (2000). Putative sites for nutrient uptake in arbuscular mycorrhizal fungi. *Plant Soil* 226, 263–274. doi: 10.1023/A:1026456818903

Besemer, J., Lomsadze, A., and Borodovsky, M. (2001). GeneMarkS: a self-training method for prediction of gene starts in microbial genomes. Implications for finding sequence motifs in regulatory regions. *Nucleic Acids Res.* 29, 2607–2618. doi: 10.1093/nar/29.12.2607

Bever, J. D., Broadhurst, L. M., and Thrall, P. H. (2013). Microbial phylotype composition and diversity predicts plant productivity and plant–soil feedbacks. *Ecol. Lett.* 16, 167–174. doi: 10.1111/ele.12024

Bhattacharyya, C., Bakshi, U., Mallick, I., Mukherji, S., Bera, B., and Ghosh, A. (2017). Genome-guided insights into the plant growth promotion capabilities of the physiologically versatile bacillus aryabhattai strain AB211. *Front. Microbiol.* 8:411. doi: 10.3389/fmicb.2017.00411

Blom, D., Fabbri, C., Connor, E. C., Schiestl, F. P., Klauser, D. R., Boller, T., et al. (2011). Production of plant growth modulating volatiles is widespread among rhizosphere bacteria and strongly depends on culture conditions. *Environ. Microbiol.* 13, 3047–3058. doi: 10.1111/j.1462-2920.2011.02582.x

Bucksch, A., Burridge, J., York, L. M., Das, A., Nord, E., Weitz, J. S., et al. (2014). Image-based high-throughput field phenotyping of crop roots. *Plant Physiol.* 166, 470–486. doi: 10.1104/pp.114.243519

Chaparro, J. M., Badri, D. V., and Vivanco, J. M. (2014). Rhizosphere microbiome assemblage is affected by plant development. *ISME J.* 8, 790–803. doi: 10.1038/ismej.2013.196

Chaudhari, N. M., Gupta, V. K., and Dutta, C. (2016). BPGA-an ultra-fast pan-genome analysis pipeline. *Sci. Rep.* 6:24373. doi: 10.1038/srep24373

Chen, X. H., Koumoutsi, A., Scholz, R., Eisenreich, A., Schneider, K., Heinemeyer, I., et al. (2007). Comparative analysis of the complete genome sequence of the plant growth–promoting bacterium bacillus amyloliquefaciens FZB42. *Nat. Biotechnol.* 25, 1007–1014. doi: 10.1038/nbt1325

Chen, Y. F., Yang, H., Shen, Z. Z., and Ye, J. R. (2022). Whole-genome sequencing and potassium-solubilizing mechanism of bacillus aryabhattai SK1-7. *Front. Microbiol.* 12:722379. doi: 10.3389/FMICB.2021.722379

Cheng, Y. T., Zhang, L., and He, S. Y. (2019). Plant-microbe interactions facing environmental challenge. *Cell Host Microbe* 26, 183–192. doi: 10.1016/j.chom.2019.07.009

Chin, C. S., Peluso, P., Sedlazeck, F. J., Nattestad, M., Concepcion, G. T., Clum, A., et al. (2016). Phased diploid genome assembly with single-molecule real-time sequencing. *Nat. Methods* 13, 1050–1054. doi: 10.1038/nmeth.4035

Chu, T. N., Bui, L. V., and Hoang, M. T. (2020). Pseudomonas PS01 isolated from maize rhizosphere alters root system architecture and promotes plant growth. *Microorganisms* 8:471. doi: 10.3390/microorganisms8040471

Deng, C., Zhang, N., Liang, X., Huang, T., and Li, B. (2022). Bacillus aryabhattai LAD impacts rhizosphere bacterial community structure and promotes maize plant growth. *J. Sci. Food Agric.* 102, 6650–6657. doi: 10.1002/jsfa.12032

Erik, J. J., Sabine, R., and Iver, J. (2000). Arbuscular mycorrhizal phosphate transport under monoxenic conditions using radio-labelled inorganic and organic phosphate. *Biotechnol. Lett.* 22, 1705–1708. doi: 10.1023/A:1005684031296

Fethel, Z. H., Santaella, C., Heulin, T., and Achouak, W. (2014). Root exudates mediated interactions belowground. *Soil Biol. Biochem.* 77, 69–80. doi: 10.1016/j.soilbio.2014.06.017

Fu, J. H., Chu, J. F., Sun, X. H., Wang, J. D., and Yan, C. Y. (2012). Simple, rapid, and simultaneous assay of multiple carboxyl containing phytohormones in wounded tomatoes by UPLC-MS/MS using single SPE purification and isotope dilution. *Anal. Sci.* 28, 1081–1087. doi: 10.2116/analsci.28.1081

Ghosh, P. K., Maiti, T. K., Pramanik, K., Ghosh, S. K., Mitra, S., and De, T. K. (2018). The role of arsenic resistant bacillus aryabhattai MCC3374 in promotion of rice seedlings growth and alleviation of arsenic phytotoxicity. *Chemosphere* 211, 407–419. doi: 10.1016/j.chemosphere.2018.07.148

Grissa, I., Vergnaud, G., and Pourcel, C. (2007). CRISPRFinder: a web tool to identify clustered regularly interspaced short palindromic repeats. *Nucleic Acids Res.* 35, W52–W57. doi: 10.1093/nar/gkm360

Han, J. I., Choi, H. K., Lee, S. W., Orwin, P. M., Kim, J., LaRoe, S. L., et al. (2011). Complete genome sequence of the metabolically versatile plant growth-promoting

endophyte Variovorax paradoxus S110. *J. Bacteriol. Res.* 193, 1183–1190. doi: 10.1128/JB.00925-10

Haney, C. H., Samuel, B. S., Bush, J., and Ausubel, F. M. (2015). Associations with rhizosphere bacteria can confer an adaptive advantage to plants. *Nat. Plants* 1, 1–9. doi: 10.1038/NPLANTS.2015.51

Idriss, E. E., Makarewicz, O., Farouk, A., Rosner, K., Greiner, R., Bochow, H., et al. (2002). Extracellular phytase activity of Bacillus amyloliquefaciens FZB45 contributes to its plant-growth-promoting effect. *Microbiology* 148, 2097–2109. doi: 10.1099/00221287-148-7-2097

Kalvari, I., Argasinska, J., Quinones-Olvera, N., Nawrocki, E. P., Rivas, E., Eddy, S. R., et al. (2018). Rfam 13.0: shifting to a genome-centric resource for non-coding RNA families. *Nucleic Acids Res.* 46, D335–D342. doi: 10.1093/nar/gkx1038

Kinsella, K., Schulthess, C. P., Morris, T. F., and Stuart, J. D. (2008). Rapid quantification of Bacillus subtilis antibiotics in the rhizosphere. *Soil Biol. Biochem.* 41, 374–379. doi: 10.1016/j.soilbio.2008.11.019

Knief, C., Delmotte, N., Chaffron, S., Stark, M., Innerebner, G., Wassmann, R., et al. (2012). Metaproteogenomic analysis of microbial communities in the phyllosphere and rhizosphere of rice. *ISME J.* 6, 1378–1390. doi: 10.1038/ismej.2011.192

Koren, S., Walenz, B. P., Berlin, K., Miller, J. R., Bergman, N. H., and Phillippy, A. M. (2017). Canu: scalable and accurate long-read assembly via adaptive k-mer weighting and repeat separation. *Genome Res.* 27, 722–736. doi: 10.1101/gr.215087.116

Korenblum, E., Dong, Y., Szymanski, J., Panda, S., Jozwiak, A., Massalha, H., et al. (2020). Rhizosphere microbiome mediates systemic root metabolite exudation by root-to-root signaling. *Proc. Natl. Acad. Sci. U. S. A.* 117, 3874–3883. doi: 10.1073/pnas.1912130117

Lau, J. A., and Lennon, J. T. (2011). Evolutionary ecology of plant–microbe interactions: soil microbial structure alters selection on plant traits. *New Phytol.* 192, 215–224. doi: 10.1111/j.1469-8137.2011.03790.x

Lazcano, C., Boyd, E., Holmes, G., Hewavitharana, S., Pasulka, A., and Ivors, K. (2021). The rhizosphere microbiome plays a role in the resistance to soil-borne pathogens and nutrient uptake of strawberry cultivars under field conditions. *Sci. Rep.* 11:3188. doi: 10.1038/s41598-021-82768-2

Li, Z., Yao, Q., Guo, X., Crits-Christoph, A., Mayes, M. A., Lebeis, S. L., et al. (2019). Genome-resolved proteomic stable isotope probing of soil microbial communities using $^{13}CO_2$ and ^{13}C-methanol. *Front. Microbiol.* 10:2706. doi: 10.3389/fmicb.2019.02706

Liang, X., Wang, Y., Zhang, Y., Zhuang, J., and Radosevich, M. (2021). Viral abundance, community structure and correlation with bacterial community in soils of different cover plants. *Appl. Soil Ecol.* 168:104138. doi: 10.1016/J.APSOIL.2021.104138

Liu, J., Cui, X., Liu, Z., Guo, Z., Yu, Z., Yao, Q., et al. (2019). The diversity and geographic distribution of cultivable bacillus-like bacteria across black soils of Northeast China. *Front. Microbiol.* 10:1424. doi: 10.3389/fmicb.2019.01424

Lombard, V., Golaconda, R. H., Drula, E., Coutinho, P. M., and Henrissat, B. (2014). The carbohydrate-active enzymes database (CAZy) in 2013. *Nucleic Acids Res.* 42, D490–D495. doi: 10.1093/nar/gkt1178

Lowe, T. M., and Eddy, S. R. (1997). tRNAscan-SE: a program for improved detection of transfer RNA genes in genomic sequence. *Nucleic Acids Res.* 25, 955–964. doi: 10.1093/nar/25.5.955

Lucke, M., Correa, M. G., and Levy, A. (2020). The role of secretion systems, effectors, and secondary metabolites of beneficial rhizobacteria in interactions with plants and microbes. *Front. Plant Sci.* 11:589416. doi: 10.3389/fpls.2020.589416

Ma, J., Li, Y., Hu, D., Peng, J. L., Ja, N., Zhang, C. M., et al. (2018). Progress on mechanism and applications of bacillus as a biocontrol microbe. *Chin. J. Bio. Con.* 34, 639–648. doi: 10.16409/j.cnki.2095-039x.2018.04.019

Maria, J. H. (2005). Signaling in the arbuscular mycorrhizal symbiosis. *Annu. Rev. Microbiol.* 59, 19–42. doi: 10.1146/annurev.micro.58.030603.123749

Mark, G. L., Dow, J. M., Kiely, P. D., Higgins, H., Haynes, J., Baysse, C., et al. (2005). Transcriptome profiling of bacterial responses to root exudates identifies genes involved in microbe-plant interactions. *Proc. Natl. Acad. Sci. U. S. A.* 102, 17454–17459. doi: 10.1073/pnas.0506407102

Mehmood, S., Khan, A. A., Shi, F., Tahir, M., Sultan, T., Munis, M. F. H., et al. (2021). Alleviation of salt stress in wheat seedlings via multifunctional bacillus aryabhattai PM34: an in-vitro study. *Sustainability* 13, 8030–8030. doi: 10.3390/SU13148030

Mendes, R., Garbeva, P., and Raaijmakers, J. M. (2013). The rhizosphere microbiome: significance of plant beneficial, plant pathogenic, and human pathogenic microorganisms. *FEMS Microbiol. Rev.* 37, 634–663. doi: 10.1111/1574-6976.12028

Mohite, B. (2013). Isolation and characterization of indole acetic acid (IAA) producing bacteria from rhizospheric soil and its effect on plant growth. *J. Soil Sci. Plant Nutr.* 13, 638–649. doi: 10.4067/S0718-95162013005000051

Moreau, D., Bardgett, R. D., Finlay, R. D., Jones, D. L., and Philippot, L. (2019). A plant perspective on nitrogen cycling in the rhizosphere. *Funct. Ecol.* 33, 540–552. doi: 10.1111/1365-2435.13303

O'Neal, L., Vo, L., and Alexandre, G. (2020). Specific root exudate compounds sensed by dedicated chemoreceptors shape Azospirillum brasilense chemotaxis in the rhizosphere. *Appl. Environ. Microbiol.* 86:e01026. doi: 10.1128/AEM.01026-20

Okutani, F., Hamamoto, S., Aoki, Y., Nakayasu, M., Nihei, N., Nishimura, T., et al. (2020). Rhizosphere modelling reveals spatiotemporal distribution of daidzein shaping soybean rhizosphere bacterial community. *Plant Cell Environ.* 43, 1036–1046. doi: 10.1111/pce.13708

Olanrewaju, O. S., Ayangbenro, A. S., Glick, B. R., and Babalola, O. O. (2019). Plant health: feedback effect of root exudates-rhizobiome interactions. *Appl. Microbiol. Biotechnol.* 103, 1155–1166. doi: 10.1007/s00253-018-9556-6

Park, Y. G., Mun, B. G., Kang, S. M., Hussain, A., Shahzad, R., Seo, C. W., et al. (2017). Bacillus aryabhattai SRB02 tolerates oxidative and nitrosative stress and promotes the growth of soybean by modulating the production of phytohormones. *PLoS One* 12:e0173203. doi: 10.1371/journal.pone.0173203

Pascale, A., Proietti, S., Pantelides, I. S., and Stringlis, I. A. (2020). Modulation of the root microbiome by plant molecules: the basis for targeted disease suppression and plant growth promotion. *Front. Plant Sci.* 10:1741. doi: 10.3389/fpls.2019.01741

Philippe, H. (2001). Bioavailability of soil inorganic P in the rhizosphere as affected by root-induced chemical changes: a review. *Plant Soil* 237, 173–195. doi: 10.1023/A:1013351617532

Richter, M., Rosselló-Móra, R., Oliver, G. F., and Peplies, J. (2016). JSpeciesWS: a web server for prokaryotic species circumscription based on pairwise genome comparison. *Bioinformatics* 32, 929–931. doi: 10.1093/bioinformatics/btv681

Roy, K., Ghosh, D., DeBruyn, J. M., Dasgupta, T., Wommack, K. E., Liang, X., et al. (2020). Temporal dynamics of soil virus and bacterial populations in agricultural and early plant successional soils. *Front. Microbiol.* 11:1494. doi: 10.3389/fmicb.2020.01494

Shao, Y., Liu, T., Eisenhauer, N., Zhang, W., Wang, X., Xiong, Y., et al. (2018). Plants mitigate detrimental nitrogen deposition effects on soil biodiversity. *Soil Biol. Biochem.* 127, 178–186. doi: 10.1016/j.soilbio.2018.09.022

Shivaji, S., Chaturvedi, P., Begum, Z., Pindi, P. K., Manorama, R., Padmanaban, D. A., et al. (2009). Janibacter hoylei sp. nov., bacillus isronensis sp. nov. and bacillus aryabhattai sp. nov., isolated from cryotubes used for collecting air from the upper atmosphere. *Int. J. Syst. Evol. Microbiol.* 59, 2977–2986. doi: 10.1099/ijs.0.002527-0

Taghavi, S., Lelie, D., Hoffman, A., Zhang, Y. B., Walla, M. D., Vangronsveld, J., et al. (2010). Genome sequence of the plant growth promoting endophytic bacterium Enterobacter sp. 638. *PLoS Genet.* 6:e1000943. doi: 10.1371/journal.pgen.1000943

Tahir, H. A., Gu, Q., Wu, H., Raza, W., Hanif, A., Wu, L., et al. (2017). Plant growth promotion by volatile organic compounds produced by Bacillus subtilis SYST2. *Front. Microbiol.* 8:171. doi: 10.3389/fmicb.2017.00171

Tzipilevich, E., Russ, D., Dangl, J. L., and Benfey, P. N. (2021). Plant immune system activation is necessary for efficient root colonization by auxin-secreting beneficial bacteria. *Cell Host Microbe* 29, 1507–1520.e4. doi: 10.1016/j.chom.2021.09.005

Upadhyay, S. K., Singh, J. S., and Singh, D. P. (2011). Exopolysaccharide-producing plant growth-promoting rhizobacteria under salinity condition. *Pedosphere* 21, 214–222. doi: 10.1016/S1002-0160(11)60120-3

Vernikos, G., Medini, D., Riley, D. R., and Tettelin, H. (2015). Ten years of pan-genome analyses. *Curr. Opin. Microbiol.* 23, 148–154. doi: 10.1016/j.mib.2014.11.016

Wagi, S., and Ahmed, A. (2019). Bacillus spp.: potent microfactories of bacterial IAA. *PeerJ* 7:e7258. doi: 10.7717/peerj.7258

Walker, B. J., Abeel, T., Shea, T., Priest, M., Abouelliel, A., Sakthikumar, S., et al. (2014). Pilon: an integrated tool for comprehensive microbial variant detection and genome assembly improvement. *PLoS One* 9:e112963. doi: 10.1371/journal.pone.0112963

Zhang, H., Murzello, C., Yan, S., Kim, M. S., and Paré, P. W. (2010). Choline and osmotic-stress tolerance induced in Arabidopsis by the soil microbe Bacillus subtilis (GB03). *Mol. Plant Microbe Interact.* 23, 1097–1104. doi: 10.1094/MPMI-23-8-1097

frontiers | Frontiers in Microbiology

TYPE Original Research
PUBLISHED 24 October 2022
DOI 10.3389/fmicb.2022.988692

Check for updates

OPEN ACCESS

EDITED BY
José David Flores Félix,
Universidade da Beira Interior, Portugal

REVIEWED BY
Judith Naamala,
McGill University, Canada
Vinay Kumar,
ICAR-National Institute of Biotic Stress Management, India

*CORRESPONDENCE
Jia Yao Zhuang
nlzjiayao@njfu.edu.cn

SPECIALTY SECTION
This article was submitted to Microbe and Virus Interactions with Plants, a section of the journal Frontiers in Microbiology

RECEIVED 14 July 2022
ACCEPTED 20 September 2022
PUBLISHED 24 October 2022

CITATION
Zheng J, Liu C, Liu J and Zhuang JY (2022) Study of the effect of bacterial-mediated legume plant growth using bacterial strain *Serratia marcescens* N1.14 X-45. *Front. Microbiol.* 13:988692. doi: 10.3389/fmicb.2022.988692

COPYRIGHT
© 2022 Zheng, Liu, Liu and Zhuang. This is an open-access article distributed under the terms of the Creative Commons Attribution License (CC BY). The use, distribution or reproduction in other forums is permitted, provided the original author(s) and the copyright owner(s) are credited and that the original publication in this journal is cited, in accordance with accepted academic practice. No use, distribution or reproduction is permitted which does not comply with these terms.

Study of the effect of bacterial-mediated legume plant growth using bacterial strain *Serratia marcescens* N1.14 X-45

Jiaxin Zheng, Chao Liu, Jiayi Liu and Jia Yao Zhuang*

Collaborative Innovation Center of Sustainable Forestry in Southern China of Jiangsu Province, Nanjing Forestry University, Nanjing, China

Soil microorganisms play an indispensable role in plant growth and are widely used to promote plant growth. However, poor microbial strains are homogeneous. The heavy application of chemical fertilizers and pesticides to agricultural soil has adversely affected the soil flora, necessitating the regulation of the soil flora to maintain soil health. In this study, X-45, a highly efficient and phosphorus-dissolving strain of the lysogenic bacterium *Serratia marcescens* N1.14 was isolated from bare rock slope soil samples from Yueyang Avenue, Hunan Province, China. We observed that microbial strain X-45 could release P from the rocks into solution when the sample rocks were used as the only phosphorus source. Furthermore, we observed that the P content in media increased by 3.08 X compared to the control. After applying X-45 as a bacterial fertilizer, the growth of potted *Indigofera pseudotinctoria* plants significantly increased, the soil physicochemical properties were significantly improved, and the relative abundance of *Bradyrhizobium* in the soil increased significantly from 1 to 42%. Besides, *Bradyrhizobium* became the most dominant genus in the soil. The indirect promotion of another beneficial microorganism by X-45 further revealed the intrinsic mechanism by which X-45 exerted its effect on plant promotion and soil improvement. Using this bacteria, the hypothesis of the superposition effect of legume plant promotion was also confirmed.

KEYWORDS

bacterial communities, bioremediation, phytoremediation, sequencing technology, soil fertility

Introduction

The restoration of high and steep exposed rock walls demands urgent attention as human activities, such as road construction and mining, have led to the exposure of high and steep slopes, adversely affecting the ecological habitat of human beings. Phytoremediation is considered the most promising restoration technology because of its low cost and environmental friendliness. However, restoration of exposed rock walls is challenging because they are mainly made of hard rocks, and their poor ground conditions make it difficult for plants to grow. The improvement of environmental conditions is crucial to the restoration of exposed high and steep slopes. Soil microorganisms have a vital role in rock weathering (Zhu et al., 2014). Besides, soil microbes enhance the release of rock nutrients and promote plant growth (Wu et al., 2017). For instance, bacteria actively solubilize phosphorus, which is then transported by mycorrhizal fungi to the plant root system (Song et al., 2021). Soil microbes also facilitate rock dissolution, creating a microenvironment conducive to plant growth (Mo and Lian, 2011). The weathering rate of minerals and rocks by microbial activities is significantly higher than in other abiotic systems (Barker et al., 2018). For instance, microorganisms play a positive role in CO_2 mineral trapping (Zhao et al., 2014). Soil microbes facilitate well-established conditions for the growth of plants by facilitating the weathering of rocks.

Currently, the regulatory function of microbial communities on ecosystem function has been extensively investigated; however, drivers of subsurface microbial communities remain largely unexplored. Microbial communities are regulated by soil nutrients. For instance, increased carbon input promotes soil microbial processes and plant growth. However, adding carbon to soil significantly increases soil microbial biomass and activity, but it has limited implications on the soil microbial community structure (Ma et al., 2012). Compared with soil conditioners, microbial addition to existing soil microbiota alters the structure of soil microbiota. Besides, adding soil microbes plays a vital role in the re-construction and regulation of subsurface microbial communities, significantly improving the abundance of beneficial soil microbes (Dong et al., 2019). Adding soil microbes also shortens the time for microbial agents to improve soil quality compared to compost (Zhuang et al., 2021). Thus, phytoremediation of exposed high steep rock walls progresses in the correct direction.

In phytoremediation, leguminous tree and shrub species are widely used due to their stress resistance, rapid regeneration, and the ability to restore a degraded environment (Mahmud et al., 2020). These plants reestablish degraded ecological functions and soil characteristics and positively affect the subsurface microbial community (Hu et al., 2015). In this study, the high steep slope of Yueyang Avenue in Hunan, China, was selected as an experimental site. Soil microbes in minerals were screened through rock weathering experiments. We studied the effects of microbial bacterial agents on the growth of legumes and soil physicochemical properties in combination with potting experiments. Besides, we also studied the intrinsic mechanism of bacteria-mediated plant growth promotion, intending to provide plant-growth promoting bacterial agents for efficient ecological restoration of challenging sites, such as high steep bare rock slopes. In a previous study, we proposed a hypothesis of "the imposed effect for promoting leguminous plant growth," including mineral weathering, nodule growth promotion, and beneficial microbial regulation, and tested by fungi Penicillium simplicissimum NL-Z1 (Zhuang et al., 2021). In this study, we focused on the effects of microbial bacterial agents on the growth of legumes and soil physicochemical properties in combination with potting experiments.

Materials and methods

Sample source

The soil samples for screening microbial monocultures were obtained from the soil of the legume *Robinia pseudoacacia* from the high steep bare rock slopes of Yueyang Avenue, Yueyang City, Hunan Province, China. These soil samples were sieved through 0.075 mm for physical and chemical properties. In addition, local rock samples were collected from the same site and transferred to the laboratory. These rock samples were cleaned, crushed, and ground for compositional analysis of rock samples and subsequent weathering experiments.

Screening and rock weathering experiments

Culture medium

(a) Phosphorus solubilizing strain isolation medium: 0.3 g sodium chloride, 0.3 g potassium chloride, 0.5 g ammonium sulfate, 0.3 g magnesium sulfate heptahydrate, 0.03 g ferrous sulfate heptahydrate, 0.3 g manganese sulfate tetrahydrate, 5.0 g calcium phosphate, 10 g sucrose, 15-20 g agar, deionized water 1,000 mL, and pH 7.0-7.5.

(b) Beef paste peptone medium: 3 g beef (dip) paste, 10 g peptone, 5 g sodium chloride, 20 g agar, 1,000 mL deionized water, and pH 7.0-7.2.

(c) Monkina organic phosphorus medium: 10 g glucose, 0.5 g ammonium sulfate, 0.3 g sodium chloride, 0.3 g potassium chloride, 0.3 g magnesium sulfate heptahydrate, 0.03 g ferrous sulfate heptahydrate, 0.03 g manganese sulfate, 5.0 g calcium carbonate, 0.3 g lecithin, 20 g agar, deionized water 1,000 mL, and pH 7.0-7.5.

(d) Monkina inorganic phosphorus medium: 10 g glucose, 0.5 g ammonium sulfate, 0.3 g sodium chloride, 0.3 g potassium

chloride, 0.3 g magnesium sulfate heptahydrate, 0.03 g ferrous sulfate heptahydrate, 0.03 g manganese sulfate, 5.0 g tricalcium phosphate, 20 g agar, 1000 mL deionized water, and pH 7.0-7.5.

(e) Modified Monkina medium: In this medium, phosphorus-containing components mentioned in mediums 3 and 4 were replaced with rock samples.

(f) LB liquid medium: 10 g peptone, yeast dip powder 5 g, sodium chloride 5 g, deionized water 1,000 mL, and pH 7.2.

Isolation and purification of strains

A tenfold serial dilution of soil samples were smeared on NA and PDA to isolate bacteria and fungi, respectively. Three replicates of each diluent were cultured at 28°C for 3 days in a constant-temperature incubator. Single strains were obtained through three rounds of purification, and the isolated strains were stored at 4°C.

Screening of phosphate-dissolving bacteria

The screening of phosphate solubilizing microbes were carried out on Monkina agar at 28°C following spot inoculation; three replicates were prepared for each strain. The plates were treated with organic and inorganic phosphorus for 5 and 7 days, respectively, at 28°C in an incubator. The results showed that the transparent circle in the medium was due to the phosphate-dissolving bacteria. The diameter of the colony (d) and of the transparent circle (D) were measured, and D/d was calculated to preliminarily evaluate the ability of the strain to dissolve phosphate, five strains of phosphate solubilizing microbes were selected for weathering experiment.

Rock weathering experiments

In this study, single microbial colonies were isolated and cultured from rocks. To isolate microbes with mineral weathering ability and understand phosphorus weathering process, screening of soil was carried out. To verify if the rock can be dissolved, five different single microbial colonies with good phosphorus dissolution effect were selected for rock weathering dissolution analysis to explore the rock weathering effect of these microbes. After culturing the microbes in nutrient agar media, these five single colonies were added to a 100 mL conical flask containing 30 mL LB medium and oscillated at 30°C and 180 RPM for three days. 1 mL bacterial culture was added to a 30 mL modified Monkina broth in an Erlenmeyer flask containing 1.5 g rock particles instead of phosphorus in the modified Monkina agar and incubated at 30°C and 180 RPM for ten days. At different time intervals (4, 7, and 10 days), samples (n = 3) after centrifugation (8000 RPM, 10 min) were collected from the inoculated group (X-4, X-8, X-11, X-14, X-45) and the control group. The resulting 5 mL of supernatant was added to 0.2 μm pour filtrate and centrifuged to determine the pH value, phosphorus (AP), potassium (k), calcium, and magnesium content. 100 mL Erlenmeyer flask containing 30 mL LB media was incubated at 30°C and 180 RPM for three days. Then, 1 mL broth of each five microbial strains was inoculated into the 30 mL modified Monkina broth media containing 1.5 g rock particles to replace the phosphorus component of Monkina agar in an Erlenmeyer flask and incubated at 30°C and 180 RPM for 10 days. Samples (n = 3) from inoculated groups (X-4, X-8, X-11, X-14, X-45) and the control group were collected on day ten and centrifuged at 8,000 RPM for 10 min. 5 mL of supernatant was filtered using a 0.2 μM membrane filter for the determination of pH, available phosphorus (AP), potassium (K), calcium (Ca), and magnesium (Mg). pH was determined using the Mettler toledo pH meter. AP was determined using the molybdenum-antimony anti-colorimetric method. K, Ca, and Mg was determined using the atomic absorption spectrometer. The shape and size of the rock particles were measured during the last sampling.

Potted plant experiment

Experimental environment

The experiment was conducted in a greenhouse at the teaching base of Nanjing Forestry University in Baima, with 65% air humidity, 450 ppm CO_2 concentration, 28°C and a maximum photosynthetic radiation of 1,850 μmol/(m^2·s). The soil was taken from the field trial fields below 20 cm at the Baima site and brought back to the laboratory to remove any gravel, dead material and roots, etc. The soil was sterilized in an autoclave at 121°C for 30 min to ensure sterility. Plastic pots with an inner diameter of 9 cm, an outer diameter of 13 cm and a height of 15 cm were used for planting *I. pseudotinctoria.*

Bacterial agent preparation

To produce bacterial X-45 inoculum, isolates were grown to a certain colony size on NA at 28°C and then inoculated into liquid medium at 30°C and 180 RPM for three days. The OD 600 of this media was measured by UV spectrophotometer, and the OD 600 value was adjusted to 0.8∼1.2. Later, the media was sealed and stored in 4°C refrigerators.

Experimental design

The bacterial strain X-45, which was effective in the weathering experiments, was selected for potting experiments to study the growth-promoting ability of this strain. The experiment was divided into a control group and an experimental group. Leguminosae *I. pseudotinctoria* were used as experimental plants. The pots were divided into two groups (CK and X-45, 3 replicates for each group) and placed in a greenhouse. Three young shoots of *I. pseudotinctoria* were planted in each pot and screened after one month of growth, keeping one healthy seedling in each pot (the same growth from pot to pot). For inoculation, the stored bacterial solution was

diluted 100 times, 60 mL of diluted bacterial solution was added to each pot, and three replicates were set for each group, while an equal amount of sterile culture solution was added to the control group. Three months later, the plants were collected and the indexes were measured.

Determination of potted plant indicators

For plants: Vernier caliper and tape were used to measure the ground diameter and height of seedlings. Measuring the quantity and quality of root nodules. The leaf area was measured using a root scanner (10 upper, middle, and lower leaves of each pot were selected to measure the leaf area). Plants were sampled and dried, and the above-ground and underground biomass of the plants were measured, respectively.

For potted soils: The hydrolytic nitrogen of the soil was determined by the alkaline diffusion method. The effective phosphorus of the soil was determined using the acid soluble-molybdenum antimony anti-colorimetric method, and the pH was determined by a Mettler Toledo pH meter (water to soil ratio of 5:1).

Microbial strain identification and macro-genome sequencing

Identification of the physiological and biochemical characteristics

Physiological and biochemical characteristics, including the morphology of the bacteria, Gram test, amylase hydrolysis test, V.P test, methyl red test, hydrogen sulfide production test, gelatin liquefaction test, milk coagulation and peptonization test, and the nitrate reduction test *Common Identification Method of Bacteria and Characteristics and Yeast Identification Manual*.

16S rDNA identification of the gene sequence

The bacterial X-45 strain was identified using morphological characterization and 16s rRNA analysis. Molecular-level identification was performed with the support of Shanghai Jinyu Medical Laboratory Co., Ltd., The collected and collated rhizobial inter-rhizosphere soil samples were sent to Shanghai Mayobio Biomedical Technology Co., Ltd., for sequencing on the Illumina Miseq platform. The sequencing primer was 515F_907R.

Identification

As shown in **Table 1**, strain X-45 is a kind of bacteria producing bright red pigment, which is motile, convex, irregular on edge, unable to ferment sugars, and positive in Starch hydrolysis, indole, methyl red, V.P., citrate and hydrogen sulfide tests.

The 16S rDNA sequence of strain X-45 was compared and analyzed by using MEGA (version 6.0) software. As shown in the **Figure 5**, the phylogenetic tree was constructed. The sequence result was similar to that of *Serratia marcescens* by BLAST, and the similarity was 99.79%. Combining the previously mentioned results, the strain X-45 was confirmed as *Serratia marcescens* N1.14.

The nucleotide sequence of X-45 and the potted soil 16S sequence have been uploaded to the NCBI database, the registration numbers are MT645673[1] and PRJNA645742[2], respectively.

Statistical analysis

The bacterial sequences were submitted to the GenBank database[3]. Raw sequence data and sequencing quality files were obtained as FASTA files, and file access was used for processing and analysis through Mothur software as described previously by Schloss (Hakim et al., 2019). To account for potted soil microbial diversity as well as the abundance of dominant species, α-diversity indices (Chao1, Simpson, and Shannon indices) and relative abundance were quantified using OTU richness. In addition, the analysis detected the relationship between environmental factors, samples, and flora using the ggplot2 package; the ggplot2 package was set as the default parameter in R, and the vegan package was set as the default parameter in R for environmental association analysis. Plant indicators and soil physical and chemical property indicators were analyzed using spss software. Analysis of function difference between groups was calculated by Welch's *t*-test (Oksanen et al., 2011). Analysis of variance (ANOVA) was performed on plant biomass and soil physicochemical property data (Systat Inc., Evanston, IL, USA), using Student Newman-Keuls significant difference ($p < 0.05$) to distinguish treatments from controls (Manly, 2018).

Results and analysis

Screening of phosphate-dissolving bacteria

According to the results of the transparent phosphate-dissolving circle on the Monkina organic phosphorus and inorganic phosphorus culture plates, a strain with the ability of phosphate-dissolving was screened out. And the diameter of the transparent dissolved phosphate rings was D.

The colony diameter is represented by d, and D/d indicates the phosphate-dissolving effect of the strain: the larger the

1 https://www.ncbi.nlm.nih.gov/nuccore/MT645673

2 https://dataview.ncbi.nlm.nih.gov/objects?linked_to_id=PRJNA645742&archive=sra

3 http://www.ncbi.nlm.nih.gov

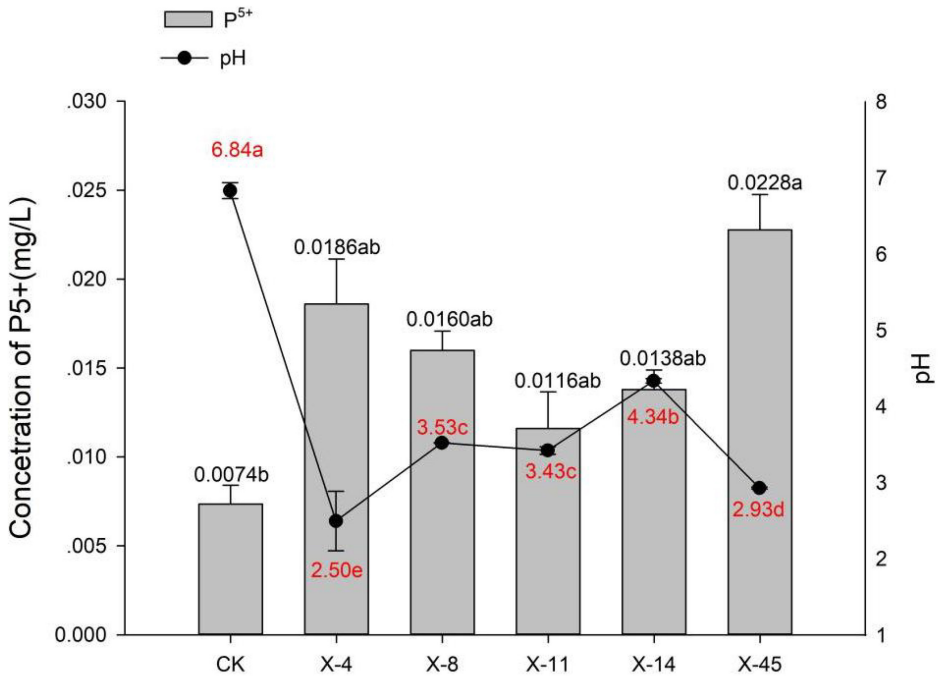

FIGURE 1
Release of active phosphorus and pH changes.

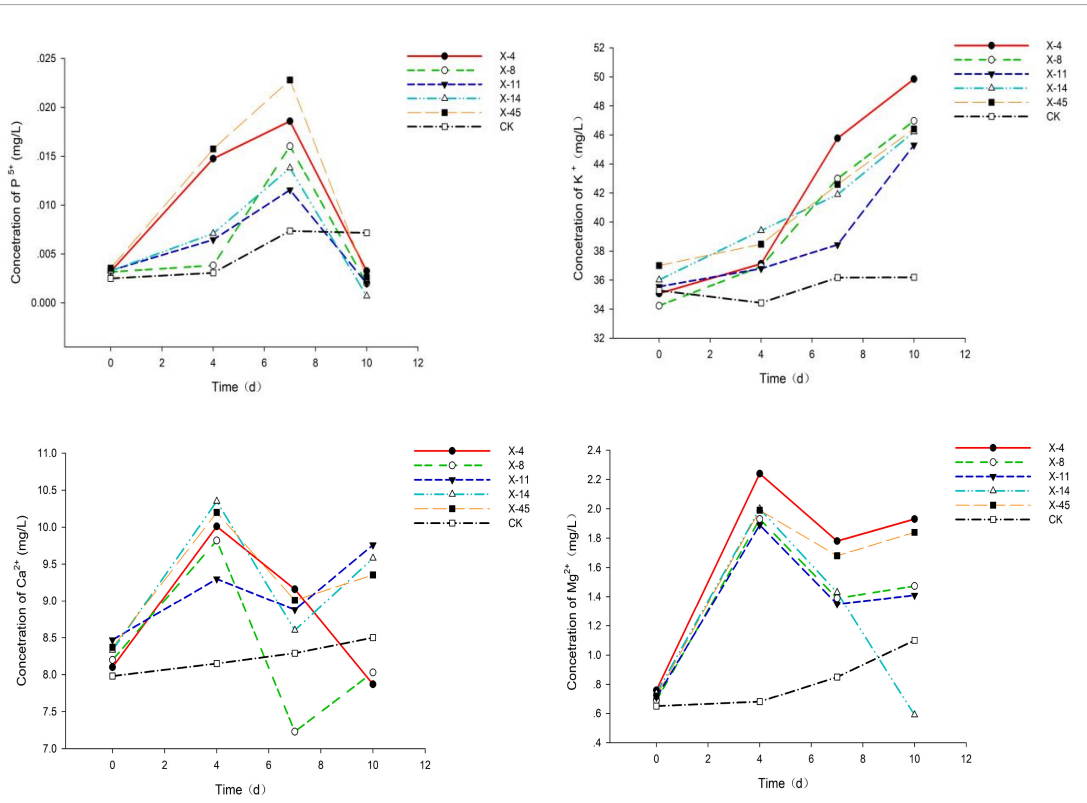

FIGURE 2
Phosphorus, potassium, calcium, and magnesium release from the fermentation broth of five strains of bacteria.

TABLE 1 Morphological physiological and biochemical characteristics of strain X-45.

Project	Characteristics	Project	Characteristics
Colony characteristics	Edge irregularity, Red, Bulge	Starch hydrolysis	+
Gram stain	Red, Negative	Indole test	+
Morphology	Short rod	Methyl red test	+
Motility	+	V.P. test	+
Glucose Fermentation(gas/acid)	−/+	Citrate test	+
Lactose Fermentation(gas/acid)	−/−	Hydrogen sulfide test	+

"+" means that the test result is positive; "−" means that the test result is negative.

TABLE 2 Primary effect of phosphate-dissolving bacteria.

Name	D/d(organic)	D/d(inorganic)	Name	D/d(organic)	D/d(inorganic)
X-4	3.61a	2.13c	X-35	—	1.27f
X-8	—	2.60bc	X-38	2.41bc	1.93c
X-11	3.06ab	4.54a	X-42	—	1.57d
X-14	3.47a	2.81b	X-43	2.83b	—
X-17	2.22c	—	X-44	1.42e	—
X-19	2.09cd	2.60bc	X-45	3.95a	1.67d
X-25	2.49b	1.53d	X-48	2.25c	—
X-27	2.50b	2.00c	X-53	1.79d	—
X-30	—	1.69d	X-55	2.22c	1.37f
X-33	—	1.50d	X-58	2.17c	—
X-34	—	1.44df			

D/d indicates the phosphate-dissolving effect of the strain: the larger the proportion, the better the effect of the dissolving phosphorus. Different letters in the columns indicate significant differences ($P < 0.05$).

TABLE 3 Composition of rock sample.

Species	K_2O	Na_2O	CaO	MgO	P_2O_5	Fe_2O_3	Al_2O_3	MnO
Concentration/percentage	3.71	1.39	0.21	1.28	0.11	6.81	15.21	0.04

proportion, the better the effect of the dissolving phosphate. A total of 58 strains of bacteria were isolated from the soil samples in this experiment. As shown in Table 2, 21 strains were screened, of which 15 were organo phosphate-dissolving bacteria, and 15 were inorganic phosphate-dissolving bacteria. Nine strains could degrade both organo phosphorus and inorganic phosphorus. Finally, five strains with good effect were selected for further study, namely X-4, X-8, X-11, X-14 and X-45.

Weathering effect of microbial strain X-45

Based on the results of the analysis of the rocks, the main components of the rock samples are shown in Table 3.

Five isolated bacteria were compared based on the release of effective phosphorus and the pH variation. With a concentration of 0.0228 mg/L, effective peak phosphorus released from microbial strain X-45 was the highest, which was 3.08 X higher than the control group (Figure 1). The pH of the fermentation broth was also determined. The pH of the group treated with X-45 decreased significantly relative to the blank control group. In addition, the X-45 microbial strain showed a greater ability to release each element into fermentation broth (Figure 2), and its peak release for potassium, calcium, and magnesium increased by 25.43, 11.71, and 155.56%, respectively, compared to the control. Overall, the release of the P, K, Ca, and Mg in the rock particles by each strain initially showed an upward trend followed by a downward trend. When the strains were in their growth phase, the concentration of the elements in the fermentation broth increased continuously. However, the strains in the growth phase would eventually consume large amounts of nutrient elements in the fermentation broth; moreover, the fermentation space is limited. Thus, the element dissolution rate is lower than the utilization rate, resulting in a downward trend. At the end of the experiment, we found that the rock particles became significantly smaller, and

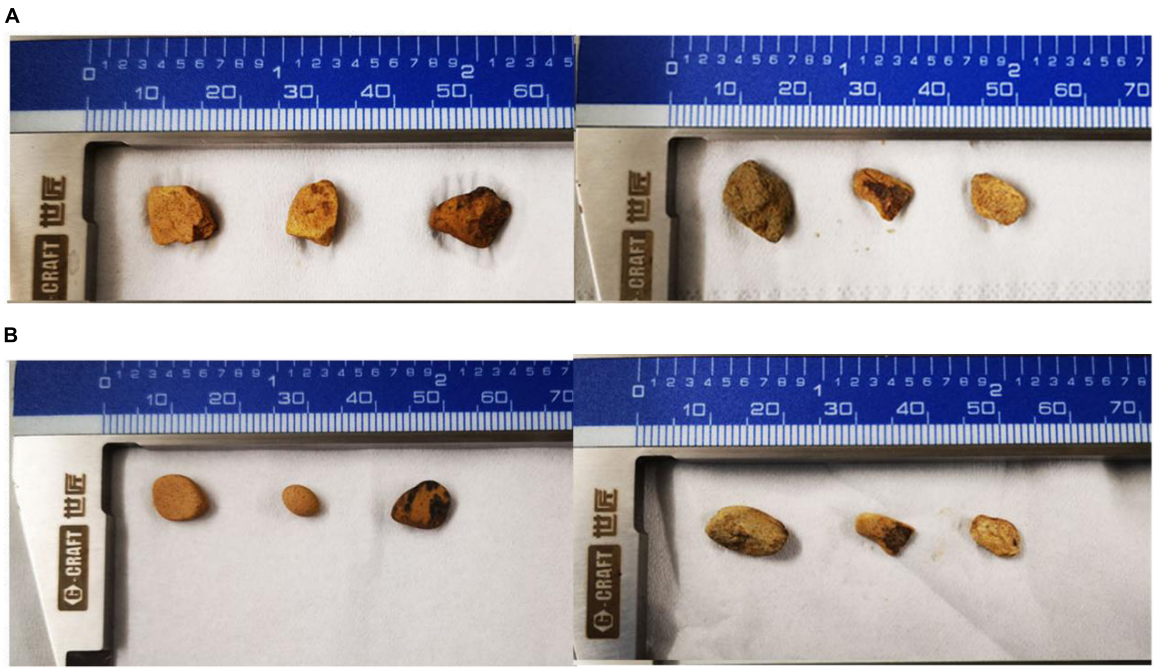

FIGURE 3
The dissolution of the rock after 10 days by *P. simplicissimum*. **(A,B)** Means three replicates in the X-45 treatment group before and after the experiment, respectively.

their morphology changed dramatically (Figure 3). The results showed that microbial strain X-45 effectively released each element and changed rock morphology significantly, indicating that X-45 can effectively promote rock dissolution.

Growth promotion of X-45

After treatment with microbial strain X-45, all above-ground indices of *I. pseudotinctoria* seedlings were higher than the sterile treatment group. With a significant increase of 22.7%, the above-ground biomass of the treated groups was 7.33 g. In addition, the ground diameter increased significantly by 23.52%, seedling height by 18.91%, and leaf area by 30.48% to the average values of 5.62 mm, 65 cm, and 6.55 cm^2 ($P < 0.05$), respectively.

In this study, the root nodules of the experimental plants were analyzed. The average number of root nodules formed in the sterile treatment group was about 8 cm, and the total mass of root nodules was about 0.19 g. The average number of root nodules formed in the seedlings treated with microbial strain X-45 was 86, and the total mass of roots of the seedlings treated with microbial strain X-45 was about 0.42 g. Compared with the control group, the number of root nodules and total mass increased significantly by 11.21 X and 121.05% in the seedlings treated with microbial strain X-45, respectively. In addition, the root biomass, root surface area, and root volume of the sterile treatment group were 1.2 g, 232.26 cm^2, and 1.71 cm^3, respectively. The root biomass of the seedlings treated with microbial strain X-45 increased by 45% to 1.74 g ($P < 0.05$), root surface area increased significantly by 13.91% to 264.57 cm^2, and root volume increased significantly by 53.8% ($P < 0.05$) to 2.63 cm^3 ($P < 0.05$).

In addition, the physical and chemical properties of *I. pseudotinctoria* potted soil also changed. With a significant increase of 22.76% ($P < 0.05$) and 19.95%, concentrations of available phosphorus and hydrolyzed nitrogen of the potted soil treated with microbial strain X-45 were 3.02 mg/kg and 248.5 mg/kg, respectively. The potted soil was acidified to a certain extent, and the pH decreased from 7.06 to 6.89. Pot experiment further confirmed that microbial strain X-45 could convert phosphorus and nitrogen in soil into forms directly absorbed and utilized by plants to promote plant growth and create an environment conducive to the growth of *I. pseudotinctoria* plants. The growth-promoting effect of X-45 microbial strain on *I. pseudotinctoria* was further verified (Table 4).

Effect of X-45 microbial strain inoculation on soil microbiota

The microbial diversity in potted soil was detected using high-throughput sequencing. The microbial community composition of potted soil was also analyzed. There was no

TABLE 4 Comparison of physicochemical properties of soil plants.

Groups (sample)	Plant (underground)			Plant (aboveground)				Soil (potted,mg/kg)		
	Total nodule weight(g)	Dry weight(g)	Root volume(cm^3)	Dry weight(g)	Ground diameter(mm)	Plant height(cm)	Average leaf area(cm^2)	AP	HN	pH
CK	0.19 ± 0.06b	1.20 ± 0.07b	1.71 ± 0.02a	5.74 ± 0.07b	4.55 ± 0.39b	54.67 ± 2.52b	5.02 ± 0.30b	2.46 ± 0.36b	207.17 ± 3.21a	7.06 ± 0.06a
X-45	0.42 ± 0.07a	1.74 ± 0.11a	2.63 ± 0.11a	7.33 ± 0.36a	5.62 ± 0.16a	65.00 ± 5.57a	6.55 ± 0.21a	3.02 ± 0.33a	248.50 ± 4.58a	6.89 ± 0.10a

The values "a, b" represent the standard deviation. Different letters represent significant differences. Abbreviations are HN: Hydrolyzable nitrogen; AP: available phosphorus.

difference in microbial community composition at the phylum level between the control group and the potted soil treated with the microbial strain X-45. However, a remarkable difference was observed in the relative abundance of microorganisms between these two groups. The Proteobacteria abundance increased from 35% to 64% (**Figure 4**). *Bradyrhizobium* (circa 46%) was found to be the dominant genus in the X-45 treated group, while the relative abundance of *Bradyrhizobium* in the control group was less than 0.5% (**Figure 5**). The student's t-test was used to test the significance of species differences at the genus level (**Figure 6**). *Bradyrhizobium* was found to be significantly different between the two treatment groups ($P < 0.05$).

Redundancy analysis

Redundancy analysis (RDA) was conducted at the genus level to reflect the relationship among environmental factors, flora, and samples (**Figure 7**; axis 1 = 95.52%, axis 2 = 1.87%). This analysis showed that community distribution was significantly and positively correlated with available phosphorus ($r^2 = 0.91$, $P < 0.01$), significantly and positively with hydrolyzed nitrogen ($r^2 = 0.99$, $P < 0.05$), and negatively with pH ($r^2 = 0.97$, $P < 0.05$). Out of the identified genera, *Bradyrhizobium* showed the strongest correlation with various environmental factors (**Figure 7**).

Discussion

The growth of plants is mainly dependent on the soil. However, the poor conditions of high and steep exposed slopes restrict the phytoremediation process. This study aimed to screen and isolate the microorganisms that could improve the soil environment and thus the efficiency of phytoremediation. In this study, the Mongina organic (inorganic) phosphorus medium screening method was used to screen phosphate-dissolving bacteria. Research has shown that the transparent circle on the Monkina plate and the available phosphate concentration in the fermentation broth can only preliminarily explain the phosphate dissolving ability of phosphate-dissolving bacteria and cannot further reliably evaluate their phosphate dissolving effect (Calvaruso et al., 2013). Therefore, in this study, rock particles were used instead of phosphate in Mongina culture medium for dissolution experiments, and the ability of the phosphate-dissolving bacteria was determined by analyzing the changes of phosphate in the fermentation broth. A considerable release of K, Ca, Mg, and active phosphorus by soil microbes in X-45 treated soil was observed through rock weathering experiments. In addition to the decrease in pH (Wang et al., 2018), previous studies have shown that microbes could secrete H + to dissolve minerals, validating the acidification effect of microbes (Azaiez et al., 2018). In

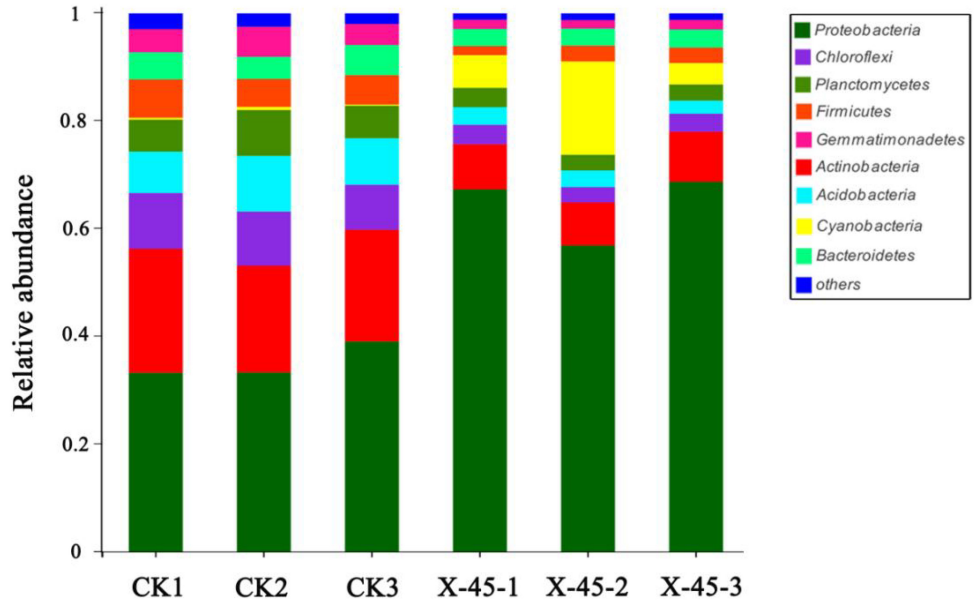

FIGURE 4
Relative abundance of bacterial communities at phylum.

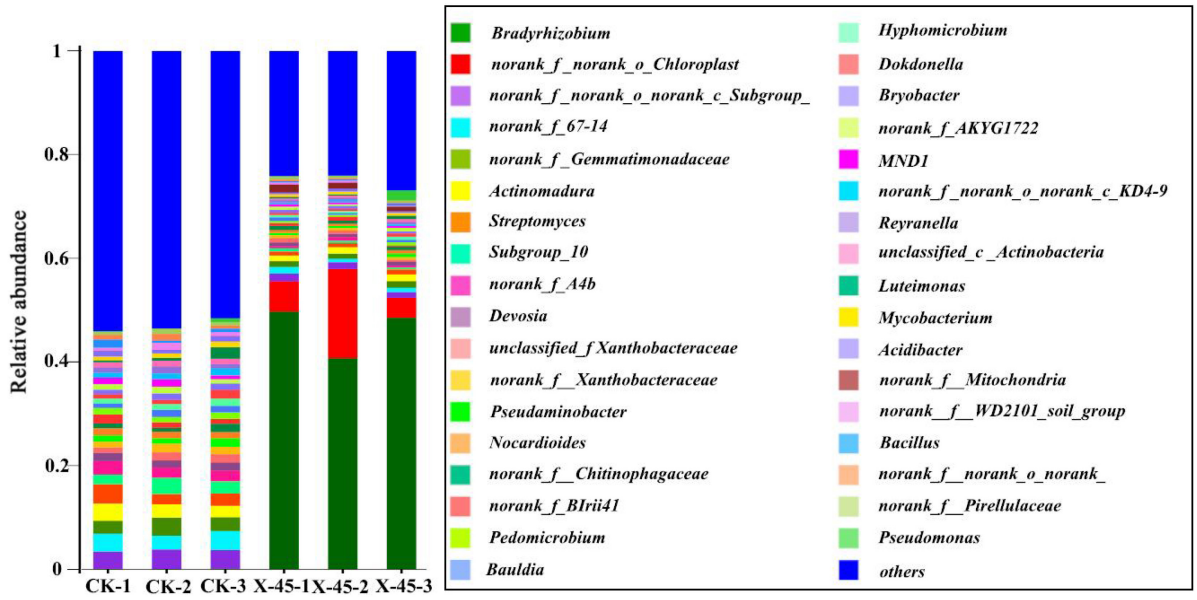

FIGURE 5
Relative abundance of bacterial communities at genus level.

this study, the rock weathering ability of microbial strain X-45 accelerated the soil formation process, improved the soil quality, and provided mineral nutrients required for plant growth.

Symbiotic nitrogen fixation of rhizobia in legume nodule injects about 40 million tons of nitrogen into the agricultural system every year (Udvardi and Poole, 2013), increasing plant nutrient content, improving soil health reclamation, and reducing synthetic nitrogen fertilizer application in agriculture (Mahmud et al., 2020). In the pot experiment, we observed that the number of root nodules of *I. pseudotinctoria* inoculated with microbial strain X-45 was 11.21X that of the control group. The total weight of root nodules increased by 121.05%, and hydrolyzed nitrogen content in pot soil increased by 19.95%. With increasing nitrogen content, X-45 microbial

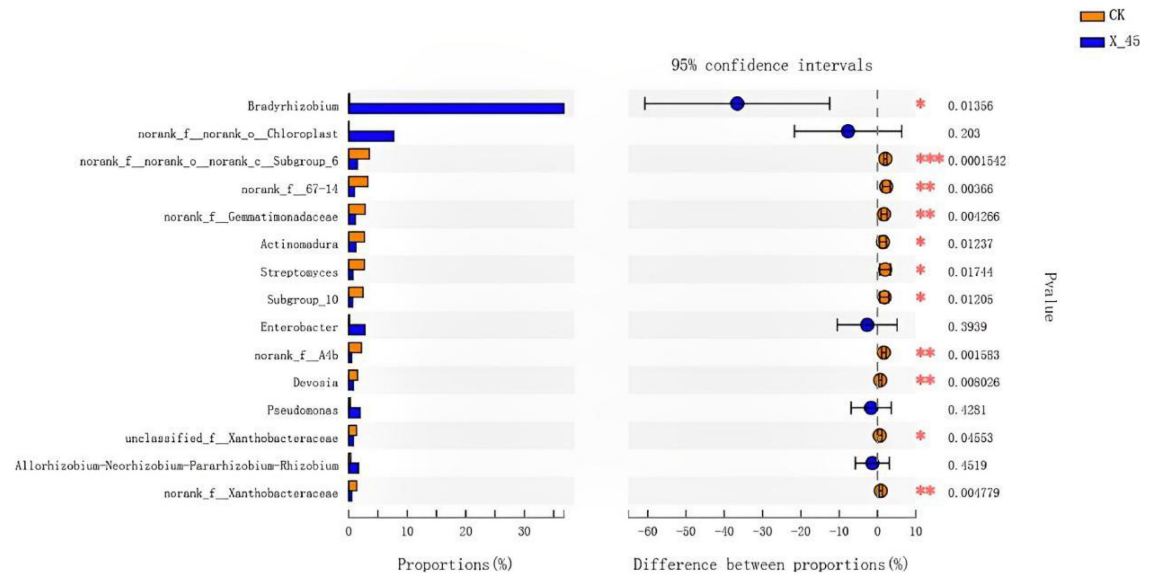

FIGURE 6
Student's *t*-test bar plot on genus level with 95% confidence intervals.

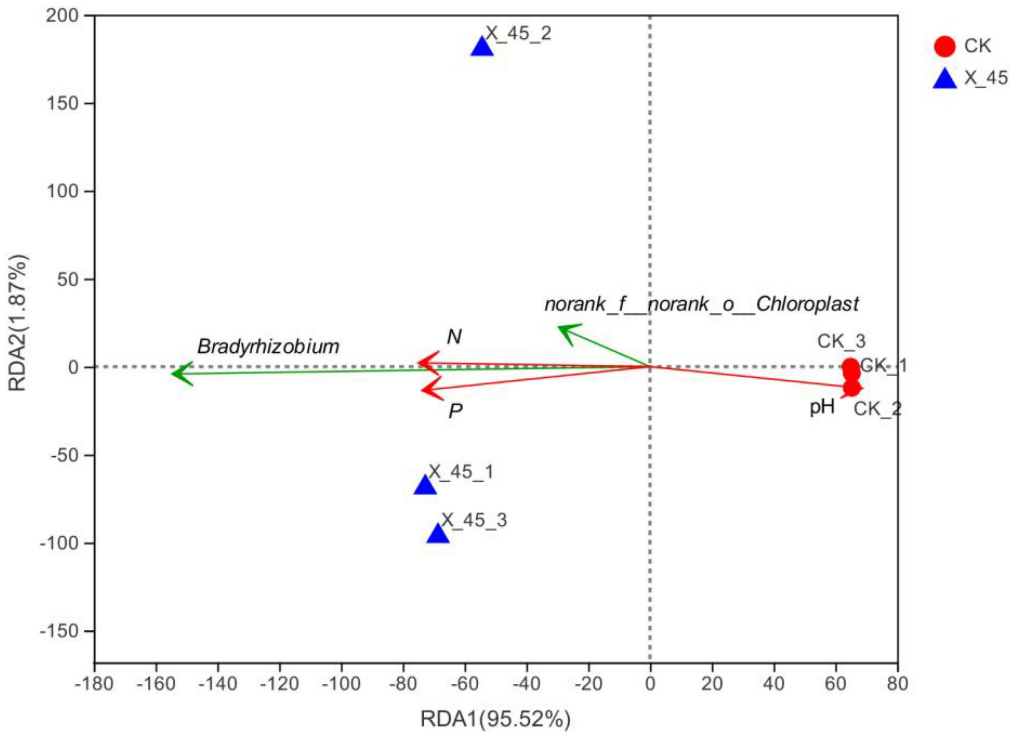

FIGURE 7
Bacterial community redundancy analysis (RDA).

strain promoted the nodulation and nitrogen fixation in *I. pseudotinctoria* (Mu et al., 2018). Thus, the symbiotic nitrogen fixation ability of root nodules and host plants was effectively brought into play.

In this study, the microbial strain X-45 converted soil phosphorus and nitrogen to a form that could be directly absorbed and used by the plant. Also, a significant improvement was noticed in the hydrolytic nitrogen and effective phosphorus

in the potted soil treated with microbial strain X-45. This validated that in this study, phosphorus-solubilizing bacteria in the experimental soil slowed down the fixation of effective phosphorus and promoted the growth of *I. pseudotinctoria* (Chungopast et al., 2021). The isolated microbial strain X-45 belongs to the genus Serratia. Previous studies have shown that it could transform insoluble phosphorus into accessible phosphorus and be used as an inoculant to increase phosphorus uptake by plants (Srinivasan et al., 2012). The above analysis proved that X-45, a phosphorus solubilizing bacterium, released phosphorus effectively. Besides, it improved soil quality and promoted plant growth. Thus, microbial strain X-45 could be used as a functional strain for phosphorus solubilization and microbial fertilizer.

Microbial agents could change soil microbial community structure. In this study, we observed that the application of microbial agent X-45 directly increased the relative abundance of *Proteobacteria*. *Serratia marcescens* (the original genus of X-45) was not found in the potted soil; however, the dominant genus was found to be *Bradyrhizobium*, which belongs to *Proteobacteria* just like microbial strain X-45. *Bradyrhizobium*, a type of rhizobium that grows in the roots of legumes, has nitrogen fixation ability (Hungria et al., 2015). Thus, it can improve the nodulation rate and nodulation amount (Masciarelli et al., 2014), increase nutrient content and dry matter accumulation (Gough et al., 2021), improve soil quality, and decrease soil degradation (Li et al., 2018). Previous studies have shown that soil microbes play an important role in the growth and health of plants. Relevant studies have shown that the relative abundance of *Proteobacteria* in healthy soil is higher than in soil infected with bacterial wilt (Yuan et al., 2020). A higher abundance of beneficial microorganisms improves soil quality and thus promotes a lower incidence of morbidity, higher nutrient content, and soil enzyme activity (Wang et al., 2017). In addition, according to the RDA analysis of environmental factors and bacterial communities, such bacterial communities as *Bradyrhizobium* are significantly positively correlated with available phosphate and hydrolyzed nitrogen, indicating that X-45 indirectly improves the release of nutrients by promoting the increase in the abundance of *Bradyrhizobium*. Therefore, X-45 can be used as a rhizobium growth promoter, and it is potentially important when planting legumes in poor soil areas for slopes protection.

In this study, we observed that X-45 microbial strain inoculant could rapidly shorten the soil improvement cycle compared with organic fertilizer. Previous studies have shown that after 35 years of field experiments with soybean compost, the abundance of beneficial microorganisms in the soil increased significantly, from less than 1 to 40% of the fungal species (Li et al., 2018). Compared with this study, experimental results of the current study showed that three months after inoculation with microbial strain X-45, the abundance of *Aspergillus* in the test group increased from 35 to 64%, and the abundance of *Bradyrhizobium* increased from less than 1 to 42%. This suggested that X-45 can rapidly shorten the time span of the improvement cycle of soil beneficial microbial populations compared to organic fertilizer application.

In a previous study, the hypothesis of "the imposed effect for promoting leguminous plant growth," including mineral weathering, nodule growth promotion, and beneficial microbial regulation, was based on the role played by fungi *Penicillium simplicissimum* NL-Z1 (Zhuang et al., 2021). This study also confirmed the hypothesis of the superposition effect of legume promotion via bacteria. According to previous studies, the inoculation of beneficial microorganisms, such as fungi and bacteria, on legume plates may differ significantly from harmful microorganisms.

Conclusion

In this study, the highly efficient phosphorus-dissolving lithotrophic bacterium X-45 was isolated from soil samples of Yueyang Avenue, Yueyang City, Hunan Province, China, by conventional methods and rock weathering experiments. The pot experiment showed that microbial strain X-45 increased the legume's symbiotic nitrogen fixation effect and promoted plant growth. The microbial analysis at the genus level showed that microbial strain X-45 substantially enhanced the growth of *Bradyrhizobium*. The ability of *Bradyrhizobium* to improve the physicochemical properties of the soil was verified using RDA analysis. Based on the above analysis, we concluded that the beneficial changes in soil flora of *I. pseudotinctoria* potted plants were due to bacterial agent X-45. Besides, the addition of X-45 for soil improvement, combined with symbiotic nitrogen fixation by legumes, indirectly regulated the abundance of beneficial soil microbes and improved soil quality. The interconnection of mineral weathering, rhizome promotion, and microbial regulation significantly promoted the growth of *I. pseudotinctoria* by improving soil quality, which is of great importance for slope restoration.

Data availability statement

The datasets presented in this study can be found in online repositories. The names of the repository/repositories and accession number(s) can be found below: The nucleotide sequence of X-45 and the potted soil 16S sequence have been uploaded to the NCBI database, the registration numbers are MT645673 and SRP271689, respectively.

Author contributions

JXZ and JYZ: conceptualization, designed the experiments, performed the experiments, analyzed the data, and wrote the draft. JXZ and JL contributed clinical advices and review and editing the manuscript. JXZ and CL designed the research study, wrote the manuscript, and supervision. All authors read and agreed to the published version of the manuscript.

Conflict of interest

The authors declare that the research was conducted in the absence of any commercial or financial relationships that could be construed as a potential conflict of interest.

Publisher's note

All claims expressed in this article are solely those of the authors and do not necessarily represent those of their affiliated organizations, or those of the publisher, the editors and the reviewers. Any product that may be evaluated in this article, or claim that may be made by its manufacturer, is not guaranteed or endorsed by the publisher.

Supplementary material

The Supplementary Material for this article can be found online at: https://www.frontiersin.org/articles/10.3389/fmicb.2022.988692/full#supplementary-material

References

Azaiez, A., Beaudoin Nadeau, M., Bertrand, A., and Khasa, D. P. (2018). In vitro selection of ecologically adapted ectomycorrhizal fungi through production of fungal biomass and metabolites for use in reclamation of biotite mine tailings. *Mycologia* 110, 1017–1032. doi: 10.1080/00275514.2018.1520036

Barker, W. W., Welch, S. A., and Banfield, J. F. (2018). "Biogeochemical weathering of silicate minerals," in *Geomicrobiology*, eds J. F. Banfield and K. H. Nealson (Berlin: De Gruyter), 391–428. doi: 10.1515/9781501509247-014

Calvaruso, C., Turpault, M.-P., Frey-Klett, P., Uroz, S., Pierret, M.-C., Tosheva, Z., et al. (2013). Increase of apatite dissolution rate by Scots pine roots associated or not with *Burkholderia glathei* PML1 (12) Rp in open-system flow microcosms. *Geochim. Cosmochim. Acta* 106, 287–306. doi: 10.1016/j.gca.2012.12.014

Chungopast, S., Thongjoo, C., Islam, A., and Yeasmin, S. (2021). Efficiency of phosphate-solubilizing bacteria to address phosphorus fixation in Takhli soil series: A case of sugarcane cultivation, Thailand. *Plant Soil* 460, 347–357. doi: 10.1007/s11104-020-04812-w

Dong, L., Li, Y., Xu, J., Yang, J., Wei, G., Shen, L., et al. (2019). Biofertilizers regulate the soil microbial community and enhance *Panax ginseng* yields. *Chin. Med.* 14:20. doi: 10.1186/s13020-019-0241-1

Gough, E. C., Owen, K. J., Zwart, R. S., and Thompson, J. P. (2021). Arbuscular mycorrhizal fungi acted synergistically with *Bradyrhizobium* sp. to improve nodulation, nitrogen fixation, plant growth and seed yield of mung bean (*Vigna radiata*) but increased the population density of the root-lesion nematode *Pratylenchus thornei*. *Plant Soil* 465, 431–452. doi: 10.1007/s11104-021-05007-7

Hakim, J. A., Morrow, C. D., Watts, S. A., and Bej, A. K. (2019). High-throughput amplicon sequencing datasets of the metacommunity DNA of the gut microbiota of naturally occurring and laboratory aquaculture green sea urchins *Lytechinus variegatus*. *Data Brief* 26:104405. doi: 10.1016/j.dib.2019.104405

Hu, G., Liu, H., Yin, Y., and Song, Z. (2015). The role of legumes in plant community succession of degraded grasslands in northern China. *Land Degrad. Dev.* 27, 366–372. doi: 10.1002/ldr.2382

Hungria, M., Nogueira, M. A., and Araujo, R. S. (2015). Soybean seed co-inoculation with *Bradyrhizobium* spp. and *Azospirillum brasilense*: A new biotechnological tool to improve yield and sustainability. *Am. J. Plant Sci.* 6, 811–817. doi: 10.4236/ajps.2015.66087

Li, F., Chen, L., Redmile-Gordon, M., Zhang, J., Zhang, C., Ning, Q., et al. (2018). Mortierella elongata's roles in organic agriculture and crop growth promotion in a mineral soil. *Land Degrad. Dev.* 29, 1642–1651. doi: 10.1002/ldr.2965

Ma, L., Huang, W., Guo, C., Wang, R., and Xiao, C. (2012). Soil microbial properties and plant growth responses to carbon and water addition in a temperate steppe: The importance of nutrient availability. *PLoS One* 7:e35165. doi: 10.1371/journal.pone.0035165

Mahmud, K., Makaju, S., Ibrahim, R., and Missaoui, A. (2020). Current progress in nitrogen fixing plants and microbiome research. *Plants* 9:97. doi: 10.3390/plants9010097

Manly, B. F. (2018). *Randomization, Bootstrap and Monte Carlo Methods in Biology: Texts in Statistical Science*. London: Chapman and Hall/CRC. doi: 10.1201/9781315273075

Masciarelli, O., Llanes, A., and Luna, V. (2014). A new PGPR co-inoculated with *Bradyrhizobium japonicum* enhances soybean nodulation. *Microbiol. Res.* 169, 609–615. doi: 10.1016/j.micres.2013.10.001

Mo, B., and Lian, B. (2011). Interactions between *Bacillus mucilaginosus* and silicate minerals (weathered adamellite and feldspar): Weathering rate, products, and reaction mechanisms. *Chin. J. Geochem.* 30, 187–192. doi: 10.1007/s11631-011-0500-z

Mu, X., Chen, Q., Wu, X., Chen, F., Yuan, L., and Mi, G. (2018). Gibberellins synthesis is involved in the reduction of cell flux and elemental growth rate in maize leaf under low nitrogen supply. *Environ. Exp. Bot.* 150, 198–208. doi: 10.1016/j.envexpbot.2018.03.012

Oksanen, J., Blanchet, F., Kindt, R., Legendre, P., O'Hara, R., Simpson, G., et al. (2011). *R package version 1.17-7. Community ecology package, vegan*. Available online at: https://cran.r-project.org/web/packages/vegan/index.html (accessed April 17, 2022).

Song, C., Sarpong, C. K., Zhang, X., Wang, W., Wang, L., Gan, Y., et al. (2021). Mycorrhizosphere bacteria and plant-plant interactions facilitate maize P acquisition in an intercropping system. *J. Clean. Prod.* 314:127993. doi: 10.1016/j.jclepro.2021.127993

Srinivasan, R., Alagawadi, A. R., Yandigeri, M. S., Meena, K. K., and Saxena, A. K. (2012). Characterization of phosphate-solubilizing microorganisms from salt-affected soils of India and their effect on growth of sorghum plants [*Sorghum bicolor* (L.) Moench]. *Ann. Microbiol.* 62, 93–105. doi: 10.1007/s13213-011-0233-6

Udvardi, M., and Poole, P. S. (2013). Transport and metabolism in legume-rhizobia symbioses. *Annu. Rev. Plant Biol.* 64, 781–805. doi: 10.1146/annurev-arplant-050312-120235

Wang, R., Zhang, H., Sun, L., Qi, G., Chen, S., and Zhao, X. (2017). Microbial community composition is related to soil biological and chemical properties and bacterial wilt outbreak. *Sci. Rep.* 7:343. doi: 10.1038/s41598-017-00472-6

Wang, Y. L., Wang, Q., Yuan, R., Sheng, X. F., and He, L. Y. (2018). Isolation and characterization of mineral-dissolving bacteria from different levels of altered mica schist surfaces and the adjacent soil. *World J. Microbiol. Biotechnol.* 35:2. doi: 10.1007/s11274-018-2573-x

Wu, Y.-W., Zhang, J.-C., Wang, L.-J., and Wang, Y.-X. (2017). A rock-weathering bacterium isolated from rock surface and its role in ecological restoration on exposed carbonate rocks. *Ecol. Eng.* 101, 162–169. doi: 10.1016/j.ecoleng.2017.01.023

Yuan, J., Wen, T., Zhang, H., Zhao, M., Penton, C. R., Thomashow, L. S., et al. (2020). Predicting disease occurrence with high accuracy based on soil macroecological patterns of Fusarium wilt. *ISME J.* 14, 2936–2950. doi: 10.1038/s41396-020-0720-5

Zhao, J., Lu, W., Zhang, F., Lu, C., Du, J., Zhu, R., et al. (2014). Evaluation of CO2 solubility-trapping and mineral-trapping in microbial-mediated CO2–brine–sandstone interaction. *Mar. Pollut. Bull.* 85, 78–85. doi: 10.1016/j.marpolbul.2014.06.019

Zhu, Y., Duan, G., Chen, B., Peng, X., Chen, Z., and Sun, G. (2014). Mineral weathering and element cycling in soil-microorganism-plant system. *Sci. China Earth Sci.* 57, 888–896. doi: 10.1007/s11430-014-4861-0

Zhuang, J., Liu, C., Wang, X., Xu, T., and Yang, H. (2021). *Penicillium simplicissimum* NL-Z1 induced an imposed effect to promote the leguminous plant growth. *Front. Microbiol.* 12:738734. doi: 10.3389/fmicb.2021.738734

frontiers | Frontiers in Microbiology

TYPE Original Research
PUBLISHED 04 November 2022
DOI 10.3389/fmicb.2022.1000222

Check for updates

OPEN ACCESS

EDITED BY
Víctor Manuel Ruíz-Valdiviezo,
Tecnológico Nacional de México/Instituto Tecnológico de Tuxtla Gutiérrez, Mexico

REVIEWED BY
Eduardo Castro-Nallar,
University of Talca,
Chile
Oskars Purmalis,
University of Latvia,
Latvia

*CORRESPONDENCE
Everlon Cid Rigobelo
everlon.cid@unesp.br

SPECIALTY SECTION
This article was submitted to Microbe and Virus Interactions with Plants, a section of the journal Frontiers in Microbiology

RECEIVED 21 July 2022
ACCEPTED 13 October 2022
PUBLISHED 04 November 2022

CITATION
da Silva MSRA, de Carvalho LAL, Braos LB, de Sousa Antunes LF, da Silva CSRA, da Silva CGN, Pinheiro DG, Correia MEF, Araújo ES, Colnago LA, Desoignies N, Zonta E and Rigobelo EC (2022) Effect of the application of vermicompost and millicompost humic acids about the soybean microbiome under water restriction conditions.
Front. Microbiol. 13:1000222.
doi: 10.3389/fmicb.2022.1000222

COPYRIGHT
© 2022 da Silva, de Carvalho, Braos, de Sousa Antunes, da Silva, da Silva, Pinheiro, Correia, Araújo, Colnago, Desoignies, Zonta and Rigobelo. This is an open-access article distributed under the terms of the Creative Commons Attribution License (CC BY). The use, distribution or reproduction in other forums is permitted, provided the original author(s) and the copyright owner(s) are credited and that the original publication in this journal is cited, in accordance with accepted academic practice. No use, distribution or reproduction is permitted which does not comply with these terms.

Effect of the application of vermicompost and millicompost humic acids about the soybean microbiome under water restriction conditions

Maura Santos Reis de Andrade da Silva[1,2], Lucas Amoroso Lopes de Carvalho[1], Lucas Boscov Braos[3], Luiz Fernando de Sousa Antunes[2], Camilla Santos Reis de Andrade da Silva[4], Cleudison Gabriel Nascimento da Silva[5], Daniel Guariz Pinheiro[1], Maria Elizabeth Fernandes Correia[6], Ednaldo da Silva Araújo[6], Luiz Alberto Colnago[7], Nicolas Desoignies[8], Everaldo Zonta[4] and Everlon Cid Rigobelo[1]*

[1]Programa de Pós-Graduação em Microbiologia Agropecuária, Universidade Estadual Paulista "Júlio de Mesquita Filho" (UNESP), Faculdade de Ciências Agrárias e Veterinárias, Jaboticabal, Brazil, [2]Universidade Federal Rural do Rio de Janeiro (UFRRJ), Seropédica, Rio de Janeiro, Brazil, [3]Faculdade de Ciências Agrárias e Veterinárias, Programa de Pós-graduação em Agronomia, Universidade Estadual Paulista (UNESP), Jaboticabal, Brazil, [4]Departamento de Solos, Instituto de Agronomia, Universidade Federal Rural do Rio de Janeiro (UFRRJ), Seropédica, Rio de Janeiro, Brazil, [5]Programa de Pós-graduação em Microbiologia Agrícola, Universidade Federal de Lavras (UFLA), Lavras, Minas Gerais, Brazil, [6]Embrapa Agrobiologia, Seropédica, Rio de Janeiro, Brazil, [7]Embrapa Instrumentação, São Carlos, São Paulo, Brazil, [8]Phytopathology, Microbial and Molecular Farming Lab, Centre D'Etudes et Recherche Appliquée-Haute Ecole Provinciale du Hainaut Condorcet, Ath, Belgium

Humic substances (HSs) are constituent fractions of organic matter and are highly complex and biologically active. These substances include humic acids (HA), fulvic acids (FA), and humin. HS are known to stimulate the root system and plant growth and to mitigate stress damage, including hydric stress. Humic acids have already been reported to increase microbial growth, affecting their beneficial effect on plants. However, there is scarce information on whether HA from vermicompost and millicompost, along with *Bradyrhizobium,* improves the tolerance of soybean to water restriction. This study aimed to evaluate the responses of soybean plants to the application of vermicompost HA (HA-V) and millicompost (HA-M) along with *Bradyrhizobium* sp. under water restriction. The experiment was carried out in a greenhouse, and the treatments received *Bradyrhizobium* sp. inoculation with or without the application of HA from vermicompost and millicompost with or without water restriction. The results showed that HA provided greater soybean growth and nodulation than the control. The application of HA-M stimulated an increase in the richness of bacterial species in roots compared to the other treatments. After the application of water stress, the difference between the treatments disappeared. Microbial taxa were differentially abundant in plants, with the fungal fraction most affected by HA application in stressed roots. HA-V appears to be more prominent in inducing taxa under stress conditions. Although the results showed slight differences between HA from vermicompost and

millicompost regarding plant growth, both humic acids promoted an increase in plant development compared to the control.

KEYWORDS

humic substances, microbiome, inoculation, water stress, humic acid

Introduction

Earthworm humus is recognized for its use in agriculture, as well as the humic acids (HA) extracted from this compound (García et al., 2018). The application of HA at low doses is capable of inducing beneficial effects on plants, improving their ability to take up nutrients and helping them overcome stress conditions (Canellas and Olivares, 2014). The role of HA in plant metabolism is closely related to the structure of these substances, and compounds from different matrices are expected to act differently in plants (Nardi et al., 2021). Another compound that has stood out for its benefit to plants is millicompost, which is produced from the processing of millipedes (*Diplopoda* sp.). These animals are able to use agricultural and urban waste, generating organic waste of great quality for plant growth. To date, there are no reports in the literature of the extraction and characterization of humic substances from millicompost.

The application of HA from different sources can increase soybean growth (Guo et al., 2015; da Silva et al., 2021a). This crop plays a key role in the world's agricultural and economic scenario, and part of the success of soybean establishment in Brazil is due to the benefits of inoculating this crop with elite *Bradyrhizobium* strains (Hungria and Mendes, 2015). This symbiosis provides all the nitrogen needed for soybeans and reduces the dependence on nitrogen fertilizers and, consequently, prevents nitrogen losses by leaching and the emission of gases into the atmosphere (Hungria and Mendes, 2015). However, biotic and abiotic stresses can reduce crop productivity – even harming the contribution of biological processes to agriculture – and are therefore a risk to global food security (De Freitas et al., 2022). The application of agrochemicals to control environmental stresses may be ineffective, and in this context, the use of biostimulants has been recommended (Hossain et al., 2020). As HA plays an important role in plant resilience in relation to abiotic stresses and in the protection of bacteria in unfavorable environmental conditions, it is plausible that the use of HA contributes to the maintenance of biological processes even under adverse environmental conditions (Canellas et al., 2020; da Silva et al., 2021a).

It is known that the phytomicrobiome has the ability to act as an extension of the plant genotype (Carrión et al., 2019) and that its composition can be influenced by external factors such as the application of biostimulants (da Silva et al., 2021b). Changes in the plant microbiome can often increase tolerance to environmental stresses. Timm et al. (2018) demonstrated that different abiotic stresses have an impact on the bacterial community, enriching specific microbial groups, which may contribute to plant protection against adverse environmental conditions. A study showed that the application of a plant stress-related amino acid (1-aminocyclopropane-1-carboxylate, ACC) can remodel the soil microbiome and promote greater plant tolerance to salt stress (Liu et al., 2020). The application of HA to rice roots also caused changes in the composition of bacterial genera associated with the plant, and the authors suggested that the enriched bacterial groups would be related to plant protection; however, experiments under stress conditions have not been performed (da Silva et al., 2021b).

Despite this knowledge, there are practically no studies on the effects of HA on the community of endogenous and plant-associated bacteria and how this relationship affects plant growth, development and protection against biotic and abiotic stresses. It is well established in the literature that plants naturally harbor a great diversity of microorganisms in their tissues, and this microbiota is involved in functions that affect plant growth and survival (Vandenkoornhuyse et al., 2015). Therefore, the aim of this study was to evaluate the composition of the endophytic community of soybean plants in relation to the application of humic acids from different sources (vermicompost and millicompost) cultivated under different water availability conditions.

Specifically, the following hypotheses were tested: (i) the application of millicompost (HA-M) and vermicompost (HA-V) HA in soybean have different effects on plant growth and (ii) select different microbial groups related to plant growth promotion in water restriction.

Materials and methods

Extraction of humic acids

Millicompost and vermicompost came from an experimental agroecological farm, called "Fazendinha Agroecológica km 47", which is a consortium between Embrapa Agrobiology, Federal Rural University of Rio de Janeiro and Pesagro. Humic acids and fulvic acids (FA) were extracted from these composts with KOH 0.1 mol L^{-1} in a ratio of 1:10 (v/v compost/solvent) under stirring for 4 h at room temperature. After that, the supernatant was separated from the humin (insoluble fraction), which was deposited at the bottom of the flask. Then, the supernatant (HA and FA) was acidified with 6 mol L^{-1} HCl to pH 1.5. Then, HA

(insoluble fraction) was separated from FA by centrifugation at 2,000*g* for 10 min. The HAs were frozen and lyophilized.

Characterization of humic acids

Humic acid samples were ground and sieved in sieves with a mesh size of 2 mm. Spectra acquisition was performed by cross polarization-magic angle spinning in a Bruker BioSpin 400 MHz spectrometer (Bruker Corporation, Billerica, United States) using a cross polarization-magic angle sample spinning sequence. Samples were placed in 4 mm probes using a rotor spinning speed of 14 kHz, and the spectra acquisition parameters were as follows: temperature of 297 K, ^{13}C NMR frequency of 100.57 MHz, acquisition time of 0.04 s, contact time of 1 ms, recycle delay of 5 s, ^{1}H and ^{13}C pulse lengths of 2.5 and 3.8 μs, respectively, and 1,000 scans.

The spectra were processed with Bruker Topspin 3.2 software, phased, smoothed with a line broadening of 100 Hz, and baseline corrected. Each spectrum was then integrated after dividing it into chemical shift regions assigned to different carbon functional groups: 0–45 ppm (alkyl-C), 45–60 ppm (O- or N-substituted alkyl-C), 60–110 ppm (O-alkyl-and di-O-alkyl-C), 110–145 ppm (aromatic-C) 145–160, phenolic-C and 160–220 ppm (carbonyl-C + carboxyl-C). Based on the NMR results, the hydrophobicity index was calculated according to Aguiar et al. (2013).

The different carbon functional groups of humic acid samples were characterized using Fourier transform infrared (FTIR) spectroscopy on an IRAffinity-1 Shimadzu® spectrometer according to the method described by Stevenson (1994). Measurements were performed using 1 mg of ground sample mixed with 100 mg of potassium bromide (KBr), operating between wavelengths from 400 to 4,000 cm^{-1}. The elemental analyses of the C, H, and N contents of the HA were analyzed by a Perkin Elmer elemental analyzer (model 2,400). The results were as follows: C, 37.1%; H, 4.5; N, 3.1; C:N ratio, 12; H:C ratio, 0.120 for HA-M and C, 32.6%; H, 4.1; N, 3.3; C:N ratio, 10; H:C ratio, 0.125 for HA-V.

Soil experiment

The experiment was set up in a randomized block design in a 3 × 2 factorial scheme, having as factors the application of humic acids and two water conditions (with and without water restriction). The experiment was carried out in a greenhouse using 5 L pots filled with red latosol, and fertilization was performed according to soil chemical analysis: pH, 6.9; C, 10 g kg^{-1}; Al, 0 mmol kg^{-1}; Ca, 79 mmol kg^{-1}; Mg, 13 mmol kg^{-1}; P, 14 mmol kg^{-1}; K, 0.7 mmolc kg^{-1}, no N source was added. Pots filled with dry soil were kept at field capacity, and irrigation, when necessary, was carried out with the same water volume for all pots until the time of water restriction. Treatments were composed as follows: (I) only inoculation of soybean seeds with commercial inoculant containing *Bradyrhizobium japonicum* SEMIA 5079 and *Bradyrhizobium diazoefficiens* SEMIA 5080; (II) inoculation of *B. japonicum* SEMIA 5079 and *B. diazoefficiens* SEMIA 5080 and application of 100 mg L^{-1} of millicompost HA in soybean seeds *via* the foliar route and (III) inoculation of *B. japonicum* SEMIA 5079 and *B. diazoefficiens* SEMIA 5080 and application of 150 mg L^{-1} of vermicompost HA in soybean seeds *via* the foliar route. A volume of 1 ml of inoculant was applied *via* soybean seeds of the ADV 4317 IPRO cultivar., and treatments that received HA had this compound added to the inoculant at the time of planting at the concentrations described above. The HA doses used in the present study were based on previous dose–response experiments of the different HAs in soybean. Each pot contained two seedlings, and foliar HA application occurred after 10 days of seed germination, with applications every 3 days. Three applications were performed at doses of 100 mg L^{-1} of millicompost HA and 150 mg L^{-1} of vermicompost HA, both diluted in water. In the treatment without HA, applications were performed only with water. After 25 days from the beginning of the experiment, a group of plants was submitted to water restriction for 5 days; in the other group with the same treatments, irrigation was maintained. Collection took place after 30 days of experimentation. The dry shoot and root mass, nodules and number of nodules, relative leaf water content (RWC) and chlorophyll and carotenoid contents were evaluated according to Wellburn (1994). Shoots and roots were collected for DNA extraction.

Soil moisture, relative leaf water content and chlorophyll and carotenoid contents

Soil samples were collected at a depth of 10 cm, with three samples per pot, to obtain the soil moisture. The soil wet mass was weighed, and later, these samples were taken to an oven for 24 h at 105°C to obtain the dry mass. These measurements were used to obtain soil moisture based on the following equation: M% = [(soil wet mass) – (soil dry mass)]/(soil wet mass) × 100.

To evaluate the relative leaf water content, 15 disks were collected from the same leaf of the penultimate trefoil of each plant as a single sample; then, its fresh weight (FW) was measured. Subsequently, the material was submerged in distilled water for 6 h. The turgid weight (TW) of leaves was obtained, and after that, the material was placed in an oven at 60°C for 48 h to obtain the dry weight (DW). The following equation was used to calculate the RWC: RWC = [(FW – DW)/(TW – DW)] × 100%.

A total of 0.025 g of fresh leaf mass was removed from the penultimate trefoil and placed in tubes filled with 80% acetone. The extraction process was carried out in triplicate. After this period, readings were taken at the following wavelengths: chlorophyll a at 663 nm (A662); chlorophyll b at 647 nm (A645) and carotenoids (carotene [c] + xanthophylls [x]) at 470 nm (A470). To calculate the chlorophyll (Chl) and carotenoid (Car) concentrations, the formulas described by Lichtenthaler (1987)

were used: Chl a + b = 7.05 A661.6 + 18.09 A644.8. Total chlorophyll (Chl a + b) and carotenoid contents were expressed as μg of pigment per gram of fresh mass (μg/g; Wellburn, 1994).

DNA extraction

To obtain the endophytic community, shoots and roots were sterilized. First, the plant material was washed in running water and then added to sterile tubes containing 50% bleach (with 0.01% Tween 20). The plant material was vortexed at maximum speed for 2 min, the disinfectant solution was removed, and 70% alcohol was added. Subsequently, stirring was carried out at maximum speed for 1 min, and then, the alcoholic solution was removed and distilled water (previously sterilized) was added, again stirring for 1 min, which step was performed twice more. The water from the last wash was inoculated into Luria Bertani (LB) solid medium, and plates were incubated for 3 days at 28°C to infer the efficiency of the sterilization process. Sterilized shoots and roots were macerated with a previously sterilized mortar and pestle in the presence of liquid nitrogen, and 80 mg of the material was used for total DNA extraction. A Qiagen DNeasy® PowerPlant® kit was used, and the methodology was performed according to the manufacturer's instructions. The quantity and quality of the total DNA extracted was evaluated in a NanoDrop® ND 1000c spectrophotometer. The DNA concentration ($ng\,\mu L^{-1}$) was measured by absorbance at a wavelength of 260 nm, and the relationship between absorbance values at 260 and 280 nm was used as an indicator of the extracted DNA quality. Integrity was assessed by 1% agarose gel electrophoresis. The gel was submitted to 70 V for 90 min and then stained with ethidium bromide and subsequently visualized with ultraviolet light in a transilluminator.

Sample sequencing

For the sequencing analysis, three replicates of root and shoot DNA samples from each treatment were used, which were sent to be sequenced at the NGS company. The hypervariable region of the 16S rRNA V4 gene was amplified with the primers 515F (5′-GTGCCAGCMGCCGCGGTAA-3′) and 806R (5′-GGACTA CHVGGGTWTCTAAT-3′; Caporaso et al., 2011), which were modified by adding degenerate nucleotides (Ns) in the 5′ region to increase the diversity of target sequences (de Souza et al., 2016). For the fungal fraction, the internal transcript spacer (ITS) was selected using ITS1f (CTTGGTCATTTAGAGGAAGTAA) and ITS2 (GCTGCGTTCTTCATCGATGC; Smith and Peay, 2014) primers. In both cases, library preparation followed previously established protocols with two-step amplification (de Souza et al., 2016; Armanhi et al., 2018). In the first PCR, the V4 prokaryotic region (16S rRNA) was amplified from the total DNA using the aforementioned primers with PNA-clamps (for the reduction of mitochondrial and chloroplast amplification; Lundberg et al., 2013). The products of this amplification were visualized on a 1.5% agarose gel. The purification of this PCR product was performed with Beckman's AMPure XP beads. After purification, Illumina adapters were ligated into a PCR. These ligation products were further purified and then visualized on a 1.5% agarose gel. The adapter binding products were quantified and normalized to the same concentration. After normalization, an equimolar pool of each sample and qPCR quantification were performed to validate and determine the final pool concentration in nM. The kit used was the KAPA Library Quantification kit for Illumina. The equipment used was the Illumina MiSeq in 2 × 250 base pair (bp) runs.

Analysis of experimentation data in the greenhouse

Experimentation data had normality and heteroscedasticity evaluated by the Shapiro–Wilk and Bartlett tests, respectively. Subsequently, analysis of variance (ANOVA) was performed, and when differences were detected, means were compared using Tukey's multiple comparison test. There was no significant difference between the blocks; therefore, this effect was disregarded.

Sequencing data processing

Processing started by assessing the quality of the data sequenced using the "FastQC" software (v.0.11.9). Subsequently, the cut-off parameters of the sequences were established. For this, the "-fastx_info," "-fastq_eestats2" and "-search_oligodb" functions from the "USEEARCH" software (v.11.0.667) were used, where the average quality thresholds and size and placement of adapters were obtained. Adapters were then removed using the "atropos" software (v.1.1.21), where sequences that did not contain them ("--discard-untrimmed") or were smaller than 200 bp ("--minimum-length = 200") were discarded. Adapter-free sequences underwent a quality control process using the "PRINSEQ-lite" software (v.0.20.3), where the final end was excluded, whose quality window ("-trim_qual_window = 3") was <20 and 18 for the "forward" (R1) and "reverse" (R2) sequences of each library, respectively. Finally, library pairs were sorted ("fastq_pair"; v.1.0) and merged ("PEAR"; v. 0.9.11). The merged sequences were submitted to the "DADA2" pipeline (v.1.22.0) through a package made available for R statistical software (v. 4.1.2; R Core Team, 2021), for the establishment of amplicon sequence variants (ASVs). The pipeline starts with a quality control ("filterAndTrim"), where sequences were filtered and truncated respecting the insert size of the 16S rRNA gene V4 region ("truncLen = 250") – for ITS sequences, whose size shows great variability, this parameter was suppressed. Then, possible sequencing errors were identified ("learnErrors") and corrected to obtain the exact ASV for each sample. Each ASV was taxonomically classified ("assignTaxonomy") based on the SILVA

10.3389/fmicb.2022.1000222

(v.138.1) and UNITE (v.8.2) reference banks for 16S rRNA and ITS libraries, respectively.

Diversity analysis and statistics

ASV counts per sample, as well as the relative taxonomic classifications, were imported as a "phyloseq" object (R package "phyloseq"; v.1.38.0) transformed into compositional data by the function "phyloseq_standardize_otu_abundance" (R package: "metagMisc" – v.0.0.4) with the "total" method, which applies total sum scaling (TSS) to the dataset. For alpha diversity, richness (Chao1) and diversity measures (Shannon and Gini-Simpson indices) were calculated using the "alpha" function of the "microbiome" R package (v.1.10.0). The existence of general differences in the alpha diversity means was evaluated with ANOVA/Kruskal–Wallis tests (depending on data distribution), and in the case of significance (p-value < 0.1), means were compared pair-to-pair with Student/Wilcoxon t-tests. Additionally, we performed a three-way ANOVA with alpha diversity measures to assess whether the interaction between the evaluated factors could influence these measures. For beta diversity, dissimilarities were calculated using the Bray–Curtis index ("distance" function of the "phyloseq" R package), from which the hierarchical clustering of samples was extracted in the form of a dendrogram, as well as a principal coordinate analysis (PCoA). The statistical significance of the separation of conditions evaluated was given through PERMANOVA, considering a p-value of 0.1. Finally, microorganisms that had significant changes in abundance among the conditions studied were identified. For this, the "DESeq2" approach was used, which implements the Wald test for the comparison of means (p-value < 0.05). For this analysis, samples were sectioned concerning plant tissue + stress condition and compared to humic acid treatments (formula = "plant tissue + stress ~ treatment"). The microbiota was collapsed at each taxonomic level and compared with the raw count sum of each taxon.

Results and discussion

Regarding the variables soil moisture, RWC and pigment content, only the stress factor differed (p-value ≤ 0.05). Soil moisture, RWC and pigment content were significantly higher in irrigated plants than in plants submitted to water restriction. Regarding plant dry mass, differences were observed between treatments with HA in both water conditions (Table 1).

In the present work, millicompost and vermicompost HA were evaluated, and to date, we have no reports of studies that have extracted and characterized millicompost HA and evaluated its effect on plants and their microbiota. The effect of millicompost and vermicompost HA on soybean growth was compared with that of the control (treatment that did not receive HA), both under favorable environmental conditions and under water deficit (Table 1).

TABLE 1 Soybean plant parameters evaluated under different water conditions.

	Without stress	With stress	
Shoot mass (g)			
HA			Overall average
HA-V	7.86Aa	3.37Aa	5.94A
HA-M	8.01Aa	3.65Aa	6.07A
Control	4.65Ba	0.82Ab	3.18B
Overall average	6.40a	2.40b	
Root mass (g)			
HA			Overall average
HA-V	1.46Aa	1.23Aa	1. 36A
HA-M	1.31Aa	0.88Aa	1.12AB
Control	0.89Aa	0.39Aa	0.70B
Overall average	1.15a	0.76a	
Nodules mass (g)			
HA			Overall average
HA-V	0.43Aa	0.11Ab	0.29A
HA-M	0.30Ba	0.15Ab	0.23A
Control	0.07Ca	0.02Aa	0.06B
Overall average	0.22a	0.09b	
No. of nodules			
HA			
HA-V	127.0Aa	44.25Ab	87.85A
HA-M	80.40Ba	35.65ABb	64.33B
Control	29.37Ca	6.00Ab	20.38C
Overall average	67.35a	26.16b	

Means followed by different letters, uppercase in the column compares HA-V with HA-M and with the control (Humic acid-HA), lowercase in the row compares the treatment with and without stress and differ from each other by the Tukey's test at 10% significance level.

Nuclear magnetic resonance and FTIR analyses revealed structural differences between HA-M and HA-V (Table 2; Supplementary Figure S1). These differences result from the biological and biochemical composting processes, in addition to differences in the composition of the source material itself. The ^{13}C NMR results show that both composts were in an advanced stage of humification with strong C aromatic and phenolic groups (Tadini et al., 2022). The HA-M and HA-V aromatic C represent ~24 and 20.3% and C-Phenolic ~10 and 7.1% of the total area NMR spectra, respectively. The higher aromatic and phenolic C contents in HA-M than HA-V may indicate differences in the original organic material sources or differences in the composting process. These differences in chemical composition might help to explain the differences related to plant performance (Table 1). HA-M has a lower proportion of C-alkyl groups, which are organic groups formed by saturated hydrocarbons and are relatively inert in the soil and contribute to increasing the hydrophobicity index (Table 2). Both composts had similar levels of C-alkyl-O (Table 2), revealing that most of their bioavailable molecules were consumed during the stabilization process.

TABLE 2 Distribution of different types of carbons, relative areas of spectral regions and the degree of aromaticity in humic acids.

	C-alkyl	C-alkyl-N/ methoxyl	C-alkyl-O	C-aromatic	C-carbonyl/ amide	Hydrophobicity Indices	C-Phenolic
	0–45	45–60	60–110	110–140	160–220		145–160
HA-M	23.0%	11.4%	22.7%	24.0%	8.9%	1.38	10.0
HA-V	30.5%	13.1%	23.1%	20.3%	5.9%	1.74	7.1

HA-M, Millicompost humic acids; HA-V, Vermicompost humic acids.

The FTIR spectra of HA-M and HA-V are similar, indicating similar chemical compositions, with the exception of the peak from 1,200 to 950 cm^{-1}, which is stronger in HA-V than in HA-M (Supplementary Figure S1). The absorbance from 3,000–3,500 is assigned to OH groups of phenolic and carboxylic acids and alcohols and NH groups of amines and amides, from 3,000 to 2,800 is assigned to C-H alkyl bonds and from 1,800 to 1,550 is assigned to C=O bonds of carbonyl, quinone, carboxylic acids, esters and amide, and the C=C vibration of aromatic molecules shows similar intensities. The band between 1,200 and 900 cm^{-1} is stronger in HA-V, indicating a larger content of C-O bonds (Osiro et al., 2004) than in HA-M, which might be due to the residual polysaccharides and lignin phenolic and O-CH_3 groups.

The concentration of millicompost HA (100 mg L^{-1}) was lower than that of vermicompost HA (150 mg L^{-1}), providing similar results on plants. These results may indicate that millicompost HA is more bioactive in plants than vermicompost HA, and this effect is possibly related to the chemical composition of these substances, as seen in Table 2, which, in turn, was influenced by the compound matrix, given that the extraction method was the same for both.

Supplementary Figure S1 shows the counts of 16S rRNA amplicon reads throughout data processing per sample (see Supplementary material). Supplementary Figure S2 shows the counts of ITS amplicon reads throughout data processing per sample. Supplementary Table S3 shows the counts of 16S rRNA amplicon reads throughout data processing, per group. Supplementary Table S4 shows the counts of ITS amplicon reads throughout data processing, per group. Supplementary Table S5 shows the counts of 16S rRNA amplicon reads classified in each taxonomic rank, and Supplementary Table S6 shows the counts of ITS amplicon reads classified in each taxonomic rank.

Regarding bacterial samples in the absence of stress, higher values (p-value ≤ 0.1) were observed for Shannon and Gini-Simpson diversity indices in leaves than in roots of the control treatment (Figure 1A). For the vermicompost and millicompost HA treatments, it was observed that roots presented greater species richness than leaves; however, unlike what was observed in the treatment without HA, the application of HA did not affect the diversity indices between leaves and roots. The imposition of stress causes these differences to disappear (Figure 1A). In addition to the evaluations of the effect of the factors separately, it is notable that the combination of the factors treatment with humic acids and stress significantly influenced the Chao1 and Shannon indices (Supplementary Table S9).

Regarding the fungal composition, in relation to the difference between roots and leaves, greater species richness and diversity were observed in roots than in leaves in the absence of stress (Figure 1B). Similar behavior was observed in stressed plants, but only in the control treatment (Chao1 and Shannon). The differences that were observed in relation to the different tissues of unstressed plants seem to have been attenuated or extinguished in stressed plants, especially in those that received HA applications (Figure 1B). In the absence of stress, application of millicompost HA showed higher Chao1 values in roots compared to treatments with vermicompost HA and the control and higher values of the diversity indices compared to the control (Figure 1A). The application of HA did not significantly alter the alpha diversity metrics (Figure 1B). However, the interaction of the three factors (HA application + plant tissue + stress) had a significant effect on the diversity indices (Shannon and Gini-Simpson; Supplementary Table S10).

Considering the taxonomic level of the family, it was observed that the highest abundance of taxa was within the family *Proteobacteria,* and the other families, present in smaller proportions, were *Firmicutes* and *Bacteroidetes* (Figure 2A). Regarding roots, it was observed that the most abundant group was *Xanthobactereaceae*, and unstressed roots that received millicompost HA showed a greater plurality of families than roots of the control and those that received vermicompost HA; in addition, there was a greater abundance of *Rhizobiaceae*. This family comprises rhizobia, bacteria associated with BNF in soybean (Breedveld and Miller, 1994). In the presence of stress, in roots with millicompost HA, there was an increase in *Xanthobactereaceae* and a relative reduction in the abundance of the other groups.

Few studies have evaluated the effect of humic acids on microbial diversity in plants. Sun et al. (2022) verified that HA application in tomatoes resulted in the best flavor compared to the other two organic fertilizers. The Chaol estimator and Shannon index showed that fertilizer addition decreased microbial diversity but increased species richness. Akimbekov et al. (2020) demonstrated that HA increased potato growth (54.9%) and tuber yield (66.4%) when compared to the control and maintained the biogeochemical stability of soils, healthy microbial community structure, and increased the agronomic productivity of potato plants. Other studies have shown that the bacterial composition during vermicomposting was split between the families *Proteobacteria*, *Bacteroidetes*, *Actinobacteria*, *Firmicutes* and *Verrucimicrobia*. *Proteobacteria* were most abundant at the

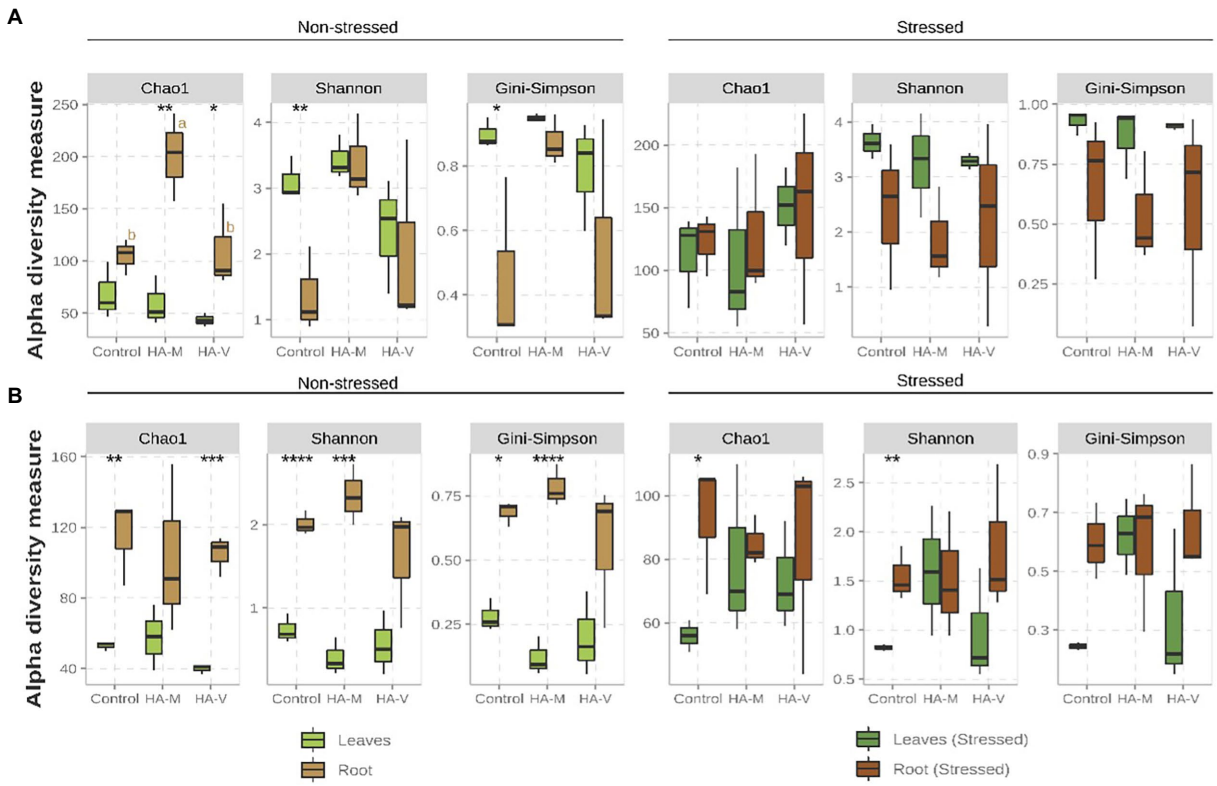

FIGURE 1
Boxplot of the alpha diversity metrics of bacterial **(A)** and fungal **(B)** fractions present in the shoot and root of soybean plants that received the application of vermicompost HA (HA-V), millicompost HA (HA-M) or that did not receive application (Control) in the presence and absence of stress. Different letters indicate significant differences between HA application within the same plant material (*post-hoc* test). Significant differences between different plant tissues under the same conditions (HA application and presence or absence of stress) can be seen by the presence of the following symbols: ****p<0.001; ***$p\leq$0.01; **$p\leq$0.05; *$p\leq$0.1. The absence of letters/symbols indicates no significant differences between contrasts.

beginning of the process, while after the 14th day, their abundance decreased but remained significant (Gómez-Brandón et al., 2011, 2012).

Regarding the effect of fertilization on the soil microbial community, Wang et al. (2017) verified the effect of organic and inorganic fertilization on the soil microbial diversity during 10 years of fertilizer applications. The results of this study show that inorganic fertilization decreased the richness of bacteria and increased the richness of fungi. The application of mineral fertilizers increased the abundance of some oligotrophic bacteria, such as *Bacteroidetes* and *Acidobacteria*. On the other hand, the application of organic fertilizers increased the abundance of coprotrophic bacteria, such as *Proteobacteria* (Wang et al., 2017), which is a heterogeneous class that includes free-living, symbiotic, and gram-positive bacteria and some integral intracellular bacteria that generally have important metabolic capabilities, such as biological nitrogen fixation and carbon fixation (Hallez et al., 2017).

Principal coordinate analysis (PCoA) using Bray–Curtis distances was performed to determine the dissimilarity of bacterial communities between shoot and root samples in the different treatments. Regardless of HA application and the presence of stress, the bacterial compositions of the shoots and roots were different ($p=0.001$; Figures 2B,C). Significance through PERMANOVA was only obtained in leaf samples, regardless of the "stress" factor (Figures 2B,C). In line with the PCoA graph, the hierarchical grouping shows the separation of the two groups (Supplementary Figure S4). Under nonstressful conditions, the variance in leaf communities and the PERMANOVA result showed a significant difference ($p=0.02$) between treatments, where it was possible to observe the separation of the two groups, in which the community of the control treatment was more distant from the communities of leaves that received vermicompost and millicompost HA. In the presence of stress, a greater distance between samples treated with different HA was observed, forming three distinct groups, indicating the difference between bacterial communities. These results indicate that the enriched bacterial groups appear to play distinct roles in plants under water stress conditions.

For fungi, the taxa identified were mostly in the family *Ascomycota*, followed by *Basidiomycota* (Figures 3A). It is noteworthy that many of the most abundant sequences could not be classified even at the phylum level, as shown in Figure 3. Unstressed leaves presented mostly members related to the family

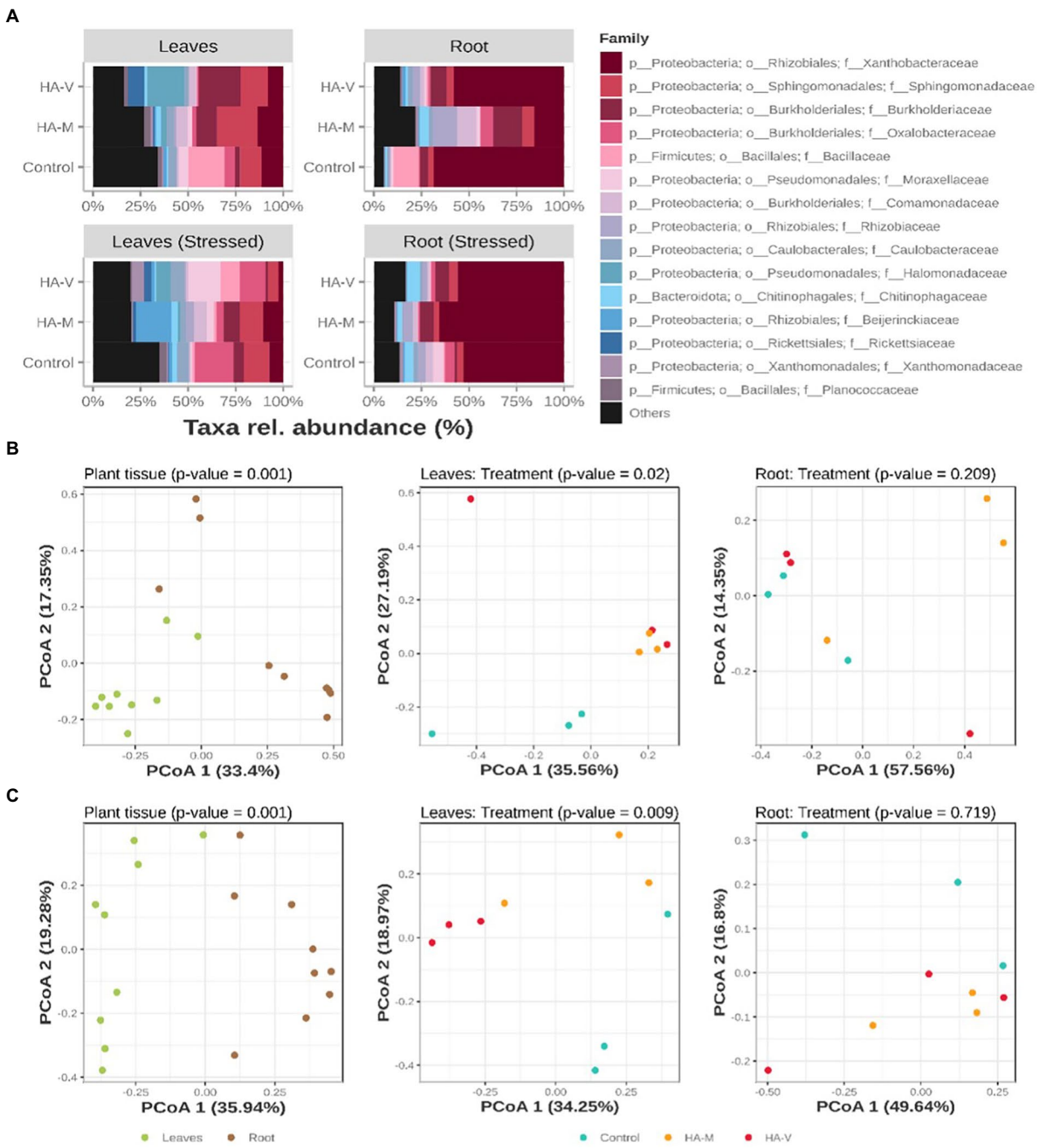

FIGURE 2
Relative abundances of the top 15 bacterial ASVs, collapsed to the taxonomic level of "family" **(A)**. Graphic representation of principal coordinate analysis (PCoA) based on the Bray–Curtis distances of samples in the absence **(B)** and presence **(C)** of stress. At the first level (on the left), the PCoAs of all samples tested in terms of separation by plant material are observed. Next (center and right), the distribution of leaf and root samples, respectively, tested according to the treatment received is observed. Treatments refer to the application of vermicompost HA (HA-V), millicompost HA (HA-M) and that did not receive application (control).

Ascomycota. Specifically, in stressed leaves that received millicompost HA, an increase in the *Erysiphaceae* family was observed. In unstressed roots, the control showed an increase in members of the *Chaetomiaceae* family compared to the other treatments. Treatment with millicompost HA presented a greater abundance of *Nectriaceae* and *Pleosporaceae*. In the presence of stress, an increase in *Chaetomiaceae* was observed in treatments with HA, and an increase in *Trichosphaeriaceae* was observed in the control. For the distribution of compositions illustrated in PCoA (Figures 3B,C) and its respective dendrograms (Supplementary Figure S5), separation of leaf and root samples was observed ($p < 0.05$).

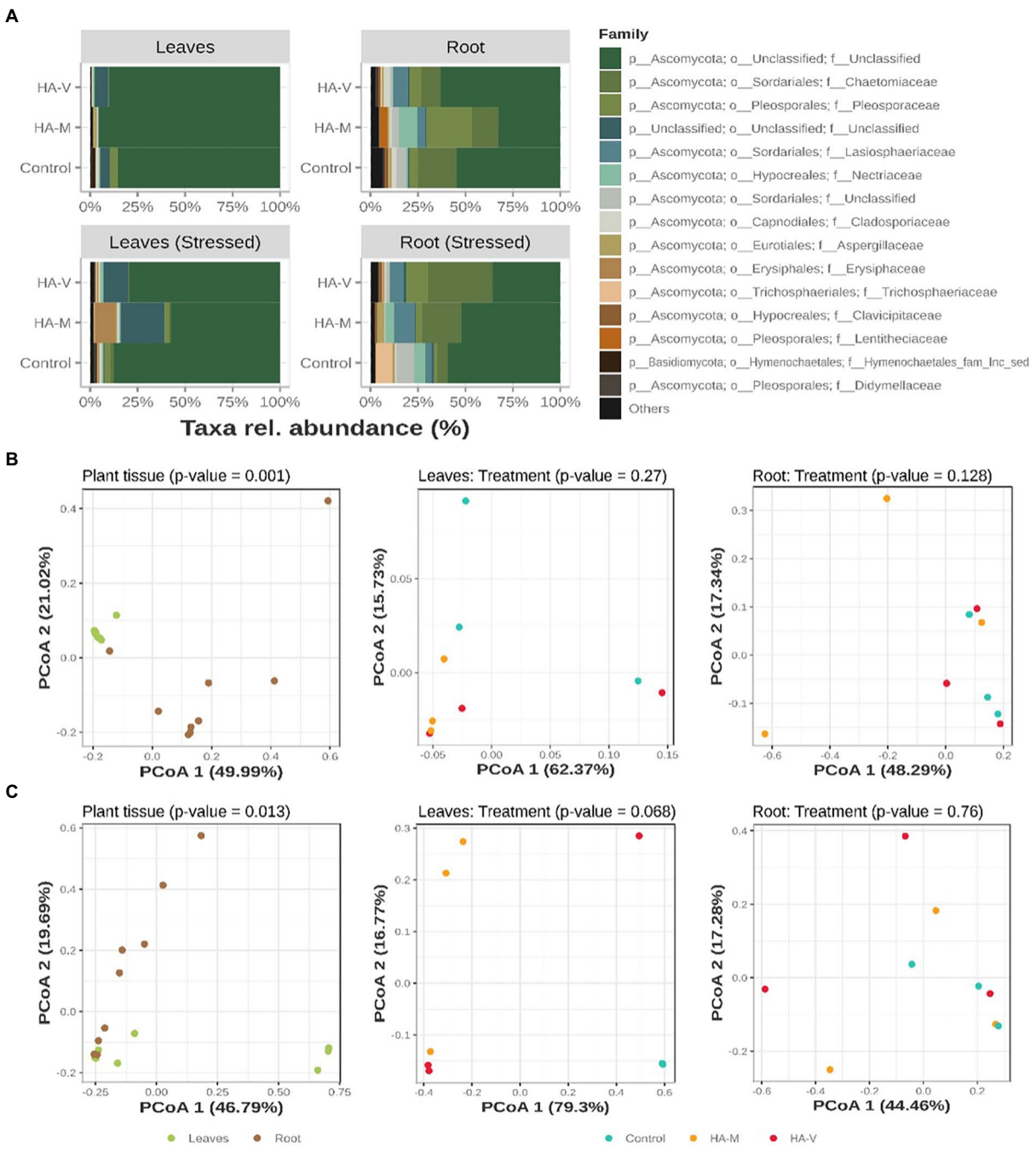

FIGURE 3
Relative abundances of the top 15 fungal ASVs, collapsed to the taxonomic level of "family" **(A)**. Graphic representation of principal coordinate analysis (PCoA) based on the Bray–Curtis distances of samples in the absence **(B)** and presence **(C)** of stress. At the first level (on the left), the PCoAs of all samples are observed and tested in terms of separation by plant material. Next (center and right), the distribution of leaf and root samples, respectively, tested according to the treatments received is observed. Treatments refer to the application of vermicompost HA (HA-V) and millicompost HA (HA-M) and that did not receive application (control).

Nectriaceae, *Pleosporaceae* and *Trichosphaeriaceae* are families of fungi that are pathogenic to Berchemia discolor, which is a drought-tolerant multipurpose tree with the potential to provide medicine, food and other commodities to drylands in several countries (Susan et al., 2022). *Chaetomiaceae* species are a wealthy source of enzymes with diverse biotechnological and industrial applications, such as PMO (polysaccharide monooxygenase), L-methioninase, β-1,3-glucanase, laccase, dextranase, lipolytic, pectinolytic, amylolytic, chitinolytic, and proteolytic enzymes. Different classes of secondary metabolites have been reported

TABLE 3 Quantifications of differentially abundant (DA) taxa related to each treatment under the experimental conditions evaluated.

	Treatment	No stress		Stressed	
		Leaves	Roots	Leaves	Roots
Bacteria	HA-V	5	15	38	33
(16S	HA-M	2	51	15	22
rRNA)	Control	22	4	1	15
Fungi	HA-V	3	9	–	27
(ITS)	HA-M	3	26	–	11
	Control	2	3	–	9

HA-V, Samples treated with vermicompost HA; HA-M, Samples treated with millicompost HA. Control refers to samples without the addition of HA.

from this family and are derived from various biosynthetic pathways, such as alkaloids, polyketides, peptides, terpenes, and polyketide-amino acid hybrid secondary metabolites. These metabolites have attracted research interest due to their fascinating structural frameworks and bioactivities (Ibrahim et al., 2021). The family *Erysiphe* (including powdery mildew fungi only known as anamorph, Pseudoidium) is the largest genus in *Erysiphaceae* and contains more than 50% of all species in this family. Little is known about the phylogenetic structure of this genus. Erysiphaceae (Ascomycete: Erysiphales) are a group of obligate parasitic fungi of plants that cause powdery mildew diseases on ~10,000 angiosperm species (Amano, 1986). With the exception of the dormant stage, their life cycle completely depends on living hosts, from which they obtain nutrients without killing the host cells and without which they are unable to survive. To maintain the obligate parasitic life cycle, *Erysiphaceae* have developed highly specific and sophisticated mechanisms to avoid the resistance system of the host, to obtain nutrient resources from the host without injuring the host cells, and to synchronize their life-cycle parameters to those of the host (Aist and Bushnell, 1991).

To evaluate the compositional differences among microbial communities present in the leaf and root samples, we detected differentially abundant (DA) taxa between control and HA-treated samples in the presence and absence of stress. The list of DA taxa, as well as for which condition and in what proportion they were identified, is available in more detail in Supplementary Tables S7 (Bacteria), S8 (Fungi).

The application of HA had a great effect on the bacterial communities. In the absence of stress, treated leaves tended to considerably reduce the abundance of certain taxa compared to the control (Table 3). In the other conditions, treatments with HA were superior in this regard, causing an increase in the abundance of specific taxa (Supplementary Tables S7, S8).

In unstressed leaves, it was observed that the application of vermicompost HA promoted an increase in the genera *Rickettsia, Candidatus hamiltonella, and Candidatus portiera* (Figure 4), recognized endosymbionts of whitefly, a pest that causes damage to soybean plants (Bello et al., 2021). Despite the presence of these taxa, the prevalence of these groups was not observed in all replicates, possibly being a punctual contamination of one of the biological replicates. Despite this, the confirmation of these microbial groups shows that insect symbionts can enter plant tissues.

The genera *Variovorax* and *Kosakonia* were DA in plants that received HA. These bacterial groups have already been isolated from soybean plants and, when evaluated *in vitro*, showed antagonistic activity against various bacterial and fungal pathogens of this crop (De Almeida Lopes et al., 2018). Members of the genera *Variovorax* and *Oxalicibacterium* have been reported to catabolize oxalate (Tamer et al., 2002). In some plants, the degradation of this compound provides protection against fungal pathogens (Müller et al., 2016). Additionally, microorganisms that degrade oxalate can also act to increase nutrient uptake by plants (Morris and Allen, 1994).

A study evaluated the foliar application of leonardite (a compound with high HA concentrations) in beetroot produced under hydroponics and in field conditions and evaluated the effect of this compound on the endophytic bacterial community. The authors observed that the genus most responsive to the application of leonardite in beetroot under both conditions was *Oxalicibacterium* (Della Lucia et al., 2021). This genus was also stimulated in plants that received vermicompost HA. Therefore, the effects observed in the treatment with leonardite may be additional (or mediated) to the effects of bacterial endophytes.

In the treatment with millicompost HA, increases in *Cupriavidus pauculus, Sphingomonas naasensis, and Massilia armeniaca* were observed, which are genera that have members related to tolerance to heavy metals, growth under low water availability, resistance to microbial agents and assistance in nutrient uptake by plants (Menon et al., 2019; Asaf et al., 2020; Zeng et al., 2020). Therefore, these bacterial groups may act on plant growth and protect against abiotic stresses. *Actinoplane luojiashanensis* was also DA in this treatment, and one of the few studies found with this species highlights its characteristic in antibiotic production (Jilian et al., 1995). This genus, *Chitinophaga,* is commonly associated with biological control (Hu et al., 2019).

Some studies found *Novosphingobium ginsenosidimutans* to be highly associated with the soybean rhizosphere (Meier et al., 2021), and HA may have favored its endophytic colonization in this plant.

In plants treated with vermicompost HA, an increase in *Acinetobacter lwoffii* was observed, which has already been described for improving bean growth through arsenic contamination (Das and Sarkar, 2018). This same work observed the effect of this species on the production of plant regulators under favorable environmental conditions, such as under stress. Additionally, it has also been successful in improving the plant's response to oxidative stress. *Sphingobium yanoikuyae* also plays a known role in protecting plants, providing tolerance to water stress (Arunthavasu et al., 2019). *Luteibacter jiangsuensis* is a bacterial species related to the degradation of complex molecules, including compounds toxic to the environment (Lin et al., 2020). Members of the genus *Devosia* have the ability to nodule legumes (Rivas et al., 2002) and may play a relevant role in this regard in relation to soybeans, since *Devosia elaeis* was DA in samples.

FIGURE 4
Differently abundant (DA) bacterial taxa. Both levels are presented ordered by the sum of relative abundances. The heatmap (left) demonstrates the relative abundance of taxa in leaves (L), roots (R), stressed leaves (LS), stressed roots (RS) by applying millicompost humic acid (HA-M), vermicompost humic acid (HA-V) and without application of HA (control). The dot plot (right) reveals in which niche differences in abundance between plant materials occurred.

Actinoplane luojiashanensis was DA in the vermicompost and millicompost HA treatments.

A study showed that the root application of HA was able to change the bacterial composition in this plant organ, providing an increase in taxa belonging to *Sphingobacteriaceae*, *Chitinophaga* and *Actinobacteria* (da Silva et al., 2021b). Similar results were found in the present work. The authors emphasize that the role of HA in inducing plant tolerance may be related to the stimulation

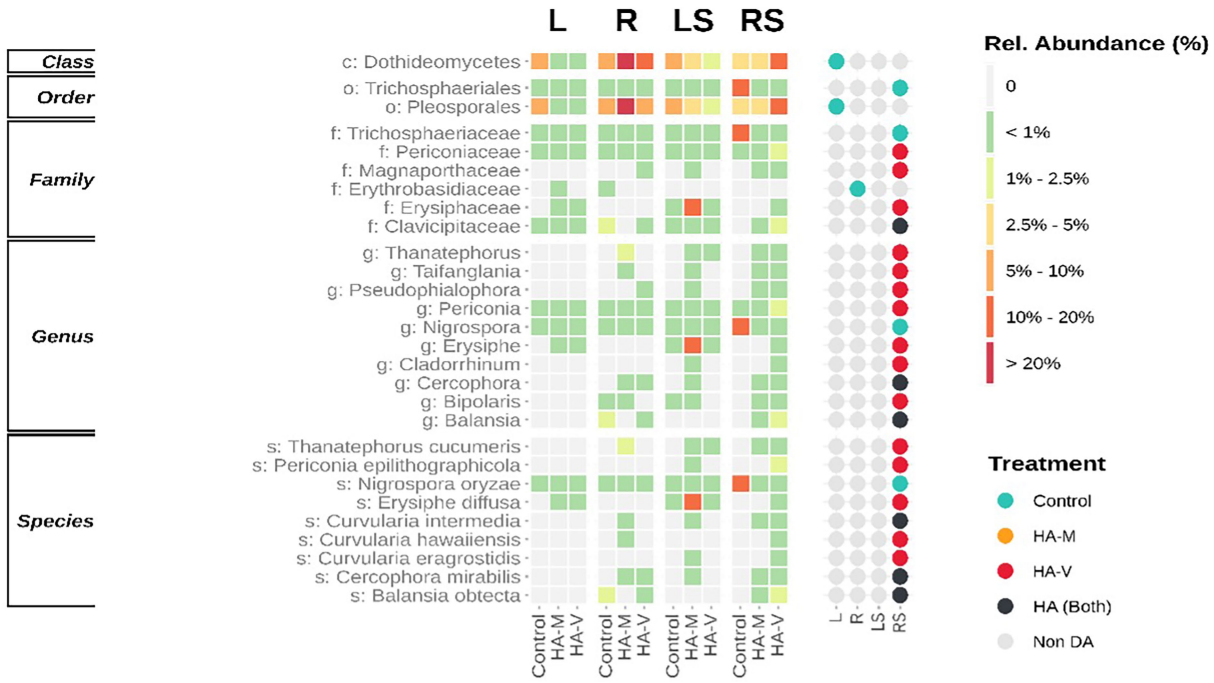

FIGURE 5
Different abundant (DA) fungal taxa. Both levels are presented ordered by the sum of relative abundances. The heatmap (left) demonstrates the relative abundance of taxa in leaves (L), roots (R), stressed leaves (LS), stressed roots (RS) by applying millicompost humic acid (HA-M), vermicompost humic acid (HA-V) and without application of HA (control). The dot plot (right) reveals in which niche differences in abundance between plant materials occurred.

of these bacteria. Therefore, it is appropriate to suggest that HA improves the physiological response of the plant to cope with environmental stresses (Canellas et al., 2020), while it also selects microorganisms with a role in promoting plant growth and protecting the plant from stress.

Regarding the fungal portion, DA groups were observed in stressed roots, where treatments with HA were more impactful, especially treatment with vermicompost HA. At the species level, treatments with HA reduced *Nigrospora oryzae* (Figure 5). Interestingly, some enriched fungal groups are related to phytopathogens, such as *Erysiphe diffusa* (McTaggart et al., 2012) and *Thanatephorus cucumeris* (Chela Fenille et al., 2002). Despite this, no disease was observed in soybean plants. It is possible that different responses to plant growth promotion and pathogenicity are related to changes in the genotype of the plant and microorganisms. Such changes can generate changes in recognition and the type of interaction between them (Schmidt et al., 2012). Furthermore, the microbiome itself can affect interactions between microorganisms and plants.

The species *Periconia epilithographicola* was enriched in the presence of HA, and its genus has members with a role in biocontrol (Verma et al., 2011). *Cercophora mirabilis*, a species of this genus, has been found to be associated with soybean roots in the field, but its function is still poorly understood (Bargaz et al., 2017). The genus *Balansia* has been reported as a pathogen, growth promoter and antagonist of agricultural pests (Clay et al., 1985; Porter et al., 1985; Ren and Clay, 2009). *Curvularia* also plays a dubious role in its effect on the plant, since this genus presents individuals who act in plant growth promotion and are capable of causing diseases in plants (Michael Tilley and Lynn Walker, 2002).

It is known that under abiotic stress, opportunistic pathogens more easily colonize previously weakened plants, reducing their defense against injuries (Tewari and Arora, 2014). Thus, the stimulation of microorganisms related to biological control is also of great relevance for plant establishment even under abiotic stresses. In nature, most plants are colonized by an enormous diversity of endophytic and pathogenic microorganisms. However, it is still unclear how the presence of multiple partners is balanced in plant roots to the point of maintaining plant growth (Niu et al., 2020).

In short, the application of millicompost and vermicompost HA helps plant growth and induces the modulation of the endophytic community. It was also shown that HA can trigger the enrichment of microorganisms with the potential to act both in plant growth and defense against pathogens and protection against abiotic stresses. These results support previous questions, such as the need for approaches to elucidate the real role of HA in plant physiology and the participation of plant microbiota. Our findings may point to the use of HA as part of a strategy to prepare plants against biotic and abiotic stresses by stimulating their defense metabolism.

It is noteworthy that perhaps the application of HA has favored the endophytic establishment of soil microorganisms, including opportunistic fungi. However, it is suggested that the organization of the microbiota is adjusted to prevent the development of diseases through these potentially pathogenic groups. Thus, the present study represents an advance in the understanding of HA-induced changes in the soybean microbiome and reinforces the potential of this compound to improve plant growth even under water restrictions. However, more studies should be developed to understand the effect of HA on the plant microbiota and its function in plants.

Conclusion

HA extracted from vermicompost and millicompost has the potential to promote the maintenance of plant growth even in adverse environmental conditions, acting in the best performance of the plant in the face of environmental stresses, as well as recruiting beneficial microorganisms to the plant. Although the results showed slight differences between vermicompost and millicompost regarding plant growth, both humic acids promoted an increase in plant development compared to the control. These substances could be used due to their beneficial function in the plant and its microbiome. HA can behave as a sustainable agricultural technology, promoting plant growth and thus reducing the need for agrochemicals.

Data availability statement

The datasets presented in this study can be found in online repositories. The names of the repository/repositories and accession number(s) can be found in the article/Supplementary material.

Author contributions

All authors listed have made a substantial, direct, and intellectual contribution to the work and approved it for publication.

Funding

This study was financed in part by the Coordination for the Improvement of Higher Education Personnel (CAPES), Brazil, Finance Code 001.

Conflict of interest

The authors declare that the research was conducted in the absence of any commercial or financial relationships that could be construed as a potential conflict of interest.

Publisher's note

All claims expressed in this article are solely those of the authors and do not necessarily represent those of their affiliated organizations, or those of the publisher, the editors and the reviewers. Any product that may be evaluated in this article, or claim that may be made by its manufacturer, is not guaranteed or endorsed by the publisher.

Supplementary material

The Supplementary material for this article can be found online at: https://www.frontiersin.org/articles/10.3389/fmicb.2022.1000222/full#supplementary-material

References

Aguiar, N. O., Olivares, F. L., Novotny, E. H., Dobbss, L. B., Balmori, D. M., Santos-Júnior, L. G., et al. (2013). Bioactivity of humic acids isolated from Vermicomposts at different maturation stages. *Plant Soil* 362, 161–174. doi: 10.1007/s11104-012-1277-5

Aist, J. R., and Bushnell, W. R. (1991). "Invasion of plants by powdery mildew fungi, and cellular mechanisms of resistance," in *The Fungal Spore and Disease Initiation in Plants and Animals*. eds. G. T. Cole and H. C. Hoch (Boston, MA: Springer), 321–345.

Akimbekov, N., Qiao, X. H., Digel, Y., Abdieva, G. Z. M., Ualieva, E. R. Z., and Zhubanova, A. Z. R. (2020). The effect of leonardite-derived amendments on soil microbiome structure and potato yield. *Agriculture-Basel*, 10.

Amano, K. (1986). *Host Range and Geographical Distribution of the Powdery Mildew Fungi* Japan Scientific Societies Press.

Armanhi, J. S. L., de Souza, R. S. C., Damasceno, N. D. B., de Araújo, L. M., Imperial, J., and Arruda, P. (2018). A community-based culture collection for targeting novel plant growth-promoting bacteria from the sugarcane microbiome. *Front. Plant Sci.* 8:2191. doi: 10.3389/fpls.2017.02191

Arunthavasu, R., Thangavel, K., and Uthandi, S. (2019). Impact of drought-tolerant rice apoplastic fluid endophyte (*Sphingobium yanoikuyae* MH394206) on the morphological and physiological characteristics of rice (CO51) grown in moisture deficit condition. *Madras Agric. J.* 106, 217–224. doi: 10.29321/MAJ.2019.000249

Asaf, S., Numan, M., Khan, A. L., and Al-Harrasi, A. (2020). Sphingomonas: from diversity and genomics to functional role in environmental remediation and plant growth. *Crit. Rev. Biotechnol.* 40, 138–152. doi: 10.1080/07388551.2019.1709793

Bargaz, A., Noyce, G. L., Fulthorpe, R., Carlsson, G., Furze, J. R., Jensen, E. S., et al. (2017). Species interactions enhance root allocation, microbial diversity and P acquisition in intercropped wheat and soybean under P deficiency. *Appl. Soil Ecol.* 120, 179–188. doi: 10.1016/j.apsoil.2017.08.011

Bello, V. H., Da Silva, F. B., Watanabe, L. F. M., Vicentin, E., Muller, C., De Freitas Bueno, R. C. O., et al. (2021). Detection of Bemisia tabaci Mediterranean cryptic species on soybean in São Paulo and Paraná states (Brazil) and interaction of cowpea mild mottle virus with whiteflies. *Plant Pathol.* 70, 1508–1520. doi: 10.1111/ppa.13387

Breedveld, M. W., and Miller, K. J. (1994). Cyclic beta-glucans of members of the family Rhizobiaceae. *Microbiol. Rev.* 58, 145–161. doi: 10.1128/mr.58.2.145-161.1994

Canellas, L. P., Canellas, N. O. A., Da, S., Irineu, L. E. S., Olivares, F. L., and Piccolo, A. (2020). Plant chemical priming by humic acids. *Chem. Biol. Technol. Agric.* 7:12. doi: 10.1186/s40538-020-00178-4

Canellas, L. P., and Olivares, F. L. (2014). Physiological responses to humic substances as plant growth promoter. *Chem. Biol. Technol. Agric.* 1:3. doi: 10.1186/2196-5641-1-3

Caporaso, J. G., Lauber, C. L., Walters, W. A., Berg-Lyons, D., Lozupone, C. A., Turnbaugh, P. J., et al. (2011). Global patterns of 16S rRNA diversity at a depth of

millions of sequences per sample. *Proc. Natl. Acad. Sci. U. S. A.* 108, 4516–4522. doi: 10.1073/pnas.1000080107

Carrión, V. J., Perez-Jaramillo, J., Cordovez, V., Tracanna, V., de Hollander, M., Ruiz-Buck, D., et al. (2019). Pathogen-induced activation of disease-suppressive functions in the endophytic root microbiome. *Science* 366, 606–612. doi: 10.1126/science.aaw9285

Chela Fenille, R., Luiz de Souza, N., and Eurya Kuramae, E. (2002). Characterization of Rhizoctonia solani associated with soybean in Brazil. *Eur. J. Plant Pathol.* 108, 783–792. doi: 10.1023/A:1020811019189

Clay, K., Hardy, T. N., and Hammond, A. M. (1985). Fungal endophytes of grasses and their effects on an insect herbivore. *Oecologia* 66, 1–5. doi: 10.1007/BF00378545

da Silva, M. S. R. de A., de Melo Silveira dos Santos, B., Hidalgo Chávez, D. W., de Oliveira, R., Barbosa Santos, C. H., Oliveira, E. C., et al. (2021a). K-humate as an agricultural alternative to increase nodulation of soybeans inoculated with Bradyrhizobium. *Biocatal. Agric. Biotechnol.* 36:102129. doi: 10.1016/j.bcab.2021.102129

da Silva, M. S. R., Tavares, O. C. H., Ribeiro, T. G., da Silva, C. S. R., García-Mina, J. M., Baldani, V. L. D., et al. (2021b). Humic acids enrich the plant microbiota with bacterial candidates for the suppression of pathogens. *Appl. Soil Ecol.* 168:104146. doi: 10.1016/j.apsoil.2021.104146

Das, J., and Sarkar, P. (2018). Remediation of arsenic in mung bean (*Vigna radiata*) with growth enhancement by unique arsenic-resistant bacterium *Acinetobacter lwoffii*. *Sci. Total Environ.* 624, 1106–1118. doi: 10.1016/j.scitotenv.2017.12.157

de Souza, R. S. C., Okura, V. K., Armanhi, J. S. L., Jorrín, B., Lozano, N., da Silva, M. J., et al. (2016). Unlocking the bacterial and fungal communities assemblages of sugarcane microbiome. *Sci. Rep.* 6:28774. doi: 10.1038/srep28774

De Almeida Lopes, K. B., Carpentieri-Pipolo, V., Fira, D., Balatti, P. A., López, S. M. Y., de Souza, R. S. C., et al. (2018). Screening of bacterial endophytes as potential biocontrol agents against soybean diseases. *J. Appl. Microbiol.* 125, 1466–1481. doi: 10.1111/jam.14041

De Freitas, V. F., Cerezini, P., Hungria, M., and Nogueira, M. A. (2022). Strategies to deal with drought-stress in biological nitrogen fixation in soybean. *Appl. Soil Ecol.* 172:104352. doi: 10.1016/j.apsoil.2021.104352

Della Lucia, M. C., Bertoldo, G., Broccanello, C., Maretto, L., Ravi, S., Marinello, F., et al. (2021). Novel effects of Leonardite-based applications on sugar beet. *Front. Plant Sci.* 12:646025. doi: 10.3389/fpls.2021.646025

García, A. C., Tavares, O. C. H., Balmori, D. M., dos Santos Almeida, V., Canellas, L. P., García-Mina, J. M., et al. (2018). Structure-function relationship of vermicompost humic fractions for use in agriculture. *J. Soils Sediments* 18, 1365–1375. doi: 10.1007/s11368-016-1521-3

Gómez-Brandón, M., Aira, M., Lores, M., and Domínguez, J. (2011). Changes in microbial community structure and function during vermicomposting of pig slurry. *Bioresour. Technol.* 102, 4171–4178. doi: 10.1016/j.biortech.2010.12.057

Gómez-Brandón, M., Lores, M., and Domínguez, J. (2012). Species-specific effects of epigeic earthworms on microbial community structure during first stages of decomposition of organic matter. *PLoS One* 7:e31895. doi: 10.1371/journal.pone.0031895

Guo, G., Yuan Xu, Y., Jiang, F., Zhen Li, B., Shui Yang, J., Tao Wang, E., et al. (2015). Nodulation characterization and proteomic profiling of Bradyrhizobium liaoningense CCBAU05525 in response to water-soluble humic materials. *Sci. Rep.* 5:10836. doi: 10.1038/srep10836

Hallez, R., Delaby, M., Sanselicio, S., and Viollier, P. H. (2017). Hit the right spots: cell cycle control by phosphorylated guanosines in alphaproteobacteria. *Nat. Rev. Microbiol.* 15, 137–148. doi: 10.1038/nrmicro.2016.183

Hossain, A., Kerry, R. G., Farooq, M., Abdullah, N., and Tofazzal Islam, M. (2020). Application of nanotechnology for sustainable crop production systems. *Nanotechnology for Food, Agriculture, and Environment* (Springer), 135–159.

Hu, W., Strom, N. B., Haarith, D., Chen, S., and Bushley, K. E. (2019). Seasonal variation and crop sequences shape the structure of bacterial communities in cysts of soybean cyst nematode. *Front. Microbiol.* 10:2671. doi: 10.3389/fmicb.2019.02671

Hungria, M., and Mendes, I. C., (2015). Nitrogen fixation with soybean: the perfect Symbiosis?, in: BruijnF. J. de (Ed.), *Biological nitrogen fixation*. John Wiley & Sons, Inc, Hoboken, NJ, 1009–1024.

Ibrahim, S. R., Mohamed, S. G., Sindi, I. A., and Mohamed, G. A. (2021). Biologically active secondary metabolites and biotechnological applications of species of the family Chaetomiaceae (Sordariales): an updated review from 2016 to 2021. *Mycol. Prog.* 20, 595–639. doi: 10.1007/s11557-021-01704-w

Jilian, H., Qiwei, Y., and Zhixian, L. (1995). A producer of new antitumor antibiotics, Actinoplanes luojiashanensis n. sp. Zhongguo Kang Sheng su za zhi = Chinese. *Journal of Antibiotics* 20, 241–245.

Lichtenthaler, H. K. (1987). "[34] chlorophylls and carotenoids: pigments of photosynthetic biomembranes" in *Methods in Enzymology*. eds. L. Packer and R. Douce Aist (Amsterdam, The Netherlands: Elsevier), 350–382.

Lin, Z., Pang, S., Zhang, W., Mishra, S., Bhatt, P., and Chen, S. (2020). Degradation of Acephate and its intermediate Methamidophos: mechanisms and biochemical pathways. *Front. Microbiol.*:11:2045. doi: 10.3389/fmicb.2020.02045

Liu, H., Brettell, L. E., Qiu, Z., and Singh, B. K. (2020). Microbiome-Mediated Stress Resistance in Plants. *Trends Plant Sci.* 25:733743. doi: 10.1016/j.tplants.2020.03.014

Lundberg, D. S., Yourstone, S., Mieczkowski, P., Jones, C. D., and Dangl, J. L. (2013). Practical innovations for high-throughput amplicon sequencing. *Nat. Methods* 10, 999–1002. doi: 10.1038/nmeth.2634

McTaggart, A. R., Ryley, M. J., and Shivas, R. G. (2012). First report of the powdery mildew Erysiphe diffusa on soybean in Australia. *Australas. Plant Dis. Notes* 7, 127–129. doi: 10.1007/s13314-012-0065-7

Meier, M. A., Lopez-Guerrero, M. G., Guo, M., Schmer, M. R., Herr, J. R., Schnable, J. C., et al. (2021). Rhizosphere microbiomes in a historical maize-soybean rotation system respond to host species and nitrogen fertilization at the genus and subgenus levels. *Appl. Environ. Microbiol.* 87, e03132–e03120. doi: 10.1128/AEM.03132-20

Menon, R. R., Kumari, S., Kumar, P., Verma, A., Krishnamurthi, S., and Rameshkumar, N. (2019). *Sphingomonas pokkalii* sp. nov., a novel plant associated rhizobacterium isolated from a saline tolerant pokkali rice and its draft genome analysis. *Syst. Appl. Microbiol.* 42, 334–342. doi: 10.1016/j.syapm.2019.02.003

Michael Tilley, A., and Lynn Walker, H. (2002). Evaluation of Curvularia intermedia (Cochliobolus intermedius) as a potential microbial herbicide for large crabgrass (Digitaria sanguinalis). *Biol. Control* 25, 12–21. doi: 10.1016/S1049-9644(02)00035-X

Morris, S. J., and Allen, M. F. (1994). Oxalate-metabolizing microorganisms in sagebrush steppe soil. *Biol. Fertil. Soils* 18, 255–259. doi: 10.1007/BF00647677

Müller, D. B., Vogel, C., Bai, Y., and Vorholt, J. A. (2016). The plant microbiota: systems-level insights and perspectives. *Annu. Rev. Genet.* 50, 211–234. doi: 10.1146/annurev-genet-120215-034952

Nardi, S., Schiavon, M., and Francioso, O. (2021). Chemical structure and biological activity of humic substances define their role as plant growth promoters. *Molecules* 26:2256. doi: 10.3390/molecules26082256

Niu, B., Wang, W., Yuan, Z., Sederoff, R. R., Sederoff, H., Chiang, V. L., et al. (2020). Microbial interactions within multiple-strain biological control agents impact soil-borne plant disease. *Front. Microbiol.* 11:585404. doi: 10.3389/fmicb.2020.585404

Osiro, D., Colnago, L. A., Otoboni, A. M. M. B., Lemos, E. G. M., Souza, A. A., Filho, H. D. C., et al. (2004). A kinetic model for Xylella fastidiosa adhesion, biofilm formation, and virulence. *FEMS Microbiol. Lett.* 236:313318. doi: 10.1111/j.1574-6968.2004.tb09663.x

Porter, J. K., Bacon, C. W., Cutler, H. G., Arrendale, R. F., and Robbins, J. D. (1985). In vitro auxin production by Balansia epichloë. *Phytochemistry* 24, 1429–1431. doi: 10.1016/S0031-9422(00)81037-7

R Core Team (2021). *R: A Language and Environment for Statistical Computing Version 3.6. 1*. Vienna: R Foundation for Statistical Computing.

Ren, A., and Clay, K. (2009). Impact of a horizontally transmitted Endophyte, Balansia henningsiana, on growth and drought tolerance of Panicum rigidulum. *Int. J. Plant Sci.* 170, 599–608. doi: 10.1086/597786

Rivas, R., Velázquez, E., Willems, A., Vizcaíno, N., Subba-Rao, N. S., Mateos, P. F., et al. (2002). A new species of Devosia that forms a unique nitrogen-fixing root-nodule Symbiosis with the aquatic legume Neptunia natans (L.f.) Druce. *Appl. Environ. Microbiol.* 68, 5217–5222. doi: 10.1128/AEM.68.11.5217-5222.2002

Schmidt, M. A., Balsanelli, E., Faoro, H., Cruz, L. M., Wassem, R., de Baura, V. A., et al. (2012). The type III secretion system is necessary for the development of a pathogenic and endophytic interaction between *Herbaspirillum rubrisubalbicans* and Poaceae. *BMC Microbiol.* 12:98. doi: 10.1186/1471-2180-12-98

Smith, D. P., and Peay, K. G. (2014). Sequence depth, not PCR replication, improves ecological inference from next generation DNA sequencing. *PLoS One* 9:e90234. doi: 10.1371/journal.pone.0090234

Stevenson, F. J. (1994). *Humus Chemistry: Genesis, Composition, Reactions (2nd ed.)*. New York: John Wiley & Sons.

Sun, C. X., Bei, K., Liu, Y. H., and Pan, Z. Y. (2022). Humic acid improves greenhouse tomato quality and bacterial richness in rhizosphere soil. *Acs Omega* 7, 29823–29831.

Susan, K., Jane, N., Steven, R., Alice, M., Joseph, M., and Phoebe, M. (2022). Molecular and morphological identification of fungi causing canker and dieback diseases on *Vangueria infausta* (Burch) subsp. rotundata (Robyns) and Berchemia discolor (Klotzsch) Hemsl in lower eastern Kenya. *Afr. J. Biotechnol.* 21, 6–15. doi: 10.5897/AJB2020.17297

Tadini, A. M., Martin-Neto, L., Goranov, A. I., Milori, D. M., Bernardi, A. C., Oliveira, P. P., et al. (2022). Chemical characteristics of soil organic matter from integrated agricultural systems in southeastern Brazil. *Eur. J. Soil Sci.* 73:e13136.

Tamer, A. Ü., Aragno, M., and Şahin, N. (2002). Isolation and characterization of a new type of aerobic, oxalic acid utilizing bacteria, and proposal of Oxalicibacterium flavum gen. Nov., sp. nov. *Syst. Appl. Microbiol.* 25, 513–519. doi: 10.1078/072320260517643

Tewari, S., and Arora, N. K. (2014). Multifunctional exopolysaccharides from Pseudomonas aeruginosa PF23 involved in plant growth stimulation, biocontrol and stress amelioration in sunflower under saline conditions. *Curr. Microbiol.* 69, 484–494. doi: 10.1007/s00284-014-0612-x

Timm, C. M., Carter, K. R., Carrell, A. A., Jun, S.-R., Jawdy, S. S., Vélez, J. M., et al. (2018). Abiotic stresses shift belowground Populus-associated bacteria toward a Core stress microbiome. *mSystems* 3, e00070–e00017. doi: 10.1128/mSystems.00070-17

Vandenkoornhuyse, P., Quaiser, A., Duhamel, M., Le Van, A., and Dufresne, A. (2015). The importance of the microbiome of the plant holobiont. *New Phytol.* 206, 1196–1206. doi: 10.1111/nph.13312

Verma, V. C., Lobkovsky, E., Gange, A. C., Singh, S. K., and Prakash, S. (2011). Piperine production by endophytic fungus Periconia sp. isolated from *Piper longum* L. *J. Antibiot. (Tokyo)* 64, 427–431. doi: 10.1038/ja.2011.27

Wang, J., Song, Y., Ma, T., Raza, W., Li, J., Howland, J. G., et al. (2017). Impacts of inorganic and organic fertilization treatments on bacterial and fungal communities in a paddy soil. *Appl. Soil Ecol.* 112, 42–50. doi: 10.1016/j.apsoil.2017.01.005

Wellburn, A. R. (1994). The spectral determination of chlorophylls a and b, as well as total carotenoids, using various solvents with spectrophotometers of different resolution. *J. Plant Physiol.* 144, 307–313.

Zeng, W., Zhang, S., Xia, M., Wu, X., Qiu, G., and Shen, L. (2020). Insights into the production of extracellular polymeric substances of Cupriavidus pauculus 1490 under the stimulation of heavy metal ions. *RSC Adv.* 10, 20385–20394. doi: 10.1039/C9RA10560C

frontiers | Frontiers in Microbiology

TYPE Original Research
PUBLISHED 15 December 2022
DOI 10.3389/fmicb.2022.1058772

Check for updates

OPEN ACCESS

EDITED BY
José David Flores Félix,
Universidade da Beira Interior,
Portugal

REVIEWED BY
Sudhir K. Upadhyay,
Veer Bahadur Singh Purvanchal University,
India
Judith Naamala,
McGill University,
Canada
Rashid Nazir,
COMSATS University Islamabad,
Abbottabad Campus,
Pakistan

*CORRESPONDENCE
Arun Kumar Devarajan
arun.kumar.devarajan@ut.ee
Sabarinathan Kuttalingam
Gopalasubramaniam
sabarimicro@hotmail.com

SPECIALTY SECTION
This article was submitted to
Microbe and Virus Interactions
with Plants,
a section of the journal
Frontiers in Microbiology

RECEIVED 30 September 2022
ACCEPTED 29 November 2022
PUBLISHED 15 December 2022

CITATION
Devarajan AK, Truu M,
Gopalasubramaniam SK,
Muthukrishanan G and Truu J (2022)
Application of data integration for rice
bacterial strain selection by combining
their osmotic stress response and plant
growth-promoting traits.
Front. Microbiol. 13:1058772.
doi: 10.3389/fmicb.2022.1058772

COPYRIGHT
© 2022 Devarajan, Truu,
Gopalasubramaniam, Muthukrishanan and
Truu. This is an open-access article
distributed under the terms of the Creative
Commons Attribution License (CC BY). The
use, distribution or reproduction in other
forums is permitted, provided the original
author(s) and the copyright owner(s) are
credited and that the original publication in
this journal is cited, in accordance with
accepted academic practice. No use,
distribution or reproduction is permitted
which does not comply with these terms.

Application of data integration for rice bacterial strain selection by combining their osmotic stress response and plant growth-promoting traits

Arun Kumar Devarajan[1]*, Marika Truu[1], Sabarinathan Kuttalingam Gopalasubramaniam[2]*, Gomathy Muthukrishanan[3] and Jaak Truu[1]

[1]Institute of Molecular and Cell Biology, University of Tartu, Tartu, Estonia, [2]Department of Plant Pathology, Agricultural College and Research Institute, Tamil Nadu Agricultural University, Killikulam, Tuticorin, India, [3]Department of Soil Science and Agricultural Chemistry, Agricultural College and Research Institute, Tamil Nadu Agricultural University, Killikulam, Tuticorin, India

Agricultural application of plant-beneficial bacteria to improve crop yield and alleviate the stress caused by environmental conditions, pests, and pathogens is gaining popularity. However, before using these bacterial strains in plant experiments, their environmental stress responses and plant health improvement potential should be examined. In this study, we explored the applicability of three unsupervised machine learning-based data integration methods, including principal component analysis (PCA) of concatenated data, multiple co-inertia analysis (MCIA), and multiple kernel learning (MKL), to select osmotic stress-tolerant plant growth-promoting (PGP) bacterial strains isolated from the rice phyllosphere. The studied datasets consisted of direct and indirect PGP activity measurements and osmotic stress responses of eight bacterial strains previously isolated from the phyllosphere of drought-tolerant rice cultivar. The production of phytohormones, such as indole-acetic acid (IAA), gibberellic acid (GA), abscisic acid (ABA), and cytokinin, were used as direct PGP traits, whereas the production of hydrogen cyanide and siderophore and antagonistic activity against the foliar pathogens *Pyricularia oryzae* and *Helminthosporium oryzae* were evaluated as measures of indirect PGP activity. The strains were subjected to a range of osmotic stress levels by adding PEG 6000 (0, 11, 21, and 32.6%) to their growth medium. The results of the osmotic stress response experiments showed that all bacterial strains accumulated endogenous proline and glycine betaine (GB) and exhibited an increase in growth, when osmotic stress levels were increased to a specific degree, while the production of IAA and GA considerably decreased. The three applied data integration methods did not provide a similar grouping of the strains. Especially deviant was the ordination of microbial strains based on the PCA of concatenated data. However, all three data integration methods indicated that the strains *Bacillus altitudinis* PB46 and *B. megaterium* PB50 shared high similarity in PGP traits and osmotic stress response. Overall, our results indicate that data integration methods complement the single-table

data analysis approach and improve the selection process for PGP microbial strains.

KEYWORDS

osmotic stress, rice phyllosphere, plant growth-promoting bacteria, data integration, strain selection

Introduction

Global food production has been significantly affected by climate change and the evolution of pests and pathogens (FAO, 2022). Rice is one of the world's most important food crops, but it is highly vulnerable to numerous abiotic and biotic stresses (Sandhu et al., 2020). Plants have several mechanisms to adapt to and establish tolerance and resistance to stress (Vats, 2018; Chauhan et al., 2022; Hidangmayum et al., 2022; Sachdev and Ansari, 2022). One such mechanism is symbiosis, wherein beneficial microorganisms living in or on plant organs directly and/or indirectly support plant growth and protect them from biotic and abiotic stresses (Shinwari et al., 2019). Given this beneficial effect, more attention has been paid to rice microbiome to increase crop yield and achieve sustainable agricultural goals. The microbial community composition of the rice rhizosphere has been extensively investigated using both culture-dependent and -independent approaches (Ding et al., 2019). Although the role of rhizobacteria in crop health improvement under abiotic stress has been widely reported (Ayuso-Calles et al., 2021; Saxena et al., 2021), the contribution of rice phyllosphere and spermosphere microbial communities and populations to this process is only partially understood (Kim and Lee, 2020).

The phyllosphere refers to a plant's total aboveground surface, representing an unstable habitat, where microbes are subjected to extreme and highly variable environmental factors, such as light intensity, ultraviolet (UV) radiation, temperature, and dryness. Bacteria dominate this habitat, and their number estimated either by cultivation or direct microscopy can be up to 10^7 cells per cm^2 on plant leaf surfaces (Vorholt, 2012; Remus-Emsermann and Schlechter, 2018). Microbial genetic and metabolic competence has been shown to help bacteria overcome and survive extreme environments (Sessitsch et al., 2012; Shu and Huang, 2022). Venkatachalam et al. (2016) demonstrated that the adaptability and functionality of culturable rice microbial communities were related to their diversity and abundance in the phyllosphere, while their ability to stimulate plant growth was strongly influenced by the rice cultivation method. *Bacillus* species can be highly resistant to extreme abiotic stress factors, such as UV radiation, high and low temperatures, and dryness, by forming resistant endospores and having higher survival rates than other bacterial species in the phyllosphere (Setlow, 2014; Saleem et al., 2017).

Under high temperatures and desiccation stress, microorganisms regularly encounter osmotic stress in the phyllosphere habitat. Under osmotic stress, most bacteria produce compatible osmolytes, such as proline, glycine betaine (GB), ectoine, trehalose, and sucrose (Santos and Da Costa, 2002). Proline reduces osmotic stress by acting as a chemical chaperone that directly breaks down the reactive oxygen species produced during stress and by means of an indirect mechanism that activates the signaling pathways that promote cell survival (Liang et al., 2013). In contrast, quaternary ammonium compounds, such as GB and choline, serve as osmoprotectants. Choline is a precursor of GB, and during osmotic stress, a certain level of choline is oxidized to GB by choline oxidase and betaine aldehyde dehydrogenase (Fitzsimmons et al., 2012). It has been demonstrated that plant growth-promoting bacteria (PGPB) that accumulate osmolytes reduce plant salinity stress (Upadhyay et al., 2011, 2012). Therefore, to understand the osmotic stress tolerance of microorganisms, it is essential to investigate their osmolyte production potential.

The levels of phytohormones in plants significantly affect their growth by regulating metabolism and defense mechanisms (Egamberdieva et al., 2017). Many plant-associated bacteria can produce beneficial phytohormones, mainly indole-acetic acid (IAA), gibberellic acid (GA), cytokinin, and abscisic acid (ABA; Belimov et al., 2014; Nutaratat et al., 2017; Baliyan et al., 2022; Mekureyaw et al., 2022). Some microbes support host plants indirectly by preventing the growth and infestation of pests and pathogens. Such microbes produce a variety of compounds that inhibit the growth of competing organisms. Some of the most important antagonistic mechanisms involve the production of hydrogen cyanide (HCN), which affects cellular respiration and siderophore production, leads to iron chelation, and limits iron accessibility to pathogens (Sayyed et al., 2013; Muthukumar et al., 2022; Singh et al., 2022). Such behavior of beneficial bacteria against host pathogens can suppress diseases in *in vitro* and *in planta* (Ramakrishna et al., 2019; Mahmud et al., 2021). Therefore, the application of phyllosphere bacteria that can produce phytohormones, have antagonistic activity against pathogens, and tolerate osmotic stress can be greatly beneficial in improving rice health through the alleviation of biotic and abiotic stress.

To select the most promising strains for plant applications, the phenotypic and, less often, the genomic data related to PGP characteristics of microbial strains are explored by applying statistical and exploratory analyses. The data obtained for microbial strains are most often examined using univariate statistical methods including *t*-tests, ANOVA, and linear models. Less frequently,

univariate data analysis methods are complemented with multivariate approaches, such as cluster analysis or principal component analysis, which allow the elucidation of patterns among strains and relationships with their properties (da Costa et al., 2014). When several types of datasets, such as PGP traits and abiotic and biotic stress response parameters, are generated to characterize the potential of PGP-microbial strains for improving plant growth and health, an integration of these datasets is needed to facilitate the simultaneous identification of important phenotypic and genomic features during strain selection.

If the properties of microbial strains are assessed using different measurement methods and experimental conditions, the data produced by a particular method can be considered single-view data. It is possible to fuse microbial strain data from different perspectives using multi-view learning (MVL), which utilizes the consensual and complementary information between different views of the same set of microbial strains. MVL, also known as data fusion or integration from multiple feature sets, is an emerging direction in multi-view machine learning that can be used to improve generalization performance (Zhao et al., 2017; Li et al., 2018). Picard et al. (2021) recently delineated data integration methods into five different integration strategies (early, mixed, intermediate, late, and hierarchical). Data integration can be applied in two ways, depending on the nature of datasets: horizontal integration, which studies the same parameters across different microbial strains, and vertical integration, which examines multiple sets of variables on the same set of strains. Generally, machine learning methods are highly effective in data integration when datasets are appropriately transformed and combined (Picard et al., 2021; Cai et al., 2022).

Thus far, data integration methods have been applied to multi-omics datasets, where the combination of different layers of molecular information obtained for plant-related microbial communities has been analyzed (Kaul et al., 2016). The suitability of this data analysis approach for characterizing and selecting PGP microbial strains using various types of datasets has not yet been explored. We hypothesized that the application of data integration methods can enhance the selection of PGP microbial strains for plant application if multiple PGP-related datasets are measured for these strains.

The main aim of this study was to test the applicability of three unsupervised machine learning-based data integration methods for simultaneous grouping and trait evaluation of osmotic stress-tolerant PGP bacterial strains isolated from the rice phyllosphere. In addition, a set of univariate and multivariate data analysis methods conventionally used for this purpose was implemented.

Materials and methods

Study design

To assess PGP traits and osmotic stress responses in eight bacterial strains isolated from the phyllosphere of drought-tolerant rice varieties grown in Paramakudi, Tamil Nadu, India (Arun et al., 2020; Devarajan et al., 2021), two sets of different assessments were conducted. The following strains (genbank[1] accession numbers in brackets) were included in this study: *Bacillus endophyticus* PB3 (MK969113), *B. australimaris* PB17 (MK979279), *B. pumilus* PB18 (MK979280), *B. safensis* PB23 (MK979280), *Staphylococcus sciuri* PB24 (MK994020), *B. altitudinis* PB37 (MK994020), *B. altitudinis* PB46 (MK979282), and *B. megaterium* PB50 (MK979284). The flowchart shows the study design in detail (Figure 1).

Assessment of PGP traits

Production of phytohormones

To estimate the production of bacterial phytohormones, the strains were inoculated in triplicate into tryptic soy broth (TSB) and allowed to grow at 37°C for 24 h. The growth temperature for bacterial strains in TSB broth was set at 37°C for all studies. This temperature was selected based on the air temperature (42°C) in this region and the fact that the crop leaf surface temperature is expected to be 5°C lower (37°C) than the atmospheric temperature (Deva et al., 2020). Extraction, purification, and quantitative determination of IAA, GA, zeatin, and ABA from different strains were carried out using the methods described by Karadeniz et al. (2006). Briefly, phytohormones were extracted from the bacterial supernatant using ethyl acetate and thin-layer chromatography (TLC) was developed using a mixture of isopropanol/ammonia/distilled water (10:1:1 v/v/v). IAA, GA, zeatin, and ABA bands and R_f (retardation factor) values of the samples were visualized under 254 nm of UV light according to the standards of IAA, GA, zeatin, and ABA. The detected bands were scraped from TLC plates and dissolved in methanol. The purified samples were analyzed by ultra-high-performance liquid chromatography (UHPLC) using an evaporative light scattering detector (ELSD) system with reversed phase C-18 column (Shimadzu, Japan) at an isocratic flow rate of 0.5 min ml^{-1} at 40°C. The wavelengths were 280, 208, 254, and 265 nm for IAA, GA, zeatin, and ABA, respectively (HiMedia, India), and the total duration for the detection of each hormone was approximately 15 min. The results of all phytohormone concentrations are expressed as µg $ml^{-1.}$

Production of siderophores

Siderophores production was evaluated in all bacterial strains. Briefly, the chrome azurol sulfonate (CAS) medium was prepared by adding the CAS solution to melted King's B agar medium at a 1:15 ratio, and 10 µl of rice phyllosphere bacterial strains actively grown in TSB at 37°C for 24 h were spot inoculated on the center of the CAS plate. Colonies with a yellow-orange halo after 3 days of incubation (28 ± 2°C) were considered positive for siderophore production (Schwyn and Neilands, 1987). For siderophore quantification, 100 µl of fresh culture was inoculated into 100 ml of

1 www.ncbi.nlm.nih.gov/genbank/

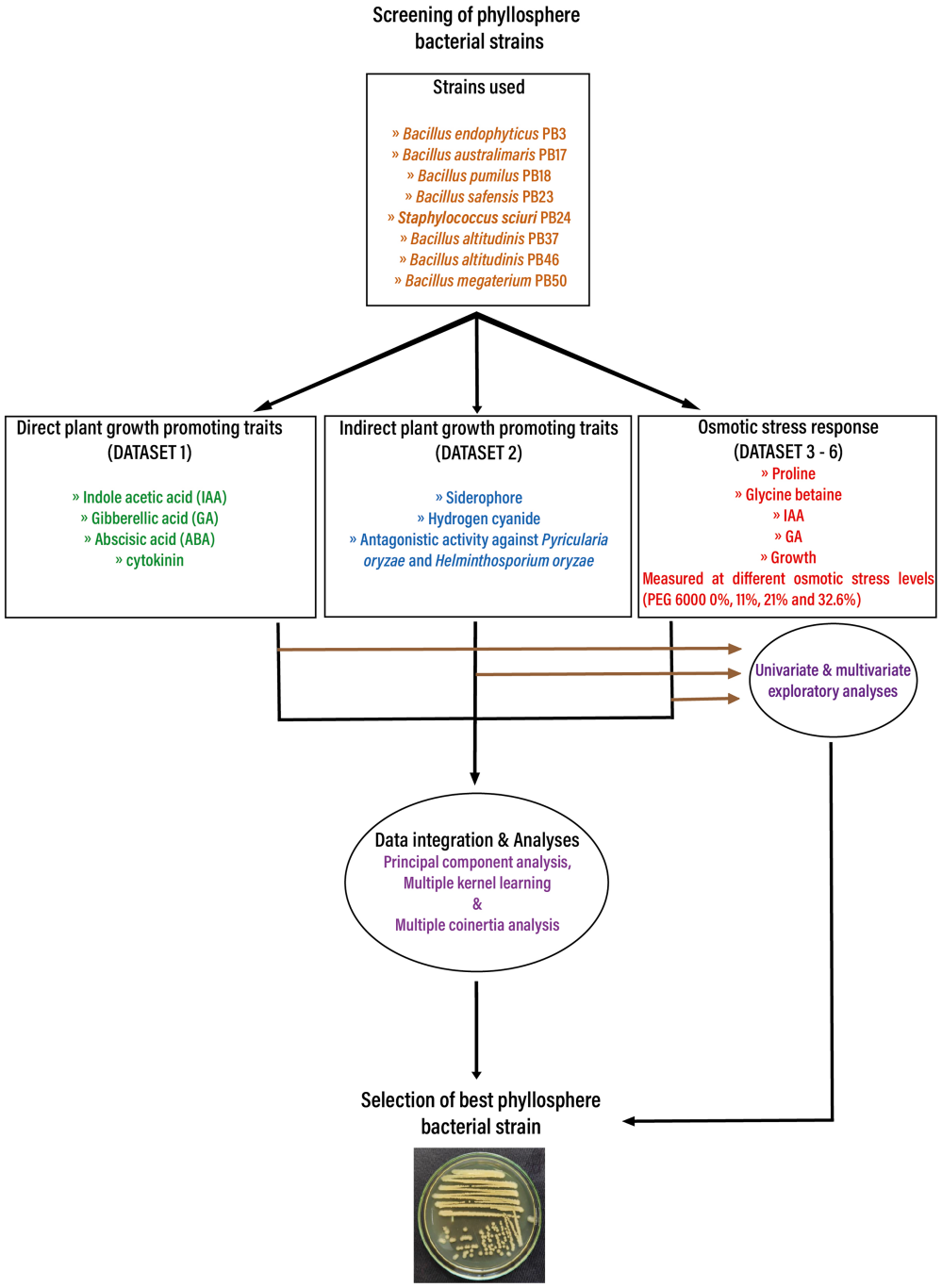

FIGURE 1
The flow chart depicts the basic workflow used in the current study to select the best phyllosphere bacterial strains for use in rice drought alleviation by screening the plant growth-promoting traits and osmotic stress response of bacterial strains. Obtained datasets were analyzed first using univariate and multivariate exploratory analyses. In the next step, the obtained datasets were integrated and analyzed using three unsupervised machine learning techniques: principal component analysis, multiple kernel learning, and multiple co-inertia analysis.

iron-free succinic broth medium and incubated in a rotary shaker at 30°C for 24 h (120 rpm). Subsequently, the broth culture was centrifuged at 10,000 rpm for 10 min. The absorbance of the supernatant was measured at 400 nm using a spectrophotometer (LAMBDA 365 UV–Vis spectrophotometer, PerkinElmer, Mumbai, India), and siderophore production was calculated using the molar extinction coefficient ($\varepsilon = 20{,}000\ M^{-1}\ cm^{-1}$). The hydroxamate- and catecholate-type siderophores were characterized using Arnow's and tetrazolium tests, respectively (Arnow, 1937). The quantification of siderophores is represented

as μM, and the presence or absence of siderophore type is expressed by the signs "+" and "−," respectively.

Production of HCN

The production of HCN by the bacterial strains was measured using the alkaline picric acid method described by Wei et al. (1991). For the qualitative measurement of HCN production, a change in the color of the filter paper strips from yellow to light brown, brown, or brick red was recorded as a mild (+), moderate (+ +), or strong (+ + +) reaction, respectively, whereas no color shift was considered as a negative (−) reaction. The color in the paper was eluted using 10 ml of distilled water, and the filter paper in a sterile medium blank was used as a control. HCN quantification was performed by measuring the absorbance of the eluted samples at 625 nm, and the results are presented as optical density (OD) units.

Evaluation of antagonistic activity

The biocontrol activity of all bacterial strains was tested against two fungal pathogens (*Pyricularia oryzae* and *Helminthosporium oryzae*) obtained from the Department of Plant Pathology, Tamil Nadu Agricultural University, Coimbatore, India, following the protocol proposed by Ji et al. (2013). In brief, the mycelial disks (5 mm diameter) of each rice pathogenic fungus were placed on the edge of potato dextrose agar media (30 mm), and each bacterium was streak inoculated close to the center of the plates that were incubated for 5–6 days at 25°C. Subsequently, the mycelial growth inhibition percentage of *P. oryzae* (PO.IP) and *H. oryzae* (HO.IP) by each bacterial strain was calculated as follows:

Inhibition percentage = [(growth of pathogen in control − growth of pathogen with bacterial strains)/growth of pathogen in control] × 100

Evaluation of osmotic stress effect on bacterial strains

Estimation of bacterial growth and sample preparation

Phyllosphere bacterial strains were inoculated in 100 ml of TSB in side-arm flasks with different concentrations of PEG 6000 (0, 11, 21, and 32.6%) and incubated at 37°C for 24 h. The optical density (OD) of the broth cultures was estimated at 600 nm, and the growth results were expressed as OD units. The cells were then centrifuged at 10, 000 rpm for 5 min and the supernatant was collected to assess IAA and GA production. Cell pellets were used to measure the accumulation of endogenous proline and GB.

Estimation of IAA and GA production

To determine IAA concentration, 2 ml of the supernatant was mixed with 4 ml of Salkowski reagent (2% of 0.5 M $FeCl_3$ in 35% $HClO_4$), and sterile TSB was used as a control (Meudt and Gaines, 1967). Subsequently, the mixtures were incubated in the dark at 25°C for 24 h. The absorbance of IAA was measured at 520 nm using a spectrophotometer. The concentration of IAA in the samples was determined using the IAA standard curve and expressed as μg ml^{-1}.

To determine GA concentrations, 2 ml of the supernatant was mixed with 2 ml of zinc acetate solution and 2 ml of potassium ferrocyanide solution before centrifugation at 8,000 rpm for 10 min (Holbrook et al., 1961). A 5-ml aliquot of supernatant was added to 5 ml of 30% hydrochloric acid and incubated at 27°C for 75 min. The absorbance was measured at 254 nm, and the GA concentration in the samples was determined using a standard GA curve and expressed as μg ml^{-1}.

Estimation of proline and GB production

The endogenous production of proline and GB was measured using the protocol described by Qurashi and Sabri (2013). The harvested cells were boiled and centrifuged to collect the supernatant. For proline estimation, 150 μl of the supernatant was mixed with 100 ml of water and 1 ml of ninhydrin reagent (0.35% ethanol), and 150 μl of sterile water was used as a control. This mixture was heated for 20 min, and then the absorbance was measured at 520 nm. The concentration of proline was calculated using a standard curve prepared with L-proline and expressed as μg ml^{-1}.

To estimate the endogenous accumulation of GB, the extracted supernatant was diluted (1:1) in boiled 2 N H_2SO_4, and sterile water was used as a control (Qurashi and Sabri, 2013). The mixture (0.50 ml) was cooled for 60 min in ice water, and 200 μl of cold KI-I_2 reagent was added with gentle vortexing. The mixture was incubated for 16 h at 4°C and gradually centrifuged for 15 min at 10,000 rpm. After carefully removing the supernatant, the resulting pellet was dissolved in 9 ml of 1,2-dichloroethane, and the absorbance was measured at 365 nm. The concentration of GB was calculated using a standard curve and expressed as μg ml^{-1}.

Statistical analysis

All experiments were conducted in triplicate, and the results are expressed as means with standard deviations. The obtained data were checked for normality and outliers and log-transformed prior to data analysis, if necessary. The following data analysis methods were used for analysis of direct and indirect microbial PGP traits: one-way ANOVA and multivariate ANOVA (MANOVA) with strain type as a single factor. Two-way ANOVA and MANOVA was applied to the set of microbial parameters (growth, production of indole-acetic acid, gibberellic acid, proline, and glycine betaine) with two factors—strain type and stress level. One-way ANOVA test was followed by Tukey's post-hoc test. The significance level was set to 0.05 for all tests. Multivariate exploratory analyses included principal component analysis (PCA), heatmaps, k-means clustering, and spectral clustering. PCA was performed separately for two datasets (direct and indirect PGP traits and osmotic stress data). Heatmaps, k-means clustering, and spectral clustering were used as additional

methods for analysis of osmotic stress dataset. The details of software packages used for the data analysis are provided in Supplementary Table S1 (Paradis et al., 2004; Lê et al., 2008; R Core Team, 2013; Meng et al., 2014; Mariette and Villa-Vialaneix, 2018; Kolde, 2019; John et al., 2020). In the case of PCA, the variables contributing significantly to the principal component (PC) axes were determined using the PCAtest package with random permutation, a bootstrap replication value of 1,000, and an alpha level of 0.05 (Camargo, 2022). The importance of the variable was ranked from each principal component axis using the total loading values.

Data integration

We used horizontal integration of the datasets to compare multiple treatment factors on similar variables and samples. We applied unsupervised machine learning techniques and implemented them using three integration techniques: early integration (PCA), mixed integration (multiple kernel learning, MKL), and intermediate integration (multiple co-inertia analysis, MCIA). Supplementary Table S10 contains information on the dataset combinations used for the integration methods.

In the case of the PCA analysis, the datasets were first combined and transformed, and then the PCA function from the factomineR package was applied to the obtained dataset (Supplementary Table S10). MCIA is a mixed integration technique in which the dataset is dimensionally reduced and transformed using ordination methods, such as PCA, correspondence analysis (COA), or non-symmetric correspondence analysis (NSCA), before being combined for analysis. In this study, the MCIA was performed on the data list (Supplementary Table S10) using the omicade4 package (Supplementary Table S1). Data dimension reduction, transformation, and analysis were performed using a single-function MCIA with singular value decomposition. The output was saved as a MCIA class object, and from that object, the variables from each dataset were visualized with regard to the sample relationship using the plotVar function.

The same data list was used in the R package mixKernel to perform MKL (Supplementary Tables S1, S10), wherein each dataset was first converted into a kernel object using the compute. kernel function with a linear kernel, thereby converting a linearly inseparable space object into a linearly separable one. The fully unsupervised MKL (UKML) method was used to combine all kernel objects, and the resulting kernels were subjected to PCA and an important variable analysis using the kernel.pca and kernel.pca.permute functions, respectively.

The results of different data integration techniques were compared using the congruence among distance matrices (CADM) approach (Campbell et al., 2011) implemented in the CADM.global function using the R package ape: analyses of phylogenetics and evolution (Supplementary Table S1).

Results

Direct and indirect PGP activities of phyllosphere bacterial strains

The analysis of direct PGP activities showed significant differences (one-way MANOVA, $p < 0.001$) in the production of phytohormones by the studied bacterial strains (Table 1; Supplementary Table S2). *Bacillus megaterium* PB50 showed the highest production of all four phytohormones, followed by *B. endophyticus* PB3, which produced the highest levels of IAA, GA, and ABA, and *B. altitudinis* PB46, which produced high levels of GA and cytokinin. The lowest levels of IAA and GA were produced by *B. australimaris* PB17 and those of cytokinin and ABA were produced by *B. safensis* PB23 and *S. sciuri* PB24, respectively.

Similarly, the studied strains significantly differed in their indirect PGP trait values (one-way MANOVA, $p < 0.001$, Table 2; Supplementary Table S2). Siderophore production was found to be the highest in *B. megaterium* PB50, followed by *B. pumilus* PB18. The characterization of siderophores revealed that only *B. megaterium* PB50 produced hydroxamate-type siderophores, whereas the remaining strains produced catecholate-type siderophores (Table 2). The analysis of HCN production results showed that *B. pumilus* PB18 produced the highest amount of HCN, while *B. safensis* PB23 and *S. Sciuri* PB24 produced the least amount of HCN. The assessment of the antagonistic activity of phyllosphere bacterial strains against the rice foliar pathogens revealed that only *B. endophyticus* PB3 and *B. australimaris* PB17 had an antagonistic activity against *P. oryzae*, and only *B. megaterium* PB50 inhibited the growth of *H. oryzae* (Table 2; Supplementary Figure S1).

Bacterial growth and production of phytohormones and osmolytes under different osmotic stress levels

Analysis of bacterial growth under different osmotic stress levels showed that under non-stressed conditions, *B. pumilus* PB18, *B. safensis* PB23, *S. sciuri* PB24, and *B. megaterium* PB50 reached the highest OD, with no significant difference between them. No significant difference was observed among *B. australimaris* PB17, *B. altitudinis* PB37, and *B. altitudinis* PB46, which had the lowest OD values (Table 3; Supplementary Table S6). The maximum growth values were achieved by *B. altitudinis* PB46 at 11 and 21% PEG 6000 concentrations and by *B. megaterium* PB50 at 32% PEG 6000 (Figure 2A). The lowest growth was observed in *B. altitudinis* PB37 at 11 and 21% PEG 6000 concentrations and in *B. australimaris* PB17 and *B. altitudinis* PB37 at 32.6% PEG 6000, with no significant difference between them.

As the PEG 6000 concentration increased, IAA and GA production decreased in all strains (Table 4; Figures 2B,C). The strain *B. megaterium* PB50 produced the highest IAA

TABLE 1 Mean and standard deviation values of the direct plant growth-promoting traits [indole-acetic acid (IAA), gibberellic acid (GA), cytokinin, and abscisic acid (ABA) production] measured for each rice phyllosphere bacterial strain (number of replicates, *n*=3).

Strains	IAA	GA	Cytokinin	ABA
	($\mu g\,ml^{-1}$)	($\mu g\,ml^{-1}$)	($ng\,ml^{-1}$)	($ng\,ml^{-1}$)
Bacillus endophyticus PB3	32.5 (0.73)^{b}	34.8 (1.2)^{b}	148.4 (4.1)^{c}	239.8 (7.8)^{b}
B. australimaris PB17	7.57 (0.37)^{g}	9.2 (0.3)^{f}	63.3 (1.5)^{e}	74.5 (2.3)^{f}
B. pumilus PB18	15.1 (0.39)^{f}	14.7 (0.4)^{d}	78.2 (0.6)^{d}	92.8 (3.4)^{e}
B. safensis PB23	20.4 (0.32)^{d}	19.8 (0.4)^{c}	28.9 (0.5)^{g}	59.3 (1.6)^{g}
Staphylococcus sciuri PB24	18.4 (0.44)^{e}	13.8 (0.4)^{d}	52.6 (1.9)^{f}	34.4 (3.3)^{h}
B. altitudinis PB37	19.5 (0.46)^{de}	10.3 (0.4)^{e}	80.2 (0.9)^{d}	124.4 (3.6)^{d}
B. altitudinis PB46	26.4 (0.35)^{c}	35.7 (0.3)^{b}	178.1 (1.0)^{b}	147.2 (2.0)^{c}
B. megaterium PB50	38.9 (0.86)^{a}	46.6 (0.4)^{a}	410 (5.2)^{a}	311.7 (30.7)^{a}

Parameter values with different letters are significantly different according to Tukey's test, $p < 0.05$.

TABLE 2 Mean and standard deviation values of the indirect plant growth-promoting traits, such as siderophore (Sid.) production, qualitative (Qual.), and quantitative (Quant.) assessment of hydrogen cyanide (HCN) production, and growth inhibition of *Pyricularia oryzae* and *Helminthosporium oryzae* measured for each rice phyllosphere bacterial strain (number of replicates, *n*=3).

Strains	Sid. production (μM)	Arnow's test	Tetrazolium test	Qual. HCN production	Quant. HCN production (OD_{625})	Inhibition percentage (%)	
						Pyricularia oryzae	*Helminthosporium oryzae*
Bacillus endophyticus PB3	46.1 (2.2)^{c}	+	–	++	0.083 (0.002)^{b}	71.2 (4.2)^{b}	0
B. australimaris PB17	38.4 (1.5)^{d}	+	–	++	0.062 (0.004)^{c}	0	0
B. pumilus PB18	65.5 (1.5)^{b}	+	–	+++	0.128 (0.003)^{a}	79.7 (2.7)^{a}	0
B. safensis PB23	14.8 (0.6)^{f}	+	–	–	0.013 (0.003)^{f}	0	0
Staphylococcus sciuri PB24	37.1 (0.6)^{d}	+	–	–	0.009 (0.001)^{f}	0	0
B. altitudinis PB37	17.3 (0.5)^{f}	+	–	+	0.041 (0.003)^{e}	0	0
B. altitudinis PB46	20.7 (0.8)^{e}	+	–	++	0.089 (0.004)^{b}	0	0
B. megaterium PB50	72.2 (3.2)^{a}	–	+	+	0.049 (0.004)^{d}	0	44.4 (5.2)^{a}

Parameter values with different letters are significantly different according to Tukey's test, $p < 0.05$.

TABLE 3 Mean and standard deviation values of growth of each rice phyllosphere bacterial strain (number of replicates, *n*=3) measured under three different osmotic stress conditions and a non-stress condition.

Strains	Growth (OD)			
	Non-stress	PEG 6000 (11%)	PEG 6000 (21%)	PEG 6000 (32.6%)
Bacillus endophyticus PB3	0.638 (0.007)^{b}	0.886 (0.01)^{d}	0.464 (0.003)^{f}	0.267 (0.003)^{e}
B. australimaris PB17	0.553 (0.008)^{c}	0.838 (0.01)^{e}	0.590 (0.003)^{e}	0.228 (0.005)^{f}
B. pumilus PB18	0.693 (0.009)^{a}	0.924 (0.01)^{c}	0.624 (0.003)^{d}	0.285 (0.007)^{d}
B. safensis PB23	0.680 (0.01)^{a}	0.924 (0.01)^{c}	0.658 (0.003)^{c}	0.333 (0.009)^{c}
Staphylococcus sciuri PB24	0.681 (0.01)^{a}	0.760 (0.01)^{f}	0.594 (0.003)^{e}	0.272 (0.01)^{de}
B. altitudinis PB37	0.539 (0.008)^{c}	0.696 (0.01)^{g}	0.395 (0.004)^{g}	0.217 (0.003)^{f}
B. altitudinis PB46	0.533 (0.009)^{c}	1.177 (0.01)^{a}	0.715 (0.004)^{a}	0.399 (0.005)^{b}
B. megaterium PB50	0.673 (0.01)^{a}	1.083 (0.01)^{b}	0.701 (0.004)^{b}	0.420 (0.007)^{a}

Parameter values with different letters are significantly different according to Tukey's test, $p < 0.05$.

amount under almost all stress conditions, except for PEG 6000 at the 21% level, when this value was the highest for *B. altitudinis* PB46. The strain *B. megaterium* PB50 also exceeded the other studied strains in the production of GA at all stress levels, followed by *B. endophyticus* PB3 at 11% PEG 6000 and *B. altitudinis* PB46 at 21 and 32.6% PEG 6000.

All studied strains showed a gradual increase in proline and GB production from non-stress to stress conditions at 21% PEG 6000, but at 32.6% PEG 6000, the production dropped below the non-stress level for both osmolytes (Table 5; Figures 2D,E). Nevertheless, substantial differences were observed for the different strains in osmolyte production at different stress levels.

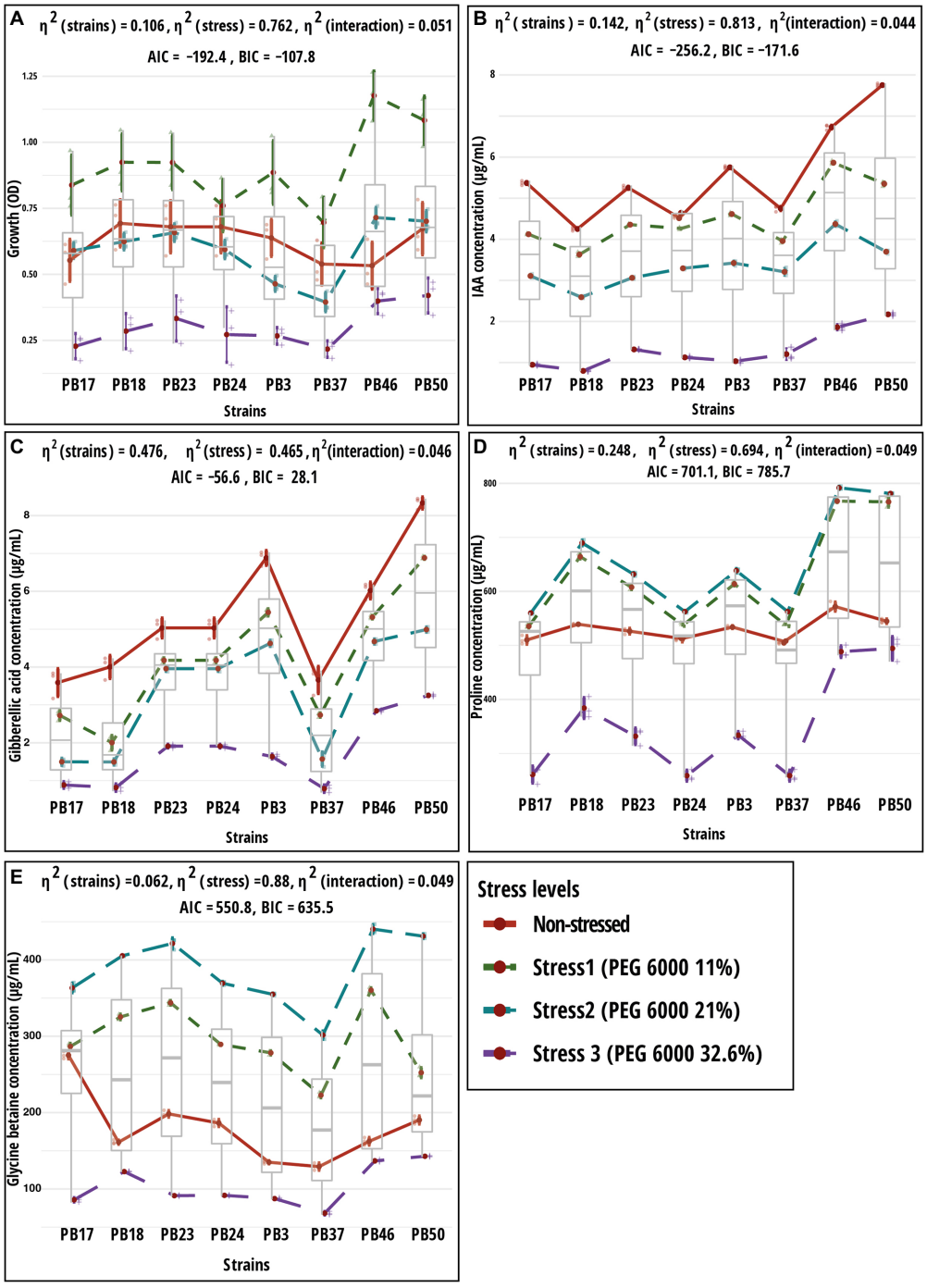

FIGURE 2
Results of two-way ANOVA showing the mean differences of dependent variables according to two independent variables (strain and stress) and their interaction. Shown are mean and standard error values for two grouping variables. Plots **(A)** growth; **(B)** indole-acetic acid (IAA); **(C)** gibberellic acid (GA); **(D)** proline; and **(E)** glycine betaine. The strain codes refer to the following strains: *Bacillus endophyticus* PB3, *B. australimaris* PB17, *B. pumilus* PB18, *B. safensis* PB23, *S. sciuri* PB24, *B. altitudinis* PB37, *B. altitudinis* PB46, and *B. megaterium* PB50. AIC, akaike information criterion; BIC, Bayesian information criterion; and η^2, effect size. Individual *p* values are given in Supplementary Table S5.

Bacillus pumilus PB18 accumulated the highest proline content under non-stress conditions, whereas *B. megaterium* PB50 accumulated the lowest amount under these conditions. Furthermore, under 11, 21, and 32.6% PEG 6000 concentrations, the bacterial strains *B. pumilus* PB18 and *B. safensis* accumulated the maximum amount of proline, with no significant difference between them. The strains *B. australimaris* PB17 and *B. altitudinis* PB37 accumulated the lowest amount of proline at all three stress levels, with no significant differences between them. Different strains showed different GB production patterns under variable

TABLE 4 Mean and standard deviation values of indole-acetic acid (IAA) and gibberellic acid (GA) production (μgml^{-1}) by each rice phyllosphere bacterial strain (number of replicates, n=3) measured under three different osmotic stress conditions and a non-stress condition.

Strains	Non-stress		PEG 6000 (11%)		PEG 6000 (21%)		PEG 6000 (32.6%)	
	IAA	GA	IAA	GA	IAA	GA	IAA	GA
Bacillus endophyticus PB3	33.0 (0.4)^{c}	47.0 (0.8)^{b}	21.3 (0.4)^{c}	31.4 (0.42)^{b}	11.7 (0.4)^{c}	20.7 (0.17)^{b}	1.07 (0.08)^{ef}	2.47 (0.77)^{c}
B. australimaris PB17	28.8 (0.6)^{d}	12.6 (1.7)^{g}	17.0 (0.2)^{e}	8.99 (0.17)^{e}	9.7 (0.3)^{e}	1.93 (0.17)^{e}	0.89 (0.04)^{fg}	0.64 (0.09)^{d}
B. pumilus PB18	18.1 (0.4)^{f}	15.9 (1.0)^{f}	13.2 (0.4)^{g}	5.87 (0.51)^{f}	6.7 (0.2)^{f}	1.23 (0.18)^{f}	0.63 (0.03)^{g}	0.52 (0.18)^{d}
B. safensis PB23	27.6 (0.6)^{d}	25.0 (0.5)^{d}	19.0 (0.2)^{d}	19.3 (0.49)^{d}	9.4 (0.2)^{e}	15.0 (0.29)^{c}	1.74 (0.03)^{c}	3.46 (0.26)^{c}
Staphylococcus sciuri PB24	17.4 (0.3)^{f}	22.1 (1.2)^{e}	18.2 (0.3)^{de}	5.5 (0.34)^{f}	10.9 (0.2)^{cd}	3.1 (0.34)^{d}	1.27 (0.06)^{de}	0.86 (0.23)^{d}
B. altitudinis PB37	22.6 (0.7)^{e}	13.1 (0.3)^{fg}	15.7 (0.4)^{f}	9.31 (0.17)^{e}	10.3 (0.6)^{de}	1.86 (0.17)^{e}	1.46 (0.36)^{cd}	0.47 (0.25)^{d}
B. altitudinis PB46	45.3 (0.9)^{b}	35.9 (0.9)^{c}	34.4 (0.6)^{b}	29.9 (0.93)^{c}	19.1 (0.6)^{a}	21.2 (0.34)^{b}	3.46 (0.30)^{b}	7.93 (0.13)^{b}
B. megaterium PB50	60.1 (0.7)^{a}	69.0 (0.9)^{a}	28.6 (0.7)^{a}	49.0 (0.45)^{a}	13.7 (0.3)^{b}	24.3 (0.51)^{a}	4.72 (0.16)^{a}	10.4 (0.63)^{a}

Parameter values with different letters are significantly different according to Tukey's test, $p < 0.05$.

TABLE 5 Mean and standard deviation values of proline and glycine betaine (GB) accumulation (μgml^{-1}) by each rice phyllosphere bacterial strain (number of replicates, *n*=3) measured under three different osmotic stress conditions and a non-stress condition.

Strains	Non-stressed		PEG 6000 (11%)		PEG 6000 (21%)		PEG 6000 (32.6%)	
	Proline	GB	Proline	GB	Proline	GB	Proline	GB
Bacillus endophyticus PB3	534 (15)^{ab}	135 (7)^{c}	614 (19)^{c}	278 (20)^{d}	638 (22)^{c}	354 (18)^{c}	334 (14)^{c}	89 (5)^{e}
B. australimaris PB17	510 (16)^{b}	275 (18)^{a}	535 (17)^{e}	287 (11)^{d}	560 (19)^{d}	363 (15)^{c}	261 (9)^{d}	86 (5)^{e}
B. pumilus PB18	571 (15)^{a}	162 (12)^{bc}	767 (14)^{a}	325 (9)^{c}	792 (15)^{a}	405 (23)^{bc}	488 (16)^{a}	123 (5)^{c}
B. safensis PB23	541 (13)^{ab}	190 (18)^{b}	766 (24)^{a}	343 (13)^{ab}	781 (17)^{a}	421 (19)^{ab}	494 (18)^{a}	91 (5)^{d}
Staphylococcus sciuri PB24	526 (18)^{b}	186 (14)^{b}	608 (25)^{c}	289 (19)^{d}	632 (32)^{c}	369 (21)^{c}	332 (12)^{c}	92 (3)^{d}
B. altitudinis PB37	534 (10)^{ab}	129 (23)^{c}	537 (13)^{e}	223 (7)^{e}	562 (11)^{d}	301 (12)^{d}	259 (6)^{d}	68 (5)^{f}
B. altitudinis PB46	539 (15)^{ab}	162 (8)^{bc}	664 (24)^{b}	360 (9)^{a}	690 (29)^{b}	440 (15)^{a}	384 (11)^{b}	137 (5)^{b}
B. megaterium PB50	384 (14)^{c}	198 (11)^{b}	585 (22)^{d}	352 (12)^{a}	610 (24)^{cd}	431 (17)^{a}	313 (18)^{c}	143 (4)^{a}

Parameter values with different letters are significantly different according to Tukey's test, $p < 0.05$.

stress conditions. Under non-stress conditions, the bacterial strain *B. australimaris* PB17 produced the highest GB, whereas *B. altitudinis* PB46 and *B. megaterium* PB50 produced the highest GB at 11 and 21% PEG 6000 levels. *Bacillus megaterium* PB50 produced the maximum GB at 32.6% PEG 6000. Under non-stress conditions as well as 11, 21, and 32.6% PEG 6000 levels, *B. altitudinis* PB37 had the lowest GB.

Two-way MANOVA revealed the significance of the interaction effect (strain–osmotic stress interaction) and the main effects (strains and osmotic stress level) in the examined parameters (Supplementary Table S3). The results of one-way MANOVA revealed that the impact of bacterial strains on microbial parameters was statistically significant at each stress level (Supplementary Table S4), except for bacterial growth, which was not significant in the non-stress conditions (Supplementary Tables S6–S9). The two-way ANOVA results showed significant ($p < 0.05$) differences in all traits tested among bacterial strains and osmotic stress levels, as well as their interaction effects (Supplementary Table S5).

The response pattern of the studied strains based on biochemical properties and growth under various osmotic stress levels was revealed by the PCA plot (Figure 3). The PCA first (PC1) axis captured 68.4% of the overall data variation, and all variables significantly contributed to the PCA first axis (Supplementary Table S11). All strains had a generally similar response pattern that consisted of a gradual change along the PCA second (PC2) axis in the case of 11 and 21% stress levels of PEG 6000, followed by a shift in the same direction along the PC1 axis when strains were exposed to 32.6% PEG 6000 (Figure 3C). The gradual change along the PC2 axis was related mainly to the increase in GB and proline production with the increase in PEG 6000 level to 21%, while the application of 32.6% PEG 6000 was characterized by a reduction in strain growth values (Figure 3D).

The heatmap based on PGP traits showed that the strains could be divided into two main groups based on their response to osmotic stress levels. At the 32% PEG 6000 level, the strains formed one group, and the strains at other stress levels formed another cluster (Supplementary Figure S4). The results of *k*-means clustering indicated four optimal clusters, of which two (stress levels 0 and 32.6%) were partially homogenous (Supplementary Figure S5A). Moreover, these results indicated that *B. altitudinis* PB46 and *B. megaterium* PB50 were the most deviant in their responses to different stress levels. Spectral clustering identified two strain groups with similar response patterns to increasing PEG 6000 stress levels. The first group consisted of four strains (*B. endophyticus* PB3, *B. pumilus* PB18,

B. altitudinis PB46, and *B. megaterium* PB50), and the second group consisted of three strains (*B. australimaris* PB17, *B. safensis* PB23, and *S. sciuri* PB24; Supplementary Figure S5B). *Bacillus altitudinis* PB37 was not included in either group. The main difference between the response dynamics of the two groups was related to a more profound stress response in the first group than in the second group and the strain *B. altitudinis* PB37. This higher stress response was more reflected at the stress levels of 11 and 21% PEG 6000 when the relative stress response magnitude was 1.5–2-fold higher in the first group than in the second group.

Integration of different datasets

Early integration approach

A PCA was used to explore the variation among strains based on a joint dataset of direct and indirect PGP variables (Figure 3). The PC1 axis explained 54.6% of the data variance, and the statistically significant variables in PCA were siderophore, IAA, GA, GB, ABA production, and *H. oryzae* inhibition percentage (Supplementary Table S11). The PC1 axis separated *B. megaterium* PB50, *B. altitudinis* PB46, and *B. endophyticus* PB3 from the other

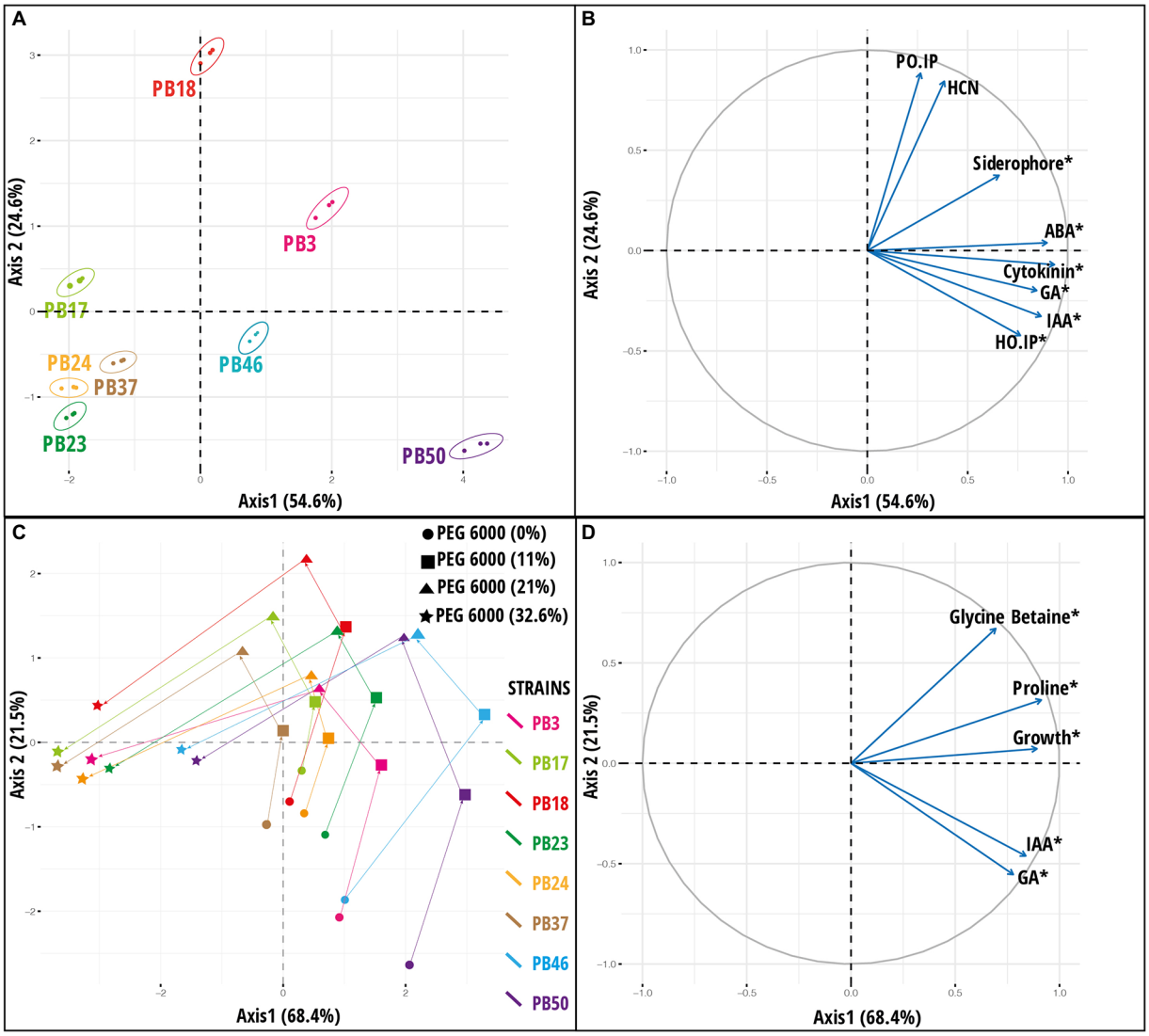

FIGURE 3
Results of principal component analysis (PCA) based on the plant growth-promoting (PGP) trait data of rice phyllosphere bacteria (number of replicates, *n*=3). **(A)** Score plot and **(B)** loading plot of variables according to first two principal component axes. Bacterial strains are indicated by 95% confidence ellipses. The plots correspond to 79.2% of the total data variance and variance proportions are shown along each principal component axis. **(C)** Score plot and **(D)** loading plot of variables along first two principal component axes based on microbial dataset [indoleacetic acid (IAA), gibberellic acid (GA), proline, glycine betaine, and growth] of rice phyllosphere bacterial strains measured at different PEG 6000 concentrations (number of replicates, *n*=3). The plots correspond to 89.9% of the total data variance, and variance proportions are shown along each principal component axis. Variables with asterisk in plot B and D are significant along the first principal component axis. Abbreviations used in plot **(B)** are, abscisic acid (ABA), hydrogen cyanide (HCN), *Helminthosporium oryzae* inhibition percentage (HO_IP), and *Pyricularia oryzae* inhibition percentage (PO_IP). The codes of the strains in plots **(A,C)** refer to the following strains: *Bacillus endophyticus* PB3, *B. australimaris* PB17, *B. pumilus* PB18, *B. safensis* PB23, *Staphylococcus sciuri* PB24, *B. altitudinis* PB37, *B. altitudinis* PB46, and *B. megaterium* PB50.

strains (Figures 3A,B). The PC2 axis emphasized the variation among strains in *P. oryzae* inhibition percentage and HCN production ability, indicating that strain *B. pumilus* PB18 exhibited the highest *P. oryzae* inhibition percentage and HCN production potential among the studied strains. A heatmap based on direct and indirect PGP traits was used to assess similarities among the studied bacterial strains (Supplementary Figure S2). Based on the intensity of the PGP response, the strains were separated into one large group of seven strains with two subclusters, whereas the *B. megaterium* PB50 strain formed a separate cluster. The large cluster comprised two sub-clusters, with *B. endophyticus* PB3, *B. pumilus* PB18, and *B. altitudinis* PB46 grouped together as moderate-performance strains, and *B. australimaris* PB17, *B. safensis* PB23, *S. sciuri* PB24, and *B. altitudinis* PB37 grouped separately because of their poor performance in PGP activities. Furthermore, *k*-means clustering led to the identification of six optimal clusters in this dataset, with *B. australimaris* PB17 and *B. altitudinis* PB37 and *B. safensis* PB23 and *S. sciuri* PB24 clustered together, and both clusters were close to each other, as shown in the PCA ordination plot (Supplementary Figure S3).

In addition to PCA on the joint PGP trait dataset (Figures 3A,B), PCA was performed by combining all osmotic stress datasets (datasets 3–6; Supplementary Table S10) and all six datasets (datasets 1–6; Supplementary Table S10). The results for PCA on all osmotic stress datasets are provided in Supplementary Figure S6, and these data were used as input later in the congruence among the distance matrices approach. The PCA results for all six datasets are shown in Figure 4. PC1 was significant ($p < 0.05$), accounting for 56% of the total variance, whereas PC2 accounted for only 12.5% of the total variance. Most variables had a significant impact on PC1 (Supplementary Table S11). The maximum variance was attributed by the variables measured at a stress level of 32.6% PEG 6000 32.6%.

Multiple co-inertia analysis

Multiple co-inertia analysis was applied to jointly analyze the six datasets (Supplementary Table S10). The graphical outputs of this analysis are shown in Figure 5; Supplementary Figure S7. The MCIA first axis captured the highest variance (78.3%) in the datasets and separated three strains, *B. endophyticus* PB3, *B. altitudinis* PB46, and *B. megaterium* PB50, from the remaining strains (Figure 5A). The MCIA second axis, explaining 16.0% of the data variation, emphasized the distinction between the strains *B. pumilus* PB18 and *B. altitudinis* PB37 and the other studied strains. The pseudo-eigenvalue space of six datasets (Figure 5D) indicates that three datasets (direct PGP traits as well as stress at PEG 6000 levels of 0 and 11%) contributed the most to the MCIA first axis, while the contribution of indirect PGP parameters was small. The datasets of the stress at PEG 6000 levels of 21 and 32.6% contributed to the MCIA second axis. Correlations

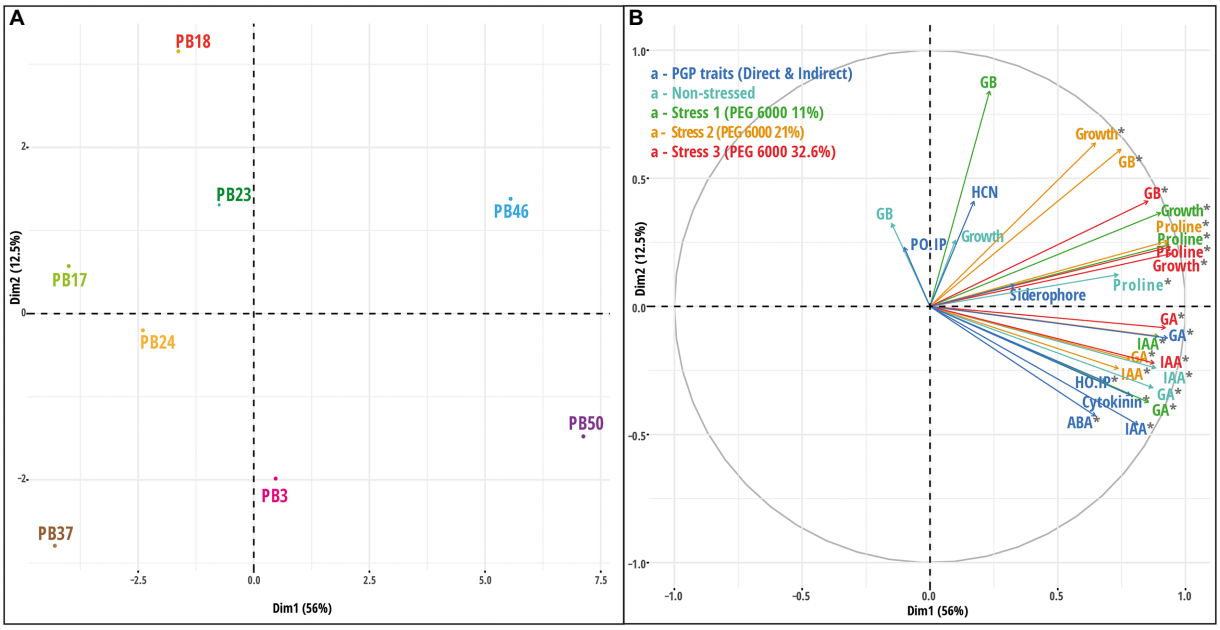

FIGURE 4
Results of principal component analysis (PCA) based on the integration of plant growth-promoting traits data and osmotic stress response parameters datasets. **(A)** Score plot and **(B)** loading plot of variables according to first two principal components. The plots correspond to 68.5% of the total data variance, and variance proportions are shown along each principal component axis. Variables with asterisk in the plot **(B)** are significant along the first principal component axis. Abbreviations used in plot **(B)** are, indoleacetic acid (IAA), gibberellic acid (GA), glycine betaine (GB), abscisic acid (ABA), hydrogen cyanide (HCN), *Helminthosporium oryzae* inhibition percentage (HO.IP), and *Pyricularia oryzae* inhibition percentage (PO.IP). The codes of the strains in plot **(A)** refer to the following strains: *Bacillus endophyticus* PB3, *B. australimaris* PB17, *B. pumilus* PB18, *B. safensis* PB23, *Staphylococcus sciuri* PB24, *B. altitudinis* PB37, *B. altitudinis* PB46, and *B. megaterium* PB50.

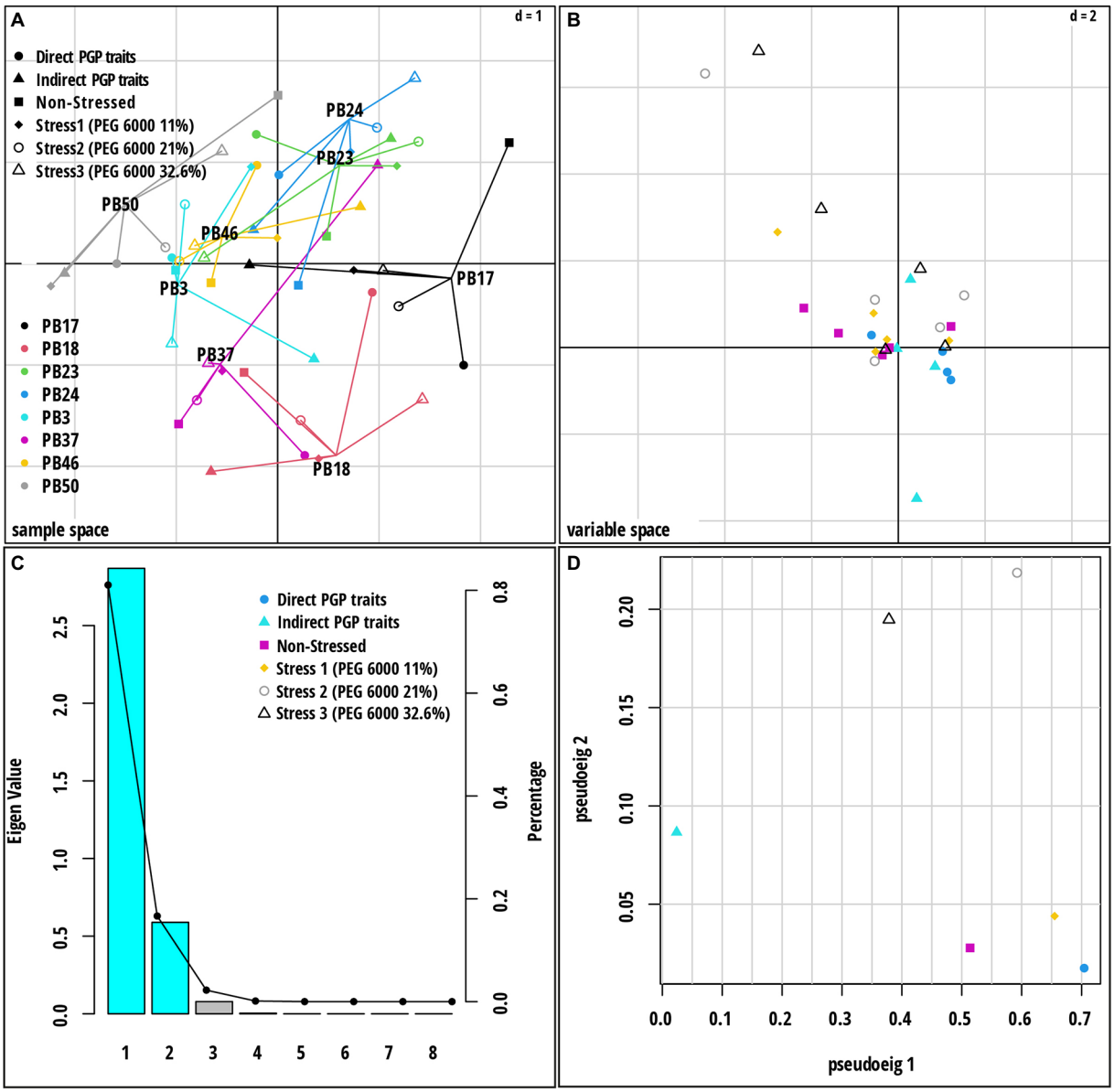

FIGURE 5
Multiple co-inertia analysis (MCIA) results based on six datasets [direct plant growth-promoting (PGP) traits, indirect PGP traits, microbial parameters under osmotic stress at PEG concentrations 0, 11, 21, and 32.6%]. **(A)** A plot of the first two components in the sample space. Each sample is represented by a shape where lines connect the six datasets for each sample to a center point (MCIA global score). **(B)** Variable space for each dataset. **(C)** A scree plot of absolute eigenvalues (bars) and the proportions of variance for the eigenvectors (line). **(D)** A plot of data weighting space that shows the pseudo-eigenvalues space of all datasets indicating the variance of an eigenvalue contributed by each dataset. The codes of the strains in plot **(A)** refer to the following strains: *Bacillus endophyticus* PB3, *B. australimaris* PB17, *B. pumilus* PB18, *B. safensis* PB23, *Staphylococcus sciuri* PB24, *B. altitudinis* PB37, *B. altitudinis* PB46, and *B. megaterium* PB50.

between datasets were the highest at the stress levels of 11, 21, and 32.6% PEG 6000 (RV = 0.71–0.76) and lowest in the case of the datasets of indirect PGP traits and stress levels of 0, 11, and 21% of PEG 6000 (RV = 0.35–0.51). Projections of all variables onto the first two MCIA axes space indicated that the strains *B. altitudinis* PB46 and *B. megaterium* PB50, and to a lesser extent, *B. endophyticus* PB3, were associated with higher IAA and GA values (Supplementary Figure S7). The concentration of GB was an important variable for the separation of strains under non-stress conditions, and it coincided with higher siderophore and cytokinin production. The dataset correlation plot based on the RV coefficient value showed that the dataset of intermediate stress level (21% PEG 6000) was highly positively correlated with the datasets of 11 and 32.6% PEG 6000 datasets (Supplementary Figure S8A). The positive correlation of the stress and non-stress datasets of 11% PEG 6000 with the datasets of PGP traits was higher than that of the other two stress levels, indicating that the stress level influenced

the function of all studied strains. Indirect PGP traits did not positively correlate with other dataset types.

Multiple kernel learning

The MKL technique was applied to the same six datasets (Supplementary Table S10), and the combined kernel principal component analysis (KPCA) was used in further exploratory analysis. The results of these analyses revealed that the majority of the overall variance in the data was captured by the first axis of KPCA, which clearly separated the two strains, *B. altitudinis* PB46 and *B. megaterium* PB50, from the rest of the strains (Figure 6A). To identify the influence of the variables on KPCA, an important variable plot was computed (Figure 6B), which showed that GA and HCN production were the most important direct and indirect PGP traits, respectively. The production of IAA and GA was important in the non-stress conditions, whereas GA was also relevant at the 11% PEG 6000 stress level. Proline production was found to be an important variable in both 21 and 32.6% PEG 6000 stress levels. The kernel correlation plot showed that the dataset correlation followed a pattern similar to that observed with the MCIA analysis, indicating that the dataset correlation was heavily influenced by stress levels (Supplementary Figure S8A).

Comparison of data analysis results

The CADM test indicated that some of the obtained distance matrices were similar (CADM global test, $p < 0.001$). The most congruent were strain groupings according to the PCA based on all datasets and the PCA based on osmotic stress data (Mantel $r = 0.54$, $p < 0.001$). In addition, the MCIA and KPCA results correlated (Mantel $r = 0.46$, $p < 0.01$). The similarities among the studied data integration methods were visualized using a dendrogram based on the Mantel test correlation values (Supplementary Figure S9). The posteriori test indicated that the strain distance matrices of the KPCA and PCA based on osmotic stress data were incongruent with the rest of the distance matrices.

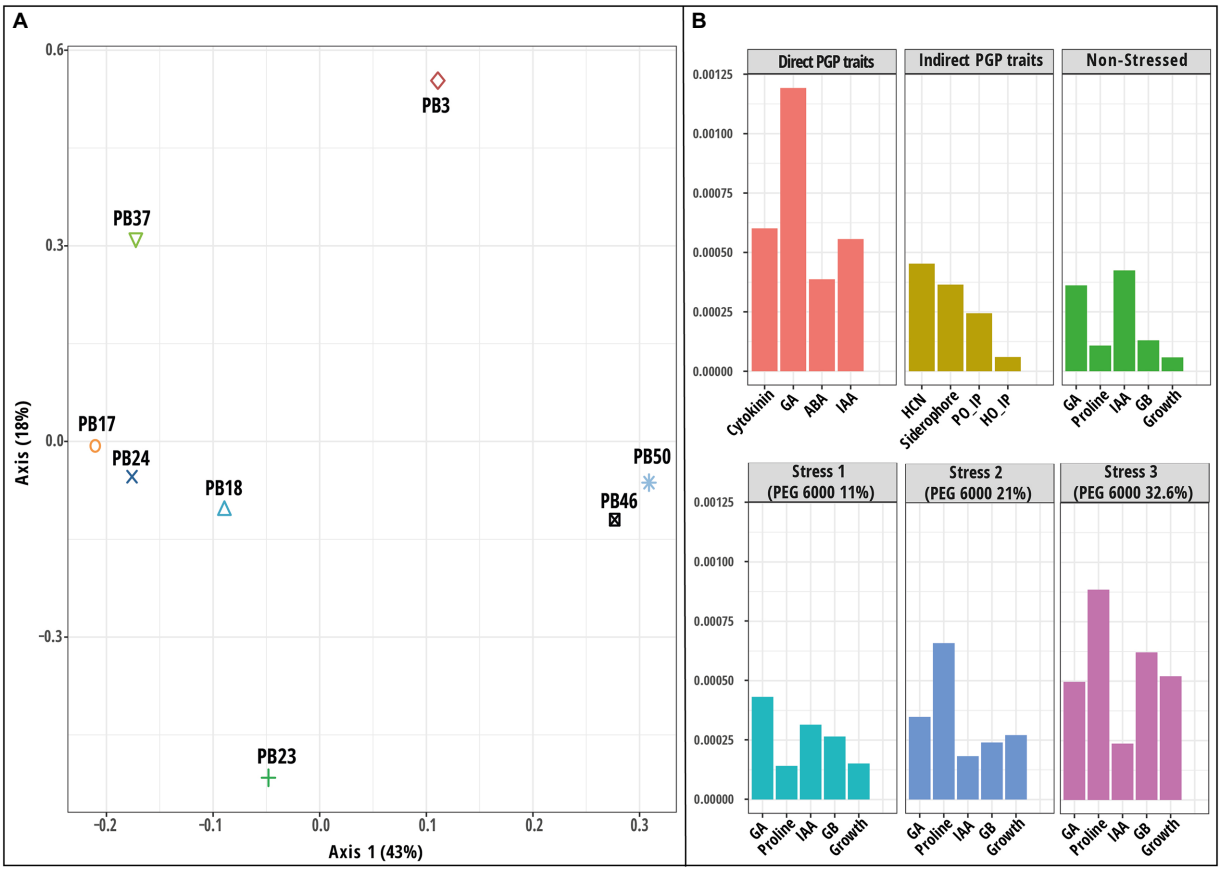

FIGURE 6
Results of multiple kernel learning analysis (MKL). **(A)** A plot of kernel principal component analysis (KPCA) based on six datasets (direct plant growth-promoting (PGP) traits, indirect PGP traits, microbial parameters under osmotic stress at polyethylene glycol (PEG) concentrations 0, 11, 21, and 32.6%). **(B)** A plot for important variables in each dataset assessed using the Crone-Crosby distance. The codes of the strains in plot **(A)** refer to the following strains: *Bacillus endophyticus* PB3, *B. australimaris* PB17, *B. pumilus* PB18, *B. safensis* PB23, *Staphylococcus sciuri* PB24, *B. altitudinis* PB37, *B. altitudinis* PB46, and *B. megaterium* PB50. Abbreviations used in plot **(B)** are indoleacetic acid (IAA), gibberellic acid (GA), abscisic acid (ABA), hydrogen cyanide (HCN), *Helminthosporium oryzae* inhibition percentage (HO_IP), and *Pyricularia oryzae* inhibition percentage (PO_IP).

Discussion

Estimating strains difference using univariate and multivariate analysis

Among the eight strains included in this study, seven were spore-forming gram-positive *Bacillus* strains that were generally resistant to the effects of dryness, heat, UV radiation, and various other environmental stressors (Nicholson et al., 2000; Tortora et al., 2019). However, the measured biochemical and microbiological indicators revealed significant differences in osmotic stress tolerance and PGP properties among the strains.

Based on the univariate analysis results, *B. endophyticus* PB3, *B. altitudinis* PB46, and *B. megaterium* PB50 stood out with their phytohormone production ability, with *B. megaterium* PB50 producing the highest amounts of all four phytohormones. The production of these phytohormones by *B. megaterium* species has been reported previously (Karadeniz et al., 2006), and this ability has been associated with the stimulation of growth and stress alleviation in plants (Shahzad et al., 2017; Sun et al., 2017; Kang et al., 2019; Zerrouk et al., 2020) by a direct effect on phytohormone levels (Vejan et al., 2016).

The production of HCN and siderophores in bacterial cells serves as a defense mechanism against other microbes. While known to be good siderophore producers that inhibit the growth of several plant pathogens, *Bacillus* species have been shown to possess moderate HCN production ability (Muthukumar et al., 2022). In this study, all *Bacillus* strains could produce siderophores; however, *B. megaterium* PB50 was the most effective siderophore producer among the studied strains and was the only strain that produced hydroxamate-type siderophores (Ferreira et al., 2019). *Bacillus megaterium* is a dominant rice phyllosphere bacterial species that has shown antagonistic activity against several predominant rice fungal pathogens *in vitro* (Islam and Nandi, 1985; Gowdu and Balasubramanian, 1988). Moreover, *B. megaterium* PB50 was among the three *Bacillus* strains that showed antagonistic activity against rice fungal pathogens in this study. However, another strain, *B. pumilus* PB18, also exhibited antagonistic activity against fungal pathogens and had the highest siderophore production activity among the strains examined in this study.

In all strains, a decrease in IAA and GA production was observed under more pronounced osmotic stress conditions; however, the production was again the highest in *B. megaterium* PB50 at different stress levels. Similarly, a higher production of IAA by *B. megaterium* at the 15% PEG level was detected by Armada et al. (2014). In addition, decreased IAA, GA, and cytokinin production under stress conditions (20% PEG 6000) compared to non-stress conditions was observed in *Azospirillum brasilense* and *B. subtilis* (Ilyas et al., 2020). In addition, to *B. megaterium* PB50, *B. altitudinis* PB46 stood out from the other strains in responding to stress levels. Similar to earlier reports for different *Bacillus* species (Paul et al., 2015; Lee et al., 2018), the growth of the two aforementioned strains was faster at 11% PEG 6000 than under non-stress conditions.

Bacterial growth and proline and GB accumulation increased with increasing osmotic stress levels of up to 21% PEG 6000 in all strains. Phytohormone production decreased with increasing proline and GB concentrations. In contrast to *B. megaterium* PB50, which showed the lowest proline accumulation and highest phytohormone production under stress, *B. pumilus* PB18 showed the highest osmolyte accumulation and lowest phytohormone production under stress. Although all studied strains were gram-positive bacteria that could synthesize endogenous proline under osmotic stress conditions by boosting the synthesis process and then degrading proline for another metabolism (Tempest et al., 1970; Deutch, 2019), and the GB is transported from an external source or converted from imported choline during stress (Onyango and Alreshidi, 2018), the results of this study suggest that osmolyte accumulation is balanced. Each bacterium uses a specific osmolyte synthesis mechanism to overcome abiotic stress (Bremer and Krämer, 2019). It has been shown earlier that under non-stress conditions, bacteria favor phytohormone synthesis rather than osmolyte accumulation, whereas the opposite occurs under stress conditions. Such a shift in metabolic activity is common in bacterial cells, allowing them to maintain homeostasis when there is an increase in osmotic pressure in the extracellular medium (Varela et al., 2004; Lahtvee et al., 2014; Cesar et al., 2020).

Integration of bacterial strain datasets

Complementary information from several types of datasets produced for microbial strains can be exploited to obtain better insights into microbial strain grouping and to elucidate factors behind strain clustering using machine-learning-based data integration methods. We applied three data-integration approaches to obtain microbial datasets: early, intermediate, and mixed integration.

In the early integration approach, several microbial datasets were combined into a single table and processed using PCA. This approach highlighted two strains, *B. altitudinis* PB46 and *B. megaterium* PB50, which were the most distinct from the other strains. At the same time, the PCA of the concatenated data did not clearly indicate the variables important for the separation of microbial strains in the PCA plot. Although the early integration approach is appealing owing to its simplicity and easy implementation, the complexity, data imbalance, and possible noise in the underlying matrix may complicate learning. As a linear dimension reduction method, PCA is the most commonly used approach for concatenated data, whereas nonlinear methods (*t*-distributed stochastic neighbor embedding,

t-SNA; uniform manifold approximation, and UMAP) may provide better performance depending on the dataset properties (Xiang et al., 2021).

For mixed data integration, we utilized the MKL technique, in which a linear kernel was first computed for each microbial dataset and then the obtained kernels were combined to produce a global similarity matrix that describes microbial strains across all included datasets (Mariette and Villa-Vialaneix, 2018). The resulting similarity matrix was used as the input for the PCA. The results of this method also emphasized the separation of the two strains, *B. altitudinis* PB46 and *B. megaterium* PB50, from the other studied strains. In addition, the analysis outcome provided estimates of the variable importance. Direct PGP traits, such as GA and proline production at stress levels of 21 and 32% of PEG 6000, were highlighted by this analysis. The MKL technique has the advantage of preserving the original properties of the data and combining different data types by applying appropriate transformations (Zampieri et al., 2019). However, the MKL analysis results may be challenging to interpret because the interactions and correlations among different datasets are not always well determined.

The third method, MCIA, is an intermediate strategy of data integration, where multiple microbial datasets are jointly integrated without prior transformation. Similar to MKL, the MCIA reduces the dimensionality and complexity of datasets. The MCIA results clearly showed the distinction of strain *B. megaterium* PB50 from the other strains. The direct PGP trait data set (particularly GA and IAA production) and stress level 11% (GA production) were the most important indicators of the variation among the microbial strains. MCIA is considered one of the best-performing algorithms for the benchmarking of joint multi-omics dimensionality reduction approaches in the case of cancer datasets and provides an effective elucidation of relationships among the studied datasets (Cantini et al., 2021). Moreover, it can be considered a variation of the canonical correspondence analysis (CCA) method (Vahabi and Michailidis, 2022). The applicability of other CCA extensions could also be tested for simultaneous feature selection and classification in microbial datasets in the future.

The three applied data integration methods did not provide a similar grouping of the studied strains, except for the ordination of microbial strains based on the PCA of concatenated data. However, all three data integration methods indicated that the strains *B. altitudinis* PB46 and *B. megaterium* PB50 had high similarity in their biochemical properties and osmotic stress response. However, when applied together with *B. endophyticus* PB3 in a rice growth experiment under drought conditions, these two strains had variable effects on plant growth, biochemical properties, and gene expression (Devarajan et al., 2021). Strain *B. megaterium* PB50, and to a lesser extent *B. altitudinis* PB46, induced elevated drought tolerance in rice plants, while *B. endophyticus* PB3 had no effect. Simultaneously, the MCIA method placed the strain *B. endophyticus* PB3 close to *B. altitudinis* PB46 and *B. megaterium* PB50. Both MCIA and MKL indicate that GA production is one of the main features of microbial strains. In addition, MCIA emphasized IAA and MKL proline production at higher osmotic stress values. Several studies have reported the importance of microbial IAA, GA, and proline production in mitigating drought stress in crops (Ashry et al., 2022; Fadiji et al., 2022; Uzma et al., 2022).

One option for improving strain selection and feature identification in the future is to apply a combination of unsupervised and supervised data integration methods (Singh et al., 2019). In such cases, the outcome of plant inoculation experiments could be included in the process of data integration. It could also be that the microbial parameters included in the current data analysis did not completely cover the microbial traits required for successful plant application. In addition to biochemical properties, different omics (genome, transcriptome, proteome, and metabolome) datasets could be produced for microbial strains. The analysis of such datasets could be challenging, although there are several data integration methods specifically designed for the analysis of different omics layers.

Conclusion

Overall, our findings suggest that when selecting bacterial strains to improve crop resilience under field drought conditions, various aspects of the PGP activity and osmotic stress tolerance of microbial strains should be considered simultaneously. Data integration methods could complement the single-table data analysis approach and may provide better insight into the microbial strain selection process. In addition, data integration allows for the exploration of complex microbial strain datasets within a single analytical framework. Currently, there are no general rules for selecting the most efficient data integration method for biological datasets. Thus, additional benchmarking of different joint data analysis methods with larger microbial strain datasets is advisable for PGP microbial strains. Another aspect of the data integration of PGP microbial strains, which needs further exploration, is related to the joint analysis of microbial biochemical and omics datasets. The integration of microbial biochemical and omics datasets may provide better insights for producing mixtures of PGP microbes that perform better than a single strain.

In this study, we used only joint data analysis to combine diverse datasets related to microbial strain properties. In the future, supervised data integration methods could be applied to combine greenhouse experiments and field trial data with PGP strain characterization data to improve the strain selection process.

Data availability statement

The raw data supporting the conclusions of this article will be made available by the authors, without undue reservation.

Author contributions

AD and SG designed the study. AD performed the experiments, assisted by SG and GM and wrote the first draft of the manuscript. AD and JT performed data analyses. MT, JT, SG, and GM read the first version of the manuscript. All authors contributed to the article and approved the submitted version.

Funding

This research was funded by the Department of Biotechnology, Ministry of Science and Technology, grant number BT/IN/Indo-US/Foldscope/39/2015; Department of Science and Technology, Science and Engineering Research Board, grant number EMR/2016/008061; and Estonian Research Council (grant numbers PRG548 and PRG916).

Acknowledgments

The authors thank the Department of Biotechnology, Foldscope Project (E28ACO), India; Department of Science and Technology, Science and Engineering Research Board (DST-SERB project E28ADI), New Delhi, India; Tamil Nadu Agricultural University, Coimbatore, India; ERDF Research Fund; and Estonian Research Council for providing financial support for this study.

Conflict of interest

The authors declare that the research was conducted in the absence of any commercial or financial relationships that could be construed as a potential conflict of interest.

Publisher's note

All claims expressed in this article are solely those of the authors and do not necessarily represent those of their affiliated organizations, or those of the publisher, the editors and the reviewers. Any product that may be evaluated in this article, or claim that may be made by its manufacturer, is not guaranteed or endorsed by the publisher.

Supplementary material

The Supplementary material for this article can be found online at: https://www.frontiersin.org/articles/10.3389/fmicb.2022.1058772/full#supplementary-material

References

Armada, E., Roldán, A., and Azcon, R. (2014). Differential activity of autochthonous bacteria in controlling drought stress in native Lavandula and salvia plants species under drought conditions in natural arid soil. *Microb. Ecol.* 67, 410–420. doi: 10.1007/s00248-013-0326-9

Arnow, L. E. (1937). Colorimetric determination of the components of 3, 4-dihydroxyphenylalanine-tyrosine mixtures. *J. Biol. Chem.* 118, 531–537. doi: 10.1016/S0021-9258(18)74509-2

Arun, K. D., Sabarinathan, K. G., Gomathy, M., Kannan, R., and Balachandar, D. (2020). Mitigation of drought stress in rice crop with plant growth-promoting abiotic stress-tolerant rice phyllosphere bacteria. *J. Basic Microbiol.* 60, 768–786. doi: 10.1002/jobm.202000011

Ashry, N. M., Alaidaroos, B. A., Mohamed, S. A., Badr, O. A., El-Saadony, M. T., and Esmael, A. (2022). Utilization of drought-tolerant bacterial strains isolated from harsh soils as a plant growth-promoting rhizobacteria (PGPR). *Saudi J. Biol. Sci.* 29, 1760–1769. doi: 10.1016/j.sjbs.2021.10.054

Ayuso-Calles, M., Flores-Félix, J. D., and Rivas, R. (2021). Overview of the role of rhizobacteria in plant salt stress tolerance. *Agronomy* 11:9. doi: 10.3390/agronomy11091759

Baliyan, N., Dhiman, S., Dheeman, S., Kumar, S., Arora, N. K., and Maheshwari, D. K. (2022). Optimization of gibberellic acid production in endophytic Bacillus cereus using response surface methodology and its use as plant growth regulator in chickpea. *J. Plant Growth Regul.* 41, 3019–3029. doi: 10.1007/s00344-021-10492-2

Belimov, A. A., Dodd, I. C., Safronova, V. I., Dumova, V. A., Shaposhnikov, A. I., Ladatko, A. G., et al. (2014). Abscisic acid metabolizing rhizobacteria decrease ABA concentrations in planta and alter plant growth. *Plant Physiol. Biochem.* 74, 84–91. doi: 10.1016/j.plaphy.2013.10.032

Bremer, E., and Krämer, R. (2019). Responses of microorganisms to osmotic stress. *Annu. Rev. Microbiol.* 73, 313–334. doi: 10.1146/annurev-micro-020518-115504

Cai, Z., Poulos, R. C., Liu, J., and Zhong, Q. (2022). Machine learning for multi-omics data integration in cancer. *iScience* 25:103798. doi: 10.1016/j.isci.2022.103798

Camargo, A. (2022). PCAtest: testing the statistical significance of principal component analysis in R. *PeerJ.* 10:e12967. doi: 10.7717/peerj.12967

Campbell, V., Legendre, P., and Lapointe, F. J. (2011). The performance of the congruence among distance matrices (CADM) test in phylogenetic analysis. *BMC Evol. Biol.* 11:64. doi: 10.1186/1471-2148-11-64

Cantini, L., Zakeri, P., Hernandez, C., Naldi, A., Thieffry, D., Remy, E., et al. (2021). Benchmarking joint multi-omics dimensionality reduction approaches for the study of cancer. *Nat. Commun.* 12:124. doi: 10.1038/s41467-020-20430-7

Cesar, S., Anjur-Dietrich, M., Yu, B., Li, E., Rojas, E., Neff, N., et al. (2020). Bacterial evolution in high-osmolarity environments. *MBio* 11, e01191–e01120. doi: 10.1128/mBio.01191-20

Chauhan, P. K., Upadhyay, S. K., Tripathi, M., Singh, R., Krishna, D., Singh, S. K., et al. (2022). Understanding the salinity stress on plant and developing sustainable management strategies mediated salt-tolerant plant growth-promoting rhizobacteria and CRISPR/Cas9. *Biotechnol. Genet. Eng. Rev.* 17, 1–37. doi: 10.1080/02648725.2022.2131958

da Costa, P. B. D., Granada, C. E., Ambrosini, A., Moreira, F., de Souza, R., dos Passos, J. F. M., et al. (2014). A model to explain plant growth promotion traits: a multivariate analysis of 2,211 bacterial isolates. *PLoS One* 9:e116020. doi: 10.1371/journal.pone.0116020

Deutch, C. E. (2019). L-proline catabolism by the high G+ C gram-positive bacterium Paenarthrobacter aurescens strain TC1. *Antonie Van Leeuwenhoek* 112, 237–251. doi: 10.1007/s10482-018-1148-z

Deva, C. R., Urban, M. O., Challinor, A. J., Falloon, P., and Svitákova, L. (2020). Enhanced leaf cooling is a pathway to heat tolerance in common bean. *Front. Plant Sci.* 11:19. doi: 10.3389/fpls.2020.00019

Devarajan, A. K., Muthukrishanan, G., Truu, J., Truu, M., Ostonen, I., Kizhaeral, S. S., et al. (2021). The foliar application of Rice phyllosphere bacteria induces drought-stress tolerance in Oryza sativa (L.). *Plants* 10:387. doi: 10.3390/plants10020387

Ding, L. J., Cui, H. L., Nie, S. A., Long, X. E., Duan, G. L., and Zhu, Y. G. (2019). Microbiomes inhabiting rice roots and rhizosphere. *FEMS Microbiol. Ecol.* 95:5. doi: 10.1093/femsec/fiz040

Egamberdieva, D., Wirth, S. J., Alqarawi, A. A., Abd Allah, E. F., and Hashem, A. (2017). Phytohormones and beneficial microbes: essential components for plants to balance stress and fitness. *Front. Microbiol.* 8:2104. doi: 10.3389/fmicb.2017.02104

Fadiji, A. E., Santoyo, G., Yadav, A. N., and Babalola, O. O. (2022). Efforts towards overcoming drought stress in crops: revisiting the mechanisms employed by plant growth-promoting bacteria. *Front. Microbiol.* 13:962427. doi: 10.3389/fmicb.2022.962427

FAO (2022). Crops and climate change impact briefs – climate-smart agriculture for more sustainable, resilient, and equitable food systems. Rome.

Ferreira, C. M. H., Vilas-Boas, Â., Sousa, C. A., Soares, H. M. V. M., and Soares, E. V. (2019). Comparison of five bacterial strains producing siderophores with ability to chelate iron under alkaline conditions. *AMB Express* 9:78. doi: 10.1186/s13568-019-0796-3

Fitzsimmons, L. F., Hampel, K. J., and Wargo, M. J. (2012). Cellular choline and glycine betaine pools impact osmoprotection and phospholipase C production in Pseudomonas aeruginosa. *J. Bacteriol.* 194, 4718–4726. doi: 10.1128/JB.00596-12

Gowdu, B. J., and Balasubramanian, R. (1988). Role of phylloplane micro-organisms in the biological control of foliar plant diseases. *J. Plant Dis. Prot.* 95, 310–331.

Hidangmayum, A., Dwivedi, P., Kumar, P., and Upadhyay, S. K. (2022). Seed priming and foliar application of chitosan ameliorate drought stress responses in Mungbean genotypes through modulation of Morpho-physiological attributes and increased Antioxidative defense mechanism. *J. Plant Growth Regul.* 1-18. doi: 10.1007/s00344-022-10792-1

Holbrook, A. A., Edge, W. J. W., and Bailey, F. (1961). Spectrophotometric method for determination of gibberellic acid. *Adv. Chemother.* 28, 159–167. doi: 10.1021/ba-1961-0028.ch018

Ilyas, N., Mumtaz, K., Akhtar, N., Yasmin, H., Sayyed, R. Z., Khan, W., et al. (2020). Exopolysaccharides producing bacteria for the amelioration of drought stress in wheat. *Sustain. For.* 12:8876. doi: 10.3390/su12218876

Islam, K. Z., and Nandi, B. (1985). Control of brown spot of rice by bacillus megaterium. *J. Plant Dis. Prot.* 92, 241–246.

Ji, S. H., Paul, N. C., Deng, J. X., Kim, Y. S., Yun, B. S., and Yu, S. H. (2013). Biocontrol activity of bacillus amyloliquefaciens CNU114001 against fungal plant diseases. *Mycobiology* 41, 234–242. doi: 10.5941/MYCO.2013.41.4.234

John, C. R., Watson, D., Barnes, M. R., Pitzalis, C., and Lewis, M. J. (2020). Spectrum: fast density-aware spectral clustering for single and multi-omic data. *Bioinformatics* 36, 1159–1166. doi: 10.1093/bioinformatics/btz704

Kang, S. M., Khan, A. L., Waqas, M., Asaf, S., Lee, K. E., Park, Y. G., et al. (2019). Integrated phytohormone production by the plant growth-promoting rhizobacterium bacillus tequilensis SSB07 induced thermotolerance in soybean. *J. Plant Interact.* 14, 416–423. doi: 10.1080/17429145.2019.1640294

Karadeniz, A., Topcuoğlu, Ş. F., and İnan, S. (2006). Auxin, gibberellin, cytokinin and abscisic acid production in some bacteria. *World J. Microbiol. Biotechnol.* 22, 1061–1064. doi: 10.1007/s11274-005-4561-1

Kaul, S., Sharma, T., and Dhar, K. M. (2016). 'Omics' tools for better understanding the plant–endophyte interactions. *Front. Plant Sci.* 7:955. doi: 10.3389/fpls.2016.00955

Kim, H., and Lee, Y. H. (2020). The rice microbiome: a model platform for crop holobiome. *Phytobiomes J.* 4, 5–18. doi: 10.1094/PBIOMES-07-19-0035-RVW

Kolde, R. (2019). pheatmap: Pretty Heatmaps. R package version 1. 0. 12. CRAN. Available at: https://cran.r-project.org/web/packages/pheatmap/index.html

Lahtvee, P. J., Seiman, A., Arike, L., Adamberg, K., and Vilu, R. (2014). Protein turnover forms one of the highest maintenance costs in Lactococcus lactis. *Microbiology* 160, 1501–1512. doi: 10.1099/mic.0.078089-0

Lê, S., Josse, J., and Husson, F. (2008). FactoMineR: an R package for multivariate analysis. *J. Stat. Softw.* 25, 1–18. doi: 10.18637/jss.v025.i01

Lee, Y. H., Jang, S. J., Han, J. H., Bae, J. S., Shin, H., Park, H. J., et al. (2018). Enhanced tolerance of Chinese cabbage seedlings mediated by *bacillus aryabhattai* H26-2 and B. siamensis H30-3 against high temperature stress and fungal infections. *Plant Pathol. J.* 34, 555–566. doi: 10.5423/PPJ.OA.07.2018.0130

Li, Y., Wu, F. X., and Ngom, A. (2018). A review on machine learning principles for multi-view biological data integration. *Brief. Bioinform.* 19, bbw113–bbw340. doi: 10.1093/BIB/BBW113

Liang, X., Zhang, L., Natarajan, S. K., and Becker, D. F. (2013). Proline mechanisms of stress survival. *Antioxid. Redox Signal.* 19, 998–1011. doi: 10.1089/ars.2012.5074

Mahmud, A. A., Upadhyay, S. K., Srivastava, A. K., and Bhojiya, A. A. (2021). Biofertilizers: a nexus between soil fertility and crop productivity under abiotic stress. *CRSUST* 3:100063. doi: 10.1016/j.crsust.2021.100063

Mariette, J., and Villa-Vialaneix, N. (2018). Unsupervised multiple kernel learning for heterogeneous data integration. *Bioinformatics* 34, 1009–1015. doi: 10.1093/bioinformatics/btx682

Mekureyaw, M. F., Pandey, C., Hennessy, R. C., Nicolaisen, M. H., Liu, F., Nybroe, O., et al. (2022). The cytokinin-producing plant beneficial bacterium Pseudomonas fluorescens G20-18 primes tomato (Solanum lycopersicum) for enhanced drought stress responses. *J. Plant Physiol.* 270:153629. doi: 10.1016/j.jplph.2022.153629

Meng, C., Kuster, B., Culhane, A. C., and Gholami, A. M. (2014). A multivariate approach to the integration of multi-omics datasets. *BMC Bioinform* 15:162. doi: 10.1186/1471-2105-15-162

Meudt, W. J., and Gaines, T. P. (1967). Studies on the oxidation of indole-3-acetic acid by peroxidase enzymes. I. Colorimetric determination of indole-3-acetic acid oxidation products. *Plant Physiol.* 42, 1395–1399. doi: 10.1104/pp.42.10.1395

Muthukumar, A., Raj, T. S., Prabhukarthikeyan, S. R., Kumar, R. N., and Keerthana, U. (2022). "Pseudomonas and bacillus: a biological tool for crop protection in New and Future Developments," in *Microbial Biotechnology and Bioengineering*. eds. H. B. Singh and A. Vaishnav (Elsevier), 145–158.

Nicholson, W. L., Munakata, N., Horneck, G., Melosh, H. J., and Setlow, P. (2000). Resistance of bacillus endospores to extreme terrestrial and extraterrestrial environments. *Microbiol. Mol. Biol. Rev.* 64, 548–572. doi: 10.1128/MMBR.64.3.548-572.2000

Nutaratat, P., Monprasit, A., and Srisuk, N. (2017). High-yield production of indole-3-acetic acid by Enterobacter sp. DMKU-RP206, a rice phyllosphere bacterium that possesses plant growth-promoting traits. *3 Biotech* 7:305. doi: 10.1007/s13205-017-0937-9

Onyango, L. A., and Alreshidi, M. M. (2018). Adaptive metabolism in staphylococci: survival and persistence in environmental and clinical settings. *J. Pathog.* 2018:1092632. doi: 10.1155/2018/1092632

Paradis, E., Claude, J., and Strimmer, K. (2004). APE: analyses of phylogenetics and evolution in R language. *Bioinformatics* 20, 289–290. doi: 10.1093/bioinformatics/btg412

Paul, S., Aggarwal, C., Thakur, J. K., Bandeppa, G. S., Khan, M., Pearson, L. M., et al. (2015). Induction of osmoadaptive mechanisms and modulation of cellular physiology help Bacillus licheniformis Strain SSA 61 adapt to salt stress. *Curr Microbiol.* 70, 610–617. doi: 10.1007/s00284-014-0761-y

Picard, M., Scott-Boyer, M. P., Bodein, A., Périn, O., and Droit, A. (2021). Integration strategies of multi-omics data for machine learning analysis. *Comput. Struct. Biotechnol. J.* 19, 3735–3746. doi: 10.1016/j.csbj.2021.06.030

Qurashi, A. W., and Sabri, A. N. (2013). Osmolyte accumulation in moderately halophilic bacteria improves salt tolerance of chickpea. *Pak. J. Bot.* 45, 1011–1016.

R Core Team (2013). R: A Language and Environment for Statistical Computing.

Ramakrishna, W., Yadav, R., and Li, K. (2019). Plant growth promoting bacteria in agriculture: two sides of a coin. *Appl. Soil Ecol.* 138, 10–18. doi: 10.1016/j.apsoil.2019.02.019

Remus-Emsermann, M. N., and Schlechter, R. O. (2018). Phyllosphere microbiology: at the interface between microbial individuals and the plant host. *New Phytol.* 218, 1327–1333. doi: 10.1111/NPH.15054

Sachdev, S., and Ansari, M. I. (2022). "Role of plant microbiome under stress environment to enhance crop productivity," in *Augmenting Crop Productivity in Stress Environment*. eds. S. A. Ansari, M. I. Ansari and A. Husen (Singapore: Springer), 205–221.

Saleem, M., Meckes, N., Pervaiz, Z. H., and Traw, M. B. (2017). Microbial interactions in the phyllosphere increase plant performance under herbivore biotic stress. *Front. Microbiol.* 8:41. doi: 10.3389/fmicb.2017.00041

Sandhu, N., Yadav, S., and Kumar, A. (2020). "Advances in developing multigene abiotic and biotic stress-tolerant rice varieties," in *Abiotic Stress in Plants. Vol. 1* eds. S. Fahad, S. Saud, Y. Chen, C. Wu and D. Wang (London, UK: INTECH Open Access Publishers), 1–20.

Santos, H., and Da Costa, M. S. (2002). Compatible solutes of organisms that live in hot saline environments. *Environ. Microbiol.* 4, 501–509. doi: 10.1046/j.1462-2920.2002.00335.x

Saxena, R., Kumar, M., and Tomar, R. S. (2021). "Plant–rhizobacteria interactions to induce biotic and abiotic stress tolerance in plants," in *Plant, Soil and Microbes*. eds. S. K. Dubey and S. K. Verma (Singapore: Springer), 1–18.

Sayyed, R. Z., Chincholkar, S. B., Reddy, M. S., Gangurde, N. S., and Patel, P. R. (2013). "Siderophore producing PGPR for crop nutrition and phytopathogen suppression," in *Bacteria in Agrobiology: Disease Management*. ed. S. D. Maheshwari (Berlin, Heidelberg: Springer), 449–471.

Schwyn, B., and Neilands, J. B. (1987). Universal chemical assay for the detection and determination of siderophores. *Anal. Biochem.* 160, 47–56. doi: 10.1016/0003-2697(87)90612-9

Sessitsch, A. N., Hardoim, P. A., Döring, J., Weilharter, A., Krause, A. N., Woyke, T. A., et al. (2012). Functional characteristics of an endophyte community colonizing rice roots as revealed by metagenomic analysis. *Mol. Plant-Microbe Interact.* 25, 28–36. doi: 10.1094/MPMI-08-11-0204

Setlow, P. (2014). Germination of spores of *bacillus* species: what we know and do not know. *J. Bacteriol.* 196, 1297–1305. doi: 10.1128/JB.01455-13

Shahzad, R., Khan, A. L., Bilal, S., Waqas, M., Kang, S. M., and Lee, I. J. (2017). Inoculation of abscisic acid-producing endophytic bacteria enhances salinity stress tolerance in Oryza sativa. *Environ. Exp. Bot.* 136, 68–77. doi: 10.1016/j.envexpbot.2017.01.010

Shinwari, Z. K., Tanveer, F., and Iqrar, I. (2019). "Role of microbes in plant health, disease management, and abiotic stress management," in *Microbiome in Plant Health and Disease*. eds. V. Kumar, R. Prasad, M. Kumar and D. Choudhary (Singapore: Springer), 231–250.

Shu, W. S., and Huang, L. N. (2022). Microbial diversity in extreme environments. *Nat. Rev. Microbiol.* 20, 219–235. doi: 10.1038/s41579-021-00648-y

Singh, P., Chauhan, P. K., Upadhyay, S. K., Singh, R. K., Dwivedi, P., Wang, J., et al. (2022). Mechanistic insights and potential use of siderophores producing microbes in rhizosphere for mitigation of stress in plants grown in degraded land. *Front. Microbiol.* 13:898979. doi: 10.3389/fmicb.2022.898979

Singh, A., Shannon, C. P., Gautier, B., Rohart, F., Vacher, M., Tebbutt, S. J., et al. (2019). Diablo: an integrative approach for identifying key molecular drivers from multi-omics assays. *Bioinformatics* 35, 3055–3062. doi: 10.1093/bioinformatics/bty1054

Sun, Z., Liu, K., Zhang, J., Zhang, Y., Xu, K., Yu, D., et al. (2017). IAA producing Bacillus altitudinis alleviates iron stress in *Triticum aestivum* L. seedling by both bioleaching of iron and up-regulation of genes encoding ferritins. *Plant Soil* 419, 1–11. doi: 10.1007/s11104-017-3218-9

Tempest, D. W., Meers, J. L., and Brown, C. M. (1970). Influence of environment on the content and composition of microbial free amino acid pools. *J. Gen. Microbiol.* 64, 171–185. doi: 10.1099/00221287-64-2-171

Tortora, G. J., Funke, B. R., and Case, C. L. (2019). *Microbiology: An Introduction 13th Edn*. Boston: Pearson Education.

Upadhyay, S. K., Singh, J. S., Saxena, A. K., and Singh, D. P. (2012). Impact of PGPR inoculation on growth and antioxidant status of wheat under saline conditions. *Plant Biol.* 14, 605–611. doi: 10.1111/j.1438-8677.2011.00533.x

Upadhyay, S. K., Singh, J. S., and Singh, D. P. (2011). Exopolysaccharide-producing plant growth-promoting rhizobacteria under salinity condition. *Pedosphere* 21, 214–222. doi: 10.1016/S1002-0160(11)60120-3

Uzma, M., Iqbal, A., and Hasnain, S. (2022). Drought tolerance induction and growth promotion by indole acetic acid producing Pseudomonas aeruginosa in Vigna radiata. *PLoS One* 17:e0262932. doi: 10.1371/journal.pone.0262932

Vahabi, N., and Michailidis, G. (2022). Unsupervised multi-omics data integration methods: a comprehensive review. *Front. Genet.* 13:560. doi: 10.3389/FGENE.2022.854752/BIBTEX

Varela, C. A., Baez, M. E., and Agosin, E. (2004). Osmotic stress response: quantification of cell maintenance and metabolic fluxes in a lysine-overproducing strain of *Corynebacterium glutamicum*. *Appl. Environ. Microbiol.* 70, 4222–4229. doi: 10.1128/AEM.70.7.4222-4229.2004

Vats, S. (ed.) (2018). *Biotic and Abiotic Stress Tolerance in Plants*. Cham, Switzerland: Springer

Vejan, P., Abdullah, R., Khadiran, T., Ismail, S., and Nasrulhaq Boyce, A. (2016). Role of plant growth promoting rhizobacteria in agricultural sustainability—a review. *Molecules* 21:573. doi: 10.3390/molecules21050573

Venkatachalam, S., Ranjan, K., Prasanna, R., Ramakrishnan, B., Thapa, S., and Kanchan, A. (2016). Diversity and functional traits of culturable microbiome members, including cyanobacteria in the rice phyllosphere. *Plant Biol.* 18, 627–637. doi: 10.1111/plb.12441

Vorholt, J. A. (2012). Microbial life in the phyllosphere. *Nat. Rev. Microbiol.* 10, 828–840. doi: 10.1038/nrmicro2910

Wei, G., Kloepper, J. W., and Tuzun, S. (1991). Induction of systemic resistance of cucumber to Colletotrichum orbiculare by select strains of plant growth-promoting rhizobacteria. *Phytopathology* 81, 1508–1512. doi: 10.1094/Phyto-81-1508

Xiang, R., Wang, W., Yang, L., Wang, S., Xu, C., and Chen, X. (2021). A comparison for dimensionality reduction methods of single-cell RNA-seq data. *Front. Genet.* 12:320. doi: 10.3389/FGENE.2021.646936/BIBTEX

Zampieri, G., Vijayakumar, S., Yaneske, E., and Angione, C. (2019). Machine and deep learning meet genome-scale metabolic modeling. *PLoS Comput. Biol.* 15:e1007084. doi: 10.1371/JOURNAL.PCBI.1007084

Zerrouk, I. Z., Rahmoune, B., Auer, S., Rößler, S., Lin, T., Baluska, F., et al. (2020). Growth and aluminum tolerance of maize roots mediated by auxin-and cytokinin-producing bacillus toyonensis requires polar auxin transport. *Environ. Exp. Bot.* 176:104064. doi: 10.1016/j.envexpbot.2020.104064

Zhao, J., Xie, X., Xu, X., and Sun, S. (2017). Multi-view learning overview: recent progress and new challenges. *Inf. Fusion.* 38, 43–54. doi: 10.1016/J.INFFUS.2017.02.007

frontiers | Frontiers in Microbiology

TYPE Mini Review
PUBLISHED 21 December 2022
DOI 10.3389/fmicb.2022.1069053

Check for updates

OPEN ACCESS

EDITED BY
José David Flores Félix,
Universidade da Beira Interior, Portugal

REVIEWED BY
Everlon Cid Rigobelo,
São Paulo State University, Brazil

*CORRESPONDENCE
Jakub Dobrzyński
✉ j.dobrzynski@itp.edu.pl

SPECIALTY SECTION
This article was submitted to Microbe and Virus Interactions with Plants, a section of the journal Frontiers in Microbiology

RECEIVED 13 October 2022
ACCEPTED 30 November 2022
PUBLISHED 21 December 2022

CITATION
Dobrzyński J, Jakubowska Z and Dybek B (2022) Potential of *Bacillus pumilus* to directly promote plant growth. *Front. Microbiol.* 13:1069053. doi: 10.3389/fmicb.2022.1069053

COPYRIGHT
© 2022 Dobrzyński, Jakubowska and Dybek. This is an open-access article distributed under the terms of the Creative Commons Attribution License (CC BY). The use, distribution or reproduction in other forums is permitted, provided the original author(s) and the copyright owner(s) are credited and that the original publication in this journal is cited, in accordance with accepted academic practice. No use, distribution or reproduction is permitted which does not comply with these terms.

Potential of *Bacillus pumilus* to directly promote plant growth

Jakub Dobrzyński*, Zuzanna Jakubowska and Barbara Dybek

Institute of Technology and Life Sciences—National Research Institute, Falenty, Poland

Plant Growth-Promoting Bacteria (PGPB) are a promising alternative to conventional fertilization. One of the most interesting PGPB strains, among the spore-forming bacteria of the phylum Firmicutes, is *Bacillus pumilus*. It is a bacterial species that inhabits a wide range of environments and shows resistance to abiotic stresses. So far, several PGPB strains of *B. pumilus* have been described, including *B. pumilus* LZP02, *B. pumilus* JPVS11, *B. pumilus* TUAT-1, *B. pumilus* TRS-3, and *B. pumilus* EU927414. These strains have been shown to produce a wide range of phytohormones and other plant growth-promoting substances. Therefore, they can affect various plant properties, including biometric traits, substance content (amino acids, proteins, fatty acids), and oxidative enzymes. Importantly, based on a study with *B. pumilus* WP8, it can be concluded that this bacterial species stimulates plant growth when the native microbiota of the inoculated soil is altered. However, there is still a lack of research with deeper insights into the structure of the native microbial community (after *B. pumilus* application), which would provide a better understanding of the functioning of this bacterial species in the soil and thus increase its effectiveness in promoting plant growth.

KEYWORDS

spore-forming bacteria, plant growth stimulation, phytohormones, sustainable agriculture, eco-friendly, soil microbiota

Introduction

Bacillus pumilus is a Gram-positive, spore-forming bacteria, which commonly occurs in various environments including marine water, deep-sea sediments, and soil (Priest, 1993; Shivaji et al., 2006; Liu et al., 2013; Pudova et al., 2022; Yakovleva et al., 2022; Zhang et al., 2022). This species exhibits significant resistance to environmental stresses, e.g., low or no nutrient availability, drought, irradiation, UV radiation, chemical disinfectants, or oxidizing enzymes (Nicholson et al., 2000). Previously, *Bacillus pumilus* was included in the *Bacillus subtilis* group. Currently, *Bacillus pumilus* belongs to the *Bacillus pumilus* group which also includes *B. altitudinis, B. australimaris, B. safensis, B. xiamenensis,* and *B. zhangzhouensis* (Chen et al., 2016).

Progressive climate change and environmental pollution are intensifying the development of eco-friendly fertilizers (Čimo et al., 2020; Dobrzyński et al., 2021; Kasperska-Wołowicz et al., 2021; Wierzchowski et al., 2021; Zielewicz et al., 2021; Heyi et al., 2022). One of the best solutions for safe fertilization appears to be fertilizers based on plant

growth-promoting bacteria (Čimo et al., 2020). Due to its properties, *Bacillus pumilus* is classified as a plant growth-promoting bacteria (PGPB; Gutiérrez-Mañero et al., 2001; De-Bashan et al., 2010; Kaushal et al., 2017). PGPB can stimulate plant growth either directly or indirectly. Mechanisms of direct action are defined as the use of bacterial traits that result in the direct promotion of plant growth, including the production of auxins, e.g., indole-3-acetic acid (IAA), 1-aminocyclopropane-1-carboxylic acid (ACC) deaminase, cytokinins, gibberellins, atmospheric nitrogen fixation (nitrogenase production), phosphorus solubilization, and iron sequestration (by production bacterial siderophores). In contrast, indirect mechanisms relate to the properties of bacteria that inhibit the functioning of one or more plant pathogenic organisms. Indirect mechanisms include, e.g., the production of antibiotics (e.g., cyclic lipopeptides), enzymes that degrade the cell wall of fungi (including chitinases and β-1,3 glucanases), and production of hydrogen cyanide (HCN) inducing plant resistance (e.g., against fungal phytopathogens; Joo et al., 2005; Cuong and Hoa, 2021; Lipková et al., 2021; Shahid et al., 2021; Bessai et al., 2022; Mirskaya et al., 2022)

The mini-review aims to summarize the current state of knowledge on the *Bacillus pumilus* plant growth promotion properties and highlight the lack in the literature on this issue.

Overall potential of *Bacillus pumilus*

Bacillus pumilus is one of the most studied bacterial strains in terms of promoting the growth of bacteria from the genus *Bacillus*. So far, it has been found that *B. pumilus* is capable of producing several phytohormones. Gutiérrez-Mañero et al. (2001) detected a few gibberellins (GA1, GA3, GA4, and GA20) in the culture of *B. pumilus* using full-scan gas chromatography and mass spectrometry assays. Joo et al. (2005) found other gibberellins derived from this species (strain no. CJ-69), including a few new ones such as GA5, GA8, GA34, GA44, and GA5. *B. pumilus* is also able to produce other traits that directly promote plant growth. Isolated from the tea rhizosphere, *B. pumilus* TRS-3 showed the production of indole 3-acetic acid (IAA), siderophore, and phosphate solubilization (Chakraborty et al., 2013). Besides, *B. pumilus* JPVS11 is capable of producing ACC deaminase which contributes to decreasing ethylene levels in the plants by degrading ACC (Kumar et al., 2021). Importantly, *B. pumilus* is also capable of fixing atmospheric N_2 by nitrogenase production which reduces this nitrogen form to ammonia (Masood et al., 2020). Other authors also detected these plant growth-promoting traits in *B. pumilus* (Hafeez et al., 2006; Murugappan et al., 2013; Upadhyay et al., 2019).

Promoting plant growth under different growing conditions

To date, several papers have been published on the effect of various *B. pumilus* strains on plant growth parameters. The inoculation efficiency of *B. pumilus* was studied in various conditions including *in vitro*, growth chambers, greenhouses, and in-field conditions. A lot of these studies focus on rice growth promotion and deal mainly with biometric parameters and chemical properties of shoots and roots (Win et al., 2018; Ngo et al., 2019; Liu et al., 2020) Importantly, both commercial strains and soil isolates are used to study on the effects of bacteria on the efficiency in promoting plant growth.

The research based on growing plants on Murashige and Skoog liquid medium has proven that the strain *B. pumilus* LZP02 is able to promote rice growth by increasing the root length, root surface area, number of nodes, root tips, forks, and chlorophyll content (Liu et al., 2020). In addition, the application of *B. pumilus* LZP02 also caused an increase in nitrogen, phosphorus, calcium, and magnesium contents in rice roots (Liu et al., 2020). Previously, it was proven that *B. pumilus* promotes rice growth under growth chamber conditions (Ngo et al., 2019) *B. pumilus* TUAT1 significantly enhanced growth, root development, and nutrient absorption in 21-day-old rice seedlings compared to the control. Interestingly, significantly better efficiency of the studied strain was obtained after inoculating plants with spores than vegetative cells (Ngo et al., 2019).

As well, it has been reported that *B. pumilus* may be a good growth promoter of other plants, including grasses, trees, and others. For instance, after the application of *B. pumilus* of *Alnus glutinosa*, higher values of parameters linked with root system (in both studied soil types) and an increase in shoot surface (in one of the studied soil types) was documented compared to control (Ramos et al., 2003). Subsequently, the application of *B. pumilus* caused an increase in plant height, number of leaves and branches in Chinese tea under *in vivo* conditions (Chakraborty et al., 2013). Moreover, after inoculation of lentils (*Lens culinaris* Medik.) by *B. pumilus*, Siddiqui et al. (2007) noted an increase in plant length and plant fresh weight. Ahmad et al. (2012) also noted that inoculation *B. pumilus* of *Lollium multiflorum* led to increased biomass and growth of plants. Inoculation of wheat (var. Orkhon) by *B. pumilus* led to increasing root length, root area, shoot dry weight, and P and N contents in aboveground plants (Hafeez et al., 2006).

Interestingly, *B. pumilus* can also be an endophytic bacteria. This species was isolated from tissue surfaces of *Ocimum sanctum* and its ability to colonize tissues was confirmed by scanning electron microscopy (SEM; Murugappan et al., 2013). Importantly, the inoculation of *Octimum sanctum* by this species also caused an increase in root and shoot length and leaves number compared to non-inoculated treatment (Murugappan et al., 2013).

Recently it has been suggested that *B. pumilus* promotes plant growth better in combination with nitrogen fertilizers (Win et al., 2018; Masood et al., 2020). Strain *B. pumilus* TUAT-1 with added nitrogen fertilization increased the height, biomass, and chlorophyll content of 21-day-old rice seedlings); (what is important, this study was conducted under field conditions (Win et al., 2018). Next, Masood et al. (2020) carried out a study to determine the main mechanisms relating to PGPB-improved N nutrition in tomatoes under greenhouse conditions. The authors

recorded an interesting pattern, namely *B. pumilus* improves tomato growth and N uptake only under N fertilization. Moreover, *B. pumilus* inoculation under nitrogen fertilization increased leaf chlorophyll contents, plant height, shoot fresh weight, and shoot dry weight in comparison with only bacteria inoculation treatment.

It was also documented that *Bacillus pumilus* is able to enhance the activity of a few antioxidant enzymes from the oxidoreductase class, including peroxidase, ascorbate peroxidase, superoxide dismutase, catalase, glutathione reductase, and adenosine triphosphatase in inoculated plants (Liu et al., 2020); (Shahzad et al., 2021). Besides, *B. pumilus* may cause an increase in soil enzyme activity such as alkaline phosphatase, acid phosphatase, urease, and β-glucosidase (Kumar et al., 2021).

Promoting plant growth under plant stress conditions

Bacillus pumilus has also been shown to promote plant growth under abiotic stress conditions (Kumar et al., 2021; Shahzad et al., 2021). Recently, it was found that *B. pumilus* can promote plant growth under salinity stress (Kumar et al., 2021). Positive effects of rice inoculation by *B. pumilus* JPVS11 (pot experiment) such as the enhancement of plant height, root length, and plant fresh weight were observed at the various values of NaCl concentration (0, 50, 100, 200, and 300 mM). Furthermore, *B. pumilus* also may promote plant growth in conditions of Cd contamination; maize seeds inoculation with *B. pumilus* contributed to an increase in the germination percentage, shoot length, leaf length, number of leaves, and plant fresh weight at different concentrations of $CdSO_4$ (Shahzad et al., 2021). In addition, Khan et al. (2016) conducted a study on plant growth-promoting properties of rice seedlings by *B. pumilus* under saline and high boron (B) conditions. In non-inoculated treatment, they observed high values of B and salt toxic ions in leaves. On the other hand, there are also studies that show the lack of plant growth promotion by *B. pumilus* under abiotic stress conditions. This phenomenon was found in a study on several plants of the *Brassica genus* under caesium-contaminated conditions (Aung et al., 2015).

Mechanisms of promoting plant growth

Importantly, inoculation of plants by *B. pumilus* may affect the expression of genes related to root development, for instance, this bacteria increased transcript abundance CRL5 (Murugappan et al., 2013), which regulates crown root formation by expression activation of the OsRR1. It is a gene of rice which encodes a negative regulator of cytokinin signaling (Radhakrishnan et al., 2017). Moreover, *B. pumilus* may decrease transcript abundance WOX11 (Ngo et al., 2019), which contributes to the repression of OsRR2 (Cheng et al., 2016). This fact indicates that the impact of *B. pumilus* on the expression of previously mentioned rice genes may be one of its mechanisms of plant growth promotion (Ngo et al., 2019).

Plant growth promotion by *Bacillus pumilus* in co-inoculation

There are also results describing the potential to promote plant growth in consortia with other microorganisms. A consortium composed of *B. pumilus* EU927414, *Pseudomonas medicona* EU927412, and *Arthrobacter* sp. EU927410 led to a 24% increase in wheat yield compared to the control under field conditions (Upadhyay et al., 2019). In addition, it has been documented that the application of the consortium of *B. pumilus* and *Bacillus subtilis* increased values of crude protein, dry matter, fat, and carbohydrate in amaranth grains. Besides, in this study, a significant increase in a few amino acid values including methionine lysine and tryptophan was recorded in the studied sample (Pandey et al., 2018). Also dos Santos et al. (2018) used a combined application of *B. pumilus* and *B. subtilis,* however, in sugarcane cultivation. There, together with mineral fertilization and filter cake compost, the solution improved shoot and root growth, as well as increased phosphorus content in soil up to 13% compared to untreated control. Another example of co-inoculation is the application of *B. pumilus* CECT 5105 in combination with *Bacillus licheniformis* CECT 5106 and mycorrhizal fungus *Pisolithus tinctorius* to enhance *Pinus pinea* seedlings growth (Probanza et al., 2001). In this study, authors did not observe a synergic effect with mycorrhizal infection, however, the inoculation by various consortiums showed an increase in a few biometric parameters of the studied plant. For example, *B. pumilus* and *Pisolithus tinctorius* combination led to an increase in aerial and root system parameters.

Effect of *Bacillus pumilus* on native soil microbiota and post-inoculation tracking of its abundance

A very important aspect related to the application of PGPB is their impact on the indigenous microbiota of the inoculated soil or rhizosphere. Assessing the impact of plant growth-promoting bacteria on the soil microbiota can be crucial to its effectiveness. So far, there are several papers considering the *B. pumilus* effect on the formation of native microbial communities. For instance, (De-Bashan et al., 2010) revealed that inoculation with *B. pumilus* may shift the bacterial community over 60 days under greenhouse conditions and documented that *B. pumilus* prefers to colonize the roots tips and root elongation area (FISH analysis). Besides, using denaturing gradient gel electrophoresis (PCR-DGGE), Kang et al. (2013) conducted a study on the reaction of soil bacterial community soil under fava beans to *B. pumilus* WP8 and its post-inoculation monitoring in soil. Their results indicated that the studied strain survived in large numbers up to 40 days in bulk soil and shifted the bacterial community, especially dominant taxon populations. However, despite the short-lived studied strain in soil, it exhibits the ability to promote fava bean seedlings for at least 90 days; the inoculation of *B. pumilus* WP8 enhanced shoot length, aboveground dry weight, root length, and root dry weight.

Interestingly, in the case of another *Bacillus* strain, *Bacillus amyloliquefaciens* NJN-6, using the qPCR technique, (Fu et al., 2017) recorded its stable abundance in the rhizosphere soil of banana plantation within 3 years of inoculation (in the range of 2.5–3.0 log copies of 16S rRNA gene per gram of soil). Also, it is worth mentioning that the survival rate of bacterial inoculants in the soil largely depends on the indigenous soil microbiota; the survival of PGPB in the soil is high when the diversity of native microbiota is low and vice versa (Mallon et al., 2015; Manfredini et al., 2021). In addition, (Bueno et al., 2022) carried out an interesting study on the persistence of *B. subtilis* in the endosphere of soybean roots, showing that after the application of concentrations of 1×10^4 CFU ml^{-1} and 1×10^{10} ml^{-1}, a higher abundance of this strain was recorded a few weeks after inoculation compared to *B. subtilis* abundance in treatment: *B. subtilis* + mineral fertilization (the study based on transformed *B. subtilis* with ampicillin resistance gene).

The PLFA (phospholipid fatty acid) technique was also used to assess the response of native soil microbiota to *B. pumilus* application. The introduction of a consortium composed of *B. pumilus* and *B. licheniformis* shifted the rhizosphere microbiota, despite the low abundance of both strains in the final phase of the study (Probanza et al., 2001). Another example of using PLFA to evaluate native microbiota reaction to *B. pumilus* inoculation is a study conducted by (Ramos et al., 2003). The authors observed changes in the rhizosphere microbial community in one of the studied soil types from *Alnus glutinosa* cultivation (Ramos et al., 2003).

The only study assessing the status of the native microbiota following the application of *B. pumilus* (strain TUAT-1) was conducted by (Win et al., 2020) using Next-Generation Sequencing (NGS). The researchers studied *B. pumilus* TUAT-1 effect on the microbiota of bulk soil, rhizosphere, and root endosphere in forage rice 2 and 5 weeks after transplantation under greenhouse conditions. *B. pumilus* TUAT-1 shifted the microbial community of rhizosphere and roots endosphere, e.g., this bacterial strain significantly contributed to an increase in the Desulfuromonadales abundance and a decrease of the abundance of Xanthomonadales 5 weeks after transplantation of rice. While in the bacterial community of root endosphere, *B. pumilus* TUAT-1 significantly enhanced the relative abundance of Acidobacteriales, Saprospirales, and Alteromonadales 2 weeks after transplanting in comparison with control treatment. However, in bulk soil, the author did not note such a significant alteration in native microbiota after the introduction of the above-mentioned PGPB. Moreover, compared to the control, *B. pumilus* TUAT-1 enhanced bacterial biodiversity, including Shannon diversity in the rhizosphere and root endosphere 2 weeks after transplanting. Importantly, using qPCR techniques, the researchers also demonstrated that *B. pumilus* TUAT-1 persisted in the rhizosphere soil 2 and 5 weeks after transplanting of rice (Win et al., 2020). Different patterns after the introduction of *B. subtilis* into the soil were noted by dos (Dos Santos et al., 2022). The authors showed that *B. subtilis* application did not affect the root endophytic microbial community of soybean (greenhouse conditions), which was also evaluated by alpha diversity metrics. Importantly, it is still unclear whether the PGPB effect on native microbiota can be long-term. This phenomenon may depend on many factors, including the soil's chemical properties, the stage of plant development, plant root exudates, or indeed the biodiversity and composition of the native microbial community. Hence, there is a need for further studies on the effects of PGPB on indigenous endophytic microbiota and soil microbiota, both for *B. pumilus* and other strains of the *Bacillus* genus (Manfredini et al., 2021).

Conclusion

Bacillus pumilus is a very interesting PGPB strain that has already been incorporated into the commercial circuit. Despite that, there are deficiencies in the literature in several areas. There is still a lot to be understood about the reaction of various plants to the inoculation of *B. pumilus*. The need for further research in this field is determined by the specificity of the plant rhizosphere microbiome, which can interact differently with *B. pumilus* strains and vice versa. In addition, it is vital to test the effectiveness of this bacterium on different soil types with different physicochemical properties. Importantly, there is a very small number of studies assessing the impact of *B. pumilus* on the native microbiota using NGS (only one paper to date). NGS offers the possibility of a more detailed analysis of the bacterial community structure than DGGE or PLFA. Hence, it is possible to find the abundance of important taxa involved in biochemical changes in the soil. e.g. whether the abundance of oligotrophic bacteria, including Acidobacteria, decreased after inoculation with the *B. pumilus* strain. Also, in order to test the effect of alterations in the native microbiota under the influence of PGPB, studies of this type should be conducted over a long period of time (even up to several years) and under field conditions. Finally, it is worth mentioning that there is also a lack of studies on the tracking of *B. pumilus* strains in soil (bulk and rhizosphere soil) or plant tissues after its introduction, especially in the long term aspect.

Author contributions

JD contributed to conception of the minireview. JD, ZJ, and BD wrote the first draft of the manuscript. All authors contributed to manuscript revision, read, and approved the submitted version.

Acknowledgments

Many thanks to Katarzyna Rafalska for English proofreading.

Conflict of interest

The authors declare that the research was conducted in the absence of any commercial or financial relationships that could be construed as a potential conflict of interest.

Publisher's note

All claims expressed in this article are solely those of the authors and do not necessarily represent those of their affiliated organizations, or those of the publisher, the editors and the reviewers. Any product that may be evaluated in this article, or claim that may be made by its manufacturer, is not guaranteed or endorsed by the publisher.

References

Ahmad, F., Iqbal, S., Anwar, S., Afzal, M., Islam, E., Mustafa, T., et al. (2012). Enhanced remediation of chlorpyrifos from soil using ryegrass (*Lollium multiflorum*) and chlorpyrifos-degrading bacterium *Bacillus pumilus* C2A1. *J. Hazard. Mater. Lett.* 237-238, 110–115. doi: 10.1016/j.jhazmat.2012.08.006

Aung, H. P., Djedidi, S., Oo, A. Z., Aye, Y. S., Yokoyama, T., Suzuki, S., et al. (2015). Growth and 137Cs uptake of four *brassica species* influenced by inoculation with a plant growth-promoting rhizobacterium *Bacillus pumilus* in three contaminated farmlands in Fukushima prefecture. *Japan. Sci. Total. Environ.* 521-522, 261–269. doi: 10.1016/j.scitotenv.2015.03.109

Bessai, S. A., Bensidhoum, L., and Nabti, E. H. (2022). Optimization of IAA production by telluric bacteria isolated from northern Algeria. *Biocatal. Agric. Biotechnol.* 41:102319. doi: 10.1016/j.bcab.2022.102319

Bueno, C. B., Dos Santos, R. M., de Souza Buzo, F., and Rigobelo, E. C. (2022). Effects of chemical fertilization and microbial inoculum on Bacillus subtilis colonization in soybean and maize plants. *Front. Microbiol.* 13:901157. doi: 10.3389/fmicb.2022.901157

Chakraborty, U., Chakraborty, B. N., and Roychowdhury, P. (2013). Plant growth promoting activity of *Bacillus pumilus* in tea (*Camellia sinensis*) and its biocontrol potential against *Poria hypobrunnea*. *Indian. Phytopathol.* 66, 387–396.

Chen, L., Liu, Y., Wu, G., Veronican Njeri, K., Shen, Q., Zhang, N., et al. (2016). Induced maize salt tolerance by rhizosphere inoculation of bacillus amyloliquefaciens SQR9. *Physiol. Plant.* 158, 34–44. doi: 10.1111/ppl.12441

Cheng, S., Zhou, D. X., and Zhao, Y. (2016). WUSCHEL-related homeobox gene WOX11 increases rice drought resistance by controlling root hair formation and root system development. *Plant Signal. Behav.* 11:e1130198. doi: 10.1080/15592324.2015.1130198

Čimo, J., Šinka, K., Tárník, A., Aydin, E., Kišš, V., and Toková, L. (2020). Impact of climate change on vegetation period of basic species of vegetables in Slovakia. *J. Water Land Dev.* 47, 38–46. doi: 10.24425/jwld.2020.135030

Cuong, P. V., and Hoa, N. P. (2021). Optimization of culture condition for iaa roduction by *Bacillus* sp. isolated from cassava field of Vietnam. *Vietnam. J. Sci. Technol.* 59, 312–323. doi: 10.15625/2525-2518/59/3/15600

De-Bashan, L. E., Hernandez, J. P., Bashan, Y., and Maier, R. M. (2010). *Bacillus pumilus* ES4: candidate plant growth-promoting bacterium to enhance establishment of plants in mine tailings. *Environ. Exp. Bot.* 69, 343–352. doi: 10.1016/j.envexpbot.2010.04.014

Dobrzyński, J., Wierzchowski, P. S., Stępień, W., and Górska, E. B. (2021). The reaction of cellulolytic and potentially cellulolytic spore-forming bacteria to various types of crop management and farmyard manure fertilization in bulk soil. *Agronomy* 11:772. doi: 10.3390/agronomy11040772

Dos Santos, R. M., Cueva-Yesquén, L. G., Garboggini, F. F., Desoignies, N., and Rigobelo, E. C. (2022). Inoculum concentration and mineral fertilization: effects on the endophytic microbiome of soybean. *Front. Microbiol.* 13:900980. doi: 10.3389/fmicb.2022.900980

Dos Santos, R. M., Kandasamy, S., and Rigobelo, E. C. (2018). Sugarcane growth and nutrition levels are differentially affected by the application of PGPR and cane waste. *MicrobiologyOpen.* 7:e00617. doi: 10.1002/mbo3.617

Fu, L., Penton, C. R., Ruan, Y., Shen, Z., Xue, C., Li, R., et al. (2017). Inducing the rhizosphere microbiome by biofertilizer application to suppress banana Fusarium wilt disease. *Soil Biol. Biochem.* 104, 39–48. doi: 10.1016/j.soilbio. 2016.10.008

Gutiérrez-Mañero, F. J., Ramos-Solano, B., Probanza, A. N., Mehouachi, J., R. Tadeo, F., and Talon, M. (2001). The plant-growth-*promoting* rhizobacteria *Bacillus pumilus* and *bacillus licheniformis* produce high amounts of physiologically active gibberellins. *Physiol. Plan.* 111, 206–211. doi: 10.1034/j.1399-3054.2001.1110211.x

Hafeez, F. Y., Yasmin,S., Ariani, D., Renseigné, N., Zafar, Y., and Malik, K. A. (2006). Plant growth-promoting bacteria as biofertilizer. *Agron. Sustain. Dev.* 26, 143–150. doi: 10.1051/agro:2006007

Heyi, E. A., Dinka, M. O., and Mamo, G. (2022). Assessing the impact of climate change on water resources of upper Awash River sub-basin. *Ethiopia. J. Water Land Dev.* 52, 232–244. doi: 10.24425/jwld.2022.140394

Joo, G. J., Kim, Y. M., Kim, J. T., Rhee, I. K., Kim, J. H., and Lee, I. J. (2005). Gibberellins-producing rhizobacteria increase endogenous gibberellins content and promote growth of red peppers. *J. Microbiol.* 43, 510–515.

Kang, Y., Shen, M., Wang, H., and Zhao, Q. (2013). A possible mechanism of action of plant growth-promoting rhizobacteria (PGPR) strain *Bacillus pumilus* WP8 via regulation of soil bacterial community structure. *J. Gen. Appl. Microbiol.* 59, 267–277. doi: 10.2323/jgam.59.267

Kasperska-Wołowicz, W., Rolbiecki, S., Sadan, H. A., Rolbiecki, R., Jagosz, B., Stachowski, P., et al. (2021). Impact of the projected climate change on soybean water needs in the Kuyavia region in Poland. *J. Water. Land. Dev.* 51, 199–207. doi: 10.24425/jwld.2021.139031

Kaushal, M., Kumar, A., and Kaushal, R. (2017). *Bacillus pumilus* strain YSPMK11 as plant growth promoter and biocontrol agent against *Sclerotinia sclerotiorum*. *3 Biotech* 7, 90–99. doi: 10.1007/s13205-017-0732-7

Khan, A., Zhao, X. Q., Javed, M. T., Khan, K. S., Bano, A., Shen, R. F., et al. (2016). *Bacillus pumilus enhances* tolerance in rice (*Oryza sativa* L.) to combined stresses of NaCl and high boron due to limited uptake of Na+. *Environ. Exp. Bot.* 124, 120–129. doi: 10.1016/j.envexpbot.2015.12.011

Kumar, A., Singh, S., Mukherjee, A., Rastogi, R. P., and Verma, J. P. (2021). Salt-tolerant plant growth-promoting *Bacillus pumilus* strain JPVS11 to enhance plant growth attributes of rice and improve soil health under salinity stress. *Microbiol. Res.* 242:126616. doi: 10.1016/j.micres.2020.126616

Lipková, N., Cinkocki, R., Maková, J., Medo, J., and Javoreková, S. (2021). Characterization of endophytic bacteria of the genus bacillus and their influence on the growth of maize (*Zea mays*) in vivo. *J. Microbiol. Biotechnol. Food Sci.* 10:e3602. doi: 10.15414/jmbfs.3602

Liu, Y., Lai, Q., Dong, C., Sun, F., Wang, L., Li, G., et al. (2013). Phylogenetic diversity of the *Bacillus pumilus* group and the marine ecotype revealed by multilocus sequence analysis. *PLoS One* 8:e80097. doi: 10.1371/journal.pone.0080097

Liu, H., Wang, Z., Xu, W., Zeng, J., Li, L., Li, S., et al. (2020). *Bacillus pumilus* LZP02 promotes rice root growth by improving carbohydrate metabolism and phenylpropanoid biosynthesis. *Mol. Plant-Microbe Interact.* 33, 1222–1231. doi: 10.1094/MPMI-04-20-0106-R

Mallon, C., Poly, F., Le Roux, X., Marring, I., van Elsas, J. D., and Salles, J. F. (2015). Resource pulses can alleviate the biodiversity – invasion relationship in soil microbial communities. *Ecology* 96, 915–926. doi: 10.1890/14-1001.1

Manfredini, A., Malusà, E., Costa, C., Pallottino, F., Mocali, S., Pinzari, F., et al. (2021). Current methods, common practices, and perspectives in tracking and monitoring bioinoculants in soil. *Front. Microbiol.* 12:698491. doi: 10.3389/fmicb.2021.698491

Masood, S., Zhao, X. Q., and Shen, R. F. (2020). *Bacillus pumilus* promotes the growth and nitrogen uptake of tomato plants under nitrogen fertilization. *Sci. Hortic.* 272:109581. doi: 10.1016/j.scienta.2020.109581

Mirskaya, G. V., Khomyakov, Y. V., Rushina, N. A., Vertebny, V. E., Chizhevskaya, E. P., Chebotar, V. K., et al. (2022). Plant development of early-maturing spring wheat (*Triticum aestivum* L.) under inoculation with *bacillus* sp. V2026. *Plan. Theory* 11:1817. doi: 10.3390/plants11141817

Murugappan, R. M., Begum, S. B., and Roobia, R. R. (2013). Symbiotic influence of endophytic *Bacillus pumilus* on growth promotion and probiotic potential of the medicinal plant Ocimum sanctum. *Symbiosis* 60, 91–99. doi: 10.1007/s13199-013-0244-0

Ngo, N. P., Yamada, T., Higuma, S., Ueno, N., Saito, K., Kojima, K., et al. (2019). Spore inoculation of *Bacillus pumilus* TUAT1 strain, a biofertilizer microorganism, enhances seedling growth by promoting root system development in rice. *Soil Sci. Plant Nutr.* 65, 598–604. doi: 10.1080/00380768.2019.1689795

Nicholson, W. L., Munakata, N., Horneck, G., Melosh, H. J., and Setlow, P. (2000). Resistance of *bacillus* endospores to extreme terrestrial and extraterrestrial environments. *Mol. Biol. Rev.* 64, 548–572. doi: 10.1128/MMBR.64.3.548-572.2000

Pandey, C., Bajpai, V. K., Negi, Y. K., Rather, I. A., and Maheshwari, D. K. (2018). Effect of plant growth promoting *bacillus* spp. on nutritional properties of *Amaranthus hypochondriacus* grains. *Saudi J. Biol. Sci.* 25, 1066–1071. doi: 10.1016/j.sjbs.2018.03.003

Priest, F. G. (1993). "Systematics and ecology of *bacillus*", in *Bacillus subtilis and Other Gram-Positive Bacteria*. eds. A. L. Sonenshein, J. A. Hoch and R. Losick (Washington, DC: American Society for Microbiology Press). 1–16.

Probanza, A., Mateos, J. L., Lucas Garcia, J. A., Ramos, B., De Felipe, M. R., and Gutierrez Manero, F. J. (2001). Effects of inoculation with PGPR *bacillus* and *Pisolithus tinctorius* on *Pinus pinea* L. growth, bacterial rhizosphere colonization, and mycorrhizal infection. *Microb. Ecol.* 41, 140–148. doi: 10.1007/s00248000008

Pudova, D. S., Toymentseva, A. A., Gogoleva, N. E., Shagimardanova, E. I., Mardanova, A. M., and Sharipova, M. R. (2022). Comparative genome analysis of two *Bacillus pumilus* strains producing high level of extracellular hydrolases. *Genes.* 13:409. doi: 10.3390/genes13030409

Radhakrishnan, R., Hashem, A., and Abd Allah, E. F. (2017). *Bacillus*: a biological tool for crop improvement through bio-molecular changes in adverse environments. *Front. Physiol.* 8, 1–14. doi: 10.3389/fphys.2017.00667

Ramos, B., Lucas García, J. A., Probanza, A., Domenech, J., and Javier Gutierrez Mañero, F. (2003). Influence of an indigenous European alder (*Alnus glutinosa* (L.) Gaertn) rhizobacterium (*Bacillus pumilus*) on the growth of alder and its rhizosphere microbial community structure in two soils. *New For.* 25, 149–159. doi: 10.1023/A:1022688020897

Shahid, I., Han, J., Hanooq, S., Malik, K. A., Borchers, C. H., and Mehnaz, S. (2021). Profiling of metabolites of *bacillus* spp. and their application in sustainable plant growth promotion and biocontrol. *Front. Sustain. Food. Syst.* 5:605195. doi: 10.3389/fsufs.2021.605195

Shahzad, A., Qin, M., Elahie, M., Naeem, M., Bashir, T., Yasmin, H., et al. (2021). *Bacillus pumilus* induced tolerance of maize (*Zea mays* L.) against cadmium (cd) stress. *Sci. Rep.* 11, 17196–17111. doi: 10.1038/s41598-021-96786-7

Shivaji, S., Chaturvedi, P., Suresh, K., Reddy, G. S., Dutt, C. B., Wainwright, M., et al. (2006). *Bacillus aerius* sp. nov., *Bacillus aerophilus* sp. nov., *bacillus stratosphericus* sp. nov. and *Bacillus altitudinis* sp. nov., isolated from cryogenic tubes used for collecting air samples from high altitudes. *Int. J. Syst. Evol. Microbiol.* 56, 1465–1473. doi: 10.1099/ijs.0.64029-0

Siddiqui, Z. A., Baghel, G., and Akhtar, M. S. (2007). Biocontrol of Meloidogyne javanica by rhizobium and plant growth-promoting rhizobacteria on lentil. *World J. Microbiol. Biotechnol.* 23, 435–441. doi: 10.1007/s11274-006-9244-z

Upadhyay, S. K., Saxena, A. K., Singh, J. S., and Singh, D. P. (2019). Impact of native ST-PGPR (*Bacillus pumilus*; EU927414) on PGP traits, antioxidants activities, wheat plant growth and yield under salinity. *CABI Agric. Biosci* 7, 157–168. doi: 10.5958/2320-642X.2019.00021.8

Wierzchowski, P. S., Dobrzyński, J., Mazur, K., Kierończyk, M., Wardal, W. J., Sakowski, T., et al. (2021). Chemical properties and bacterial community reaction to acidified cattle slurry fertilization in soil from maize cultivation. *Agronomy* 11:601. doi: 10.3390/agronomy11030601

Win, K. T., Okazaki, K., Ohkama-Ohtsu, N., Yokoyama, T., and Ohwaki, Y. (2020). Short-term effects of biochar and *Bacillus pumilus* TUAT-1 on the growth of forage rice and its associated soil microbial community and soil properties. *Biol. Fertil. Soils* 56, 481–497. doi: 10.1007/s00374-020-01448-x

Win, K. T., Oo, A. Z., Ohkama-Ohtsu, N., and Yokoyama, T. (2018). *Bacillus Pumilus* strain TUAT-1 and nitrogen application in nursery phase promote growth of Rice plants under field conditions. *Agron. J.* 8:216. doi: 10.3390/agronomy8100216

Yakovleva, G., Kurdy, W., Gorbunova, A., Khilyas, I., Lochnit, G., and Ilinskaya, O. (2022). *Bacillus pumilus* proteome changes in response to 2, 4, 6-trinitrotoluene-induced stress. *Biodegradation* 33, 593–607. doi: 10.1007/s10532-022-09997-8

Zhang, Q., Lin, Y., Shen, G., Zhang, H., and Lyu, S. (2022). Siderophores of *Bacillus pumilus* promote 2-keto-L-gulonic acid production in a vitamin C microbial fermentation system. *J. Basic Microbiol.* 62, 833–842. doi: 10.1002/jobm.202200237

Zielewicz, W., Swędrzyński, A., Dobrzyński, J., Swędrzyńska, D., Kulkova, I., Wierzchowski, P. S., et al. (2021). Effect of forage plant mixture and biostimulants application on the yield, changes of botanical composition, and microbiological soil activity. *Agronomy* 11:1786. doi: 10.3390/agronomy11091786

frontiers | Frontiers in Microbiology

TYPE Original Research
PUBLISHED 02 February 2023
DOI 10.3389/fmicb.2023.1064358

Check for updates

OPEN ACCESS

EDITED BY
Reiner Rincón Rosales,
Tuxtla Gutierrez Institute of Technology, Mexico

REVIEWED BY
Hongjun Liu,
Nanjing Agricultural University, China
Betsy Peña-Ocaña,
National Institute of Cardiology Ignacio Chavez, Mexico
Clara Ivette Rincón Molina,
Instituto Tecnológico de Tuxtla Gutiérrez/TecNM, Mexico

*CORRESPONDENCE
Youming Zhang
✉ zhangyouming@sdu.edu.cn
Qiang Tu
✉ qiang.tu@siat.ac.cn

SPECIALTY SECTION
This article was submitted to Microbe and Virus Interactions with Plants, a section of the journal Frontiers in Microbiology

RECEIVED 08 October 2022
ACCEPTED 17 January 2023
PUBLISHED 02 February 2023

CITATION
Ni H, Wu Y, Zong R, Ren S, Pan D, Yu L, Li J, Qu Z, Wang Q, Zhao G, Zhao J, Liu L, Li T, Zhang Y and Tu Q (2023) Combination of *Aspergillus niger* MJ1 with *Pseudomonas stutzeri* DSM4166 or mutant *Pseudomonas fluorescens* CHA0-*nif* improved crop quality, soil properties, and microbial communities in barrier soil.
Front. Microbiol. 14:1064358.
doi: 10.3389/fmicb.2023.1064358

COPYRIGHT
© 2023 Ni, Wu, Zong, Ren, Pan, Yu, Li, Qu, Wang, Zhao, Zhao, Liu, Li, Zhang and Tu. This is an open-access article distributed under the terms of the Creative Commons Attribution License (CC BY). The use, distribution or reproduction in other forums is permitted, provided the original author(s) and the copyright owner(s) are credited and that the original publication in this journal is cited, in accordance with accepted academic practice. No use, distribution or reproduction is permitted which does not comply with these terms.

Combination of *Aspergillus niger* MJ1 with *Pseudomonas stutzeri* DSM4166 or mutant *Pseudomonas fluorescens* CHA0-*nif* improved crop quality, soil properties, and microbial communities in barrier soil

Haiping Ni[1,2], Yuxia Wu[1,3], Rui Zong[2], Shiai Ren[2], Deng Pan[1], Lei Yu[4], Jianwei Li[4], Zhuling Qu[2], Qiyao Wang[5], Gengxing Zhao[5], Jianzhong Zhao[6], Lumin Liu[2], Tao Li[4], Youming Zhang[1,3]* and Qiang Tu[1,3]*

[1]Helmholtz International Lab for Anti-Infectives, Shandong University–Helmholtz Institute of Biotechnology, State Key Laboratory of Microbial Technology, Shandong University, Qingdao, China, [2]Qingdao Hexie Biotechnology Co., Ltd., Qingdao, China, [3]CAS Key Laboratory of Quantitative Engineering Biology, Shenzhen Institute of Synthetic Biology, Shenzhen Institute of Advanced Technology, Chinese Academy of Sciences, Shenzhen, China, [4]Shandong Agricultural Technology Extension Center, Jinan, China, [5]National Engineering Laboratory for Efficient Utilization of Soil and Fertilizer, College of Resources and Environment, Shandong Agricultural University, Tai'an, China, [6]Shandong Rural Economic Management and Service Center, Jinan, China

Soil salinization and acidification seriously damage soil health and restricts the sustainable development of planting. Excessive application of chemical fertilizer and other reasons will lead to soil acidification and salinization. This study focus on acid and salinized soil, investigated the effect of phosphate-solubilizing bacteria, *Aspergillus niger* MJ1 combined with nitrogen-fixing bacteria *Pseudomonas stutzeri* DSM4166 or mutant *Pseudomonas fluorescens* CHA0-*nif* on crop quality, soil physicochemical properties, and microbial communities. A total of 5 treatments were set: regular fertilization (T1), regular fertilization with MJ1 and DSM4166 (T2), regular fertilization with MJ1 and CHA0-*nif* (T3), 30%-reducing fertilization with MJ1 and DSM4166 (T4), and 30%-reducing fertilization with MJ1 and CHA0-*nif* (T5). It was found that the soil properties (OM, HN, TN, AP, AK, and SS) and crop quality of cucumber (yield production, protein, and vitamin C) and lettuce (yield production, vitamin C, nitrate, soluble protein, and crude fiber) showed a significant response to the inoculated strains. The combination of MJ1 with DSM4166 or CHA0-*nif* influenced the diversity and richness of bacterial community in the lettuce-grown soil. The organismal system-, cellular process-, and metabolism-correlated bacteria and saprophytic fungi were enriched, which were speculated to mediate the response to inoculated strains. pH, OM, HN, and TN were identified to be the major factors correlated with the soil microbial community. The inoculation of MJ1 with DSM4166 and CHA0-*nif* could meet the requirement of lettuce and cucumber growth after reducing fertilization in acid and salinized soil, which provides a novel candidate for the eco-friendly technique to meet the carbon-neutral topic.

KEYWORDS

phosphate-solubilizing, biological nitrogen fixation, fertilizer reduction, bacterial community, green

Introduction

Soil salinization and acidification are commonly seen as soil barrier that breaks soil health and restricts the sustainable development of planting. According to the statistical data, the area of global saline-alkali land has reached 9.55×10^8 hm^2, and the area in China is about 9.91×10^7 hm^2. The micropores of the saline-alkali soil are large containing a variety of soluble salts, including chloride, sulfate, carbonate, calcium, magnesium, potassium ions, etc. Meanwhile, insufficient drainage would result in the accumulation of salt ions. High concentrations of salt ions could affect the soil structure, reduce the penetration of water into the soil pores, and therefore induced soil compaction. In addition, high concentrations of salt ions in the soil will reduce the relative activity of mineral elements, thereby reducing their uptake by plants and affecting plant growth. On the other hand, soil acidification is also a challenging problem for global agriculture. The long-term and excessive application of chemical fertilizers, especially the excessive application of nitrogen, has become one of the important reasons for the aggravation of soil acidification. Studies have found that long-term NPK fertilizers can improve soil comprehensive fertility and economic yield, but at the same time led to soil acidification (Zhu et al., 2018; Bai et al., 2020; Yan et al., 2020; Aasfar et al., 2021). Soil acidification results in a series of hazards. First, the uneven distribution of soil nutrients leads to poor growth of above-ground crops during planting, which reduces the productivity and economic benefits. Meanwhile, great damages were exerted in soil micro-ecosystems and other functions. There was a lack of scientific guidance for the application of organic fertilizers, which is also another fatal factor resulting in the large difference in the fertilizer effects. Exploring novel fertilizer strategies to improve the productivity of barrier soil and the production of crops is of urgent need.

Phosphorus in the soil is easily integrated with metal ions, such as calcium, iron, and aluminum, and formed insoluble metal minerals, which results in the reduced availability of phosphorus and further limits its uptake by plants (Wu et al., 2019). The level of total phosphorus in the soil is always found to be much higher than available phosphorus, and in order to improve the yield, a huge number of phosphate fertilizer was applied to the soil. According to previous data, less than 20% phosphate fertilizer can be used by crops, therefore leading to the increasing accumulation of phosphorus in the soil (Li et al., 2015). Excessive phosphorus in the soil could enter the aquatic system through runoff, inducing eutrophication and aggravating non-point pollution. Moreover, excessive phosphorus is also a major inducing factor of soil acidification, due to the fact that some kinds of phosphate fertilizer like calcium superphosphate, could produce free acid into the soil, which results in the decreasing soil pH. Therefore, the conversion of insoluble phosphorus into soluble forms and reducing excessive accumulation of phosphorus in soil are of urgent need to be solved.

Phosphate-solubilizing microorganisms (PSMs) in the soil could transform the insoluble P into the form that can be utilized by plants. Hitherto, numerous PSMs have been isolated from different kinds of soil, and the number of fungi was larger than that of bacteria. The mechanism of phosphate solubilization by PSMs varies from different strains, including the secretion of phytases, nucleases, phosphatases, and organic acid (Rawat et al., 2021). *Aspergillus niger* MJ1 is a PSM isolated from alkaline soil, which was demonstrated to improve the content of available phosphorus through dissolving organic and inorganic phosphorus (Schneider et al., 2010; Xiao et al., 2015; Klaic et al., 2021). Therefore, the application of *A. niger* MJ1 might ameliorate the deficiency of phosphorus in the soil and benefit crop production.

With the increasing food requirement, the amount of nitrogen fertilizers applied in agriculture also grew rapidly. However, the utilization of nitrogen fertilizers is unsatisfactory. According to recent data, only 30–50% of the applied fertilizers can be utilized, and the residuals were left in the soil (Xu et al., 2012; Wang et al., 2018). Excessive nitrogen would induce a series of soil degradation problems, such as soil acidification and compaction. Biological nitrogen fixation is one of the major sources of soil nitrogen, where N_2 was reduced to ammonia by nitrogen-fixing microorganisms. The nitrogen-fixing (*nif*) gene cluster is a typical nitrogen fixing-correlated gene that encodes the components of the nitrogenase enzyme and catalyzes the biological nitrogen fixation process (Curatti and Rubio, 2014; Thiel, 2019). Previous studies have identified a series of diazotrophs with various genetic components and arrangements of *nif* genes, such as *Paenibacillus brasilensis* PB24, *Klebsiella oxytoca* M5a1, and *Azotobacter vinelandii* AvOP (Mahmud et al., 2020; do Carmo Dias et al., 2021). Increasing studies have been devoted to investigating the genetics and regulation of *nif* genes in some functional bacteria that play roles in the circulation of other elements. For instance, in *Leptospirillum ferrooxidans*, an acidophile iron-oxidizing bacteria, a variety of nitrogen fixation-correlated genes were identified, including the specific member of the *nif* family, *nifA*, indicating its potential in biological nitrogen fixation (Parro and Moreno-Paz, 2004). *Pseudomonas stutzeri* DSM4166 was identified as a diazotroph isolated from the rhizosphere of a Sorghum nutans cultivar (Yu et al., 2011). In our previous work, we have established a mutant strain of *Pseudomonas fluorescens* CHA0 through integrating a *nif* cluster with a length of 49 kb from *P. stutzeri* DSM4166 into the genome of *P. fluorescens* CHA0 by biparental conjugation, which makes *P. fluorescens* CHA0 possess the potential ability of nitrogen fixation (Yu et al., 2019; Jing et al., 2020).

Soil microorganisms play vital roles in regulating the physiochemical properties and biophysical processes of the soil, which would indirectly influence plant growth. The structure of the soil microbial community could disclose the mechanism of fertilization application and indicate the healthy condition of the soil. In previous studies, the soil bacterial community was suggested to be sensitive to the soil nutrients as well as some exogen pollutants and fertilization, such as biochar, chemical fertilizers, and organic fertilizers (Balkhair, 2016; Zhang et al., 2019, 2021). Hence, the addition of PSMs or diazotrophs might affect the composition and structure of soil bacteria, which could provide more functional bacteria and reveal the mechanism underlying the applied bacteria.

This study aimed to clarify the following questions: (1) evaluating the effect of the combination of *Aspergillus niger* MJ1, *P. stutzeri* DSM4166, and *P. fluorescens* CHA0-nif mutant strain on the quality of lettuce and cucumber and the properties of barrier soil; (2) revealing the response of soil bacteria to the application of modified fertilization strategies; (3) exploring the optimal strain combination to provide the theoretical basis for improving production and quality of lettuce and cucumber.

Materials and methods

Field experiment

The field experiment was conducted in Haofeng base, Jimo District, Qingdao, Shandong Province, China (36.38°N, 120.33°E). The acid field was grown with lettuce (pH 5.5–6.1) and the salinization field was grown

with cucumber (pH 7.6–7.9, soluble salt 0.14–0.19%). The lettuce (*Lactuca sativa* L. planting density 3,300 trees per mu) was transplanted at the four-leave stage on 21st, August 2020, while the cucumber (*Cucumis sativus* L. planting density 3,500 trees per mu) was seeded on 22nd, June 2020. The quality and production of the plants were added up on the 9th, October 2020, and 20th, August 2020, respectively. The soil samples were also collected at different layers (0–20 and 20–40 cm) at the same time.

The completely randomized block design was applied with five treatments and three triplicates of each. Each block possessed an area of 30 m^2 (length of 6 m and width of 5 m). The specific application fertilization and strains of each treatment were summarized in Table 1. Regular fertilization was composed of 675 kg/ha. The microbial inoculants were used with a concentration of 600 L/ha. No fertilization in other periods.

Earthworm surveys were conducted using cubes of soil (length 1.0 m, width 2.0 m, and height 0.3 m) excavated manually in the field after harvest, all earthworms were counted.

Strains

The *A. niger* MJ1 was isolated from the from alkaline soil, which had been deposited in CCTCC (China Center for Type Culture Collection) on 5th, January 2015 (CCTCC No: M2015004), routinely solid cultivated with aeration at 30°C in the PDA medium (pH 7.0, Potato 200 g/L, Dextrose 20 g/L, and Agar 20 g/L). The wild-type strain *P. stutzeri* DSM4166 (deposited in DSMZ: Deutsche Sammlung von Mikroorganismen und Zellkulturen, No: DSM4166) and its derived strain CHA0-*nif* (deposited in CGMCC: China General Microbiological Culture Collection Center on 31st, July 2017, No: CGMCC 14476) used in this study were routinely cultivated with aeration at 30°C in the KB medium (pH 7.0, K_2HPO_4 1.5 g/L, $MgSO_4{\cdot}7H_2O$ 1.5 g/L, peptone 20 g/L, glycerin 10 ml/L). At least 200 million colony-forming units per ml (CFU/ml) of *P. stutzeri* DSM4166 or CHA0-*nif* were added to the soil during the sowing of the crop's seeds. While 5 million CFU/ml of *A. niger* MJ1 spore powder was applied to the soil.

Soil and plant analysis

The major physicochemical properties of collected soil samples, including pH, organic matter (OM), hydrolysis nitrogen (HN), total nitrogen (TN), available phosphorus (AP), available potassium (AK), soluble salt (SS), microbial biomass carbon (MBC), microbial biomass nitrogen (MBN), and microbial biomass phosphorus (MBP) were analyzed with regular methods according to previous reports.

The total weight of the cucumber and lettuce was evaluated after the harvest and converted to the yield per hectare. The weight and height of lettuce heads and the characteristics of the lettuce vanes (length and width) were measured to estimate the lettuce quality. The soluble protein, sugar, and nitrates in lettuce were analyzed according to reported methods (Aasfar et al., 2021). The content of vitamin C was assessed according to Li et al. with a UV-spectrophotometer (Sánchez-Rangel et al., 2013).

DNA isolation and sequencing

DNA extraction was carried out with the E.Z.N.A. soil kit (Omega Bio-Tek, United States) according to the manufacturer's protocols. After evaluating the purity and concentration of isolated DNA with NanoDrop 2000 (Thermo Fisher, United States), the amplification process was conducted by PCR system. The primer sequences are as follows: 338F 5′-ACTCCTACGGGAGGCAGCAG-3′ and 806r 5′-GGACTACHVGGGTWTCTAAT-3′ for bacterial V3–V4 region of bacterial 16S rRNA gene, ITS1F 5′-CTTGGTCATTTAGAGGAAGTAA-3′ and ITS2R 5′-GCTGCGTTCTTCATCGATGC-3′ for fungal ITS hypervariable regions. The Illumina Miseq sequencing process was performed on an Illumina Miseq platform (Illumina, United States) by Novogene Bioinformatics Technology Co. (Beijing, China) according to the standard protocols. The quality control of raw data was conducted with Trimmomatic and merged by FLASH.

The Illumina sequencing was performed with a MiSeq PE250 sequencer (Illumina, United States). The USEARCH method (Edgar et al., 2011) was applied for the stitching, filtering, deduplication, and clustering of the data. With the help of the UPARSE algorithm, the sequences with similarity of over 97% were classified into the same OTU. Then, the sequences were classified and annotated to establish the taxonomic tree and phylogenetic tree. The alpha- and beta-diversity indexes were calculated with the rarefied OTUs. The alpha-diversity index includes Chao1, species, Shannon, Simpson, Faith, Pielou, and coverage, which were calculated by the R-package in QIIME2. For the further beta-diversity analysis, the principal coordinate analysis (PCoA) was conducted with four distance algorithms.

TABLE 1 The fertilization and strain application of each treatment.

		Regular fertilization	*Aspergillus niger* MJ1	*Pseudomonas stutzeri* DSM4166	*Pseudomonas fluorescens* CHA0-*nif*
Lettuce	L1	+	–	–	–
	L2	+	+	+	–
	L3	+	+	–	+
	L4	Reduce 30%	+	+	–
	L5	Reduce 30%	+	–	+
Cucumber	C1	+	–	–	–
	C2	+	+	+	–
	C3	+	+	–	+
	C4	Reduce 30%	+	+	–
	C5	Reduce 30%	+	–	+

Statistical analysis

The obtained data were represented as mean value ± SD and analyzed by SPSS 26.0 software. The difference between groups was evaluated with one-way ANOVA followed by the Duncan *post-hoc* test. The microbial data were analyzed with the R software (Version 2.15.3) including the following parts. The alpha-diversity was estimated by the Ace and Shannon index and compared with the ANOVA. The beta-diversity was assessed through the principal coordinate analyses based on weighted and unweighted unifrac distance algorithms. The Lefse analysis was performed to identify differential microbial communities or species between different treatments. The correlation between soil physicochemical properties and microbial community was analyzed with RDA analysis. The function analysis was also performed to further predicted the potential functional role of identified microorganisms. PICRUSt is a bioinformatics tool that uses marker genes to predict the functional content of microorganism. In this study, this method was employed to predict the potential functions of each sample based on 16S rRNA sequencing data. We used the KEGG database and performed closed reference OTU picking using the sampled reads against a Greengenes reference taxonomy (Greengenes database Version). The 16S copy number was then normalized, molecular functions were predicted and final data were summarized into KEGG pathways. $p < 0.05$ indicates statistical significance.

Results

Effect of inoculated strains on barrier soil properties

Compared with regular fertilization, the inoculation of the studied strains dramatically influenced the OM, HN, TN, AP, AK, and SS contents in the barrier soil with various depths. The detailed soil physiochemical properties are summarized in Table 2.

Specifically, in the 0–20 cm of the salinized soil with cucumber, the MJ1 significantly improved the content of TN, AP, and AK. Meanwhile, the co-inoculation of CHA0-*nif* showed a significant promoted effect on TN in comparison with the co-inoculation of DSM4166. After reducing 30% of the regular fertilization, the inoculation of MJ1 with DSM4166 or CHA0-*nif* increased the soil content of TN, AP, and AK relative to treatment with regular fertilization, and no significant difference was observed between the DSM4166 and CHA0-*nif*. For the 20–40 cm soil, the contents of HN, TN, AP, and AK were found to elevate in the presence of MJ1 co-inoculated with DSM4166 and CHA0-*nif*, and the enhanced effect of CHA0-*nif* was significantly stronger than DSM4166 in the content of HN and AK. The TN in the soil with co-inoculation of MJ1 and DSM4166 or CHA0-*nif* was significantly higher than the regular fertilization, and the difference between the co-inoculations was insignificant. While MJ1 and DSM4166 could increase the HN content after reducing 30% of fertilization, the co-inoculation with DSM4166 or CHA0-*nif* after 30%-reducing fertilization showed no significant effects.

In the acid soil grown with lettuce, compared with the regular fertilization, the co-inoculation of MJ1 with CHA0-*nif* significantly improved OM, HN, TN, AP, and AK in the 0–20 cm of soil, while only the contents of HN and AP were elevated by MJ1 with DSM4166 and the promoted effect of CHA0-*nif* was stronger than that of DSM4166 in soil AP. After reducing 30% of fertilization, the combination of MJ1 and DSM4166 could improve soil SS, while MJ1 with CHA0-*nif* was found to improve soil AP. DSM4166 inoculating with MJ1 dramatically enhanced the HN and AP in 20–40 cm soil, while the soil treated with CHA0-*nif* with MJ1 possessed a higher content of HN, TN, and AK than DSM4166, $p < 0.05$. For the treatment with 30%-reducing fertilization reduction, the combination of DSM4166 or CHA0-*nif* with MJ1 could keep the soil content of TN, AP, and AK from reducing, and DSM4166 could improve HN and AK content.

Effect of inoculated strains on crop quality

For the yield production of cucumber, all treatments showed significantly enhanced effect even the treatments with a 30% reducing regular fertilization, the treatment of MJ1 and CHA0-*nif* combination showed the maximum production of 5542.36 ± 14.60 kg/acre. For the content of protein and vitamin C in cucumber, MJ1 combined with DSM4166 or CHA0-*nif* showed a dramatically promoted effect in the presence of regular fertilization. Interestingly, after reducing 30% fertilization, the treatments of MJ1 and CHA0-*nif* combination showed the maximum contents of protein (0.737 ± 0.021%) and vitamin C (4.287 ± 0.032 mg/kg) in all treatments (Table 3).

The production of lettuce was increased by the combination of MJ1 and CHA0-*nif* under regular fertilization, and no significant difference was observed between different strain combinations. The quality of lettuce was assessed from two aspects, including growth indexes and physiological indexes. The lettuce that grew under the fertilization combined with MJ1 and CHA0-*nif* possessed the highest head weight of 0.269 ± 0.046 kg but was insignificantly different from other inoculated treatments. For the other growth indexes, no significant difference was observed in the lettuce vanes' width, length, and the height of lettuce heads. Physiologically, the content of vitamin C, nitrate, soluble protein, and crude fiber of lettuce was significantly improved in the presence of MJ1 and CHA0-*nif*, while the combination of MJ1 with DSM4166 was only found to enhance the content of nitrate, which was insignificantly different from CHA0-*nif* (Table 3).

Effect of inoculated strains on microbial biomass of barrier soil

In salinized soil, the co-inoculation of MJ1 with DSM4166 or CHA0-*nif* significantly increased the MBC and MBN in 0–20 cm depth and the MBN in 20–40 cm in the presence of regular fertilization, and there was no significant difference in the effect between DSM4166 and CHA0-*nif*. In the presence of 70% of regular fertilization, the combination of MJ1 and DSM4166 or CHA0-*nif* markedly improved the MBN of 20–40 cm soil, and their effects on the MBC, MBN, and MBP in 0–20 cm soil were not obvious (Table 4).

According to the data, the co-inoculation of MJ1 with DSM4166 or CHA0-*nif* exerted an enhanced effect on the MBP level of 0–20 cm acid soil under regular fertilization. While only MJ1 inoculating with CHA0-*nif* was found to improve the level of MBC and MBN of 20–40 cm soil, the effect of DSM4166 was insignificant. After reducing regular fertilization, the combination of MJ1 with DSM4166 or

10.3389/fmicb.2023.1064358

TABLE 2 Basic physicochemical properties of soil at different depths grown with cucumber or lettuce.

Crop	Depth	Group	pH	OM (g/kg)	HN (mg/kg)	TN (g/kg)	AP (mg/kg)	AK (mg/kg)	SS (%)
Cucumber	0–20 cm	C1	7.75 ± 0.10a	20.28 ± 0.54a	150.07 ± 4.11a	1.07 ± 0.10c	49.08 ± 0.79b	278.70 ± 11.06c	0.183 ± 0.012a
		C2	7.71 ± 0.06a	20.43 ± 2.03a	155.07 ± 9.30a	1.53 ± 0.04b	61.50 ± 7.30a	417.10 ± 12.10a	0.173 ± 0.017a
		C3	7.71 ± 0.08a	20.97 ± 1.23a	159.86 ± 6.04a	1.74 ± 0.19a	63.24 ± 5.51a	439.33 ± 27.49a	0.168 ± 0.005a
		C4	7.67 ± 0.10a	20.47 ± 0.75a	150.36 ± 3.10a	1.41 ± 0.05b	49.55 ± 0.50b	341.80 ± 15.33b	0.176 ± 0.019a
		C5	7.70 ± 0.12a	20.32 ± 0.22a	150.76 ± 5.69a	1.42 ± 0.12b	50.56 ± 1.77b	348.70 ± 34.25b	0.173 ± 0.004a
	20–40 cm	C1	7.86 ± 0.09a	12.12 ± 0.24a	103.27 ± 3.74c	0.94 ± 0.04c	28.50 ± 6.78b	236.20 ± 16.20c	0.167 ± 0.018a
		C2	7.82 ± 0.10a	12.85 ± 1.63a	119.04 ± 1.58b	1.19 ± 0.10ab	39.70 ± 4.41a	335.10 ± 11.62b	0.142 ± 0.010a
		C3	7.76 ± 0.10a	13.20 ± 0.76a	128.24 ± 5.05a	1.27 ± 0.05a	37.53 ± 2.09a	387.00 ± 2.20a	0.141 ± 0.014a
		C4	7.85 ± 0.14a	12.56 ± 0.52a	114.24 ± 5.28b	1.12 ± 0.11b	28.24 ± 4.43b	243.37 ± 31.00c	0.147 ± 0.018a
		C5	7.84 ± 0.05a	12.80 ± 0.25a	104.16 ± 4.62c	1.10 ± 0.06b	28.37 ± 5.01b	256.25 ± 14.45c	0.145 ± 0.020a
Lettuce	0–20 cm	L1	5.53 ± 0.11a	13.71 ± 0.47b	109.92 ± 6.30b	0.98 ± 0.02b	67.84 ± 3.65c	208.97 ± 10.55b	0.061 ± 0.006a
		L2	5.74 ± 0.29a	13.66 ± 0.37b	123.81 ± 6.48a	1.01 ± 0.05b	91.29 ± 2.43a	184.80 ± 13.55b	0.057 ± 0.001ab
		L3	5.60 ± 0.17a	14.84 ± 0.57a	121.24 ± 3.98a	1.12 ± 0.12a	78.00 ± 4.48b	387.00 ± 2.20a	0.057 ± 0.004ab
		L4	5.87 ± 0.24a	13.78 ± 0.61b	109.57 ± 6.38b	0.96 ± 0.03b	75.72 ± 5.28bc	205.62 ± 25.32b	0.053 ± 0.001b
		L5	5.78 ± 0.10a	13.94 ± 0.33b	105.49 ± 3.45b	0.95 ± 0.03b	77.30 ± 5.64b	192.77 ± 13.54b	0.054 ± 0.004ab
	20–40 cm	L1	5.95 ± 0.09a	11.74 ± 0.60a	86.94 ± 4.30d	0.87 ± 0.02b	67.97 ± 7.50b	166.00 ± 2.57b	0.050 ± 0.003a
		L2	6.00 ± 0.12a	12.15 ± 0.89a	94.99 ± 4.04bc	1.00 ± 0.17b	83.09 ± 5.31a	164.17 ± 11.91b	0.049 ± 0.006a
		L3	6.08 ± 0.05a	13.20 ± 0.76a	128.24 ± 5.05a	1.27 ± 0.05a	67.53 ± 2.09b	195.03 ± 9.11a	0.048 ± 0.002a
		L4	6.03 ± 0.14a	11.82 ± 0.76a	95.81 ± 3.16b	0.87 ± 0.02b	67.25 ± 3.32b	193.05 ± 0.75a	0.045 ± 0.005a
		L5	6.06 ± 0.09a	11.82 ± 1.09a	87.76 ± 4.57cd	0.87 ± 0.03b	75.42 ± 6.57ab	160.53 ± 14.35b	0.045 ± 0.007a

Different letters indicate significant difference.

CHA0-*nif* could protect the MBC, MBN, and MBP levels from declining (Table 4).

Effect of inoculated strains on the alpha-diversity of barrier soil microbial community

Among the critical alpha-diversity indexes, there were no significant changes were observed in the bacterial richness and diversity between different groups of salinized soil (Supplementary Figure S1A). For the fungal community, the co-inoculation of MJ1 with DSM4166 or CHA0-*nif* was found to reduce the number of observed species and Shannon indexes, but the differences were not significant (Supplementary Figure S1B). Although there was no significant effect of inoculated strains was observed on the microbial diversity and richness, an increasing number of earthworms was found in the cucumber-grown soil (Supplementary Figure S2).

While in the acid soil, in the treatments with regular fertilization, the co-inoculation of MJ1 and DSM4166 or CHA0-*nif* significantly improved the number of bacterial species and the Shannon indexes, indicating the improving bacterial richness and diversity. After reducing 30% of regular fertilization, the combination of MJ1 and CHA0-*nif* showed a markedly promoted effect on the bacterial richness and diversity, but the effect of DSM4166 was insignificant (Supplementary Figure S1C). For the fungal community, the inoculation of MJ1 with DSM4166 or CHA0-*nif* slightly elevated the observed species number and Shannon index, but the changes were not of statistical significance (Supplementary Figure S1D).

Effect of inoculated strains on the beta-diversity of barrier soil microbial community

Based on two distance algorithms, the microbial community structure of soil with different treatments were evaluated (Figure 1). In the bacterial community of salinized soil, the combination of MJ1 with DSM4166 or CHA0-*nif* under 30%-reducing regular fertilization was found to significantly separate from the regular fertilization group in the results of weighted unifrac (total explanation rate of 56.69%) and unweighted unifrac (total explanation rate of 37.05%; Figure 1A). The fungal community structure of the soil with the MJ1-CHA0-*nif* combination was found to separate from the regular fertilization from the results of weighted unifrac (total explanation rate of 48.85%) and unweighted unifrac (total explanation rate of 22.86%; Figure 1A).

While the bacterial and fungal community structure of the acid soil showed a stronger response to the inoculated strains. Specifically, both the weighted unifrac (total explanation rate of 60.53%) and unweighted unifrac (total explanation rate of 20.25%) demonstrated the clear separation between the regular fertilization treatment and the other treatments with different co-inoculations. The combination of MJ1 with CHA0-*nif* under regular fertilization and the combination of MJ1 with DSM4166 in the presence of 70% regular fertilization was found to be more different from the regular fertilization (Figure 1B). Meanwhile, a clear separation was also observed in the fungal community between the fertilization group and the various combinations of MJ1 and DSM4166 or CHA0-*nif* through the weighted unifrac (total explanation rate of 59.90%) and unweighted unifrac (total explanation rate of 23.69%).

10.3389/fmicb.2023.1064358

TABLE 3 The quality indexes of cucumber and lettuce in different groups.

	Crops													
	Cucumber						Lettuce							
	Protein (%)	Vitamin C (mg/kg)	Yield production (kg/acre)	Head weight (kg)	Vanes width (cm)	Vanes length (cm)	Head height (cm)	Vitamin C (mg/kg)	Nitrate (mg/kg)	Soluble protein (mg/kg)	Soluble sugar (mg/kg)	Crude fiber (%)	Yield production (kg/acre)
C/L-1	0.487 ± 0.012d	2.057 ± 0.021e	3555.95 ± 13.97e	0.210 ± 0.027b	13.93 ± 0.50a	14.03 ± 0.57a	11.53 ± 0.50a	58.33 ± 2.54c	404.71 ± 13.42d	2842.42 ± 153.88d	8.10 ± 0.05a	1.217 ± 0.064c	1005.97 ± 134.03b
C/L-2	0.610 ± 0.010b	2.227 ± 0.012d	4679.59 ± 6.13b	0.240 ± 0.026ab	14.11 ± 1.12a	14.95 ± 1.41a	12.53 ± 1.54a	66.67 ± 2.30bc	536.53 ± 3.98a	2947.72 ± 73.06cd	8.80 ± 1.71a	1.663 ± 0.258bc	1200.00 ± 132.29ab
C/L-3	0.570 ± 0.026c	2.963 ± 0.045b	5542.36 ± 14.60a	0.269 ± 0.046a	14.41 ± 0.55a	14.71 ± 0.48a	12.23 ± 0.64a	83.33 ± 10.43a	555.37 ± 13.22a	3090.64 ± 1.96bc	9.72 ± 0.16a	2.207 ± 0.146ab	1342.60 ± 231.90a
C/L-4	0.617 ± 0.015b	2.337 ± 0.023c	4073.55 ± 73.01d	0.231 ± 0.017ab	14.01 ± 0.74a	14.09 ± 1.10a	11.61 ± 1.66a	58.33 ± 1.84c	480.88 ± 14.18c	3617.15 ± 135.61a	10.29 ± 2.09a	2.583 ± 0.947ab	1152.37 ± 84.62ab
C/L-5	0.737 ± 0.021a	4.287 ± 0.032a	4571.46 ± 44.84c	0.242 ± 0.036ab	14.07 ± 0.55a	14.53 ± 1.10a	11.90 ± 0.40a	75.66 ± 3.01ab	502.64 ± 1.61b	3233.55 ± 92.00b	10.60 ± 2.78a	2.980 ± 0.580a	1208.33 ± 180.42ab

The difference is marked with a letter. If the difference is not significant, the same letter a will be marked until the average number with significant difference is met, followed by the letter b, and so on. $p < 0.05$ indicates statistical significance.

MJ1 combined with CHA0-*nif* was found to mostly affect the fungal community structure under regular or reduced fertilization (Figure 1B).

The enriched differential microorganisms

In the acid soil, two bacterial and three fungal biomarkers were identified between different treatments. Moreover, in the presence of regular fertilization, five fungal biomarkers were screened under the combination of MJ1 with DSM4166 or CHA0-*nif*. After reducing 30% of fertilization, three bacterial biomarkers were screened (Supplementary Figures S3A, B). For different strain combinations, five bacterial biomarkers and six fungal biomarkers were identified in the presence of MJ1 with DSM4166, while seven fungal biomarkers were identified under the combination of MJ1 with CHA0-*nif*. No microbial biomarker was observed between DSM4166 and CHA0-*nif* in the presence of 70% fertilization with MJ1 (Supplementary Figures S4A, B).

In the salinized soil, one bacterial biomarker were screened between different treatments. Additionally, in the presence of regular fertilization, one differential bacterium was identified, while two differential bacteria were observed after a 30% reduction of the fertilization (Figures 2A, B). One fungal biomarker was identified between DSM4166 and CHA0-*nif* in the presence of regular fertilization with MJ1, and one bacterial biomarker was screened after reducing 30% fertilization (Supplementary Figures S5A, B).

Function prediction of enriched microorganisms

The top 10 most abundant functions of enriched bacteria or fungi in the soil with different treatments were predicted and annotated. It was revealed that the functions of bacteria in both the salinized (Figure 3A) and acid (Figure 3B) soil were mainly associated with metabolism, genetic and environmental information processing, cellular processes, and a small part of human disease and organismal systems. The abundance of involved functions was relatively average between different treatments (Supplementary Figures S6A, B). The functions of the fungi community in both salinized (Figure 3C) and acid (Figure 3D) soil were mainly enriched as saprotrophs, especially the wood saprotroph-correlated function, such as plant and animal pathogen (Supplementary Figures S6C, D).

The PCA analysis on bacterial function enrichment of salinized soil showed that there was a clear separation of fertilization reduction treatments (MJ1 with DSM4166 or CHA0-*nif*) from the regular fertilization (Supplementary Figure S7A), while the difference in the fungal function was not obvious (Supplementary Figure S7B). Similarly in the acid soil, the bacterial functions of the reduction fertilization with MJ1 combined with DSM4166 or CHA0-*nif* were obviously separated from other groups (Supplementary Figure S7C). The fungal function under the regular fertilization with MJ1 combined with DSM4166 and the 30% reducing fertilization with MJ1 combined with CHA0-*nif* were separated from the other treatments (Supplementary Figure S7D).

Association of soil physicochemical properties and microbial community

In the salinized soil, the interpretation rates of RDA1 for the bacterial and fungal communities were 54.51 and 47.58%, respectively,

TABLE 4 Biomass soil grow with cucumber or lettuce in the presence of different inoculated strains.

		Cucumber			Lettuce		
		MBC (mg/kg)	MBN (mg/kg)	MBP (mg/kg)	MBC (mg/kg)	MBN (mg/kg)	MBP (mg/kg)
0–20 cm	C/L-1	418.33 ± 28.71b	46.91 ± 3.75c	46.58 ± 0.71a	345.38 ± 31.20b	46.76 ± 6.44a	51.36 ± 5.54b
	C/L-2	500.11 ± 36.67a	71.17 ± 6.91a	51.63 ± 5.66a	371.20 ± 21.09ab	47.88 ± 4.66a	62.85 ± 5.00a
	C/L-3	495.38 ± 11.50a	66.94 ± 5.86ab	49.84 ± 1.90a	394.56 ± 9.35a	50.84 ± 4.81a	58.27 ± 4.90ab
	C/L-4	426.91 ± 23.80b	55.75 ± 5.07c	46.94 ± 4.57a	369.96 ± 12.85ab	48.26 ± 5.50a	57.48 ± 6.05ab
	C/L-5	452.92 ± 24.76ab	57.80 ± 7.91bc	48.80 ± 5.18a	335.87 ± 25.07b	45.68 ± 4.88a	54.76 ± 6.93ab
20–40 cm	C/L-1	328.98 ± 34.04a	38.85 ± 4.86b	37.86 ± 2.34abc	287.65 ± 26.87b	36.03 ± 5.54b	46.14 ± 6.18ab
	C/L-2	367.43 ± 44.64a	47.91 ± 3.50a	41.72 ± 1.52a	310.35 ± 19.24b	33.49 ± 4.63b	51.18 ± 3.73a
	C/L-3	378.98 ± 42.39a	50.84 ± 4.81a	40.97 ± 0.72ab	378.98 ± 42.39a	48.71 ± 4.53a	40.97 ± 0.72b
	C/L-4	347.97 ± 42.84a	48.58 ± 4.12a	37.77 ± 1.53bc	310.53 ± 30.09b	36.29 ± 5.29b	47.89 ± 6.79ab
	C/L-5	331.04 ± 28.89a	49.62 ± 6.35a	34.81 ± 3.55c	322.45 ± 3.92b	35.47 ± 4.73b	53.93 ± 3.45a

The difference is marked with a letter. If the difference is not significant, the same letter a will be marked until the average number with significant difference is met, followed by the letter b, and so on. $p < 0.05$ indicates statistical significance.

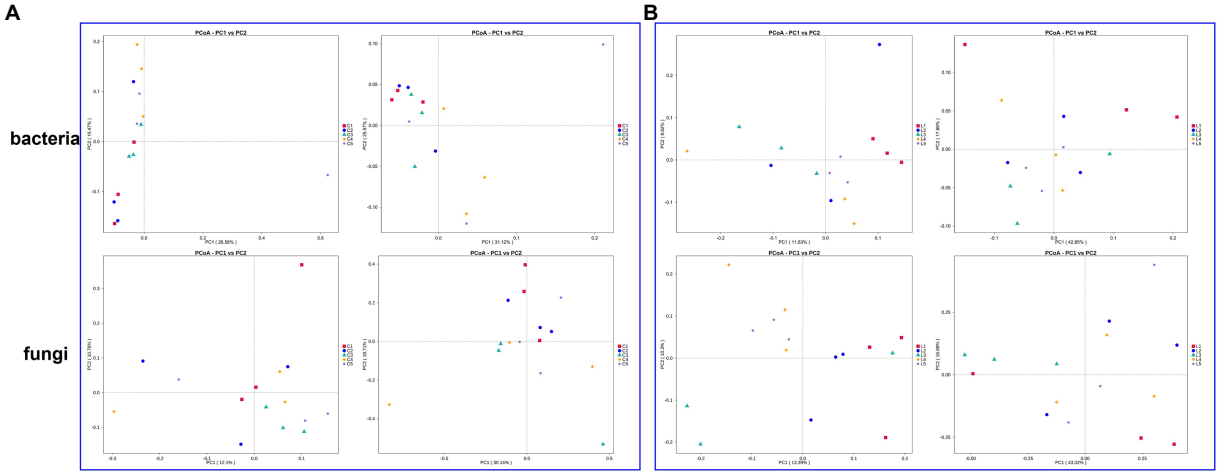

FIGURE 1
PCoA based on the weighted and unweighted unifrac distance algorithm. **(A,B)** The bacterial and fungal community of salinized **(A)** and acid **(B)** soil. The left rows of each part represented the results of unweighted unifrac distance and the right rows represented the results of the weighted unifrac distance algorithm.

while the interpretation rates of RDA2 were 26.24 and 25.39%, respectively (Figure 4A). pH, HN, TN, and OM were demonstrated as the major affected factors associated with the bacterial and fungal community. The total interpretation rates of RDA were 85.79 and 82.93% for the bacterial and fungal communities in lettuce-grown soil, respectively (Figure 4B). The most correlated factors were also revealed as pH, HN, TN, and OM.

Using the CCA and RDA functions in the vegan package, we can calculate the r^2 and p values of each environmental factor's impact on species distribution through the envfit function, and then use the selected environmental factors with significant impact to do CCA and RDA analysis. In the salinized groups, pH was positively correlated with the *Bacillus* and negatively related to the *Caldicoprobacter*, *Sedimentibacter*, *Tissierella*, *Syntrophomonas*, and *Fastidiosipila* genus. The *Lactobacillus* was positively correlated with OM, while TN and HN showed no significant correlation with abundant bacterial genus (Figure 5A). pH showed a significantly negative correlation with the fungal genus, including *Cylindrocarpon*, *Lophotrichus*, and *Preussia*. The OM-correlated genus involved *Macroventuria*, *Lysurus*, and an unidentified *Mortierellales* genus. The correlation of TN or HN with fungal genera was consistent, where the *Pseudogymnoascus*, *Melanospora*, *Stagonosporopsis*, *Trichoderma*, and *Asepergillus* genera were all positively correlated with TN and HN (Figure 5B).

In the acid soil, *Pseudoxanthomonas*, *Arthrobacter*, and *Massilia* genus were positively correlated with soil pH, while the *Bryobacter* genus showed a significant negative correlation. OM was found to be positively correlated with an unidentified *Gemmatimonadaceae* genus, and HN was negatively correlated with *Gemmatimons* genus, which was also negatively correlated with TN as well the *Rhodanobacter*, *Flavisolibacter*, and *Pseudomonas* (Figure 5C). For the fungal genus, pH was found to be positively correlated with the *Dixhotomophthora* and *Plectosphaerella*, while OM showed significant correlation with a variety of genera, such as *Olpidium*, *ideriella*, *Trichocladium*, and several unidentified genera. Both TN and HN were negatively correlated with the Pseudogymnoascus genus, and TN also showed a positive correlation with the *Microidium* genus (Figure 5D).

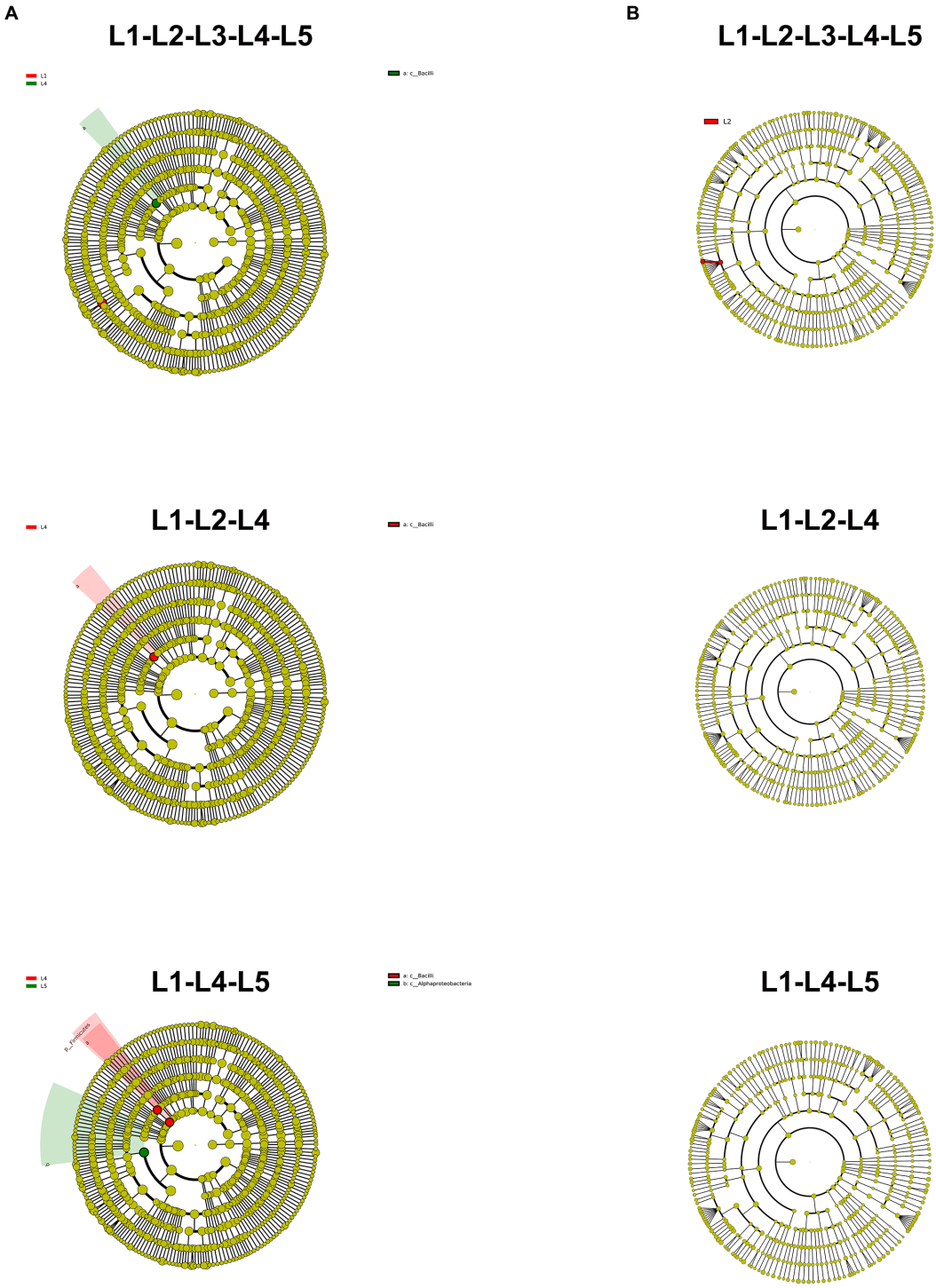

FIGURE 2
Lefse analysis to identify microbial biomarkers in each treatment of acid soil. **(A,B)** The results of bacterial **(A)** and fungal **(B)** communities. The yellow node represents that the species is not significantly enriched, and the nodes of other colors represent that the species are enriched in the corresponding treatment.

Discussion

Effect of inoculated strains on barrier soil properties and crop quality

Due to the diversity of microbial function, the inoculated strains could ameliorate the soil environment and benefit the cycles of nutrients. For example, the inoculation of nitrogen-fixing microorganisms could fix the nitrogen elements in the air to meet the requirement of nitrogen and promote its uptake by plants (Reis and Teixeira, 2015; Dellagi et al., 2020; Aasfar et al., 2021). Phosphorus-solubilizing microorganisms could decompose a variety of organic acids, which can react with insoluble phosphates to convert them into available phosphorus (Alori et al., 2017). Consistently, although the inoculation of MJ1 with

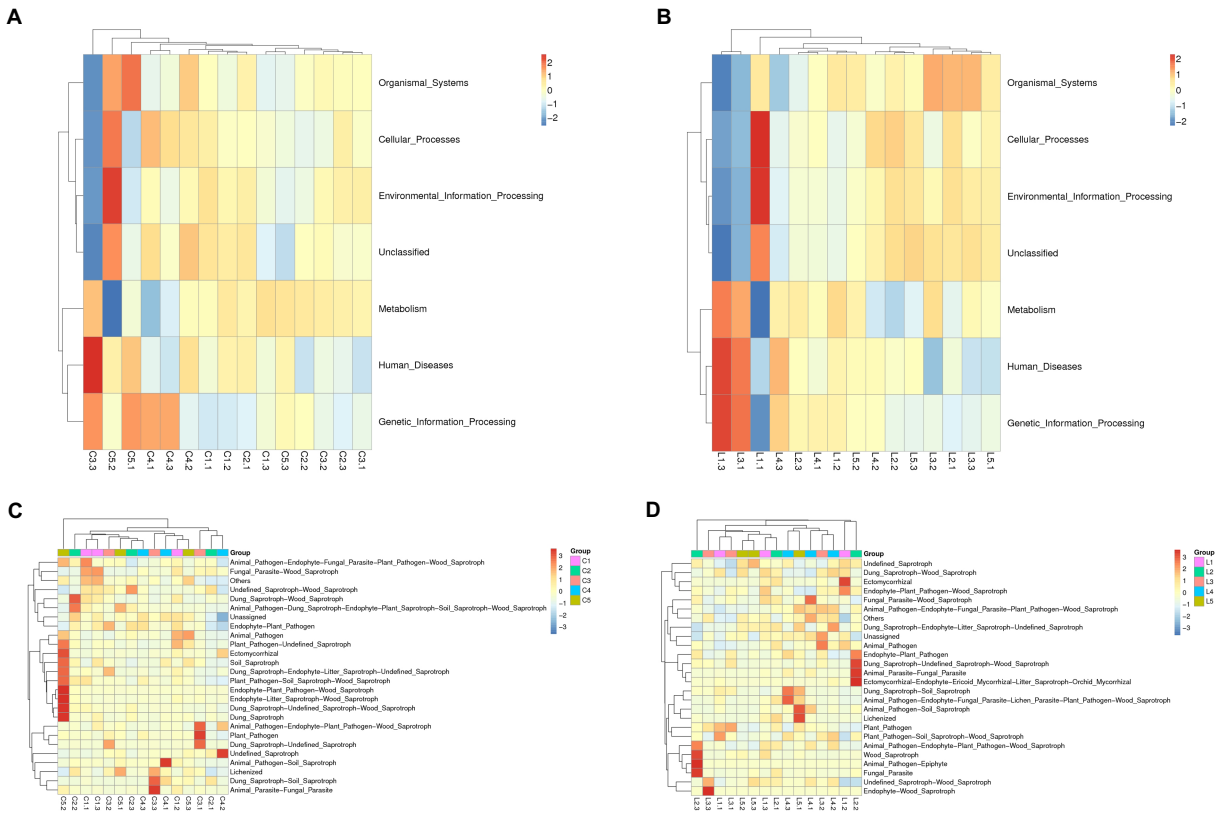

FIGURE 3
Heatmap of bacterial and fungal function prediction. **(A,B)** Function prediction of abundant bacteria in the salinized **(A)** and acid **(B)** soil. **(C,D)** Function prediction of abundant fungi in the salinized **(C)** and acid **(D)** soil.

DSM4166 or CHA0-*nif* showed insignificant effect on soil pH, it dramatically elevated the contents of HN, TN, AP, and AK in shallow and deep soil layers.

Under regular fertilization, the combination of MJ1 with CHA0-*nif* was found to show a stronger enhancement than DSM4166. Additionally, after reducing 30% of regular fertilization the inoculated strains could keep or even elevated the nutrient contents in different soil layers, the difference in the effect of DSM4166 and CHA0-*nif* was not significant, indicating that the inoculation of MJ1 with DSM4166 or CHA0-*nif* could help reduce the application of regular fertilization and meet the requirement of carbon-neutral and environment friendly of the current status of agriculture. It is worthy to note that the effect of inoculated strains was distinct in different barrier soil. The combination of MJ1 with CHA0-*nif* was more effective to improve the content of nitrogen of salinized soil and the content of phosphorus in acid soil. Low availability of phosphorus is the typical barrier of acid soil due to the formation of precipitation with metal ions. Although there were no significant changes in pH of acid soil, the improved availability of soil nutrients also suggested the potential of inoculated strains in barrier soil remediation.

Microorganisms could produce a variety of metabolites, which could regulate plant growth and improve their ability to pest resistance. For example, it was reported that the inoculation of *Azospirillum brasilense* DSM-1843 could improve the content of chlorophyII and biomass, increase Fe in the cucumber leaves, and therefore promote the recovery of cucumbers from the Fe-deficiency (Pii et al., 2015). The application of microbiological fertilization significantly improved the content of nitrate and vitamin C in *Lactuca sativa* L. (Stojanovic et al., 2020). The production, protein content, and Vitamin C content of cucumber were promoted by the inoculated strains, meanwhile, the cucumber under 30%-reduction fertilization with MJ1 combining CHA0-*nif* showed the maximum contents of protein and Vitamin C. Therefore, this combination could benefit the target of "reducing fertilization and increasing production." Although the effect of inoculated strains on lettuce production was not significant, the contents of Vitamin C, nitrate, soluble protein, and crude fiber of lettuce were dramatically improved by the combination of MJ1 with DSM4166 or CHA0-*nif*, especially the combination of MJ1 with CHA0-*nif* under regular or reducing fertilization. The increasing content of nitrate suggested that the fertilization can be reduced over 30% in the presence of inoculated strains, or the engineering bacteria can be established by knockout related regulator genes.

Effect of inoculated strains on barrier soil microbial community

The secretion and metabolites of microorganisms play critical roles in affecting the microbial community (Tyc et al., 2017). Yuan et al. (2017) reported that *Bacillus amyloliquefaciens* NJN-6 released volatile organic compounds that dramatically affected soil bacterial and fungal communities and decreased the alpha-diversity of soil microbial community. The exogenous strains have also been revealed to affect the microbial community. For instance, in a cucumber-planting soil, the *myxobacterium Corallococcus* sp. strain EGB could regulate soil

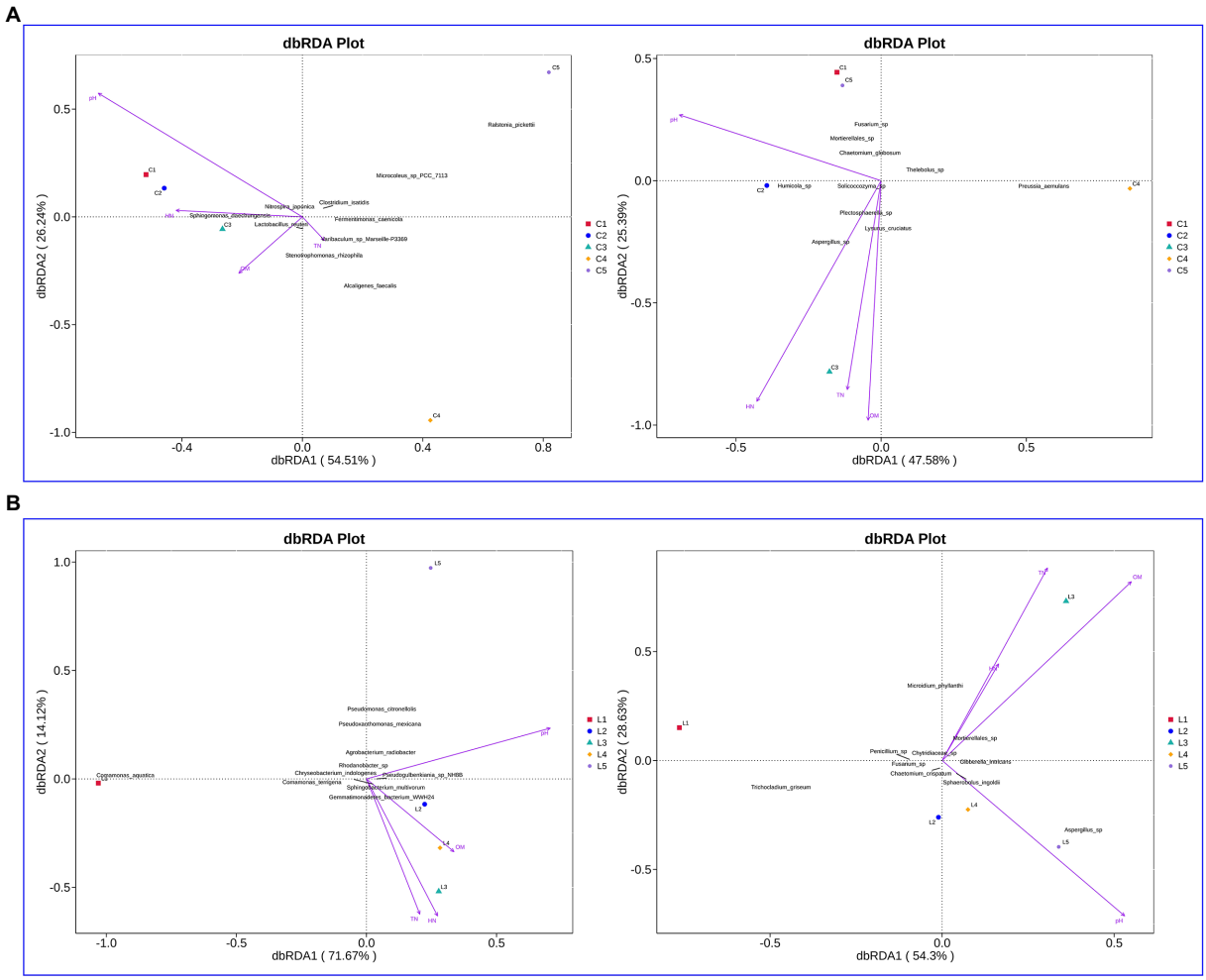

FIGURE 4
Evaluation of the association between soil physicochemical properties and microbial communities. **(A,B)** Effect of soil physicochemical properties on bacterial (left rows) and fungal (right rows) in the salinized **(A)** and acid **(B)** soil.

microbial community and further control cucumber Fusarium wilt (Ye et al., 2020). The application of the *Trichoderma hamatum* strain MHT1134 in the soil with continuous cropping obstacles could alleviate the reducing microbial diversity and abundance and improve microbial community structure (Mao and Jiang, 2021).

The application of fertilization could also affect the soil microbial community, and the fertilization amount is a critical factor associated with its effect. A recent study demonstrated that the long-term application of chemical fertilization would dramatically destroy the soil microbial community, which resulted in reduced bacterial diversity and increased soil healthy problems (Xu et al., 2020). Herein, the inoculation of MJ1 with DSM4166 or CHA0-nif was found to improve soil microbial biomass C, N, and P, especially in the deeper soil layers. It was observed that the reduction of regular fertilization did not affect the bacterial and fungal diversity of soil grown with cucumber. The inoculation of MJ1 with DSM4166 or CHA0-*nif* significantly affected the bacterial community of acid soil, where the inoculated strains improved the richness and diversity of soil bacteria. Although the effects were not significant, the inoculation of MJ1 with DSM4166 or CHA0-*nif* could also slightly improve fungal diversity and richness of acid soil. Additionally, the protective effect of inoculated strains on soil ecology was revealed in the salinized soil, where an increasing number of earthworms was observed even reducing the application of fertilization. The inoculated strains could keep or improved the microbial diversity after reducing fertilization application.

The weighted and unweighted unifrac distances were employed in the present study to evaluate the microbial community structure of the soil with different treatments, which could represent the kinship and the abundance of different species (Lozupone and Knight, 2005). The effect of exogenous strains on soil microbial beta-diversity has been previously reported. For example, *Rhizobium alamii* was revealed to improve significantly modified the beta-diversity of water stress soil and improved the tolerance of rapeseed (Tulumello et al., 2021). The inoculation of *Pigmentiphaga* sp. D-2 dramatically affected the bacterial community structure of an acetamiprid-contaminated area and improved the activity of acetamiprid degradation-related bacteria (Yang et al., 2021). The inoculated trains dramatically changed the microbial community structure of salinized soil, especially in the presence of 30%-reducing fertilization. Similarly, in acid soil, the response of bacterial and fungal community structure to inoculated strains was stronger than the cucumber-grown soil. Both the weighted unifrac and unweighted unifrac results showed significant changes in the bacterial and fungal community structure of lettuce-grown soil, indicating that the inoculation of MJ1 with

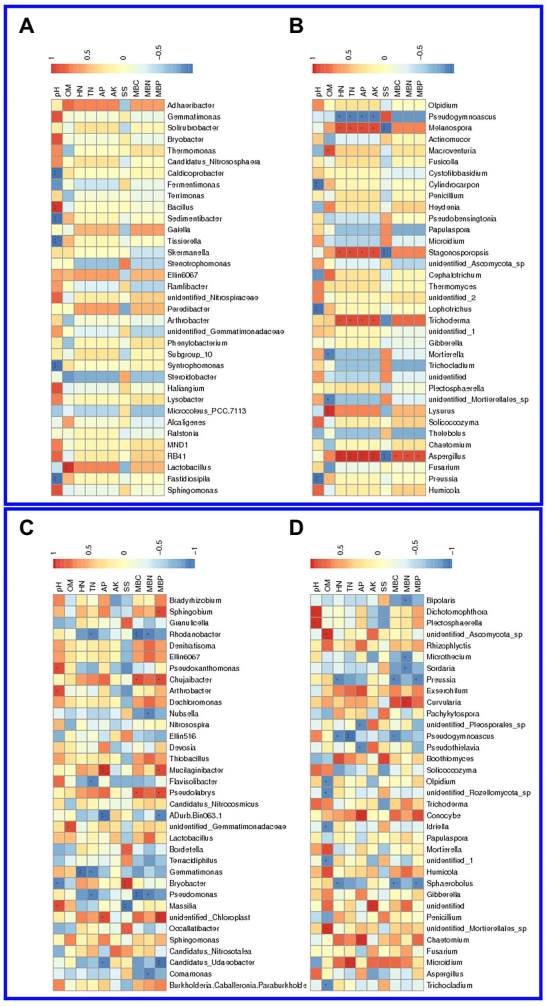

FIGURE 5
Association of soil physicochemical properties with microbial genera in the barrier soil. **(A,B)** The correlation of soil properties with bacteria **(A)** and fungi **(B)** genera in the salinized soil. **(C,D)** The correlation of soil properties with bacteria **(C)** and fungi **(D)** genera in the acid soil.

DSM4166 or CHA0-*nif* could affect the relationship and abundance of bacteria and fungi.

Interestingly, except for the effect of inoculated strains, it was found that the reduction of regular fertilization significantly influenced the structure of the microbial community in cucumber-grown and lettuce-grown soil. Previously, the application of nitrogen fertilization was illustrated to drive the beta-diversity of soil archaea, bacteria, and fungi, and affected the microbial abundance (Li et al., 2020). The bacterial and fungal beta diversity in the soil was also found to be influenced by the application of biofertilizer (Yang et al., 2022). Therefore, the changes in the beta-diversity of soil bacteria and fungi after reducing fertilization also indicated the response of soil bacteria and fungi to fertilization, and the differential microorganisms might help explain the mechanism.

Potential functions of enriched microorganisms

According to the Lefse analysis, several microbial biomarkers were identified in different treatments. *Pyrinomonadaceae* and *Blastocatellia* were enriched in the combination of MJ1 with DSM4166 in salinized soil. A previous study observed the relatively high abundance of these two genera, and *Blastocatellia* was demonstrated to be sensitive to soil pH, carbon, nitrogen, and drought (Wust et al., 2016; Ivanova et al., 2020; Huber et al., 2022). The enriched fungi were *Motiereallaes* and *Mortierellomycetes*, which were reported to be enriched in the shallow soil layers and negatively correlated with nitrogen in the soil (Zhou et al., 2021; Wang et al., 2022). For the different combinations of MJ1 with DSM4166 or CHA0-*nif*, *Mortierellomycetes* and *plectosphaerellaceae* were found to play vital roles in the inoculation of CHA0-*nif* and DSM4166, respectively, in the presence of regular fertilization. Interestingly, the identified biomarker microorganisms were significantly different between DSM4166 and CHA0-*nif* combined with MJ1 after reducing fertilization, indicating the different mechanism of the combinations of MJ1 with DSM4166 or CHA0-*nif* to meet the nutrients requirements of cucumber after reducing fertilization.

In the acid soil, *Bacilli* was identified as a major biomarker of different treatments, which plays a critical role in the combination of MJ1 with DSM4166 in the presence of regular fertilization or 30%-reducing fertilization. *Bacilli* have been widely applied as a nitrogen-fixing engineering bacteria and biopesticides due to its outstanding ability to fix nitrogen and antibacterial (Perez-Garcia et al., 2011). While *Sordariales* and *Burkholderiales* were enriched in the combination of MJ1 with DSM4166 under regular fertilization and 30%-reducing fertilization, respectively. Although few studies have reported the function of *Sordariales* and *Burkholderiales* in soil microbial communities, the function of enriched microorganisms was evaluated in the present study. Similar functions of enriched microorganisms were observed between salinized and acid soil, which were mainly associated with metabolism, genetic information processing, cellular processes, and human disease, and fungi were mainly related to the saprotroph process. The inoculated strains MJ1, DSM4166, and CHA0-*nif* were able to solubilize phosphorus and fix nitrogen. The different functional role of inoculated strains was considered the major reason for different enriched microorganism. Moreover, the regulatory effects of inoculate strains on correlated genes or procedures also contributed to the response of various functional microorganisms to the inoculations.

Effect of soil properties on soil microbial community

A recent investigation focused on the effect of fertilization patterns on soil microbial community revealed that the fertilization patterns could affect the nutrient status, which further affected the soil microbial biomass and microbial community structure (Li et al., 2022). In the present study, pH, OM, HN, and TN were identified to be the major factors correlated with the soil microbial community, which were found to strongly respond to the inoculated strains.

Although no significant changes were observed in the presence of different inoculated strains, pH was revealed to be the major effect factor in the salinized soil bacterial community, which correlated with several genera, including *Bacillus*. *Bacillus* was previously demonstrated to be alkaliphilic and possess the ability to solubilize phosphorus (Krulwich et al., 1999; Saeid et al., 2018). In terms of the fugal

community, *Aspergillus*, *Pseudogymnoascus*, *Melanospora*, *Stagonosporopsis*, and *Trichoderma* were found to be more sensitive to soil properties, which were correlated with HN, TN, AP, AK, and SS. *Aspergillus* was also found to respond to soil biomass C, N, and P. These identified fungi have also been reported to play various functions in plant growth, including serving as pathogens and promoting crop production (Marin-Felix et al., 2018; Dou et al., 2019; Dong et al., 2021; Urbina et al., 2021). In the inoculated strains, MJ1 is a typical phosphorus-solubilizing bacteria, and the other strains DSM4166 and CHA0-*nif* were able to fix nitrogen, which improves the nutrient provision for the parasitic fungi. The acid soil properties-correlated bacterial genus was reported to play role in the rhizosphere, and the fungal genus was mainly involved in the plant diseases (Cho et al., 2017; Huq, 2019; Lee et al., 2019; Al-Sadi, 2021), which are consistent with the results of function prediction. Previously, Ren et al. (2021) tried to use organic fertilizer to replace chemical fertilizer and found that the effect of organic fertilizer on soil physicochemical properties influenced the microbial community and directly or indirectly affected the activity of soil enzymes. Therefore, it was speculated that the inoculated strains might affect the microbial community *via* regulating soil physicochemical properties.

Outlook

This study focused on the growth and development of cucumber planting on salinized soil and lettuce on acid soil, which lacks negative controls. There have been some intolerant plants of salinized, acid, or other barrier soils identified in previous studies. Therefore, investigating the optimized fertilization or other management strategies would be beneficial and of urgent needs to improve the growth and development of sensitive plants on barrier soil.

Conclusion

The cucumber (yield production, protein, and vitamin C) and lettuce quality indexes (yield production, vitamin C, nitrate, soluble protein, and crude fiber) and soil properties (OM, HN, TN, AP, AK, and SS) showed a significant response to the inoculation of phosphorus-solubilizing bacterium MJ1 with nitrogen-fixing bacteria DSM4166 and CHA0-*nif*. The combination of MJ1 with DSM4166 or CHA0-nif influenced the diversity and richness of bacterial community in the acid soil and showed no significant effects on the salinized soil microbial community and the fungal community of acid soil. The organismal system-, cellular process-, and metabolism-correlated bacteria and saprophytic fungi were enriched, which were speculated to mediate the response to inoculated strains. pH, OM, HN, and TN were identified to be the major factors correlated with the soil microbial community. The inoculation of MJ1 with DSM4166 and CHA0-*nif* could meet the requirement of cucumber and lettuce growth after reducing fertilization, which provides a novel candidate for the eco-friendly technique to meet the carbon-neutral topic.

Data availability statement

The datasets presented in this study can be found in online repositories. The names of the repository/repositories and accession number(s) can be found in the article/Supplementary material.

Author contributions

HN, YZ, and QT: conceptualization. HN and YW: methodology. HN, RZ, SR, and ZQ: software. HN, YW, RZ, and DP: validation. HN, LY, and JL: formal analysis. HN, YW, QW, GZ, LL, TL, and QT: investigation. TL, YZ, and QT: resources. HN: data curation and visualization. HN and QT: writing—original draft preparation. YZ and QT: writing—review and editing, supervision, and funding acquisition. All authors contributed to the article and approved the submitted version.

Funding

This research was supported by funding from the National Key R&D Program of China (Grant No. 2019YFA0904000); the Recruitment Program of Global Experts (1000 Plan); Shandong Key Research and Development Program (2019JZZY010724); Qingdao Science and Technology Benefit People (Grant no. 21-1-4-ny-22-nsh); Natural Science Foundation of Shandong Province (ZR2021QC170), and the Program of Introducing Talents of Discipline to Universities (B16030).

Acknowledgments

We thank Nannan Dong and Xiangmei Ren of the Core Facilities for Life and Environmental Sciences, State Key laboratory of Microbial Technology of Shandong University for data analysis and guidance in fermentation.

Conflict of interest

HN, RZ, SR, ZQ, and LL are employed by Qingdao Hexie Biotechnology Co., Ltd.

The remaining authors declare that the research was conducted in the absence of any commercial or financial relationships that could be construed as a potential conflict of interest.

Publisher's note

All claims expressed in this article are solely those of the authors and do not necessarily represent those of their affiliated organizations, or those of the publisher, the editors and the reviewers. Any product that may be evaluated in this article, or claim that may be made by its manufacturer, is not guaranteed or endorsed by the publisher.

Supplementary material

The Supplementary material for this article can be found online at: https://www.frontiersin.org/articles/10.3389/fmicb.2023.1064358/full#supplementary-material

References

Aasfar, A., Bargaz, A., Yaakoubi, K., Hilali, A., Bennis, I., Zeroual, Y., et al. (2021). Nitrogen fixing *Azotobacter* species as potential soil biological enhancers for crop nutrition and yield stability. *Front. Microbiol.* 12:628379. doi: 10.3389/fmicb.2021.628379

Alori, E. T., Glick, B. R., and Babalola, O. O. (2017). Microbial phosphorus solubilization and its potential for use in sustainable agriculture. *Front. Microbiol.* 8:971. doi: 10.3389/fmicb.2017.00971

Al-Sadi, A. M. (2021). *Bipolaris sorokiniana*-induced black point, common root rot, and spot blotch diseases of wheat: a review. *Front. Cell. Infect. Microbiol.* 11:584899. doi: 10.3389/fcimb.2021.584899

Bai, Y. C., Chang, Y. Y., Hussain, M., Lu, B., Zhang, J. P., Song, X. B., et al. (2020). Soil chemical and microbiological properties are changed by Long-term chemical fertilizers that limit ecosystem functioning. *Microorganisms* 8:694. doi: 10.3390/microorganisms8050694

Balkhair, K. S. (2016). Microbial contamination of vegetable crop and soil profile in arid regions under controlled application of domestic wastewater. *Saudi J. Biol. Sci.* 23, S83–S92. doi: 10.1016/j.sjbs.2015.10.029

Cho, G. Y., Lee, J. C., and Whang, K. S. (2017). *Rhodanobacter rhizosphaerae* sp. nov., isolated from soil of ginseng rhizosphere. *Int. J. Syst. Evol. Microbiol.* 67, 1387–1392. doi: 10.1099/ijsem.0.001825

Curatti, L., and Rubio, L. M. (2014). Challenges to develop nitrogen-fixing cereals by direct nif-gene transfer. *Plant Sci.* 225, 130–137. doi: 10.1016/j.plantsci.2014.06.003

Dellagi, A., Quillere, I., and Hirel, B. (2020). Beneficial soil-borne bacteria and fungi: a promising way to improve plant nitrogen acquisition. *J. Exp. Bot.* 71, 4469–4479. doi: 10.1093/jxb/eraa112

do Carmo Dias, B., da Mota, F. F., Jurelevicius, D., and Seldin, L. (2021). Genetics and regulation of nitrogen fixation in *Paenibacillus brasilensis* PB24. *Microbiol. Res.* 243:126647. doi: 10.1016/j.micres.2020.126647

Dong, Z. Y., Huang, Y. H., Manawasinghe, I. S., Wanasinghe, D. N., Liu, J. W., Shu, Y. X., et al. (2021). *Stagonosporopsis pogostemonis*: a novel ascomycete fungus causing leaf spot and stem blight on *Pogostemon cablin* (Lamiaceae) in South China. *Pathogens* 10:1093. doi: 10.3390/pathogens10091093

Dou, K., Gao, J., Zhang, C., Yang, H., Jiang, X., Li, J., et al. (2019). Trichoderma biodiversity in major ecological systems of China. *J. Microbiol.* 57, 668–675. doi: 10.1007/s12275-019-8357-7

Edgar, R. C., Haas, B. J., Clemente, J. C., Quince, C., and Knight, R. (2011). UCHIME improves sensitivity and speed of chimera detection. *Bioinformatics (Oxford, England)* 27, 2194–2200. doi: 10.1111/1751-7915.13335

Huber, K. J., Vieira, S., Sikorski, J., Wüst, P. K., Fösel, B. U., Gröngröft, A., et al. (2022). Differential response of acidobacteria to water content, soil type, and land use during an extended drought in African Savannah soils. *Front. Microbiol.* 13:750456. doi: 10.3389/fmicb.2022.750456

Huq, M. A. (2019). *Sphingobium chungangianum* sp. nov., isolated from rhizosphere of *Pinus koraiensis*. *Antonie Van Leeuwenhoek* 112, 1341–1348. doi: 10.1007/s10482-019-01266-8

Ivanova, A. A., Zhelezova, A. D., Chernov, T. I., and Dedysh, S. N. (2020). Linking ecology and systematics of acidobacteria: distinct habitat preferences of the acidobacteria and *Blastocatellia* in tundra soils. *PLoS One* 15:e0230157. doi: 10.1371/journal.pone.0230157

Jing, X., Cui, Q., Li, X., Yin, J., Ravichandran, V., Pan, D., et al. (2020). Engineering pseudomonas protegens Pf-5 to improve its antifungal activity and nitrogen fixation. *Microb. Biotechnol.* 13, 118–133. doi: 10.1111/1751-7915.13335

Klaic, R., Guimarães, G. G. F., Giroto, A. S., Bernardi, A. C. C., Zangirolami, T. C., Ribeiro, C., et al. (2021). Synergy of *Aspergillus niger* and components in biofertilizer composites increases the availability of nutrients to plants. *Curr. Microbiol.* 78, 1529–1542. doi: 10.1007/s00284-021-02406-y

Krulwich, T. A., Guffanti, A. A., and Ito, M. (1999). pH tolerance in bacillus: alkaliphiles versus non-alkaliphiles. *Novartis Found. Symp.* 221, 167–179. doi: 10.1002/9780470515631.ch11

Lee, J. C., Song, J. S., and Whang, K. S. (2019). *Sphingobium pinisoli* sp. nov., isolated from the rhizosphere soil of a Korean native pine tree. *Antonie Van Leeuwenhoek* 112, 815–825. doi: 10.1007/s10482-018-01215-x

Li, H., Liu, J., Li, G., Shen, J., Bergstrom, L., and Zhang, F. (2015). Past, present, and future use of phosphorus in Chinese agriculture and its influence on phosphorus losses. *Ambio* 44, 274–285. doi: 10.1007/s13280-015-0633-0

Li, Y., Tremblay, J., Bainard, L. D., Cade-Menun, B., and Hamel, C. (2020). Long-term effects of nitrogen and phosphorus fertilization on soil microbial community structure and function under continuous wheat production. *Environ. Microbiol.* 22, 1066–1088. doi: 10.1111/1462-2920.14824

Li, L., Xiang, D., Wu, Y. F., Huang, Y. D., Li, H., Zhang, X. M., et al. (2022). Effects of long-term different fertilization patterns on soil nutrients and microbial community structure of tomato in a solar greenhouse. *Ying Yong Sheng Tai Xue Bao* 33, 415–422. doi: 10.13287/j.1001-9332.202202.027

Lozupone, C., and Knight, R. (2005). UniFrac: a new phylogenetic method for comparing microbial communities. *Appl. Environ. Microbiol.* 71, 8228–8235. doi: 10.1128/AEM.71.12.8228-8235.2005

Mahmud, K., Makaju, S., Ibrahim, R., and Missaoui, A. (2020). Current Progress in nitrogen fixing plants and microbiome research. *Plants* 9:97. doi: 10.3390/plants9010097

Mao, T., and Jiang, X. (2021). Changes in microbial community and enzyme activity in soil under continuous pepper cropping in response to *Trichoderma hamatum* MHT1134 application. *Sci. Rep.* 11:21585. doi: 10.1038/s41598-021-00951-x

Marin-Felix, Y., Guarro, J., Ano-Lira, J. F., Garcia, D., Iller, A. N., and Stchigel, A. M. (2018). *Melanospora* (Sordariomycetes, Ascomycota) and its relatives. *MycoKeys* 44, 81–122. doi: 10.3897/mycokeys.44.29742

Parro, V., and Moreno-Paz, M. (2004). Nitrogen fixation in acidophile iron-oxidizing bacteria: the nif regulon of *Leptospirillum ferrooxidans*. *Res. Microbiol.* 155, 703–709. doi: 10.1016/j.resmic.2004.05.010

Perez-Garcia, A., Romero, D., and de Vicente, A. (2011). Plant protection and growth stimulation by microorganisms: biotechnological applications of bacilli in agriculture. *Curr. Opin. Biotechnol.* 22, 187–193. doi: 10.1016/j.copbio.2010.12.003

Pii, Y., Penn, A., Terzano, R., Crecchio, C., Mimmo, T., and Cesco, S. (2015). Plant-microorganism-soil interactions influence the Fe availability in the rhizosphere of cucumber plants. *Plant Physiol. Biochem.* 87, 45–52. doi: 10.1016/j.plaphy.2014.12.014

Rawat, P., Das, S., Shankhdhar, D., and Shankhdhar, S. C. (2021). Phosphate-solubilizing microorganisms: mechanism and their role in phosphate solubilization and uptake. *J. Soil Sci. Plant Nutr.* 21, 49–68. doi: 10.1007/s42729-020-00342-7

Reis, V. M., and Teixeira, K. R. (2015). Nitrogen fixing bacteria in the family Acetobacteraceae and their role in agriculture. *J. Basic Microbiol.* 55, 931–949. doi: 10.1002/jobm.201400898

Ren, J., Liu, X., Yang, W., Yang, X., Li, W., Xia, Q., et al. (2021). Rhizosphere soil properties, microbial community, and enzyme activities: short-term responses to partial substitution of chemical fertilizer with organic manure. *J. Environ. Manag.* 299:113650. doi: 10.1016/j.jenvman.2021.113650

Saeid, A., Prochownik, E., and Dobrowolska-Iwanek, J. (2018). Phosphorus solubilization by *Bacillus* species. *Molecules* 23. doi: 10.3390/molecules23112897

Sánchez-Rangel, J. C., Benavides, J., Heredia, J. B., Cisneros-Zevallos, L., and Jacobo-Velázquez, D. A. (2013). The Folin-Ciocalteu assay revisited: improvement of its specificity for total phenolic content determination. *Anal. Methods* 5, 5990–5999. doi: 10.1039/c3ay41125g

Schneider, K. D., van Straaten, P., de Orduña, R. M., Glasauer, S., Trevors, J., Fallow, D., et al. (2010). Comparing phosphorus mobilization strategies using *Aspergillus niger* for the mineral dissolution of three phosphate rocks. *J. Appl. Microbiol.* 108, 366–374. doi: 10.1111/j.1365-2672.2009.04489.x

Stojanovic, M., Petrovic, I., Zuza, M., Jovanovic, Z., Moravcevic, D., Cvijanovic, G., et al. (2020). The productivity and quality of *Lactuca sativa* as influenced by microbiological fertilisers and seasonal conditions. *Zemdirbyste-Agriculture* 107, 345–352. doi: 10.13080/z-a.2020.107.044

Thiel, T. (2019). Organization and regulation of cyanobacterial nif gene clusters: implications for nitrogenase expression in plant cells. *FEMS Microbiol. Lett.* 366:fnz077. doi: 10.1093/femsle/fnz077

Tulumello, J., Chabert, N., Rodriguez, J., Long, J., Nalin, R., Achouak, W., et al. (2021). Rhizobium alamii improves water stress tolerance in a non-legume. *Sci. Total Environ.* 797:148895. doi: 10.1016/j.scitotenv.2021.148895

Tyc, O., Song, C., Dickschat, J. S., Vos, M., and Garbeva, P. (2017). The ecological role of volatile and soluble secondary metabolites produced by soil bacteria. *Trends Microbiol.* 25, 280–292. doi: 10.1016/j.tim.2016.12.002

Urbina, J., Chestnut, T., Allen, J. M., and Levi, T. (2021). *Pseudogymnoascus* destructans growth in wood, soil and guano substrates. *Sci. Rep.* 11:763. doi: 10.1038/s41598-020-80707-1

Wang, Y. Y., Cheng, Y. H., Chen, K. E., and Tsay, Y. F. (2018). Nitrate transport, signaling, and use efficiency. *Annu. Rev. Plant Biol.* 69, 85–122. doi: 10.1146/annurev-arplant-042817-040056

Wang, J., Liao, L., Wang, G., Liu, H., Wu, Y., Liu, G., et al. (2022). N-induced root exudates mediate the rhizosphere fungal assembly and affect species coexistence. *Sci. Total Environ.* 804:150148. doi: 10.1016/j.scitotenv.2021.150148

Wu, W. L., Yan, J. L., Jiang, T., and Wei, S. Q. (2019). Natural organic matter-metal ion/oxide-phosphorus complexes in environment: a review. *J. Ecol. Rural Environ.* 35, 1089–1096. doi: 10.19741/j.issn.1673-4831.2018.0636

Wust, P. K., Foesel, B. U., Geppert, A., Huber, K. J., Luckner, M., Wanner, G., et al. (2016). *Brevitalea aridisoli*, *B. deliciosa* and *Arenimicrobium luteum*, three novel species of Acidobacteria subdivision 4 (class Blastocatellia) isolated from savanna soil and description of the novel family Pyrinomonadaceae. *Int. J. Syst. Evol. Microbiol.* 66, 3355–3366. doi: 10.1099/ijsem.0.001199

Xiao, C., Wu, X., and Chi, R. (2015). Dephosphorization of high-phosphorus iron ore using different sources of *Aspergillus niger* strains. *Appl. Biochem. Biotechnol.* 176, 518–528. doi: 10.1007/s12010-015-1592-4

Xu, G., Fan, X., and Miller, A. J. (2012). Plant nitrogen assimilation and use efficiency. *Annu. Rev. Plant Biol.* 63, 153–182. doi: 10.1146/annurev-arplant-042811-105532

Xu, Q., Ling, N., Chen, H., Duan, Y., Wang, S., Shen, Q., et al. (2020). Long-term chemical-only fertilization induces a diversity decline and deep selection on the soil bacteria. *mSystems* 5:e00337-20. doi: 10.1128/mSystems.00337-20

Yan, P., Wu, L., Wang, D., Fu, J., Shen, C., Li, X., et al. (2020). Soil acidification in Chinese tea plantations. *Sci. Total Environ.* 715:136963. doi: 10.1016/j.scitotenv.2020.136963

Yang, H., Zhang, Y., Chuang, S., Cao, W., Ruan, Z., Xu, X., et al. (2021). Bioaugmentation of acetamiprid-contaminated soil with *Pigmentiphaga* sp. strain D-2 and its effect on the soil microbial community. *Ecotoxicology* 30, 1559–1571. doi: 10.1007/s10646-020-02336-8

Yang, L. Y., Zhou, S. Y., Lin, C. S., Huang, X. R., Neilson, R., and Yang, X. R. (2022). Effects of biofertilizer on soil microbial diversity and antibiotic resistance genes. *Sci. Total Environ.* 820:153170. doi: 10.1016/j.scitotenv.2022.153170

Ye, X., Li, Z., Luo, X., Wang, W., Li, Y., Li, R., et al. (2020). A predatory myxobacterium controls cucumber Fusarium wilt by regulating the soil microbial community. *Microbiome* 8:49. doi: 10.1186/s40168-020-00824-x

Yu, F., Jing, X., Li, X., Wang, H., Chen, H., Zhong, L., et al. (2019). Recombineering pseudomonas protegens CHA0: an innovative approach that improves nitrogen fixation with impressive bactericidal potency. *Microbiol. Res.* 218, 58–65. doi: 10.1016/j.micres.2018.09.009

Yu, H., Yuan, M., Lu, W., Yang, J., Dai, S., Li, Q., et al. (2011). Complete genome sequence of the nitrogen-fixing and rhizosphere-associated bacterium pseudomonas stutzeri strain DSM4166. *J. Bacteriol.* 193, 3422–3423. doi: 10.1128/JB.05039-11

Yuan, J., Zhao, M., Li, R., Huang, Q., Raza, W., Rensing, C., et al. (2017). Microbial volatile compounds alter the soil microbial community. *Environ. Sci. Pollut. Res. Int.* 24, 22485–22493. doi: 10.1007/s11356-017-9839-y

Zhang, M., Muhammad, R., Zhang, L., Xia, H., Cong, M., and Jiang, C. (2019). Investigating the effect of biochar and fertilizer on the composition and function of bacteria in red soil. *Appl. Soil Ecol.* 139, 107–116. doi: 10.1016/j.apsoil.2019.03.021

Zhang, M., Zhang, L., Riaz, M., Xia, H., and Jiang, C. (2021). Biochar amendment improved fruit quality and soil properties and microbial communities at different depths in citrus production. *J. Clean. Prod.* 292:126062. doi: 10.1016/j.jclepro.2021.126062

Zhou, J. B., Jin, Z. J., Xiao, X. Y., Leng, M., Wang, X. T., and Pan, F. J. (2021). Investigation of soil fungal communities and functionalities within karst Paddy fields. *Huan Jing Ke Xue* 42, 4005–4014. doi: 10.13227/j.hjkx.202011164

Zhu, Q., Liu, X., Hao, T., Zeng, M., Shen, J., Zhang, F., et al. (2018). Modeling soil acidification in typical Chinese cropping systems. *Sci. Total Environ.* 613–614, 1339–1348. doi: 10.1016/j.scitotenv.2017.06.257

Frontiers in Microbiology

Explores the habitable world and the potential of microbial life

The largest and most cited microbiology journal which advances our understanding of the role microbes play in addressing global challenges such as healthcare, food security, and climate change.

Discover the latest Research Topics

See more →

Frontiers

Avenue du Tribunal-Fédéral 34
1005 Lausanne, Switzerland
frontiersin.org

Contact us

+41 (0)21 510 17 00
frontiersin.org/about/contact